

Environmental Science and Technology

(2016)

Volume 2

Edited by

George A. Sorial

Jihua Hong

ISBN 978-1-5323-2260-0

Library of Congress Cataloging-in-Publication Data

Environmental Science and Technology 2016 Vol. 2

Proceedings from the 8th International Conference on Environmental Science and Technology, held on June 6-10, 2016 in Houston, Texas, USA

Includes bibliographical references

ISBN: 978-1-5323-2260-0

I. Sorial, George A.

II. Hong, Jihua

III. International Conference on Environmental Science and Technology
(8th : 2016 : Houston : Texas)

Printed in the United States of America

Copyright © 2016 American Science Press. All rights reserved. This document, or parts thereof, may not be reproduced in any form without the written permission of the American Science Press. Requests for permission or further information should be addressed to the American Science Press, 9720 Town Park Dr. Ste. 18, Houston, TX 77036, USA

Email: press@AASci.org

Website: www.AASci.org/conference/env

ISBN 978-1-5323-2260-0

© 2016 American Science Press

Environmental Science and Technology (2016)

Volume 2

Edited by

**George A. Sorial
Jihua Hong**

American Science Press, Houston, USA

TABLE OF CONTENTS

LAND (SOIL, SOLID WASTE) POLLUTION AND REMEDIATION	1
<i>Contaminants in the Subsurface</i>	
Improving Soil Chemical Properties and Maize Growth in Southeastern Nigerian Ultisol Using Spent Grain Ash. <i>Ogbonna, Emmanuel Ahamefula and Osodeke, Victor Emmanuel</i>	2
Variable Behaviour of Mass Transfer Coefficient with Velocity, Length and Dispersion of Reactive Solute. <i>Deepak Swami, Abhimanyu Sharma</i>	9
Preliminary Study of Heavy Metal Pollution in Soil of Industrial Zone of Surat – India. <i>Tank Shantilal K, Mehra Bhavna K</i>	10
Transport and Adsorption of Colloids in Soils: A MRI Approach. <i>Alizée P. Lehoux, Eric Michel, Pamela Faure, Denis Courtier-Murias, Stéphane Rodts, Philippe Coussot</i>	11
Vertical Distributions of Elements in the Soil (Albic Luvisol) of Sanjiang Plain in China. <i>Wei Ouyang, Hongguang Cheng, Chunye Lin</i>	12
<i>Natural Attenuation of Contaminants</i>	
Modeling of Phosphorus Sorption and Buffering Mechanisms in Selected Soils of Fiji. <i>Muni Sangeeta Goundar, John Morrison and Satyanarayan Shashtri</i>	13
<i>In-Situ Remediation</i>	
Innovative In-Situ Oxidation Technologies for Treating Groundwater Contaminated by Chlorinated Solvents and 1,4-dioxane. <i>Hua Zhong, Mark Brusseau, Ni Yan, Lina Zhang, and Peng Cui</i>	19
Utilizing Plants to Limit the Migration of Contaminants from Fracking-Water Spill Sites. <i>Amanda Shores, Brittany Hethcock, Dr. Melinda Laituri</i>	20
<i>Solid Waste Management / Polymer Waste Recycling and Management</i>	
Bio-drying of Green Wastes. <i>Ertan Durmusoglu, Mutala Mohammed, and Ismail Ozbay</i>	21
A New Concept for Utilization of Industrial Solid Wastes in Building Structures. <i>Arunima Shukla and Ashok N. Bhaskarwar</i>	27
Recovery of Copper from Waste Printed Circuit Boards (PCBs) using Electrowinning Process. <i>Pradeep Kumar, Shashi Bhushan Kumar, Poornima Pandey and Roli Saini</i>	33
Waste: A Raw Material for Soil Amendment and an Employer of Labour. <i>Ogbonna, Emmanuel Ahamefula and Isinguzo, Nnadozie Sunday</i>	38
The Effects of Different Condensation Temperatures on Waste Tire Pyrolysis, <i>Neslihan Doğan-Sağlamtimur, Ahmet Bilgil, Tuğçe Aykanat, Öznur Çalışkan, Funda Yolcu, Elif Dilan Yıldırım, Türkan Vural, Halime Ötgün and Büşra Arıcan</i>	44
The Impact of Saw Dust Biochar on Soil PH and Crop Yields for Climate Change Mitigation. <i>Lukong Pius Nyuykonge and George Elambo Nkeng, Lenzemo Wirnkar Venasius</i>	45
Impacts of Waste Disposal Methods on Household Health Conditions in Kenya. <i>Emmanuel Donkor, Stephen Onakuse, Joe Bogue</i>	46

The Challenges of Sustainable Management of Electronics Waste and the Risk Assessment of Improper Management Practices. <i>E. Sahle-Demessie, Teri' Richardson, Joshua Dietrich.</i>	47
<i>On-site / Off-site Remediation</i>	
On-Situ Remediation of Nitro Compound Contaminated Soil by Biological-Ecological Method. <i>Quanlin Zhao, Zhengfang Ye, Zhongyou Wang and Zengxiong Li.</i>	48
Fenton Oxidation of Polycyclic Aromatic Hydrocarbons in the Concentrates Obtained From the Decontaminated Soil. <i>Malika Bendouz, Lan Huong Tran, Lucie Coudert, Guy Mercier and Jean-François Blais.</i>	49
<i>Landfill / Pemeable Reactive Barriers/</i>	
Dredged Material as Restoration Substrate in Landfill Surface Sealing Systems <i>Gert Morscheck, Gert, Astrid Lemke, Michael Henneberg.</i>	50
Treatment of Sanitary Landfill Leachate by Membrane Distillation. <i>Yasemin Melek Tilki, Gizem Sahin, Berna Kiril Mert, Coskun Aydiner, Esra Can Dogan.</i>	60
Environmental Monitoring of Landfills by a Downscaling Approach. <i>Mei Alessandro, Manzo Ciro, Paciucci Lucia, Allegrini, Alessia, Petracchini Francesco, Romagnoli Paola, Bassani Cristiana.</i>	61
<i>Waste Fuel Site Remediation / Waste Recycling</i>	
Performance of Vegetative Bioretention System for Greywater Reuse in the Arid Climates. <i>Rezaul Chowdhury, Taoufik Ksiksi, Mohamad M A Mohamed and Jameelu Abaya.</i>	62
Bio-Waste Recycling in Germany. <i>M. Nelles, A. Schüch, A. Lemke, G. Morscheck.</i>	68
Utilization of Woodwaste as Container Media by Accelerated Composting. <i>Hoda Bakhshizadeh, H. Borazjani, R. C. Sloan, and S. S. Worthey.</i>	78
Novel Coupled Surface Modification and Froth Flotation Separation of Halogenated Plastics from Hazardous Waste (ASR/ESR) Plastics with Nanoscale Metallic Calcium Composite. <i>Srinivasa Reddy Mallampati, Je Haeng Heo and Min Hee Park.</i>	79
Characterization of Carbon-Based Biochar from Grapeseed Pyrolysis. <i>Nathaniel F. Adegboyega & William C. Hockaday, Chris Cunningham & Mark Kelm.....</i>	80
Effect of Tire Rubber Ash on Bituminous Mixes Used for Roadway Pavement. <i>Tapash Kumar Roy</i>	81
Struvite Recovery from Wastewater and Reuse as Amendment for Heavy Metals Immobilization in Soil. <i>Hao Wang, Xuejiang Wang, Jing Zhang, Jingke Song.</i>	85
Hydrothermal Synthesis of Zeolite A from Bottom Ash of Sugar Industry Its Crystallization. <i>Noor-ul-Amin and Yousaf Hameed.</i>	86
Recycling Spent Lithium-Ion Battery for Function Material Development. <i>Fu-Shen Zhang, Meng-Meng Wang.</i>	87
Reuse of Green Walnut Shell to Produce Dye, <i>Ruhsar Arabacioğlu, Neslihan Doğan-Sağlamtimur and Ersen Turaç.</i>	88
Recycling Mercury-Impacted Scrap Metal: Key Issues and Research Needs. <i>Molly E. Finster and Corrie E. Clark.</i>	89
<i>Radioactive Waste and Land Pollution</i>	
The Potential of Effective Microorganism (EM) to Promote the Phytoremediation of Uranium Polluted Water. <i>Jing Zhu, Ke Chen, Renhua Huang, Xiaoming Chen, Gangxue Luo.</i>	90

Grass and Microbial Combined Remediation to Uranium-Contaminated Soil, <i>Xiaoming Chen, Xuegang Luo, Xichao Hao, Ke Chen</i>	91
---	----

Phytoremediation of Organic Pollutants

Potentially Useful Plants for Phytoremediation of Hydrocarbons in Subtropical Zone: Cameroon Case. <i>Matsodoum N. P., Wanko N. A., Ndemba Etim S. G., Djumyom Wafo G. V., Djougoue P. F., Kengne Noumsi I. M.</i>	92
Ex-Situ Phytoremediation of Hydrocarbon Contaminated Soil with <i>Crotalaria Pallida</i> Ait. <i>Partha Pratim Baruah, Plabita Baruah, and Suresh Deka</i>	93
Assessment for Removing Multiple Pollutants by Plants in Bioretention Systems Based on ISPA Model. <i>Xiaohua Yang, Yi Ye, Meishui Li</i>	94

Polymer Waste Recycling and Management

Synthesis and Properties of Biodegradable Polyesters Based On Biomass Monomers. <i>Yang Zhang, Jun Xu, Baohua Guo</i>	95
---	----

ECOSYSTEM ASSESSMENT AND RESTORATION

Ecosystem Assessment

An Ecological Study of Reproduction in <i>Coringa</i> Mangrove Forest, Andhra Pradesh, India. <i>Aluri Jacob Solomon Raju</i>	97
Some Risk Assessments at Nuclear Power Plants (NPP). <i>Alexander Valyaev, Gurgen Aleksanyan, Alexey Valyaev, Oleg Arkhipkin</i>	135
The Elbe Estuary: Balance between a High Frequented Waterway and the Provision of ESS. <i>Carolin Schmidt-Wygasch, Uwe Schröder, Elmar Fuchs, Rainer Marggraf, Jan Barkmann, and Uta Sauer</i>	143
Novel Taxa Are Dominant in Mangrove Swamp of Niger Delta, Nigeria. <i>Chika Christiana Nwankwo., Gideon Chijioko Okpokwasili</i>	144
Phylogenic Diversity of Microorganisms in the Mangrove Swamp under Crude Oil Perturbation. <i>Onyinyechika Christiana Nwankwo</i>	145
Stress Factors to Fish Habitat in Urban Rivers. <i>Yuta Yamauchi, Tetsuya Nakata, and Yutaka Sakakibara</i>	146

Nutrients and Functions of Ecosystems

The Impact of Alternative Measures of Riverbank Fixation on Climate Change and Water Quality. <i>Lars Symmank, Katharina Raupach, Mathias Scholz and Christiane Schulz-Zunkel</i>	147
---	-----

Restoration of Ecosystems

State Transitions and Feedback Mechanisms during Ecosystem Development in the Constructed Catchment 'Chicken Creek'. <i>Wolfgang Schaaf, Christoph Hinz, Werner Gerwin, Markus K. Zaplata, Reinhard F. Huettl</i>	148
Ecosystem Assessment and Restoration. <i>Elvis Obeng Boateng</i>	149

Urban Ecosystems

Land Surface Temperature Variation and Land Cover Changes Based on Satellite Imagery Data. <i>Kim-Anh Nguyen, Yuei-An Liou, and Ming-Hsu Li.</i>	150
Causes of Dampness in Residential Building Walls in Jos Metropolis, Plateau State, Nigeria. <i>Kalada Itelima.</i>	157

WETLANDS

Wetland Conservation

Restoration of a Tropical Wetland through Low-Cost Technology. <i>Shadananan Nair</i>	159
Spatial Distribution of Wetland Vegetation and its Ecological Function on Riparian Zone of Riverscape. <i>Lixin Wang.</i>	160
Impact of Urban Sprawling on East Kolkata Wetland and on the Ecosystem Functioning of Sundarbans Mangrove Ecosystem, India. <i>Susanta Kumar Chakraborty, Poulami Sanyal, Nandan Bhattacharyya, Ratnadip Roy and Sumana Bandhopadhayay.</i>	161

Wetlands for Wastewater Treatment

Behavior of Antibiotics with Corresponding Resistance Genes in Constructed Wetland Coupled with Microbial Fuel Cell. <i>Shuai Zhang and Hai-liang Song</i>	162
--	-----

SEDIMENTS

Assessment of Sediments

The Elbe Estuary (Germany): Resistance of the Sediments to Hydrodynamic Forces on Microscale. <i>Nina Stoppe, Thomas Neugebauer, Rainer Horn, Uwe Schröder, Elmar Fuchs, and Carolin Schmidt-Wygasch.</i>	173
Development and Evaluation of New Indices for Sediment-Associated Contaminants. <i>Nsikak U. Benson, Adebayo E. Adedapo, Omowunmi H. Fred-Ahmadu, Akan B. Williams and Abaas A. Iajire</i>	174
Geochemical Speciation and Risk Assessment of Trace Metals in Sediments from Coastal Ecosystems off Equatorial Atlantic Ocean. <i>Nsikak U. Benson, Essien D. Udosen, Winifred U. Anake, Akan B. Williams, Oyeronke A. Akintokun, Adebayo E. Adedapo and Abaas A. Olajire</i>	175
Milling Conditions Effect on Contaminated Sediments Treatment by Pozzolanic Materials. <i>Rabah Hamzaoui, Othman Bouchenafa, Abdelkrim Bennabi, Johan Colin.....</i>	176
Surface Water and Sediment Quality Assessment in the Gbaran-Ubie Integrated Oil & Gas Project, Niger Delta, Nigeria. <i>Seiyaboh, E.I., Gijo, A.H and Sikoki, F.D.</i>	177

Remediation of Contaminated Sediments

Distribution of Organochlorine Pesticide Residues in Epipellic and Benthic Sediments from Lagos Lagoon, Nigeria. <i>Akan Williams, Nsikak Benson and Egbenya Shaibu-Imodagbe</i>	178
Development and Testing of Next Generation Sorbent Polymer Extraction and Remediation from Sediments (SPEARS) Technology. <i>Robert DeVor, Phillip Maloney, and Jacqueline Quinn.</i>	187

GLOBAL WARMING AND CLIMATE CHANGE

Global Warming and Its Impacts

Forest Fire - A Global Scenario Identification and Sustainable Management Using Geo Information Technology. *Jose T. M, Subin K. Jose, G. Madhu.* 189

Reducing Global Warming In Africa through Traditional African Architecture: Challenges and the Way Forward. *Iwuagwu, Ben Ugochukwu; Onyegiri, Ikechukwu; Iwuagwu, Ben Chioma.* 196

Enhancement of Wastewater Facilities for Long Term Global Climate Changes. *Amirthaganth Amithalingam, and D. S. Mahamah.* 202

An Integrated Assessment of Low Carbon Emission Scenarios proposed in Climate Policy. *Sascha Hokamp and Mohammad Mohammadi Khabbazan.* 203

Carbon Discharge Reduction

Leapfrogging Carbon Capture Sequestration. *Adel J. Al-Khalifah* 204

Aerobic and Nitrite-Dependent Methane Oxidizers in the Zoige Wetland of the Tibetan Plateau. *Anzhou Ma, Guoqiang Zhuang, Mengmeng Cui.* 205

Energy Conservation Helps in Mitigation of Adverse Effects of Climate Change. *Mehboob Alam Khan.* 206

METALS

Metal Distribution

Spatial and Temporal Distribution of Heavy Metals in Coastal Red Sea Sediments. *Bandar Almur, Andrew Quicksall, Ahmed M. Al-Ansari.* 208

Vertical Distribution and Chemical Behavior of Uranium in the Tailings Material of Schneckenstein (Germany). *Taoufik Naamoun and Broder Merkel.* 215

Synergetic Effects of Cd²⁺ and Cu²⁺ on Chlorophyll Fluorescence of *Microcystis Aeruginosa*. *Cui Jiansheng*, Song Yanyan* 216

Characteristics of Heavy Metal Pollution from Antimony Mining, Ore Dressing and Smelting Process in China. *Mengchang He.* 217

Metal Removal and Remediation

Citric Acid Enhanced Metal Uptake in Reed Seedlings in Acid Mine Drainage Solutions. *Lin Guo, Teresa J. Cutright.* 218

Silver Recovery: Silver Ion Toxicity. *S. Syed.* 223

Removal of Hg(II) By Encapsulated Thiophosphinic Extractants. *Janette Alba, Ricardo Navarro, Imelda Saucedo, and Eric Guibal.* 235

Technologies for Reducing Uptake and Transport of Heavy Metals into Rice Grain. *Yongchao Liang and Tingqiang Li, Alin Song, Zhaojun Li, and Fenliang Fan, Xionghui Ji.* 236

Speciation, Bioavailability and Accumulation/ Phytoremediation

Levels of Heavy Metals in Organs of *Oreochromis Niloticus* from Great Kwa River, South-East Nigeria. *Philomena Asuquo and Lynda-Uta Okon, Juliet Yakubu.* 237

Effect of Selected Heavy Metals on the Germination and Early Seedling Growth of *Jatropha Curcas* (Linnaeus). *Ogunbanjo O.R., Akintola O.O. and Awotoye O.O.* 238

Studies on Effect of Mixed Cropping Technique on the Phytoextraction Potential of Vegetables over Hyperaccumulators. <i>Tank Shantilal</i>	245
--	-----

CHLORINATED AND OTHER PERSISTENT ORGANIC COMPOUNDS

Characterization of Organic Pollutants

Biological and Instrumental Analysis of Emerging Contaminants of Concern: In Single and Multiple Profiling. <i>Momoh A. Yakubu, Nina Brinkley, Syntia Kwende, Sara Munyu, Chioma Ihemadu, Fatemeh Bidabadi, Bhavin Rena, Joan Tran, Naga Naidu, and Gloria Okome</i>	247
Analysis of Nonylphenol Compounds in Aquatic Environment Using Gas Chromatography-Mass Spectrometry. <i>Seçil Ömeroğlu, Fadime Kara Murdoch and Faika Dilek Sanin</i>	248

Degradation of Persistent Organic Pollutants

Photolytic and Photocatalytic Decomposition of Pharmaceuticals in Water by Ultraviolet Light-Emitting Diode. <i>Burhanuddin Khuzema Zaveri, Mohammad Reza Eskandarian, Mostafa Fazli, Mohammad Hossein Rasoulifard, Hyeok Choi</i>	249
In-situ Decomposition of Biological Toxins on Nitrogen-Doped Nanostructured TiO ₂ Films under Solar Radiation. <i>Hesam Zamankhan Malayeri and Hyeok Choi</i>	254
Dechlorination of DDT and its Products Using Palladized Bacterial Cellulose in a Reactor. <i>Sumathi Suresh and Vyjayanthi J. P.</i>	259
The Potential of Spore Forming Bacteria in Heavy oil Spill Clean Up. <i>Biji Shibulal, Saif Al-Bahry, Yahya Al-Wahaibi, Abdulkadir Elshafie, Ali Al-Bemani, Sanket J.</i>	266
Separation of Polybrominated Diphenyl Ethers in Fish for Compound-Specific Stable Carbon Isotope Analysis. <i>Yanhong Zeng, xiaojun Luo and Bixian Mai</i>	267

MODELING

Environmental Simulation

Design Optimization of Gas-To-Liquid Biosludge Management Systems. <i>Rana Abbass, Emad Imam</i>	269
Probing the Water Quality Transformation of Underground Caverns in a Tropical Region Using ELCOM-CAEDYM Model. <i>Ming Chen, Jian Li, and Xiaosheng Qin</i>	276
Depth Filtration through Porous Media. <i>Hooman Fallah</i>	283
Environmental Quality and Foreign Trade in Turkey: A Cointegration Analysis with a Structural Break. <i>Nilgün Çil</i>	292
Environmental Kuznets Curve Hypothesis and Structural Breaks: Evidence from Turkey. <i>Burcu Kıran</i>	297
A Linear Genetic Programming Approach for Discharge Forecasting. <i>Jonathan Barge and Hatim Sharif, Jonathan Barge and Hatim Sharif</i>	304
Vulnerability Assessment of the Central Gulf of Mexico Coast using a Multi-dimensional Index Approach. <i>David E. Dismukes and Siddhartha Narra</i>	306
Predicting the Long-Term Leaching Behavior of Coal Ash Deposits in Mine Site: A Column Study. <i>Mina Mohebbi, Farshad Rajabipour, and Barry E Scheetz</i>	307

Water Quality Modeling

Investigation, Modeling and Prediction of Triclosan and Carbamazepine in Surface Waters: A Case Study in the Shahe Stream. <i>Xiao Yuan, Shiyu Li, Jiatang Hu, Yuying Li, Ziyun Wang and Jia Huang.</i>	308
Space/Time Geostatistical Estimation of Chloride along Maryland Rivers Using a Covariance Model with River Distances. <i>Prahlad Jat, Marc L Serre.</i>	323
Modeling of Spreading of Submarine Mine Tailings in a Norwegian Fjord. <i>Øyvind Leikvin, Venkat Kolluru, Guttorm N. Christensen, Magdalena Kempa, Torulv Tjomsland.</i>	324

GIS, DATABASE, AND REMOTE SENSING

GIS for Environmental Assessment / Data Management and Statistics / Environmental Remote Sensing Applications

Estimation of Crop Coefficients using Remote Sensing and GIS: A Case Study of Khuskera-Bhiwari Neemrana Investment Region, Rajasthan, India. <i>Rohit Goyal, Kuldeep Tiwari and Priyamitra Munoth.</i>	326
Geospatial Mapping of Groundwater Quality Using GIS. <i>Prachi Singh, Raj Mohan Singh.</i>	333
Development and Application of the Integrated Water Distribution Management System. <i>Patryk Wójtowicz, Andrzej Ziółkowski and Janusz Studziński.</i>	340

ENVIRONMENTAL ANALYSIS AND MEASUREMENTS

Environmental Analysis

Sustainability Evaluation of Food and Bioplastic Waste Management Options. <i>Shakira R. Hobbs, Prathap Parameswaran, and Amy E. Landis.</i>	342
Deuterated Monitoring Compounds for Better Accuracy and Precision Measurement of GC/MS Environmental Data. <i>Charles Appleby.</i>	348
Pretreatment Method for Total Organic Carbon (TOC) Analysis of Suspended Solids-Containing Water Samples. <i>Han-Saem Lee, So-Hui Kim, and Hyun-Sang Shin, Jin Hur, Keun-Heon Lee.</i>	349

Field Measurement Technologies

Experimental Study on Stream Flow Measurement Using Large Scale Particle Image Velocimetry Techniques. <i>Aadhi Naresh and M. Gopal Naik.</i>	350
Radiosonde Launch under High Surface Wind. <i>Boris S. Yurchak.</i>	359
The Critical Parameters for How to Address Oil/Hydrocarbon Based Material Spills. <i>Steven Pedigo.</i>	364

New Method Applications

An Alternative Method to Overcome Inconsistent Cellulolytic Screenings when using Gram's Iodine. <i>Joshua OHair, Terrance Johnson, Anthony Ejiofor and Suping Zhou.</i>	365
--	-----

Environmental Monitoring

Landscape Changes in Lopé National Park, Gabon: To what is the extent of Savannah thickening? <i>Gilbert Gauci.</i>	366
---	-----

SOCIETY AND THE ENVIRONMENT

Society and the Environment

Public Perception and Acceptance of Fertilizers from Human Urine among Turkish Citizens Holding University Degrees. <i>Ayse D. ALLAR, Nihan YILDIZ-DOGAN, Bilsen BELER-BAYKAL.</i>	368
Fragmented Stakeholders: Unaccountable Representatives. <i>Yaw Amo Sarpong, Nelson Owusu Ansah, Emmanuel Marfo, Francisca Amoatema.</i>	375
Some Remarks to Risk Assessments of Nuclear Power Plants (NPP). <i>Alexander Valyaev, Gurgen Aleksanyan, Alexey Valyaev.</i>	376
Cost-Risk Analysis of Solar Radiation Management. <i>Mohammad Mohammadi Khabbazan, Elnaz Roshan, and Hermann Held.</i>	377
In Light of Infrastructure and Construction Affordability, Can Southeast Queensland Cater for Current Population Forecasts? <i>Kirsty Miller, David Hood.</i>	378

Environmental Ethics and Laws

Science, Political Polarization, and How Hydraulic Fracturing Is Framed as Environmentally Safe or Risky. <i>Michelle L. Edwards.</i>	379
Implementation of Environmental Laws and Ethics in India. <i>C.V. Rajeswari.</i>	386

Environmental Education

Environmental Education at the Maritime Education Training, <i>Tanzer Satır and Neslihan Doğan-Sağlamtimur.</i>	387
Education Program to the Environment: An Advocacy of a Travel Agency in Avo City, Philippines. <i>Lilia F. Panchito, Ruben A. Neri, Recto B. Campos, Elisa P. Madrazo.</i>	388
Students' Attitudes towards the Environment. <i>Mile Srbinovski, Veton Latifi & Zamir Dika.</i>	389
Does Viewing Documentary Films Affect Environmental Perceptions and Behaviors? <i>Henry Janpol, Rachel Dilts.</i>	390

ENVIRONMENTAL PLANNING AND MANAGEMENT

Environmental Quality and Planning

A Study on the Vulnerability of Alahsa Governorate to Generate Urban Heat Islands. <i>Ilham Elsayed.</i>	392
Optical-Electronic Equipments of Ecological Dedication. <i>Ruben Asatryan, Hamlet Karayan, Norayr Khachatryan.</i>	399
An Approach for Environmental Risk Assessment of Engineered Nanomaterials Using Analytical Hierarchy Process (AHP) and Fuzzy Inference Rules. <i>Emel TOPUZ, C.A.M. van Gestel.</i>	400

Energy-related Environmental Problems

What Is Ethical? --- An Analysis of the Opposing Forces of Environmental. <i>Terry L. Polen, Carri Coleman Tucker.</i>	401
Climate Variability and Sustainable Development: The Case of Nigeria's Niger Delta Region. <i>Chika Ubaldus Ogbonna.</i>	407
Urban Environmental Overall Planning and Its Role in Urban Sustainable Development in China. <i>Luyan Wang, Yang Zhao, Lina Tang, and Jingzhu Zhao.</i>	414
Performance Enhancement of Evaporative Cooling Technology in the Company of Lower Environmental Impact. <i>S.P. S. Rajput and Amrat Kumar Dhamneya.</i>	415
Adaptation Strategies to Mitigate Climate Change Impacts on Urban Stormwater. <i>Ashantha Goonetilleke, An Liu, and Erick R. Bandala.</i>	416
Environmental and Social Sustainability. <i>Sukhmander Singh.</i>	417
Ecotourism and Sustainable Development; Evidence from Lope National Park, Gabon. <i>CORNELIUS Frimpong.</i>	418

Environmental Policy and Management

Stakeholder Participation in Integrated Watershed Management: Models and Process. <i>Aysegul Tanik & Cigdem Kanber.</i>	419
Effectiveness of South Africa's Biodiversity Policies in Protecting the Indigenous Vegetation of the Soutpansberg Region. <i>Priscilla Ntuchu Kephe and Brilliant M. Petja.</i>	426

RENEWABLE ENERGY DEVELOPMENT

Water Energy Nexus / Wind Energy / 16-3 Solar Energy

Photogalvanic Cell: An Efficient Device for Photochemical Conversion and Storage of Solar Energy. <i>Chhagan Lal.</i>	428
The Environmental Benefits of Achieving High Solar Penetrations in the United States. <i>Ryan Wisner, Trieu Mai, Dev Millstein, Jordan Macknick, Alberta Carpenter, Stuart Cohen, Wesley Cole, Bethany Frew, Garvin Heath.</i>	434

Bio-fuels

Energy Consumption Pattern and Greenhouse Gases Emission: A Case Study on Potentiality of Biogas as a Renewable Energy Technology and its Role in Reducing Greenhouse Gases Emission. <i>Poudel M., Adhikari P. and Singh R. M.</i>	435
Cloning of Genes Encoding for Cellulolytic Enzymes from Metagenome in Goat's Rumen. <i>Santosh Thapa, Hui li, Suping Zhou, Sarabjit Bhatti and Roger J. Sauvé.</i>	442
Anaerobic and Subsequent Photosynthetic Process for Biohydrogen and Bioplastic (PHB) Production. <i>Arun. A, Dinesh. G. H and Satheesh Murugan. R.S. Karthik Sundaram.</i>	443
Algal Oil Production Potential under Different Municipal Wastewater Delivery Scenarios. <i>Tyler Brown and Yiwen Chiu.</i>	444
Economics of Green versus Dry Forest Harvest Residue Feedstock for the Aviation Fuel Supply Chain. <i>Rene Zamora-Cristales and John Sessions.</i>	445
Cloning and Characterization of Genes Encoding Cellulolytic Enzymes Screened From Goat Rumen Metagenome. <i>Santosh Thapa, Hui Li, Sarabjit Bhatti, and Suping Zhou.</i>	446

Special Energy Development

Preparation and Properties of MA-PA/EG Composite Phase Change Material for Energy Storage. <i>Wu Jianyun, Zhou Wenhe, Yuan Yanping, Yuan Yaguang.</i>	447
Eco-Economical Non-Conventional Method for Electricity Generation. <i>Seema Vats.</i>	455

**LAND (SOIL, SOLID WASTE) POLLUTION
AND
REMEDICATION**

IMPROVING SOIL CHEMICAL PROPERTIES AND MAIZE GROWTH IN SOUTHEASTERN NIGERIAN ULTISOL USING SPENT GRAIN ASH

Ogbonna Emmanuel Ahamefula (DOTECON Nigeria Limited, Lagos, Nigeria)¹
OSODEKE, Victor Emmanuel (Michael Okpara University of Agriculture, Umudike, Abia, Nigeria)

ABSTRACT: A pot experiment was conducted at the Michael Okpara University of Agriculture, Umudike, Abia State, Southeastern Nigeria to determine the effect of spent grain ash on chemical properties of an acid Ultisol; its effect on the growth and nutrients uptake of maize. Six treatment levels of spent grain ash: 0 (control), 1, 2, 3, 4, and 5 ton/ha were applied and replicated three times in Completely Randomized Design (CRD) in a total of 18 pots. The effects of the treatments on soil pH, exchange acidity, exchangeable bases, available phosphorus, total nitrogen and organic matter were evaluated using standard laboratory procedures. Maize parameters measured were plant height, number of leaves, leaf area, number of roots, root lengths, stem diameter, moisture content and dry matter yield. The results showed that all the treatments significantly ($P < 0.05$) increased soil pH and reduced exchange acidity, with 5ton/ ha of spent grain ash being more effective than the other treatments. For the plant parameters, 5 ton/ha of spent grain ash gave the highest significant ($P < 0.05$) values except for leaf area. For soil parameters after planting, 5 ton/ha of spent grain ash significantly ($P < 0.05$) increased soil pH and reduced exchange acidity. There was generally significant positive correlation between soil pH and plant parameters except for root length and dry matter weight. The study also showed that 5 ton/ha of spent grain ash was more effective in amelioration of soil acidity and enhancing the growth of maize, confirming its liming potential in an Ultisol of Umudike area of Southeastern Nigeria.

INTRODUCTION

Soil acidity has been identified as a major problem to world food production due to the drastic reduction in crop yield as a result of depletion of basic cations (Tang *et al.*, 2003) and increase in hydrogen and aluminum ions (Mullins, 2005). Soils of Southeastern Nigeria are formed predominantly from the coastal plain sand parent materials, which are mainly Ultisols (Onwuka and Ogbonna, 2009). These soils are highly weathered and acidic in nature with a low pH, generally less than 5.5 (Osodeke, 2000). Consequently, soil acidity inhibits root growth, with the root apex being the primary affected part. It also plays a central role in aluminum and manganese toxicity and tolerance (Matsumoto, 2000).

In order to ameliorate these negative effects of acidity and ensure the sustainability of food basket in affected regions, liming practice is often employed to neutralize soil acidity and raise soil pH. Presently, attention is being shifted to the use of non-conventional liming materials and this is because it is cheaper and it is the best way of recycling such materials (Owolabi *et al.*, 2003).

The objectives of the study were to determine the effect of spent grain ash on some soil properties of an acid Ultisol and to determine the effect of spent grain ash on the growth of maize and nutrient uptake.

MATERIALS AND METHODS

Experimental site. The experiment was conducted in Michael Okpara University of Agriculture, Umudike located between ($05^{\circ} 29'N$; $07^{\circ} 33'E$) with an altitude of 122m above the sea level (NRCRI Met. Station, 2012). The area is characterized by a humid tropical rainforest and climate with marked wet and dry season and an average rainfall of 2135.9mm per annum distributed over eight months period, ranging from March to November with bimodal peaks in July and September. The soil is deep, porous and dark in colour and derived from coastal plain sand thus classified as Typic kandiodult. Table 1 shows some initial soil properties. It was sandy loam texture with low CEC and pH.

Field Method. Augered surface (0-15 cm) samples were taken randomly from the study site and bulked together to form a composite. The composite soil sample was air dried at room temperature and passed

through sieved with 2mm sieve then 50g were weighed into 12 liter capacity buckets each perforated at the bottom and properly labeled.

TABLE 1. PHYSICAL AND CHEMICAL PROPERTIES OF THE SOIL USED FOR THE EXPERIMENT BEFORE THE APPLICATION OF LIME.

Physiochemical Properties	Values
Sand (g/kg)	845.3
Silt (g/kg)	62.7
Clay (g/kg)	92.0
Textural Class	Sandy loam
pH (H ₂ O)	4.43
pH (CaCl ₂)	3.72
Organic Carbon (g/kg)	18.0
Organic Matter (g/kg)	31.0
Total Nitrogen (g/kg)	1.50
Aluminum Saturation (%)	26.57
Calcium Saturation (%)	42.14
Available Phosphorus (mg kg ⁻¹)	10.24
Exchangeable Calcium (cmol kg ⁻¹)	2.35
Exchangeable Magnesium (cmol kg ⁻¹)	0.78
Exchangeable Potassium (cmol kg ⁻¹)	0.13
Exchangeable Sodium (cmol kg ⁻¹)	0.10
Exchange acidity (cmol kg ⁻¹)	2.00
Exchangeable Aluminum (cmol kg ⁻¹)	1.50
Exchangeable Hydrogen (cmol kg ⁻¹)	0.50
ECEC (cmol kg ⁻¹)	5.36
Base Saturation (%)	62.69
Ca:Al Ratio	1.57

Laboratory Methods. The sieved samples were analyzed before and after the pot experiment. The particle size analysis was determined by the Bouyoucos (1962) hydrometer method using sodium hexametaphosphate. Soil pH was determined using Eel glass electrode pH meter (Mclean, 1982) while organic carbon was determined using dichromate wet oxidation method (Nelson and Sommer, 1982). Exchange acidity was determined by Kamprath (1976) method and total nitrogen was assessed by micro-kjeldahl digestion method as modified by Jackson (1996). Basic cations were determined by extracting 5g of soil with 30ml IN NH₄OAC. Potassium and Sodium were determined using flame photometer while calcium and magnesium were determined by titrating with EDTA (Tel and Hagarty, 1984). Effective cation exchange capacity was measured through the summation of exchangeable bases and acidity. The treatment, spent grain ash (by-product of brewery subjected to combustion) was analyzed before it application so as to ascertain its chemical properties, Table 2.

TABLE 2. CHEMICAL PROPERTIES OF THE SPENT GRAIN ASH USED FOR THE EXPERIMENT

Properties Of The Spent Grain Ash	Values
pH (H ₂ O)	9.21
pH (CaCl)	8.21
% P	0.27
% OM	3.64
Ca (%)	0.92
Mg (%)	0.24
K (%)	0.35
Na (%)	0.02
N (%)	0.32

RESULTS AND DISCUSSION

Table 3 shows the effects of spent grain ash on some soil properties after harvesting the maize plant. The results showed that spent grain ash significantly ($P<0.05$) increased the soil pH in water when compared to the control. The results indicated that spent grain ash significant ($P<0.05$) reduced exchange acidity while five tonnes per hectare ash gave the highest reduction value of 0.90. For the exchangeable aluminum and exchangeable hydrogen, there were significant ($P<0.05$) differences among the treatments and five tonnes per hectare gave the lowest significant ($P<0.05$) values of 0.67 and 0.23 respectively. This result is an agreement with Onwuka *et al.* (2007) and Onwuka and Ogbonna (2009) who stated that the application of ash increased soil pH and reduced exchange acidity, exchangeable aluminum and exchangeable hydrogen. There was significantly ($P<0.05$) increased of soil organic carbon when compared to the control while 5 ton/ha gave the highest value of 5.32% organic carbon. The increase in the soil organic carbon could be attributed to the liming effect of spent grain ash, resulting in favoured environment for decomposing microbes (Badolucco *et al.* 1992). But, this result was in contrast to the findings of Voundi Nkama *et al.* (1998) who reported that lime application did not significantly increase soil organic.

Significant total nitrogen values above the critical level of 0.15% (Adeoye and Agboola, 1984) were obtained. This could be attributed to the increase in soil pH as a result of the treatments which in turn increase microbial activities and rates (Dee *et al.*, 2003), especially the nitrifiers, which are involved in the transformation of organic nitrogen thus increasing the amount of nitrogen. Five ton/ha gave the highest significant value of 1.27 mg kg⁻¹ which could be ascribed to the large quantity of the treatments. This result was in agreement with Adu-Dupaal *et al.* (1994) finding, who reported that increasing the application rate of ash increases soil potassium.

TABLE 3. EFFECT OF SPENT GRAIN ASH ON SOME SOIL CHEMICAL PROPERTIES AFTER MAIZE PLANT HARVEST IN THE POT EXPERIMENT

SPENT GRAIN ASH (TON/HA)	PH H ₂ O	EX. ACIDITY	EXCH. AL	EXCH. H	OC ←	OM (%)	N →	P ←	K (CmolKg ⁻¹)	NA →
0	5.89	1.90	1.44	0.46	3.47	5.99	0.30	12.07	0.13	9.80
1	6.13	1.41	0.98	0.43	4.74	8.16	0.41	15.27	0.50	10.30
2	6.16	1.32	0.91	0.41	4.71	8.13	0.41	13.87	0.43	9.23
3	6.29	1.20	0.86	0.34	4.68	8.07	0.40	16.01	0.83	9.37
4	6.35	1.10	0.79	0.31	4.47	7.71	0.39	14.43	1.17	9.70
5	6.40	0.90	0.67	0.23	5.32	9.17	0.46	15.17	1.27	10.07

* Ex = Exchange; Exch. = Exchangeable; OC = Organic carbon; OM = Organic matter

The effects of spent grain ash on maize plant height in the pot experiment are shown in Table 4. The result indicated that the treatments significantly ($P<0.05$) increased the maize plant height when compared with the control. Five tonnes per hectare of spent grain ash application gave the highest significant ($P<0.05$) values of 40, 60.1 and 96.8 cm at 2, 4, and 6 WAP respectively. The highest significant ($P<0.05$) value of 110.9 cm was obtained from the treatment means at 8 WAP. This increase in the maize plant height could be attributed to the reduction of the soil exchange acidity by the spent grain ash. This finding was in agreement with what was earlier reported by Njoku *et al.* (1986), who indicated that liming increased the plant height in Umudike area of South East Nigeria.

The effect of spent grain ash on the number of leaves in the pot experiment is shown in Table 5. The results stated that at 4, 6 and 8 WAP, the values from all the treatments significantly ($P<0.05$) increased the number of leaves when compared to the control. Five tonnes per hectare of spent grain ash gave the highest values (16 leaves) across the treatments. This significant increase in the number of leaves of the maize plant could be attributed to the high content of nitrogen, above the critical level of 0.15% as indicated in the soil analysis after planting. This positive effect of nitrogen in the number of leaves could be ascribed to the increase in soil pH as a result of the application of various treatments, which in turn increase of microbial activities and rates (Dee *et al.*, 2003).

Figure 1 shows the effects of spent grain ash on maize leaf area in the pot experiment. From the figure, there was no significant difference among the values obtained except at 8 WAP where all the treatments significantly ($P<0.05$) increased the leaf area when compared to the control. The control and 1

ton/ha of spent grain ash significantly ($P < 0.05$) gave the lowest and highest significant values respectively and both treatments maintained this trend throughout the experimental period.

TABLE 4. EFFECTS OF SPENT GRAIN ASH ON MAIZE PLANT HEIGHT IN THE POT EXPERIMENT AT 2, 4, 6 AND 8 WEEKS AFTER PLANTING (WAP).

SPENT GRAIN ASH (TON/HA)	PLANT HEIGHT (CM)			
	2 WAP	4 WAP	6 WAP	8 WAP
0	17.2	30.3	57.3	60.9
1	36.1	52.3	84.1	108.0
2	26.9	41.5	65.9	87.5
3	35.4	52.3	83.1	105.0
4	28.4	45.0	70.1	94.4
5	40.0	60.1	96.8	110.9
LSD (0.05)	11.85	16.38	16.63	19.18

TABLE 5. EFFECTS OF SPENT GRAIN ASH ON THE NUMBER OF LEAVES IN THE POT EXPERIMENT AT 2, 4, 6 AND 8 WEEKS AFTER PLANTING (WAP).

SPENT GRAIN ASH (TON/HA)	NUMBER OF LEAVES			
	2 WAP	4 WAP	6 WAP	8 WAP
0	4	6	9	12
1	4	9	11	15
2	4	8	10	13
3	4	8	10	14
4	4	7	10	13
5	5	9	13	16
LSD (0.05)	NS	NS	NS	NS

*NS = No significant difference.

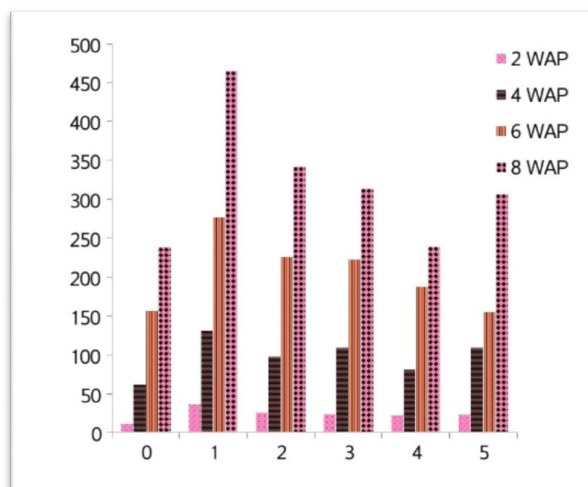


FIGURE 1. EFFECTS OF DIFFERENT RATES OF SPENT GRAIN ASH ON MAIZE LEAF AREA IN THE POT EXPERIMENT

Table 6 shows the effects of spent grain ash on plant growth and nutrients uptake in maize plant after harvest. The result indicated that spent grain ash significantly ($P < 0.05$) increased the maize plant girth (cm) when compared with the control. This increase could be attributed to the potassium content of the spent grain ash, which according to Chude, *et al* (2004), is responsible for the development of the stalks.

For maize root number, spent grain ash significantly ($P<0.05$) increased the number of maize root when compared to the control. The result showed that both 1 and 2 ton/ha of spent grain ash gave the same number of maize root while the highest number of maize root was recorded in the 5 ton/ha treatment application. This could be attributed to the fact that the calcium in the spent grain ash suppressed the toxicity of aluminum in the soil (Franco and Munns, 1982), thus enhancing the activities of the root by creating a better environment for phosphorus release.

From Table 6, the result indicated that there were no significant differences among the values of maize root lengths obtained from the different treatments. Table 6 also indicated that the treatments significantly ($P<0.05$) increased both fresh weight yield (FWY) and dry matter yield when compared to the control. Three tonnes per hectare of spent grain ash gave the highest significant ($P<0.05$) values for both fresh weight yield and dry matter yield. The treatments significantly ($P<0.05$) increased the moisture content when compared to the control and 3 ton/ha of spent grain ash significantly ($P<0.0$) gave the highest value of 2.31% when compared to other treatments.

TABLE 6. EFFECTS OF SPENT GRAIN ASH ON PLANT GROWTH AND NUTRIENT UPTAKE

Spent Grain Ash (ton/ha)	Girth (cm)	MRN	RL (cm)	FWY (g/pot)	DMY (g/pot)	MC (%)	N (%)	P (mg/kg)	K (mg/kg)
0	1.38	16	18.96	64	7.2	0.57	27.94	94	31
1	1.9	27	17.6	232	17.8	2.14	111.07	422	106
2	1.35	27	16.68	168	13.7	1.54	75.90	311	104
3	1.66	23	17.29	253	22.9	2.31	92.52	508	168
4	1.48	22	18.18	204	19.2	1.85	103.10	496	147
5	1.95	29	19.35	236	21.5	2.15	73.96	745	179
LSD (0.05)	0.44	6.8	5.51	103.9	10.1	94.2	1.43	80.5	62.3

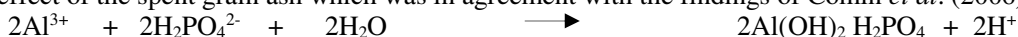
* Root length (RL); Fresh weight yield (FWY); Dry matter yield (DMY) Moisture content (MC); Root length (RL); Maize root number (MRN)

Table 6 showed the effects of spent grain ash on plant growth and nutrients (N, P and K) uptake in maize plant after harvest in the pot experiment. The results indicated that all the treatments significantly ($P<0.05$) increased the nitrogen uptake when compared to the control, 5 ton/ha of spent grain ash significantly ($P<0.05$) reduced the amount of nitrogen in the maize plant. This reduction of nitrogen in the maize plant could be as a result of the effective utilization of nitrogen in the pots by the maize plant thus giving rise to high vegetative growth of the maize plant. But this significant ($P<0.05$) increase in nitrogen could be attributed to the increase in soil pH as a result of the treatments which in turn increase the activities of microorganisms and bacterial rates (Dee *et al*, 2003), especially the nitrifiers, which are involved in the transformation of nitrogen thus increasing the amount of nitrogen.

Table 6 showed the effects of spent grain ash on plant growth and nutrients (N, P and K) uptake in maize plant after harvest in the pot experiment. The results indicated that all the treatments significantly ($P<0.05$) increased the nitrogen uptake when compared to the control, 5 ton/ha of spent grain ash significantly ($P<0.05$) reduced the amount of nitrogen in the maize plant. This reduction of nitrogen in the maize plant could be as a result of the effective utilization of nitrogen in the pots by the maize plant thus giving rise to high vegetative growth of the maize plant. But this significant ($P<0.05$) increase in nitrogen could be attributed to the increase in soil pH as a result of the treatments which in turn increase the activities of microorganisms and bacterial rates (Dee *et al*, 2003), especially the nitrifiers, which are involved in the transformation of nitrogen thus increasing the amount of nitrogen.

From Table 6, all the treatments significantly ($P<0.05$) increased the plant phosphorus uptake. Five tonnes per hectare of spent grain ash significantly ($P<0.05$) gave the highest value of phosphorus uptake. It is obvious that there is high phosphorus fixation at low pH by aluminum (Osodeke, 2000), resulting in the formation of aluminum-phosphate complex that is insoluble and unavailable to plants. This increased in phosphorus could be attributed to the application of liming material which increased the soil pH, thus increasing phosphorus availability.

For the potassium, spent grain ash significantly ($P < 0.05$) increased the soil potassium uptake when compared to the control. Five tonnes per hectare of spent grain ash significantly ($P < 0.05$) gave the highest value of 179 mg kg^{-1} of the potassium uptake. This increase in potassium uptake could be as a result of liming effect of the spent grain ash which was in agreement with the findings of Comin *et al.* (2006).



The correlation matrix showing the relationship between soil chemical properties and maize growth parameters is shown in Table 7. The result showed that soil pH correlated positively and significantly with almost all the maize growth parameters except root length, fresh weight yield (FWY) and dry matter weight. Table 7 also indicated highly significant and positive correlation between soil pH, plant height and number of leaves. There was no correlation between soil acidity indices (exchange acidity, exchangeable aluminum and exchangeable hydrogen) and the maize growth parameters. Total nitrogen gave a positive and significant correlation with some maize growth parameters except for plant girth and root length. For the available phosphorus, there was no significant correlation with the maize growth parameters except with the number of leaves (where the correlation was highly significant ($P < 0.001$)), plant height and plant girth. Potassium gave a positive and significant correlation with plant height and Dry matter yield and only exchangeable sodium was positively and significantly correlated with root length ($P < 0.001$). From the table below, there was significant and positive correlation between soil organic matter and maize parameters except for plant girth and root length.

TABLE 7. CORRELATION MATRIX SHOWING THE RELATIONSHIPS BETWEEN SOIL PROPERTIES AND SOME MAIZE GROWTH PARAMETERS

SOIL PROPERTIES	MAIZE GROWTH PARAMETERS						DRY WEIGHT MATTER
	PLANT HEIGHT	NUMBER OF LEAVES	PLANT GIRTH	ROOT NUMBER	ROOT LENGTH	FWY	
PH (H ₂ O)	0.624**	0.641**	0.472*	0.512*	-0.168 ^{NS}	0.433 ^{NS}	0.318 ^{NS}
EX. ACIDITY	0.141 ^{NS}	0.133 ^{NS}	0.048 ^{NS}	0.382 ^{NS}	0.248 ^{NS}	0.157 ^{NS}	0.090 ^{NS}
EX. AL	0.066 ^{NS}	0.167 ^{NS}	0.110 ^{NS}	0.325 ^{NS}	0.200 ^{NS}	0.093 ^{NS}	0.004 ^{NS}
EX. H	0.165 ^{NS}	-0.006 ^{NS}	-0.078 ^{NS}	0.222 ^{NS}	0.161 ^{NS}	0.154 ^{NS}	0.165 ^{NS}
N	0.586*	0.559*	0.284 ^{NS}	0.544*	-0.198 ^{NS}	0.647**	0.541*
AV. P	0.555*	0.642**	0.514*	0.446 ^{NS}	-0.260 ^{NS}	0.373 ^{NS}	0.319 ^{NS}
K	0.547*	0.434 ^{NS}	0.319 ^{NS}	0.379 ^{NS}	0.211 ^{NS}	0.455 ^{NS}	0.504*
NA	0.182 ^{NS}	0.216 ^{NS}	0.279 ^{NS}	0.087 ^{NS}	0.594**	-0.233 ^{NS}	-0.217 ^{NS}
OM (%)	0.574*	0.552*	0.271 ^{NS}	0.530*	-0.220 ^{NS}	0.640**	0.539*

** = Significant at $P < 0.001$; * = Significant at $P < 0.05$; NS = Not significant

CONCLUSION AND RECOMMENDATION

The goal of the pot experiment was to know the effects of spent grain ash on some soil chemical properties and growth of maize (*Zea mays*) in an Ultisol of Southeastern Nigeria. The result showed that all the treatments significantly ($P < 0.05$) increased soil pH and reduced exchange acidity while five tonnes per hectare of spent grain ash gave the best positive effects on soil chemical properties and also revealed the potential of spent grain ash on the average improved plant parameters. Five tonnes per hectare gave the overall best results in terms of amelioration of soil acidity and the growth of maize. It is therefore recommended that 5 ton/ha should be used for the reduction of soil acidity and improvement of maize performance in Umudike area of southern Nigeria.

ACKNOWLEDGEMENT

This research was supported by the Almighty God for His inspiration, guidance and protection in the course of the entire study. I specially appreciate the assistance made by my mentor, Dr. C. F. Isinguzo financially and my supervisor Prof. V. E. Osodeke. I equally appreciate the contributions of my lecturers, Dr. M. I. Onwuka and Dr. O. I. Nwachukwu for their support and care. I am obliged to extend my gratefulness to my beloved family, mostly my mother, Mrs. M. U. Ogbonna; sister (Chichi), brother (Chibueze) and my dearest father, Mr. L. E. Ogbonna of blessed memory.

REFERENCES

- Adeoye, G. O. and Agboola, A. A. 1984. "Critical Level for Soil pH, Available P, K, Zn and Mn and Maize Content of P; Cu; Mn in the Sedimentary Soils of Southwestern Nigeria". *Fertilizer Research*. 6:65-71.
- Adu-Dupaal, H. K; Cobbina, J. and Asare, E. O. 1994. "Effect of Cocoa Pod Ash on the Growth of Maize". *Journal of Agricultural Science*. 122: 13-33.
- Bouyoucos, G. A. 1962. "Hydrometer Method Improved for making Particle Size Analysis of Soils". *Agronomy Journal*. 54: 464 -465.
- Chude, V. O; Melgori, W.B. Amapu I.Y and Ano, O. A. 2004. "Manual on Soil Fertility Assessment". Published by Federal Fertilizer Department in Collaboration with National Special Programme for Food Security Abuja-Nigeria.
- Comin, J. J; Barloy, J; Hallaire, V; Zanette, F. and Miller, P. R. M. 2006. "Effects of Aluminum on the Adventitious Root System, Aerial Biomass and Grain Yield of Maize Growth in the Field and in a Rhizotron". *Experimental Agriculture*. 42(3): 351-366.
- Dee, B. M; Haynes, R. J. and Graham, M. H. 2003. "Change in Soil Acidity and the Size and Activity of the Microbial Biomass in Response to the Addition of Sugar Mill Waste". *Biology Fertility Soils*. 32:47-54.
- Franco, A. A. and Munns, D. N. 1982. "Acidity and Aluminum Restraints on Nodulation Nitrogen Fixation and Growth of Phaseoln Vulgaria in Nutrient Solution". *Soil Science Society of American Journal*. 46: 296-301.
- Jackson, M.L. 1996. *Soil Chemistry Analysis - Advanced Course*. Published Department of Soil Science, University of Wisconsin, Madison, Wisconsin.
- Kamprath, E. J. 1976. "New Buffer pH Method for Rapid Estimation of Exchange Acidity and Lime Requirement of Soils". *Communications in Soil Science and Plant Analysis*. 7: 637 - 652.
- Matsumoto H. 2000. "Cell Biology of Tolerance and Toxicity in Higher Plants". *International Review of Cytology*. 200: 1 - 46.
- Mclean, E.O. 1982. "Soil pH and Lime Requirement". In: Payer AL, Editor. "Methods of soil Analysis, Part 2. 2nd Ed". *Agronomy. Monog*. 9:199-224.
- Mullins, G. L. 2005. *Sources of Lime for Acid Soil in Virginia*, Department of Crop and Soil Environmental Sciences, Virginia.
- National Root Crop Research Institute, Umudike. 2012. Meteorological Station. Nigeria.
- Njoku, B. O., Enwezor, W. O. and Onyeankwe, B. I. 1986. "Chemical Factors Affecting Maize Growth in Acid Ultisols of Eastern Nigeria". *Proceedings of the 14 Annual Conference of Soil Science Society of Nigeria held in Markurdi. 19th-22nd Oct. Edited by V. O. Chude*. Pp. 119-125.
- Onwuka, M. I. and Ogbonna, E. A. 2009. "Effect of Different Kitchen Residue Ash Sizes on Soil Acidity Amelioration in an Ultisol". *Proceedings of the 33rd Annual Conference of the Soil Science Society of Nigeria held at Ekiti State*. Pp 184 - 186.
- Onwuka, M. I., Osodeke, V. E. and Okolo, N. 2007. "Amelioration of Soil Acidity Using Cocoa Husk Ash for Maize Production in Umudike Area of Southeastern Nigeria". *Tropical and Subtropical Agroecosystem*. 7: 41-45.
- Osodeke, V. E. 2000. "Potentials of Biofertilizers for Soil Fertility Management in Southeastern Nigeria". *Food and Fiber Production in Nigeria, Umuahia*, Pp. 277-282.
- Owolabi, O., Adeleye, A., Oladejo, B. T. and Ojeniyi, S. O. 2003. "Effect of Wood Ash on Soil Fertility and Crop Yield in South West Nigeria". *Nigeria Journal of Soil Science*. 13:55-60.
- Tang, C; Asseng, S; Diatloff, E. and Rengel, Z. 2003. "Modeling Yield Losses of Aluminum Resistant and Aliminum-Sensitive Wheat due to Subsurface Soil Acidity Effects of Rainfall, Liming and Nitrogen Application". *Plant and Soil*. 254:349-360.
- Tel, D.A. and Hargarty, M. 1984. *Soil and Plant Analysis*, IITA, University of Ghelph.
- Voundi Nkama, J. C. V; Demeyer, A. and Verloo, M. G. 1988. "Chemical Effects on Wood Ash on Plant Growth in Tropics Acid Soils". *Bioresource Technology*. 63: 251-260.

**VARIABLE BEHAVIOUR OF MASS TRANSFER COEFFICIENT WITH VELOCITY,
LENGTH AND DISPERSION OF REACTIVE SOLUTE**

Deepak Swami, Abhimanyu Sharma
(IIT Mandi, HP, INDIA)

This work represents the experimental and numerical investigation performed on the transport of reactive solute through stratified porous media. Numbers of experiments are performed using reactive solute (solution of NaF) transport through experimental model of stratified porous media of different lengths. The motive of the study is to correlate the effect of scale of hydraulically connected mobile-immobile region and velocity on the estimation of first order mass transfer coefficient for reactive solute transport. During the experimentation variable velocity provided for different lengths of stratification for understanding the behavior of mass transfer coefficient, under variable head gradient. The estimated values of mass transfer coefficient are analyzed for interdependency with length, velocity and dispersion coefficient. The contour plots between velocity, length of mobile-immobile interface, mass transfer coefficient and dispersion coefficient interestingly revealed the correlation in between earlier presumed independent parameters. It is observed that mass transfer coefficient has an inverse relationship with dispersion coefficient. Also first order mass transfer coefficient exhibited varying behavior with length of mobile-immobile region and velocity. Finally, variable behavior of mass transfer coefficient is obtained when the transport media is under the influence of physical non-equilibrium. The study concludes a very important relation of mass transfer between, scales of heterogeneous porous media, velocity and dispersion coefficient. It is also observed that constant first order mass transfer input in higher modelling approach does not comply with the scale effect, and need to be modified.

**PRELIMINARY STUDY OF HEAVY METAL POLLUTION IN SOIL OF INDUSTRIAL ZONE
OF SURAT – INDIA**

Tank Shantilal K

(Department of Biosciences, Veer Narmad South Gujarat University, Surat - 395007, Gujarat, India)

Mehra Bhavna K.

(Detox Corporation Pvt. Ltd., Surat – 395001, Gujarat, India)

Aggregate chemical characteristics and metal concentration in the sub surface soil (12 inch) of two industrial zones of Surat city, known as a part of large industrial belt of Gujarat and as the Textile hub of India , were investigated for evaluating the suitability of soil for plantation. According to WHO- SEARO (South East Asia Regional Office) the urban population of Asia is expected to double between 2000 & 2030. Soil being one of the repositories for anthropogenic and industrial wastes needs to be prevented from large quantities of pollutants being continuously introduced. Hence the present study was focused to carry out a preliminary analysis of the chemical profile and heavy metal contamination of soil in two industrial zones of Surat city. The study was carried out in the Pre- Monsoon period.

Results of soil investigation of the present study are compared to the normal content interval and maximum allowable limits (MAL) established by Kloke (1980) to calculate compliance Index (I_c) for Plantation. Compliance index I_c is the ratio between the observed concentration of metal in soil samples and the maximum accepted limits. Though the concentration of metals like Pb,Cd, Co,Zn, Cu, & Cr is found to be within the Maximum Allowable limits , the degree of soil pollution established based on the Compliance Index calculated with reference to the Maximum acceptable limits (Kloke,1980) , shows that Cd, Co, Zn & Cu show a Significant Pollution Level 1(PS1) ($1.0 < I_c < 5.0$), Pb shows Potentially Significant Pollution (PPS) ($0.7 < I_c < 1.0$) and Cr shows Insignificant Pollution (PN) ($I_c < 0.7$) at all the target locations viz, L1,L2,L3 & L4, L5, L6 in the two separate Industrial Zones of Surat City.

TRANSPORT AND ADSORPTION OF COLLOIDS IN SOILS: A MRI APPROACH

Alizée P. Lehoux, Eric Michel

(INRA, Avignon, France)

Paméla Faure, Denis Courtier-Murias, Stéphane Rodts, Philippe Coussot

(Laboratoire Navier, Champs sur Marne, France)

The ability to predict transport and retention of colloidal particles is a major environmental concern as such particles can carry adsorbed pollutants towards the groundwater or be pollutants themselves. The models currently used to predict the fate of colloids in soils are based on mechanisms inferred from breakthrough curves (evolution of concentration as a function of pore volume or time) after injection of particles into a column of porous media. In this study we aim to complement this knowledge with internal measurements by Magnetic Resonance Imaging (MRI).

MRI provides spatial distribution of colloidal particles and water content in time along the sample axis during transport experiment through a porous medium of 20 cm height. We injected several pulses of superparamagnetic nanoparticles in columns of porous media of increasing complexity: glass beads, sand, soil aggregates, and undisturbed soil.

We were able to follow suspended and adsorbed particles in glass beads and sand with MRI. From these experiments we show that dispersion of suspended particles is less important than predicted from standard measurements (breakthrough curves). This is due to entrance effects inducing an initial radial flow heterogeneity which appears as a significant dispersion in the breakthrough curve. With charged particles able to adsorb we were able to follow the adsorption dynamics as the solution advances through the porous medium.

Experiments in soil aggregates showed a strong adsorption but also a constant release, which indicates that more complex mechanisms are occurring in soil aggregates, due to heterogeneities of surface charges and complex porosity. We propose a model to explain this particular behaviour. In the last step of our study, we follow water content and particle concentration during a rain simulation under undisturbed soil.

**VERTICAL DISTRIBUTIONS OF ELEMENTS IN THE SOIL (ALBIC LUVISOL) OF
SANJIANG PLAIN IN CHINA**

Wei Ouyang*, Hongguang Cheng, Chunye Lin

(State Key Joint Laboratory of Environmental Simulation and Pollution Control, School of Environment,
Beijing Normal University, Beijing, China)

The vertical distributions of elements in soils are critical to understand their origins and transports in soil forming processes. The objectives of this study were to investigate the vertical distribution of elements in the Albic Luvisol of Sanjiang Plain to identify the origin of toxic elements in the soil. Soil cores (0 to 50 cm depth) were collected at 33 sites in the northeastern agricultural field of Sanjiang Plain and then sliced into 10 cm slices. The concentrations of SOM and 19 elements were determined. The results showed that the concentrations of SOM, P, Ca, Cd, Hg, and Mn in the soil generally decreased with depth, while Al, Fe, Mg, K, Ti, Cr, Cu, Ni, Sc, and V concentrations roughly increased with depth. The concentrations of As, Co, Pb, and Na were higher in the middle layers than bottom and top layers. Correlation analysis showed that As and Co were significantly correlated to the mineral matrix elements Mn and Fe. Cd was significantly correlated to SOM and the mineral matrix P and Ca. Hg was significantly correlated to SOM. Pb was significantly correlated to the mineral matrix elements Mn, Al, and Fe. Cr and Ni were significantly correlated to the mineral matrix elements Al and Fe. Cu was significantly correlated to SOM and the mineral matrix elements Al and Fe. Whereas the maximal concentrations of toxic trace elements As, Cd, Cr, Cu, Hg, Ni, and Pb in the soil of Sanjiang Plain were lower than the environmental quality standards for the agricultural soils in China, Cd and Hg in the soil partially originated from anthropogenic sources. In details, about 37% of Cd and 31% of Hg in the 0 to 10 cm depth originated from anthropogenic sources. Major anthropogenic source of Cd might be phosphate fertilizer, while the anthropogenic source of Hg might be from atmospheric Hg deposition. Therefore, the long-term accumulation of Cd and Hg in the soil may be a concern in future and should be monitored regularly.

MODELING OF PHOSPHORUS SORPTION AND BUFFERING MECHANISMS IN SELECTED SOILS OF FIJI

Muni Sangeeta Goundar^{*}, Satyanarayan Shashtri (Fiji National University, Lautoka, Fiji)
and R. John Morrison (University of Wollongong, NSW 2522, Australia)

*Email:sangeeta1g@yahoo.com

ABSTRACT: Mechanisms by which P is retained in the soil include precipitation and ligand exchange, lattice diffusion and anion exchange, which have a strong effect on the bioavailability and the transport potential of P. The main objective of this research was to use phosphorus buffer index (PBI) as an indicator of the P status of selected sugarcane growing soils in Fiji to reduce the risk of excessive fertilizer applications and leaching of P into the waterways, thus minimizing contamination of the environment. Soils used in this study were Inceptisols, Mollisols, Alfisols, Oxisols and Ultisols. PBI and phosphorus isotherm measurements were performed on selected soils. Pearson's correlation, performed using Statistix (Version 10) showed that PBI has a significant negative correlation with soil pH ($R = -0.67$, $p = 0.017$). The P sorption maxima obtained using the Langmuir equation ranged from 480 to 1314 mg/kg and Pmax had a moderate positive correlation with PBI ($R = 0.70$, $p = 0.01$). The isotherm data had a significant fit to the Freundlich sorption model, with R values ranging from 0.82 to 0.97.

Keywords: Phosphorus, phosphorus buffer index, soils, fertilizers, phosphorus sorption mechanisms

INTRODUCTION

The phosphorus status of Fijian soils along with other soil properties is declining due to the intensive cultivation of sugarcane (Morrison et al, 2005). The Fiji sugar industry has been long dependent on the use of fertilizers to improve crop production, mainly due to the low concentrations of available P and total P in most soils. However, improper long- term application of fertilizers could lead to P accumulation in agricultural soils to levels greater than those required for healthy plant growth, thus leading to the elevated soil potential for P loss to water bodies (McLaughlin et al, 2011). Fine soil particles with sorbed P may be transported via erosion and surface runoff to waterways promoting eutrophication. Furthermore, excessive applications of P fertilizer are a waste of limited resources.

Previous research on phosphate adsorption on soils of Fiji has shown that significant quantities of added P are strongly adsorbed by soils, and only 20 to 30 percent of applied P fertilizer are utilized by the plants (Chee et al, 1978; Dandy and Morrison, 1980). Adsorption reactions are considered as key processes for governing P fertilizer efficiency but then precipitation processes become important at higher level of P (McLaughlin et al, 2011). The mechanisms by which P is retained in the soil include precipitation and ligand exchange (adsorption), lattice diffusion and anion exchange. The fixation/sorption of P in soil is mechanistically complex and sorption is a term used when the mechanism of P retention is undefined (Sims and Pierzynski, 2005). Adsorption can be reversible and irreversible, fast or slow, conditional to buffering capacity of the soil and the contact time with the solution (Bhadha et al, 2012),. The concentration of P in the soil solution is controlled by the adsorption/desorption and precipitation/dissolution equilibria which are affected by the pH, anions competing with phosphate for ligand exchange sites and the levels of Fe, Al and Ca that form precipitates with phosphate ions.

Numerous studies have investigated the P sorption in the soils for environmental or agronomic purposes (e.g., Barrow, 1974; Pant et al, 2002). One issue encountered with isotherms is that the soil phosphate solution interaction is not a true equilibrium, as the soil continues to take phosphate slowly after an initial rapid pseudo-equilibrium is reached and both true chemical and surface adsorption are involved. However, the results obtained from the initial rapid uptake of phosphate from the solution can be treated using the mathematical expressions which are derived assuming that a true equilibrium is reached. The two commonly used sorption models for P sorption isotherm data are the Langmuir and Freundlich equations,

which provide information such as binding energy, and sorption capacity and these equations have been developed from simple dynamic models of gas-solid interface processes (Sims and Pierzynski, 2005).

The P sorption assessment methods include: P sorption isotherms, P buffering capacity (PBC) measures (slope between equilibrium P concentration of 0.25 and 0.35 mg P/L), the single-point P-buffering indices (PBI), with methods either adjusted or unadjusted for current P fertility (Burkitt et al, 2008). It was found that the PBI values, which were calculated without the extractable P adjustments, were very reliable (Burkitt et al, 2002). In this study, a simpler method is used to determine the buffer index capacity of some selected Fijian soils.

MATERIALS AND METHODS

Soil Sampling Methods. Approximately 1 kg of composite soil samples were collected from three sugarcane farms in each sampling site on Viti Levu (Rarawai Mill-R, Lautoka Mill- Lt, Penang Mill- P) and Vanua Levu (Labasa Mill-La). The R, Lt, P and La sampling sites were selected on the basis of obtaining soil samples from the different soil orders based on the USDA Soil Taxonomy (Soil Survey Staff, 1999). The soil samples selected belonged to the Inceptisols, Mollisols, Alfisols, Oxisols and Ultisols. Three farms were selected from each mill area based on the soil orders that were found to be the most extensive in that area. Inceptisols were found to be the most extensive (40%) group of soils in Fiji. Mollisols were found to be the second most extensive (24%) followed by Alfisols (10%) and Oxisols (9%).

Soil Sample Preparation. The field samples were air dried in trays at <40°C after removing roots, stones, living organisms, and homogenized and subsampled by coning and quartering techniques. Representative sub-samples were ground to <2 mm size for most analyses, and <250 µm sieve for carbon and nitrogen analyses. The analytical data reported represents the average of duplicate analyses of each composite.

Methods for Soil Analysis. Soil samples were analysed using standardised methods for pH (1:5 & 1:2.5 soil/water suspension), organic carbon (Walkley Black method), total P (strong acid digest), particle size distribution by the pipette method, oxalate-extractable aluminium (Al) and iron (Fe), exchangeable bases by ammonium acetate method, extractable P by a modified Troug method, and P sorption isotherms, as summarized in Goundar (2013). The equilibrium P concentration (EPC) for each soil type was obtained from the line of best fit of sorption curves by putting $y = 0$. The P_{max} (phosphorus sorption maximum) values were assessed using the Langmuir equation and the data were also fitted to the Freundlich sorption model using Microsoft Excel.

RESULTS AND DISCUSSION

Chemical Parameters And Pbi For Sampled Soils. Table 1 presents the chemical parameters measured for the sampled soils. The PBI results obtained for the topsoils tested are given in Figure 1. Overall results of the PBI of the soils studied showed low to moderate rates of PBI. The PBI values of the soils studied decreases in the following order; Oxisols > Mollisols > Ultisols > Alfisols > Inceptisols. Inceptisols showed a low PBI possibly tended to leach a higher P to the waterways (Burkitt et al, 2008).

The PBI analyses indicate that different soils have different P sorption capacities, so a common fertilizer application will not meet the P requirements for different soils. These results showed that Oxisols had the highest mean PBI of 152 ± 25 implying that P will be fixed strongly in Oxisols rendering it unavailable for plant uptake as found by Syers et al (1971) for P fixation in highly weathered soils such as Oxisols and Ultisols. Different Oxisols have a range of PBI values due to the other factors, such as, soil pH, soil texture, fertilizer application rates, the content of other elements present, and degree of weathering and vegetation as these affect the P sorption capacities in soils.

Relationship of Pbi With Other Soil Properties for Topsoils. There is a positive correlation between the % clay content of soil with PBI ($R = 0.76$, $p = 0.005$) as found by other researchers (e.g., Burkitt et al, 2002). Inceptisols had the lowest clay content and the lowest PBI while the commonly clay rich Oxisols have high PBIs. Pearson's correlation showed that PBI has a moderate negative significant correlation with pH ($R = -0.67$, $p = 0.017$) while soil pH had a moderate positive correlation with the available P ($R = 0.63$, $p = 0.026$). This indicates that the availability of P in soil is pH-dependent and the reactions that occur in

acidic and basic soils produce insoluble P compounds (precipitates). Inceptisols (pH 6.8) had the lowest P fixation as expected according to the reviewed literature and P fixation is minimal at pH 6.5. The PBI is inversely proportional to the available P.

Table 1: Chemical parameters and PBI of 12 Fiji soils (0-29 cm). Note: Where the soils are Alf- Alfisols, Oxi- Oxisols, Mol- Mollisols, Inc- Inceptisols and Ult- Ultisols.

Mill Area	Soil Type	pH H ₂ O (1:5)	Oxal-Fe (%)	Oxal-Al (%)	Avail P (mg/kg)	PBI	Total P %	Ex-Ca cmol/kg	TEB cmol/kg	CEC cmol/kg
Lt Mill	Alf	5.9	0.78	0.25	44.4	64	0.166	11.86	19	23
Lt Mill	Oxi	5.2	0.14	0.33	7.2	170	0.091	4.86	8	14
Lt Mill	Mol	4.9	1.76	0.30	51.5	90	0.138	14.51	19	28
R Mill	Mol	5.4	1.81	0.38	116.2	72	0.227	15.21	20	27
R Mill	Inc	5.4	1.20	0.27	76.0	54	0.201	10.68	15	21
R Mill	Mol	4.9	1.92	0.43	51.8	106	0.181	13.11	18	29
P Mill	Mol	5.1	1.16	0.32	7.8	82	0.083	9.28	15	23
P Mill	Alf	6.2	1.22	0.46	16.8	62	0.073	15.76	22	27
P Mill	Inc	6.8	1.05	0.48	242.9	33	0.145	20.80	27	31
La Mill	Ult	5.1	1.12	0.43	54.2	70	0.134	16.70	22	32
La Mill	Oxi	4.7	0.34	0.35	11.2	134	0.055	2.00	4	14
La Mill	Mol	5.9	0.91	0.43	59.5	63	0.088	19.02	25	31

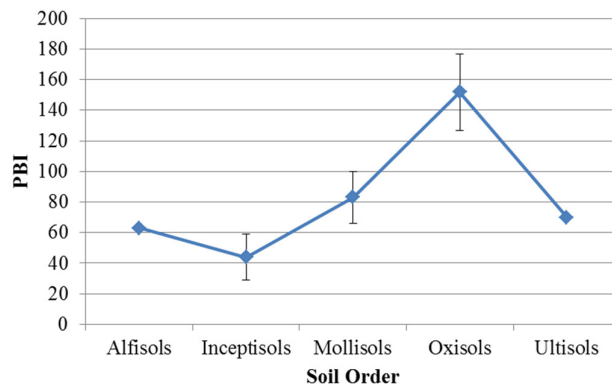


Figure 1. PBI values for different soil orders in Fiji sugarcane soils

PBI has a relatively good correlation with Fe_{ox} (R = 0.70, p = 0.02) and a moderate correlation (R = 0.65, p = 0.04) with Al_{ox} + Fe_{ox} when correlation is performed after the exclusion of the high values for Oxisols. The relationships of Al_{ox} and Fe_{ox} with P soption capacity are well documented in the literature (e.g., Pant et al., 2002). According to Weng et al (2012), the factors which control the fixation of phosphate to Fe oxyhydroxides under normal soil conditions are pH, organic matter and calcium concentration. PBI

displayed a relatively strong negative correlation with exchangeable Ca ($R = -0.79$, $p = 0.002$) and the PBI also displayed a relatively strong negative relationship with TEB ($R = -0.76$, $p = 0.0039$). PBI also displayed a weak negative relationship with the cation exchange capacity (CEC).

P Sorption Isotherms for Topsoils. The sorption curves (Figure 2) obtained after various additions of P showed the soils with the highest sorption of P were Oxisols and the lowest sorbing P soils were Inceptisols. The effect of the available P in different soil types is understandable in the isotherm curves as soils with the high available P most probably due to the fertilizer applications resulting in less amount of P adsorbed - produces a lower curve. The PBI data compare well with the generated isotherm curves for the different soil types.

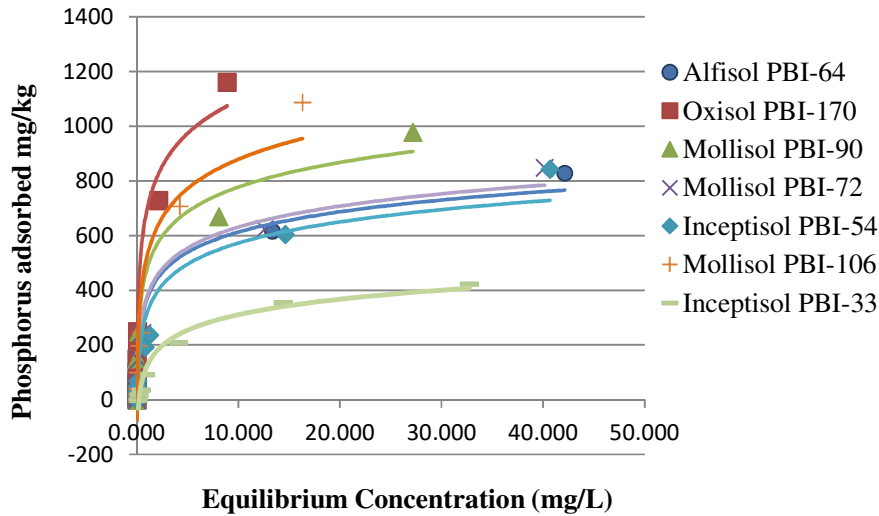


Figure 2. Sorption curves generated on different soils from soil isotherm experiments.

Equilibrium P Concentration (Epc) for Topsoils. The EPC values obtained in this study ranged from 0.006 to 0.224 mg/L (Table 2). Most soil types had very low values except for the few soil types such as Inceptisols from Penang Mill, and Inceptisols and Mollisols from Rarawai Mill which had high values due to the high available P. EPC values had very strong positive correlation with the available P ($R = 0.92$, $p < 0.01$) whereas a negative relationship is observed with PBI.

Langmuir Model for Topsoils. The Langmuir sorption model showed a highly significant fit to the isotherm data, with R^2 values of 0.77 or higher. Most soils fitted well to the Langmuir model, particularly the Inceptisols of Penang mill which had an R of 0.996. The P sorption maxima obtained using the Langmuir equation ranged from 480 to 1314 mg/kg (Table 2) and P_{max} had a moderate positive correlation with PBI ($R = 0.70$ & $p = 0.01$) indicating that soils with a high sorption capacity will require greater amount of P fertilizer compared to soils with low sorption capacity. The P_{max} obtained from the Langmuir isotherms showed a systematic decrease for soils in the following order; Oxisols, Mollisols, Alfisols, Inceptisols and Ultisols.

Freundlich Model for Topsoils. All soils fitted well to the Freundlich model except for the Mollisols which showed low R values compared with the other soil types. EPC and intercept of Freundlich model showed a strong negative correlation with $R = -0.79$ and $p = 0.002$. The y intercept of the Freundlich model correlated well to the PBI data. The soils with the lowest PBI such as Inceptisols from Penang had the lowest energy of sorption while Oxisols had the highest y intercept indicating the highest energy of sorption. It was also proven in this study that these soils had a high PBI.

Table 2. Data obtained from P isotherm curves and two models for twelve different topsoils of Fiji.

Mill Area	Soil Type	EPC (mg/L)	P max (mg/kg) (Langmuir)	Slope of Freundlich equation	Intercept of Freundlich equation
Lt Mill	Alf	0.032	850	0.350	2.400
Lt Mill	Oxi	0.019	1314	0.457	2.703
Lt Mill	Mol	0.026	1002	0.380	2.486
R Mill	Mol	0.033	861	0.441	2.322
R Mill	Inc	0.058	878	0.494	2.217
R Mill	Mol	0.034	1227	0.586	2.476
P Mill	Mol	0.003	809	0.502	2.949
P Mill	Alf	0.017	657	0.431	2.403
P Mill	Inc	0.224	480	0.631	1.804
La Mill	Ult	0.034	597	0.699	2.469
La Mill	Oxi	0.006	711	0.768	3.099
La Mill	Mol	0.014	539	0.617	2.610

CONCLUSIONS

Sorption curves and the PBI data were comparable so the PBI could be considered as a simple and efficient test variable to predict the P sorption of the different soils. The P isotherm data fitted very well to both Langmuir and Freundlich models. The Inceptisol (P Mill) had the lowest P maximum (480 mg/kg) and the lowest y intercept (1.804) indicating that this soil is the lowest P sorber. Furthermore, the isotherm curve of Inceptisols (P Mill) occupied the lowest position when all the isotherm curves of the different soils were plotted in a single graph. In contrast, the Oxisols had the highest PBI with the highest P maxima and high y intercepts (1314 mg/kg & 2.703 respectively). There is a good link between the two extensively used sorption models (Langmuir and Freundlich) with the PBI results. The Inceptisols had the PBI values as low as 33 indicating that these soils have the greatest potential of P leaching to the environment. Assessments of the long-term accumulation of P in soils should be carried out at representative sites by examining the available P, PBI, total P along with an accurate data on P fertilizer or other material additions.

ACKNOWLEDGEMENTS

The University of the South Pacific Research Office and the Faculty of Science, Technology and Environment are gratefully acknowledged for providing the financial support for this research. The staff of Sugar Research Institute of Fiji and Fiji Sugar Corporation is thanked for technical assistance. The Fiji Ministry of Primary Industries) provided particle size analyses and The University of the South Pacific, Institute of Applied Science (IAS) assisted with total nitrogen and aluminium analyses.

REFERENCES

- Barrow, N. J. 1974. The effect of previous additions of phosphate on phosphate adsorption by soils. *Soil Sciences* **118**, 82-89.
- Bhadha, J. H., Daroub, S. H. and Lang, T. A. (2012). Effect of kinetic control, soil:solution ratio, electrolyte cation, and others, on equilibrium phosphorus concentration, *Geodema* 173-174, 209-214.
- Burkitt, L. L., Moody, P. W., Gourley, C. J. P., Hannah, M. C. 2002. A simple phosphorus buffering index for Australian soils. *Australian Journal of Soil Research* **40**, 497-513.
- Burkitt, L. L., Sale, P. W. G., Gourley, C. J. 2008. Soil phosphorus buffering measures should not be adjusted for current phosphorus fertility. *Australian Journal of Soil Research* **46**, 676-685.
- Chee, M.T., Fergusson, J.E., Campbell, A.S. and Richmond, T.R. 1978. Phosphate sorption properties of

- some Fiji soils. *N.Z. Journal of Science* **21**, 157-166..
- Dandy, A. J. and Morrison, R. J. 1980. Phosphate sorption isotherms of some South Pacific soils. *N.Z. Journal of Science* **23**, 399-406.
- Goundar, M. S. 2013. *Phosphorus Status of Different Soils in the Sugarcane Belt of Fiji*. MSc Thesis, The University of the South Pacific, Suva, Fiji.
- McLaughlin, M. J., Mcbeath, T. M., Smernik, R., Stacey, S. P., Ajiboye, B., & Guppy, C. 2011. The chemical nature of P accumulation in agricultural soils--implications for fertiliser management and design: An Australian perspective. *Plant and Soil* **349**, 69-87.
- Morrison, R. J., Gawander, J. S. and Ram, A. N. 2005. Changes in the properties of a Fijian Oxisol over 25 years of sugarcane cultivation. In: *D.M. Hogarth (Editor) Proceedings International Society of Sugar Cane Technologies XXV Congress, Guatemala* **2**, 139-146.
- Pant, H. K., Nair, V. D., Reddy, K. R., Graetz, D. A., Villapando, R. A. 2002. Influence of flooding on phosphorus mobility in manure-impacted soils. *Journal of Environmental Quality* **31**, 1399-1405.
- Sims, J. T and Pierzynski, G. M. (2005). *Chemistry of Phosphorus in Soils in Chemical Processes in Soils*, Dick, W. A, Tabatabai, M. A, and Sparks, D. L eds., Soil Science Society of America Inc., Wisconsin, USA.
- Syers, J. K., Evans, T. D., Williams, D. H., Murdock, J. T. 1971. Phosphate Sorption parameters of Representative Soils from Rio Grande do sul, Brazil, *Soil Science* **112**, 267-275.
- Soil Survey Staff. 1999. *Soil Taxonomy: A basic system of soil classification for making and interpreting soil surveys*. Second Edition. USDA Handbook No. 436. Washington, DC.
- Weng, L., Van Riemsdijk, W. H., & Hiemstra, T. 2012. Factors controlling phosphate interaction with iron oxides. *Journal of Environmental Quality* **41** (3), 628-635.

**INNOVATIVE IN-SITU OXIDATION TECHNOLOGIES FOR TREATING GROUNDWATER
CONTAMINATED BY CHLORINATED SOLVENTS AND 1,4-DIOXANE**

Hua Zhong, Mark Brusseau, Ni Yan (The University of Arizona, Tucson, AZ, USA)
Lina Zhang, Peng Cui (Hunan University, Changsha, Hunan, China)

Contamination of groundwater by chlorinated-solvent constituents, 1,4-dioxane, and related compounds is ubiquitous, and remains a significant human-health and water-resource sustainability issue for many industrialized regions. For example, in Arizona, chlorinated-solvent constituents are the primary contaminants of concern for 44 of the 50 state and federal Superfund sites. Extensive dissolved-phase groundwater contaminant plumes typically form at sites contaminated by these compounds. Clean-up of these sites will require many decades or longer under current methods. Hence, alternatives are needed for cost-effective, long-term management of sources and plumes at these sites. We are developing two approaches based on the application of in-situ chemical oxidation (ISCO) for direct treatment. Method 1 employs a permeable reactive barrier supplemented with persulfate oxidant. The barrier would be placed downgradient of a control plane (source zone or plume edge), and is for sites with shallower groundwater. Method 2 is for deeper groundwater, and comprises creation of a treatment zone wherein the natural attenuation capacity of the sediment is enhanced through injection of oxidant solutions and activators. Bench-scale batch and column transport experiments were conducted to evaluate technology potential. A variety of Fe-based media, including iron filings, Fe₃O₄ solids, and several Fe-containing geomeia, were tested for in situ activation of persulfate. The use of a persulfate-H₂O₂ binary oxidant system was examined for contaminant degradation enhancement. Emplacement of Fe₃O₄ and zero-valent iron nanoparticles in porous media for activation of persulfate for deep groundwater treatment was also studied. The results showed that all these methods, though to different extents, caused in situ activation of persulfate and successfully enhanced degradation of chlorinated-solvent and 1,4-dioxane contaminants.

**UTILIZING PLANTS TO LIMIT THE MIGRATION OF CONTAMINANTS FROM
FRACKING-WATER SPILL SITES**

Amanda Shores, Brittany Hethcock, Melinda Laituri
(Colorado State University, Fort Collins, CO 80525, United State of America)

Plants provide an economical and in situ remediation method for removal of organic contaminants from soils, thereby limiting their spread to groundwater. Contaminants of particular recent interest are ones found in the produced water from hydraulic fracturing methods (fracking). Produced-water spills occur on a daily basis in Colorado and release a variety of organic contaminants in high concentrations into the environment, such as benzene, toluene, ethyl benzene, *m*-xylene (BTEX) and naphthalene, all known toxins. These contaminants are mobile in soil and have the potential to reach groundwater used for drinking. Inorganic salts in produced water are found in extremely high concentrations also, often above levels in sea water. At a produced-water spill site, vegetation dies and reestablishes only after some time, possibly after the salts have been leached out by rain. I propose the use of salt-resistant local grass species to vegetate fracking sites and facilitate the degradation of the abovementioned aromatic organic compounds. To develop this technology I will conduct two greenhouse studies. The first will test the ability of seven grasses native to Colorado to thrive on local soil spiked with salt levels commonly found in water produced from fracking in Colorado. The second will test the ability of the selected salt-resistant grasses to remediate BTEX and naphthalene from CO soil spiked with these compounds at environmentally relevant levels. Soil, root and shoot tissue concentrations of BTEX and naphthalene will be assessed using gas chromatography mass spectrometry (GC-MS) to determine if the selected plant species takes up the contaminant, where the contaminant is sequestered and which species is most effectively dissipating the contaminants. I hypothesize the plant uptake of BTEX and naphthalene will be sequestered in mainly root tissue and that the presence of these selected plants will reduce the overall contaminants in the soil. This research takes steps towards limiting toxins at a produced-water spill site from migrating to groundwater, reducing human and environmental health risks associated with such spills.

BIO-DRYING OF GREEN WASTES

Ertan Durmusoglu, Mutala Mohammed and Ismail Ozbay
(University of Kocaeli, Izmit, Kocaeli, Turkey)

ABSTRACT: In this study, the effect of bio-drying process on green waste was investigated at a laboratory scale. Four different sets of bio-drying processes were conducted and the impact of bulking agent was evaluated. The laboratory scale experiment consisted of a 0.8 m³ bio-drying reactor equipped with a matrix temperature measuring and air supply system. A 50 kg of green waste was placed in the reactor with an uninterrupted airflow rate of 1.4 m³/h. The results obtained indicated that the bio-drying reduced the water content of waste with bulking agent (BA) by 27% more than green waste alone after 7 days, allowing the production of bio-dried waste with a net calorific value of 6,270 kJ/kg wet weight, 55% higher than its initial value and 38% decrease in weight in the original mass of the waste. Although on the average, bio-drying of green waste alone showed significant reduction in volume (87%), weight (55%) and increase in calorific value (150%), bio-dried matrix with BA was the most preferred option since the process produced no leachate and generated the highest calorific value.

INTRODUCTION

The World Bank estimates that Municipal Solid Waste (MSW) generation is expected to increase to 4.3 billion tonnes by the year 2025 from the current 3 billion tonnes per year, based on population and economic rates. As developing countries continue their rapid pace of development and urbanization, these figures are expected to increase considerably. Food waste is the third largest component of generated waste and second largest component of discarded waste. Unfortunately, food waste contains high water content (Cheng et al., 2007; Zhang et al., 2008) and the indiscriminate disposal of such biodegradable waste leads to serious environmental consequences as well as significant damage to water resources when disposed in landfills. In curbing this menace, a number of innovative technologies for waste treatment such as composting, landfilling, anaerobic digestion, biodrying and thermal methods have been developed with landfilling as the most preferred option. However, as a result of the several drawbacks presented by waste landfilling and the introduction of the European Union Landfill Directive (1999/3/EC), this has led to significant reduction in the quantity of biodegradable waste disposed at landfills (European Commission, 1999; Torretta et al., 2014; Zhao et al., 2014). Henceforth, the generation of fuel from MSW by biodrying concept has recently found a new interest among researchers with the possibility to produce solid recovered fuel (SRF) (Ragazzi and Rada, 2012; Velis et al., 2013; Zawadzka et al., 2010).

Biodrying, a concept similar to composting, aims at removing or reducing water from biodegradable waste with high water content and increasing the treatability and subsequent utilization value of the Solid Recovered Fuel (SRF). The removal or reduction of moisture contents in bio-drying process involves evaporation of liquid water through aerobic decomposition of the organic material or reduction of water vapour by air flow (Cai et al., 2013; Huet et al., 2012; Velis et al., 2010). This mechanism is accomplished by relying on microorganisms, both bacteria and fungi to biologically degrade the organic component in order to reduce the moisture content while maintaining the biomass energy (Sadaka et al., 2011). Compared to traditional composting process, the essential distinguish feature of biodrying is the application of a higher ventilation rate to reduce moisture content by using the heat generated during the aerobic degradation process as well as forced aeration (Tambone et al., 2011). Also, the output from composting is stabilized organic material whereas that of biodrying is partially stabilized. Biodrying also has added advantage of pre-treating the waste at the lowest possible retention time to produce a high quality SRF. Besides these benefits, the biodrying process also renders the output material more suitable for short-term storage and lessens the transportation cost by reducing its weight through from moisture loss and partially biostabilizing it.

Initial moisture content, air-flow rate, porosity of the waste, permeability, retention time, mixing, the presence of BA and temperature have been identified by researchers as the main factors that affect biodrying process (Adani et al., 2002; Frei et al., 2004; Navaee-Ardeh et al., 2006). Among these, air-flow

rate and initial moisture content are paramount with extensive research and information available on these two parameters currently for biodrying. Air-flow rate has a direct influence on the matrix temperature and drying efficiency. Adani et al. (2002) and Roy (2005) established that high air-flow rate contributes to effective and fast drying, and high calorific value. Huilindir and Villegas (2015), studied the simultaneous effect of initial moisture content and airflow rate on biodrying of sewage sludge, and found that initial moisture content has a stronger effect on biodrying, affecting the temperature and improving the water removal. Additionally, the use of BA plays a crucial role in biodrying process. The use of BA adjusts the initial moisture content and facilitates air movement due to the increase in voids ratio. Its effects on biodrying has been demonstrated by some researchers including Frei et al., 2004; Zhao et al., 2011; Yang et al., 2014 and Zhao et al., 2012).

Currently, most studies on biodrying have been mainly focused on MSW, agricultural and sewage sludge. However, to the best of our knowledge, no studies of biodrying has been reported on neither green nor food waste. The present work was conducted to assess the biodrying of green waste of very high moisture content at constant air-flow rate and, the effect of BA on biodrying and leachate generation.

MATERIALS AND METHODS

Bio-Drying Materials and Analytical Analysis. In this study, green waste (lettuce) collected from a canteen of University of Kocaeli was used as the raw material for biodrying. Pruning waste of 15 mm in diameter was used as BA. Four different sets of biodrying processes were performed in this study. In the first (T1) and second (T2) trial, the objective was to identify the difference in moisture and weight reduction between shredded (15-20 mm) and non-shredded (80-90 mm) green waste. These investigations were undertaken by filling the reactor with 50 kg of the shredded and non-shredded green waste. For the third (T3) and fourth (T4) trial, the reactor was filled with the same amount of green waste (shredded and non-shredded) and 10% pruning waste as BA (initial moisture content of 10.20%) was added to evaluate the effect of BA in terms of weight loss and moisture reduction on biodrying of green waste. The ratio of green waste/pruning waste was 4:1 and the total waste of feedstock was 50 kg. All trials were performed at a constant and uninterrupted air-flow rate (1.4 m³/h) for seven days. The characteristics of the raw materials used in this study are presented in Table 1. The moisture content of the feedstock were analyzed following the ISO 5068-1 standard using moisture analyser (Precisa, XM 50), whereas the heat value of the biodried material was determined using IKA C-7000 model calorimeter (IKA Laboratory Equipment, Werke Staufen, Germany), in accordance with ISO 1928 standard. Elemental analysis was analyzed using Thermo Scientific Flash 2000 Elemental Analyzer (Thermo Fisher Scientific Inc., Bremen, Germany).



FIGURE 1. Bio-reactor used for the Experiment

Experiment Procedure. The biodrying process was conducted using an adiabatic box of 0.8 m³ made from a stainless steel with a leachate collection system at the bottom. The detail design of the bioreactor used in this study is presented in Fig. 1. The reactor was placed on an electronic balance to monitor the waste loss during the biodrying process. The matrix temperature was monitored with a thermometer sensor inserted in the reactor (5 cm above the bottom of the perforated plate). For aeration purposes, a whirlpool pump and an air-flow meter located in the horizontal duct from the air blower to the air chamber were used. The air

compressor or blower was used to supply aeration through the matrix at a constant rate while the air-flow meter monitored the air-flow rate. At the end of each trial, the final height and weight were determined.

TABLE 1. Characteristic of the Raw Materials

Parameter	LW ^a	PW ^b
Moisture content (%)	92.00	10.20
Bulk density (kg/m ³)	68.59	13.72
Calorific value (kJ/kg)	1,180	14,440

^a Lettuce waste; ^b Pruning waste

RESULTS AND DISCUSSION

Moisture Content and Volume Reduction of Waste Matrix. Table 2 summarizes the results obtained from the biodrying process of green waste operated for seven days. The moisture content of the biodried products were 82.5%, 71.5%, 45.0% and 57.0% for T1, T2, T3 and T4 process respectively. After the biodrying, the T3 process had the highest extent of moisture reduction (48.9%), followed by T4 (29.6%), T2 (13.9%) and T1 (10.3%). Commercial biodrying processes have been reported to be completed within 7-15 days with moisture losses around 25-30% (w/w) (Velis et al., 2009). For trial T1 and T2, moisture removal in the first few hours was principally achieved through leachate formation. As clearly indicated, moisture loss during biodrying process is by exothermic microbial reaction and airflow. Because biodrying is an aerobic process, the cell structure of the shredded waste matrix was destroyed, decreasing the water holding capacity which resulted in some amount of water been leaked in trial T1 and T2. However, the present of BA increased the porosity and facilitated the aerobic fermentation of the waste matrix with minimal biodegradation.

TABLE 2. Summary of the Results obtained from Biodrying Process

Experiment	MC (%)		Weight (kg)		CV ^e (kJ/kg)	
	Initial	Final	Initial	Final	Initial	Final
T1 ^a	92.0	82.5	50	21.6	1,050	2,290
T2 ^b	83.0	71.5	50	23.4	1,300	3,650
T3 ^c	88.0	45.0	50	26.5	3,770	6,860
T4 ^d	81.0	57.0	50	28.0	4,360	5,670

^a shredded waste; ^b non-shredded waste; ^c shredded waste + BA; ^d non-shredded waste + BA; ^e Calorific Value

Clearly, the lower the moisture content, the higher the calorific or energy content of waste. The increase in calorific value of the biodried material in the present study reached 181% for T1, which corresponds to 2,290 kJ/kg. T3 had 6,680 kJ/kg, nevertheless the increase was smaller, 82% (Table 2), in agreement with previous study by Stasta et al. (2006). A mixture of green waste and BA had higher initial average calorific value, 2 times more than green waste alone. This was attributed to the higher calorific value of the BA (pruning waste) as well as the lower initial moisture content in T3 and T4. Even though the percentage increase in calorific value of the waste matrix were in the order of T2 > T1 > T3 > T4, nonetheless T2 attained the second lowest initial calorific value.

Weight Loss Profile. Final weight loss rates after 168 hours of biodrying were 56.8%, 53.2%, 39.2% and 36.7% for T1, T2, T3 and T4 trials respectively, with an average highest weight reduction of 4.06 kg/day for T1 and 3.14 kg/day for T4 as the lowest. In contrast, the final volume loss rates were 82.9%, 84.9%, 65.0% and 77.1% for T1, T2, T3 and T4 respectively. Leachate was generated only in T1, T2 and T3. The highest weight loss was recorded in T3 (22.92 kg) as a result of leachate formation in T1 (31.69%) and T2 (26.32%) as percentage weight loss by leachate to the total weight loss, in agreement with report previously by Robles Martinez et al., (2012). This was because the mechanical shredding of the waste matrix disintegrated the structural components such as lignins and cells present in the waste and subsequently released the bound water, thus releasing large amount of leachate (Binod et al., 2012). Additionally, during biodrying process, weight loss occurred mainly through water and solid loss from leaching, moisture from

evaporation and oxidation of organic carbon or solid vitalization (Robles-Martinez et al., 2012). The results in this study established positive correlation between moisture and weight reduction. Weight loss of waste matrix for all four trials conducted in this study followed the order of T3 > T4 > T2 > T1, however, the waste matrix with BA recorded the highest moisture content reduction and weight loss, implying that waste matrix with different sizes and bulking agent could have influence on biodrying efficiency. Figure 2 shows weight loss percentages against time during seven days of biodrying. It was observed that the highest weight losses were achieved during the first two days with T1, T2 and T3 following a similar pattern.

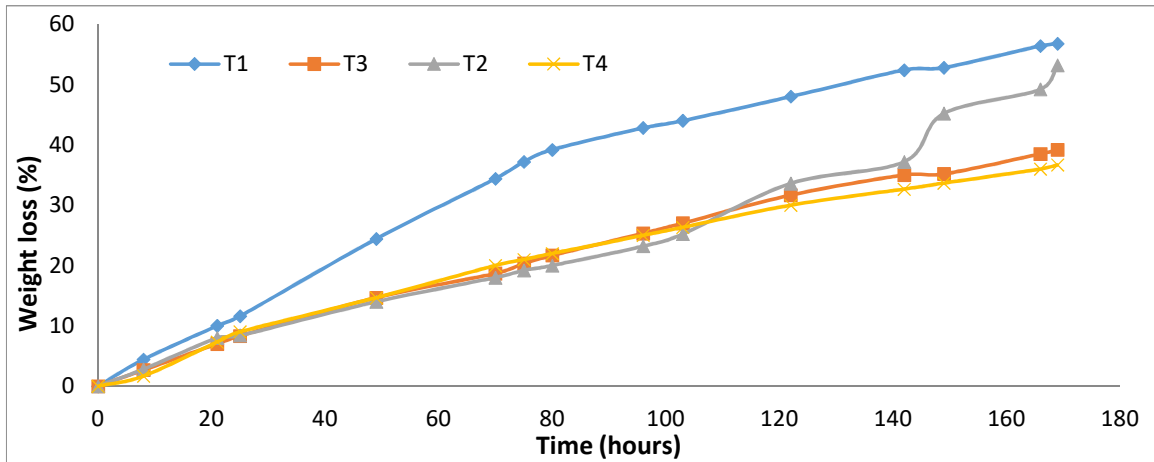


FIGURE 2. Weight Loss Percentage Profile against Time

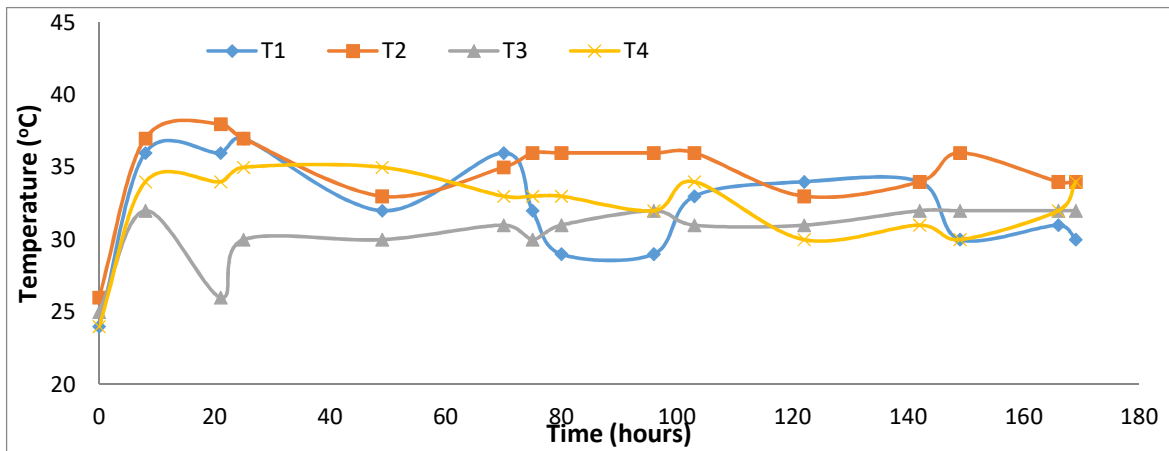


FIGURE 3. Dynamics of Temperature during the Biodrying Process

Matrix Temperature Evolution. The temperature profile of the matrix is presented in Fig. 3. The highest temperature recorded during the biodrying process was 38 °C for T2 on the 20th hour while T1 and T4 recorded the lowest as the initial temperatures, similar to that reported by Sen and Annachatre (2015). Also, the character of changes of temperature for T1, T2 and T4 followed a similar pattern, which clearly indicated three different cycles of temperature rise and fall during the entire biodrying process. At the end of the trial processes, T1 and T2 saw a decreasing trend in temperature, with T3 maintaining a linear pattern and an increasing trend in temperature for T4, 4 °C and 2 °C more than T1 and T3 respectively. The low temperatures obtained as well as the observed increase in temperature could be attributed to lack of turning or mixing, different structural composition of the matrix and inadequate air-flow. It also evident from the temperature profile (Fig. 3) that maximum self heating of the matrix occurred within the first 24 hours (i.e. highest temperatures) showing an intense microbial activity, which is an indication that the initial period of the biodrying process is crucial.

CONCLUSIONS

This study showed that biodrying is an effective approach for moisture and weight reduction of green waste, preserving most of its energy contents. Biodried matrix with BA (T3 and T4), recorded a higher decrease in moisture, 27% more than the matrix without BA. The use of BA had a positive impact on biodrying of green waste, both in terms of moisture reduction and calorific value increase. Calorific value of biodried matrix with BA increased, even though the results in this study revealed significant reduction of weight and volume. This implies lower cost for waste transportation and handling, nonetheless, the biodried material could not be suitable for energy generation since the calorific values, which is one of the parameters considered for SRF classification, obtained were below the required limit for solid-recovered fuel (SRF) generation. However, the effect of BA on both raw and biodried material on calorific value showed promising results. A mixed green waste with BA was found to be preferable since it provided real porosity which was crucial for moisture reduction with no leachate generation. Hence, further research or innovation is required to maximize the full utilization of bulking agent in order to preserve or increase the energy value of the biodried material. This could be achieved by varying the amount of BA.

ACKNOWLEDGEMENTS

The authors are grateful to the Research Unit of University of Kocaeli for funding this research.

REFERENCES

- Adani, F., D. Baido, E. Calaterra and P. Genevini. 2002. "The Influence of Biomass Temperature on Biostabilization – Biodrying of Municipal Solid Waste." *Bioresource Technol.* 83:173-179.
- Binod, P., M. Kuttiraja, M. Archana, K. U. Janu, R. Sindhu, R. K. Sukumaran and A. Pandey. 2012. "High Temperature Pretreatment and Hydrolysis of Cotton Stalk for Producing Sugars for Bioethanol Production." *Fuel* 92:340-345.
- Cai, L., T. B. Chen, D. Gao, G. D. Zheng, H. T. Liu and T. H. Pan. 2013. "Influence of Forced Air Volume on Water Evaporation during Sewage Sludge Bio-Drying." *Water Res.* 47(13):4767-4773.
- Cheng, H.F., Y. G. Zhang, A. H. Meng and Q. H. Li. 2007. "Municipal Solid Waste Fueled Power Generation in China: A Case Study of Waste-to-Energy in Changchun City." *Environ. Sci. Technol.* 41:7509-7515.
- European Commission. 1999. "Council Directive, 1999/317 EC of 26 April 1999 on the Landfill of Waste. Official Journal of the European Communities, L 182 16/07/1999.
- Frei, K. M., D. Cameron and P. R. Stuart. 2004. "Novel Drying Process Using Forced Aeration Through a Porous Biomass Matrix." *Dry Technol.* 22(5):1191-1215.
- Huet, J., C. Druilhe, A. Trémier, J. C. Benoist and G. Debenest. 2012. "The Impact of Compaction, Moisture Content, Particle Size and Type of Bulking Agent on Initial Physical Properties of Sludge-Bulking Agent Mixtures before Composting." *Bioresource Technol.* 114:428-436.
- Huilinir, C., and M. Villegas. 2015. "Simultaneous Effect of Initial Moisture Content and Airflow Rate on Biodrying of Sewage Sludge." *Water Res.* 82:118-128.
- Mohajer, A., A. Trémier, S. Barrington, J. Martinez, C. Teglia and M. Carone. 2009. "Microbial Oxygen Uptake in Sludge as Influenced by Compost Physical Parameters." *Waste Manage.* 29:2257-2264.
- Navae-Ardeh, S., F. Bertrand and P. R. Stuart. 2006. "Emerging Biodrying Technology for the Drying of Pulp and Paper Mixed Sludges." *Drying Technol.* 24:863-878.
- Ragazzi, M., and E. C. Rada. 2012. "RDF/SRF evolution and MSW bio-drying." *WIT Trans. Ecol. Environ.* 163:199-208.
- Robles-Martinez, F., E. M. Silva-Rodriguez, T. Espinosa-Solares, B. Pina-Guzaan, C. Calixto-Mosquoda, F. J. Colomer-Mendoza and E. Duran-Paramo. 2012. "Biodrying under Greenhouse Conditions as Pretreatment for Horticultural Waste." *J. Environ. Protection* 3:298-303.
- Roy, G. 2005. "Modélisation Technique et Economique d'un Réacteur de Bioséchage Discontinue (In French). Technical and Economic Modelling of a Biodrying Batch Reactor." MSc Thesis, Ecole Polytechnique de Montréal, Montréal, Canada.
- Sadaka, S., K. VanDevender, T. Costello and M. Sharara. 2011. "Partial Composting for Biodrying Organic Materials." *Agricultural and Natural Resources*, University of Arkansas, FSA1055. <http://www.uaex.edu>.

- Sen, R., and A. P. Annachhatre. 2015. "Effect of Air Flow Rate and Residence Time on Biodrying of Cassava Peel Waste. *Int. J. Environmental Technol. and Manage.* 18(1):9-29.
- Stasta, P., J. Boran, L. Bebar, P. Stehlik and J. Oral. 2006. "Thermal Processing of Sewage Sludge." *Appl. Therm. Eng.* 26(13):1420-1426.
- Tambone, F., B. Scaglia, S. Scotti and F. Adani. 2011. "Effects of Biodrying Process on Municipal Solid Waste Properties." *Bioresource Technol.* 102(16):7443-7450.
- Torretta, V., G. Ionescu, M. Raboni and G. Merler. 2014. "The Mass and Energy Balance of an Integrated Solution for Municipal Solid Waste Treatment." *WIT Trans. Ecol. Environ. Res.* 180:151-161.
- Velis, C. A., P. J. Longhurst, G. H. Drew, R. Smith and S. J. T. Pollard. 2010. "Production and Quality Assurance of Solid Recovered Fuels Using Mechanical-Biological Treatment (MBT) of Waste: A Comprehensive Assessment." *Crit. Rev. Env. Sci. Tec.* 40(12):979-1105.
- Velis, C. A., P. J. Longhurst, G. H. Drew, R. Smith and S. J. T. Pollard. 2009. "Biodrying for Mechanical-Biological Treatment of Wastes: A Review of Process Science and Engineering. *Bioresource Technol.* 100(11):2747-2761.
- Velis, C. A., S. Wagland, P. J. Longhurst, B. Robson, K. Sinfield, S. Wise and S. J. T. Pollard. 2013. "Solid Recovered Fuel: Materials Flow Analysis and Fuel Property Development during the Mechanical Processing of Biodried Waste." *Environ. Sci. Technol.* 47(6):2957-2965.
- Yang, B., L. Zhang and D. Jahng. 2014. "Importance of Initial Moisture Content and Bulking Agent for Biodrying Sewage Sludge. *Drying Technol.* 32:135-144.
- Zawadzka, A., L. Krzystek, P. Stolarek and S. Ledakowicz. 2010. "Biodrying of Organic Fraction of Municipal Solid Wastes." *Drying Technol.* 28:1220-1226.
- Zhang, D. Q., P. J. He, L. M. Shao, T. F. Jin and J. Y. Han. 2008. "Biodrying of Municipal Solid Waste with High Water Content by Combined Hydrolytic-Aerobic Technology." *J. Environ. Sci.* 20(12):1534-1540.
- Zhao, L., W. Gu, L. M. Shao and P. J. He. 2012. "Sludge Bio-Drying Process at Low Ambient Temperature: Effect of Bulking Agent Particle Size and Controlled Temperature. *Drying Technol.* 30:1037-1044.
- Zhao, L., W. M. Gu, P. J. He and L. M. Shao. 2011. "Biodegradation Potential of Bulking Agents Used in Sludge Bio-Drying and their Contribution to Bio-Generated Heat." *Water Res.* 45(6):2322-2330.
- Zhao, P., Y. Shen, S. Ge, and K. Yoshikawa. 2014. "Energy Recycling from Sewage Sludge by Producing Solid Biofuel with Hydrothermal Carbonization." *Energy Convers. Manage.* 78:815-821.

A NEW CONCEPT FOR UTILIZATION OF INDUSTRIAL SOLID WASTES IN BUILDING STRUCTURES

Arunima Shukla and Ashok N. Bhaskarwar

(Department of Chemical Engineering, Indian Institute of Technology, Delhi, Hauz Khas, New Delhi 110 016, INDIA)

ABSTRACT: The solid-waste management is one of the important issues of present times due to rapid industrialization. Research studies reveal that globally, a total estimated annual industrial solid-wastes generation was about 11 billion tons for 2002, which is expected to increase in the coming years (Chavan and Patil, 2013).

We have developed a new technology for making light-weight aerated concrete blocks, which allows the integration of industrial solid wastes. In the present study, solid waste of autoclaved aerated concrete (AAC) industries and a by-product of coal-fired power plants known as fly ash have been successfully integrated into colloidal-gas aphrons (CGA) based aerated slurry. Experimental results have shown that it is possible to utilize flyash up to 75 % and AAC solid waste up to 25 % with respect to total mass of solids in aerated concrete.

INTRODUCTION

Nowadays, industrial solid waste is one of the major environmental issues. The construction materials can be established as secondary industry in the area of solid waste and recycling (Chavan and Patil, 2013). There is

plenty of literature available on the generation and utilization of flyash. In USA, the annual production of flyash is 71 metric tons, of which only 31% is being utilized (Singh and Gupta, M Singh, 2013). In India, the percentage utilization of flyash is around 10 to 15%, where more than 88 million tons of fly ash is getting generated per year (Siddique, 2004). Due to high demand of energy, the quantity of fly ash, as a solid waste, is also increasing (Singh and Gupta, M Singh, 2013). In the autoclaved aerated concrete (AAC) manufacturing industries, a considerable amount of solid-waste, to the tune of at least about 10 to 12 % of total production, is generated because of breakage due to thermal stresses arising during autoclaving, and during handling and transportation.

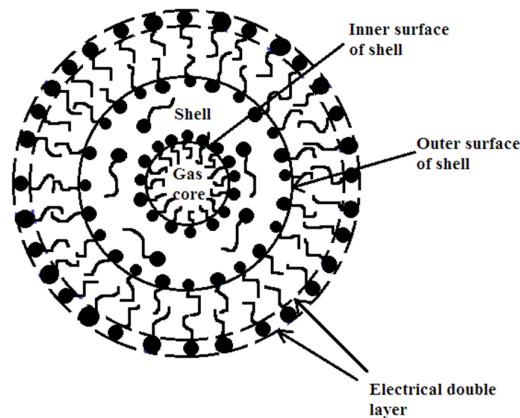


Figure 1. Conceptual diagram of CGA, as explained by Sebba

Considering the above factors, we have developed a new technology which will simultaneously manufacture light weight aerated concrete blocks, and utilize considerable amount of solid wastes generated by various industries. Aerated concrete is known for its insulating properties, as well as for its structural properties (Narayanan and Ramamurthy, 2000). Its properties mainly depend on the method of aeration, as void in the matrix is the key ingredient of light weight aerated concrete. We are working with

colloidal gas aphanes (CGAs) as an aerating medium for creating the voids in the cement matrix. CGAs are micro-bubbles, typically in the range of 10 to 100 μm diameter, having high interfacial area, flow properties similar to water, and high stability (Jauregi, Mitchell, and Varley, 2000; Sebba, 1987). The conceptual diagram of CGAs is shown in Figure 1. Sebba had proposed that CGAs have inner gas phase, surrounded bi-layer of surfactant and an electrical double layer.

MATERIALS AND METHODS

Raw Material. Sodium lauryl sulfate (Fisher scientific), ordinary portland cement (43 grade), flyash, autoclaved aerated concrete waste (Biltech Ltd.) of two sizes.

Equipment. Accelerated curing tank (Ferrotek equipments); Stirrer (Remi elektrotechnik Ltd., 220/230 V, 1 phase, 50 Hz); Hot air oven (Macro scientific works pvt. Ltd.); Optical microscope (Motic microscope) SEM (Hitachi, TM 3000, tabletop microscope)

Experimental Set-Up. The experimental set-up for CGA formation consists of a spinning disc CGA generator which is an open cylindrical vessel, attached with inverted L-shaped baffles. Stirring is done by a circular disc mounted on stirrer.

METHODOLOGY

Sodium lauryl sulfate was mixed with fixed volume of ordinary tap water for 15 minutes at 1500 rpm, in order to form a homogenous solution. This is followed by increasing the rpm of stirrer to 5500 rpm, which causes generation of waves at the surface of surfactant solution. The generated waves create thin film of gas, which being unstable, break up into small sized droplets, known as CGAs. Continuous recirculation of surfactant solution led to increase in the air hold up (up to 0.70 to 0.80) in CGAs. The CGAs generated were mixed with solid waste and cement. The samples were allowed to set for 24 hours, followed by de-moulding and steam curing at 65°C for 4 to 5 hours. The samples were then dried in oven for 24 hours, to measure oven dried weight at $110\pm 10^\circ\text{C}$.

RESULTS AND DISCUSSION

Colloidal Gas Aphanes. The CGAs were prepared by using anionic surfactant, sodium lauryl sulfate ($\text{NaC}_{12}\text{H}_{25}\text{SO}_4$). Photomicrographs of CGAs were taken using optical microscope, as shown in Figure 2. Motic software was used to determine the sizes of the micro-bubbles.

SOLID WASTE. Fly ash was obtained from two different resources in order to study its effect on the properties of aerated concrete. The SEM images of fly ash are shown in Figure 3. It was observed that the type 1 flyash was finer as compared to type 2. The solid waste from AAC was utilized in the form of pebbles and granules, in order to obtain re-integrated blocks of aerated concrete. Higher densities of aerated concrete were targeted to get the intact blocks in case of AAC solid waste utilization. The SEM images of different AAC waste were observed (Figure 4) to study the surface morphology of the waste. The needle-like and plate-like structures were observed in pebbles, which indicate that ettringite and calcium silicate hydrate were already developed (Stutzman, 2001). However, in case of granules, such kind of structures could not be observed.

EFFECT OF FLY ASH ON THE PROPERTIES OF AERATED CONCRETE. The aerated slurry has variations in the CGA distribution, which results in difference in the properties of concrete blocks. Thus, the samples, in each set of experiments, were characterized based on pouring of samples, the 1st poured was named as 1st cut, similarly, the 2nd and 3rd poured were named as 2nd and 3rd cut respectively. The weight percentages of cement, flyash and water were kept constant, within the range of $\pm 0.15\%$. It was observed that the 1st cut was lighter, as compared to 2nd and 3rd cut, because of more air hold-up. Thus with increase in air weight % in slurry, dry density of the sample decreases, as shown in Figure 5. It was also noted that with the increase in air weight % in slurry, the compressive strength of the samples initially decreases till 0.1 air weight % w/w, and then increases slightly, as shown in Figure 6. The increase is more significant in type 2 flyash samples. This is due to the fact that porosity directly influences compressive

strength (Erniati et al., 2015; Zhao et al., 2014) and the colloidal gas aphrons provide a well distributed pore size distribution in the cement matrix.

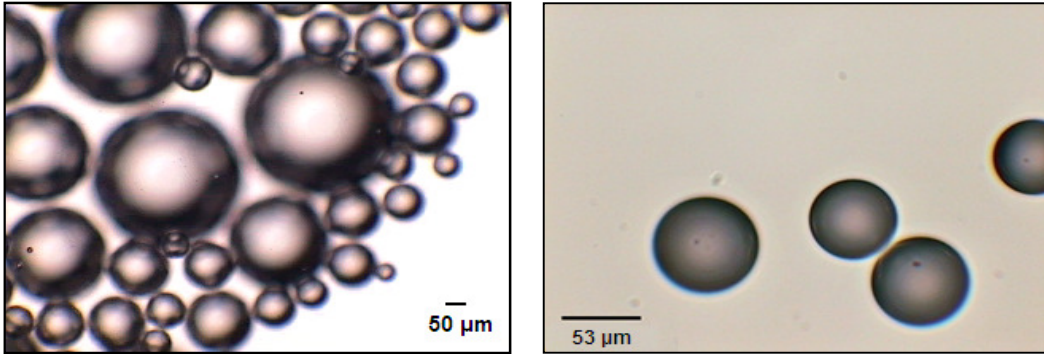


Figure 2. Photomicrographs of CGAs at different magnification: (a) At 10X; (b) At 40 X.

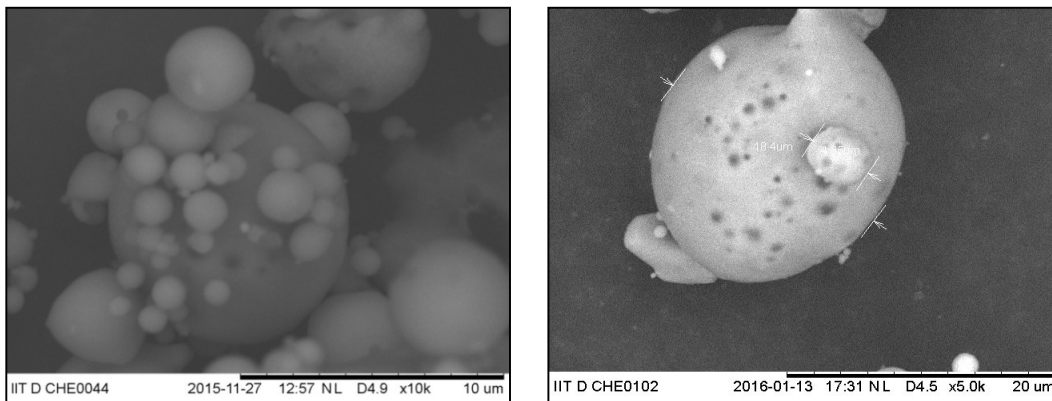


Figure 3. Scanning electron micrographs of fly ash type 1 (left) and type 2 (right).

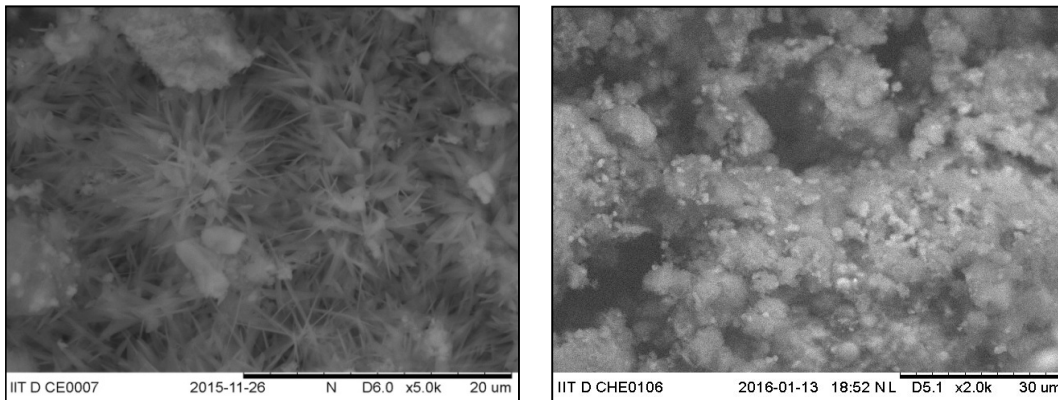


Figure 4. Scanning electron micrographs of autoclaved aerated concrete solid wastes in the form of pebbles (left) and granules (right).

All the data points were plotted (Figure 7), based on cuts, in order to check the correlation between density and compressive strength, as it was reported that compressive strength increases linearly with density (Narayanan and Ramamurthy, 2000). The range of densities from 712 to 1112 kg/m³ and compressive strengths 1.01 MPa to 3.49 MPa were observed for the fly ash type 1, and densities range of 392 to 1072 kg/m³ and compressive strengths 0.52 MPa to 4.6 MPa were observed for fly ash type 2, respectively. Type 2 flyash shown more linear trend as compared to type 1.

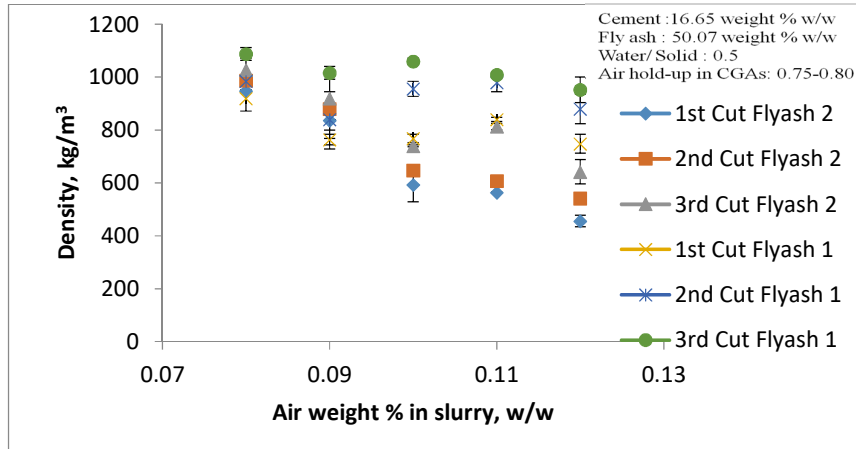


Figure 5. Density vs. air weight % w/w in slurry.

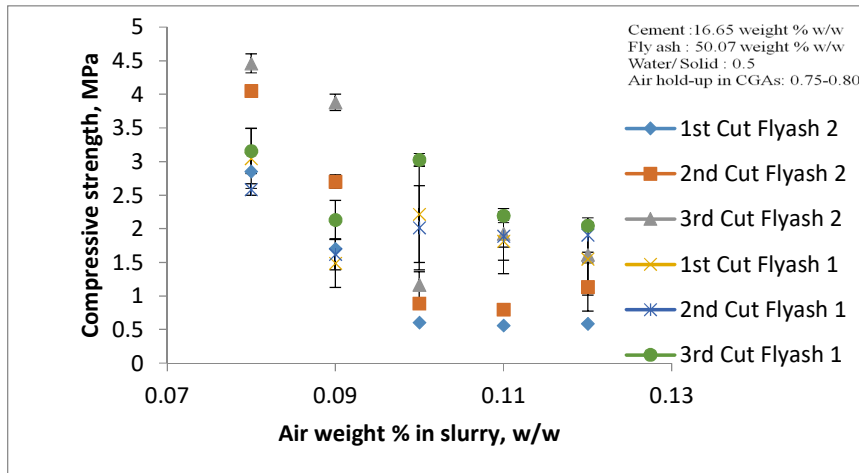


Figure 6. Compressive strength vs. air weight % w/w in slurry.

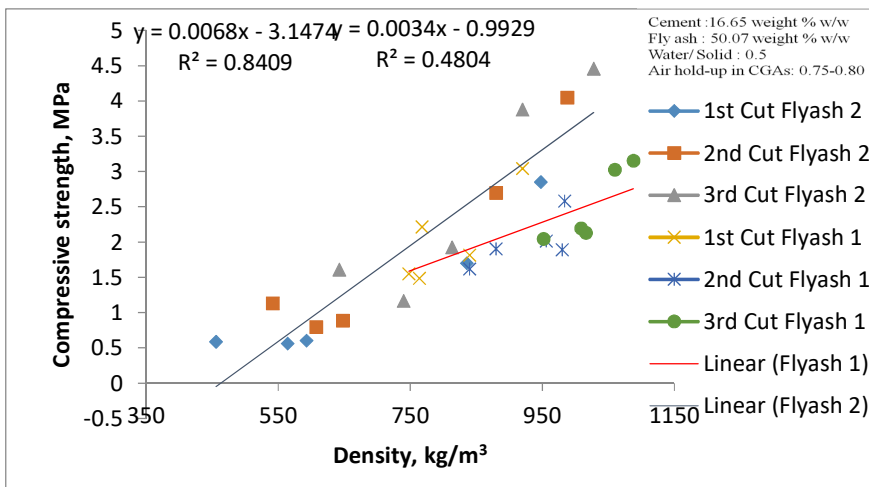


Figure 7. Variation in compressive strength vs. density based on pouring of samples.

Autoclaved Aerated Concrete Solid Waste. The solid waste from autoclaved aerated concrete industries was incorporated into the CGAs based slurry, varying from 5 to 25 weight % of total solid mass. The water to solid ratio was fixed as 0.5. The variation in the composition is given in Table 1.

Table 1. Varying percentages of composition with solid AAC waste

S.No.	AAC waste (% of total solid mass)	Cement (weight %)	Flyash (weight %)	Water (weight %)	Air (weight %)
1	5	21.09	42.19	33.31	0.06
2	10	19.98	39.98	33.31	0.06
3	15	18.88	37.76	33.32	0.05
4	20	17.77	35.54	33.32	0.05
5	25	16.66	33.32	33.32	0.04

All the samples were intact without any deformation. A good bonding between solid waste and aerated slurry was observed without any crack formation, as shown in Figure 8. The color difference between AAC waste and slurry was observed, which was marked on the sample using a marker, in order to take the SEM image of interface.

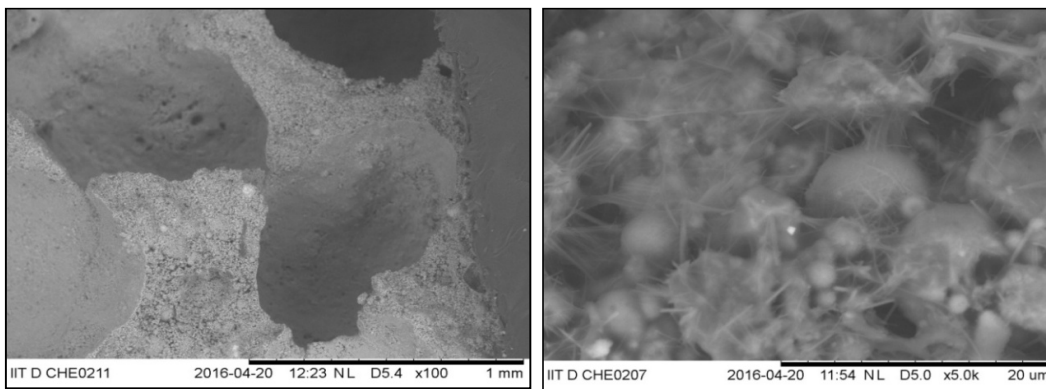


Figure 8. Scanning electron micrographs of bonding between AAC solid waste and CGAs based aerated slurry, at lower magnification (left) and at higher magnification (right) respectively.

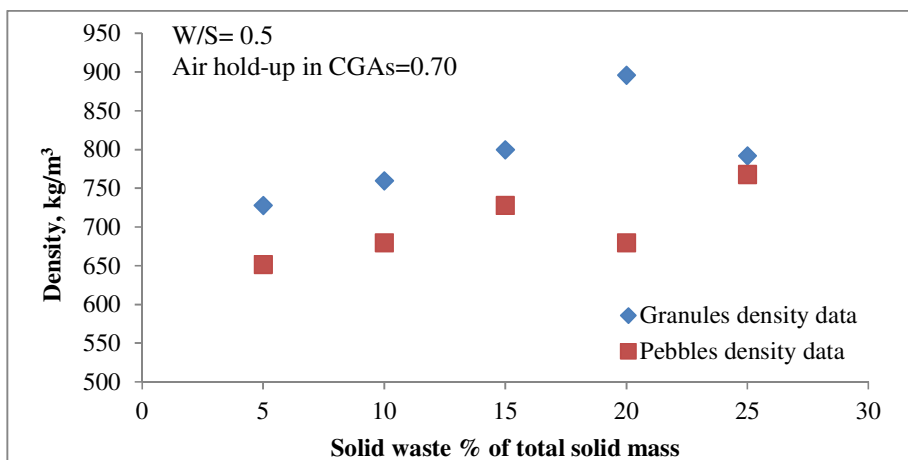


Figure 9. Density vs. solid waste percentages of autoclaved aerated concrete (AAC) sample.

The densities and compressive strengths of the samples were also measured and plotted in Figure 9 and Figure 10, respectively. The ranges of densities were from 652 to 896 kg/m³ and compressive strengths 0.26 MPa to 0.75 MPa.

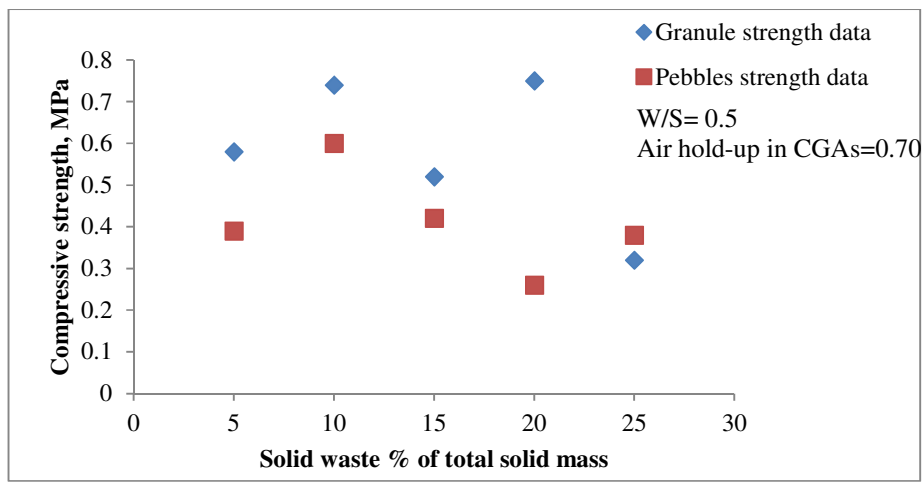


Figure 10. Compressive strength vs. solid waste percentage of autoclaved aerated concrete (AAC) samples.

CONCLUSIONS

The results revealed that the industrial solid wastes such as fly ash, and aerated concrete, in the form of granules and pebbles, can be utilized using CGAs based technology. A wide range of strengths and densities were observed using varying composition and densities. It is, thereby, possible to utilize up to 25% of AAC solid waste with respect to total mass of solid. Moreover, there is a lot of scope for the improvement of compressive strength of the AAC solid waste sample in future, as well as utilization of other industrial solid wastes.

ACKNOWLEDGEMENT

The authors would like to thank and acknowledge foundation for innovation and technology transfer (FITT), India for their support in patenting the work and Biltech Building Elements Limited, Palwal, India for their help in getting solid waste.

REFERENCES

- Chavan, P G, and S B Patil. 2013. "Substantial Use of Solid Waste." *International Journal of Advanced Technology in Civil Engineering* 2(1): 61–63.
- Erniati, M. Wihadi Tjaronge, Zulharnah, and Ulva Ria Irfan. 2015. "Porosity, Pore Size and Compressive Strength of Self Compacting Concrete Using Sea Water."
- Jauregi, Paula, Geoffrey R. Mitchell, and Julie Varley. 2000. "Colloidal Gas Aphrons (CGA): Dispersion and Structural Features." *AIChE Journal* 46(1): 24–36.
- Narayanan, N., and K. Ramamurthy. 2000. "Structure and Properties of Aerated Concrete: A Review." *Cement and Concrete Composites* 22(5): 321–29.
- Sebba, F. 1987. *Foams and Biliquid Foams-Aphrons*. Wiley, Chichester, Ž. England.
- Siddique, Rafat. 2004. "Performance Characteristics of High-Volume Class F Fly Ash Concrete." *Cement and Concrete Research* 34(3): 487–93.
- Singh, S P, and S P Gupta, M Singh. 2013. "Fly Ash Production and Its Utilization in Different Countries." *Ultra Chemistry* 9(1): 156–60.
- Stutzman, Paul E. 2001. "Scanning Electron Microscopy in Concrete Petrography." *Materials Science of Concrete Special Volume*: 59–72.
- Zhao, Haitao, Qi Xiao, Donghui Huang, and Shiping Zhang. 2014. "Influence of Pore Structure on Compressive Strength of Cement Mortar." *TheScientificWorldJournal* 2014: 1–12.

RECOVERY OF COPPER FROM WASTE PRINTED CIRCUIT BOARDS (PCBS) USING ELECTRO-WINNING PROCESS

Pradeep Kumar, Shashi Bhushan Kumar, Poornima Pandey, Roli Saini

(Department of Chemical Engineering & Technology, Indian Institute of Technology, Banaras Hindu University, Varanasi, Uttar Pradesh, India – 221005)

ABSTRACT: Solid waste management is seemingly a great significance topic. The constituent component part of Electronic waste (E-waste) is increasing the solid waste. The newer technology has to be developed to deal with e-waste separately. It contains hazardous substances which precipitate in to environment, if they are not handled properly. Cadmium, lead, arsenic, and chromium are most toxic metals present in e-waste. It contains some valuable materials (base metals such as iron, copper, aluminium etc.) which should be recovered. Hydrometallurgical method is suitable technique for copper recovery of metal from used PC or mobile phone. It consists of two steps first leaching and second metal recovery from the leaching solution. The mechanical processing (size reduction and magnetic separation) is an efficient preliminary operation to obtain a concentrated (Fe as the magnetic fraction and Cu as the conductive fraction in primarily phase) fraction of a specific metal from E-waste.

In present study, hydrometallurgical technique was used for recovery of copper from printed circuit boards (PCBs). Leaching was carried out in HNO₃ which showed a great possibility for recovery of copper. The effect of temperature, residence time, normality of leaching agent, size of PCBs, and finally solid-liquid ratio was studied in leaching operation. Electro-winning process was performed to separate copper from leaching solution. Current supply in electro-winning process was delivered by DC source across 0.37 V. The maximum copper recovery from the leachate solution in the electro-winning was obtained as 73.14 %. Overall copper recovery from PCBs to the final stage was obtained 8.641 gm/Kg of E-waste (PCBs).

Keywords: E-waste, printed circuit boards, electro-winning process, copper

INTRODUCTION

Printed circuit boards are basic component of each electronic goods, which made from polymers, ceramics and metals, mainly Cu (Calgaro et al., 2015). With cutting age technology, demand of new electronic goods increases the higher amount (approx. 20-25 million per year) of E-waste generation, which require recycling (Robinson, 2009, Orlins and Guan, 2016). Because it contained various hazardous and non-hazardous metals, these released to atmosphere and caused harmful effects on living beings (Sthiannopkao and Wong, 2013). There are several methodology available for recovery of metal from E-waste same as from ores such as pyrolysis, hydrometallurgical leaching and bioleaching in initial step. Then the finally metal from leachate will be processed by solvent extraction, cementation, activated carbon, bio-sorption and ion exchange post treatments (Cui and Zhang, 2008, Pant et al., 2012). Before recovery of metal, some basic pre-treatment steps (hammer mill, grinder mill, knife cutter, magnetic separation) are used for size reduction, separation of ferrous and non-ferrous metals (Bizzo et al., 2014). In present article, hydrometallurgical technique was used for recovery of copper in solid phase from printed circuit boards (PCBs), followed by Electro-winning process.

MATERIALS AND METHODS

Electronic Waste (E-waste). Printed circuit boards from used and discarded electronic goods were segregated and collected as E-waste from “Department of Chemical Engineering, IIT (BHU) Varanasi.

Materials. The chemicals (AR Grade) involved during leaching of copper were nitric acid (HNO₃, purity 69-70%) procured from Fischer Scientific Limited as leaching agent and NaOH granules from SD Fine

Chemicals Ltd. as flow of charge in Electro-winning process. Distilled water was prepared in the laboratory usage for dilution of leaching agent.

Experiment method. First of all PCBs (about 1 kg) having metal strip had reduced into small pieces 10 mm × 10 mm or smaller using grinder mill and knife cutter. These contained both magnetic and non-magnetic materials, which were manually separated through magnet bar. In this article, copper was main concern metal which obtained in non-magnetic materials. This was leached out by dissolving non-magnetic materials in concentric nitric acid (HNO₃) as leaching agent. After filtration process, the leachate solution was treated by Electro-winning process. For this process, the cell was prepared by consisting of a copper cathode (10 mm × 20 mm) and a stainless steel plate as anode as shown in Figure 1. It was connected through wire to the DC electric source. Characterization of leachate was done by Inductive couple plasma (ICP) for determination of trace elements in a sample.

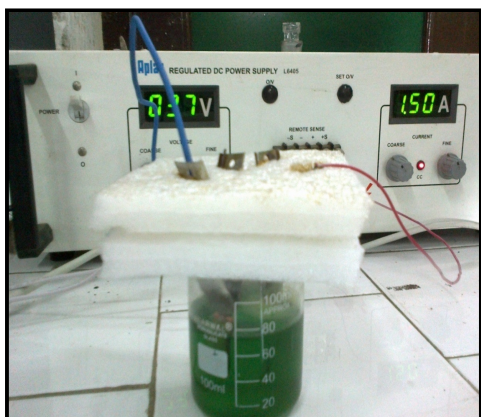


Figure 1. Set up of Electro-winning process

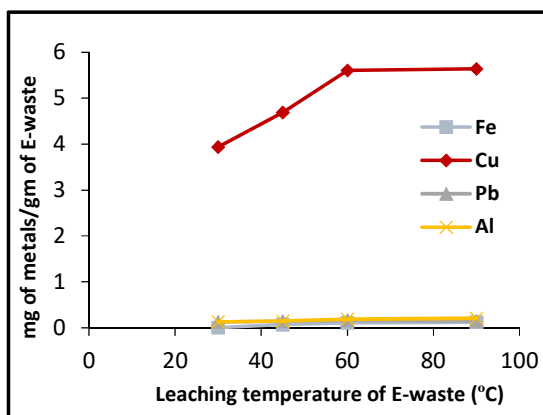


Figure 2. Effect of temperature on leaching of metals, Experimental condition: Sample (E-waste) = 12 gm, Solid liquid ratio = 1:3, Residence time = 180 min, Normality of the solvent (HNO₃) = 15.66 N

RESULTS AND DISCUSSION

All experiments were conducted using waste printed circuit boards (PCBs) as electronic wastes (E-wastes). These were also done by variation of different parameters like temperatures, solid liquid ratios, size of PCBs, residence time, and acid concentrations on copper leaching from PCBs specimen. The obtained results were discussed below.

Effect of Temperature. The effect of temperature on the leaching of PCBs was studied at different temperatures of 30, 45, 60 and 90 °C or other parameters such as solid liquid ratio 1:3 (25.5 ml of HNO₃), residence time 180 min and normal size of PCBs (over size particle of mesh size 6) were used. 12 gm of four samples were taken for leaching experiments. The results are shown in the Figure 2 that rising of the temperature has positive effect on leaching of metal in leaching solution. Leaching rate increases as temperature increases, but becomes constant at 60 to 90 °C. Initially more concentrated acid penetrate the solid material easily, but above 60 °C temperature increases viscosity of the solvent decreases rather than leaching rate becomes slow. It becomes almost constant as leaching is exothermic reaction, the heat sensitivity of solute, volatility of the solvent and possible thermal effects on the inert or residue solid limit the temperature of the reaction. At elevated temperatures, the flow of leaching agent in to pore becomes slow it cannot penetrate the solid pore.

Effect of Solid Liquid Ratio. The effect of solid-liquid ratio on leaching of PCBs was studied by taking four samples of equal weight (10 gm of each). Samples were maintained under solid liquid ratio 1:2, 1:3, 1:5, 1:10 by changing volume of HNO₃, but amount of samples were remain same. For all the four samples, other parameters were kept constant such as temperature 30 °C, leaching time 180 min and normality of

solvent (HNO_3) 15.66 N. From Figure 3 shows that leaching rate increases on increasing solid liquid ratio. However, after certain limit it decreases because it became saturated, as further liquid molecules cannot penetrate the solid material.

Effect of Particle Size of (PCB). The effect of particles of crushed size of PCBs on leaching rate was studied by using particle of size greater than 3.35 mm, equal to 3.08 mm and less than 2.81 mm. 30 gm of crushed PCBs were taken and classify by different particle size with help of two sieves of BS5 and BS4. After shaking, three different particle sizes of E-waste samples were obtained. One was upper portion of the first sieve, another was in between the two sieves and finally last one was on the pan. These three samples were taken separately and weighted. It was found 12 gm upper side, 10 gm in between the sieves and remaining in the pan. Temperature of experiment was maintained constant 30 °C as well as solid liquid ratio 1:3 and residence time 180 min.

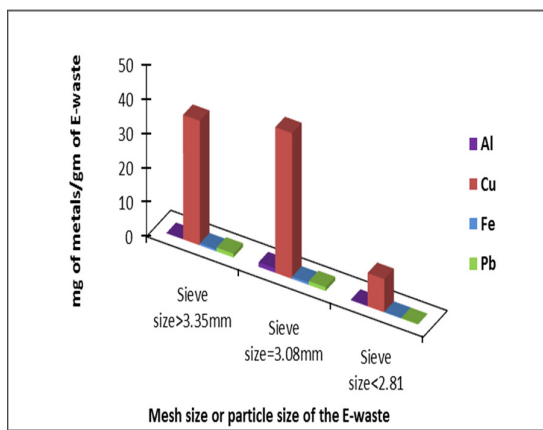
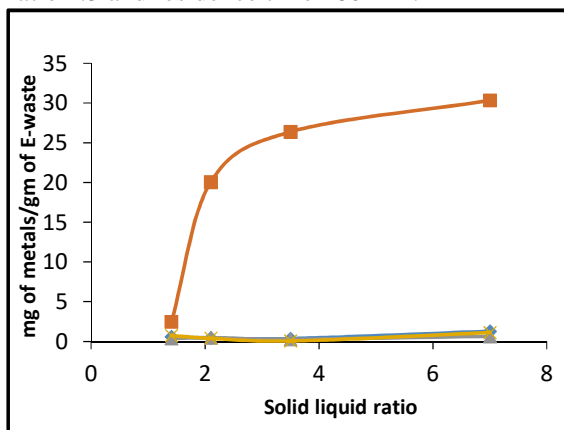


Figure 3. Effect of solid to liquid ratio (w/v) on the recovery of metals during leaching. Experimental condition: Residence time = 180 min, Temperature = 30°C, Normality of the solvent (HNO_3) = 15.66 N.

Figure 4. Effect of particle size of E-waste on the recovery of metals during leaching. Experimental condition: Residence time = 180 min, Temperature = 30°C, Solid liquid ratio = 1:3 and Normality of the solvent (HNO_3) = 15.66 N.

Figure 4 shows that as sizes of PCBs decreases extent of leaching decreases. But in real case as the size of the material decreases recovery increases because pores and surface area both increases. The leaching is directly proportional to pores and surface area. But this experiment result was not obtained as real. The reason behind that the grinder machine which was not working so effective. It crushes PCBs present but the metal strip remains greater size. When sample was separated by sieve maximum metal part remains on the upper and the middle of the sieve. On leaching sample, more metals were obtained in bigger size particle, not in smaller particle size.

Effect of Residence Time. Each sample (average particle of 10 mm × 10 mm) having weight of 10 gm were poured in to a beaker separately. Solid liquid ratio was 1:3 (470 gm/L) as constant for entire experiment. All four samples were filtered after time duration of 2, 4, 6, 24 hr. From Figure 5 it is observed at the beginning leaching rate increased with residence time very fast. After 4 hr leaching rate of PCBs in leaching solvent becomes constant as because the competition between different metals ions in solution. Initially there was large number of pores and surface area available, as well as no resisting material so it can penetrate solid easily, therefore leaching rate decreases after 4 hr.

Effect of Normality of Leaching Agent. Four samples of each 10 gm were taken for analysis of effect of normality of leaching agent during leaching. Other parameters were particle size (10mm × 10mm), temperature 30 °C, solid liquid ratio 1:3 (470 gm/L) and residence time 2 hr. Leaching rate of copper is found to increase with increase acid concentration from Figure 6, but latter it becomes constant due to the competition caused by leaching of copper at high acidity leading to increase in the viscosity of the solution that consequently inhibits the leaching process.

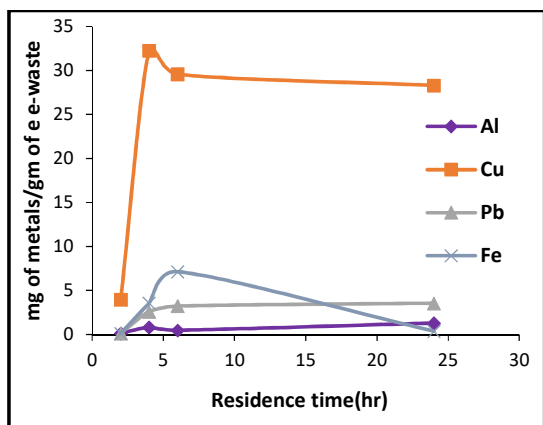


Figure 5. Effect of residence time on recovery of metals during leaching. Experimental Condition: Temperature = 30 °C, Solid liquid ratio = 1:3 and Normality of the solvent (HNO₃) = 15.66 N.

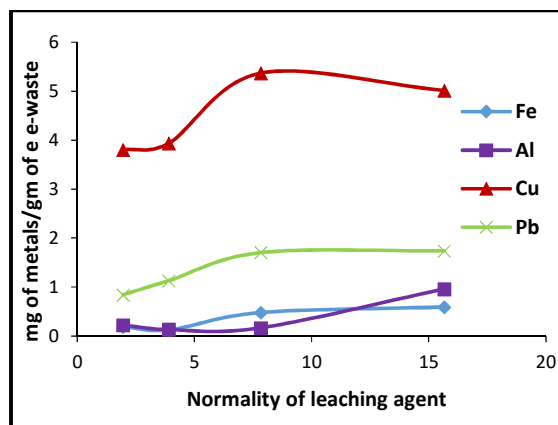


Figure 6. Effect of normality of leaching agent on recovery of metals during leaching. Experimental Condition: Residence time = 180 min, Temperature = 30 °C and Solid liquid ratio = 1:3.

Recovery of copper from the leaching solution. It was final stage of copper recovery from E-waste leachate. Electro-winning process was performed to obtained copper from leaching solution to solid form. The copper recovery in the overall process is 8.641 gm/Kg of e-waste (73.14 %).

CONCLUSION

The article had studied on the recovery of copper from the waste printed circuit boards (PCBs) as E-waste using leaching followed by electro-winning process. Analysis by inductively coupled plasma (ICP) had characterized the presence of Cu, Pb, Fe, Zn, Fe, Mg, Al, and Ca in the leachate sample of PCBs in different proportions. Leaching of PCBs was carried out in HNO₃ as leaching agent which showed a great possibility for recovery of copper. The variation of different parameters like temperature, residence time, normality of leaching agent, size of PCBs, and finally solid-liquid ratio was studied in leaching operation. It further revealed that best operating condition for the leaching of copper from PCBs at temperature 60°C, normality of HNO₃ acid 10 N, residence time 4 hr and size of PCBs about 3.08 mm. After that electro-winning process was performed in order to separate copper from leaching solution. Using DC source across 0.37 V, current supply was delivered in electro-winning process. The maximum copper recovery from the leachate solution in the electro-winning was obtained as 73.14 %. Overall copper recovery from PCBs to the final stage was obtained 8.641 gm/Kg of E-waste (PCBs). The article delivered the idea for formal recycling of devastating E-waste which could be adopted by developing countries to reduce exploitation of resources.

ACKNOWLEDGMENTS

The authors would like to gratefully acknowledge to the Department of Chemical Engineering and Technology, I.I.T. (B.H.U.), Varanasi for offering facilities for characterization and MHRD which funded the research.

REFERENCES

- B. H. Robinson. 2009. "E-waste: An assessment of global production and environmental impacts". *Science of the Total Environment*, 408: 183–191.
- C.O. Calgaro, D.F. Schlemmer, M.D.C.R. da Silva, E.V. Maziero, E.H. Tanabe and D.A. Bertuol. 2015. "Fast copper extraction from printed circuit boards using supercritical carbon dioxide". *Waste Management*, 45: 289-297.
- D. Pant, D. Joshi, M. K. Upreti, R. K. Kotnala. 2012. "Chemical and biological extraction of metals present in E waste: A hybrid technology". *Waste Management*, 32: 979–990.
- J. Cui, L. Zhang. 2008. "Metallurgical recovery of metals from electronic waste: A review". *Journal of Hazardous Materials*, 158: 228–256.

- S. Orlins and D. Guan. 2016. "China's toxic informal e-waste recycling: local approaches to a global environmental problem". *Journal of Cleaner Production*, 114: 71-80.
- S. Sthiannopkao and M. H. Wong. 2013. "Handling e-waste in developed and developing countries: Initiatives, practices, and consequences". *Science of the Total Environment*, 463-464: 1147-1153.
- W. A. Bizzo 1, R. A. Figueiredo and V. F. de Andrade. 2014. "Characterization of Printed Circuit Boards for Metal and Energy Recovery after Milling and Mechanical Separation". *Materials*, 7: 4555-4566.

WASTE: A RAW MATERIAL FOR SOIL AMENDMENT AND AN EMPLOYER OF LABOUR

*Ogbonna, Emmanuel Ahamefula** and Isinguzo, Nnadozie Sunday
(DOTECON Nigeria Limited, Lagos, Nigeria)

ABSTRACT: A demonstration waste control pilot project was carried out at the Ado Ekiti, Ekiti State, Southwest Nigeria, to justify the concept of waste management and environmental sustainability through youth engagement for poverty reduction in the area. The project involved a standard waste handling method which ensures a cleaner and greener environment thus reducing the harmful effects of pollution; and also, the transfer of wastes into soil amendment thereby generating cash for the sustenance of the youth through their engagement in the project. Three designated colour coded wheeler bins (green, blue and brown) of 250 each were used for collecting organic, recyclables and toxic wastes respectively through waste segregation from source of generation thus ensuring the project concept of “**3R**”: reduction, recycle and re-use of wastes. A total of 750 wheeler bins were distributed to different household and designated places. Polythene bags were assigned to the green coded wheeler bins in order to forestall the spilling of organic waste. Wastes inventory, sensitization campaign of waste management, construction of a compost plant – greenhouse, transfer of composting technology or skill acquisition program, employment of young people for waste management and production of compost for agricultural purposes were employed. The recyclables wastes were sold for re-use or recycling while the toxic wastes were disposed by the government waste agent. The organic wastes were transformed into compost and sold at an affordable rate which made it readily available to the farmers for their small holder vegetable farm which had little or no previous soil amendment/conservation practices; thus justifying the need for amendment with compost. A total of 2tons of compost was turned over within 30 days interval using modified thermo aerobic biodegradation technology at the compost farm consisting of 12 cells measuring 60 square meters. A demonstration farm with *Amanranthus spp* as the test crop was used to show the effectiveness of the compost. A public training was conducted for general awareness and on the handling of waste management and compost production, during which about 500 persons received the training and a total of 20 waste handlers was employed in the pilot project.

INTRODUCTION

The need for soil amendment and productivity, sustainable environment, organic farming and waste management for pollution reduction/eradication has called for effective and efficient disposal and conversion (composting) of wastes into useful products thus engaging manpower for a better living. The initiation of this project was aimed at showcasing the possibility of conversion of wastes to raw materials and jobs concept through segregation of wastes at source and composting. Historically, composting as an ancient biotechnology (Birendra, and Lourduraj, 2007) is a recognized practice dates to at least the early Roman Empire since Pliny the Elder (AD 23-79) and its modernization has dated since the year 1920s in Europe as a tool for organic farming (Heckman, 2006).

PROJECT CONCEPT

The concept of this project is based on the following:

- Reduction of waste generation and segregation of wastes at source
- Zero waste discharge or disposal through the 3Rs concept therefore achieving cleaner environment
- Conversion of wastes to valuable product (compost) therefore, revenue creation
- Encouragement and improvement of organic farming
- Poverty alleviation (providing food and revenue)
- Creating job opportunities for the youths thus reducing/eradicating youth restiveness

MATERIALS AND METHODS

Project Area Description. The project was executed at the Ado Ekiti GRA (within the coordinates, N07°36'29" E005°16'28" and N07°37'54" E005°16'29) and Erifun Compost Center (approximately N07°036', Ado Ekiti, Ekiti State, Southwest Nigeria with land area of two square kilometers and a near population of 50,000 people and over 10,000 residential homes, industrial building, business area such as market and shops. Generally, Ekiti State is known for agricultural activities such as hunting and farming of much, arable (vegetable) farming.

Field Method. Augured surface (0-30 cm) samples were taken randomly from the study site and bulked together to form a composite. The composite soil sample was air dried at room temperature and passed through sieved with 2mm sieve and properly labeled. Borehole water and soil samples were analyzed for both physicochemical and microbiological properties of the study area so as to know the baseline of the environment and specific nutritional needs of the areas concerned.

Project Resources: Both skilled and unskilled manpower (youth) resources were employed. The unskilled resources involved in waste collection, segregation at various receptacles including the composting stage and transfer of wastes to labour whereas the skilled human resources were employed for both awareness and skill acquisition training in the course of this project. Materials used for the project were bill boards, PPEs, hand bills, colored coded wheeler bins, degradable or compostable wastes, composting materials among others.

Enlightenment, Awareness and Training: The enlightenment involved development of training strategy, procurement of sensitization materials such as posters, bill boards and media advertisement. Awareness on the need/importance of the project as well as the benefits was disclosed professionally. The training was conducted for the public for general awareness and for the waste handlers for specific skill acquisition in both wastes segregation, reduction, reuse and recycle as well as compost production. Aggressive house to house sensitization was done during bin distribution. A large number (over 100) of trainees were trained during the public training section. A total of 30 trainees were employed with an in-house training on waste management system and composting, equipped with personal protective equipment (PPEs) as well as training manual for the operations. Hand bills, material translation, coloured coded bins, bill boards, PPEs, training package and materials etc. were used to facilitate the training, awareness and enlightenment in the project geographical areas as shown Figure 1.



Bin Distribution: Demographic census and survey were carried out in the study area as shown in Figure 2. A total of 750 homes were identified and a total of 750 colored coded wheeler bins were supplied. The bins were categorized into three using coloration such as green, blue and brown of 250 each for collection of organic, recyclables and toxic wastes respectively. A set of each colored coded wheeler bin was distributed to each home so as to achieve wastes segregation at source. Branded polythene bags to be placed inside the green bins were distributed to forestall the spilling of the organic wastes.



FIGURE 2. DEMOGRAPHIC CENSUS, SURVEY AND BIN DISTRIBUTION

Project Infrastructure/Strategy: The infrastructures for the project were compost plant (greenhouse of a total capacity and turnover of 2.5 tons of compost per week at optimal capacity production), size reduction diesel machine (so as to increase the surface area of raw material (wastes) and speed degradation rate), borehole water, office, test farm, farm implements, waste collection and transportation system among others. The compost plant was designed to allow for adequate aeration, minimal heat loss and optimized microbial activities therefore facilitating the rate of decomposition (Figure 3). The waste collection and transportation system involved the use of transportation and waste handlers to collect the segregated wastes from homes and transport the organic wastes (green bins) to the compost plant for composting. At the point of waste collection the polyethene bags were replaced by the waste handlers. Two levels of transportation of segregated wastes were employed from the “source segregation system”. Segregated wastes were transported from the “source segregated point” to the transfer center by the residents using waste silo trucks or garbage vans and finally to the waste segregation/inventory site thereafter to the recycling/composting plants. The organic wastes were weighed on delivery while the recyclables were sold for reuse or as raw material to other areas of production therefore creating avenue for income to the youth. The transportation system involved the use of compactors, carts or wheel barrows, pipes for liquid wastes (which were re-introduced back to the composting system), drainages and waste bags.



FIGURE 3. PROJECT INFRASTRUCTURE

Project Technology: The bio-technology was employed for the composting. This involved thermo-aeration biodegradation process using organic additives and natural catalyst by enzymatic actions of aerobes (microorganism) so as to ascertain an environmental friendly condition. A semi-intensive system of mechanization was employed due to the limited power supply thus sustainability of the project.

RESULTS AND DISCUSSION

Physicochemical and Microbiological Properties of the Study Area: An initial analysis of the physicochemical and microbiological properties of the site was carried out and the result is presented in the Table 1, 2, 3 and 4. This analysis was important to know the specific nutritional needs of the areas concerned and also because the composting area is representative of a typical agricultural land area in Ekiti State; this fact is evident in the frequency at which neighboring land areas are cultivated.

The result indicated that the average concentration of Nitrogen in the soil is quite low. This important nutritional element must be adequately provided for any arable crop to do well in this area and by extension Ekiti State. Armed with this knowledge the Brown (Carbonaceous) and the Green (Nitrogenous) materials were collected, sorted, mixed and layered.

With the exception of chloride and sulfate values most parameters were low. The physical environment was predominantly clay in texture, hence further demonstrating the relatively higher levels of chloride and the rocky nature that was experienced during the borehole drilling.

TABLE 1. MEAN VALUES OF CATIONS AND ANIONS (mg/L) IN SOIL SAMPLES

Sample	pH	Mg	K	Na	Cl	SO ₄	PO ₄	NO ₃
Composite sample	5.7	0.040	0.020	0.011	19.52	2.97	0.05	0.12

TABLE 2. AVERAGE MICROBIAL POPULATION/DOMINANT SPECIES OF SOILS FROM COMPOST PLANT SITE

SAMPLES		SPECIES	
		AVERAGE MICROBIAL COUNT (cfu/gm)	
		<i>Bacillus spp</i>	<i>Fungal spp</i>
SAMPLE 1	Control	7.5 x 10 ⁶	2.0 x 10 ³
SAMPLE 2	Composite (compost site)	10.0 x 10 ⁶	4.8 x 10 ⁴

There were many bacterial and fungal populations in the environment but the most outstanding and readily isolated were the *Bacillus* species. The control site was taken from a farm land which was about 100 meters away from the seasonal swamp.

Physical and chemical analysis of the compost site borehole water is showed in Table 3. However all the levels are within higher levels of regulatory target limits. Water sample analysis revealed absence of coliforms and presence of heterotrophic bacteria and fungi (Table 4).

TABLE 3. PHYSICOCHEMICAL PROPERTIES OF COMPOST SITE BOREHOLE WATER

Sample	pH	Mg	K	Na	Cl	SO ₄	PO ₄	NO ₃
		←			Mg/l			→
Composite sample	6.70	3.495	0.089	ND	80.60	44.80	28.50	20.10

TABLE 4. RESULT OF MICROBIOLOGICAL CHARACTERISTICS OF COMPOST SITE BOREHOLE WATER SAMPLE

S/NO	GROUPS OF MICROOGANISMS ISOLATED	READINDS Cfu/ml
1	Total heterotrophic bacteria	1.40 X 10 ²
2	Total heterotrophic fungi	1.00 X 10 ¹
3	Total faecal coliforms	0.00

Composting. The urgency for environmental sustainability, youth engagement and plant nutritional need called for the compost production. The composting involved collection of segregated wastes, layering, watering, turning, temperature monitoring, air drying, sieving, weighing, bagging, sealing and marketing for agricultural purposes (Figure 4). The high demand for compost due to its environmental friendly nature led to rapid turnover per week. This aforementioned informed our decision to lay wastes based on our knowledge of their degradation rate, introduce certain already degrading wastes and additives to speed up the development of the microbes as well as the decomposition process, scavenge for more wastes and also to cover stacked-degrading-wastes' surface with dark colored tarpaulin which traps heat within the degrading wastes thereby encouraging microbial activity and warding of excessive odor and flies in the composting area. The degradation processes were observed and tested so as to ascertain different stages of the composting and daily temperature reading were also done. At maturity stage of the compost, percentage composition of the nutrient elements in the produced compost was recorded as showed in Table 5. Their impacts in a test crop (*Amarantus spp*) farm showed over 100% increase in vegetable yield when applied (Figure 4.).

Production and Market Potentials of Compost. There is enough market for the up-to-date composted residues from kitchens, farms, gardens and markets in Ado-Ekiti. The market potential shows at the minimum double the size than the maximum compost production potential. The agricultural sector alone would be large enough in nearly all to take up the entire compost production. Even the non-agricultural sector (e.g. landscaping, hobby gardens) shows already a sufficient market potential. Market problems in some places were caused mainly by low compost qualities and the lack of experience and knowledge about compost and the potential customers. End-of-waste standards can act in this respect beneficially by raising the awareness of the importance of the compost quality in the waste sector as a precondition for successful application and marketing.



FIGURE 4. COMPOST PROCESSES, EFFECTS ON TEST CROP AND INAUGURATION

TABLE 5: BASIC PROPERTIES OF THE MANUFACTURED COMPOST

ITEM	ELEMENTS	PERCENTAGE COMPOSITION
1	Nitrogen	32.2%
2	Phosphorus	44.2%
3	Potassium	23.6%

Project Impact on Youths. Generally, a positive impact of the project was recorded on the youths. Apart from those already trained and employed thus ensuring positive living standard, the rate of youth restiveness and crime rate of the environment were reduced to the minimal level. More interest has been shown by other youths for training which now converted the project as a training or skill acquisition centre. Consequently, there comes the need for expansion or replication of the project across the nation and world at large. Some trained youths have now used their garden for composting to improve their farming system as well as getting cash into their pockets through sales of the compost.

CONCLUSION

Conclusively, although several methods of composting exist; but with due consideration to cost, time, quality and quantity, the Indore method (thermo-aerobic technology) that we have employed here would most likely be the best. Composting materials such as organic wastes from homes and markets, poultry droppings, cow dung, pig dung, saw dust and so on are readily available without cost in Ekiti State and Nigeria in general, the market for compost also abound both in Ekiti State and outside the state. The technology we have applied is simple and can be easily replicated with little cost, all these we have passed on to the trainees given to us by Ekiti State. In addition, the compost when sold yielded revenue for the waste trainees and the State Government. These crops of young people will no doubt run with this vision of turning waste to cash while making the environment cleaner.

In addition, it is very obvious that the availability and cost of buying inorganic fertilizer is readily unavailable and high respectively thus creating difficulty to the farmers consequently very low yield being harvested. Fortunately, compost (organic fertilizer) is readily available, cheap and even more environmentally friendly when compared with the inorganic fertilizer.

This shows that all organic wastes from our domestic sources can be converted to wealth. We have proven that a zero organic waste disposal can be achieved while creating employment opportunities for the youth and facilitating a cleaner and greener environment in the Ekiti GRA environment. Last and not the least was a record of over 100% improvement in the vegetable harvest from the in situ trials.

ACKNOWLEDGEMENT

This research was supported by DOTECON Nigeria Limited. I thank the Almighty God for His inspiration, guidance and protection in the course of the entire study. I specially appreciate the efforts and contributions of Dr. N. S. Isinguzo in the achievement of this study. I specially appreciate the assistance made by my mentor, Dr. C. F. Isinguzo financially. I am grateful to my lecturers, Dr. O. I. Nwachukwu and Dr. M. I. Onwuka for their support and care. I am obliged to extend my gratefulness to my beloved family, mostly my mother, Mrs. M. U. Ogbonna; brother (Chibueze) and my dearest father, Mr. L. E. Ogbonna of blessed memory.

REFERENCES

- Birendra, K.Y and Lourduraji, A. C. 2007. *In Organic Farming and Mycorrhizae in Agriculture*. I.K International Publishing House Pvt. Ltd, New Delhi, pp 37-58.
- Heckman, J. 2006. "A History of Organic Farming: Transitors from Sir Albert Howards War in the Soil to USDA National Organic Program". *Renew Agric. Food Syst.* 21:143-150.

THE EFFECTS OF DIFFERENT CONDENSATION TEMPERATURES ON WASTE TIRE PYROLYSIS

Neslihan Doğan-Sağlamtimur, Ahmet Bilgil, Tuğçe Aykanat, Öznur Çalışkan, Funda Yolcu, Elif Dilan Yıldırım, Türkan Vural, Halime Ötügen and Büşra Arıcan

(Department of Environmental Engineering, Engineering Faculty, Niğde University, Niğde, 51240, Turkey)

Despite the efforts made for the solutions, the disposal of waste tires (WTs) representing over 2% of total solid waste still remains as an important health and environmental problem. WTs have high volatile and fixed carbon contents with heating values greater than that of coal and biomass making them an ideal raw material for energy valorization process. Pyrolysis, an endothermic process, could be a good solution to WT problem because of obtained valuable solid and liquid products as well as generated low emissions.

The raw materials to be used for the pyrolysis experiments are samples of WTs rubber shreds, which will be supplied by collecting firms from Niğde, Turkey. In this study, it is aimed to obtain two phases that are liquid (pyrolytic oil) and solid (carbon black). The non-volatile carbon black remains as a solid residue, and therefore it can be recycled in worthwhile applications. The derived oils can be used as fuels or a source of refined chemicals.

The heating and cooling temperatures of WTs are important parameters that affect the reaction time, product yield and product quality. As the temperature changes, the phase of the product also changes. Lower pyrolysis temperatures usually produce more liquid products, while higher temperatures favour the production of gases. In this study, the pyrolysis reactor was designed, including modified oven for heating and its condenser units for cooling. The pyrolysis has been planned to perform five different decomposition (200, 300, 400, 500 and 600 °C) and condensation (-20, -10, 0, 10 and 20 °C) temperatures, respectively. An optimum design will be achieved for these temperature combinations. According to the results, ± 50 °C intermediate values will also be examined. Expecting the values of the carbon black to remain stable, in this study, the effect of condensation temperatures for obtaining more pyrolytic oil and less gas release will be found.

THE IMPACT OF SAW DUST BIOCHAR ON SOIL PH AND CROP YIELDS FOR CLIMATE CHANGE MITIGATION

Lukong Pius Nyuykonge and **George Elambo Nkeng**

(Ecole Nationale Supérieure des Travaux Public (ENSTP) Yaounde, Cameroon),

Lenzemo Wirnkar Venasius

(Institute of Agricultural Research for Development, Bamenda, Cameroon)

Farmers in some regions of Cameroon are faced with the problem of high and unstable soil acidity (pH<5 in general) leading to low yields of agricultural products. The main objective of this work is to test the effect of biochar on soil pH in the central region of Cameroon (3° 51' 2" N, 11° 7' 30" E,) as a mechanism attracting carbon storage. Biochar obtained from the pyrolysis of saw dust from Iroko timber (*Milicia excels*) at a temperature of 500 °C after analysis was found to contain 44 %C, 4.6 %Ca, 1.1 %N, 0.2 %P, 1.9 %K, with a pH of 9.0, an acid neutralising capacity of 15 %CaCO₃, CEC of 49 cmol(+)/kg and other exchangeable cations (Ca: 8.3, K: 36, Mg: 2.8) Ca/Mg ratio 2.9. The biochar was applied in a field experiment at the rate of (5t/hectare without fertilizer, 5t/hectare with fertilizer, and the case of fertilizer alone used as the control). The biochar treatments were found to increase the final biomass, root biomass, plant height and number of leaves of Maize plant (*Zea mays*). The soil pH increased from 5.0 to 6.1 in the case of biochar without fertilizer, from 5.0 to 5.6 in the case of biochar with fertilizer and a slight decrease in pH from 5.0 to 4.9 was observed in case of fertilizer alone, in the first harvesting season (12 weeks after planting). In the next harvesting season, the treatment of biochar without fertilizer continued from 6.1 to 6.8 while that with fertilizer increased from 5.6 to 7.1 with the case of fertilizer alone increasing from 4.9 to 5.2. The greatest biomass increase due to biochar addition was found in the soils with biochar with fertilizer (23N + 10P + 5K + 3S + 2MgO + 0.3Zn) which stood at 150 % rather than biochar alone (95 %) in the first season. Over the next season, the impact increased in the case of biochar alone (from 95 to 202 %) and the treatment of biochar with fertilizer remained almost stable. The results of this study showed that biochar can be used as a soil buffer reducing the cost of expensive limestone often used thereby attracting farmers in storing carbon, a mechanism which can help mitigate against the effects of climate change.

IMPACTS OF WASTE DISPOSAL METHODS ON HOUSEHOLD HEALTH CONDITIONS IN KENYA

Stephen Onakuse, *Emmanuel Donkor*, Joe Bogue

(Centre for Sustainable Livelihoods, and Department of Food Business and Development, University College Cork, Cork, Ireland)

Waste management has attracted the attention of most researchers in developing countries due to the health implications attached to improper waste disposal. This paper therefore examines the impacts of waste disposal methods on health conditions of 370 households in Kenya. The Probit regression model was employed to relate waste disposal methods used by households to their health conditions. The survey reveals that majority of the households in Kenya dispose their refuse in rivers/drainage, common garbage heap, latrine whilst others use waste collectors. The incidence of water borne diseases such as cholera, malaria and typhoid is prevalent in the Kenya. Households that dispose refuse into river/drainage, common garbage heap and latrine have higher probability to contract water borne diseases as compared to those that pay waste collectors to manage their waste. Presence of health care providers in community was also found to reduce contraction of water borne diseases. The study recommends that sensitization of the health implications of improper waste disposal should be created among households so as to reduce water borne incidences.

THE CHALLENGES OF SUSTAINABLE MANAGEMENT OF ELECTRONICS WASTE AND THE RISK ASSESSMENT OF IMPROPER MANAGEMENT PRACTICES

E. Sahle-Demessie^a, Teri' Richardson^a, Joshua Dietrich^b

(^a Office of Research and Development, NRMRL, US Environmental Protection Agency, Cincinnati, OH, USA; ^bChemical Engineering Program, Department of Biomedical, Chemical, and Environmental Engineering, University of Cincinnati, Cincinnati, OH, USA)

Electronic waste (e-waste) is currently the fastest growing waste stream, and it continues to be an important global environmental and health issue. The average useful life of electronic products has continued to decline and obsolete products are being stored or discarded with an increasing frequency. As a result, new challenges related to the management of electronic waste (e-waste) have become apparent. E-waste is hazardous, complex and expensive to treat in an environmentally sound manner. Of the more than 400 million electronic items per year that discarded, less than 20 percent is recycled in the U.S. And although, e-waste represents only two percent of America's trash in landfills, it contributes a disproportionate 70 percent of all toxic waste.

The growth in the electronics industry and the increasing trans-boundary movement of E-waste requires collaborative endeavors to ensure sustainable management. Currently, the stewardship of electronics products across their lifecycle is not sustainable, and only a fraction of E-waste is refurbished, reused or recycled. Most electronic products contain a combination of hazardous materials, toxic materials, and valuable elements such as precious metals and rare earth elements. There are risks to human health associated with the disposal of E-waste in landfills, or treatment by incineration. Innovative solutions that integrate electronics manufacturing with recycling are needed to sustainably manage the electronics currently in use, while continuing to promote the future development of innovative technologies to meet market challenges. Hence, there is increasing challenge of reducing the use of virgin materials, recovering useful elements from the waste and protecting human health and the environment from the harmful effects associated with the unsafe handling and disposal of these products (*National Strategy for Electronic Stewardship, NSES*).

EPA/ORD has current research tracking the flow e-waste materials at different stages of their life cycle, to better determine their environmental and economic impact. The collected information and data will later be used to develop a web-based information to enable domestic movement and material flow analysis of e-waste. We are also studying the health and environmental risks of the current improper management of e-waste such as open burning and land filing.

**ON-SITU REMEDIATION OF NITRO COMPOUND CONTAMINATED SOIL BY
BIOLOGICAL-ECOLOGICAL METHOD**

Quanlin Zhao, Zhengfang Ye, and Zengxiong Li (Peking University, Beijing, China)
Zhongyou Wang (Beijing Institute of Cooperation and Innovation, Beijing, China)

Biological-ecological method was conducted to on-situ remediate nitro compound contaminated soil. High performance microorganism coupled with water and nutrients was added to the contaminated soil to biodegrade the nitro compounds. At the same time, alfalfa and reed were used for phytoremediation. The results showed that biological-ecological method can efficiently degrade nitro compound in the contaminated soil. For the contaminated soil, the average concentration of nitro compound was 877.88 mg/kg. After 12 months' remediation, the average concentration of nitro compound in alfalfa and reed remediation site decreased to 13.09 and 400.03 mg/kg, respectively. The removal efficiency of nitro compound in alfalfa remediation site was higher than that in reed remediation site, which may be caused by its developed root system.

**FENTON OXIDATION OF POLYCYCLIC AROMATIC HYDROCARBONS IN THE
CONCENTRATES OBTAINED FROM THE DECONTAMINATED SOIL**

Malika Bendouz, Lan Huong Tran, Lucie Coudert, Guy Mercier and Jean-François Blais
(INRS-ETE, Quebec University, Quebec, QC, Canada)¹⁸

The decontamination of soils contaminated by Polycyclic Aromatic Hydrocarbons (PAHs) compounds, using attrition process generates concentrates containing high concentrations of PAHs. These concentrates are considered as hazardous waste and the management costs would be high.

The degradation of PAHs is a difficult task due to their low solubility, and their refractory character. However, the degradation of PAHs can be achieved through several treatment methods, such as advanced oxidation processes (AOPs). Among the AOPs, the Fenton oxidation process represents the most common, and involves the generation of hydroxyl radicals (OH[•]), the strongest oxidant with a redox of 2.8V.

The main objective of this study focuses to degradation of 27 PAHs and to reduce the overall toxicity in these concentrates. Different parameters have been tested to determine the operating conditions for optimal destruction of PAHs.

The results allow operating the process on the large-scale and include the study of the technical economic feasibility of the process in comparison to other concentrates management options of PAHs.

DREDGED MATERIAL AS RESTORATION SUBSTRATE IN LANDFILL SURFACE SEALING SYSTEMS

Morscheck, Gert¹, Astrid Lemke¹, Michael Henneberg²

¹(University of Rostock, Department of Waste Management and Material Flow, 18051 Rostock, Germany. gert.morscheck@uni-rostock.de

²(Steinbeis Transferzentrum Applied Landscape Planning, 18051 Rostock, Germany) michael.henneberg@uni-rostock.de

ABSTRACT: The German Landfill Ordinance requires proof of a sufficiently large field capacity for recultivation layers. In Mecklenburg-Vorpommern humus-rich and fine-grained substrate is prepared from the dredging of shipping lanes and has been used for about 15 years as landfill recultivation substrate. On four landfill sites the production and effectiveness of recultivation layers made out of matured dredged material (DM) were examined. For this purpose the used dredged material was analysed. The current functionality of the recultivation layers was examined by soil chemical and soil mechanical investigations.

Keywords: dredged material, recultivation, restoration, landfill, sealing system, field capacity, HELP

INTRODUCTION

Landfills must be secured after operation. This closure, "encapsulation" from the environment, is performed using a surface sealing system. The upper layer of this system is composed of a recultivation substrate.

The Landfill Ordinance (Ordinance on Landfill Sites and Long-Term Storage Facilities - Landfill Ordinance) (DepV 2012) sets out requirements for the recultivation layer (function and substrate).

Additional requirements on the recultivation layer are described in the recommendations of the German Geotechnical Society (DGGT - Deutsche Gesellschaft für Geotechnik e.V.; recommendations E 2-31 and E 2-32) (GDA 2006; GDA 2010) and Nationwide Quality Standards (BQS 7-1 2011; BQS 7-2 2011).

Currently, the feasibility of soil physical demands arising from the Landfill Ordinance is discussed extensively. It is checked what challenges arise for the life praxis of landfill construction thereof. In Mecklenburg-Vorpommern more than ten landfills have already been restored with matured dredged material from coastal waters since the late 90s.

Due to the new requirements for substrates for recultivation layers by the current landfill regulations, already sealed landfills with matured dredged material were examined. It was examined, whether the already existing recultivation layers meet these requirements.

Can matured dredged material be installed in recultivation layers in the future?

ORIGIN AND QUALITY OF THE DREDGED MATERIAL

The dredged material comes from waterways and harbours. Only the dumping of sand and marl in the Baltic Sea is allowed. Dredged Material with rich content of humus, silt and clay must be disposed of on land in mono disposal sites (including dewatering/flushing fields).

In Rostock this dredged material is classified, dewatered and processed in specially-developed inland disposal sites. The conditioned dredged material can be used for different purposes. The material is similar to an organic-rich, clayey-silty soil or loam.

Since the late 70s of last century, research is being conducted in Rostock for an environmentally responsible use of dredged material. The inland disposal sites of the Hanseatic City of Rostock were converted mid-90's to an industrialised dewatering and treatment system. Thus, environmentally sound and efficient management of dredged material is possible. Law requirements are met. Since 2000, Rostock

utilized his dredged material (rich in organic matter and silt/clay) to 100% onshore. The recovery takes place mainly in landscaping and landfill restoration (Fig. 1).

Particle Size Distribution (Soil Texture). The dredged sediments are flushed into confined disposal facilities (CDF) via pipeline. The dredged material has a water content of approximately 95%. A confined disposal facilities is a diked area on land, used to contain dredged material. The CDF are used interchangeably.

The particles classify in the CDF along the water stream. Stones, gravel and sand are not carried away by the water very far, at the end of the flowing water the finer and lighter components are deposited (silt, clay and organic matter) (Table 1).

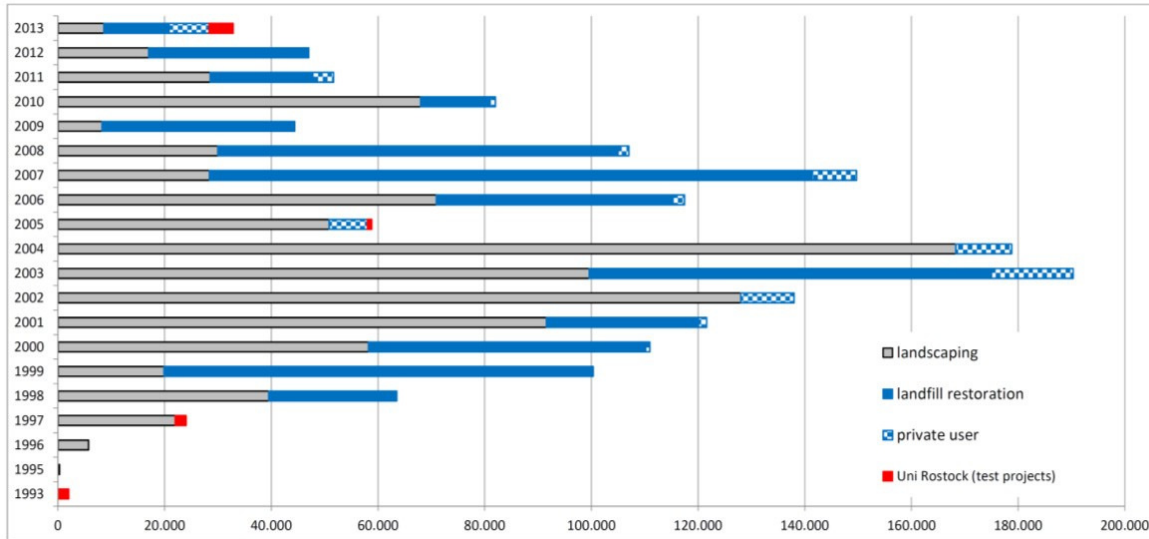


Fig. 1. Development of the utilisation of the Rostock dredged material (tons per year)

Table 1. Particle size distribution (%) of the matured dredged material (DIN ISO 11777) (arithmetic mean value = average)

	Coarse sand	Medium sand	Fine sand	Coarse silt	Medium silt	Fine silt	Clay
average silt	1,1	8,7	29,9	10,8	15,5	11,5	23,6
average mixed soil	1,4	16,3	56,4	8,5	57,0	3,0	8,3
maximum silt	3,0	22,0	49,0	18,0	27,0	19,0	46,0
maximum mixed soil	3,6	28,9	70,9	14,2	103,0	4,6	15,1
minimum silt	0,0	1,0	7,0	7,0	8,0	6,0	13,0
minimum mixed soil	0,4	7,7	45,7	3,5	26,0	1,5	3,0

The sands and gravels can be used in the construction industry. Far along in the water stream a mix of different particle sizes will settled down (mixed soils = sand-silt mixtures) and farthest from the inlet the fines particles settle down (clay-silt mixtures with organic matter). The classification along the current leads to two suitable fractions for landfill restoration (**mixed soils** and clay-silt mixtures with organic matter, called **silt**).

Chemical Characterization of Wet Dredged Material. The origin of the dredged material from the coastal area leads to naturally elevated salinities (SK) (Table 2).

The dredged material in Rostock is mainly influenced by the river Warnow. The Warnow flows into the Baltic Sea near Rostock. The river Warnow has a rural drainage area.

The wastewater of the entire drainage area is cleaned in sewage treatment plants. Therefore, the pollutant content in the dredged material is relatively low. After classification of the dredged material in the up-land CDF the silt is more polluted than the mixed soil (Table 3; Table 4). Compliance with the specific utilization limit and guideline values allows a wide range of applications such as the use in landfill restoration.

Table 2. Nutrient and salt content of silt and mixed soil

	DM	pH	SK	Cl ⁻	Na ⁺	SO ₄	OM	CaCO ₃	anorg. N	P	K	Mg	total N	exchange capacity
	%		%	mg/100 g soil				%		mg/100 g			%	mval/100g soil
			DM	DM	DM	DM	DM	DM	DM	DM	DM	DM	DM	
average silt	58,2	7,3	1,9	429	346,1	514,8	11,1	8	2,5	2	31,4	127,8	0,5	26,1
average MS	71,3	7,4	1,2	140,9	114,5	264,2	5,3	5,6	0,9	1,8	12,8	67,7	0,2	9,2
maximum silt	71	8	4	1340	905	1428	18	16	9	5	56	226	1	36
Maximum MS	87,5	7,9	2,5	678,8	422	541,9	11	9,8	2	4,4	19,5	125	0,5	14,6
minimum silt	47	7	1	69	104	163	4	2	1	0,4	9	72	0	16
minimum mixed soil	60,1	7,0	0,4	11,5	28,0	82,0	0,9	2,5	0,5	0,4	7	14,8	0,1	4,4

OM – organic matter; DM – dry matter; SK – salt, MS – mixed soil

Table 3. Pollutant content of silts and mixed soils; and limit values

	Pb	Cd	Cr	Cu	Ni	Hg	Zn	As	EOX	IR-H*	PAH	PCB
	mg/kg DM											
average silt												
	21,2	0,4	35,2	22,4	14,5	0,3	100,5	9,6	0,7	225,3	0,9	0,033
average mixed soil	9,5	0,2	15,8	12,0	6,7	0,2	44,2	5,8	0,7	108,7	0,6	0,028
maximum silt												
	35,0	0,8	63,5	37,0	18,0	0,9	177,0	25,0	1,0	715,0	2,18	0,074
maximum mixed soil	23,8	0,3	32,8	28,5	10,0	0,4	94,0	12,5	1,3	281,0	3,3	0,066
minimum silt												
	10,0	0,0	12,0	14,0	11,0	0,0	36,0	5,0	0,0	28,0	0,0	0,009
minimum mixed soil	4,0	0,1	44,0	4,6	3,0	0,0	16,0	3,6	0,4	19,4	0,0	0,009
BBodSchV												
VSW sand	40,0	0,4	30,0	20,0	15,0	0,1	60,0				3,0	0,050
70%	28,0	0,3	21,0	14,0	10,5	0,07	42,0				2,1	0,035
BBodSchV												
VSW loam/silt	70,0	1,0	60,0	40,0	50,0	0,5	150,0				3,0	0,050
70%	49,0	0,7	42,0	28,0	35,0	0,35	105,0				2,1	0,035
DepV (recultivation layer)	140	1	120	80	100	1	300				5	0,1

DM – Dry Matter; BBodSchV - Federal Soil Protection and Contaminated Sites Ordinance; DepV – Landfill Ordinance; VSW - precautionary value; IR-H* - IR-hydrocarbons

USE OF MATURED DREDGED MATERIAL IN LANDFILL RESTORATION

Since the late 90's treated dredged material (mixed soil and silt) is used in landfill restoration. Dredged material (mainly silt) is even used in gardening, landscaping and agriculture. Especially silt has very good characteristics (nutrient holding capacity, erosion stability).

The use of the dredged material in landfill cover systems was approved individually by the authorities. Exceptions are necessary since the dredged material contains great amounts of salt and organic matter. The recommended values of the Landfill Ordinance are significantly exceeded.

Table 4. Pollutant content (eluate) of the silts and mixed soils and limit values according landfill ordinance

	pH	Lf μS/cm	Chloride mg/l	Sulphate mg/l	Pb	Cd	Cr	Cu	Ni μg/l	Hg	Zn	As
average silt	7	4044	542	2022	9,1	0,6	2,3	28,8	10,6	n.n.	75,8	3,4
average mixed soil	7.1	2975	259	1596	4,6	0,2		11,3	6	n.n.	21,7	2,2
DepV (recultivation layer)	6.5 - 9	500	10	50	40	2	30	50	50	0,2	100	10

Lf – conductivity; DepV – Landfill Ordinance; VSW - precautionary value; n.n. - undetectable

The dredged material is suitable for both, forming the landfill, as well as, for building a restoration and water management layer. In Mecklenburg-Vorpommern soil material is needed for the closure of landfills and as cover of contaminated sites.

The Landfill Ordinance defines properties, which the recultivation layer has to fulfil. The recultivation layer should offer a high water storage and good plant available water capacity, helping so to reduce leachate formation. Even a temporary cover has to minimize leachate formation. The recultivation substrate also needs to ensure an adequate plant growth, a field capacity of at least 140 mm, based on the total thickness of the recultivation layer, is required (Landfill Ordinance, Appendix 1, section 2.3.1). When establishing a water regime layer, the Landfill Ordinance calls for a field capacity of at least 220 mm, based on the total thickness of the water regime layer. In addition, the seepage may not exceed 10 percent of the long-term average of precipitation (usually 30 years), not more than 60 mm per year (Landfill Ordinance, Appendix 1, section 2.3.1.1). Matured dredged material also has to fulfil the requirements for landfill replacement construction materials (DepV, Annex 3, Table 2, item 9 of Table 1).

To continue the use of mature dredged material in the landfill restoration, it has to be tested on already reclaimed landfills if the new requirements of the Landfill Ordinance (for example available water content) are complied. Observations on reclaimed landfills and experience in other fields of application of dredged material give reason to believe that the material is able to comply with the new Landfill Ordinance.

In a lysimeter test the leachate quantity was reduced up to 25% compared to loamy sand by using dredged material (silt) incorporated in the soil.

RESULTS – TEST OF RESTORATION LAYERS

For the investigations four disposal sites covered with dredged material were selected.

Following parameters at the four sites were tested:

- Current situation (leachate quantity, special problems)
- Visual assessment of the cover layer (plant growth, erosion, settlement, landslide ...)
- soil sampling (disturbed and undisturbed samples) to evaluate the residual shrinkage of the dredged material and to determine the root depth and intensity
- Geotechnical investigations under Landfill Ordinance or German Geotechnical Society recommendation (water contents, densities, shear strength on site, current field capacity (field capacity and available water content), coefficient of permeability (in-situ and laboratory), pH, organic matter, lime content
- Assessment of pollutants in the dredged material
- Investigation of the material displacement, especially salts transfer in the profile
- Examination of humus forms in the dredged material and its stability (AT4 respirometric activity)

– Modelling the water balance with the Hydrologic Evaluation of Landfill Performance Model (HELP version 3.90D)

The age of the recultivation layers was different. The landfills have been covered two to 16 years ago. The matured dredged material used for the restorations varies in its chemical and physical properties, because it comes from different dredging. None of the test fields had the same dredged material; all studies were carried out on already secured landfills.

Current Situation. During and after the restoration the landfills were visited often. Among others the maintenance state after restoration was recorded. If the landfills were mowed annually, grasses form the dominant plant species. If there is no maintenance (no mowing) for years, herbs and brushes grow, and first trees grow. At all landfills dense vegetation exists (high soil fertility of the substrate dredged material despite the increased salinity).

None of the landfills showed mechanical changes on the surface (erosion, slides or subsidence). The very intense rainfall of 2011 could not harm the recultivation layers. Leachate in the drainage layer of the sealing system could be observed only in one landfill. In excavation tests, cracks in the restoration layer could be observed. This was especially the case when the water content was too high during installation of the dredged material. The cracks reach several decimetres in the restoration layer. However, the shrinkage cracks are filled with soil particles. The recultivation layers are very well rooted and are tapped for water supply of the plants and evaporation loss.

Evaluation of Chemical and Biological Characteristics of the Recultivation Layers. Each of the four investigated landfills was sampled at two points in the entire restoration layer (about one meter deep). The measurements and the sampling were performed in three depths.

The water movements in the restoration layer led to material relocation. Especially salt and magnesium ions usually show an increase in their content with the depth. The contents of total organic carbon and lime show similar high levels as during the installation of the dredged material. The high lime content receives long-term neutral pH values (high buffering capacity). The high level of total organic substance shows the very good stability of the organic matter. The respirometric activity (AT4) is well below the specification of the landfill ordinance (5 mg O₂/g dry matter). The relevance of origin-related high salt content in the dredged material has already been highlighted.

But individual decisions enable the reasonable use of the dredged material. The relatively low levels of available nitrogen (compared to the large supply of nitrogen in the soil) in the upper mineral recultivation layer are sufficient to enable a strong plant growth. The dredged material is low in available mineral nitrogen (0.5 to 2 mg N_{min}/100 g of soil; about 20 - 80 kg N/ha in the upper restoration layer of 0 - 30 cm). The levels of plant-available phosphorus are low, as known from the fresh dredged material. To satisfy the plant's needs, the content is sufficient. The levels of plant-available potassium are adequate. There is no additional fertilization required. The levels of plant-available magnesium are high to very high (35-100 mg/100 g soil). Freshly processed dredged material contains even more than 150 mg /100 g soil) (Table 5). The investigation of soil chemical parameters shows that the dredged material has a very good soil fertility determining properties for plant growth. (Table 5).

Due to the good binding capacity (high contents of total organic content and clay) as well as the excellent water holding capacity no increased discharge of salt ions and nutrients is expected.

Evaluation of Physical Properties in the Recultivation Layers. The Landfill Ordinance and the Nationwide Quality Standards BQS 7-1 "recultivation layers" and BQS 7-2 "water regime layers" (BQS 7-1 2011; BQS 7-2 2011) require compliance with soil physical parameters (see Chap. 3). These parameters were tested in order to prove whether the further use of the treated and matured dredged material (mixed soil and silt) for landfill closure can be allowed.

Shear Strength. The in-situ shear strengths (investigated with Field Vane Shear Apparatus) vary considerably depending on the installation of the dredged material in the restoration layer. On landfills where the dredged material was slightly compacted during installation or where marl was installed as the top layer of restoration layer, high shear strengths of 70 to 80 kPa and even 100 to 120 kPa were measured, also in the top layer. The measurements on other landfill recultivation layers have a clear depth-related graduation. In the upper, loosely built layer, the determined shear strengths were only about 20 to 33 kPa.

This looseness is particularly due to the high content of organic matter and the intensive rooting. In the underlying layers shear strengths were measured by more than 100 kPa (Table 6).

Table 5. Chemical characteristics of recultivation layers

landfill	depth	dry matter	pH	salt	Cl ⁻	Na ⁺	SO ₄ ²⁻	organic matter		AT ₄	CaCO ₃	N _{am}	P	K	Mg
								grav. %	%						
M1	100	78,7	7,2	0,19	1,9	1,2	138,2	4,8	1,0	1,0	3,6	1,3	4,5	1,7	37
	350	78,3	7,4	1,03	2,0	1,3	174,3	4,8	0,7	0,7	3,2	0,8	1,7	1,0	34
	700	75,2	7,5	1,13	0,7	3,8	187,1	6,9	1,0	1,0	3,8	0,9	1,9	9	74
M2	150	71,1	7,3	0,8	0,5	1,1	66,8	7,6	1,0	1,0	3,1	0,7	5,1	1,6	44
	400	73,2	7,4	1,05	2,0	2,0	179,4	5,6	0,9	0,9	3,3	0,3	2,2	1,0	37
N1	750	67,8	7,5	1,13	1,4	3,9	207,5	7,8	1,1	1,1	4,7	0,4	1,5	9	72
	150	61,8	7,5	1,1	4,4	7,4	284,8	8,2	1,5	1,5	3,4	0,8	1,2	1,7	37
N2	450	66,8	7,7	1,4	59,4	90,0	271,7	7,4	0,6	0,6	3,4	1,6	0,8	1,3	79
	850	62,9	7,6	1,6	152,5	149,0	307,8	7,0	1,1	1,1	2,4	2,2	0,7	1,4	76
T1	150	76,9	7,6	1,1	11,5	11,0	205,5	7,4	0,8	0,8	3,8	1,2	1,0	2,2	40
	400	72,1	7,6	1,6	103,1	128,0	274,9	8,7	1,3	1,3	2,9	1,8	0,7	1,2	92
	850	69,9	7,6	2,0	329,1	218,8	286,1	9,8	0,8	0,8	2,7	1,7	1,3	1,7	102
T2	1200	66,5	7,7	1,7	210,3	159,1	283,3	8,3	3,0	3,0	3,0	1,5	0,5	2,0	95
	400-500	75,5	7,6	1,1	8,2	13,7	227,5	5,3	0,4	0,4	5,1	0,9	0,7	9	54
G1	800-850	70,2	7,6	1,3	35,1	55,1	262,4	6,5	0,6	0,6	4,2	1,1	0,6	1,3	77
	350-450	63,1	7,6	1,19	11,7	27,3	287,5	9	0,8	0,8	4,8	1,3	0,7	11	82
G2	800-850	72,2	7,6	1,21	17,4	34,3	249,9	6,1	0,6	0,6	4,6	1,0	0,6	11	71
	100-200	74,4	7,6	1,12	5,0	8,8	219,4	9,7	1,8	1,8	2,7	0,9	0,9	16	58
	400-500	66,5	7,6	1,26	14,2	29,5	244,8	8,9	0,9	0,9	2,0	0,9	0,6	13	95
G2	800	62,2	7,6	1,54	102,8	110,3	298,4	9,8	2,6	2,6	2,4	1,0	0,4	2,0	100
	950	64,2	7,6	1,51	95,0	103,9	307,5	8,6	1,8	1,8	1,8	0,9	0,4	2,0	97
G2	200-250	74,4	7,6	1,11	7,3	9,4	232,3	11,3	1,9	1,9	2,6	1,3	0,6	1,4	48
	550	58,7	7,6	1,53	79,4	116,2	331,5	12,8	2,0	2,0	4,8	1,5	0,3	2,3	110
	800	57,1	7,6	1,62	130,1	148,1	349,2	11,8	1,9	1,9	4,3	1,4	0,3	2,5	105

Table 6. In-situ shear strength of the restoration layers (field vane test)

Landfill	Depth	Dry Matter	In-Situ Shear Strength	Bulk Density
	mm	%	kPa	g/cm ³
M 1	150	78,7	26,5	1,11
	700	75,2	156,8	1,14
M 2	100	71,1	18,4	1
	350	73,2	21,3	0,98
	650	67,8	116,6	1,05
N 1	450	66,8	30,3	0,9
	1000	62,9	35,0	0,9
N 2	150	76,9	32,7	0,9
	400	72,1	116,7	0,9
	850	69,9	109,1	0,9
T 1	400 - 500	75,5	116,7	1,1
	800 - 850	70,2	109,1	1,0
G 1	100 - 200	74,4	122,0	0,9
	400 - 500	66,5	136,0	0,9
	800	62,2	124,0	0,9
G 2	200 - 250	74,4	103,5	0,82
	550	58,7	92,8	0,77
	800	57,1	97,1	0,83

Hydraulic conductivity. The determination was carried out in the field with a Double ring infiltrometer (unsaturated conductivity) and in the laboratory (saturated conductivity) with sampling rings (500 cm³ or 250 cm³).

The hydraulic conductivity of the recultivation layers is very low. There was no targeted consolidation of the built-in layers. The installation was done with bulldozer or excavator. The hydraulic conductivity varies as a function of the analytical method between 8.1×10^{-6} and 1.2×10^{-7} m/s (laboratory method) or 2.18×10^{-6} and 1.98×10^{-8} m/s (field method) and decreases from top to bottom.

Pore volume and soil bulk density. The total pore volume (total porosity) of the restoration layers (matured dredged material) is even after several years (including losses due to possible minor settling after installation) usually about 50%, often over 60%. This large pore volume is also shown in the very low bulk densities of mostly 0.8 to 1.1 g/cm³ (Table 7). Both are independent of the depth. After installation no significant settlements of the recultivation layers have occurred.

Field capacity, available water capacity and air capacity. The high total pore volume also enables high field capacity and available water capacity. Because of the high quantity of medium and fine pores (silty-clayey dredged material; silt), the majority of the total pore volume can hold water against gravity (very high field capacity, often more than 50%).

Often, more than half, but at least more than 35% of the pore volume is available for plants. The available field capacity is almost always more than 20% by volume, in some cases even more than 30% by volume. The requirements of the Landfill Ordinance by 140 mm (recultivation layer) or 220 mm (water regime layer) field capacity are always satisfactory, even years after the installation of the recultivation layer. Water regime layers can also be produced from dredged material (Table 7).

The low bulk density also results from the large air pore volume. In the top soil layer (0-30 cm) the air pore volume (air capacity) is partly greater than 10%. In combination with the very good water supply (very high available field capacity) and adequate available nutrients excellent conditions for rapid plant growth are given.

Field capacity and available field capacity fulfil the requirements of the Landfill Ordinance (DepV 2012), the recommendations E 2-31 and E 2-32 of the German Geotechnical Society (GDA 2006; GDA 2010) and the uniform nationwide Quality Standards BQS 7-1 and BQS 7-2 (BQS 7-1 2011; BQS 7-2 2011). The field capacity reaches up to 500 to 610 mm and the available field capacity reaches up to 230 to 290 mm by using matured silt in the entire restoration layer. These values were also measured in ten years old recultivation layers!

Table 7. Soil physical properties of the restoration layers

land-fill	depth	dry matter	organic matter	Ca- CO ₃	bulk density	density	PV	WV	AV	FC	aFC	aFC/FC
mm		%	%	%	g/cm ³	g/cm ³			Vol %			%
M 1	100	78,7	4,8	3,6	1,11	2,52	56,1	37,9	6,1	50,0	33,7	67,4
	350	78,3	4,8	3,2	1,10	2,52	56,2	43,6	8,8	47,4	29,5	62,3
	700	75,2	6,9	3,8	1,14	2,47	53,8	49,1	0,8	53,0	23,4	44,1
M 2	150	71,1	7,6	3,1	1,00	2,49	59,7	37,4	4,8	54,9	37,2	67,9
	400	73,2	5,6	3,3	0,98	2,51	61,2	41,0	11,8	49,4	29,1	59,0
	750	67,8	7,8	4,7	1,05	2,47	57,3	45,4	4,2	53,2	20,5	38,6
N 1	150	61,8	8,2	3,4	0,88	2,42	63,8	49,3	12,5	51,3	25,9	50,5
	450	66,8	7,4	3,4	1,03	2,45	58,1	46,7	5,6	52,4	24,1	45,9
	850	62,9	7,0	2,4	0,89	2,45	63,8	55,8	7,9	55,9	35,1	62,8
N 2	150	76,9	7,4	3,8	0,87	2,48	64,7	32,0	25,6	39,1	21,1	54,1
	400	72,1	8,7	2,9	0,90	2,43	62,8	43,3	9,7	53,1	30,2	56,8
	850	69,9	9,8	2,7	0,88	2,42	63,6	42,3	8,9	54,7	28,7	52,5
T 1	400 - 500	75,5	5,3	5,1	1,12	2,54	51,4	49,7	6,1	45,3	20,2	44,5
	800 - 850	70,2	6,5	4,2	1,01	2,48	59,5	51,3	4,2	55,2	25,0	45,3
T 2	350 - 450	63,1	9,0	4,8	0,99	2,42	59,3	60,1	-3,0	62,4	24,6	39,4
	800 - 850	72,2	6,1	4,6	1,14	2,51	51,6	48,4	1,6	50,1	20,4	40,1
G 1	100 - 200	74,4	9,7	2,7	0,88	2,40	63,3	44,0	10,9	52,4	23,0	43,9
	400 - 500	66,5	8,9	2,0	0,89	2,42	63,4	55,3	3,3	60,1	28,7	47,7
	800	62,2	9,8	2,4	0,88	2,43	63,8	55,2	4,2	59,6	24,5	41,1
G 2	200 - 250	74,4	11,3	2,6	0,82	2,35	65,0	41,2	7,2	57,8	28,1	48,7
	550	58,7	12,8	4,8	0,77	2,32	66,8	59,9	0,8	66,0	24,2	36,6
	800	57,1	11,8	4,3	0,83	2,45	66,1	56,9	4,8	65,2	22,9	35,0

PV- pore volume; WV - water volume; AV - air volume; FC - field capacity; aFC - available field capacity

Simulation of the water balance with the Land-fill Model HELP. The Landfill Ordinance requires proofing the percolation rates. Such a simulation of the water balance can be carried out with the model HELP (Hydrologic Evaluation of Landfill Performance).

This simulation was also done at the investigated recultivation layers (Berger 2012). The simulations were performed with the meteorological data of the standard period 1961 to 2010 and also carried out with the data from 2000 to 2010. The decade 2000 to 2010 shows significant changes with respect to the factors that are particularly challenging to the effectiveness of a restoration layer. The first decade of this century shows significantly higher annual rain- fall amounts (about 10%) and significantly higher mean annual temperatures (about 1°C) in all meteorological stations.

The calculated (decade 2000 to 2010) average annual seepage from the recultivation layer is located at the landfill site **N** at around 60 mm. The landfills **M** and **G** achieve average seepage of around 120 to 130 mm per year. The highest infiltration rates occur in landfill with around 150 to 165 mm / a (Table 8). These simulation results are very surprising. Field capacity and available field capacity are very high and on the landfills no seepage water processes from the recultivation layers were observed.

The matured dredged material with its high organic matter content seems not to behave like “ordinary” mineral soil. But the modelling approaches of HELP are based on “ordinary” mineral soils. “Whether the water holding capacity of the dredged material is higher than the capacity modelled in HELP and thus the infiltration of HELP is slightly overrated, remains a speculation” (Berger 2012, p 8). Nevertheless the results clearly show the positive characteristics of the dredged material compared to marl.

However, the question remains how ordinary substrates (soil types) should fulfil the requirements of the Landfill Ordinance. If we believe in the results of the HELP calculations even a substrate with extremely high field capacity and available field capacity seems not to be able to comply with the Landfill Ordinance.

In summary: matured dredged material (mixed soil and silt) meets in practice the soil physical requirements of the Landfill Ordinance.

Table 8. Mean annual water balance of the restoration layers (years 2000 - 2010) (Berger 2012)

parameters [mm]	T 1	T 2	M 1	M 2	G 1	G 2	N 1	N2
precipitation		653,1		620,5		662,4		631,3
surface runoff	7,8	8,1	3,1	3,3	11,7	14,5	2,7	2.5
PET		665,6		654,0		678,6		753,3
AET	478,2	493,9	491,6	486,0	519,6	510,2	558,3	558,7
seepage	165,3	148,9	122,2	127,8	122,4	130,7	61,8	61,2
ΔWg	1,8	2,2	3,5	3,3	8,8	7,0	8,4	8,9
field capacity	431	464	504	526	576	617	535	495
available field capacity	169	170	283	282	253	233	290	268

PET - Potential evapotranspiration; AET - Actual evapotranspiration; ΔWg - Change of soil water retention

SUMMARY

In Mecklenburg-Vorpommern landfill sites are restored with matured dredged material since 15 years. This substrate comes from waterways and harbours. The used and tested dredged material originates from the port of Rostock, from the dredging of the waterways. This dredged material is classified, de-watered and processed in specially-developed inland disposal sites. Coarse components (gravel and sand) are used in the construction industry. The mixed soils are used in landscaping.

The organic-rich, silty and clayey substrates are used after dehydration and aging in recultivation layers of landfill sealing systems. The Rostock dredged material is not contaminated with pollutants.

The German Landfill Ordinance requires the proof of the water storage capacity (field capacity and available field capacity) for landfill recultivation layers. Whether the dredged material fulfils the demands of the Ordinance was examined on landfills already sealed with matured dredged material.

On four landfills, 2 to 15 years after their restoration, the chemical and physical status was determined (hydraulic conductivity, pore-size distribution, mechanical properties and chemical composition). It could be demonstrated that the requirements of the Landfill Ordinance regarding field

capacity and available field capacity are reliably observed even many years after the restoration. The use of matured dredged material (mixed soil and silt) in recultivation layers should be continued.

REFERENCES

- Berger, K. (2012) Simulation des Wasserhaushalts mit HELP, 3.90 D für vier Deponiestandorte in Mecklenburg- Vorpommern. Berechnungen an der Universität Ham- burg; Gutachten vom 13.04.2012, unveröffentlicht.
- BQS 7-1 (2011) Bundeseinheitlicher Qualitätsstandard 7-1 "Rekultivierungsschichten in Deponieoberflächenabdich- tungssystemen" vom 23.05.2011.
- BQS 7-2 (2011) Bundeseinheitlicher Qualitätsstandard 7-2 "Wasserhaushaltsschichten in Deponieoberflächenab- dichtungen" vom 20.10.2011.
- GDA (2006) GDA-Empfehlung E2-31 Rekultivierungs- schichten (2006) Deutsche Gesellschaft für Geotechnik <http://www.gdaonline.de/pdf/E2-31.pdf>, 22:07:2012.
- GDA (2010) GDA-Empfehlung E2-32 Gestaltung des Be- wuchses auf Abfalldeponien (2010) Deutsche Gesell- schaft für Geotechnik <http://www.gdaonline.de/pdf/E2- 32.pdf>, 22:07:2012.
- DepV (2012) Landfill Ordinance - Verordnung über Depo- nien und Langzeitlager (Deponieverordnung - DepV) vom 27.04.2009, BGBl. I S. 900), die zuletzt durch Arti- kel 5 Absatz 28 des Gesetzes vom 24. Februar 2012.

TREATMENT OF SANITARY LANDFILL LEACHATE BY MEMBRANE DISTILLATION

Gizem Sahin and Berna Kiril Mert (Sakarya University, Sakarya, TURKEY)

*Yasemin Melek Tilki** and Coskun Aydiner (Gebze Technical University, Gebze, TURKEY)

Esra Can Dogan (Kocaeli University, Kocaeli, TURKEY)²⁰

As one of the most difficult wastewaters to be treated, sanitary landfill leachate has complex pollutant contents of high concentrations, and thus its treatment by novel processes has quite significance for environmental protection, economical preferences and time saving. In this regard, proactive researches on increasing of technical and economic achievements in the leachate management are encouragingly able to be pursued by promising technologies. In this work, treating the leachate from sanitary municipal solid waste landfill was aimed to achieve the appropriate effluent quality standards for direct discharge to natural receiving waters using membrane distillation (MD) in direct contact mode lying between innovative and developing membrane technologies. The experiments were carried out for conventional treatment effluent using lab-scale MD system operated at intermittent (a) and continuous (b) operating modes to determine the best conditions for 6h duration time and long-term efficiency for 6h per day at a time period of 10 days, respectively. In experiments (a), the influences of membrane type, membrane pore size, cross-flow rate, distillate temperature, trans-temperature difference, flow hydrodynamics (pulse and continuous) on the MD performance were examined. The best operating conditions were established as PTFE membrane, 0.45 μm , 200 L/h, 40 °C, 20 °C and pulse flow regime for the mentioned order of process parameters, respectively, in which rejection efficiencies of 99.96% TDS, 99.26% COD, 99.80% TOC and 99.50% NH_4^+ were observed as well as distillate flux of 29.8 L/m²h. In experiment (b), the leachate was continuously filtrated under the best conditions determined in the (a), in which membrane cleaning was also applied at the end of filtration cycle in each day using 1% HCl, 1% NaOH and distillate for a full time of 60 min. Long-term MD operation was consistently maintained along 10 days with the performances of 24.9 L/m²h flux and 99.97%, 99.60%, 99.60% and 98.85% rejections in the abovementioned order. The produced water quality was appropriate to meet the discharge criteria according to the receiving water standards described in Turkish Water Pollution Control Regulations. Using the long-term experimental data, a simulation study on full-scale application of the leachate treatment by MD process was carried out for a real-scale sanitary landfill facility having a leachate flow of 500m³/d by using process design software with cost estimation module. In simulations, it was assumed that the heat demand required for heating raw leachate stream as MD feed could be met from methane gas being produced in the landfill area. Accordingly, it was calculated that the feed stream would be able to be theoretically heated up to 142 °C using all biogas in the facility and hence 20% of the produced biogas could be met the heat requirement. The process simulation indicated that for directly discharging into receiving waters, the conventional effluent would be effectively treated with a unit treatment cost of 0.30\$/m³ in MD that is implementable in single step for waste concentrate minimization. This study finally proved that MD-included novel treatment application seemed to be a favorable technological solution for both enviable management of leachate discharges and sustainable protection of environment.

ENVIRONMENTAL MONITORING OF LANDFILLS BY A DOWNSCALING APPROACH

Mei Alessandro, Manzo Ciro, Paciucci Lucia, Allegrini, Alessia, Petracchini Francesco, Romagnoli Paola, Bassani Cristiana (Tecnologist of Institute of Atmospheric Pollution Research - CNR (National Research Council of Italy), Research Area of Rome 1 Via Salaria Km 29.300, Monterotondo (00016), Rome, Italy)

Landfills are an important part of urban society and an accurate analysis of these area are fundamental to improve decision making strategies for planning anthropic activities. The optimization of new techniques for the monitoring of landfills represents a crucial issue since usual investigation methods are expensive and time-consuming. The application of remote sensing improves the monitoring of different environmental matrices and the assessment of gas and leachate migration. Reflectance spectroscopy approach can be adopted to investigate the stressed vegetation or soil pollution due to waste deposits developing site-depending spectral indices which are linked to bio-chemicals factors .

This paper describes a multi-source approach based on the use of remote sensing data and spatial processing techniques to monitor the environmental condition around landfill. The study area is located in the landfill of San Giovanni in Fiore Municipality (CS) in the Southern Italy (Calabria District). Multi-source data was adopted for the application of a downscaling and multi-temporal analysis. In particular the dataset was composed by orthophotos (2000, 2006 and 2012), Worldview 2 (2012) and Pléiades (2014 and 2015) satellite imagery and aerial thermal data from Multispectral Infrared and Visible Imaging Spectrometer (MIVIS) (2011). Moreover, a field survey was performed collecting overnight thermal images and photo in photogrammetric configuration.

The orthophoto dataset supported the multi-temporal analysis not covered by spectral imagery showing a general increase of land consumption and highlights area with no-/senescent vegetation cover. The visible and near-infrared spectral regions allowed to adopt indices descriptive of vegetation and to retrieve anomalies on the land cover. The analysis of vegetation changes is performed applying an image differencing of the Normalized Difference Vegetation Index (NDVI) which analyses the spectral regions sensitive to chlorophyll absorption of red light and reflection of NIR energy scattered by cell structure. This index was calculated in both satellite and aerial imagery. Moreover Thermal InfraRed (TIR) spectral domain of MIVIS was adopted for detection of possible leakage migration and presence of biogas into the ground.

The validation of evidences of ground anomalies was accomplished by field surveys and nocturne thermal acquisitions. In addition, a photogrammetric survey was performed by pole in order to improve the analysis of both vegetation and thermal anomalies that have been detected. The integration of the visible, infrared and thermal optical sensors with field nocturnal thermal analysis and photogrammetric surveys for 3D models generation is performed. The 3-D model of some sections of the landfill supported the comprehension of the site topography and anomalies.

This study has allowed the implementation of a landfill investigation procedure integrating geomatic tools of remote and *in situ* data. The outcomes of the proposed multi-source analysis highlight warning areas inside and around the studied area. The presented approach can be considered an innovative and a performing methodology of investigation than the current classical methods, which require a great deal of work at local scale.

PERFORMANCE OF VEGETATIVE BIORETENTION SYSTEM FOR GREYWATER REUSE IN ARID CLIMATES

Rezaul Chowdhury, Taoufik Ksiksi, Mohamad M. A. Mohamed and Jameelu Abaya
(United Arab Emirates University, Al Ain, United Arab Emirates)

ABSTRACT: Water Sensitive Urban Design (WSUD) technologies are acknowledged to play a significant role in improving the quality of stormwater in the urban landscape. However, findings have shown that greywater, the residential wastewater except that originates from toilet and kitchen, could be used to operate the vegetative bioretention system in the arid climates. A positive signal was received when investigated in the laboratory settings, however, a better picture and a more representative result can be obtained if the system is studied in a field scale. The study intended to explore further, the effectiveness of using the vegetative bioretention to treat urban greywater. This WSUD system can play a dual role in improving greywater quality and landscape aesthetics. Selection of appropriate plants for them is also an important research question. Twelve different species of native and exotic plants in triplet planted in 36 prototype bioretention columns in the laboratory. The columns were irrigated by synthetic greywater and the removal efficiency of heavy metals and other common water quality parameters were monitored on a regular basis. The retention of heavy metals in the water, plants (leaves, stem and roots) and soil were also investigated. It was found that the *Pennisetum seateceum* provides more consistency and efficiency in removing heavy metals from greywater.

INTRODUCTION

The debate and the need for action on climate change will continue over time. Although a milestone was reached by adopting the Paris agreement in December 2015, the challenges, particularly concerning water in arid regions of the world will remain and can become worse if proper water management practices were not implemented. The United Arab Emirates (UAE) is one of the most water-scarce countries, but their water consumption rate is significantly high. Water consumption in the Abu Dhabi Emirate ranges between 170 and 200 Lpcd in flats and between 270 and 1,760 Lpcd in the villas (Environment Agency – Abu Dhabi, 2009). In a recent study, Chowdhury and Rajput (2015) observed that the water consumption in traditional villas in Abu Dhabi is more than 2500 Lpcd. Out of this, more than 80% is used for outdoor activities (gardening, car washing, for example). Because of rapid population growth in its major cities, desert greening and agricultural expansion policies and for the anticipated climate change scenarios, it is considered that water resources in the UAE will be significantly stressed in the future. Moreover, since rainfall and urban runoff are not abundant sources of water in the UAE, recycling and reuse of wastewater or greywater is considered as a potential alternative. The key technical challenges of their harvesting and reuse are appropriate treatment, storage, supply to end users at cost effective manner and their risk assessment.

Previous studies showed that reuse of alternative water resources is an economically viable solution for water demand reduction in water scarce countries (Chowdhury et al., 2015, McIntosh et al., 2013a, 2013b). Greywater (residential wastewater excluding toilet and kitchen wastewater) is becoming popular as an alternative water source in many arid and water scarce regions. Greywater generation in cities across the world is in the range of 40-80% (Allen et al. 2010; Jamrah et al. 2006; Chowdhury et al., 2015) of the indoor water consumption. Investigation on indoor average water consumption in the Al Ain city was found to be 280 Lpcd and average greywater generation estimated at 192 Lpcd in the villas. Higher water consumptions are observed in the shower (33%), dish wash (16%), toilet flush (14%) and in ablution (12%).

Further findings show that about 30% of potable water can be saved by the reuse of greywater for toilet flushing and irrigation (Chowdhury et al., 2015).

The Water Sensitive Urban Design (WSUD) systems involve several cost-effective, natural and low energy required treatment technologies for source control of stormwater runoff. Most popular WSUD systems are swales, infiltration trench, bioretention basin, permeable pavement and constructed wetlands. WSUD provides two benefits – source control of urban runoff and landscape architectural benefits to the society (Beecham and Chowdhury, 2012). Since rainfall and urban runoff are not abundant in the arid regions and that greywater is technically abundant and contains less organic loads, it is paramount to explore the applicability of its usage through WSUD.

The WSUD systems used in these studies are Permeable pavement and vegetative bioretention system. Permeable pavement is an alternative paving surface generally designed to filter stormwater runoff through voids into an underlying stone reservoir where it is temporarily stored for reuse or infiltrated into ground water (Myers et al., 2009). While bioretention systems are low depth landscaped areas, which are normally underdrained and rely on engineered soils, vegetation and filtration to improve water quality and reduce runoff downstream. They are generally aimed at sustainably managing and treating runoffs from rainfall events.

Earlier studies conducted at laboratory scale by (Chowdhury et al., 2015) show that two WSUD treatment technologies, namely the vegetative bioretention basin and permeable pavement with underlying reservoir could improve most of the greywater quality parameters fit for irrigation end use. However, application-test-bed studies are essentially required for investigation that is more rigorous and which represent in a better way the real conditions of operation (Hatt et al., 2008). Another aspect is the selection of appropriate plants, which is critical to the long-term landscape amenity, functional performance, and structural integrity of WSUD systems (Australian Northern Territory Government, 2009). Plants have a functional role in treatment and for erosion protection of WSUD systems. Vegetation planted in bioretention systems need to tolerate condition where water ponds temporarily, but will drain relatively quickly.

The pilot study involving permeable pavement and bioretention system will investigate the potential soil and groundwater pollution from greywater-based irrigation. Meanwhile, analysis within the replicas with respect to plants and within the plants with respect to the water quality parameters of the column experiment will aid in selecting the most effective species from the set of plants studied. Overall, the outcomes of these studies will help to implement the multi-functional WSUD systems in the arid landscape in recycling and reusing of greywater for potable water savings.

MATERIALS AND METHODS

Thirty-six number prototype bioretention columns were constructed and 12 different species of selected plants in triplet were planted. Firstly, the system was nursed for two months irrigating using tap water to allow the plants adapt to their new environment. Then, irrigated uniformly using measured quantities of greywater over a period. The heavy metals in the water, plants (leaves, stem and roots) and the soil were analyzed using the method of atomic absorption spectrometry. Sampling of the water effluent is twice in every month and where necessary, preserved with concentrated nitric acid and kept refrigerated before the lab analysis. Minimum of 50g dried soil sample, 0.3g dried stem and leaf samples taken at the end of every month. The sampling of the roots is only twice, in the beginning and at the end of the experimental period.

The length of the column is 60cm and the diameter is 15.8cm. The effective length is 54cm, while the 6cm (free board) left would contain the irrigation water. At the bottom is the drainage layer, 5.3 cm thick and filled with 2-5 mm aggregate. The 8 cm thick transition layer have soil with grain size in the range of 0.50 - 0.2 mm. Filter media, 40 cm thick contains well graded soil 0.075 - 4.75 mm, mixed on-site in the following percentage: sand, 25%; black soil, 20%; 0.5-2mm, 35% and 2-5mm, 20%. The columns were constructed using the PVC pipes and water drained through the tap at the bottom of the system. The system was built in multiple layers in order to avoid intoxication of plants by hydrogen sulfide and other substances

released in the anaerobic breakdown of organic matter typical of a single layer bioretention system (Trowsdale and Simcock, 2011).



FIGURE 1. Photos of thirty-six prototype bioretention columns located at the UAE University

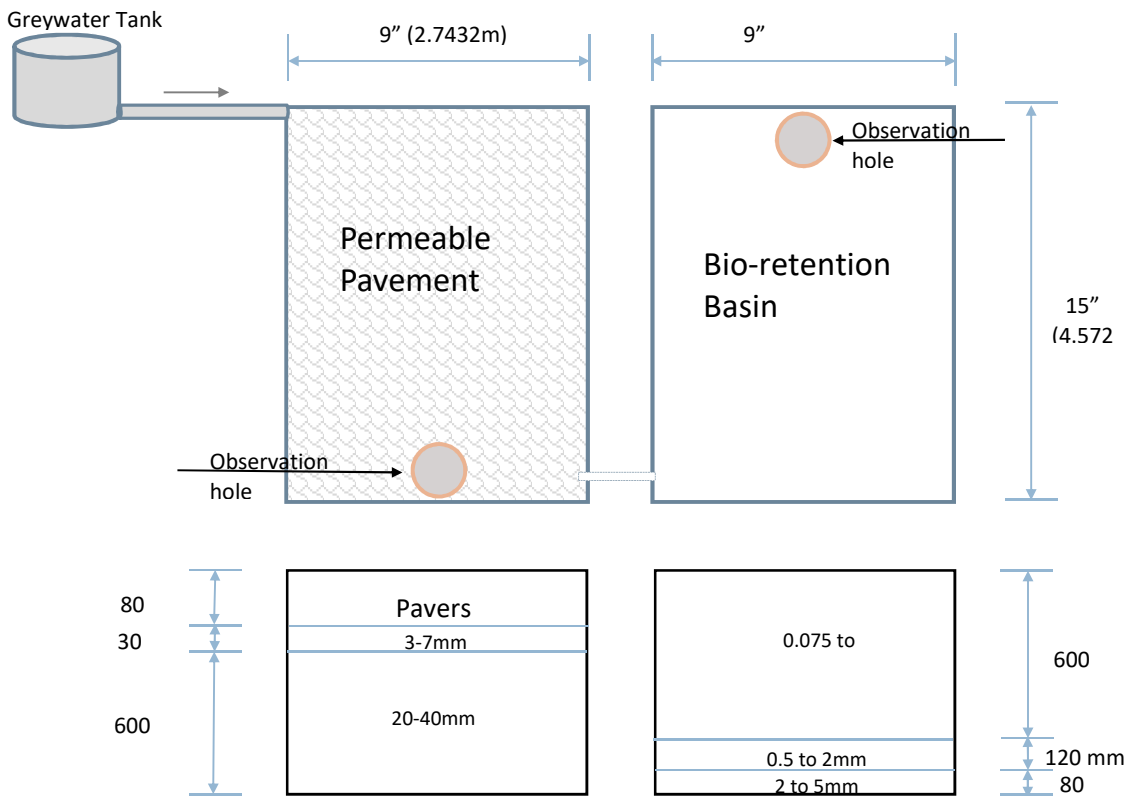


FIGURE 2. Layout of permeable pavement and bioretention basin constructed on the Falaz Hazza campus of the UAE University

There are 12 selected species of the plants, namely: 1. *Dodonaea viscosa* (Dod) 2. *Vitex agnus* (Vit) 3. *Ficus nitida* (Fic) 4. *Jasmine sambac* (Jas) 5. *Pennisetum seateceum* (Pen) 6. *Ixora coccinea* (Ixo) 7. *Hibiscus rosa sinensis* (Hib) 8. *Vinca rosea* (Vin) 9. *Lantana camara* (Lan) 10. *Canna indica* (Can) 11. *Alternanthera ficoidea* (Alt) and 12. *Rhoeo discolor* (Rho). Irrigated with tap water, the plants had 55 days (11-09-2015 to 05-11-2015) after plantation to normalize with their new environment. Subsequently, and depending on the weather a measured quantity of greywater at a uniform rate used for the irrigation. Within the period of growth, the following amounts of fertilizers were applied three times on each plant: NPK, 1.53 g/ml; MgSO₄, 0.83g/ml and CaNO₃, 0.55g/ml.

Figures 2 and 3 shows the specification and a photo, respectively, of the constructed bioretention system in the field. The bioretention system has three layers. First, the filter layer consists of 60 cm of well-graded (0.075 to 4.75 mm) sand. Then a 12 cm transition layer of coarse sand and a drainage layer of 8cm at the bottom (2 to 5 mm gravel). The topmost layer of the system contains a wide range of soil grading. The well-graded soil is a blend of different classes of soil grades in the following ratio: normal sand (45%); 0.2 -2mm sand (35%) and 2-5mm coarse sand/crushed stone (20%). After the excavation, plastic lining was placed to prevent the seepage of water out of the system. Then, different strata in the system placed layer after layer.

On-site monitoring of some water quality parameters using a multi-parameter water quality meter would help in defining the effectiveness of the system in improving the water quality. The parameters are pH, Oxidation Reduction Potential (ORP), Turbidity, Salinity, Conductivity, Dissolved Oxygen (DO) and Total Dissolved Solids (TDS). Furthermore, additional test for Total Organic carbon (TOC), Total Nitrogen (TN), Total Phosphorous (TP) and heavy metals (Zinc, cadmium and chromium) are carried out concurrently. This applied to both permeable pavement and bioretention systems.



FIGURE 3. The constructed field scale vegetative bioretention systems

RESULT AND DISCUSSION

Some plants like *Dodonaea viscosa*, *Vitex agnus* and *Alternanthera ficoidea* has shown some comfort since planting and after the experiment began. However, some other plants such as *Ficus nitida*, *Canna indica* and *Hibiscus Rosa sinensis* shows a little stress after plantation, they then revived during the normalization period. The stress was identified as a sign of nutrient deficiency, which was corrected using fertilizer. The water needs of the plants vary. While *Rhoeo discolor* is comfortable with small amount of irrigation water, other plants such as *Canna indica* needs a little bit more to stay healthy. Interestingly, plants like *Vitex agnus* and *Dodonaea viscosa* seems to have much tolerance to both drought and wet conditions preferred by *Rhoeo* and *Canna*, respectively.

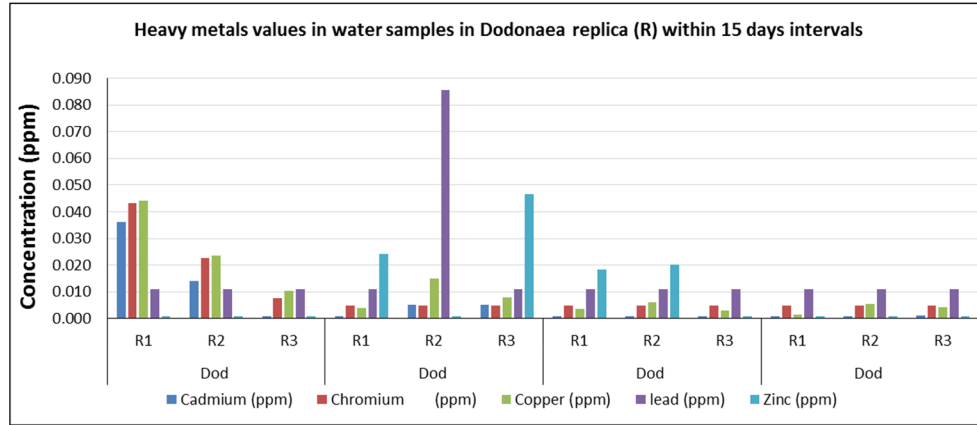


FIGURE 4. Heavy metals values in water samples in columns having the *Dodonaea viscosa* (Dod)

The study is still under investigation. The first compartment in **Error! Reference source not found.4** and **Error! Reference source not found.5** is the baseline readings (raw greywater) and followed by the subsequent readings in serial order. The chromium content in the effluent seems always near the same as that of the raw greywater (about 0.0050 ppm). This implies that it is neither absorbed nor retained in the system. In addition, it is unlikely that the water dissolved the chromium in the soil. The cadmium concentration in effluents follows the similar trend of chromium. In most of the cases, the cadmium concentrations remains 0.0010 ppm for both the raw greywater and the effluent. In a few occasions, it gets down to 0.0007 ppm. For Zinc and Copper, it appears that about 99.5% of their concentration sunk into the system in all plants. Observation shows that *Pennisetum seateceum* provides more consistency and efficiency of removal compared to other plants.

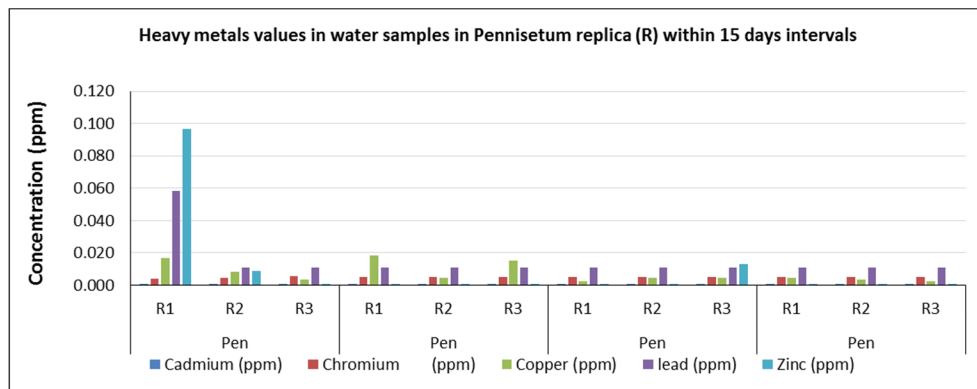


FIGURE 5. Heavy metals values in water samples in columns having the *Pennisetum seateceum* (Pen)

CONCLUSION

The two experiments are to run for a year; as such, it is now too early to conclude how different plants behave in different columns of bioretention prototypes. However, preliminary results from the column experiment hinted that the some plants have a better removal capacity and consistency. Unlike chromium and cadmium, a greater percentage of zinc and copper do not drain out of the bioretention system unhindered. Furthermore, the field tests of both systems will be useful to compare the results obtained in the laboratory and in the field conditions.

ACKNOWLEDGEMENT

The study is supported by the UAEU National Water Center interdisciplinary research grant (31R045-Research Center- NWC -2-2014) on “Greywater Reuse in Arid Climate through the Water Sensitive Urban Design Systems”.

REFERENCES

- Australian Northern Territory Government. 2009. *Water Sensitive Urban Design Vegetation Selection Guide*. Northern Territory Department of Planning and Infrastructure, Darwin, Australia.
- Beecham, S. and Chowdhury, R. 2012. “*Effects of Changing Rainfall Patterns on WSUD in Australia.*” *Water Management* 165(5):285-298.
- Beecham, S. and Myers, B. 2007. “*Structural and Design Aspects of Porous and Permeable Block Pavements.*” *JAustCeramSoc.* 43(2):74-81.
- Chowdhury, R. K. and Rajput, M. A. 2015. “*Water Consumption Patterns in the Traditional Villas of Abu Dhabi.*” 21st International Congress on Modelling and Simulation, Gold Coast, Australia, 29 Nov to 4 Dec 2015. www.mssanz.org.au/modsim2015.
- Chowdhury, R.K., Beecham, S. and Sharvelle, S. 2015. “*Greywater Quality Changes in a Permeable Pavement Reservoir.*” *Water Management*, DOI: 10.1680/wama.14.00107.
- Chowdhury, R.K., El-Shorbagy, W., Ghanma, M. and Al-Ashkar, A. 2015. “*Quantitative Assessment of Residential Water End Uses and Greywater Generation in Al Ain City.*” *Water Science and Technology: Water Supply* 15(1):114-123.
- Hatt, B. E., Fletcher, T. D., & Deletic, A. 2009. “*Hydrologic and Pollutant Removal Performance of Stormwater Biofiltration Systems at the Field Scale.*” *Journal of Hydrology* 365(3):310-321.
- Jamrah, A., Al-Omari, A., Al-Qasem, L. and Abdel Ghani, N. 2006. “*Assessment of Availability and Characteristics of Greywater in Amman.*” *Water International* 31(2):210-220.
- McIntosh, B.S., Aryal, S., Ashbolt, S., Sheldon, F., Maheepala, S., Gardner, T., Chowdhury, R., Gardiner, R., Hartcher, M., Pagendam, D., Hodgson, G., Hodgen, M. and Pelzer, L. 2013a. *Urbanisation and Stormwater Management in South East Queensland – Synthesis and Recommendations*. Technical Report No. 106, Urban Water Security Research Alliance, CSIRO, Australia.
- McIntosh, B.S., Hodgen, M., Aryal, S., Laredo, L., Wolf, L., Gardner, T., Chowdhury, R. and Maheepala, S. 2013b. *Ripley valley – An Application of GIS based Runoff Modelling to Strategic Stormwater Harvesting Assessment*. Technical Report No. 109, Urban Water Security Research Alliance, CSIRO, Australia.
- Myers, B., Beecham, S., van Leeuwen, J. and Keegan, A. 2009. “*Depletion of E. coli in Permeable Pavement Mineral Aggregate Storage and Reuse Systems.*” *Water Science and Technology* 60(12):3091-3099.
- Trowsdale, S. A. and Simcock, R. 2011. “*Urban Stormwater Treatment Using Bioretention.*” *Journal of Hydrology* 397(3):167-174.

BIO-WASTE RECYCLING IN GERMANY

M. Nelles^{1,2*}, A. Schüch^{1,2}, A. Lemke¹, G. Morscheck¹

¹ University of Rostock, Department of Waste Management and Material Flow, Germany
E-mail: michael.nelles@uni-rostock.de

² German Biomass Research Centre GmbH (DBFZ)

ABSTRACT: German biodegradable waste is collected separately, recycled and ecologically and economically used. Compost and digestate are used as organic fertilizer or replace peat in potting soil and plant substrates. The bio-waste recycling may also directly contribute to climate protection if the methane produced during the fermentation is used for energy production.

Around the world biodegradable waste in landfills is the main factor for the generation of the greenhouse gas methane. This environmental impact can be significantly reduced by the separate collection and recycling/use of organic waste. The separate collection of bio-waste is also a precondition for reutilizing of organic matter and nutrients. Only from separately collected bio-waste it is possible to produce high-quality compost and digestate, which are suitable for agricultural or horticultural use.

The separate collection of bio-waste from households affects the amount and composition of the residual waste. By separating bio-waste the remaining amount of waste is reduced up to a third. At the same time the residual waste contains less wet ingredients, which facilitate the waste sorting and makes the treatment in waste incineration plants more effective or even possible.

Both, the recycling of compost and digestate on soils, as well as the energy recovery of bio-waste, contribute to climate protection and resource conservation. The operation of the treatment plants determines how much of the greenhouse gases methane, nitrous oxide and ammonia is released during the process. Some plant operators need to be awakened and their awareness of climate-relevant emissions from their bio-waste treatment plants has to be raised. Also the amount of collected organic waste should be further reinforced. In 2015 the separate collection of bio-waste has to improve!

Keywords: Bio-waste, Compost, Digestion, Recycling, Germany

INTRODUCTION

Germany has implemented a separate collection for waste, household and other kinds of waste, more than twenty years ago. Diverse environmental damages, lack of landfill space and the use of finite resources led in the early 90s to a rethink in waste management. Today, climate change and energy demand are important arguments for the separate collection and utilisation of all kinds of organic wastes.

In response to the EU's waste framework directive, the Waste Management Act of 2012 (KrWG) in § 11 paragraph 1 obligates waste producers and mandated waste management authorities to collect bio-waste separately at the latest as of January 1st 2015. The term "bio-waste" in § 3 KrWG comprises yard, park, and landscape management waste as well as food and kitchen waste. The requirement in the Waste Management Act (KrWG) to collect bio-waste separately (§ 11/2 KrWG) is concretised in the Bio-waste Ordinance (BioAbfV).

This article tries to discuss all kind of organic waste but is focused on the bio-waste from private households that is collected by using bio-waste bins. Wastes collected through bio-waste bins, especially food, kitchen and yard waste, are monitored according to the European Waste Catalogue (The European Commission 2014.) laid down in the Commission Decision 94/3/EC and the German waste index regulation

(AVV) under the waste classification key 200308 (biodegradable kitchen and canteen waste, with animal residues) (Deutsche Bundesregierung 2001).

The German Bio-waste Ordinance (Ordinance on the Recovery of Bio-waste on Land used for Agricultural, Silvicultural and Horticultural Purposes) (Deutsche Bundesregierung 2013) defined bio-waste in general: *Waste of animal or plant origin or from fungal materials for recovery purposes, which can be degraded by microorganisms, soil-borne organisms or enzymes, including wastes for recovery purposes with high organic content of animal or plant origin or fungal materials (details in Annex 1 Bio-waste Ordinance)*

This article will use:

- Bio-waste (collected in bins): separately collected (in bio-waste bins or bags) food and kitchen waste, and yard waste from private households.
- Green waste: Separately collected yard waste from private households, and waste generated in municipal parks and in landscape management (Krause et al. 2014).
- “Organic waste” is used for all kinds of biodegradable wastes.

For the treatment of separate collected bio-waste (composting and digestion) the important laws are given with (BGK 2014):

Bio-waste Ordinance (BioAbfV 1998, revised in 2012): The amended Bio-waste Ordinance (BioAbfV) of 2012 covers the application of treated and untreated bio-wastes and mixtures on land which is used for agricultural, silvicultural and horticultural purposes. It also covers suitable raw materials, quality and hygiene requirements, and treatment and investigations of such bio-wastes and mixtures. The Bio-waste Ordinance regulates – from a precautionary perspective – the waste side (e.g. heavy metals) of the application, whereas the fertiliser law regulates the nutrient part.

Fertiliser Law (DüV 2007): Gives the frame for the good code of practice of fertilising and shows special requirements for organic fertilisers. It includes the restrictions for the application of fertilisers with essential nitrogen contents in winter periods.

Fertiliser Ordinance (DüMV 2012): Compost from biodegradable waste is subject to the fertiliser ordinance as a secondary raw material fertiliser (or seldom as soil improving agent). A declaration of the fertiliser type, raw material, nutrients and other product properties is obligatory. Threshold values for contaminants like PFT, PCCD or dl-PCB, included in the Fertiliser Ordinance are obligatory for compost and digestate, too.

Federal Soil Protection Law (BBodSchG 1998/BBodSchV 1999): Ensures the soil function and gives among others precautionary requirements for the contamination of soils. The soil protection law is relevant for the application of compost and digestate for landscaping and recultivation.

WHAT TO DO WITH ORGANIC WASTE?

Organic materials which the holder discards or intends or is required to discard become organic waste. The organic waste can be disposed of or used in different ways. The type of disposal determines the possibilities of utilization.

BIO-WASTE RECYCLING IS CLIMATE PROTECTION

The federal government targets to reduce the German emissions of greenhouse gases by 40 percent compared to 1990 levels until 2020. This objective can only be achieved by a sustainable energy economy - saving energy, renewable energy generation and efficient use of energy.

What could the waste industry additionally do, to achieve the resource, energy and climate objectives in the future? In particular, the use of organic waste can contribute to achieving the objectives. Today waste management saves annually about 56 million tons of carbon dioxide equivalent compared to 1990 and contributes significantly to the achievement of the climate protection goals. This has been achieved through the waste separation in the households, which is established in Germany since more than two decades. The separate collection of bio-waste and green waste takes a leading position in comparison across Europe.

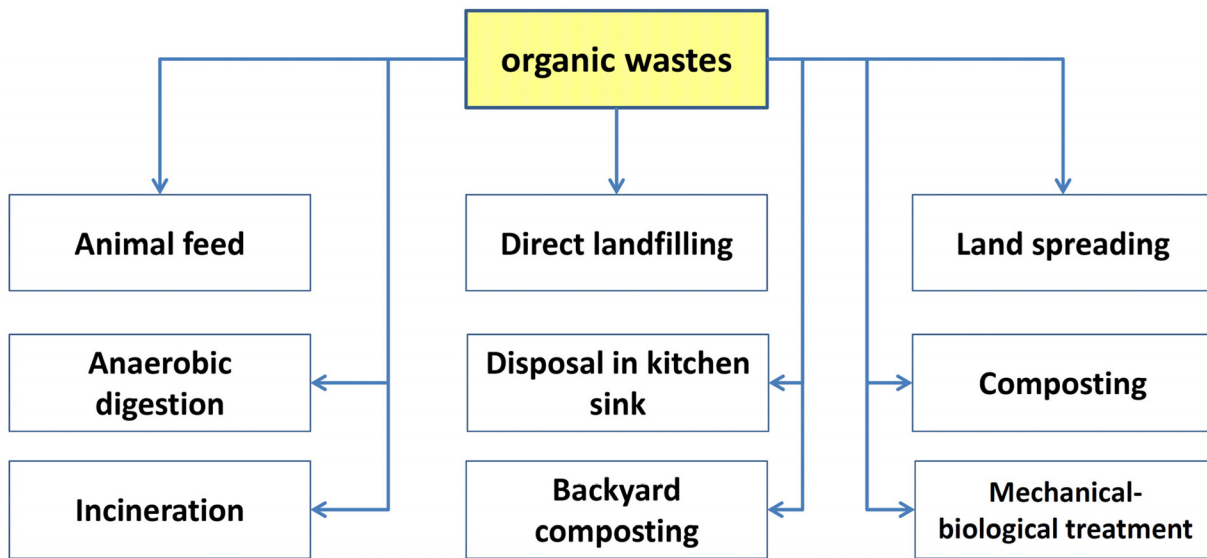


Figure 1. “Treatment” options of organic wastes (not all practised in Germany)

The share of renewable energy (such as by energy crops) in energy production should be increased further. The cultivation of energy crops is however in competition with food and feed production. For this reason the combined energy and material use of bio-waste and green waste is of particular interest.

A sustainable management of biogenic material flow combined material and energy recovery paths (nutrient and carbon recycling, energy supply, reducing carbon dioxide emissions by replacing fossil fuels, reducing the peat demand and lower treatment costs with extended regional added value).

Important questions are:

- what can be done to optimize collection and recycling of bio-waste
- which additionally exploitable potential exists
- how much work is required
- which benefits in relation to expenses is achieved.

The potential benefits of all biodegradable wastes should be utilized as much as possible and for this purpose the optimal combination of treatment methods has to be used.

Annually around 100 million tons of biodegradable wastes from, for example, forestry, agriculture or wastewater and waste management, arise nationwide. Of these, approximately 65 percent are technically and ecologically sensible usable, a potential of four to five percent of primary energy demand in Germany. Realising this residue potential is a significant part of the municipality’s responsibility.

ECOLOGICAL ASPECTS OF COMPOSTING AND ANAEROBIC DIGESTION OF ORGANIC WASTES

The utilization of organic waste reduces the release of greenhouse emissions compared to landfilling or incineration of wet organic waste in waste incineration plants.

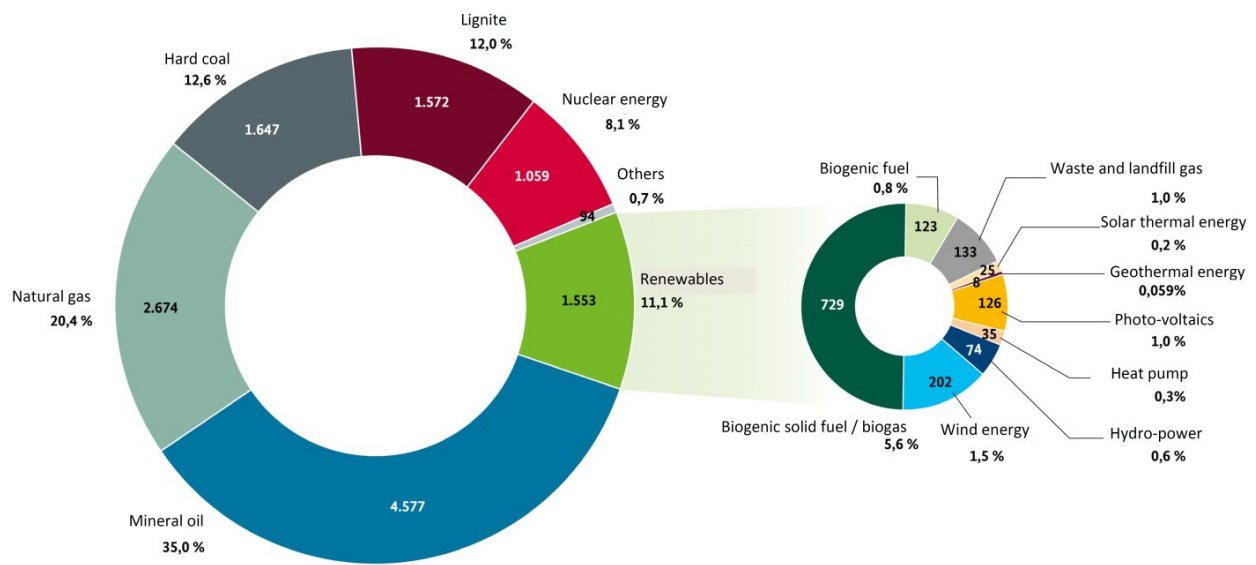
The potential environmental benefits of a consistent recovery of bio-waste in Europe could achieve CO₂-Eq savings of up to 50 million tons. The AD of organic waste would reach up to 7% of the overall EU target for renewable energy in 2020. Up to 42% of the bio-fuel target could be attained by the produced biogas. The AD of biodegradable waste is not only successful climate protection policy and independent energy production but also a relevant contribution to the humus formation of agriculturally used soils in

Europe. Limited resources, such as raw phosphate, can be protected by the recycling of the plant nutrients in the compost.

Not more than 11.1% of the primary energy consumption comes from renewable energy sources; less than 10% of the renewable energy comes from wastes. In the electricity sector the share of renewable energy climbed to 25.3% of the total (gross) electricity production.

Utilisation means composting and anaerobic digestion (AD) of bio-waste or incineration of woody dry green waste. But even these uses emit greenhouse gases. Emissions can be reduced by a good process control and plant construction.

The formation of greenhouse gases (GHG) as methane (CH₄), nitrous oxide (N₂O), ammonia (NH₃) and non-methane volatile organic compounds (NMVOC) in composting and digestion processes of organic waste depends primarily on the carbon and nitrogen content in the raw material, the structure as well as the process conditions. “It depends less on the technical standard and procedural features of the treatment plant itself. The anaerobic metabolism product methane occurs also in the aerobic composting processes; the generated amounts depending on the released anaerobic activity and oxygen supply” (Cuhls et al. 2015).



Quellen: Arbeitsgemeinschaft Energiebilanzen (AGEB), Arbeitsgruppe Erneuerbare Energien-Statistik (AGEE-Stat)

Figure 2. Share of renewable energy of primary energy consumption in Germany 2014 (AGEB 2015)

It is important that digestion plants use the total potential of the biogas. Tanks and basins with anaerobic activity, e.g. liquid fermentation residue (digestate), should be encapsulated and connected to the biogas network. Slightly with methane contaminated air flows should be used in the combined heat and power unit as combustion air or re-used as process air within the fermentation plant. In order to safely dispose of methane, exhaust air flows with high loads of methane should be combusted. On site existing biomass power stations or other combustion plants contribute to the emission control synergy (Cuhls et al. 2015).

High emissions to the atmosphere result mostly from mistakes in operation. For the biogas process reasons might be:

- inappropriate feeding system (processes in uncovered storage)
- leakage (biogas fermenter, biogas storage, pipes, valves)
- high biogas potential of the digestate (insufficient biodegradation).

In the composting or post-composting (after anaerobic digestion) process, reasons for emissions include:

- unfavourable dimensions of windrows
- insufficient use of strengthening material
- inadequate turning intensity
- high water content
- insufficient air porosity.

In the composting process all of these conditions result in a lack of air (oxygen) supply.

A closed composting process with active ventilation and exhaust gas cleaning enables a process control to reduce emissions. In practice the existing modes of operation often do not aim to reduce emissions of GHG methane and nitrous oxide (Cuhls et al.2015).

Methane is not or only slightly decomposed in biofilters. A further development of biological processes to remove methane (e.g. in downstream methane oxidation filters) is needed.

Nitrous oxide is formed within the biofilter by NH₃ conversion and its secondary products (nitrification). Therefore a removal of NH₃ before the ammonia-rich gas reaches the biofilter is necessary. The solution could be acid scrubbers. The product is a dilution of ammonium sulphate, which can be concentrated and recycled as fertilizer. This applies especially to ammonia emissions from AD plants. The process conditions are crucial for the GHG emissions. With regard to the reduction of GHG emissions open windrows as well as closed composting plants (with or without AD) can be improved.

The formation of nitrous oxide can only be suppressed preventive in the biological treatment process (in situ). A subsequent reduction is not possible in any exhaust gas purification (end-of-pipe). Currently there is a lack of technical and operational requirements for a low-emission operation, in particular in order to reduce methane. Treatment of organic wastes and bio-waste management reduces the emissions of GHG, but produces also a share of the total GHG emissions.

Important are the total greenhouse gas emissions from the treatment process as well as the storage and spreading of compost and digestate in the recycling of bio-waste and green waste.

The extrapolation of the greenhouse gas emissions of CH₄ and N₂O and the effective indirect greenhouse gas NH₃ from the operated bio-waste treatment plants (Input about 9 million tons of organic waste per year), including the emissions from the storage and spreading of compost and fermentation products results in a percentage of Germany's total greenhouse gas emissions for methane of 0.591%, nitrous oxide 0.293% and by ammonia of 0.33%. The contribution of the biological treatment and recycling of bio-waste and green waste based on the sum of total greenhouse gas emissions (CO₂-equivalent) in Germany amounts to 0.066% (Kehres 2015).

SEPARATE COLLECTION OF BIO-WASTE IN BINS, BAGS OR CONTAINERS

The waste management system in Germany is carried out in a so-called "dual system". Residual waste and organic waste are in the responsibility of the mandated waste management authorities (public administration, öRE) other recyclable household waste fractions are disposed of by private waste management companies.

In 2012, the amount of bio-waste separately collected from private households and landscape management of public land in Germany amounted to 9.1 million Mg. A part of 4.3 million Mg of this amount were collected using bio-waste bins and 4.8 million Mg were green waste, collected by the mandated waste management authorities (öRE).

The population specific average amount of bio-waste collected (in bins or bags) Germany-wide reaches 54 kg/capita/year and green waste 59 kg/capita/year. The collected amounts vary significantly across the German federal states (Krause et al. 2014, see Figure 3).

The mandated waste management authority can collect bio-waste in a pick-up or drop-off method. The authority has the choice to use bio-waste bins or bags as a collection container. Still not every household (waste-producer) in Germany is able to participate in separate bio-waste collection!

In 2010, private households in only 287 districts had access to a comprehensive separate collection system that uses bio-waste bins and is operated by mandated waste management authorities.

While 39 districts offered separate collection in some parts of the waste management area, 76 districts offered no bio-waste bin service at all (Oetjen-Dehne et al. 2014).

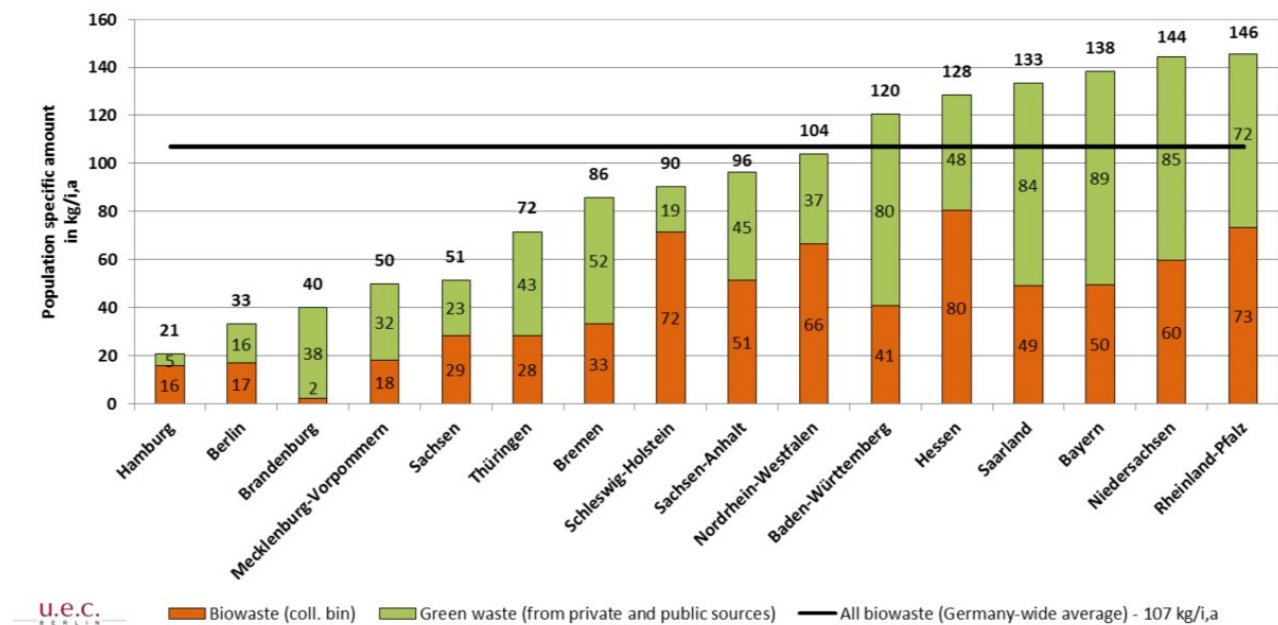


Figure 3. Separately collected amounts of bio-waste in German states in 2010 (Krause et al. 2014).

Separate collection systems for private yard waste, however, are in place in most districts. Only seven districts do not have the possibility to dispose of green waste separately through mandated waste management authorities. In addition to various “bring systems” (green waste collection, green waste containers, mobile collection sites, etc.) and “pick-up systems” (kerbside collection system) for selected green waste (street collection, collection of bags of leaves, collection of Christmas trees, bundles collection etc.) are offered.

A survey among public waste management authorities in 2012 (Krause et al. 2014) revealed that the actual rate of access of private households to separate bio-waste collection using bio-waste bins amounts to roughly 52% Germany-wide. This number increases to 65% in areas of comprehensive separate collection systems. Nearly 40 million people in Germany do not use the bio-waste bin!

As Figure 4 shows the total amount amounts bio-waste and green waste collected in the different districts ranges from 5 to more than 200 kg/capita.

In 2015 57 to 69 administrative districts will offer no compost bin! The collection of organic waste must be further strengthened. The resource Organic waste must be used more extensive.

Only 35% (green waste and bio-waste, 3.4 and 3.9 million tons) of the theoretical bio-waste potential (21.1 million tons) has been separate collected by the public waste management authorities in bins, bags or containers in 2010, while roughly 23% (4.8 million tons) were collected with the residual waste. Another significant amount was disposed of in private back-yards composting and in non-recorded private business bio-waste treatment facilities.

As residual waste analyses confirm, normally most organic material contained in residual waste consists of kitchen and food waste. Further separation efforts of residual waste should therefore focus on the separation of kitchen waste from households and gastronomy. The comparison of residual waste composition in areas with and without bio-waste bins shows that already established bio-waste bin collection reduces the amount of residual waste by 15 to 20 kg of organic matter per person and year.

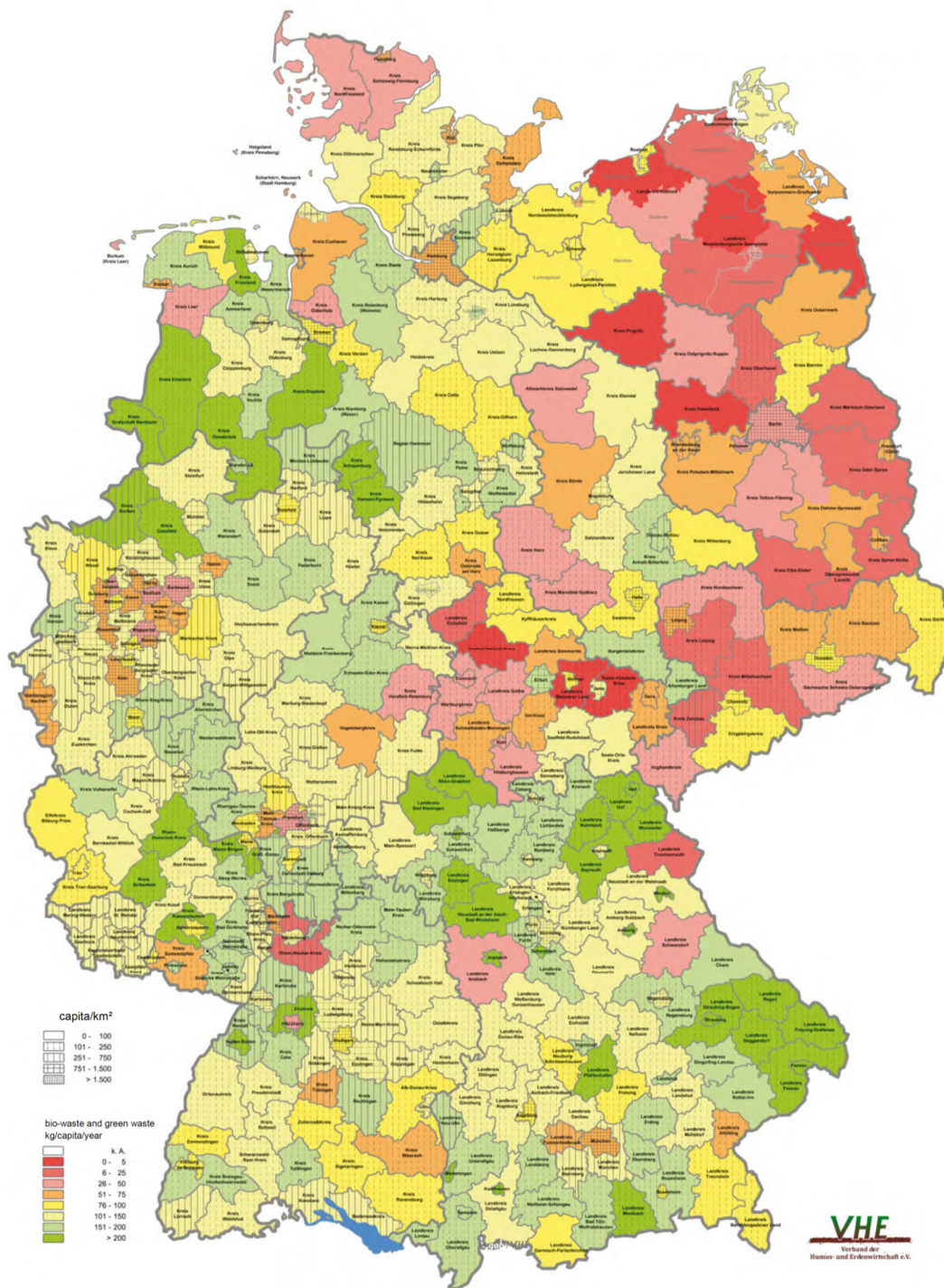


Figure 4. Population specific amounts of collected in German districts in kg/capita/year (2008 - 2011, according availability) (VHE 2012).

Additionally, yard waste is getting into bio-waste bins that would otherwise be individually composted, be illegally disposed of, or get burned. Broadly speaking, 1 kg of organic matter that is getting separated from residual waste will lead waste management authorities to gain 2 kg in yard bio-waste.

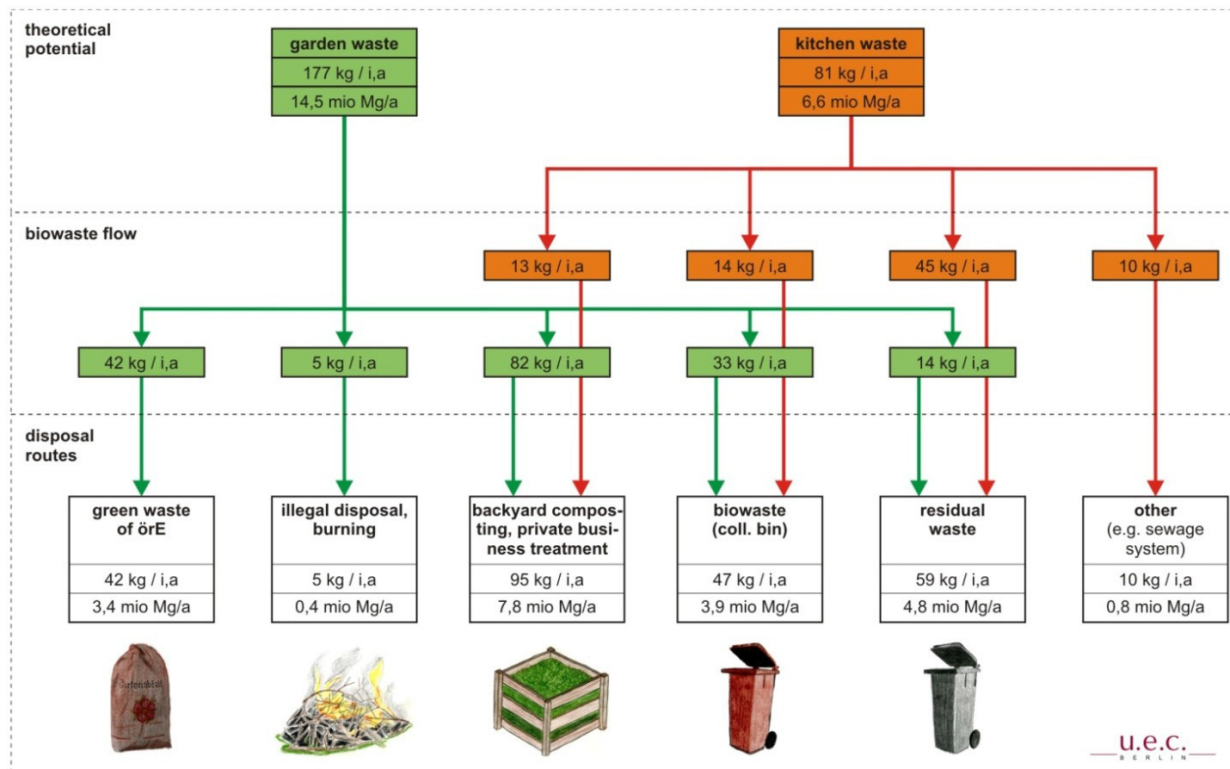


Figure 5. Bio-waste disposal routes of kitchen and yard waste in Germany in 2010 (Krause et al. 2014).

Oetjen-Dehne et al. (2014) and Krause et al. (2014) describe the bio-waste disposal situation in 2010 by using a bio-waste flow model (Figure 5).

Nevertheless, even in optimal separate collection systems and in the case of efficient use of the bio-waste bin, yearly 15 to 20 kg/capita of organic matter will usually go into residual waste, but today 59 kg/capita. In total 28.4 % (per year: 6 million tons; 74 kg/capita) of the organic waste are not collected separately!

Positive is that per year already 15.1 million tons of organic waste (184 kg/capita) are (collected), treated and used (42 kg/capita green waste; 95 kg/capita backyard composting and private business treatment; 47 kg/capita separate bio bin collection). Which is more than the by the European Union estimated collectable emergence of 150 kg/capita. EU-wide previously only 50 kg/capita organic wastes are collected per year.

The collection and recycling of bio-waste can also be profitable. Electricity from bio and green waste can be reimbursed according to §27a EEG up to 50 - 75 € per ton. But the substitution effects by material recycling of bio-waste are not promoted. Currently only 5 - 15% of the organic waste is used for the production of biogas. The total potential of fermentable organic waste amounts to 11.7 million tons (Struwe 2010).

WAYS TO INCREASE THE COLLECTION OF BIO-WASTE

In Germany the biological waste treatment looks back to a successful tradition and has become firmly established on an advanced level with about 9 million tons of separately collected organic waste as part of the municipal solid waste (bio-waste in the bio bin and green waste). However, in principle an increase in collection of 2 to 4 million tons is possible.

Basically are two **collecting systems** available.

Kerbside collection system - householders are encouraged to separate targeted recyclables from their general waste and deposit this at the kerbside for regular collection.

Bring systems - are also known as fixed point systems or drop-off centres, and they comprise large recycling containers in easily accessible places (household waste recycling centres or supermarkets).

The bio bin is part of a kerbside collection system, green waste, especially woody green waste is collected by a bring system.

In response to the EU's waste framework directive, the Waste Management Act of 2012 (KrWG) in § 11 paragraph 1 obligates waste producers and mandated waste management authorities to collect bio-waste separately at the latest as of January 1st 2015.

As outlined in the preceding presentation, improved organic waste collection is necessary. The introduction or expansion of separate collection of bio-waste in regions without or with only a small level of connection to the organic waste collection is very important.

In areas with separate collection of bio-waste could be offered measures to increase coverage rates and quality of the material flows. Objectives must be:

- the widespread removal of bio-waste and green waste from the residual waste
- optimizing of material and energy use by separation of organic waste streams for the most appropriate recovery operation.

Among other things the success depends on the following conditions:

- compulsory connection and usage of bio-waste collection systems
- regional structures of the collection area
- waste-fee system (users and pay in proportion of waste amount) for residual waste and bio-waste
- increasing the collection volumes of green waste, better collection system, banning the burning of (woody) green waste
- Better public relations work.

Expansion of the separated collection system "Bio bin" only makes sense with high quality recycling of the organic waste (high-quality recycling by material and energetic utilization).

The best recovery can be realized by fermentation (AD) followed by composting of solid fermentation residues (cascade use). Environmentally sustainable fermentation:

- Except the woody ingredients all the bio-waste is fermented
- Low-emission fermentation (including closed halls, gas-tight Storage of liquid digestate, optimized gas usage)
- Use of heat from the conversion of biogas to electricity!

Although in Germany the bio bin is already successfully introduced, there are not yet connected to the bio-waste collection authorities and people concerns about the bio-waste collection.

The resistances are against the compulsory introduction of bio-waste collection since January 2015. Separate collection results in higher costs. These costs are acceptable and must to be defrayed by the waste producer. The backyard composting captures and recycles not enough organic waste. Too much bio-waste is located in the residual waste. More than 100 kg bio-waste is collectable in bio bins even in areas with low population.

In the worldwide comparison the use of bio-waste in Germany is of a good level. The tasks for the coming years can be summarized as follows:

- All counties and cities (mandated waste management authorities - öRE) have to introduce or improve the separate bio-waste collection (bio bin and green waste);
- Possibly higher waste fees are economically viable;
- The share of fermentation (AD) of organic wastes needs to be increased;
- The management of digestate must be improved to reduce the release of greenhouse gases;
- The use of heat from biogas electricity production needs to be increased.

REFERENCES

1. AGEBA - Arbeitsgemeinschaft Energiebilanzen. 2015. <http://www.ag-energiebilanzen.de/>
2. BGK – German Compost Quality Assurance Organisation 2014. Presentation of the Bundesgütegemeinschaft Kompost e.V. <http://www.kompost.de/>
3. Cuhls, C., Mähl, B., Clemens, J. 2015. Ermittlung der Emissionssituation bei der Verwertung von Bioabfällen. UBA (Germany's main environmental protection agency). Text 39/2015
4. Deutsche Bundesregierung (editor). 2001. Abfallverzeichnis-Verordnung vom 10. Dezember 2001 (BGBl. I S. 3379), die zuletzt durch Artikel 5 Absatz 22 des Gesetzes vom 24. Februar 2012 (BGBl. I S. 212) geändert worden ist. Berlin
5. Deutsche Bundesregierung (editor). 2013. Bioabfallverordnung in der Fassung der Bekanntmachung vom 4. April 2013 (BGBl. I S. 658), die zuletzt durch Artikel 5 der Verordnung vom 5. Dezember 2013 (BGBl. I S. 4043) geändert worden ist. Berlin
6. Kehres, B. 2015. Emissionssituation bei der Bioabfallverwertung. Bundesgütegemeinschaft Kompost e.V. www.kompost.de
7. Krause, P., Oetjen-Dehne, R., Dehne, I., Dehnen, D. & Erchinger, H. 2014. Compulsory implementation of separate collection of bio-waste Federal Environment Agency (Germany), TEXTE 84/2014. Berlin
8. Oetjen-Dehne, R., Krause, P., Dehnen, D. & Erchinger, H. 2014. Obligatory introduction of separate collection of bio-waste. Müll und Abfall. 6. 2014. 309 – 316
9. Struwe, J. 2010. Gesamtökologischer Vergleich von stofflicher und energetischer Verwertung. Abfalltag Baden-Württemberg 2010. <http://www.prognos.com>
10. The European Commission (editor). 2014. COMMISSION DECISION of 18 December 2014 (2014/955/EU) amending Decision 2000/532/EC on the list of waste pursuant to Directive 2008/98/EC of the European Parliament and of the Council
11. United States Environmental Protection Agency. 2014. EPA CFR40/503 Biosolids PART 503—STANDARDS FOR THE USE OR DISPOSAL OF SEWAGE SLUDGE Subpart B—Land Application
12. VHE. 2012. Bio- und Grünguterfassung in Deutschland. <http://www.vhe.de/fileadmin/vhe/pdfs/Publikationen>. 17.05.2015

UTILIZATION OF WOODWASTE AS CONTAINER MEDIA BY ACCELERATED COMPOSTING

Hoda Bakhshizadeh¹, **H. Borazjani**², R. C. Sloan³, and S. S. Worthey³

1 Former graduate student, Mississippi State University, Department of Sustainable Bioproducts. Current address: Soybean Plant Pathology Lab, Bayer CropScience, Memphis, TN 38120, USA

2 Mississippi State University, Department of Sustainable Bioproducts, Box 9820, Mississippi State, MS 39762, USA

3 Mississippi State University, Northeast Research & Extension Center, Box 9389, Mississippi State, MS 39762, USA

The objectives of this study were: To determine the suitability of quick composted forest products woodwastes as ornamental plant media. In a 3-month accelerated composting study, woodwastes were amended with (20% & 40%) poultry litter, (1% & 2%) ammonium nitrate, or non-amended. Composting was run in fifteen 130-liter containers outdoor and samples were collected at day 90 for compost maturity (toxicity), carbon-to-nitrogen ratio and green house evaluations. The amendments containing 40% poultry litter showed significantly higher mass weight and vigor grading in transplanted zinnia and gardenia than other treatments and was comparable to commercial media. Overall, results indicated that the amendment of woodwastes with poultry litter could produce a comparable product to currently used commercial container media.

NOVEL COUPLED SURFACE MODIFICATION AND FROTH FLOTATION SEPARATION OF HALOGENATED PLASTICS FROM HAZARDOUS WASTE (ASR/ESR) PLASTICS WITH NANOSCALE METALLIC CALCIUM COMPOSITE

Srinivasa Reddy Mallampati, Je Haeng Heo and Min Hee Park

(Department of Civil and Environmental Engineering, University of Ulsan, Daehak-ro 93, Nam-gu, Ulsan 680-749, Republic of Korea)

ELVs (End of Life Vehicles) and WEEE/E-waste (Waste Electric and Electronic Equipment), are increasingly important secondary sources of ferrous metals, nonferrous metals and plastics. About 1 million ELVs are generated every year in Korea and the generation of WEEE has rapidly increased in recent years. The most problematic fractions of WEEE and ELV recycling treatments that have been mainly landfilled/incinerated in the past are shredding residues (SRs): automobile shredder residue (ASR) from ELVs and electronic waste shredder residue (ESR) from WEEE, composed of plastics, small metals, wires, rubber, textiles, etc.. Plastics are the most important portion of ASR and ESR; around 30% of WEEE plastics contain fire retardants, which are mostly based on polybrominated aromatic compounds. Approximately 50% of waste WEEE plastics are high-impact polystyrenes, with the next largest fraction being acrylonitrile-butadiene-styrene (ABS) copolymer; poly (vinyl chloride) PVC also comprise around 6–8 wt% of the total mixed plastics in ASR/ESR. The disposition and management of ASR and ESR is an emerging environmental issue of concern to the solid waste community in Korea and around the world. A Korean directive regarding resource recycling of electrical and electronic equipment and vehicles set a recycling target, including thermal recycling, at 85% by 2006 and 95% by 2015. When halogenated plastics such PVC and ABS are subjected to incineration or uncontrolled burning processes for disposal, their high bromine/chlorine content can contribute to the formation of highly toxic and persistent chlorinated/brominated dioxins. Furthermore, some of its chemical additives may leach, during landfilling. Therefore, any end-of-life product or waste stream involving products containing hazardous halogenated plastics must be separated/recovered in a way that minimizes the potential impact on human health and the environment.

Selective surface hydrophilization of PVC by a nanometallic Ca/CaO composite was successfully demonstrated in this study as a means to allow separation of PVC from other E-waste plastics. Nanometallic Ca/CaO treatment enhanced the wettability of the PVC surface; the treatment made all plastics tested more hydrophilic, but was quite selective for PVC, decreasing its water contact angle by 18°. SEM images of the plastics showed that the treatment considerably changed the surface morphology and roughness of PVC compared to other plastics. SEM-EDS elemental analysis showed that the amount of Cl detectable on PVC plastic surface significantly decreased after nanometallic Ca/CaO treatment. XPS analysis confirmed an increase of the hydrophilic functional groups C–O, C=O, and (C=O)–O on the PVC plastic surface after nanometallic Ca/CaO treatment. The treatment allowed PVC to be separated from other E-waste plastics by means of froth flotation; the plastics were separated into a PVC fraction and a PVC-free fraction, even though the plastic particles were of nonuniform size and shape. Under the condition of 100 rpm mixing, 100% of the PVC settled, and the settled fraction was 96.4% PVC; thus, the floating fraction was 100% PVC-free. The total recovery of non-PVC plastics was nearly 100%, which is greatly improved from the 20.5 wt% of light plastics that are recovered by conventional wet gravity separation. Therefore, the hybrid nanometallic Ca/CaO treatment and froth flotation separation developed herein is a simple and effective method to separate hazardous halogenated plastics from ASR/ESR. This convenient method will facilitate the industrial application of plastics flotation, and the present work provides technical insights into the process of hazardous halogenated plastics recycling. *This work was supported by National Research Foundation of Korea (NRF), funded by the Ministry of Education (2014R1A1A2055487).*

CHARACTERIZATION OF CARBON-BASED BIOCHAR FROM GRAPSEED PYROLYSIS

Nathaniel F. Adegboyega & William C. Hockaday (Baylor University, Waco, TX, USA)
Chris Cunningham & Mark Kelm (Constellation Brands Inc., Madera, CA, USA)²⁶

We report on the morphological, chemical, and spectroscopic characteristics of carbon-based biochar manufactured by the pyrolysis of grape seed wastes (from the winemaking industry). The morphology of grape seeds is such that the embryo and endosperm, which comprise starches, lipids, and protein are encased in a ligno-cellulosic seed coat. The spatially-segregated chemistry of the seed make for an interesting precursor for multi-functional carbon-based sorbents. In this study we use combination of microscopy and spectroscopy to characterize the pyrolytic transformation of grape seeds to biochar carbons. Scanning electron microscope (SEM) images revealed that the general seed morphology remains intact after pyrolysis. The cell wall structure integrity is maintained while the development of an extensive ``pores`` network is restricted to the endosperm.

Pyrolysis at 350 °C resulted in an increase in elemental C concentration from 54.04 wt % to about 71.74 wt %. An extended drying (pretreatment) of grape seed sample before pyrolysis did not significantly influence the C content after pyrolysis. The solid state¹³ C NMR of biomass before pyrolysis showed abundant liquid-like resonances in the range 14 to 34 ppm and 128 – 129 ppm attributable to unsaturated fatty acids in grape seed oils. Pyrolysis at 350 °C caused an increase in the concentration of both aliphatic and aromatic carbons at the expense of oxygen-substituted carbons. Aromatic carbon concentrations increased further at higher pyrolysis temperatures and longer duration of heating. Biochars formed at both 350 °C and 500 °C exhibited extreme hydrophobicity (poor wettability), as revealed by a simple water droplet test.

EFFECT OF TIRE RUBBER ASH ON BITUMINOUS MIXES USED FOR ROADWAY PAVEMENT

Tapash Kumar Roy

(Indian Institute of Engineering Science and Technology Shibpur Howrah-711103, W.B., India)

ABSTRACT: Scrap tires are abundant and alarming waste throughout the globe. Massive stockpiles of such tires occupied valuable land and also pollutes environment. Further steady increase in traffic intensity, overloading of commercial vehicle and the significant variation in daily and seasonal temperature demands the improved quality of the road for overcoming the early development of distresses in the flexible pavement constructed by conventional bituminous mix. Modification of bituminous mix by utilizing of such waste tires for construction of flexible pavement is the prime objective of this investigation. Outcome of the experimental study indicated that waste tire modified bituminous mix shows the lesser consumption of bitumen with better stability value of amounting more than 142% compared to that of conventional mix with much reduction in flow characteristics.

INTRODUCTION

The road needs to be updated to meet the quality and quantity of performance to sustain repeated vehicle loadings, climatic changes and riding quality. In India, it is estimated that over 42 lakh kilometers of road exists which carries close to 90% of passenger traffic and 70% of freight transport. The major part of such roads are flexible in nature, deteriorated rapidly during their design life in some parts of India due to different causes e.g. high traffic intensity, overloading of commercial vehicle, improper drainage system etc. resulting early development of distress condition in the form of cracks, rutting, raveling etc. So modification in the bituminous mixtures is needed to sustain the stresses of vehicles with other changes in properties. On the other hand, due to the worldwide growth of the automobile industry and the increasing use of cars as the main means of transport have tremendously boosted tire production in recent decades. This has generated massive stockpiles of used tires. Extensive research projects were carried out on how to use used tires in different applications. The benefits of stabilizing the stone mastic asphalt (SMA) mixture in flexible pavement with shredded waste plastic was developed by Bindu & Beena (2010). Performance of rubber as an asphalt concrete modifier was evaluated by performing experiments on the shear flow properties and creep rupture behavior (Zaman et al 1995). So the reutilization of such wastes could be a suitable way of solving environmental concerns, offering low-cost recycled resources of polymer. This investigation deals with the utilization of crumb tire rubber for producing better bituminous mix by enhancing their properties.

MATERIALS USED AND THEIR PROPERTIES

Present study involves the use of materials like aggregate, bitumen, and waste rubber for producing bituminous mixes.

Aggregate. The mineral aggregate used in this study were obtained from Pakur (Jharkhand) quarry. Representative samples have been tested in the laboratory and results are presented in Table-1.

Bitumen. In this study, 60/70 pen grade bitumen has been selected. The physical properties of the same are given in table 2 along with their permissible limits as per IS specifications.

Waste Rubber. Sources of waste rubber are the various commercial vehicles like trucks, busses, and trailers. In this study, waste tire of buses was used as rubber waste. Collected rubber waste has been

powdered by the grinding machine and subjected to mechanical sieve analysis to get the desired particle size passes from 150 mm sieves and retained in 75 mm size. Composition of such waste rubber has been summarized in the Table 3.

TABLE 1. Physical properties of aggregate

Test	Result
Impact value	21.81%
Flakiness Index	15.9%
Elongation Index	14.3%
Abrasion Value	23.24%
Specific gravity	2.78
Water absorption	0.14

TABLE 2. Physical properties of Bitumen

Type of test	Test Value	Permissible Limit
Penetration Value at 25 ⁰ c (1/10 mm)	68	60-70
Ductility Value at 25 ⁰ c (cm)	>100	>75
Softening Point (°C)	54	40-55
Specific gravity (kg/m ³)	1.04	>0.99

TABLE 3. Composition of bus tire

Materials	Composition in%
Rubber/Elastomer	45
Carbon black	22
Metal	25
Zinc oxide	2
Sulphar	1
Additives	5

SAMPLE PREPARATION

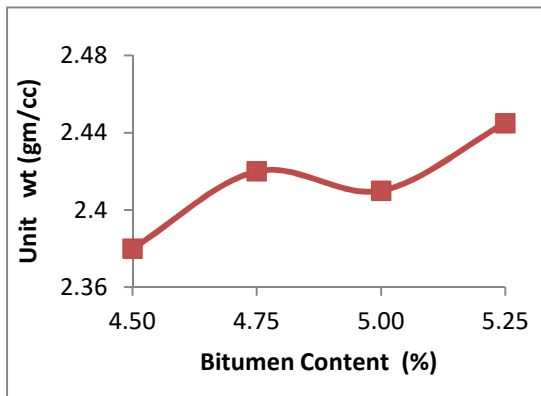
The mix design for Dense Bituminous Macadam (DBM) with Grading-I have been selected for this investigation by using the Marshall method. Primarily conventional bitumen was weighted and mixed with various percentages of waste tires (0%, 6%, 8%, and 10%) by weight of bitumen. Then the wastes added bitumen was kept in the mechanical stirrer for 1 hr. at 3500-4000 rpm at 180°C to 200°C temperature to convert the same into homogeneous modified bitumen. Next they were mixed with the preheated aggregate and filler for preparing the samples. Then Marshall Test was performed for evaluating optimum bitumen content (OBC) and other Marshall Parameters.

RESULTS AND DISCUSSION

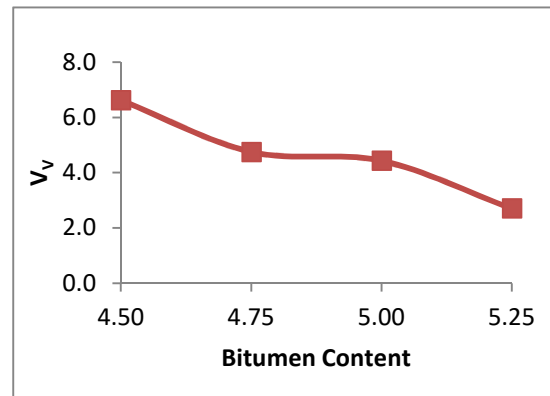
Specimens were prepared by using cement as filler @ 2% by wt. of aggregate with varying bitumen contents of 4.5%, 4.75%, 5.00% and 5.25% and tested and OBC was determined. Evaluated results are given in Figure 1 and Table 4.

Experimental results indicated that optimum bitumen conten of DMB mix is 5.08%. Other Marshall Properties like stability and flow value are 21.35 kN and 2.97 mm respectively which satisfied the standard specifications recommended by MORT&H.

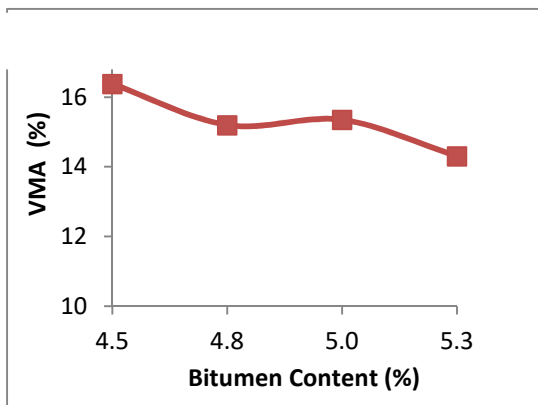
Further Marshall Properties along with Optimum bitumen content were determined by mixing various % of waste Rubber ranging as 0%, 6%, 8%, and 10% with the bitumen by following the Marshall method and tested results have been furnished in the table 5.



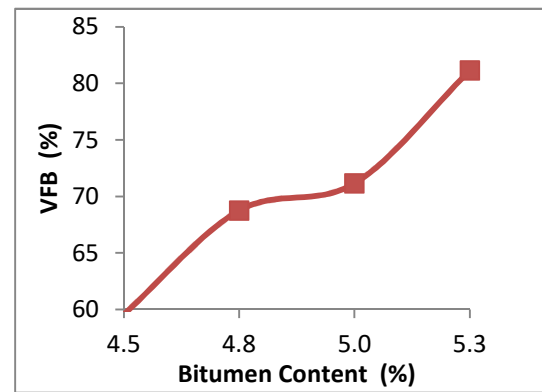
(a) Bitumen Content Vs Unit Wt



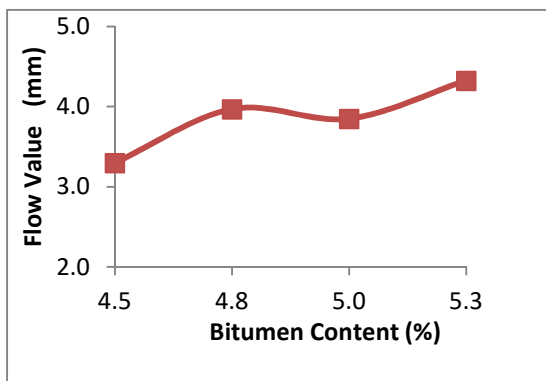
(b) Bitumen Content Vs V_v



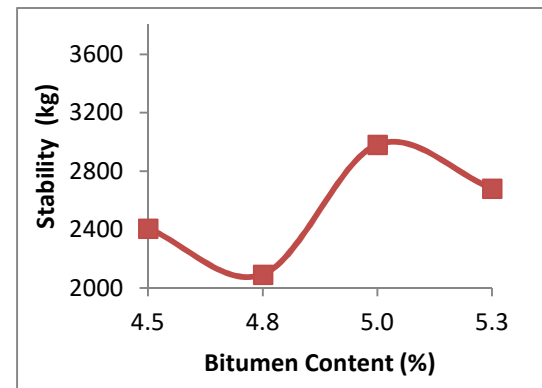
(c) Bitumen Content Vs VMA



(d) Bitumen Content Vs VFB



(e) Bitumen Content Vs Flow Value



(f) Bitumen Content Vs Stability

FIGURE 1. Comparison between Different Marshall Parameter Vs Bitumen Content

Marshall Properties as evaluated in table 5 indicates that maximum stability value of amounting 51.8 kg is obtained for adding 8 % of waste rubber ash as modifier by keeping the flow value as 3.8 mm. Where optimum bitumen content remained as 4.78% for DBM mix by using said waste tire rubber ash as modifier. In comparison with the conventional mix of DBM, it is observed that waste tire modified bituminous mix shows the lesser consumption of bitumen with better stability value of amounting more than 142%. All other evaluated parameters also satisfy the standard specification of MORTH.

TABLE 4. Evaluated Marshall Properties of DBM against OBC

Filler	Optimum Bitumen Content (%)	Vv(%)	VMA(%)	VFB (%)	Stability (KN)	Flow (mm)
Cement	5.08	4.15	15.36	73	21.35	2.97

TABLE 5. Evaluated Marshall Properties by using Rubber ash as modifier

Modifier	Quantity (%)	OBC (%)	Marshall Parameters					Unit Wt (gm/cc)
			Stability (kg)	Flow (mm)	VMA (%)	VFB (%)	V _v	
Rubber Content	6	4.95	47.0	3.75	14.0	73	3.7	2.41
	8	4.78	51.8	3.8	15.1	75	3.2	2.41
	10	4.82	48.7	3.91	18.3	72	5.1	2.37

CONCLUSION

From the above investigation it may be concluded that the scrap tires discarded in the environment, including tire composition, adverse environmental effects, threats to public health and safety, and solid waste management. However, addition of such waste in construction of dense bituminous macadam reduces the optimum bitumen content compared to the conventional mix. Significant observation is made for utilizing tire rubber of 8% in the DBM mix, where stability values increased more than 142% by reducing the flow value along with the reduction in optimum bitumen content. So use of 8% tire rubber in construction of dense bituminous macadam in roadway pavement may be encouraged as a cost effective mix proportion by achieving better performance along with environmental benefits.

REFERENCES

- Bindu, C.S., K.S., Beena, (2010) "Waste plastic as a stabilizing additives in stone mastic asphalt", *International Journal of Engineering and Technology*, Vol.2(6), pp.379-387.
- IRC:37-2001, Guidelines for the Design of flexible pavements, *Indian Roads Congress*.
- IS: 1202-1978, "Methods for Testing Tar and Bituminous Materials; Determination of Specific Gravity", *Bureau of Indian Standards*, India.
- IS: 1203-1978, "Methods for Testing Tar and Bituminous Materials; Determination of Penetration", *Bureau of Indian Standards*, India.
- IS: 1205-1978, "Methods for Testing Tar and Bituminous. Materials; Determination of Softening Point", *Bureau of Indian Standards*, India.
- IS: 1208-1978, "Methods for Testing Tar and Bituminous Materials; Determination of Ductility", *Bureau of Indian Standards*, India.
- Zaman, A.A., A.L., Fricke, and C.L., Beatty, (1995), "Rheological properties of rubber modified asphalt", *J.Transp. En.*121, pp.461-467.

STRUVITE RECOVERY FROM WASTEWATER AND REUSE AS AMENDMENT FOR HEAVY METALS IMMOBILIZATION IN SOIL

Hao Wang, Xuejiang Wang, Jing Zhang, Jingke Song
(Tongji University, Shanghai, P.R.China)

Ammonia nitrogen (AN) and phosphorus (P) were recovered from rare-earth wastewater by using the formation of struvite, which was used as the amendment with plant ash (PA) for immobilization of copper (Cu), lead (Pb) and chromium (Cr) in contaminated soil. AN removal efficiency and residual P reached to $95.32 \pm 0.73\%$ and $6.14 \pm 1.72 \text{ mg L}^{-1}$ under optimal conditions: $\text{pH}=9.0$, $n(\text{Mg}):n(\text{N}):n(\text{P}) = 1.2:1:1.1$, which were obtained from response surface methodology (RSM). The effects of mass ratio of precipitates and plant ash, immobilization time, soil pH, humic acid (HA) and fulvic acid (FA) on available concentration of Cu, Pb and Cr were investigated. It was shown that immobilization was most effective with the mass ratio of PP/PA at 1:3, while the PA addition further led to pH increase, which was beneficial for heavy metal immobilization in the bulk soil. The minimum available concentration of Cu, Pb and Cr separately reduced to $320.82 \text{ mg kg}^{-1}$, $190.77 \text{ mg kg}^{-1}$ and $121.46 \text{ mg kg}^{-1}$ with the increasing of immobilization time. HA and FA were beneficial to Cu immobilization, but both of which showed no effect or even a negative effect on the immobilization of Pb and Cr.

HYDROTHERMAL SYNTHESIS OF ZEOLITE A FROM BOTTOM ASH OF SUGAR INDUSTRY ITS CRYSTALLIZATION

Noor-ul-Amin and Yousaf Hameed

(Department of Chemistry, Abdul Wali Khan University, Mardan, 23200 Pakistan)²⁹

Zeolite A is indirectly synthesized from bottom ash of sugar industry using hydrothermal conversion method. Active SiO_2 and Al_2O_3 were obtained from bottom ash and aluminium sulphate respectively. The synthesis involve the dissolution of amorphous aluminosilicate releasing $[\text{SiO}_2(\text{OH})_2]_2$ and $\text{Al}(\text{OH})_4$, formation of sodium aluminosilicate gel and crystallization of zeolite A. The obtained zeolite was characterized using X-ray diffraction (XRD), X-ray fluorescence (XRF), Scanning electron microscope (SEM) and Fourier Transform Infrared spectroscopy (FTIR). The results showed that the amorphous silica obtained from ash was dissolved completely during the first hour of the crystallization stage. With the increase in crystallization time up to 3 h, a rapid growth of pure zeolite crystals reached its maximum limit. An excess time resulted in further dissolution of zeolite A and replacement by hydroxyl sodalite.

RECYCLING SPENT LITHIUM-ION BATTERY FOR FUNCTION MATERIAL DEVELOPMENT

Fu-Shen Zhang, Meng-Meng Wang

(Research Center for Eco-environmental Sciences, Chinese Academy of Sciences, 18 Shuangqing Road, Beijing 100085, China)

In the current study, an environmental benign process namely mechanochemical approach was developed for cobalt and lithium recovery from spent LIBs. The main merit of the process is that neither corrosive acid nor strong oxidant was used. In the proposed process, lithium cobalt oxide (obtained from spent LIBs) was co-grinded with various additives in a hermetic ball milling system, followed by a water leaching procedure. Experiment results indicated that EDTA was the most suitable co-grinding reagent, and 98% of Co and 99% of Li were respectively recovered under optimum conditions: LiCoO₂ to EDTA mass ratio 1:4, milling time 4 h, rotary speed 600 r/min and ball-to-powder ratio 80:1, respectively. Mechanisms study implied that lone pair electrons provided by two nitrogen atoms and four hydroxyl oxygen atoms of EDTA could enter the empty orbit of Co and Li by solid-solid reaction, thus forming stable and water-soluble metal complexes Li-EDTA and Co-EDTA. Moreover, the separation of Co and Li could be achieved through a chemical precipitation approach. This study provides a high efficiency and environmentally friendly process for Co and Li recovery from spent LIBs.

REUSE OF GREEN WALNUT SHELL TO PRODUCE DYE

Ruhsar Arabacıođlu, *Neslihan Dođan-Sađlamtimur* and Ersen Turađ
(Niđe University, Niđe, Turkey)

In terms of environmental technologies, in the pyramid of waste management hierarchy, conversion of waste to another product is named as reuse. Each year very large quantities of walnut shells are released as herbal originated waste after selling walnut seeds. Therefore, development of new using areas for these wastes is required under the concept of industrial ecology. In this study, for obtaining dye from green walnut shells, following experimental steps have been planned; (a) chopping small pieces from the green wallnut shells, (b) eliminating of humidity from the chopped shells after dried in oven, (c) grinding of these shells by using grinding mill to increase of contact surface and decrease of piece size, (d) extraction processing with methods of Soxhlet extraction by using of ethanol solution, (e) evaporating of ethanol solution in controlled way. New experimental designs can be arranged in accordance to obtained results from these experiments.

The aim of this study is to obtain of natural dye from wasted green wallnut shells for dye industry. It is believed that it should be a positive step to meet the need of dye in our country. In terms of new and advanced technology, conversion of wasted green walnut shells to dye has acquired an important place in recent years.

RECYCLING MERCURY-IMPACTED SCRAP METAL: KEY ISSUES AND RESEARCH NEEDS

Molly E. Finster and Corrie E. Clark
(Argonne National Laboratory, Lemont, IL 60439, USA)

The recycling of mercury-impacted scrap metal can emit measurable amounts of mercury; however, existing characterization data are insufficient to fully understand the origin, key sources, and concentrations of mercury within scrap metal and the recycling process. Currently, industry-specific mercury emissions guidance values exist for many known anthropogenic mercury sources (e.g., coal-fired utility plants and waste incinerators), but are largely nonexistent for scrap metal processing and recycling facilities. Given the lack of significant guidance for recycling mercury-impacted scrap metal, these other values can provide a useful framework to potentially guide the development of mercury acceptance and release criteria/limits for recycling facilities. To better assess measures to protect human and environmental health from potential hazards that might be posed by the processing and melting of mercury-impacted metal, information on the origin, source, nature, and extent of mercury-impacted metal in scrap is also important for assessing measures to protect scrap metal recycling workers from potential health and safety hazards that might be posed by the processing and melting of mercury-impacted metal.

THE POTENTIAL OF EFFECTIVE MICROORGANISM (EM) TO PROMOTE THE PHYTOREMEDIATION OF URANIUM POLLUTED WATER

Jing Zhu, Ke Chen, Renhua Huang, Gangxue Luo

(State Defense Key Laboratory of Fundamental Science on Nuclear Wastes and Environment, Southwest University of Science and Technology; School of Life Science and Engineering, Southwest University of Science and Technology, Mianyang, Sichuan, China)

The influence of effective microorganism (EM) on uranium accumulation and endurance in *Eichhornia crassipe*, *Pistia stratiotes* L. *Lemna minor* L. were investigated in uranium polluted solutions. With applied EM, the dismutase (SOD), catalase (CAT) and peroxidase (POD) activities of *E. crassipe* and *P. stratiotes* L. increased more significantly than those of the control without EM applied. In addition, the uranium accumulation amount in root, accumulation factor and transfer factor of *P. stratiotes* L. increased with 22.6%, 74.0% and 160.0% respectively, as well as the maximum uranium accumulation factor of *E. crassipes* increased with 172.7% compare to the control without EM applied. The results indicated that the EM applied are positive to the resistance, enrichment and transfer ability of *E. crassipes* and *P. stratiotes* to the uranium stress. However, the applied EM appeared to be negative to the uranium resistance and accumulation of *L. minor* L. with the activities of CAT, POD and SOD decreased, contents of malondialdehyde and proline increased and especially the chlorophyll contents and biomass decreased drastically. Therefore, our results suggested the aquatic plants *E. crassipes* and *P. stratiotes* L. combined with EM might effectively promote the potential of phytoremediation of uranium polluted water.

GRASS AND MICROBIAL COMBINED REMEDIATION TO URANIUM-CONTAMINATED SOIL

Xiaoming Chen and *Xuegang Luo*

(State Defense Key Laboratory of Fundamental Science on Nuclear Wastes and Environment,
Southwest University of Science and Technology, Mianyang, Sichuan, China)

Xichao Hao and Ke Chen

(Southwest University of Science and Technology, College of Life Science and Engineering, Mianyang,
Sichuan, China)

In order to build a grass and microbial combined remediation system for uranium-contaminated soil, the grass seeds germination, the growth and uranium enrichment ability of the grass plant under uranium stress pot soil, screening of microbe combination, and the effect of grass and microbial combined remediation were investigated respectively. The results showed seven species of grass seeds from 24 species had a relatively high germination rates at uranium stress condition. There was a promotion ability for seed germination rate at the uranium concentration less than 50 mg·L⁻¹, while the uranium concentration more than 100 mg·L⁻¹, had an obvious inhibition effect. The different species of grass plant had a significant growth difference under different uranium concentration. *Lolium multiflorum* had a high pot accumulation rate (10.36 mg·pot⁻¹ uranium) at uranium concentration of 150 mg·kg⁻¹, while *Lolium perenne* had the highest pot accumulation (3.58 mg·pot⁻¹ uranium) at uranium concentration of 50 mg·kg⁻¹. And *L. multiflorum* had the highest transfer factor (0.87) at uranium concentration of 100 mg·kg⁻¹. The microbe combination including 20% *Bacillus mucitagnosus* and 10% *Bacillus subtilis* was screened out, which had a high yield of IAA, ACC deaminase and siderophore. *Lolium multiflorum* Lamk connected with this microbe combination could promote the uranium accumulation rate up to 50% than control. In conclusion, the connection of grass and microbes have a effective remediation ability to uranium-contaminated soil.

**POTENTIALLY USEFUL PLANTS FOR PHYTOREMEDIATION OF HYDROCARBONS IN
SUBTROPICAL ZONE: CAMEROON CASE**

Matsodoum N. P. , Wanko N. A.

(University of Strasbourg, Strasbourg, France)

Ndemba Etim S. G., Djumyom Wafo G. V., Djocgoue P. F., Kengne Noumsi I. M.

(University of Yaounde I, Yaounde, Cameroon)

Identification of plants is prerequisite in the development of phytoremediation process. 4 cities in Cameroon have been investigated for the circumstance. The methodology consisted of studying vegetation of 26 sites of 36 m² each (polluted and unpolluted) in each city through floristic survey. 106 species belonging to 76 genera and 30 families have been identified in polluted sites, unlike the control sites where floristic diversity was much higher with a total of 166 species contained in 125 genera and 50 families. Among the most represented families in both sites, Cyperaceae (10), Asteraceae (8) and Amaranthaceae (5) have higher taxonomic richness in polluted sites compared to the control. Species richness and Shannon diversity index in hydrocarbon-polluted sites (8 to 18 species and 1.6 to 2.7 bits/ind.) are significantly lower than the control sites (24 to 34 species and 2.7 to 3.2 bit/ind.). Based on their relative frequency (Fri > 10%) and their relative abundance (A > 10% and 10% > A > 7%) on hydrocarbon-polluted sites, pollutant-tolerant or plants potentially useful for phytoremediation of hydrocarbons are dominated by Poaceae (*Eleusine indica* (L.) Gaertn., *Cynodon dactylon* (L.) Pers., *Acroceras zizanioides* (Kunth) Dandy, *Panicum maximum* Jacq. and *Axonopus compressus* (SW) P.Beauv.) ; followed by Amaranthaceae (*Amaranthus spinosus* (L.), *Alternanthera sessilis* (L.) R. Br. ex DC†); Asteraceae (*Vernonia cinerea* (L.), *Synedrella nodiflora* (L.) Gaertn.) ; Euphorbiaceae (*Euphorbia hirta* L., *Phyllanthus amarus* Schum. & Thonn.) ; Commelinaceae (*Commelina benghalensis* L.) ; Cyperaceae (*Cyperus esculentus* L.) ; Capparaceae (*Cleome ciliata* Schum. & Thonn.) and Acanthaceae (*Asystasia gangetica* (L.) T. Anderson). These plants could be tested in preliminary trials of phytoremediation to cleanup hydrocarbon-polluted soils in subtropics.

**EX-SITU PHYTOREMEDIATION OF HYDROCARBON CONTAMINATED SOIL WITH
CROTALARIA PALLIDA AIT.**

Partha Pratim Baruah and Plabita Baruah (Gauhati University, Guwahati, Assam, INDIA)
Suresh Deka (Institute of Advanced Study in Science and Technology, Guwahati, Assam, INDIA)

The total petroleum hydrocarbon (TPH) contamination has been recognised as a serious threat to natural ecosystems. The affect of which has been frequently felt in the oil exploration, drilling and production areas as well as in the spillages, leakages and accident sites during transportation. To overcome the constraints of other competing physical and chemical alternatives, application of phytoremediation of TPH is being explored. As the selection of suitable plant species is one of the main criteria for success in phytoremediation and for development of viable remediation technology, the present endeavour explored for selecting a suitable candidate from natural habitat and identified *Crotolaria pallida* Ait. as one of the potential plant species for the purpose. Result revealed that maximum dissipation of TPH was upto 87.05 % from the soil in a progressive way in relation to growth of the plant and time which was evidenced by concomitant reduction of pH and total organic carbon and subsequent increase of water holding capacity.

**ASSESSMENT FOR REMOVING MULTIPLE POLLUTANTS BY PLANTS IN
BIORETENTION SYSTEMS BASED ON ISPA MODEL**

Xiaohua Yang, Yi Ye, Meishui Li

(School of Environment, Beijing Normal University, Beijing, China)

Bioretention system is a complex uncertain system for removing multiple pollutants by plants. To select the best plant species for removing multiple pollutants rationally in bioretention systems, an improved set pair analysis (ISPA) model, is established, in which set pair analysis theory is introduced and the weights are determined by use of the maximum entropy principle and the improved analytic hierarchy process method. And the index systems and criteria of the bioretention systems assessment are established in this study. ISPA model is used to assess five plants for removing multiple pollutants in bioretention systems. Certain and uncertain information quantity of the bioretention system is calculated by connection numbers in the ISPA model. Results show that ISPA model can fully take advantage of certain and uncertain knowledge, subjective and objective information. Finally, we make some suggestions for the bioretention system management in Beijing. This study will provide a simple and useful guide for the comprehensive assessment of multiple pollutant removal by plants in complex ecological systems.

SYNTHESIS AND PROPERTIES OF BIODEGRADABLE POLYESTERS BASED ON BIOMASS MONOMERS

Yang Zhang, Jun Xu, Baohua Guo
(Tsinghua University, Beijing, China)

With increasing worldwide concern about greenhouse effects and white pollution of polymers, biobased monomers and biodegradable polymers made from renewable sources have attracted much attention recent years. Chemicals in furan family and succinic acid have been regarded as the most important building blocks derived from biomass. In our work, polyesters possessing two type molecular chain structure (random and block) which show different thermal and mechanical properties are synthesized. First, random copolymer poly(butylene succinate-*co*-butylene furandicarboxylate) (PBSF) with weight average molecular weight ranging from 55 000 to 13 000 g/mol were synthesized from 2,5-furandicarboxylic acid, succinic acid and 1,4-butanediol via polycondensation. The glass transition temperature increases continuously with increasing BF unit content from -38 °C to 37 °C. The melting temperature decreases from 113.4 °C to 69.1 °C then rise again up to 164.3 °C with increasing BF unit content from 0-100 % mol. As a result, the introducing of furan rings increases the rigidity of molecular chains and the melting temperature can be adjusted by altering the contents of furan rings in a wide temperature range through random copolymerization. Furthermore, multiblock copolymer poly (2,5-furandimethylene succinate)-*b*-poly (butylenes succinate) (PFS-PBS) were synthesized from 2,5-dihydroxymethylfuran, 1,4-butanediol and succinic acid by chain-extension reaction of dihydroxylated poly (2,5-furandimethylene succinate) and poly (butylenes succinate) using 1,6-hexamethylene diisocyanate as chain extender. The weight average molecular weight of PFS-PBS with different composition is range from 72 000 to 14 000 g/mol. The melting temperature remains relatively unchanged at 109 °C but the crystallizability decreases with increasing PFS content. Thus, the structure and properties of PFS-PBS can be modulated from a crystalline polymer with good tensile strength (13-33MPa) to an amorphous polymer of high elongation (800-1100%). So, biodegradable PFS-PBS can maintain a high end-use temperature because of unchanged molecular length of crystalline PBS block and widely tunable mechanical properties are achieved only by changing the composition of two different blocks via block copolymerization.

**ECOSYSTEM ASSESSMENT
AND
RESTORATION**

**AN ECOLOGICAL STUDY OF REPRODUCTION IN CORINGA MANGROVE FOREST,
ANDHRA PRADESH, INDIA**

Aluri Jacob Solomon Raju

(Department of Environmental Sciences, Andhra University, Visakhapatnam 530003, India)

ABSTRACT: Mangroves are dynamic and unique inter-tidal ecosystems, common in tropical and subtropical coastal environments. They are among the world's most productive ecosystems and are important in protecting coasts from erosion by fierce tides, in promoting the diversity of marine organisms and fisheries by contributing a quantity of food and providing favourable habitats for animals. These economic uses of mangroves indicate that they play an important role in the lives and economies in the coastal regions of different countries. Mangrove forests are under immense threat worldwide due to their multiple economic uses and alterations of freshwater inflows by various upstream activities in catchment areas. Mangrove plants with unique adaptations play a crucial role in sustaining life in mangrove forests. Their reproductive biology is central to understanding the structural and functional components of mangrove forests. The success of sexual reproduction and subsequent population expansion in mangrove plants is linked to flowering timings, pollinators and tidal currents. Viviparous and cryptoviviparous plants are true mangroves while non-viviparous ones are mangrove associates. The dispersal propagule is seedling in viviparous and non-viviparous plants while it is seed in nonviviparous plants. In this study, viviparous and crypto-viviparous species were included for study. These species are self-compatible, self-pollinating and also cross-pollinating; such a breeding system is a requirement for the success of sexual reproduction and subsequent build up and expansion of population. They are entomophilous in the study region. The viviparous plants include *Ceriops tagal*, *C. decandra*, *Rhizophora apiculata*, *R. mucronata*, *Bruguiera gymnorrhiza* and *B. cylindrica*. The non-viviparous plants include *Avicennia alba*, *A. marina*, *A. officinalis*, *Aegiceras corniculatum* and *Aegialitis rotundifolia*. Sexual reproduction and regeneration events are annual in these plants and are dependent on local insects, tidal currents and nutrient content in estuarine environment. In recent times, erratic and insufficient rainfall together with industrial pollutants released into rivers is causing negative effects on the growth, development and regeneration of mangrove flora. In effect, there is a gradual decrease in mangrove cover. Added to this is continuous exploitation of mangrove plants for fuel wood, creation of shelters for cattle and changes for industrial establishments and aquaculture development in estuarine regions. As a consequence, the existing mangrove cover is struggling to survive and also not in a position to support local needs and provide livelihood opportunities through fishery resources. Further, reduced mangrove cover is showing catastrophic effects on fishing communities who live along the shore line during the period of cyclonic surges and tsunami events.

Key words: Mangroves, pollination, sexual system

INTRODUCTION

Mangrove plants are the key constituents and play a crucial role in sustaining life in mangrove forests. They display special adaptations in root system, shoot system, leaf characteristics and reproductive biology to live in the harsh environment (Tomlinson, 1986). Further, they exhibit peculiarities in seedling development and dispersal by way of vivipary. Vivipary is a functional characteristic defined as the precocious and continuous growth of the offspring when still attached to the maternal parent (Goebel, 1905); it is the norm in true mangrove plants (Tomlinson, 1986).

There are two types of vivipary, true and crypto-vivipary. True vivipary refers to a situation where embryo penetrates through the fruit pericarp and grows to a considerable size before dispersal, while crypto-vivipary is a condition in which the embryo grows continuously, but does not emerge from the fruit before dispersal. These peculiar seedling characteristics present in mangrove plants could be adaptive features to overcome the harsh tidal environment for seedling establishment (Elmqvist and Cox, 1996). Therefore, reproductive biology of mangrove plants is central to understanding the structural and functional components of mangrove forests. Further, this knowledge is essential for the restoration of degraded mangrove areas. The focus on the reproductive biology of mangrove plants has almost exclusively been on the fruit, seed or seedling dispersal stage. Surprisingly, less is known about floral biology, pollination, breeding systems and success rate of propagule production, although knowledge of the effectiveness of floral mechanics and genetic isolating mechanisms is an important prerequisite to the study of successful dispersal and establishment (Juncosa and Tomlinson, 1987; Clarke and Meyerscough, 1991; Ge et al., 2003; Chiou-Rong et al., 2005; Coupland et al., 2006).

In India, a few studies provide some preliminary accounts of floral biology and pollination in some mangrove plants (Solomon Raju, 1989; Solomon Raju et al., 1994; Subba Reddi and Solomon Raju, 1997; Pandit and Choudhury, 2001; Solomon Raju et al., 2006; Solomon Raju and Jonathan, 2008). Therefore, a more complete understanding of the reproductive biology of mangroves is useful, mainly due to the growing pressures on mangroves from coastal environment and for effective mangrove rehabilitation programmes.

The present paper is an attempt to provide information on the reproductive ecology of the genera *Ceriops*, *Rhizophora*, *Bruguiera* (viviparous), *Avicennia*, *Aegiceras*, *Aegialitis* and *Scyphiphora* (crypto-viviparous), *Excoecaria*, *Lumnitzera*, *Sonneratia*, *Xylocarpus*, *Brownlowia*, *Sarcolobus* and *Suaeda* (non-viviparous) occurring in Godavari and Krishna mangrove forests in the state of Andhra Pradesh, India. Floral biology, sexual system, breeding system, floral rewards, pollinators and their foraging behaviour have been investigated in these plant species. Further, fruit and seedling ecology, dispersal strategies and establishment have also been studied in these species. This knowledge is of high value for understanding the reproductive biology of the studied plant species and for conservation and management of these species. This knowledge is also useful for the restoration of degraded mangrove areas.

MATERIAL AND METHODS

Flowering phenology was examined by conducting field trips at selected short intervals for study on all chosen plant species. Inflorescence flowering phenology was recorded by tagging some inflorescences that have not anthesed yet and then following them daily until they ceased anthesis permanently. Daily anthesis schedules and anther dehiscence schedules were carefully observed. Intrafloral events were recorded chronologically by marking some flowers at bud stage on different conspecific plants.

The aspects included flowering stage, flower organs wilting order, sepal/petal development, stamens and stigma stages and nectar production. Pollen output per anther/flower was determined as per the method given by Dafni et al. (2005). Ovule counting was made by crushing the pistil or splitting it gently and longitudinally with a blade on a glass slide spotted with lactophenol cotton blue and counting the ovules under a dissecting microscope. With the obtained pollen output and ovule number per flower, pollen-ovule ratio was determined. Stigma receptivity was examined visually and by H₂O₂ tests (Dafni et al., 2005). The amount of nectar secreted per flower was measured and expressed as μ l of nectar/flower. The nectar sugar concentration was measured by using a Hand Sugar Refractometer (Erma, Japan) (Dafni et al., 2005). Nectar analysis for sugar types was done as per the paper chromatography method of Harborne (1973). Nectar analysis for amino acid types was done as per the paper chromatography method of Baker and Baker (1973).

Breeding systems were investigated by following the protocols given by Dafni et al. (2005). Different sets of inflorescences prior to their flowering were used for determining natural fruit set rates. Foraging schedule and forage type collected by flower visitors were observed following the methods of Solomon Raju (1989). Observations on foraging behaviour versus pollination by flower visitors were made visually. To judge the foraging activity of flower visitors, the total foraging visits of each species for the

day on certain plant species were expressed in percentage. Based on this data, the percentage of foraging visits made by each species for the day was calculated. Field observations were also made regarding seed dispersal modes and subsequent establishment in mangrove forest.

RESULTS

***Ceriops tagal* (Rhizophoraceae).** It is an evergreen shrub/tree that flowers during November-February. The flowers are born in condensed short-stalked cymes formed from dichotomizing panicles, which arise from the axils of leaves on the terminal nodes of new shoots. Flowers are short-stalked, small, white, cup-shaped, strongly fragrant, bisexual and zygomorphic. Sepals are five, small, yellowish green, valvate enclosing the inner parts until anthesis and not reflexed after anthesis. Petals are five, free, white, pubescent, two lobed, and alternating with the sepals. The lower margins of adjacent petals are held together by patches of tightly intertwining, helically coiled hairs. Each petal has three distinct clavate appendages on its distal margins. Stamens are ten, five of them antisepalous, five others antipetalous and all ten inserted on the rim of the calyx cup. Each petal encloses the antipetalous stamen and an adjacent antisepalous stamen; the two stamens remain in the petal under tension enclosed above by the clavate appendages even after anthesis. Style is slender and terminated into minute separate stigmatic lobes. The stigma stands at the height of the stamens. Disc within the stamen ring is well developed and anther lobes enclose the base of the thick filaments. Ovary is semi-inferior, three-carpelled and three-locular with a total of six ovules. The mature buds open between 1630-1800 h. The calyx lobes separate at anthesis and diverge to expose the petals. The petals with the stamens inside, two per petal do not unfold naturally throughout the flower life, but remain in a tension with the spring-loaded stamens hooded above by clavate appendages. Anther dehiscence occurs in the bud. Pollen grains are triangular, light yellow, exine smooth and 15 μ in diameter. A flower produces 14,681 + 25.62 pollen grains. The pollen-ovule ratio is 2,446:1. The stigma attains receptivity on the second day and remains receptive up to six days. But, peak receptivity occurs in third-fifth day. In this period, the white petals turn red gradually from the top to the base. A flower produces 5.65 + 1.0 μ l of nectar. The nectar sugar concentration is 35-50% and the common sugars include fructose, sucrose and dextrose with the first relatively more dominant.

The nectar contains 12 amino acids which include tyrosine, glycine, methionine, proline, lysine, aspartic acid, glutamic acid, serine, cysteine, alanine, threonine and arginine. Of these, glycine, serine, cysteine, alanine and threonine are relatively dominant. The amino acids such as phenylalanine, valine, leucine, iso-leucine, tryptophan and histidine were not found in the nectar. The unpollinated flowers fall off on the seventh day. In pollinated flowers, the petals, stamens, the style and stigma drop off in this order in three-four weeks, while the fruit is in a growing stage. The sepals are persistent, become warty and spiny gradually and remain on the plant even after the shedding of propagules. The buds produced proceed to open without abortion. In open flowers, abortion rate is 42%. Of the twenty inflorescences bagged, eight flowers set fruits and, thus, the fruit set in bagged flowers is 3%. Of the sixty four open inflorescences tagged, only 115 flowers set fruit, constituting 16.3% natural fruit set. Fruit set per inflorescence varied from one to five but one and two-fruited inflorescences were more common. The pollinated flowers take four weeks to produce mature fruits with only one seed. Fruits are conical by the extrusion of the upper part of the ovary, with brown and roughened surface.

The seed has no dormancy and produces hypocotyls while on the mother tree in a span of about two months. The cotyledonary yellow cylindrical collar appears from the fruit about ten days prior to detachment of the hypocotyls. The hypocotyl is 26 cm long, distinctly ridged and hangs downwards. It is initially green, after the development of the collar, it shows a gradual colour change to brownish purple from hypocotyl end to plumule. The mature hypocotyls separate from the fruit, leaving the latter attached to the mother plant. The detached hypocotyls were found to settle in the vicinity of the mother plant. The flowers do not expose the stamens naturally but the latter attains tensed condition in the delicate petals for release by a delicate external touch. The foragers included honeybees, *Apis cerana indica*, *A. florea*, the fly, *Chrysomya megacephala* and the butterfly *Tirumala limniace*. They showed foraging activity throughout

the day but with varying percentage of foraging visits and also species-wise, the percentage of foraging varied. Of these, honeybees foraged for pollen and nectar occasionally while the fly and butterfly foraged for the nectar consistently until the floral source exhausted. All the species approached the flower from above and probed for nectar, causing a sudden release of stamens from the petals. In effect, the pollen from the already dehiscent anthers was ejected forcibly and deposited on the underside of the foraging bee or fly. Body washings for pollen revealed the presence of pollen grains which varied from 231 to 413 per bee and from 79 to 147 per fly, suggesting that both bees and the flies have an important role in petal explosion and pollination. In case of bees, they also carried pollen loads in pollen baskets present on their legs. As each petal is independently enclosing two stamens, a single foraging visit of the bee or fly did not result in the explosion of all five petals.

Both the bees and the fly tended to visit more than one flower on the same inflorescence or different inflorescences on the same plant before flying away to visit the neighbouring trees and may return back again to visit the same flowers later. As they tended to move back and forth between trees, their foraging activity may result in substantial self- and cross-pollination. The honey bees were found to concentrate principally on *Bruguiera gymnorhiza* and *Aegiceras corniculatum*, while the fly species exclusively on *Ceriops tagal*. The explosion of petals in open flowers was also triggered by the action of wind. The plant grows in the seaward zone and hence high winds are the characteristic of the site. Of the twenty four flowers observed, four flowers had shown petal explosion triggered by wind action indicating that 16.6% of flowers may achieve pollination by wind action. In such flowers also, the explosion of all five petals did not take place at one time.

It had not been possible to study whether wind could trigger petal explosion in the flowers located on the branches facing landward direction and mixed with the canopy where wind becomes relatively ineffective. Wind triggered petal explosion may result in autogamy.

***Ceriops decandra* (Rhizophoraceae).** It is an evergreen, semi-understory, and small to moderate tall tree with perfect flowers. It produces numerous branches from the main stem. A typical tree of 1.5 meters contains as many as 20-21 primary branches and each primary branch bears 11-15 secondary branches. It occurs mainly in the inside of the mangrove vegetation and certain individuals occur along the creeks/estuarine banks. The tree shows budding, flowering and fruiting continuously throughout the year but there is a burst of concentrated flowering during November. Some young trees show alternate flowering and fruiting phases. The production rate of flowers and fruits are more robust on trees growing in the interiors of the forest when compared to those on trees growing along the creeks/estuarine banks. The flowers are borne in condensed cymes formed from dichotomizing panicles, which arise from the axils of leaves.

The mechanical and biological features of this type of inflorescence provide continuous protection for the youngest units by a successive series of bracts, bracteoles and sepals. An inflorescence produces 5-31 flowers depending on the number of divisions of inflorescence axes. The cymes with more number of flowers are more common on the trees growing in the inner mangrove vegetation. The inflorescence takes sixteen days to complete its flowering life. Flowers are small, white, cup-shaped, odorless, bisexual and zygomorphic. Sepals are five, free, small, light green, six mm long, valvate enclosing the inner parts until anthesis and not reflexed after anthesis. Petals are five, free, two-lobed, alternating with the sepals, five mm long, light green in mature bud stage and white at anthesis. They are inter-locked marginally by basal short hairs and this circumstance produces a short corolla tube crowned by the series of clavate filamentous appendages.

Stamens are ten, five of them antesealous, five others antepetalous and all ten inserted on the rim of the calyx cup. Each stamen is two mm long, free and extends beyond the height of the stigma; the filaments are green, while anthers are light brown, dorsifixed and longer than filaments. Disc within the stamen ring is well developed and anther lobes enclosing the base of the stamens. The ovary is semi-inferior, three-carpelled and three-locular with a total of six ovules. Style is slender, green, one mm long and terminated into minute separate stigmatic lobes. The mature buds open during 0430-1100 h. The calyx lobes

separate at anthesis and diverge to expose the petals, which adopt various configurations. Anther dehiscence occurs at anthesis. Pollen grains are ovate, triangular, light yellow and 16.6 μm in diameter. A flower produces $12,810 + 30.87$ pollen grains. The pollen-ovule ratio is 2,135:1. The stigma attains receptivity about six hours prior to anthesis and remains receptive up to six days; but very active receptivity occurs in one-day and two-day old flowers. The stigma receptivity is notable even after six days but that receptivity appears to be non-functional in terms of pollen germination. Nectar is produced in trace amounts. The petals and stamens fall off on the seventh day of flower life. The sepals are persistent, become warty and spiny gradually and remain on the tree even after the shedding of propagules. The style and stigma dry up and drop off after ten days in fertilized flowers. The flowers that were not pollinated fall off on the fourth day. Hand pollination tests for breeding system indicated that *C. decandra* fruits through xenogamy only; the fruit set rate is 92%. Bud and flower abortion rate is 42% and 31% respectively. In open-pollinations, the fertilized flowers did not show a premature fruit drop. Fruit set per inflorescence varies from one-fruit but not fruited inflorescences are more common. The pollinated flowers produce mature fruits in 50-55 days. Fruits are light green, 1.5 cm long, ovoid, conical and blunt apically. They are distinct with five-lobed persistent calyx and produce a single seed only. The embryo has no dormancy and penetrates through the seed coat and the fruit pericarp and grows to a considerable size into a spindle-shaped hypocotyl structure before dispersal while still attached to the maternal parent. This type of hypocotyl growth constitutes true vivipary.

The hypocotyl grows upright and takes 85-90 days before detachment from the fruit. It is slender, clearly ribbed, angular, sulcate, 15 cm long and broadened at the lower end. Usually, they are entirely green and occasionally purple on one side; rarely yellow hypocotyls are also produced. The green hypocotyls seem to have the potential to photosynthesize actively with water and necessary nutrients drawn from the parent tree. The purple and yellow hypocotyls seem to lack chlorophyll partly or wholly and hence doubtful that they will have a successful establishment when detached from the parent tree. Very rarely, a single fruit produces two hypocotyls which may have arisen from two seeds resulting from two ovules out of actual six ovules per flower. In fully grown hypocotyls, fruit is separated from collar which emerges shortly before detachment. The fruit set rate per inflorescence shows a pattern in accordance with the number of flowers produced and area where the tree grows within the mangrove forest. An inflorescence produces one-six fruits. The trees growing near creeks/estuarine banks produce one-four fruits per inflorescence, one-fruited ones being 51%, two-fruited 34%, three-fruited 12% and four-fruited 3%. The trees growing in the inner mangrove areas produce one-six fruits per inflorescence, two-fruited ones are 45%, three-fruited 26%, one-fruited 22%, four-fruited 5% and five-fruited and six-fruited, 1% each. The foragers included *Nomia* sp., *Ceratina simillima* (bees), *Odynerus* sp. and *Polistes* sp. (wasps). The bees were quite common during September-October, while the wasps during November-December. The bees were found to collect nectar and pollen, while the wasps only nectar. These foragers visited the flowers during 1030-1630 h, more frequently during 1300-1400 h coinciding well with the availability of the number of flowers, because anthesis period is relatively lengthy and the new flowers with nectar and pollen accumulate by that time.

Nomia and *Odynerus* species made more percentage of foraging visits. Bees approached the flowers in an upright position, landed in the cup-shaped flowers and probed for nectar and pollen in the same or different foraging visits. In doing so, their ventral side contacted the stamens first and then stigma effecting pollination. During pollen collection, these bees rotated around the flower to collect pollen from the anthers, which are situated in one whorl against the sepals and petals. They took three-five seconds to collect the forage from each newly opened flowers and two-three seconds from differently aged flowers. Their body washings for pollen revealed that they carry $1262.7 + 428.7$ (Range 35-1570) pollen grains and hence have an important role in pollination. In addition to this pollen, they also carried pollen loads in pollen baskets present on their legs. The bees were found to move between trees of *C. decandra* to collect both nectar and pollen and this inter-tree movement was considered to effect cross-pollination. As the number of new flowers per day is small in number, the bees were forced to collect forage from different trees of *C. decandra* and this flowering strategy is expected to promote cross-pollination. Wasps are about the size of a fly and construct their nest cells in sand heaps or in cavities of trees, lining them with

agglutinated grains of sand or mud. The female wasps are known to feed on floral nectar after mating for the maturation of the eggs. The wasps observed on *C. decandra* collect nectar and such wasps were considered to be females. The study shows that *C. decandra* is a potential nectar source for female wasps. Wasps approached *C. decandra* flowers in an upright position, landed on the cymes, gradually moved to individual flowers and probed for nectar. They were found to move between individual trees in quest of more nectar. While probing the flower, they contacted the stamens and stigma with their underside and this resulted in pollination. The body washings for pollen indicated that they are pollen carriers; the pollen carry over ranges of eight to 49.

The number of bees and wasps visiting the flowers vary in different months, but both species occur continuously. Considering the changing number of bees and wasps in different months, both categories seem to be equally important as pollinators. The stigmatic pollen loads were analyzed to evaluate the rate of pollen deposition per stigma. The analysis indicated that each stigma receives $40.60 + 37.21$ (Range 5-170) pollen grains in open-pollinations but how much of it is xenogamic pollen is not known. The pollen deposition rate from the flowers was also analyzed to evaluate the role of foragers (after four-five flower visits) to empty the anthers and subsequent transportation to the receptive stigmas. The analysis showed that $10,243.7 + 1735.6$ (Range 7660-12,400) pollen grains were depleted against the pollen output by 12,810 per flower suggesting that both bees and wasps are capable of transferring pollen and effecting pollination very effectively.

Field studies indicated that *C. decandra* is used as firewood and for the constructions. Further, this species is important for its reddish brown coloured bark. The bark is known for its high tannin content ranging from 68 to 75% and dyeing with this tannin gives brown colour. The fishermen extract a reddish liquid from the bark and use it to protect cotton fishing nets from decay for a longer period. Some fishermen are involved in the trade of this bark and wood to make up their livelihood. About 80% of fishermen in 30 shore-based villages adjacent to the Godavari Delta mangrove forests depend on fishing activity for their livelihoods. They use mostly cotton nets for catching fishery sources in backwaters, while nylon nets for fishing activity in open sea water. The advantages of cotton nets include inexpensiveness and readily available because they are made locally. Nylon nets are not readily available and they are also expensive. The treatment of cotton nets is necessary to prevent damage to cotton threads due to soaking in saline water and to extend the length of its durability.

***Rhizophora apiculata* (Rhizophoraceae).** It is a medium to tall evergreen tree with profusely spreading branches, growing to a height of more than 10-12 m. The leaves are large and dark glossy green. It flowers throughout the year with profuse flowering during August-September. Flowers are borne in pairs on a stubby axis, borne below the leafy crown, that is, in the axil of a leaf scar. They are sessile and erect in position. Flowers are light yellow, 8-12 mm long, 10-14 mm wide, cup-shaped, odourless, bisexual and zygomorphic; they are situated below the leaf clusters. Calyx is characteristically hard, yellow to brown, six-eight mm long and three-four mm wide, basally cup-like, with four sepals pointed towards apex and persistent. Petals are four, alternating with sepals, five-seven mm long, creamy-white, odourless, lanceolate, glabrous and delicate. Stamens are 12, sessile, dull white to dull brown, free, anthers are five-six mm long, bilobed, introrse and sagittate. The ovary is inferior, globose with two carpels each with two glabrous ovules on axile placentation; style is thick and short, creamy white, with two creamy white to light pink stigmatic lobes. The mature buds open at 1000-1100 h; the sepals diverge least but expose the inconspicuous petals and sex organs. The petals remain flat and do not recurve. The anthers are multicellular, dehisce introrsely via the adaxial flap which falls against the base of the style in mature bud stage.

The glabrous petals do not accumulate pollen from the dehisced anthers. Stigmatic lobes are appressed in mature bud and diverged gradually after anthesis; the diverged state of stigmatic lobes indicates the commencement of receptivity and ceases around noon of the second day. The stigma has no special modifications to capture the wind borne pollen but it is thickly coated with pollen even in mature bud. The style and stigma fall off after fruit initiation. The stamens and petals drop off on the second day. The calyx remains attached to the growing fruit, expands and reflexes backward. The pollen output per

anther is $46,527.1 \pm 2,411.9$ (Range 42,681-49,854) and per flower is 5.58.326. Pollen grains are tricolporate, dullwhite, powdery, ornamentation finely reticulate, the reticulum becoming progressively less distinct from pole to equator and $16.6 \mu\text{m}$ diameter. The pollen-ovule ratio is 1.39.581:1. The pollen protein content per anther is $8.6 \mu\text{g}$ and per flower is $104 \mu\text{g}$. Nectar is secreted in trace amount around the ovary.

The results of breeding systems indicate that the flowers are self-compatible and self-pollinating. The fruit set is 72.5% in spontaneous autogamy, 86% in handpollinated autogamy, 92% in geitonogamy, 93.3% in xenogamy and 55% in open pollination. The flowers release pollen into the air; the sepals and petals in open flowers sprinkled with pollen due to wind action. A delicate manual disturbance to the flowers resulted that caused the release of a cloud of pollen out of the flower. Bees were the exclusive foragers and they were *Nomia* sp., *Trigona iridipennis* and *Halictus ligatus*. They foraged during day time from 0800-1700 h for pollen and nectar from partially and completely opened flowers. Their foraging activity was consistent during profuse flowering period while it is sporadic at other times of the year. Of the total number of foraging visits of bees, *H. ligatus* made 44% followed by *Nomia* 41% and *Trigona* 15%. These bees first landed on the sepals, then investigated the flower for pollen and nectar; while doing so, their head and ventral side of the body touched the stamens and stigma and in the process they got coated with pollen. Further, they loaded pollen into pollen baskets. As all three bee species are pollen collecting bees, they made frequent visits to flowers situated on different plants which are closely and distantly spaced in order to collect more pollen. The fresh flowers available per day on a given tree are small in number and the bees made visits to different trees to collect more forage from as many flowers as possible. Further, the body washings of the bee species revealed the presence of pollen; the average number of pollen grains per bee for each species varied from 561.6 to 1006.9. It was found that thrips breed in buds and emerge when a flower opening occurs. They collected both pollen and nectar. During August-September, a single mature bud was usually found to contain many thrips moving out of the floral base when disturbed manually. Thrips were found to effect pollination as they moved in the entire flower touching the stigma. Pollinated and fertilized flowers initiate fruit development immediately and take 35 days to produce mature fruits.

Of the four ovules in a flower, one ovule produces seed. Fruit is one-seeded with persistent light green calyx. A fruit producing two seeds and hence two hypocotyls is a rare occurrence. The seed produces 550 mm long, cylindrical elongate, light green, hypocotyl with a sharp end in a time span of 55-60 days. A light brown collar emerges between fruit and hypocotyl about a month prior to the detachment of the latter. The persistent calyx and fruit part remain in place on the parent tree while the hypocotyl detaches at the collar for dispersal. The hypocotyls fall and anchor vertically in the substratum at low tide when the forest floor gets exposed; they float in water and disperse by tidal currents at high tide until settled in the mud. The radicle side of hypocotyl penetrates the soil and produces root system while plumule side produces new leaves and subsequent aerial system.

***Rhizophora mucronata* (Rhizophoraceae).** It is a medium to tall evergreen tree with profusely and horizontally spreading branches, growing to a height of more than 15 m. It flowers during June-November. The inflorescence is a four-flowered pedunculate dichotomized cyme borne in leaf axils; the flowers are pedicellate, pendulous and hanging downwards. Flowers are creamy white, 15 mm long, 10 mm wide, cup-shaped, odourless, bisexual and zygomorphic; they are situated below the leaf clusters. Calyx is characteristically hard, creamy white, 12 mm long and seven mm wide, basally cup-like, with four sepals pointed towards apex and persistent. Petals are four, alternating with sepals, ten mm long, white, hairy, odourless, lanceolate, and delicate. Stamens are eight, sessile, four opposite to petals, another four opposite to sepals, dull white to dull brown, free, anthers are seven mm long, bilobed, introrse and sagittate. Ovary is semi-inferior, globose with two carpels each with two glabrous anatropous ovules on axile placentation; style is thick and short, creamy white, with two creamy white to light pink stigmatic lobes. The mature buds open at 1000-1600 h; the sepals diverge gradually exposing the petals and sex organs. The petals also diverge and slightly reflex backwards. The anthers are multilocular, dehisce introrsely via the adaxial flap which falls against the base of the style in mature bud stage.

The hairy petals accumulate pollen from the dehisced anthers. Stigmatic lobes are appressed in mature bud and diverged gradually after anthesis; the diverged state of stigmatic lobes indicates the commencement of receptivity and ceases around noon of the second day. The stigma has no special modifications to capture the wind borne pollen, but it is thickly coated with pollen even in mature bud. The style and stigma fall off after fruit initiation. The stamens and petals drop off on the second day. The calyx remains attached to the growing fruit, expands and reflex backwards. The pollen output per anther is $34,986.6 \pm 527.34$ (Range 34,007-35,729) and per flower is 2,79,893. Pollen grains are tricolporate, dull-white, powdery, and $24.9 \mu\text{m}$ long and $12.2 \mu\text{m}$ in diameter; their surface sculpture is rather smooth, with numerous small and shallow depressions. The pollen-ovule ratio is 69,973.2:1. The pollen protein content per anther is $10.2 \mu\text{g}$ and per flower is $82 \mu\text{g}$. Nectar volume per flower is $1.03 \pm 0.26 \mu\text{l}$ (Range 0.8-1.5) and accumulated around the ovary.

The results of breeding systems indicate that the flowers are self-compatible and self-pollinating. The fruit set is 52.5% in spontaneous autogamy, 63.3% in hand-pollinated autogamy, 71.4% in geitonogamy, 85% in xenogamy and 53.3% in open pollination. The flowers release pollen into the air; the sepals and petals in open flowers were found to be sprinkled with pollen due to wind action. A delicate manual disturbance to the flowers resulted caused the release of a cloud of pollen out of the flower. The flowers were foraged consistently during day time from 0800-1700 h exclusively by bees. The bees included *Nomia* sp., *Trigona iridipennis*, *Halictus ligatus*, *Ceratina simillima* and *Xylocopa pubescens*. An unidentified moth was also found to collect nectar occasionally. Bees collected both pollen and nectar from partially and completely opened flowers. Each bee species contributed 11-24% of total foraging visits. These bees first landed on the sepals, then entered the flower to collect pollen and nectar; while doing so, their head and ventral side of the body touched the stamens and stigma and in the process they got coated with pollen. Further, they loaded pollen into pollen baskets.

All the bee species except *Xylocopa*, are pollen collecting bees, they made frequent visits to flowers situated on different plants which are closely and distantly spaced in order to collect more pollen. *Xylocopa* bees are fast fliers and made inter-tree flight in quest of more nectar from as many flowers as possible. The fresh flowers available per day on a given tree are small in number and for this reason, the bees were compelled to make visits to different trees for more forage. Further, the body washings of the bee species revealed the presence of pollen; the average number of pollen grains per bee for each species varied from 189.3 to 951.6. Thrips breed in buds and emerge when flower opening occurs. They collected both pollen and nectar. A mature bud contained numerous thrips moving out of the floral base when disturbed manually. Thrips were found to carry pollen on their bodies and moving in the entire flower including the stigma during which they transferred pollen onto the stigma. The flowers with huge pollen production together with pollen characteristics described above were considered to be anemophilous. Further, the pollen being powdery was found to be dispersed easily due to wind action. A simple manual disturbance to flowers made the latter to release pollen into the air. Pollinated and fertilized flowers initiate fruit development immediately and take 40 days to produce mature fruits.

In fertilized flowers, only one ovule out of four ovules produced seeds. Fruit is one-seeded with woody, persistent light green and reflexed calyx. Seed produces 680 mm long, cylindrical elongate, light green, warty hanging hypocotyl in a time span of 60- 65 days. A light yellow tubular collar (20 mm long) emerges between fruit and hypocotyl about a month prior to detachment of the latter. The hypocotyl detaches at the collar for dispersal. Later, the entire fruit part also falls off. The hypocotyls settle in the substratum immediately at low tide when the forest floor gets exposed; they float in water and disperse by tidal currents at high tide until settled in the soil. The radicle side of hypocotyl penetrates the soil and produces root system, while plumule side produces new leaves and subsequent aerial system. The fruit also falls off eventually from the maternal parent.

***Bruguiera gymnorrhiza* (Rhizophoraceae).** It is a medium to tall evergreen tree with much diffused spreading branches, growing to a height of more than ten m. It flowers throughout the year with profuse flowering during April-June. Flowers are solitary, single flower in each peduncle, located in the leaf axils,

usually positioned at the first (or rarely second) node below the apical shoot. Flowers are pedicellate, typically recurved, pointing away from the terminal vegetative bud, pendulous, 30-35 mm long, 19-20 mm wide, pinkish to reddish white, tubular, odourless, bisexual and zygomorphic. Calyx is characteristically hard, smooth or with grooves above lobe junctures, pinkish to reddish white, basally cup-like, rarely ribbed, with 11-14 lobes, acutely pointed, narrow and persistent. Petals are 14, bilobed, 15 mm long and four mm wide, creamy-white in mature bud, orange-brown on maturation, delicate with marginal interlocking hairs, the tips of lobes acute commonly with three filamentous appendages distally usually with a rigid straight four mm long bristle between them. The base of each petal has a cluster of smooth silky hairs. Stamens are 28 enclosed in petal pouches, two stamens in each petal, filament creamy white, ten mm long and two mm wide, anthers are creamy white initially and turn to golden brown at maturity; bilobed and basifixed. Ovary is inferior, cup-shaped with six light brown, smooth ovules; style is slender, white to light brown, filiform with three or four, 15 mm long, whitish-yellow stigmatic lobes containing small papilla and secreting mucilage; the stigma remains attached to fruit at maturity. The mature buds open at 0700-0900 h; the sepals diverge gradually presenting the closed, erect petals in the cocked position. The petals conceal the stamens in a tensed state due to the pressing of the latter against the interlocked margins of the petals. The petals bend back and remain in an erect position by the adherent ventral margins. Marginal hairs appear to be important in holding the petals in the folded position. The stamens dehisce in mature bud stage by longitudinal slits. The petal margins unzip instantaneously when triggered by external touch; then they fly apart releasing the stamens which catapult the loose pollen as a visible cloud toward the centre of the flower. If the external touch is caused by a forager, then much of the pollen would be projected onto the head and the body of the forager. Each petal explodes independently and hence multiple visits are required to trip all the petals of a flower.

Individual flowers with combinations of closed and tripped petals were found. After the petal tripping, the petals lie back against the calyx lobes with empty stamens twisted and disorganized. Petals and stamens persist for up to seven days and eventually fall off as threefour units. Untripped petals retain their tension for up to eight days, and they eventually fall off without ever opening. Stigmatic lobes are receptive from second to fourth day and show signs of withering after the petals and stamens have fallen. The pollen output per anther is $9,005.4 \pm 834.95$ (Range 8,004-10,469) and per flower is 2,51,856 pollen grains. Pollen grains are tricolporate, pale yellow, elliptic in equatorial view, circular in polar view, exine smooth with numerous small and shallow depressions, 29.6 μm long and 16.6 μm diameter. The pollenovule ratio is 41,976:1. The pollen protein content per anther is 1.77 μg and per flower is 49.6 μg . Copious nectar accumulates in the deep calyx cup and is retained by the petal base and its associated hairs. In newly open flowers, five-ten μl of nectar is secreted and it is continuously produced even after the abscission of petals and stamens in some flowers while it is not produced continuously in some other flowers. The flowers with the former situation were designated as un-pollinated ones while those with the latter situation were designated as pollinated flowers. A flower produces 10.49 ± 5.2 (Range 5.2 - 24) μl of nectar with a sugar concentration of $23.48 \pm 4.80\%$ (Range 18-31); glucose and fructose were present. In unvisited flowers, it overflows onto the petals where it becomes viscous by evaporation and so inhibits the explosive mechanism. The total sugar content in the nectar of a flower is 2.58 ± 1.20 (Range 1.06-5.39) mg. The nectar protein content per flower is 78.68 ± 48.56 μg (Range 44.8- 147). The nectar contains eight amino acids which include alanine, aspartic acid, glutamic acid, arginine, histidine, lysine, glycine and serine. All these amino acids are abundant except lysine. The results of breeding systems indicate that the flowers are self-compatible and selfpollinating. The fruit set is 40% in manipulated autogamy, 60% in geitonogamy, 90% in xenogamy and 87% in open pollination. The flowers are characterized by explosive pollination mechanism. They were foraged consistently during day time from 0700-1700 h exclusively by bees.

The bees included *Apis dorsata*, *A. cerana*, *A. florea*, *Nomia* sp. and *Halictus ligatus*. Bees collected both pollen and nectar from partially and completely opened flowers. Of the total number of foraging visits of bees, *A. florea* contributed 25%, *A. cerana* and *Nomia* each 20%, *A. dorsata* 18% and *H. ligatus* 17%. All the bees turned their heads upward to collect nectar located in the calyx cup; while doing so, they tripped

the tensed petals to release a cloud of pollen explosively without being disturbed by the explosion. A single foraging visit did not result in tripping all the petals at a time. Petal explosion was found to be effected by touching sensitive basal hairs, especially those which project in the centre of the flower over the entrance to the calyx cup. The tip of the petal and its apical appendages were not sensitive but petal tripping was stimulated by fairly vigorous probing into the calyx cup.

The bees took different positions while probing and collecting nectar in relation to stamens and style. Each foraging visit invariably contacted the style and stigma and resulted in the deposition of pollen on the foraging bee. The bees were also found to collect nectar from empty flowers which are devoid of petals and stamens. They were found to move frequently between plants seeking more nectar and/or pollen as few rewarding flowers are available daily per tree. Such a foraging behaviour could make them as effective pollen dispersers causing both self- and crosspollination. Further, the body washings of all foraging bee species revealed the presence of pollen; the average number of pollen grains per bee for each species varied from 198 to 1,389. Pollinated and fertilized flowers initiate fruit development immediately and take 30-35 days to produce mature fruits. Fruit is one-seeded fleshy berry with persistent reddish calyx. Seed produces 141 ± 9 mm long, cylindrical elongate, stocky, dark green, coriaceous hanging hypocotyl with blunt apex in a time span of 45-50 days. In a sample of 200 hypocotyls, 5% were found to be damaged especially at the terminal part by the Rose-ringed Parakeet, *Psittacula krameri*; the damaged part was fleshy and hence eaten by the bird. The persistent calyx remains attached even after mature hypocotyl falls from the mother tree.

The hypocotyls settle in the substratum immediately at low tide when the forest floor is exposed; they float and disperse by tidal currents at high tide until settled in the soil. The radicle side of the hypocotyl penetrates the soil and produces root system while plumule side produces new leaves and aerial system.

***Bruguiera cylindrica* (Rhizophoraceae).** It is a medium to tall evergreen tree with diffused spreading branches, growing to a height of more than 12 m. The flowering occurs during September-March. The inflorescence is a simple pedunculate dichasium cyme with pedicellate erect flowers; each cyme is three-flowered and borne in leaf axils. Flowers are greenish-white, 10-12 mm long, short-tubed, odourless, bisexual and zygomorphic. Calyx is tubular, funnel-like (five-seven mm long and two mm wide), smooth, light green, with seven-eight pointed lobes, characteristically hard and persistent. Petals are seven-eight, initially creamy white, later turning to light brown from the tip towards the base, alternating with sepals, shortly bilobed, each lobe three mm long and one mm wide, delicate with marginal interlocking minute hairs, the tips of lobes acute commonly with three filamentous appendages distally usually with a rigid straight bristle between them. The base of each petal has a cluster of smooth silky hairs. Each petal encloses a pair of stamens, filament creamy white, two mm long and one mm wide, anthers are creamy white initially and turn to light brown at maturity; bilobed and basifixed. Ovary is inferior, cup-shaped, with four light brown, smooth ovules; style is slender, white to light brown, filiform with two creamy white to yellow stigmatic lobes, two mm, situated below the height of stamens, stiff and remains attached to fruit at maturity.

The mature buds open at 0700-0900 h; the sepals diverge gradually presenting the closed, erect petals in the cocked position. The petals conceal the stamens in tensed state due to the pressing of the latter against the interlocked margins of the petals. The petals are retained in an erect position by the adherent ventral margins. Marginal hairs appear to be important in holding the petals in the folded position. The stamens dehisce in mature bud stage by longitudinal slits. The petal margins unzip instantaneously when triggered by a delicate touch; then they fly apart releasing the stamens which catapult the loose pollen toward the centre of the flower. If the external touch is caused by a forager, then much of the pollen would be projected onto the head and body of the forager. Each petal explodes non-violently and independently. In an observed set of flowers, most flowers had all petals tripped. After the petal tripping, the petals lie back against the calyx lobes with the empty stamens twisted and disorganized. Petals and stamens persist for up to three days and eventually fall as three-four units. Untripped petals retain their tension for up to six days, and they eventually fall off without ever opening. Stigmatic lobes are receptive on the second and third day and show signs of withering after the petals and stamens have fallen. The pollen output per anther is 1,289.7

± 299.29 (Range 1,021-1,828) and per flower is 20,635 pollen grains. Pollen grains are tricolporate, light yellow, powdery, ornamentation finely reticulate, the reticulum becoming progressively less distinct from pole to equator and $16.6 \mu\text{m}$ long. The pollen-ovule ratio is 5,158:1. The pollen protein content per anther is one μg and per flower is 16 μg . Nectar accumulates in the deep calyx cup and is retained by the petal base and its associated hairs. A flower produces $1.43 \pm 0.31 \mu\text{l}$ (Range 0.9-2) of nectar with a sugar concentration of $15.2 \pm 1.57\%$ (Range 10-21); glucose, fructose, sucrose and maltose were present but the first sugar is dominant. The total sugar content in the nectar of a flower is 0.11 ± 0.03 (Range 0.04-0.17) mg. The results of breeding systems indicate that the flowers are self-compatible and selfpollinating. The fruit set is 40% in unmanipulated autogamy, 56% in manipulated autogamy, 63.3% in geitonogamy, 80% in xenogamy and 64.4% in open pollination. The flowers are characterized by explosive pollination mechanism. They were foraged consistently during 0700 to 1700 h by *Nomia* bee and the wasps, *Odynerus* sp. and *Polistes humilis*. The bee collected both pollen and nectar while the wasps collected only nectar. Of the number of foraging visits of bees, *Nomia* contributed 38% while the remaining percentage by the wasps. These foragers approached the flowers in upright position and probed the flowers for nectar and/or pollen; they tripped the tensed petals without being disturbed by the explosion.

One or two visits of the foragers resulted in the explosion of all flower petals. Petal explosion was found to be effected by touching sensitive basal hairs, especially those which project into the centre of flower over the entrance to the calyx cup. The tip of the petal and its apical appendages were not sensitive but petal tripping was stimulated by vigorous probing into the calyx cup. Each foraging visit invariably contacted the style and stigma and resulted in the deposition of pollen on the foraging bee. They were found to move frequently between plants seeking more nectar and/or pollen as few rewarding flowers are available daily per tree. Such a foraging behaviour could make them as effective pollen dispersers causing both self and cross pollination. Further, the body washings of all foragers revealed the presence of pollen; the average number of pollen grains per forager for each species varied from 262 to 448.2. Pollinated and fertilized flowers initiate fruit development immediately and take 18-20 days to produce mature fruits. Of the four ovules, only one ovule produces seed in fertilized flowers. Rarely, two ovules produce seeds; in such fruits, twin hypocotyls are produced per fruit. Fruit is one-seeded, creamy white, 20 mm long; persistent creamy white calyx lobes stick out at right angles to the fruit. Seed produces 136 ± 16 mm long, cylindrical elongate, slightly curved, green to purple, pendulous hypocotyl with blunt apex in a time span of 30-35 days. The persistent calyx remains attached after mature hypocotyl falls from the parent tree.

The hypocotyls settle in the mud at low tide during which the forest floor gets exposed; they float in water and disperse by tidal currents at high tide. The radicle side of the hypocotyl produces root system while plumule side produces new leaves and subsequent aerial system.

***Avicennia alba* (Avicenniaceae).** Small evergreen tree with irregular branches, growing to a height of more than 10-12 m. Following monsoon showers in June, it initiates flowering and continues flowering until the end of August. Individual trees flower for 35 ± 4 (Range 32- 48) days. Inflorescence is a terminal and axillary spicate raceme. An inflorescence produces, on average, 52.34 ± 26.96 flowers (Range 15-123) anthesing from the base to top over a period of 25 days (Range 24-28). The flowers are sessile, small (four mm long; three mm diameter), orange yellow, fragrant, actinomorphic and bisexual. Calyx is short, elliptic and has four ovate, green, pubescent, two mm long, one mm wide, sepals with hairs on the outer surface; it is persistent. Corolla has four thick, orange yellow ovate, four mm long and two mm wide petals forming a short tube at the base. Stamens are fur, epipetalous, one mm long, occur at the throat of the corolla. The anthers are dorsifixed, introrse and arranged alternate to petals. The ovary is very small (two mm long), flask-shaped, conspicuously hairy but lower part includes glandular hairs, bicarpellary syncarpous with four imperfect locules and each locule contains one pendulous ovule.

It is terminated with a one mm long glabrous style tapered to the bifid hairy stigma. The light yellow style and stigma arise from the centre of the flower and stand erect throughout the flower life. The mature buds open throughout the day but most buds opening during 0900-1200 h. The petals slowly open and take three-four hours for complete opening to expose the stamens and stigma. The petals emit fragrance at

anthesis. The stamens bend inward overarching the stigma at anthesis and dehisce $\frac{1}{2}$ hour after anthesis. All the four anthers dehisce at the same time by longitudinal slits. The stigma is well seated in the centre of the flower. After anthesis, the stigma grows gradually and becomes bifid on the morning of the second day. The bifid condition of stigma is an indication of beginning of stigma receptivity and it remains receptive for two days. The stigmatic lobes recurve completely. A flower lasts for six days. The petals, stamens and stigma drop off while the calyx is persistent. The pollen production per anther is $1,967 \pm 31,824.3$ (Range 1,929-2,010) and per flower is 7,868. The pollen grains are light yellow, granular, tricolporate, reticulate, muri broad, flat, thick; lumina small irregularly shaped, colpi deeply intruding and $24.9 \mu\text{m}$ in size. The pollen-ovule ratio is 1,967:1. The flowers begin nectar secretion along with anther dehiscence. The nectar secretion occurs in minute amount which is accumulated at the ovary base and on the yellow part of petals; the nectar glitters against sunlight. A flower produces $0.5 \pm 0.1 \mu\text{l}$ (Range 0.4-0.7) of nectar with a sugar concentration of 40%.

The sugar types included glucose and fructose and sucrose with the first as dominant. The results of breeding systems indicate that the flowers are self-compatible and self-pollinating. The fruit set is 17.5% in spontaneous autogamy, 40% in handpollinated autogamy, 62.5% in geitonogamy, 64.28% in xenogamy and 42% in open pollination. The flowers were foraged consistently during day time from 0700-1700 h by insects. The insects included *Apis dorsata*, *A. florea*, *Nomia* sp., *Chrysomya megacephala*, an unidentified fly, *Danaus chrysippus* and *Everes lacturnus*. The fly species visited the flowers in groups. The pollen was collected by bees only; they also collected nectar throughout the flower life depending on the availability. All other insects collected nectar only. Each forager species made 8.5-21% of foraging visits. All the insects probed the flowers in upright position to collect the forage. Butterflies landed on the petals, stretched their proboscis to collect nectar aliquots on the petals and at the flower base. In this process, all the insects invariably touched the anthers and the stigma; the ventral side of all insects was found with pollen. Further, the body washings of the all insect species revealed the presence of pollen; the average number of pollen grains per insect for each species varied from 67.6 to 336.2. As the nectar is secreted in minute amount, the insects made multiple visits to most of the flowers on a tree and moved frequently between trees to collect nectar. Such a foraging behaviour was considered to effect self- and cross-pollination. Pollinated and fertilized flowers initiate fruit development immediately and take about five-six weeks to produce mature fruits. In fertilized flowers, only ovule produces seed. Fruit is a one-seeded leathery pale green capsule with persistent reddish brown calyx; 40 mm long, 15 mm wide, abruptly narrowed to a short beak and hairy throughout.

Seed produces light green, hypocotyl which completely occupies the fruit cavity. An inflorescence produces three \pm one fruits (Range 1-5); one-fruited ones constituted 54% followed by two-fruited ones (23%) and three-fruited (10%) and four-fruited (5%) and five-fruited (2%). Of these, 6% were damaged by the Rose-ringed Parakeet, *Psittacula krameri*; it was found to feed on the concealed hypocotyl in fruits and these fruits were subsequently empty. The fruit together with hypocotyl falls off the mother plant; it was found to settle in the substratum immediately at low tide period when the forest floor is exposed; it floats in water and disperses by tidal currents at high tide period until settled somewhere in the soil. The radicle side of hypocotyl penetrates the soil and produces root system while plumule side produces new leaves and subsequent aerial system. The fruit pericarp detaches and disintegrates when plumular leaves are produced.

***Avicennia marina* (Avicenniaceae).** It is a small evergreen tree with irregular spreading branches, growing to a height of more than three-eight m. Following monsoon showers in June, it initiates flowering and continues flowering until the end of August. Individual trees flower in 32-35 days. Inflorescence is a compound axillary or terminal cyme. An inflorescence shoot produces, on average, 47 ± 13.97 flowers (Range 26-76) anthesing from the base to top over a period of 22 days (Range 15-22). The flowers are sessile, small (six mm long; five mm diameter), orange yellow, sweet scented, actinomorphic and bisexual. Calyx is short, elliptic and has four ovate light green, two mm long sepals with hairs on the outer surface; it is persistent. Corolla has four thick, orange yellow ovate four mm long and two mm wide petals forming a short tube at the base.

The petals are glabrous inside and hairy outside. Stamens are four, epipetalous, two mm long, occur in the throat of the corolla. The anthers are basifixed, exerted, introrse and arranged alternate to petals. The ovary is very small (two mm long), conspicuously hairy, bicarpellary syncarpous with four imperfect locules and each locule contains one pendulous ovule. It is terminated with a one mm long glabrous style tapered to the bifid hairy stigma. The light yellow style and stigma arise from the center of the flower and stand erect throughout the flower life. The mature buds open throughout the day but most buds open during 1000-1300 h. The petals slowly open and take two-three hours for complete opening to expose the stamens and stigma. The petals emit a sweet fragrance at anthesis. The stamens bend inward overarching the stigma at anthesis and dehisce half an hour after anthesis. All the four anthers dehisce at the same time by longitudinal slits. The stigma is well seated in the center of the flower. After anthesis, the stigma grows gradually and becomes bifid on the morning of the second day. The bifid condition of stigma is an indication of beginning of stigma receptivity and it remains receptive for two days. The stigmatic lobes recurve completely. A flower lasts for five days. The petals, stamens and stigma drop off while the calyx is persistent. The pollen production per anther is 1643.2 ± 31.8 (Range 1600-1690) and per flower is 6572.8. The pollen grains are light yellow, granular, tricolporate, reticulate, muri broad, flat, thick; lumina small irregularly shaped, colpi deeply intruding, and $33.2 \mu\text{m}$ in size. The pollen-ovule ratio is 1,643.2:1.

The flowers begin nectar secretion along with anther dehiscence. The nectar secretion occurs in minute amount which has accumulated at the ovary base and on the yellow part of petals and it glitters against sunlight. It is quite prominent during the entire period of stigma receptivity. A flower produces $0.4 \pm 0.08 \mu\text{l}$ (Range 0.3-0.5) of nectar with a sugar concentration of 38%. The sugar types included glucose and fructose and sucrose with the first as dominant. The results of breeding systems indicate that the flowers are self-compatible and self-pollinating. The fruit set is 12% in spontaneous autogamy, 33.33% in hand-pollinated autogamy, 40% in geitonogamy, 68% in xenogamy and 55% in open pollination. The flowers were foraged consistently during day time from 0700-1700 h by insects. The insects included *Halictus* sp., *Chrysomya megacephala*, *Eristalinus arvorum*, *Rhyncomya* sp., an unidentified fly, *Polistes humilis* and *Catopsilia pyranthe*. Individuals of each fly species were numerous on each tree. Bees were the exclusive pollen feeders. They also collected nectar throughout the flower life depending on the availability. All other insects collected nectar only. Each forager species made 11.5 to 17.5% of foraging visits. Percentage of foraging activity of insect organisms on *Avicennia marina* species. All the insects probed the flowers in upright position to collect the forage. *C. pyranthe* landed on the petals, stretched its proboscis to collect nectar aliquots on the petals and at the flower base. In this process, all the insects invariably touched the anthers and the stigma; the ventral side of all insects was found with pollen. Further, the body washings of the all insect species revealed the presence of pollen; the average number of pollen grains per insect for each species varied from 63.1 to 227.4. As the nectar is secreted in minute amount, the insects made multiple visits to most of the flowers on a tree and moved frequently between trees to collect nectar. Such a foraging behaviour was considered to effect self- and crosspollination. Pollinated and fertilized flowers initiate fruit development immediately and take about a month to produce mature fruits.

In each fertilized fruit, only one ovule produces seed. Fruit is a one-seeded leathery grayish green capsule with persistent reddish brown calyx; 30-35 mm long, 25 mm wide, abruptly narrowed to a short beak and hairy throughout. Seed produces light green, hypocotyls, which completely occupies the fruit cavity. An inflorescence produces 6.88 ± 2.96 fruits (Range 3-20). The Rose-ringed Parakeet, *Psittacula krameri* was found to feed on the hypocotyl by damaging the fruit pericarp; the percentage of damaged fruits is 4%. The fruit together with hypocotyl falls off the maternal parent, it settles in the substratum immediately at low tide period, it floats in water and disperses by tidal currents at high tide period until settled somewhere in the soil. The radicle side of hypocotyl penetrates the soil and produces root system while plumule side produces new leaves and subsequent aerial system. The fruit pericarp detaches and disintegrates when plumular leaves are produced.

***Avicennia officinalis* (Avicenniaceae).** It is a tall evergreen tree with irregular spreading branches giving crowned globose appearance. It grows to a height of more than 15- 20 m. The summer showers or early

monsoon rains trigger flowering response. The rains vary in their occurrence and intensity even over a short distance; consequently the flowering period varies from place to place. The flowering season extends until August. The flowering density is almost uniform throughout the flowering season. Inflorescence is a terminal or axillary trichotomous panicle; each panicle produces 32 ± 11 flowers which anthes over a period of 16-25 days. Flowers are small, orange-yellow, ten mm long, ten mm wide, cup-shaped, have foetid smell, bisexual, slightly zygomorphic and oriented erect or partly horizontal. Calyx is shorter and has four ovate light green sepals with hairs on the outer surface; it is persistent. The corolla has four thick, light to orange yellow glabrous petals forming a short tube at the base; the petal margins are dull white. The adaxial petal is the broadest and shallowly bilobed. Stamens are four, epipetalous, three mm long and inserted basally on corolla.

The anthers are basifixed, exserted, introrse and arranged alternate to petals. The ovary is very small (seven mm long), conspicuously hairy, bicarpellary syncarpous with four imperfect locules and each locule contains one pendulous ovule. It is terminated with a two mm long glabrous style tapered to the unequal bifid hairy stigma; both the style and stigma are light yellow throughout the flower life. The entire female structure is over-arched by stamens above. The style is bent, situated below the adaxial corolla lobe but not in the centre of the flower. The mature buds open throughout the day with most mature buds opening during 0800- 1100 h. The petals slowly open and take two-three hours for complete opening to expose the stamens and stigma. The petals emit foetid smell at anthesis. The stamens bend inward overarching the stigma at anthesis and dehisce 0.5 h after anthesis. All the four anthers dehisce at the same time by longitudinal slits. Gradually, they become erect and bend backwards; to achieve this, they take three days. Then, the anthers became dark brown and petals turn light orange. Gradually, the bent stigma grows, becomes erect and is bifid on the morning of the third day. The bifid condition of stigma is an indication of beginning of stigma receptivity and it remains receptive until the fifth day. A flower lasts for seven days. The petals, stamens and stigma drop off while the calyx is persistent. The pollen production per anther is $2,444 \pm 202.4$ (Range 2078-2604) and per flower is 8,837. The pollen grains are light yellow, granular, tricolporate, reticulate, muri broad, flat, thick; lumina small irregularly shaped, colpi deeply intruding, and $33.2 \mu\text{m}$ in size. The pollen-ovule ratio is 2,209.3:1. The flowers begin nectar secretion along with anther dehiscence. The nectar secretion occurs in minute amount of the yellow part of petals and it glitters against sunlight. It is quite prominent during the entire period of stigma receptivity. A flower produces 0.65 ± 0.09 (Range 0.5-0.8) μl of nectar with a sugar concentration of $39.75 \pm 1.89\%$ (Range 36-43%).

The sugar types included sucrose, glucose and fructose with the first as dominant. The nectar amino acids included aspartic acid, cysteine, alanine, arginine, serine, cystine, proline, lysine, glycine, glutamic acid, threonine and histidine. All of these are prominent except lysine, glycine and proline. The results of breeding systems indicate that the flowers are self-compatible and self-pollinating. The fruit set is 21.42% in spontaneous autogamy, 42.85% in hand-pollinated autogamy, 63.33% in geitonogamy, 67.85% in xenogamy and 58.13% in open pollination. The flowers were foraged consistently during day time from 0700-1700 h by insects. The insects included *Apis dorsata*, *Xylocopa pubescens*, *Xylocopa* sp., *Eristalinus arvorum*, *Chrysomya megacephala*, *Sarcophaga* sp., *Euploea core*, *Danaus chrysippus*, *D. genutia*, *Junonia lemonias*, *J. hierta*, a fly and a wasp (unidentified). Individuals of each fly species were numerous at the flowers. *A. dorsata* was the only pollen feeder. It also collected nectar throughout the flower life depending on the availability. All other insects collected nectar only. Each forager species made 5.5 to 12.5% of foraging visits. All the insects probed the flowers in upright position to collect the forage. In case of *Xylocopa* bees, they made audible buzzes while collecting nectar aliquots from the petals. The butterflies landed on the petals, stretched their proboscis to collect nectar aliquots on the petals. In this process, all the insects invariably touched the anthers and the stigma; the ventral side of all insects was found with pollen. Further, the body washings of the all insect species revealed the presence of pollen; the average number of pollen grains per insect for each species varied from 73 to 550.2. As the nectar is secreted in minute amount, the insects made multiple visits to most of the flowers on a tree and moved frequently between trees to collect nectar. Such a foraging behaviour was considered to effect self- and cross-pollination. Pollinated

and fertilized flowers initiate fruit development immediately and take about a month to produce mature fruits.

In fertilized flowers, only one ovule produces seed. Fruit is a one-seeded leathery capsule with persistent reddish brown calyx; 30 mm long, 25 mm wide, abruptly narrowed to a short beak and hairy throughout. Seed produces light green, hypocotyl which completely occupies the fruit cavity. The fruit pericarp dehisces when the hypocotyl is ready for dispersal and when the latter is still on the mother tree. The entire dehisced fruit with hypocotyl inside falls off from the mother tree. The fruit pericarp together with hypocotyl settles in the substratum immediately at low tide period; it floats in water and disperses by tidal current at high tide period until settled in the soil. The radicle side of hypocotyl penetrates the soil and produces root system while plumule side produces new leaves and subsequent aerial system. The fruit pericarp detaches and disintegrates when plumular leaves are produced.

***Aegiceras corniculatum* (Myrsinaceae).** It is a small evergreen shrubby tree with spreading diffused branches, growing to a height of four-five m. It flowers mainly from second week of February to second week of April; sporadic flowering occurs outside this period, especially during rainy season. The plant species such as *Bruguiera gymnorhiza* (year-long bloomer), *B. cylindrica* (seasonal bloomer, September-March), *Ceriops decandra* (year-long bloomer) and *Excoecaria agallocha* (seasonal bloomer, July-August) occur in association with *A. corniculatum*. In *A. corniculatum*, an individual tree flowers for 22-25 days. Inflorescence is a simple umbel which arises in the shoot apex or in axillary branches. An inflorescence produces 21.53 ± 4.42 flowers (Range 14-36). There is considerable synchrony of flower development in one umbel and in this state, the flowers appear in ball-like clusters. The umbels open in acropetal succession. Flowers are pedicellate, pointed in bud condition, 17 mm long, seven mm wide, white, cup-shaped, fragrant, bisexual and zygomorphic. Sepals are five, small, five mm long, creamy white, twisted, free, coriaceous, round apex and persistent. Petals are five, free, five mm long, white, twisted to the left, slightly fused at base to form short tube of five-six mm length, mouth with a dense web of hairs and capitate hairs at the base.

Stamens are five, opposite to petals, epipetalous, adnate to the base of the corolla tube, filament creamy white, five mm long, base united to form a tube with a ring of internal and external hairs at the level of the mouth of the corolla tube. The anthers are bilobed, two mm long, inserted, sagittate, introrse and medifixed. Ovary is superior, conical, eight mm long, single-loculed with 35 ovules arranged on free central placentation in one chamber. Style is terminal, elongated, creamy white with dark brown dots, three mm long and extends beyond the mouth of the corolla tube. It has pedicellate glands at the base of the style and a nectariferous area at the base of the ovary, glabrous, soft, gradually tapering; stigma is apiculate. The mature buds open at 0600 h by slightly unfolding the petals. Gradually, the erect petals take horizontal position and finally reflex backwards exposing stamens and the single style; this entire process takes place in a time span of three hours. The anthers enclose the style and stigma and are bend towards it; both parts attain almost the same height. Anther dehiscence occurs one hour after anthesis by longitudinal slits. The pollen output per anther is $15,221 \pm 1528.09$ (Range 12,864-18,336) and per flower is 76,105. Pollen grains are spheroidal, tricolporate with distinct annulus, dull white, exine smooth, thick and $33.2 \mu\text{m}$ in size. The pollen-ovule ratio is 2,174:1. The pollen protein content per anther is $5.6 \mu\text{g}$ and per flower is $28 \mu\text{g}$. Pollen grains are viable for 3.5 days. The stigma attains receptivity almost at the time of anther dehiscence and continues up to the evening of the third day. A flower produces $4.08 \pm 0.6 \mu\text{l}$ (Range 2.2-5) of nectar from the ring of tissue at the base of the ovary.

The nectar sugar concentration is $36.46 \pm 3.7\%$ (Range 32-40%) and the common sugars include fructose and glucose with the former relatively more dominant. There is no significant correlation between nectar volume and sugar concentration ($r = 0.462$ at $p > 0.05$ significance level). The total sugar content in the nectar of a flower is $1.73 \pm 0.39 \text{ mg}$ (Range 0.76-2.63). The nectar contains 13 amino acids which include tyrosine, glycine, proline, lysine, aspartic acid, glutamic acid, serine, cysteine, cystine, alanine, threonine, arginine and histidine. The flowers not pollinated fall off on the fifth day. In pollinated flowers, the petals and stamens drop off on the fourth day while the fruit is in a growing stage. The sepals and style

are persistent, and remain on the plant even after the shedding of propagule. Floral bud abortion is 2%. The results of breeding systems indicate that the flowers are self-compatible and self-pollinating. The fruit set is 7% in wind-pollinated flowers, 15.8% in spontaneous autogamy, 40.0% in insect-assisted pollination and 54.6% in open pollination. Fruit set per inflorescence in open pollination is 13.96 ± 5.05 (Range 5-24). The flowers are unspecialized and the stamens and style become exposed when the petals reflex backward. They were foraged during day time from 0600-1700 h. The foragers included bees (*Apis dorsata*, *A. cerana*, *A. florea*, *Amegilla* sp., *Nomia* sp., *Megachile* sp., *Xylocopa pubescens*, *X. latipes*, *Xylocopa* sp.), wasps (*Delta campaniforme*, *Polistes humilis* and *Odynerus* sp.), a fly species, *Chrysomya megacephala* and butterflies (*Catopsilia pomona*, *Euploea core* and a Hesperiid). All these started their forage collection from 0600 h and continued until 1700 h with varying number of foraging visits at each hour. Bees collected both pollen and nectar throughout the day and accordingly the number of foraging visits were found to be nearly consistent.

In the afternoon hours, bees were found to collect primarily pollen. Wasps, the fly and butterflies collected only nectar. They made a number of foraging visits during forenoon hours and gradually their visits were reduced towards the end of the day. Of the total number of foraging visits of insects, bees made 71%, wasps 17.1%, the fly 5.5% and butterflies 6.4%. Further, *A. dorsata* and *Xylocopa* species individually made higher percentage of foraging visits. All these insects while probing the flower for nectar and/or pollen invariably contacted the style, stigma and stamens.

These insects while probing for nectar contacted the sex organs with their ventral and/or dorsal side. In case of butterflies, the proboscis usually contacted the sex organs; the head and wings rarely contacted the floral sex organs. Bees while collecting pollen always made contact with their ventral side. Body washings of insects revealed the presence of pollen grains; the mean number varied from 51.9 to 1552. Bees were found to carry more number of pollen grains than all other categories of insects; the number of pollen grains found appeared to be related to the size of the bee species. Wasps with their smooth bodies were found to carry a small number of pollen grains. The fly was found to carry relatively more number of pollen grains than the wasps. Butterflies were found to transfer pollen grains principally through their proboscis; the proboscides were found with an average number of 93.3-117.3 pollen grains. Bees were also found to forage for pollen and nectar of *Bruguiera gymnorrhiza* occasionally. *Nomia* bees and *Odynerus* wasps also collected forage from *Ceriops decandra* occasionally. High winds prevailing in the plant area enabled the medifixed anthers with free movement to release light, dry and powdery pollen grains into the air easily. Pollinated and fertilized flowers initiate fruit development immediately and take 30-35 days to produce mature fruits. Of the 35 ovules, only one ovule enlarges and the others remain undeveloped.

The developing ovule displaces the placenta laterally while the young seed elongates. Fruit is an elongated, one-seeded capsule, light green to pink, 65 ± 5 mm long (Range 50-80), completely curved with pointed apex, persistent calyx and filled at maturity by the embryo with extended radicle and attached laterally by a long funicle-like structure. Seed coat is hard, brown, hairy with placental remains attached to mature seed coat and at the hypocotyl tip. Hypocotyl comes out of the seed coat but it does not pierce the pericarp. Mature fruit with well developed hypocotyl inside hangs downwards. They are water-buoyant and dispersed by tidal waters. After detachment from the mother plant, fruit pericarp dehisces longitudinally by absorbing water. The hypocotyl is not water-buoyant without fruit pericarp. In dehisced fruit, the green hypocotyl is exposed and produces a new plant when settled in a suitable substratum. The radicle side of hypocotyl penetrates the soil and produces root system while plumule side produces new leaves and subsequent aerial system.

***Aegialitis rotundifolia* (Plumbaginaceae).** It is a soft-wooded evergreen shrub species, growing to three m height with a basally swollen fluted axis. It occurs in association with *Ceriops decandra*, *C. tagal*, *Bruguiera gymnorrhiza* and *Excoecaria agallocha*. Its leaves excrete salt which in turn gets crystallized on the leaf surface on sunny days. The flowering occurs from second week of February to third week of April. An individual tree flowers for 20-22 days. The flowers are produced in terminal, irregular one-sided cymes with pairs of opposite linear bracteoles. An inflorescence produces 6.2 ± 1.6 flowers (Range 4-10) over a

period of six or seven days. Flowers are pedicellate, small, 18 mm long, 11 mm wide, white, cup-shaped, odourless, bisexual and zygomorphic. Sepals are five, small, nine mm long, green, united basally and free apically, glabrous, coriaceous, valvate and persistent. Petals are five, alternate to sepals, 12 mm long, white, herbaceous, free above with bluntly rounded lobes, fused basally to form a corolla tube of three mm long. Stamens are five, 12 mm long, free, inserted on the corolla tube alternately with the petals. The filaments are seven mm long, whitish, glabrous, slender, forming short hollow tube with a ring of internal and external hairs at the level of the mouth of the corolla tube. The anthers are bilobed, two mm long, inserted, sagittate, introrse and basifixed.

The ovary is superior, oblong, onechambered with a single basally attached anatropous ovule. It has five grooves each extending into a lobe which in turn extending into a free style. The styles are five, free, white, each style ten mm long with an extended oblique peltate stigma initially facing inward and later facing outward. The mature buds open at 0700-0930 h by slightly unfolding a single petal first followed by the second petal and other petals within two hours. Petals reflex backward partially exposing the stamens and the styles. The styles and stigmas stand slightly below the height of the anthers, face inward at anthesis and diverge gradually moving away from the anthers but reaching closer to the petals. The anthers dehisce by longitudinal slits along with anthesis. The pollen output per anther is 288.6 ± 40.27 (Range 240-372) and per flower is 1443. Pollen grains are large, spheroidal, tricolporate characterized by prominent central wart-like sculptures, light yellow, exine rough, thick and $119.52 \pm 10.49 \mu\text{m}$ in size. The pollen-ovule ratio is 1443:1. The pollen protein content per anther is $6.08 \mu\text{g}$ and per flower is $30.04 \mu\text{g}$. Pollen grains are viable for 2.5 days. The stigma attains receptivity two hours after anthesis and continues up to the evening of the third day.

A flower produces 6.50 ± 0.8 (Range 5-7.8) μl of nectar at the flower base by the time of anthesis. The nectar sugar concentration is $46.2 \pm 5.4\%$ (Range 36-53%) and the common sugars include fructose and glucose which occur in almost equal amounts. There is no significant correlation between nectar volume and sugar concentration ($r = -0.386$ at $p > 0.05$ significance level). The total sugar content in the nectar of a flower is 3.60 ± 0.49 (Range 3.07-4.64) mg. The nectar contains 16 amino acids which include tyrosine, glycine, lysine, aspartic acid, glutamic acid, serine, cysteine, cystine, alanine, threonine, arginine, phenylalanine, proline, tryptophan, valine and histidine. The corolla gradually turns from white to dark red from day one to day four. The dark red corolla together with stamens and styles remain in place for two to three weeks during which the calyx bulges due to growing fruit inside. The calyx is persistent and inseparable from fruit. The flowers not pollinated fall off on the fourth day. The results of breeding systems indicate that the flowers are self-compatible and self-pollinating. The fruit set is 9% in wind-pollinated flowers, 25% in spontaneous autogamy, 47% in insect-assisted pollination and 60% in open pollination. Fruit set per inflorescence in open pollination is 2.62 ± 1.41 (Range 1-7). The flowers are unspecialized; the stamens and styles to become exposed when the petals reflex backward partially. They were foraged during day time from 0700-1600 h. The foragers were exclusively bees which included honey bees, *Apis dorsata*, *A. cerana*, *A. florea* and the Stingless bee, *Ceratina simillima*. All the bees collected pollen and nectar in the same and/or in a different foraging visit. Their foraging activity was primarily concentrated in the forenoon period and gradually decreased towards the end of the day. Of the total number of foraging visits of insects, *A. dorsata* and *A. florea* together made 64.5% while the other two bee species made the remaining percentage of visits. All the bees while probing the flower for nectar and/or pollen invariably contacted the styles and stamens. The *Apis* bees were also found to forage for pollen and nectar of *Bruguiera gymnorrhiza* while *C. simillima* collected pollen and nectar of *Cerriops decandra*. High winds prevailing in the plant area enabled the anthers to release light, dry and granular pollen grains into the air easily. Pollinated and fertilized flowers initiate fruit development immediately and take 30-45 days to produce mature fruits. Fruit is an elongated, bluntly pointed one-seeded capsule, light green to brown, 72 ± 4 mm (Range 65-83) long, enveloped basally by persistent calyx, funicular tube attached to seed and enlarging hypocotyl which protrudes from the seed coat but not the pericarp. Seed coat is hard, brown, embryo elongated with an extended hypocotyl. Mature fruit with well developed hypocotyl stands upright. Fruit

pericarp is thin but thickened somewhat distally. It is water-buoyant and dispersed by tidal waters. It detaches along with the quadrangular calyx.

The hypocotyls settle at the mother plant if the site is not inundated due to tidal water and float in tidal waters, especially during high tide periods. In fruits that float in tidal waters, the pericarp becomes soft and ruptures longitudinally to expose the hypocotyl to saline water. The hypocotyls devoid of fruit pericarp did not float while those with it floated. Such hypocotyls float until they find suitable substratum which is sticky and silty mud. The radicle side of hypocotyl penetrates the soil and produces root system while plumule side produces new leaves and subsequent aerial system. In the study area, very few propagules were found to settle, establish and produce new plants.

DISCUSSION

***Ceriops tagal* and *Ceriops decandra*.** It is strictly a winter bloomer whereas its closely related species, *C. decandra* is a year-long bloomer with alternate flowering and fruiting phases (Solomon Raju et al., 2006). Aksornkoae et al. (1992) reported that the occurrence of the two species at the same site is rare; we also found similar situation at the Krishna mangrove forests. The distribution of *C. tagal* in this forest indicates that it has a distinct seaward zonation and prefers well drained high saline soils, suggesting that the species is a salt tolerant mangrove with the competitive ability to grow in highly saline and partly inundated locations (Aziz and Khan, 2001). The site is flooded with water only during high tides and is well drained during low tides indicating that *C. tagal* is a higher inter-tidal mangrove specialist and the plants occurring in such sites are inundated about twenty times a month (Duke et al., 1998). Further, in such sites, rainfalls make no differences and hence, the salt content of the soil remains high and approximately uniform throughout the year. Duke et al. (1998) reported that *Excoecaria agallocha* becomes more common in the absence of *C. tagal* in such sites. At the study site, a few trees of *C. tagal* occur with some naked habitat and *E. agallocha* grows here and there in its association. On the contrary, *C. decandra* is not a strict seaward mangrove plant and it occurs commonly even in areas of tidal zone far away from sea shore (Tomlinson, 1986). Field studies here showed that *C. tagal* is absent in Godavari mangrove forest, while a few trees still survive in Krishna mangrove forests. Therefore, *C. tagal* being a seaward mangrove, it is highly unsuccessful to establish a good population size, while its sister species, *C. decandra*, with flexibility to survive in tidal zones even far away from the seashore, is highly successful to build up its populations to the extent of becoming a common constituent of mangrove forests.

In *C. tagal*, the floral characteristics such as white flowers, strong fragrance, complex petal-stamen configuration and production of moderate amount of nectar suggest an elaborate and specialized floral mechanism. The petals require an external delicate touch for the explosive release of stamens. The helically coiled hairs at the lower margins of the petals help to propagate explosive pollen release effectively (Juncosa and Tomlinson, 1987). The petal clavate appendages of petals in *C. tagal* lack hydathodes and abundant xylem which are characteristically present and have a role in flower function under extreme water pressure deficits during the day in *C. decandra* (Juncosa and Tomlinson, 1987). Such a state may make appendages very light and provide necessary trigger for petal explosion by delicate touch by the forager in *C. tagal*. Explosive pollination mechanism has also been reported in *Bruguiera* species for which the flower tripping agents are birds and butterflies (Tomlinson et al., 1979; Ge et al., 2003). Tomlinson (1986) reported night-flying insects, especially moths, as probable pollinators. Meeuse and Morris (1984) described the characteristics of moth flowers which include flower opening in the evening, display of overwhelming fragrance at that time, light flower colour, absence of landing platform, fringed petals for guidance, visual and olfactory nectar-guides, long and narrow corolla tube, abundance of nectar and short-tongued visitors. Baker and Baker (1983) reported that hawk moth flowers produce sucrose-rich or dominant nectar with low sugar concentration. Cruden et al. (1983) reported that small moth flowers produce relatively small volume of nectar with small amount of sugar. They also stated that moth flowers initiate nectar secretion one-three hours or even ten or more hours prior to the activity period of moths. In the *C. tagal*, nectar guides and tubular corolla are lacking, the nectar secretion begins an hour after anthesis; it is in moderate volume,

hexose-rich with high sugar concentration. These characters together with the shallow nature of flowers are suitable for foraging by short-tongued bees and flies (Baker and Baker, 1983; Cruden et al., 1983).

In this study, there was no foraging activity of hawk moths or settling moths at the flowers after anthesis till late evening (up to 2200 h) and the absence of moths could be due to nonavailability of nectar at anthesis and reduced opportunities for food and breeding opportunities in harsh mangrove habitats. *C. tagal* with a few trees and a few numbers of flowers per unit of time per tree does not constitute a potential nectar station for moths. Further, adult moths do not survive for longer periods and in particular, hawk moths may survive for a period exceeding a month (Opler, 1983). Within that life span, the availability of nectar in the habitat is crucial and since *C. tagal* is unable to attract and supply its nectar requirements, the moths might have disappeared or migrated to other reliable food-rich habitats. *Apis* bees and *Chrysomya* flies make up day-time foragers for *C. tagal*. With a small number of trees and again each tree with a small number of flowers per day, *C. tagal* is not a potential pollen and nectar source for honey bees. Yao et al. (2006) also reported that this plant species is a minor pollen and nectar source for honey bees. In the study site, *Aegiceras* and *Bruguiera* flowers attract honey bees and the latter were found concentrating on these species. *Chrysomya* flies frequent the flowers of *C. tagal* daily effecting pollination but they have limited pollen transport capacity; this however, is compensated by their numbers and could bring about substantial geitonogamy and xenogamy (Faegri and van der Pijl, 1979). The petal colour change may act as a nectar guide for the flies to visit the flowers for several days. The close proximity between trees of *C. tagal* at the study site also facilitates xenogamy. The fly is present throughout the year unlike periodic bees and moths; but its presence depends on local opportunities for breeding sites (Faegri and van der Pijl, 1979). The butterfly is an occasional forager and has no role in pollination. Our observations suggest that *Chrysomya* is the primary and consistent pollinator, while honey bees are secondary and occasional pollinators. Petal explosion also occurs sporadically in nature due to wind action and this is evident in bagging experiment in which there is a negligible fruit set and also in natural conditions to some extent. The role of wind in tripping explosive pollination has also been reported in *Hyptis suaveolens* (Lamiaceae) (Solomon Raju, 1989) and *Shorea robusta* (Dipterocarpaceae) (Aluri et al., 2004). Therefore, petal explosion and subsequent pollination events are primarily vector-dependent and inadequate numbers or non-availability of pollinators are bound to result in reduced or no fruit set in *C. tagal*. Less is known about the importance of amino acids in floral nectars to foragers. Amino acids are the second most abundant class of the compounds after sugars to be found in nectar (Gardener and Gillman, 2002). Their concentrations in nectars are considerably lower than sugar concentrations. But even the slightest concentrations are important nutritionally and also contribute to the “taste” of the nectar (Baker and Baker, 1983). Honey bees respond to differences in amino acid concentration and detect amino acids. They prefer certain amino acids and their presence makes nectar more attractive (Dress et al., 1997). Tyrosine is not an essential amino acid, but may be important in the formation of sclerotin (Gardener and Gillman, 2002). Phenylalanine is a precursor of specific honey aroma component, phenylethanol (Thawley, 1969), iso-leucine is required for rapid breeding (Slansky and Feeny, 1977). Flies also prefer amino acids in nectar. In the flies, *Boettcherisca peregrina* and *Phormia regina*, proline stimulates salt receptor cells, methionine and valine stimulate sugar receptors, methionine also elicits a feeding response from flies and glycine and serine invoke an extension of the proboscis (Shiraishi and Kuwabara, 1970; Goldrich, 1973). *C. tagal* flowers with a mix of floral characteristics of moth, bee and fly flowers contain conventional protein building amino acids such as tyrosine, glycine, methionine, proline, lysine, aspartic acid, glutamic acid, serine, cysteine, alanine, threonine and arginine but are devoid of other proteinbuilding amino acids such as phenylalanine, valine, leucine, iso-leucine, tryptophan and histidine. The nectar provides an instant supply of methionine, lysine and arginine for honey bees and flies; moths if occur in the habitat also make use of this nectar for protein building. The presence of several amino acids in this nectar source stimulates feeding and may also be an important source for flower foragers. *C. decandra* as a common species in most of the regions and its distribution range may have achieved distinct out-crossing rates and accordingly, it has been reported to be an outcrosser (Solomon Raju et al., 2006). On the contrary, *C. tagal* with a small number of individuals at

the study site can produce offspring with mixed mating system only if it fails to attract potential and adequate pollinators.

In line with this, we have found that it possesses such a system to produce fruit set even through autogamy. But, autogamy is negligible as realized in bagging experiment. In *Kandelia candel* and also in a crypto-viviparous species, *Avicennia marina*, negligible self-pollination has been reported in bagging experiments (Sun et al., 1998; Clarke and Myerscough, 1991). The fruit set in *C. tagal* is through geitonogamy and xenogamy. The long flower life and stigma receptivity and high pollen-ovule ratio (Cruden, 1977) indicate that the plant is primarily out-crossing. However, the close proximity of the existing trees at the study site in the course of time could bring about genetic uniformity and if this happens, then the survival of this species becomes doubtful. In *C. decandra*, the floral characteristics such as small white flowers lacking fragrance, simple stamen-petal configuration, short, thick filaments and production of trace amount of nectar suggest a simple floral mechanism. Juncosa and Tomlinson (1987) stated that the short basal hairs of petal edges have no evident function in *C. decandra*, but these hairs are well developed and help to propagate explosive pollen release effectively in fragrant flowers of *C. tagal*, in which the petal-stamen configuration is elaborate and specialized. Further, these authors reported that petal clavate appendages in *C. decandra* have abundant xylem elements with a significant reservoir of water and hydathodes at or near the termini; they have significance in flower function under extreme water pressure deficits during the day in mangrove swamps. Abundant xylem is absent in petal appendages in *C. tagal* and *K. candel*, which are pollinated at night or early in the morning (Juncosa and Tomlinson, 1987). Therefore, the abundant xylem and hydathodes and their function in petal appendages of *C. decandra* suggest that the latter is adapted for pollination during the day. Tomlinson (1986) suggested that wasps and flies are suitable for pollination in *C. decandra*. Juncosa and Tomlinson (1987) noted that trigonid bees and small insects visit *C. decandra* flowers.

In the present study, bees while collecting pollen and nectar and wasps while collecting nectar pollinate *C. decandra* flowers consistently. Female bees of *Nomia* and worker bees of *Trigona* collect pollen voraciously for brood provisioning. Female wasps collect nectar after mating for the maturation of the eggs. The plant produces a small number of flowers daily and accordingly, the pollen and nectar available is also in small quantities. Further, the anthesis process is gradual and the accumulation of new flowers with pollen and nectar begins to appear from late morning. As a consequence, bees and wasps also delay their foraging activity and appear from late morning onwards and stop foraging in the early evening. As flower number and floral rewards are small at the plant level, both bees and wasps fly between individuals of *C. decandra* in quest of more forage and this foraging behaviour brings about cross-pollination. Hand-pollination tests showed that it is an obligate outcrosser. The protandry, long period of stigma receptivity and long flower life substantiate this; pollination by bees and wasps favours outcrossing (Tomlinson, 1986). The pollen recovered from the body washings of these foragers suggests that they effect pollination. Earlier reports on bees, flies, wasps or even other insects as pollinators (Tomlinson, 1986; Juncosa and Tomlinson, 1987) and the present study on bees and wasps as pollinators suggest that *C. decandra* is strictly entomophilous and utilizes different locally available insects as pollinators. The commonness of *C. decandra* at Coringa mangrove forest provides ample opportunities for effective outcrossing and the genetic variation thus achieved would permit the species to survive well in the harsh mangrove environment. In *C. tagal*, the number of fruits per inflorescence varies from one to five, but one- and two-fruited inflorescences are most common.

The fruited flowers produce only one seed against the actual number of six ovules as in *C. decandra* and all other viviparous species of Rhizophoraceae. This characteristic may permit these plants to save resources and use them to produce one-seeded viable fruits. Despite this effort by *C. tagal*, a few propagules lack green pigment and becoming entirely yellowish or yellowish on one side and purplish on another side. Such hypocotyls have been referred to as “albino” forms which also occur in *C. decandra* and *Bruguiera gymnorrhiza* (Solomon Raju et al., 2006; Allen and Duke, 2006). These propagules are non-viable, cannot photosynthesize and die after depleting reserves if settled in the habitat. The propagules that are green first and brownish purple later are healthy and grow to their actual size. The length of hypocotyls in *C. tagal* is

almost double the length of hypocotyls in *C. decandra*. Both the species of *Ceriops* show a short period of attachment to the maternal plant (Solomon Raju et al., 2006) and this characteristic is not in agreement with the report of Bhosale and Mulik (1991) that the hypocotyls of true viviparous mangrove species remain attached to the mother plant for a full year. The hypocotyl grows upward in *C. decandra* in which flowers are sessile (Solomon Raju et al., 2006), while in *C. tagal*, it grows downward which seems to be because of stalked flowers and more weight of the hypocotyls. This is an important field characteristic feature to distinguish *C. tagal* from *C. decandra*. The downwardly hanging hypocotyl is also a characteristic of *Bruguiera*, *Rhizophora* and *Kandelia* species. In *C. tagal*, the cotyledonary yellow cylindrical collar emerges from the fruit about ten days prior to the detachment of the hypocotyl while this structure is entirely absent in *C. decandra* (Solomon Raju et al., 2006). The cotyledonary collar is a characteristic also in *Rhizophora* in which it is reddish brown and in *Kandelia* in which it is yellow and the hypocotyl is about double the length of *C. tagal* (Aksornkoae et al., 1992). Fruit in *C. tagal* grows continuously and the seed also has no dormancy like in other mangrove species of Rhizophoraceae (Farnsworth and Farrant, 1998). This form of fruit growth and seed germination leading to the formation of hypocotyl while still attached to the mother plant represents “vivipary”, the opposite of “ovipary” in which seed dormancy is the rule. The viviparous condition has been considered as an evolutionary loss of seed dormancy (Farnsworth and Farrant, 1997), however, it is an adaptive feature for the plant to overcome the harsh tidal environment for seedling establishment in the parental sites but it is not considered adaptive for dispersal either in time or space (Sun et al., 1998). The other adaptive values of vivipary include facilitation of early rooting (MacNae, 1968), buoyancy during sea dispersal (Rabinowitz, 1978), transfer of maternal nutrients to the hypocotyls (Pannier and Pannier, 1975), maintenance of embryonic osmotic equilibrium and establishment in coarse grained environments. On the other hand, vivipary incurs maternal costs to supply water and necessary nutrients. Numerous attached seedlings may constitute a substantial carbon sink to the maternal plant, a concentrated apparent resource for herbivores (Farnsworth and Farrant, 1998). *C. tagal* at the study site was found to produce 20 to 60 hypocotyls per tree and it is not known whether this small number could attract herbivores. Kairo et al. (2001) reported that viviparous mangrove species use self-planting or stranding strategy for establishment depending on forest conditions tide and stability of the soils. The self-planting strategy dominates in undisturbed mangrove forests but stranding strategy is dominant in exploited and open or naked forests (Dahdouh-Guebas et al., 1998). *C. tagal* with epigeal seed germination, elongated and pointed hypocotyls with straight curvature (Clarke et al., 2001) fall freely from the mother plant and plant themselves into the mud at the same site during low tide period.

The hypocotyls if fallen during high tides float to another site for settlement. But, our field studies do not show settlement of hypocotyls away from the mother plants suggesting that *C. tagal* uses self-planting strategy only. This is further substantiated by McGuinness (1997), who also reported that the hypocotyls of *C. tagal* in Northern Australia dispersed to very short distances; only 9% moved more than three m from the parent tree. He also mentioned that within that short distances, a high percentage of them were either damaged or eaten by animals. *C. tagal* at the study site may also be experiencing the damage or consumption by animals, especially crabs as the latter have been reported to show high predation on hypocotyls in high inter-tidal areas (Duke et al., 1998). Some of the fallen hypocotyls settled at the mother plants showed signs of weathering. Therefore, the study suggests that *C. tagal* though occurring in undisturbed and human-free site, is almost unable to add new plants and the presence of only a few individuals at the site attests this contention.

The work reported in this paper is important for initiating studies on the genetic structure of *C. tagal* population. The genetic marker analysis helps to understand the variability within and between populations. Introduction of *C. tagal* from the mangrove forests of the Sundarbans, Andaman and Nicobar islands to this site would help to enhance gene flow in order to maintain the gene diversity and expansion of population size of *C. tagal* in Krishna mangrove forests. The pollinated flowers initiate fruit growth and development immediately and produce mature fruits in about two months. Fruits are light green, ovoid, conical and blunt apically. They are distinct with five-lobed persistent calyx and produce only a single seed. The seed has no dormancy and it immediately produces spindle-shaped hypocotyls within three months,

while still attached to the maternal parent. Then, it detaches from the residual fruit. The hypocotyl is slender, green, clearly ribbed, angular, sulcate, 15 cm long and broadened at the lower end. The short period of hypocotyl attachment to the maternal parent is a characteristic of cryptoviviparous species (Bhosale and Mulik, 1991). However, *C. tagal* shows this characteristic, being a true viviparous species (Selvam and Karunakaran, 2004). Further, the hypocotyl in *C. decandra* grows upright and is an important characteristic to distinguish it from *C. tagal* in which the hypocotyl grows downward (Kathiresan and Rajendran, 2003). In *C. decandra*, the hypocotyl is characteristically green and seems to have the potential to photosynthesize actively with water and necessary nutrients drawn from the parent tree. Viviparous reproduction allows hypocotyls to develop some salinity tolerance before being released from the parent tree. It provides a store of nutrients before the hypocotyls fall-off from the plant and helps in quick rooting in the muddy environment. The hypocotyl characteristics also help to develop buoyancy for distribution of the seedlings and structural stability to protect seedling from damage (Kathiresan, 2003). Therefore, vivipary could be an adaptive feature of the plant to overcome the harsh tidal environment for seedling establishment, especially in the parental sites. The small upright hypocotyls, when detached from the mother plant, float in water and settle at different places depending on the direction and extent of movement of tidal water. Such dispersal characterizes “Stranding Strategy”. Pollinator species of *C. tagal* and *C. decandra* need a special mentioning here. The fly pollinators have rich sources of breeding and feeding materials in the forests, but the breeding materials are subject to flooding during high tide periods and during rainy season. Bees and wasps use above ground plant materials such as live/dead branches/wood. But, these materials are usually collected by local people for use as fuel wood. The forage collection from plants occurring in windy areas is a difficult task for them and hence these foragers tend to collect the forage from the plants occurring landward. These foragers have no difficulty to collect forage from *C. decandra* as the latter is distributed principally landward. In case of *C. tagal*, it occurs seaward where wind blows at high speed which usually prevents or minimizes the foraging activity of honeybees. In consequence, the bees tend to collect the forage from the flowers covered by the branches and foliage where there is reduced wind speed.

The importance of bark of *C. decandra* in dyeing the cotton and fishing nets here is driving the fishermen to cut down trees indiscriminately and the tree cutting rate is further driven by the trade concept in some fishermen. Most of the areas where *C. decandra* occurs have been partly cleared for its bark and wood. The cleared areas show the stumps or the basal part of the cut trees and these areas are gradually being invaded by the oviparous weed species, *Excoecaria agallocha*. Further, some such areas are being used as cattle shelters by some villagers. Therefore, such areas cleared of *C. decandra* trees and the still existing stretches of *C. decandra* are an important consideration for the concerned forest authorities with regard to conservation, management and artificial regeneration of this species in naked and semi-naked mangrove habitats in order to provide a continuous supply of bark tannin for fishermen for treating their cotton fishing nets.

***Rhizophora apiculata* and *Rhizophora mucronata*.** These species are polyhaline, evergreen true viviparous tree species. The former species blooms throughout the year, but shows profuse flowering for two months during August-September while the latter species flowers for about six months with profuse to sparse flowering during August-September. Mulik and Bhosale (1989) reported that *R. mucronata* flowers throughout the year with intense flowering during September-November. The flowers are sessile and borne in pairs below the leafy cluster in *R. apiculata*, while they are pedicellate and borne in four-flowered cymes within the leafy cluster in *R. mucronata*. With foliage background, the flowers of *R. mucronata* are also quite prominent and may be more attractive to flower foragers when compared to those of *R. apiculata*. In the latter species, bee foraging activity has been found to be consistent during profuse flowering period than at other times of the year. This suggests that greater floral displays during profuse flowering period have an important role in attracting bee pollinators. The year-long flowering allows the plant to set fruit continuously and this may be a fail-safe strategy against pollination limitation and propagule predation. In both the species of *Rhizophora*, the flowers exhibit certain adaptations for anemophily. The flowers are pendulous, point downward at maturity and situated below or within the leafy crown; this floral orientation

is important to minimize interference of foliage for effective pollen dispersal by wind. The sepals diverge least, while the petals are glabrous, do not recurve or retain pollen grains in *R. apiculata*. But, in *R. mucronata* and in all other *Rhizophora* species, the petals are equipped with marginal hairs which have been shown to be promoters of anemophily by their hygroscopic movements (Tomlinson, 1986). Late morning anthesis, high pollen/ovule ratio, light powdery pollen, absence of an attractive colour and odour, absence of abundant pollinators and the presence of traces or minute quantity of nectar are some important characteristics for anemophily in the genus *Rhizophora* in general (Tomlinson, 1986) and in the studied species of *Rhizophora* in particular. Further, anther dehiscence and pollen release occur in mature bud in both *Rhizophora* species. In both, the late morning anthesis is another important characteristic for the effective dispersal of dry powdery pollen grains from the already dehiscent anthers due to moderate levels of temperature and humidity present at that time. The anthesis period noted in this study for *R. mucronata* does not agree with the report by Kondo et al. (1987) that the anthesis occurs in the afternoon from 1500 to 1700 h. These two plant species occur as pure stands mostly and are located in a windy environment along the creeks. This form of distribution may facilitate effective dispersal of pollen between individual trees and receptive sites of flowers receive wind-borne pollen. Kondo et al. (1987) reported that the pollen grains also have evolved characteristics for anemophily. Tomlinson et al. (1979) also experimentally proved that wind-borne pollen is abundant and hence anemophily is most efficient in such pure stands of other *Rhizophora* species.

Although both *R. apiculata* and *R. mucronata* have several adaptations for anemophily, their stigma is not elaborated in the manner usual for wind-pollinated species to capture wind-borne pollen. Similar structure of the stigma has been reported in all other *Rhizophora* species (Tomlinson, 1986). The absence of marginal hairs on petals, lack of elaboration of stigma, absence of odour and presence of traces or minute quantity of nectar seem to be vestigial characteristics of entomophily. Kress (1974) also related these characteristics to entomophily in *R. mangle* and *R. stylosa*. The flowers of *R. apiculata* attract the bees such as *Nomia*, *Trigona* and *Halictus*, while those of *R. mucronata* attract the bees such as *Nomia*, *Trigona*, *Halictus*, *Ceratina* and *Xylocopa*, and a moth species. Kondo et al. (1987) reported that *R. mucronata* is anemophilous, but is also pollinated by small insects like *Camponotus* sp., *Onychostylus pallidiolus* and a Collembola. In both the plant species, pollen is the principal reward since it is produced in huge amount. Further, the flowers are nectariferous but the nectar is secreted in traces or in minute quantity and hence has little importance for the foragers. The pollen and/or nectar feeding behaviour of these bees and the moth would contribute to pollination. But, their pollen feeding activity may considerably reduce the availability of airborne pollen and hence may affect the efficiency of anemophily. The copious production of pollen at flower level may compensate to some extent the pollen loss caused by pollen collecting bees. Further, thrips have been found in the floral buds of both *R. apiculata* and *R. mucronata*. Their presence in the buds indicates that egg deposition by female thrips takes place prior to bud formation; the eggs hatch, produce larvae or adult thrips by the time the buds mature. These thrips represent the suborder Terebrantia of the order Thysanoptera. The females of this group of thrips have an ovipositor with which they cut slits into plant tissue in order to insert their eggs, one egg per slit. With this ability, these thrips raise their offspring in floral buds. They are short-distance flyers, but windy areas extend their travel distance to a great extent. They feed on both nectar and pollen and in so doing contribute to both self- and cross-pollination, but the latter mode is more effective in areas where pure stands of *Rhizophora* species occur. The study suggests that the pollination mechanism in the studied *Rhizophora* species is originally entomophilous and is now being transformed to anemophily. This transitional stage of pollination mechanism is advantageous for these plant species to utilize both wind and insects as pollinating agents for the success of sexual reproduction. Tomlinson (1986) stated that animal pollination predominates in mangrove communities and in such a situation anemophily enables these species to escape the competition for insect pollinators and to set fruit in the total absence of insect pollinators. Tomlinson (1986) reported that *Rhizophora* exhibits weak protandry and is self-compatible. He found that the isolated greenhouse plants set fruit. He has not mentioned what species of this genus are weakly protandrous and self-compatible. Coupland et al. (2006) reported that *Rhizophora* species show low rates of fruit set due to lack of autogamy. Ghosh et al. (2008) mentioned that

a distinct trend for self-incompatibility exists in *Rhizophora*. In this study, *R. apiculata* and *R. mucronata* show anther dehiscence in mature bud and commencement of stigma receptivity soon after anthesis, suggesting that they are weakly protandrous. Tomlinson et al. (1979) reported that in these species, the petals and stamens fall off the flower on the day of anthesis leaving the central stigma alone in the empty flower. These authors also stated the stigma lacks any secretion or divergence of its two lobes. Kondo et al. (1987) reported that the stigma is two-lobed; each tip contains small papilla and secretes mucilage.

In this study, it is found that the stigmatic lobes diverge soon after anthesis and since then it is in receptive stage to receive pollen. The stigmatic lobes are mucilaginous and have minute papilla, which may aid in capturing and retaining pollen readily. Tomlinson et al. (1979) reported that in *Rhizophora stylosa*, an individual flower is generally incapable of self-pollination. Hand-pollination results suggest that *R. apiculata* and *R. mucronata* are capable of self-pollination either by gravitational fall of pollen or by wind driven pollen fall on the stigma. Further, these plants set fruit through allogamy, autogamy and geitonogamy (Kondo et al., 1987). The significantly low fruit set evidenced in open-pollinations is attributable to the intense pollen feeding activity of bees and also to the wastage of pollen due to wind activity. Coupland et al. (2006) also reported low fruit set to the extent of 13% in open-pollinations.

The ability to set fruit through self- and cross-pollination is the characteristic of pioneering species in mangrove communities. *R. apiculata* and *R. mucronata* with this ability may become established as isolated individuals in new environments remote from parental source. Like in *Bruguiera cylindrica*, the flowers are four-ovuled in both *Rhizophora* species, but only one ovule develops into mature seed in fertilized and fruited flowers. The production of one-seeded fruits may be due to maternal resource constraint or maternal regulation of seed set. Fruits mature within four to six weeks and are not enclosed by the persistent and expanded calyx at any stage. The calyx therefore seems to have no role in protecting the fruit. As the fruit is thick with hard pericarp, it does not require protection from the calyx. In both *R. apiculata* and *R. mucronata*, the single seed formed in the fruit is not dormant and germinates immediately to produce a cylindrical hypocotyl or seedling, while still on the maternal parent. The hypocotyl emerges out of seed and fruit pericarp and remains naked until it is detached from the maternal parent. This is a characteristic of “true viviparous” species (Tomlinson, 1986). While still attached to the maternal parent, the seedling develops chlorophyll and actively photosynthesizes; the parent tree supplies the water and necessary nutrients (Selvam and Karunakaran, 2004). The seedling hangs downward and detaches from the residual fruit at the collar end, leaving behind its cotyledons, and falls from the maternal parent. Christensen and Wium-Andersen (1977) speculated that in *R. apiculata*, the development from visible flower buds to mature propagules lasts about two years while Muniyandi (1986) reported that the propagule takes eight months to grow to full length after fertilization. But, in this study, it is found that this species produces mature seedlings from flower buds in a time span of about four months only. Muniyandi (1986) say that the seedlings of *R. mucronata* take 16 months to grow to full length after fertilization in *R. mucronata*. But, in this study, it is found that this species produces mature seedlings from flower buds in a time span of about four months only. The fallen seedlings of *R. apiculata* and *R. mucronata* plant themselves into the mud in the vicinity of the maternal parent or are stranded and planted away from maternal parent. In the latter case, the seedlings sink after some period of dispersal and exhibit growth under water (Rabinowitz, 1978). The study shows that the seedlings disperse through self-planting and stranding strategies.

Although dispersal distances have not been measured in this study, the available information shows that most viviparous seedlings do not disperse more than one km from their point of origin (Clarke, 1993), and in certain instances, as little as 65 m (Chan and Husin, 1985) or even three m (McGuinness, 1997). Davis (1940) found that *Rhizophora mangle* propagules carried by ocean currents could disperse at least 100 km. Smith (1987) reported seedling predation prior to and after detachment from the maternal parent in *R. apiculata* and *R. mucronata*. Monkeys and insects attack seedlings prior to their detachment, while crabs attack seedlings when they later fall in the mud or tidal water. Monkeys, insects and crabs collectively contribute to more than 83% of seedling predation. Bosire et al. (2005) reported that seedling predation is a mechanism to regulate individual species colonization, but in case of *R. mucronata*, the seedling predation is the least since they are very large and are not preferred by crabs. In this study, there is no seedling

predation prior to detachment from the maternal parent in both the species of *Rhizophora*. Seedling predation by crabs may be there since different species of crabs have been found. The locals use crabs as a source of food and livelihood.

***Bruguiera gymnorrhiza* and *Bruguiera cylindrica*.** Both the species of *Bruguiera* are polyhaline, evergreen true viviparous tree species. *B. gymnorrhiza* is a year-long bloomer with concentrated flowering during April-June, while *B. cylindrica* shows flowering during September-March during which flowering level is almost uniform. On *B. gymnorrhiza*, pollinator activity is consistently intense during concentrated flowering period, while it is sporadic at other times of the year. On the contrary, pollinator activity is not consistent and also not intense at any point of time on *B. cylindrica*. This finding stated that pollinators preferentially visit plants with greater floral display. Therefore, fruit set is largely a function of pollinator activity during concentrated flowering period in *B. gymnorrhiza*. However, the characteristic of year-long or extended flowering in these two tree species is an important adaptation for additional fruit set; this characteristic would enable them to compensate the low fruit set rate which may result from pollinator limitation and also to compensate the loss of seedlings due to predation. Tomlinson (1986) reported that *B. gymnorrhiza* represents the large, solitary-flowered group, while *B. cylindrica* represents the small, many-flowered group. The present study shows that it is true in case of *B. gymnorrhiza* but it is not so in *B. cylindrica* in which the flowers are small, but borne in three-flowered cymes. The flowers are pendulous in *B. gymnorrhiza*, while they are either horizontal or downward or slightly erect and located outward in the crown of leaves in *B. cylindrica*; these different orientations enable the pollinators to collect the forage comfortably. In both species, the anthesis period is the same, is confined to morning hours and quite appropriate for pollination by day-active pollinators.

The field studies also indicate that their flowers receive visits exclusively from day-active pollinators. The flowers are red in *B. gymnorrhiza* while they are greenish-white in *B. cylindrica*. In both the species, the floral characteristics such as large or small flowers with concealed nectar, elaborate complex petal-stamen configuration, presence of basal clumps of hairs and marginal hairs suggest specialized explosive floral mechanism which is functional only when pollinating agents are involved. The same elaborate specialized mechanism is present in all other species of *Bruguiera* (Tomlinson et al., 1979). In *B. gymnorrhiza*, the petals are 14 and each petal encloses two stamens; this petal-stamen configuration requires multiple visits of pollinators for the explosion of all petals. In *B. cylindrica*, the flowers have only seven or eight petals with 14 or 16 stamens and closely spaced; this arrangement with reduced number of petals in relation to the small flower size is an important adaptation for the explosion of all petals of the flower and subsequent pollination in a single or two visits of the pollinator insects. Petal explosion is characteristically violent in *B. gymnorrhiza*, while it is non-violent in *B. cylindrica*. Further, similar explosive mechanism is present also in another mangrove Rhizophoraceae member, *Ceriops tagal*. Therefore, the floral mechanism in all the species of *Bruguiera* and in *C. tagal* is highly specialized and reflects an advanced state when compared to the simple floral mechanism that is present in *Ceriops decandra*, *Rhizophora* species and *Kandelia candel* - all belonging to mangrove Rhizophoraceae (Tomlinson, 1986; Juncosa and Tomlinson, 1987). Further, explosive pollination mechanism has been reported in a number of non-mangrove families such as Lamiaceae, Fabaceae, Onagraceae, Loranthaceae, Marantaceae, Urticaceae, Ericaceae, Fumariaceae, Musaceae, Cornaceae, Acanthaceae and Orchidaceae (Solomon Raju and Subba Reddi, 1995; 1996). In *Bruguiera*, the explosive floral mechanism involves different functional aspects. At the time the flower opens, each petal pouch enclosing a pair of anthers includes loose pollen due to anther dehiscence during mature bud stage and stays in cocked position due to floral expansion and pressing of stamens against the interlocked margins of the petals. Marginal hairs appear to be important in holding the petals in the folded position. The petal explosion occurs due to release of tension by a slight touch at its hairy base by the probing pollinator during its vigorous search for nectar in the floral cup. During explosion, the petal unzips instantly, scattering a cloud of pollen, most or part of which falls on the pollinator. In each flower, individual petals work independently and this requires more than one visit of the same pollinator species or more than one pollinator species. This observation is substantiated by the occurrence of closed and open

petals in each flower. The flowers with unexploded petals due to non-receipt of foraging visit(s) fall off without pollination or without ever-opening. In *B. gymnorrhiza*, the following characters suggest adaptations for bird pollination: the flowers are recurved and typically point backwards into the crown of the tree; this facilitates an approach by a perching bird. Nectar is produced in abundance and held in the deep floral cup. The calyx is red, a colour attractive to birds. Large flowers with a heavy construction are suitable for a powerful pollinator like a bird (Faegri and van der Pijl, 1979). Azuma et al. (2002) examined *B. gymnorrhiza* flowers for scent characteristics and reported that the floral scent is lacking and the floral characteristics are indicative of bird pollination. Ghosh et al. (2008) also reported that the flowers are adapted to a range of flower visitors such as birds for pollination. Kondo et al. (1987) reported that this species is pollinated by honeyeaters, white eye and insects. Ge et al. (2003) mentioned that the flowers are pollinated by birds or butterflies. Solomon Raju (1989) reported that the flowers are exclusively pollinated by three species of passerine birds, *Nectarinia asiatica*, *N. zeylonica* and *Zosterops palpebrosus* at the Godavari mangrove site; then this site was ecologically healthy and there was little human interference.

The present study finds that this site is now ecologically degraded and fragmented due to land use changes. With this present situation, *B. gymnorrhiza* is now pollinated exclusively by pollen and nectar collecting bees consisting of *Apis*, *Nomia* and *Halictus* genera. These bees trip the tensed petals to release the stamens which in turn eject a cloud of pollen from the already dehiscent anthers. During this process, the bees get a pollen shower all over their body, especially on their dorsal side. Further, the bees fly between individual trees in quest of more forage; this foraging activity is important to bring about cross-pollination. The production of a small number of fresh flowers daily at tree level may also compel the pollinator bees to make inter-tree flights and effect cross-pollination. Their body washings indicated that they carry pollen and transfer the same to other flowers they visit. The study suggests that *B. gymnorrhiza* is strictly melittophilous and this mode of pollination is as efficient as ornithophily; but the pollen feeding activity of bees may affect the pollen availability rate for the receptive stigmas at the population level which in turn may affect the natural fruit set rate. However, the bees are reliable pollinators when compared to bird pollinators. The ability of the plant to utilize birds and bees is certainly adaptive and is also essentially required for the survival, colonization and expansion of its geographical range (Tomlinson, 1986). Tomlinson et al. (1979) stated that small-flowered *Bruguiera* species including *B. cylindrica* is pollinated by butterflies. These authors also mentioned the following characteristics as adaptations for butterfly pollination: small flowers in nearly erect state and displayed to the outside of the tree crown; thin branchlets which are insufficient for bird perching; greenish-yellow petals; flat calyx cup with a small quantity of nectar; and pollen release by delicate, distal stimulation of petals. In this study, the flowers have been found to have three different orientations while all other characteristics remain the same. A careful examination of these characteristics as Faegri and van der Pijl (1979) does not conform to the characteristics of butterfly-flowers. Tomlinson (1986) reported that this species is pollinated by small insects including butterflies. In this study, *B. cylindrica* has been found to be pollinated by bee and wasp species only. *Nomia* bees, *Odynerus* and *Polistes* wasps during nectar collection and the first species also during pollen collection trip all petals of a flower mostly in a single visit; then these insects get a pollen drizzle all over their body, especially on their dorsal side. Further, they fly between individual trees to collect more forage and in so doing they carry pollen on their bodies; this foraging activity is important to bring about self and cross-pollination. Therefore, *B. cylindrica* is bee- and wasp-pollinated but not butterfly-pollinated. Tomlinson (1986) mentioned that bees and wasps represent a group of pollinators that nest in mangroves, and some populations are completely dependent on mangal for their existence. Ghosh et al. (2008) reported that some wasps and flies are highly dependent on mangroves for nesting. In the light of these reports, it is not unreasonable to suggest that bees and wasps are reliable pollinators since they nest in mangroves and collect forage from the same plants for their nutrition. In the present study, both the species of *Bruguiera* with specialized floral mechanism offer pollen and nectar as rewards to their pollinators. Pollen grains are very dry even at the time of flower-opening. Their surface sculpture is finely reticulate; they are tricolporate with numerous small and shallow depressions, and easily adhere to the body of insect pollinator so that the latter can easily transfer pollen (Kondo et al., 1987). They contain some protein content and are important in the

nutrition of bee pollinators. In *B. gymnorhiza*, nectar production is continuous in some flowers, while it is not so in some other flowers. Such nectar production pattern indicates that nectar secretion ceases in pollinated flowers, while its secretion is continuous until the stigma loses receptivity or until the flower is pollinated. The production of copious amount of nectar with dilute sugar concentration is the characteristic of bird-pollinated flowers (Baker and Baker, 1983). But, the nectar of *B. gymnorhiza* is copious with moderate sugar concentration; it is suitable for bee pollinators as the latter tend to prefer sugar concentrations of 30 to 50% (Waller, 1972). The sugars present in the nectar include only hexoses. Roubik (1995) stated that nectar with only hexose sugars is rarely reported. Baker and Baker (1983) segregated bee flowers into those adapted to “short-tongued” bees (with less than six mm in length) and those adapted to “long-tongued” bees. These authors also reported that nectars of flowers pollinated by short-tongued bees are usually hexose-rich, while those pollinated by long-tongued bees are usually sucrose-rich. In line with this, the bees observed have tongues less than five mm length, are short-tongued and utilize the hexose nectar of *B. gymnorhiza*. De Groot (1953) reported that insects in general and bees in particular require ten essential amino acids - threonine, valine, methionine, leucine, isoleucine, phenylalanine, lysine, histidine, arginine and tryptophan. The nectar of *B. gymnorhiza* has three of these essential amino acids, lysine, histidine and arginine. The presence of these amino acids and also other non-essential amino acids, alanine, aspartic acid, glutamic acid, glycine and serine may have a role in giving the “taste” to the nectar (Baker and Baker, 1982). The nectar also has some protein content. Therefore, the nectar of *B. gymnorhiza* with these amino acids and protein content has high nutritional value and bee pollinators are attracted to this floral source, especially during concentrated flowering period.

In *B. cylindrica*, the nectar is produced in small quantity, hexose-dominant and the sugar concentration is low. Bees and wasps utilize this nectar until exhausted. This observation is in partial agreement with the generalizations made by Baker and Baker (1982; 1983) who stated that the production of a small quantity of nectar with high sugar concentration is the characteristic of bee-flowers, and that the nectars of flowers adapted for pollination by short-tongued bees are hexose-rich, while those adapted for pollination by wasps are sucrose-rich. Tomlinson (1986) mentioned that pollination may favour outcrossing in *B. gymnorhiza*. Kondo et al. (1987) reported that this species produces fruit through allogamy, autogamy and geitonogamy and hence, it might be outcrossing and inbreeding. Ge et al. (2003) stated that this species has mixed mating system with outcrossing as a main system. In this study also, *B. gymnorhiza* has been found to set fruit through allogamy, geitonogamy and autogamy, but all modes are functional only when petal explosion is manipulated; this suggests that pollination is essentially vector-dependent and fruit set is completely a consequence of the foraging activity of bee pollinators. The fallen flowers with some or a few unexploded petals evidenced in this study indicate that wind is not an agent of pollination. Fruit set through vector-mediated autogamy or geitonogamy indicates that *B. gymnorhiza* is self-compatible and self-pollinating. But, protandrous condition and stigma showing receptivity commencing from day two and extending its receptivity until day four indicate that it is primarily adapted for cross-pollination. The small papilla and mucilage secreted by stigmatic lobes are special adaptations to retain pollen readily; these are especially important for capturing cross-pollen (Kondo et al., 1987). Therefore, *B. gymnorhiza* with mixed mating system is adapted for pollination by biotic agents, the classes of which may change from time to time in the same habitat depending on the local land use changes. Similar vector-dependent mixed mating system and stigma function exists in *B. cylindrica*. Such a mating system facilitates fruit set in the presence of pollinators even in isolated trees of both the species of *Bruguiera*. With the ability to set fruit through self-pollination, these species can colonize new areas and expand their distribution range. *B. cylindrica* has scattered distribution in the study sites and also here and there it has established small patches representing pure stands. This finding is in agreement with Tomlinson (1986) who stated that it may form pure stands. In mangrove Rhizophoraceae, the flowers have been reported to contain six or four ovules (Tomlinson, 1986). The flowers are six-ovuled in *B. gymnorhiza* and four-ovuled in *B. cylindrica*; but only one ovule develops into mature seed in fertilized and fruited flowers in both the species. The production of one-seeded fruits may be due to maternal resource constraint or maternal regulation of seed set. Fruits mature within a month. The persistent and expanded calyx gives protection to the fruit; the mature fruit is well seated within

the calyx and hence is not directly exposed to sunlight. Therefore, the calyx has an important role in protecting the fruit from desiccation.

In both the species of *Bruguiera*, the single seed formed in the fruit is not dormant and germinates immediately to produce a cylindrical hypocotyl or seedling, while still on the maternal parent. The hypocotyl emerges out of seed and fruit pericarp and remains naked until it is detached from the parent plant. This is a characteristic of “true viviparous” species (Tomlinson, 1986). While still attached to the maternal parent, the seedling develops chlorophyll and actively photosynthesizes; the parent tree supplies the water and necessary nutrients (Selvam and Karunakaran, 2004). The seedling hangs downward and detaches from the residual fruit, leaving behind its cotyledons, and falls from the maternal parent. Viviparous reproduction allows seedlings to develop some salinity tolerance before being released from the parent tree. This reproduction provides a store of nutrients before the seedlings fall off from the maternal parent and may help in quick rooting in the muddy environment. The seedling characteristics also help to develop buoyancy for dispersal and structural stability for protection against damage (Kathiresan, 2003). Therefore, vivipary is an adaptive feature to overcome the harsh tidal environment for seedling establishment. The study shows that seedlings of *Bruguiera* fall off the maternal parent freely and plant themselves into the mud or stranded and planted away from parent tree. La Rue and Muzik (1954), Rabinowitz (1978) and Van Speybroeck (1992) reported similarly for this species. Kairo et al. (2001) reported that the mode of seedling dispersal depends on the forest conditions, tides, as well as the stability of the soils. Further, Van Speybroeck (1992) reported that the seedlings can plant themselves into the mud if they are dropped from maternal parent at low water or low tide. He termed it as self-planting strategy. He also reported that the seedlings float to another site to settle and develop if they fall in the water at high tide and he termed it as stranding strategy. The study shows that the seedlings of *Bruguiera* disperse through self-planting and stranding strategies; the former strategy is functional at low tide while the latter strategy is functional at high tide. Van Speybroeck (1992) reported that the self-planting strategy dominates in undisturbed mangrove forest whereas the stranding strategy is dominant in an exploited and open forest. The stranding strategy is especially important for regeneration and colonization of naked or semi-naked habitats and also for expanding the distribution range of the species. The study found that the Roseringed Parakeet feeds on the softest part of the seedlings of *B. gymnorrhiza* prior to their detachment from the parent tree.

The seedlings attacked by this parakeet have not established new plants; their percentage however did not exceed 5%. The feeding on these seedlings by the parakeet may be partly attributable to the scarcity of food. There is no seedling predation prior to detachment from the maternal parent in *B. cylindrica*. Sousa and Mitchell (1999) reported that after detachment from the maternal parent, seedlings experience mortality due to crab predation. Crabs prefer to feed on small propagules as the latter facilitate easy burial in burrows, have high nutritive value and low concentration of inhibiting chemicals such as tannins. Since the seedlings of both the species of *Bruguiera* are long, crabs may not utilize them as food source but further study is required to confirm this.

***Avicennia alba*, *Avicennia marina* and *Avicennia officinalis*.** All the three *Avicennia* species studied are principally polyhaline evergreen tree species. *A. alba* and *A. marina* are small trees while *A. officinalis* is a tall tree. These tree species show flowering response to monsoon showers in June; the first monsoon showers seem to provide the necessary stimulus for flowering. Opler et al. (1976) and Ewsie (1980) have reported such a flowering response to light rains in summer season in a number of plants occurring in coastal environments. The flowering period extends until August in all the three species of *Avicennia* at the study sites, indicating that the flowering season is only for three months in a year. On the contrary, WiumAndersen and Christensen (1978) reported that in *A. marina*, flowering occurs during April-May. Further, Mulik and Bhosale (1989) noted that the flowering in this species is from April to September. These authors also mentioned that the flowering occurs during March-July in *A. officinalis*. The variation in the schedule and length of flowering season in these species may be a response to local environmental conditions and to avoid competition for the available pollinators depending on the flowering seasons and

population size of the constituent plant species which vary with each mangrove forest. In all the three species, the flowers are borne either in terminal or axillary inflorescences. But, the average number of flowers per inflorescence varies with each species; it is the highest in *A. alba*, moderate in *A. marina* and the least in *A. officinalis*. This flower production rate at inflorescence level may serve as an important taxonomic characteristic for the identification of these three species.

In all, the flowers are strongly protandrous and the stamens with dehisced anthers over-arch the stigma. The stigma shows post-anthesis growth. It is erect and seated in the centre of the flower in *A. alba* and *A. marina* while it is bent and situated below the adaxial corolla lobe in *A. officinalis*. The erect stigma does not change its orientation throughout the flower life in *A. alba* and *A. marina* while the bent stigma becomes erect on day three. The stigma is bifid and appressed on the day of anthesis in all the three species; it remains in the same state also on day two in *A. officinalis*. The stigma commences receptivity by diverging in dorsi-ventral plane; it is receptive on day two and three in *A. alba* and *A. marina*, and on day three, four and five in *A. officinalis*. The timing of commencement of stigma receptivity in *A. officinalis* strongly contradicts with an earlier report by Subba Reddi et al. (1995) that the stigma attains receptivity three hours after anthesis with the bent stigma becoming erect. In *A. officinalis*, stigma behaviour is more advanced towards achieving cross-pollination. In all the three species, self-pollination of individual flowers is unlikely on the day of anthesis due to protandry but the stamens with dehisced anthers over-arching the stigma may facilitate the fall of pollen on the receptive stigma when the latter attains receptivity. In effect, self-pollination may occur and the same is evidenced through fruit set in bagged flowers without manual self-pollination. Further, the sequence and synchrony of flowering, and pollinator behaviour at tree level contribute to geitonogamy (Clarke and Meyerscough, 1991). Hand-pollination results indicate that it is self-compatible and fruit set occurs through autogamy, geitonogamy and allogamy. The hermaphroditic flowers with strong protandry and long period of flower life in these species suggest that they are primarily adapted for cross-pollination. Clarke and Meyerscough (1991) also reported that *A. marina* is protandrous, self-compatible and self-pollinating but the fruits resulting from spontaneous self-pollination showed a higher rate of maternal abortion reflecting an inbreeding depression. Coupland et al. (2006) reported that in *A. marina*, autogamy is most unlikely and emphasized the importance of pollen vectors to the reproductive success.

This report is not in agreement with the results obtained in handpollination experiments on *A. marina*. Primack et al. (1981) suggest that protandry promotes out-crossing in mangroves, and that insect pollination facilitates it. They also suggested that geitonogamy in coastal colonizing plants would allow some fruit set in isolated colonizing plants, and thereafter the proportion of such pollinations would decline as pollen is transferred between plants. Pollen transfer between plants in such situations would still result in sibling mating. However, this is counteracted by dispersal of propagules, canopy suppression of seedlings and irregular yearly flowering among trees in close proximity. Clarke and Meyerscough (1991) reported that in *A. marina*, some trees flower and fruit every year while some others do not flower every year. Those with complete canopy crops did not produce another large crop the following year. A similar pattern observed within a tree where fruit is produced on one branch and in the following year heavy flowering shifts to another branch. In the present study, all the three species of *Avicennia* flowered annually and the flowering is uniform on all branches within a tree. The study suggests that annual mass flowering, protandry, self-compatibility and self-pollination ability are important adaptations for *Avicennia* species to successfully colonize new areas and expand their distribution range as pioneer mangroves. All the three species of *Avicennia* are hermaphroditic and have similar floral architecture. In *A. officinalis*, the flowers are foetid and slightly zygomorphic while in the other two species, they are scented and actinomorphic. In all, the flowers are of open type and shallow with small aliquots of nectar which is exposed to rapid evaporation resulting in increased nectar sugar concentration. Corbet (1978) considered these characteristics as adaptations for fly pollination. Hexose-rich nectar is present in *A. alba* and *A. marina* while sucrose-rich nectar in *A. officinalis*. Hexose-rich nectar is the characteristic of fly- and shorttongued bee-flowers while sucrose-rich nectar is the characteristic of wasps and butterflies (Baker and Baker, 1982, 1983). The nectar sugar concentration is high and ranged from 38 to 40% in all the three *Avicennia* species.

Cruden et al. (1983) reported that high nectar sugar concentration is the characteristic of bee-flowers while low nectar sugar concentration is the characteristic of butterfly-flowers. Baker and Baker (1982) reported that the floral nectar is an important source of amino acids for insects. Dadd (1973) stated that insects require ten essential amino acids of which arginine, lysine, threonine and histidine are present in the nectar of *A. officinalis*. He also reported that proline and glycine are essential amino acids for some insects; these two amino acids are also present in the nectar of *A. officinalis*. He further stated that other amino acids such as alanine, aspartic acid, glutamic acid, glycine and serine while not essential do increase insect growth. All these amino acids are also present in the nectar of *A. officinalis*. Shiraishi and Kuwabara (1970) reported that proline stimulates salt receptor cells in flies. Goldrich (1973) reported that histidine elicits a feeding response while glycine and serine invoke an extension of the proboscis. The nectars of *A. alba* and *A. marina* have not been analyzed for amino acids and hence this aspect has not been discussed. The flowers of all the three species of *Avicennia* with differences in their structural and functional characteristics as stated above have been able to attract different classes of insects - bees, wasps, flies and butterflies. Of these, bees while collecting pollen and nectar while all others collecting nectar effected pollination and their ability to carry pollen has been evidenced in their body washings. Flies are known as short distance fliers and such behaviour largely results in autogamy or geitonogamy. Since these flies visit the flowers as large groups, there is automatically a competition for the available nectar which is secreted in small aliquots on the petals of all the three *Avicennia* species. In consequence, they shift from tree to tree in search of nectar forage and in the process they contribute to both self- and cross-pollination. All other insects are habitual long-distance fliers and affect both self- and cross-pollination. An earlier report by Subba Reddi et al. (1995) showed that only bees and flies are the pollinators of *A. officinalis* at the study sites. Tomlinson (1986) mentioned that *Avicennia* flowers are beepollinated. In Australia, *A. marina* is pollinated by ants, wasps, bugs, flies, bee-flies, cantharid beetles and moths (Clarke and Meyerscough, 1991). It is surprising to note that thrips are absent both in bud and flower stage in all the three species of *Avicennia*.

A study on this aspect is needed to understand why thrips avoided these flowers for breeding or for forage collection. Tomlinson (1986) documented that *A. alba*, *A. marina* and *A. officinalis* have very similar flowers and hence may well be served by the same class, if not by the same species of pollinators; when these species grow together, there is evidence of non-synchrony in flowering times, which might minimize the competition for pollinators (probably bees) and at the same time spread the availability of nectar over a more extended period. In the present study, these plant species grow together, flower synchronously, but served by the same classes of insects. There is no competition for pollen among different classes of insects since only bees collect pollen while all other classes of insects collect only nectar. Fly pollinators with their swarming behaviour at the flowers may enable the plant species to set fruit to the extent possible. Flies and bees are usually consistent and reliable when compared to wasps and butterflies. Therefore, the study shows flies and bees play an important role in the success of sexual reproduction in all the three species of *Avicennia*. Despite being pollinated by different classes of insect pollinators and having the ability to self-pollinate even in the absence of insect activity as evidenced in bagged flowers, the natural fruit set stands at 42-58% in these plant species. This low fruit set could be due to maternal abortion of self-pollinated fruits as reported by Clarke and Meyerscough (1991), non-availability of sufficient pollen to receptive stigmas due to pollen feeding activity of bees and the nutritional resource constraint to the maternal parent. Coupland et al. (2006), while reporting on fruit set aspects of *A. marina* in Australia mentioned that fruit set is not pollinator limited but resource limited. In Avicenniaceae, the flowers have been reported to contain four ovules (Tomlinson, 1986). In the present study, all the three species of *Avicennia* are four-ovuled but only one ovule develops into mature seed in fertilized and fruited flowers as in Rhizophoraceae. The production of one-seeded fruits may be due to maternal resource constraint or maternal regulation of seed set. Fruits grow and mature within five-six weeks in *A. alba* and within four weeks in the other two *Avicennia* species. The duration of fruit maturation is not in agreement with the report of Wium-Andersen and Christensen (1978) who stated that the development from flower bud to mature fruit takes a few months. The calyx is persistent in all the three species but it does not expand to enclose the growing fruit. Therefore, the calyx has no role in sheltering or protecting the fruit. As the fruit is a leathery capsule, it does not require

any protection from the calyx. The single seed formed in the fruit is not dormant and germinates immediately to produce chlorophyllous seedling, which remains within the fruit, while still on the maternal parent. This is a characteristic of “crypto-viviparous” species; a similar situation exists in other genera such as *Aegiceras*, *Aegialitis*, *Nypa* and *Pelliciera* (Tomlinson, 1986). In all these species, fruit is the propagule; the seedling occupies the fruit cavity. The chlorophyllous seedling actively photosynthesizes while the maternal parent supplies the water and necessary nutrients (Selvam and Karunagaran, 2004). In *Avicennia* species, the propagules are small, light and the entire embryo is buoyant after detachment from the maternal parent.

Gradually, the fruit pericarp is lost exposing the leathery succulent cotyledons to tidal water. Rabinowitz (1978) reported that *A. marina* has an absolute requirement for a stranding period in order to establish since its propagules always float in tidal water. He also felt that the propagules must have freedom from tidal disturbance in order to take hold in the soil. In consequence, this species is restricted to the higher ground portions of the swamp where the tidal inundation is less frequent. In the present study, *Avicennia* species exhibit self-planting strategy at low tide and stranding strategy at high tide. However, their seedlings disperse widely in tidal water but establishment is mainly stationed in the polyhaline zone. Duke et al. (1998) reported that *Avicennia* seedlings disperse widely and are genetically uniform throughout their range. In the study areas, genetic studies are required to know whether all the three species studied are genetically uniform. When the seedlings settle, radicle penetrates the sediment before the cotyledons unfold. The first formal leaves appear one month after germination and the second pair one to two months (Wium-Andersen and Christensen, 1978). Coupland et al. (2006) reported that *Avicennia* propagules are a rich source of nutrients and attract a diverse range of insect predators which in turn influence the rate of seedling maturation. Resource constraints and insect predation on developing fruit and seedling may both act to reduce fruit set. In *A. marina* and *A. germinans*, the seedlings tend to be high in nutritive value and have relatively few chemical defences (Smith, 1987; McKee, 1995). These species tend to exhibit a pattern of very rapid initial predation (Allen et al., 2003). In the present study, seedling predation has been evidenced in *A. alba* and *A. marina* only; in both the species, the Rose-ringed Parakeet, *Psittacula krameri* attacks propagules prior to their detachment from the maternal parent. Seedling predation by crabs after detachment from the maternal parent may be expected since different species of crabs have been found in the study areas. Therefore, seedling predation may reduce the success of seedling establishment in all the three species of *Avicennia*.

***Aegiceras corniculatum*.** The plant is a mesohaline evergreen species. The flowering occurs during the dry season; sporadic flowering also occurs at other times of the year but it is especially significant during the rainy season. The floral characteristics such as morning anthesis, scent production, zygomorphic symmetry, short-tubed corolla with sexual organs exposed, pollen structural features and nectar production are adaptations for pollination by any class of animals (Baker and Baker, 1983; Cruden et al., 1983). Different workers reported different insects as pollinators of *A. corniculatum* - bees without mentioning the species by Tomlinson (1986); the bees *Trigona iridipennis* and *Pseudapis oxybeloides* at Coringa mangrove forest by Solomon Raju (1989); butterflies, bees, wasps and flies, and also birds in the Orissa mangrove forest by Pandit and Choudhury (2001). The present study shows that bees, wasps, flies and butterflies are the pollinators; *Xylocopa* bees are the most efficient pollinators due to their ability to collect forage quickly from each umbel and to their quick mobility between plants for want of more forage. The bees are pollen and nectar collectors while all others are nectar feeders. Pollen is a source of protein for bees and the pollen of *A. corniculatum* with some protein content is important for them. The small volume of nectar with high sugar concentration consisting of only two hexose sugars, fructose and glucose in *A. corniculatum* is stated to be a requirement for bees, flies and butterflies while sucrose-rich nectar is the requirement for wasps (Baker and Baker, 1983).

This study shows that wasps also utilize short-tubed flowers with nectar containing only hexose sugars. Further, the nectar contains four of the ten essential amino acids required by insects (De Groot, 1953). They are arginine, lysine, threonine and histidine. It also has some non-essential amino acids. These

essential and non-essential amino acids in the nectar of *A. corniculatum* serve as important nutrient source for all the insects. Near synchronous anthesis in one umbel and acropetal succession of flowers resulting in the extension of flowering period are energetically beneficial and provide forage continuously until the cessation of flowering. All the insects carry pollen and pollinate the flowers without fail. *A. corniculatum* with its unspecialized flowers is capable of utilizing the locally available insect species for fruit set; the insects are especially important for cross-pollination. The pollen grains being light and dry, and small in size facilitated by the medifixed versatile anthers are carried away by wind action and this wind-driven pollen movement also contributes to a small percent of fruit set. Therefore, both insects and wind are the pollinators of this plant. In *A. corniculatum*, the anthers and stigma of a flower mature simultaneously; anthers dehisce an hour after anthesis while stigma remains receptive for the next two days. Pandit and Choudhury (2001) mentioned that the flowers of this plant would be able to self-pollinate with the simultaneous anther dehiscence and stigma receptivity, and with the stigma position at the level of the anthers. The plant is self-compatible and capable of autogamy, but suggested that insect pollinators are required for a higher level of fruit set. They also substantiated their suggestion by stating that pollen-ovule ratio falls within the range of facultative xenogamy according to Cruden (1977). Further, these authors observed low levels of genetic variation in this plant occurring in China; this may be an indication that fruit set in this plant is largely a function of self-pollination. Solomon Raju (1989) also reported that autogamy is a mode of self-pollination for fruit set in this plant. In the present study, hand-pollination results indicate that fruit set occurs through autogamy, wind and insects, but fruit set is highest only in the flowers pollinated by insects. All of this indicates that the plant though self-compatible and capable of setting fruit through autogamy is largely dependent on insects for maximizing fruit set rate.

The pollen viability and stigma receptivity for more than three days indicate are additional adaptations to achieve cross-pollination through foraging activity of insects. In this context, Primack and Tomlinson (1980) argued that if the plant is primarily a colonizing species, it would retain the need for self-fertility if it is to establish populations in isolated localities. Therefore, *A. corniculatum* with self-compatible option would be able to establish populations even in isolated localities and utilize locally available flower visiting insects for both self- and cross-pollination. In *A. corniculatum*, flower bud abortion is negligible and its occurrence may be due to defective origin. Numerous flattened ovules are embedded in the rounded, somewhat fleshy, and short-stalked free central placenta; it may cause an underestimation of ovule number. The present study shows that the ovules in an ovary are only thirty five but only one ovule produces seed in each fruit. Fruit maturation takes a month or slightly more than a month's time. Seed is not dormant and produces a hypocotyl within the fruit pericarp. The fruits hang downwards in this plant whereas the fruits stand upwards in *Aegialitis rotundifolia*. The entire fruit of *A. corniculatum* falls off when due for dispersal. Hypocotyls float only if they are with the fruit pericarp. Self-planting and stranding strategies are effective for the dispersal and establishment of hypocotyls. Therefore, the plant displays scattered occurrence and also forms pure stands in certain mesohaline areas of the mangrove forest. Bosire et al. (2005) reported higher rate of crab predation in this plant. In the present study, this aspect was not examined but the hypocotyls being small in size may contain high nutrient content and low fiber content may attract crab predators prior to their establishment.

***Aegialitis rotundifolia*.** The genus *Aegialitis* represents only two shrub species, *A. annulata* and *A. rotundifolia*. It is recently segregated as the family Aegialitiaceae because of some distinctive features from other genera of Plumbaginaceae. Some features include anomalous secondary thickening, abundant sclereids, incipiently viviparous seeds, monomorphic pollen and homostylous flowers (Weber-El Ghobary, 1984; Tomlinson, 1986). The two species do not occur together in the same forest and have distribution in different parts of the world. *A. annulata* is distributed in Australia and eastern Malaysia (Tomlinson, 1986) while *A. rotundifolia* in South Africa and South-East Asia (Kathiresan and Bingham, 2001). *A. rotundifolia* has been reported to occur in Burma, Bengal and the Andamans by Tomlinson (1986). Later, Naskar and Mandal (1999) reported this species as occurring in the Sundarbans, Andaman and Nicobar islands and Mahanadi Delta of Orissa only. Ramasubramanian et al. (2003) have not mentioned about the occurrence

of *A. rotundifolia* in their published book on the mangrove flora of Krishna and Godavari deltas of Andhra Pradesh.

The present study revealed the presence of *A. rotundifolia* in Nachugunta Reserve Forest of Krishna Mangroves in Andhra Pradesh and hence it is the first record of *A. rotundifolia* from Andhra Pradesh. Tomlinson (1986) stated the fact that *Aegialitis* species prefer or require exposed sites and withstand waves and tidal action. Further, he also mentioned the fact that *A. rotundifolia* does not occur within closed mangrove communities but it may occur as back mangal if soil is highly saline. Aksornkoae et al. (1992) also reported similarly about the habitat requirements of *A. rotundifolia*. At the study site also, this species occurs in seaward, euhaline and exposed sites. As the habitat of *A. rotundifolia* is highly saline, salt in high concentrations in plant tissues is toxic and hence, must be excluded by some mechanism. The absorbed salt is excreted metabolically via salt glands present on the leaf blade (Scholander, 1968). The salt evaporates or crystallizes in a conspicuous manner on the surface of leathery leaf blade of *A. rotundifolia*. Later, the crystallized salt blows away or washes off during cool periods by the absorption of atmospheric moisture and by rain. Therefore, *A. rotundifolia* with salt excretion mechanism is highly specialized to withstand high saline soils.

The plant is a dry season bloomer but it completes flowering prior to the onset of extreme dry conditions in the month of May. During this period, fluvial discharge from rivers to the sea is almost negligible and this would result in increased salinity of seawater. A steep increase in salinity levels can be expected at the site of the plant which is characteristically seaward in occurrence. Increased salinity of seawater reportedly prevents fruiting and causes senescence of immature flowers and buds (Qureshi, 1993). This may be an important factor for the plant to cease flowering by the mid-April and supply the available resources to the growing fruits to realize maximum fruit set. *A. rotundifolia* species with anthesis during morning hours and odourless flowers indicates that it is adapted for pollination during daytime. The floral characteristics of this plant species such as short-tubed corolla with anthers at the flower entrance, the styles and stigmas situated slightly below the anthers, production of slightly moderate volume of nectar with high sugar concentration and the presence of only hexose sugars in nectar are adaptations for bee-pollination (Baker and Baker, 1983; Opler, 1983). Further, the nectar has the essential amino acids such as arginine, lysine, phenylalanine, threonine, tryptophan, valine and histidine; and also some non-essential amino acids. De Groot (1953) showed that insects in general and honeybees in particular require ten essential amino acids and seven of them are present in the nectar of this plant. The pollen also has some protein content. The flower visitors recorded are exclusively honeybees and stingless bees; the latter is also honey producers. These bees collect both pollen and nectar from the flowers. They carry pollen on their bodies and pollinate the flowers while probing for the forage. As they require more quantity of forage for honey production and brood rearing, they collect forage from as many flowers as available on *A. rotundifolia* and hence, contribute to both self- and cross-pollination. Naskar and Mandal (1999) mentioned that this plant is pollinated by the honey bee, *Apis dorsata* in the Sundarban mangroves. Bhattacharya et al. (2006) also noted that the pollen of this plant is dominant in honey collected from the Sundarbans region. Therefore, *A. rotundifolia* is primarily melittophilous. *A. rotundifolia* species flowers are weakly protandrous, self-compatible and selfpollinating. The protandry does not contribute to autogamy in the first two hours period of flower life as the stigmas lack receptivity during that period. Gradually, the stigmas diverge and stand away from the anthers while they attain receptivity to pollen. Individual flowers with this situation produce fruit through autogamy with the aid of wind or honeybees.

The pollen grains are very large and fall down on the stigmas gravitationally due to wind action, the result of which is autogamy; if there are flowers of the same age side by side in the same or adjacent inflorescences, geitonogamy may occur. However, the flower function with reference to protandry, movement of stigmas and duration of stigma receptivity suggests that the plant is primarily evolved for outcrossing. Hand-pollination results also indicate the same and the fruit set rate is highest in open-pollinations which are largely a function of foraging activity of bees. Despite high fruit set rate in this plant, its population size is small. Pollination among the individuals of this small population may lead to a reduction in genetic diversity and molecular studies on its genetic structure would enable to know the

existing level of genetic variation. Transplanting the propagules from other mangrove forests like mangrove of the Mahanadi Delta of Orissa and the Sundarbans to the study site would help to enhance gene flow in order to enable the plant to build up a stable and sustainable population size. The flowers produce singled-ovuled ovary and the ovule invariably produces a single seed in fertilized flowers. This character is advantageous for the plant to save and use the resources for higher fruit set rate. Seed is not dormant and produces hypocotyl within the fruit pericarp while still on the parent plant; it is a characteristic of crypto-viviparous species (Carey, 1934; Das and Ghose, 2003). The fruit with hypocotyl inside grows upward like the upwardly growing naked hypocotyl of *C. decandra*. Since the hypocotyl is concealed, the entire capsule-like fruit falls off when due for dispersal. Fruit pericarp is essential for the hypocotyl to float until it is settled. Self-planting and stranding strategies are functional for the dispersal of hypocotyls. But, field studies indicate that only a few of those hypocotyls which have fallen at the parental sites settled well and showed further growth. Clarke and Kerrigan (2002) reported that the small-sized hypocotyls contain high nutrient content and low fiber content. The crabs prefer to consume such hypocotyls and feed on them prior to establishment. They also reported that 80% of the propagules failed to establish due to predation by crabs in *Aegialitis annulata*. In the study site of *A. rotundifolia* also, crabs are common and they may be consuming most of the hypocotyls prior to their establishment and hence, affecting the recruitment process of the plant.

CONCLUSIONS

Both viviparous and crypto-viviparous species exhibit mixed mating system and adaptations for entomophily. In case of *B. gymnorhiza*, the floral features suggest ornithophily but locally the plant is found to be melittophilous. The mixed mating system coupled with entomophily appears to be adaptive for the success of sexual reproduction in harsh environment which is characteristic of mangrove forest. The seed is usually the stage of the life cycle at which dispersal and the colonization of new areas occurs. It contains a reserve of food, providing the embryo with a temporary continuation of maternal support. In contrast, in both true and crypto-viviparous tree species, the seed lacks dormancy and does not perform any of these roles. The unit of dispersal in these species is not the seed but the young seedling (hypocotyl); it is naked in true viviparous species while it remained within the fruit pericarp in crypto-viviparous species suggesting that the zygote is not dependent on stored nutritional support from the endosperm or carpal tissues, but instead may be nourished directly from the maternal plant. In all the plant species, the dispersal of propagules takes place via self-planting and stranding strategies. The self-planting strategy is important in undisturbed sites while the stranding strategy is effective in exploited and open forest sites of mangroves. Therefore, the detailed information included in this paper is useful for framing effective measures for conservation and management of the studied mangrove plants as these are the characteristic species of mangrove forest. The study further provide basis for taking up extensive studies on mangrove plants for the sustainability of mangrove forest.

REFERENCES

- Aksornkoae S., Maxwell G. S., Havanond S. and Panichsuko S., 1992 – Plants in Mangroves, Chalongrat Co., Ltd., Thailand, 120.
- Allen J. A. and Duke N. C., 2006 – *Bruguiera gymnorhiza* (large-leafed mangrove): Species Profiles for Pacific Island Agroforestry, www.traditionaltree.org
- Allen J. A., Krauss K. W. and Hauff R. D., 2003 – Factors limiting the intertidal distribution of the mangrove species *Xylocarpus granatum*, *Oecologia*, 135, 110-121.
- Aluri J. B., Venkata Ramana S. P. and Subba Reddi C., 2004 – Explosive pollen release, windpollination and mixed mating in the tropical tree *Shorea robusta* Gaertn. F. (Dipterocarpaceae), *Current Science*, 86, 1416-1419.
- Aziz I. and Khan M. A., 2001 – Experimental assessment of salinity tolerance of *Ceriops tagal* seedlings and saplings from the Indus Delta, Pakistan, *Aquatic Botany*, 70, 259-268.

- Azuma H., Toyota M., Asakawa Y., Takaso T. and Tobe H., 2002 – Floral scent chemistry of mangrove plants, *Journal of Plant Research*, 115, 47-53.
- Baker H. G. and Baker I., 1973 – Some anthecological aspects of evolution of nectar-producing flowers, particularly amino acid production in nectar, in *Taxonomy and Ecology*, Heywood V. H. (ed.), Academic Press, London, 243-264.
- Baker H. G. and Baker I., 1982 – Chemical constituents of nectar in relation to pollination mechanisms and phylogeny, in *Biochemical aspects of evolutionary biology*, Nitecki H. M. (ed.), University of Chicago Press, Chicago, 131-171.
- Baker H. G. and Baker I., 1983 – A brief historical review of the chemistry of floral nectar, in *The Biology of Nectaries*, Bentley B. and Elias T. (eds), Columbia University Press, New York, 126-152.
- Bhattacharya K., Majumdar M. R. and Bhattacharya S. G., 2006 – *A Textbook of Palynology (Basic and Applied)*, New Central Book Agency (P) Ltd., Kolkata, 126-152.
- Bhosale L. J. and Mulik N. G., 1991 – *Proceedings of the International Seed Symposium*, David N. S. and Mohammad S. (eds), Jodhpur, 201-205.
- Bosire J. O., Kairo J. G., Kazungu J., Koedam N. and Dahdouh Geubas F., 2005 – Predation on propagules regulates regeneration in a high-density reforested mangrove plantation, *Marine Ecology Progress Series*, 299, 149-155.
- Carey G., 1934 – Further investigations on the embryology of viviparous seeds, *Proceedings of Linnean Society of New South Wales*, 59, 392-410.
- Chan H. T. and Husin N., 1985 – Propagule dispersal, establishment, and survival of *Rhizophora mucronata*, *Malaysian Forester*, 48, 324-329.
- Chiou-Rong S., Yong J. W. H. and Yang Y. P., 2005 – The *Brugueira* (Rhizophoraceae) species in the mangroves of Singapore, Especially on the new record and the rediscovery, *Taiwania*, 50, 251-260.
- Christensen B. and Wium-Andersen S., 1977 – Seasonal growth of mangrove trees in southern Thailand, I, The phenology of *Rhizophora apiculata* Bl., *Aquatic Botany*, 3, 281-286.
- Clarke P. J., 1993 – Dispersal of gray mangrove (*Avicennia marina*) propagules in southeastern Australia, *Aquatic Botany*, 45, 195-204.
- Clarke P. J. and Meyerscough P. J., 1991 – Floral biology and reproductive phenology of *Avicennia marina* in south eastern Australia, *Australian Journal of Botany*, 39, 283-293.
- Clarke P. J. and Kerrigan R. A., 2002 – The effects of seed predators on the recruitment of mangroves, *The Journal of Ecology*, 90, 726-736.
- Clarke P. J., Kerrigan R. A. and Westpal C. J., 2001 – Dispersal potential and early growth in 14 tropical mangroves: do early life history traits correlate with patterns of adult distribution?, *Journal of Ecology*, 89, 648-659.
- Corbet S. A., 1978 – Nectar, insect visits, and the flowers of *Echium vulgare*, in *The Pollination of Flowers by Insects*, Richards A. J. (ed.), Academic Press, London, 21-30.
- Coupland G. T., Paling Eric I. and McGuinness Keith A., 2006 – Floral abortion and pollination in four species of tropical mangroves from northern Australia, *Aquatic Botany*, 84, 151-157.
- Cruden R. W., 1977 – Pollen-ovule ratios: a conservative indicator of breeding systems in flowering plants, *Evolution*, 31, 32-46.
- Cruden R. W., Hermann H. M. and Peterson S., 1983 – Patterns of nectar production and plant-pollinator coevolution, in *The Biology of Nectaries*, Bentley B. and Elias T. (eds), Columbia University Press, New York, 80-125.
- Dadd R. H., 1973 – Insect nutrition: current developments and metabolic implications, *Annual Review of Entomology*, 18, 881-420.
- Dafni A., Kevan P. G. and Husband B. C., 2005 – *Practical Pollination Biology*, Enviroquest Ltd., Canada, 590.
- Dahdouh-Guebas F., Verneirt M., Tack J. F., Van Speybroeck D. and Koedam N., 1998 – Propagule predators in Kenyan mangroves and their possible effect on germination, *Manual of Freshwater Research*, 49, 345-350.

- Das S. and Ghose M., 2003 – Seed structure and germination pattern of some Indian mangroves with taxonomic relevance, *Taiwania*, 48, 287-298.
- Davis J. H., 1940 – The ecology and geologic role of mangroves in Florida, *Papers from the Tortugas Laboratory of the Carnegie Institution of Washington*, 32, 303-412.
- De Groot A. P., 1953 – Protein and amino acid requirements of the honey bee (*Apis mellifera* L.), *Physiologia Comparata et Oecologia*, 3, 197-285.
- Dress W. J., Newell S. J., Nastase A. J. and Ford J. C., 1997 – Analysis of amino acids in nectar from pitchers of *Sarracenia purpurea* (Sarraceniaceae), *American Journal of Botany*, 84, 1701-1706.
- Duke N. C., John A. H. B., Goodall J. A. and Ballment E. R., 1998 – A genetic structure and evolution of species in the mangrove genus *Avicennia* (Avicenniaceae) in the Indo-west pacific, *Evolution*, 52, 1612-1626.
- Elmqvist T. and Cox P. A., 1996 – The evolution of vivipary in flowering plants, *Oikos*, 77, 3-9.
- Ewusie J. Y., 1980 – *Tropical Ecology*, Heinemann Educational Books Ltd., London, 243.
- Faegri K. and van der Pijl L., 1979 – *The Principles of Pollination Ecology*, Pergamon Press, New York, 243.
- Farnsworth E. J. and Ellison A. M., 1997 – Global pattern of pre-dispersal propagule predation in mangrove forests, *Biotropica*, 29, 316-330.
- Farnsworth E. J. and Farrant J. M., 1998 – Reductions in abscisic acid are linked with viviparous reproduction in mangroves, *American Journal of Botany*, 85, 760-769.
- Gardener M. C. and Gillman M. P., 2002 – The taste of nectar - a neglected area of pollination ecology, *Oikos*, 98, 552-557.
- Ge J., Cai B. and Lin P., 2003 – Mating system and outcrossing rates of four *Bruguiera gymnorhiza* populations of mangrove in China, *Nature and Science*, 1, 42-48.
- Ghosh A., Gupta S., Maity S. and Das S., 2008 – Study of floral morphology of some Indian mangroves in relation to pollination, *Research Journal of Botany*, 3, 9-16.
- Goebel K. E., 1905 – *Organography of Plants*, Hafner, New York.
- Goldrich N. R., 1973 – Behavioural responses of *Pharmia regina* (Meigen) to labellar stimulation with amino acids, *Journal of General Physiology*, 61, 74-88.
- Harborne J. B., 1973 – *Phytochemical Methods*. Chapman and Hall, London.
- Juncosa A. M. and Tomlinson P. B., 1987 – Floral development in mangrove Rhizophoraceae, *American Journal of Botany*, 74, 1263-1279.
- Kairo J. G., Dahdouh-Guebas F., Bosire J. and Koedam N., 2001 – Restoration and management of mangrove systems - a lesson for and from the East African regions, *South African Journal of Botany*, 67, 383-389.
- Kathiresan K., 2003 – Biology of Mangroves in Biodiversity in Mangrove Ecosystems, Kathiresan K. and Subramanian A. N. (ed.), *UNU-UNESCO International Training Course Manual*, Annamalai University, Parangipettai, 74-90.
- Kathiresan K. and Bingham B. L., 2001 – Biology of mangroves and mangrove ecosystems, *Advances in Marine Biology*, 40, 81-251.
- Kathiresan K. and Rajendran N., 2003 – Mangroves, in *UNU-UNESCO International Training Course on Biodiversity in Mangrove Ecosystems*, Course Manual Kathiresan K. and Subramanian A. N., (eds), Annamalai University, 138-147.
- Kondo K., Nakamura T., Tsuruda K., Saito N. and Yaguchi Y., 1987 – Pollination in *Bruguiera gymnorhiza* and *Rhizophora mucronata* (Rhizophoraceae) in Ishigaki Island, The Ryukyu Islands, Japan, *Biotropica*, 19, 377-380.
- Kress W. J., 1974 – The floral biology of *Rhizophora mangle* in south Florida, Undergraduate Honors Thesis. Biology Department, Harvard University.
- LaRue C. D. and Muzik T. J., 1954 – Does mangrove really plant its seedling?, *Nature*, 114, 661-662. 52.
- MacNae W., 1968 – A general account of the flora and fauna of mangrove swamps and forests in the Indo-West pacific regions, *Advances in Marine Biology*, 6, 73-270.

- McGuinness K. A., 1997 – Dispersal, establishment and survival of *Ceriops tagal* propagules in the north Australian mangrove forest, *Oecologia*, 109, 80-87.
- McKee K. L., 1995 – Mangrove species distribution and propagule predation in Belize: An exception to the dominance-predation hypothesis, *Biotropica*, 27, 334-345.
- Meeuse B. and Morris S., 1984 – *The Sex Life of Flowers*, Facts on File, New York, 152.
- Mitchell R. J., Karron J. D., Holmquist K. G. and Bell J. M., 2004 – The influence of *Mimulus ringens* floral display size on pollinator visitation patterns, *Functional Ecology*, 18, 116-124.
- Mulik N. G. and Bhosale L. J., 1989 – Flowering phenology of the mangroves from the west coast of Maharashtra, *Journal of Bombay Natural History Society*, 86, 355-359.
- Muniyandi K., 1986 – Studies on mangroves of Pitchavaram (South East Coast of India), Ph.D. Thesis, Annamalai University, Parangipettai, India.
- Naskar K. and Mandal R., 1999 – Ecology and biodiversity of Indian Mangroves Part - I Global Status, Daya Publishing House, New Delhi, 361.
- Opler P. A., 1983 – Nectar production in a tropical ecosystem, in Bentley B. and Elias T. (eds), *The Biology of Nectaries*, Columbia University Press, New York, 30-79.
- Opler P. A., Frankie G. W. and Baker H. G., 1976 – Rainfall as a factor in the release, timing and synchronization of anthesis by tropical trees and shrubs, *Journal of Biogeography*, 3, 231- 236.
- Pandit S. and Choudhury B. C., 2001 – Factors effecting pollinator visitation and reproductive success in *Sonneratia caseolaris* and *Aegiceras corniculatum* in the mangrove forest in India, *Journal of Tropical Ecology*, 17, 431-447.
- Pannier F. and Pannier R. F., 1975 – Physiology of vivipary in *Rhizophora mangle* L. *Proceedings of International Symposium on Biology and Management of Mangroves*, 2, 632- 639.
- Primack R. B. and Tomlinson P. B., 1980 – Variation in tropical forest breeding systems, *Biotropica*, 12, 229-231.
- Primack R. B., Duke N. C. and Tomlinson P. B., 1981 – Floral morphology in relation to pollination ecology in five Queensland coastal plants, *Austrobaileya*, 4, 346-355.
- Qureshi M. T., 1993 – Rehabilitation and management of mangrove forests of Pakistan, in *Towards the Rational Use of High Salinity Tolerant Plants*, 1, Leith H. and Al Masoom A., (eds), Kluwer Academic Publishers, The Netherlands, 89-95.
- Rabinowitz D., 1978 – Mortality and initial propagules size in mangrove seedlings in Panama, *Journal of Ecology*, 66, 45-51.
- Ramasubramanian R., Ravishankar T. and Sridhar D., 2003 – Mangroves of Andhra Pradesh, Identification and Conservation Manual, M. S. Swaminathan Research Foundation, Chennai.
- Roubik D. W., 1995 – Pollination of Cultivated Plants in the Tropics, *FAO Agricultural Services Bulletin*, 118.
- Scholander P. F., 1968 – How mangroves desalinate water, *Physiologia Plantarum*, 21, 251- 261.
- Selvam V. and Karunakaran V. M., 2004 – Coastal Wetlands: Mangrove Conservation and Management. Orientation Guide 1. Ecology and Biology of Mangroves, M. S. Swaminathan Research Foundation, Chennai.
- Shiraishi A. and Kuwabara M., 1970 – The effects of amino acids on the labellar hair chemosensory cells of the fly, *Journal of General Physiology*, 56, 768-782.
- Slansky F. and Feeny P., 1977 – Stabilization of the rate of nitrogen accumulation by larvae of the cabbage butterfly on wild and cultivated food plants, *Ecological Monographs*, 47, 209-228.
- Smith T. J., 1987 – Seed predation in relation to tree dominance and distribution in mangrove forests, *Ecology*, 68, 266-273.
- Solomon Raju A. J., 1989 – Reproductive ecology of *Ocimum americanum* L. and *O. basilicum* L. (Lamiaceae) in India, *Plant Species Biology*, 4, 107-116.
- Solomon Raju A. J. and Subba Reddi C., 1995 – Explosive pollen release and pollination in flowering plants, *Proceedings of Indian National Science Academy*, B61, 323-332.

- Solomon Raju A. J. and Subba Reddi C., 1996 – The explosive floral-mechanism and pollination in the genus *Hyptis* (Lamiaceae), Proceedings of Indian National Science Academy, B62, 117-124.
- Solomon Raju A. J. and Jonathan K. H., 2008 – Reproductive ecology of mangrove trees *Ceriops decandra* (Griff.) Ding Hou and *Ceriops tagal* (Perr.) C. B. Robinson (Rhizophoraceae), Acta Botanica Croatica, 67, 201-208.
- Solomon Raju A. J., Jonathan K. H. and Lakshmi A. V., 2006 – Pollination biology of *Ceriops decandra* (Griff.) Ding Hou (Rhizophoraceae), an important true viviparous mangrove tree species, Current Science, 91, 1235-1238.
- Sousa W. P. and Mitchell B. J., 1999 – The effect of seed predators on plant distributions: is there a general pattern in mangroves?, Oikos, 86, 55-66.
- Subba Reddi C. and Solomon Raju A. J., 1997 – Reproductive biology of three mangrove plant species, Indian Journal of Forestry, 20, 153-157.
- Subba Reddi C., Solomon Raju A. J. and Reddy S. N., 1995 – Pollination ecology of *Avicennia officinalis* L. (Avicenniaceae), Journal of Palynology, 31, 253-260.
- Sun M., Wong K. C. and Lee J. S. Y., 1998 – Reproductive biology and population genetic structure of *Kandelia candel* (Rhizophoraceae), a viviparous mangrove species, American Journal of Botany, 85, 1631-1637.
- Thawley A. R., 1969 – The components of honey and their effects on its properties: A review, Bee World, 50, 51-60.
- Tomlinson P. B., 1986 – The Botany of Mangroves, Cambridge University Press, New York.
- Tomlinson P. B., Primack R. B. and Bunt J. S., 1979 – Preliminary observations on floral biology in mangrove Rhizophoraceae, Biotropica, 11, 256-277.
- Van Speybroeck D., 1992 – Regeneration strategy of mangrove along the Kenyan coast, Hydrobiologia, 247, 243-251.
- Waller G. D., 1972 – Evaluating responses of honeybees to sugar solution using an artificial flower feeder, Annals of Entomological Society of America, 6, 857-862.
- Weber-El Ghobary M. O., 1984 – The systematic relationships of *Aegialitis* (Plumbaginaceae) as revealed by pollen morphology, Plant Systematics and Evolution, 144, 53-58.
- Wium Andersen S. and Christensen B., 1978 – Seasonal growth of mangrove trees in southern Thailand, II, Phenology of *Bruguiera cylindrica*, *Ceriops tagal*, *Lumnitzera littorea* and *Avicennia marina*, Aquatic Botany, 5, 383-390.
- Yao Y., Bera S., Wand Y. and Li C. S., 2006 – Nectar and pollen sources for honeybee (*Apis cerana cerana* Fabr.) in Qingian Mangrove Area, Hainan Island China, Journal of Integrative Plant Biology, 48, 1266-1273.

SOME RISK ASSESSMENTS AT NUCLEAR POWER PLANTS (NPP)

Alexander Valyaev (Nuclear Safety Institute of Russian Academy of Sciences, Moscow, Russia)

Gurgen Aleksanyan (Yerevan State University, Yerevan, Armenia)

Alexey Valyaev (University of Sydney, Australia)

Oleg Arkhipkin (Corporative University "Samruk-Kazyna" Almaty, Kazakhstan)

ABSTRACT: Today NPP energy production is intensive increased in the world with the growth of different threats under its exploitation. This growth is caused by different natural and manmade factors, including possible directed terrorist attacks. It is necessary to perform correct assessments of corresponding risks levels for the individual NPP. Early we predicted the irradiation doses and corresponded risks for population under implementation of Russian Federal Program: "Development of Russian atomic energy industrial complex on 2007-2020 years at 10 homeland NPP that operated in normal non-disasters regimes during two last decades. But such data are absent for NPP, that have been or will be under non prognostic emergencies. It is connected with the following facts. The part or total of needed information may be obtained only after NPP disasters. Some NPP are located in the dangerous regions and exposed to intense negative natural responses (earthquakes, tsunami, etc.) and manmade ones, when NPP are located in some dangerous conflicts zones with high level of possible terrorism threats. Here the using of classic methods of expertise risk NPP assessments are not correct and often impossible at all. Some needed thematic data may be obtained from primary virtual computer tests of individual NPP with imitation of possible disasters. It allows to plan the actions for NPP operators and special services under serious NPP disasters or may be to prevent them at all.

INTRODUCTION

Every NPP is presented the unique very complex object for energy production. Its normal exploitation is possible under the observation of many thematic laws and rules. NPP disasters may create the great different damages with the exclusive negative and often non reversible consequences for population and environment. Usually NPPs are located in density populated industrial regions, where there is the great need in energy consumption. Besides the NPP specific technological cycle demands a lot of water and all NPP are located near the large natural or artificial water objects (WO), that greatly increase possible risks and damages, caused by NPP disasters. The constant WO management is needed especially in urgent risk situations [1-5].

Early we used our method for prediction of irradiation doses for population under implementation of Russian Federal Program: "Development of Russian atomic energy industrial complex on 2007-2020 years" [6, 7]. Only the normal non disasters regimes of 10 Russian NPP exploitation have been under the detail consideration. The representative statistic data, obtained for 2 last decades of its exploitation, were sufficient for such consistent prediction.

Here we demonstrate and analyze some possibilities of using of our method for assessments of radiation dose for population under some possible NPP disasters. The following NPP Japan Fukusima, Russian Seversk in Tomsk region, Armenian and the future NPP in Kazakhstan are under consideration.

RESULTS AND DISCUSSION

The total vector of limited damages under NPP exploitation has been used for the fixed time interval under the following assumptions: (1) at initial state the object is in normal (non accidents) exploitation; (2) the different kinds of accidents may be occurred as noticed $i=2, 3, \dots, m$, where m is the total number of possible accidents ($m=1$ is corresponded to the normal regime); (3) every accident may

create the different kinds of damages: (4) realization of i accident creates the damage of j kind with P_{ij} probability,

$$\bar{a}_{lim} = P(1)\bar{a}_{1n} + \sum_{i=2}^m \hat{P}_{ij}\bar{a}_j \quad (1)$$

Here j is the kind of damage with a_j value. Then $j = 1, 2, \dots, n$, where n is the total number of possible kinds of damage; where $P(1)$ is the probability of loss formation under normal exploitation; \bar{a}_{1n} is the vector of limited damage under regular exploitation. $P_{ij}a_j$ coordinate vector value in sum is equal the damage value of j kind under realization of i kind accident. Thus the matrix of loss probabilities is determined. Under absent of accidents (normal regime of exploitation) \bar{a}_{lim} is determined only the first part of (1) formula.

The main problem is P_{ij} values assessment. Usually the representative statistic data for its assessment are present only for long duration of NPP normal exploitation period. Such data are absent for NPP non prognostic emergencies, when some information may be obtained only after disasters.

Some NPP are located in regions with negative natural responses such as earthquakes, tsunamis, etc.) in Armenian, Japan, California NPP and the others. The serious negative manmade factors with the global wide scale treats exist for some NPP in the dangerous conflicts zones with high probability of possible terrorist attacks, including using of explosives. Using of classic methods of expertise assessments for NPP disaster are not correct (often impossible) in these cases. Some needed data may be obtained from primary virtual computer tests of concrete NPP with imitation of possible disasters. It allows to assess risk values and also to plan the actions for NPP operators and special emergency services under serious NPP disasters or may be to prevent it at all. Effectively of liquidation of any disaster, including NPP one, is determined by qualification and professional actions of special save emergency services. Especially, when the determined disaster is in the stage of its developing. In some cases developing of the happened disaster may be stopped at all. But in any case it will help to minimize and soft of its negative consequences. Also it is often necessary to transform these consequences from its possible irreversible state in reversible ones.

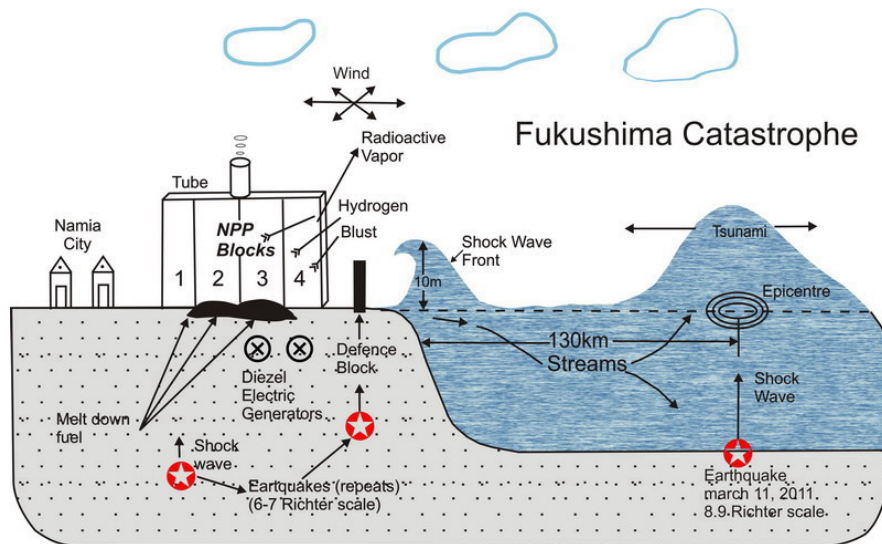


Figure 1. Scheme of tsunami response on FNPP.

Risks and possible ecological and economic damages from large-scale natural and manmade catastrophes in ecology-hazard regions of Central Asia and the Caucasus are presented in [8-10] with some problems of nuclear safety for U - tailing storages.

Now we pay some attention to Fukushima NPP (FNPP) catastrophe. Today FNPP presents the wide scale suitable polygon for complex detail researching of all possible NPP disasters, because it includes many events, close connected natural and manmade reasons from the stage of the catastrophe's appearance and its developing. The scheme of tsunami response on FNPP with its consequences after the earthquake on March 11, 2011 is presented in Fig.1. The main reason FNPP catastrophe was the first shock huge water wave (HWW) resulted after the earthquake, located down ocean bottom. HWW front height at the beach was about 10-15 m with its 965 km/h speed. The most dramatic scenario has taken place, when NPP external its diesel underground electric generators have been totally over dammed. The outside electric supplement from external sources, such as high voltage electric lines, was destroyed and the inside energy supplement from generators were stopped at all. The total all emergency systems (hydrogen defense, emergency cooling water injection pumps of NPP blocks, the systems of fire-protection, industrial seismic-protection, the signal system about temperature's access have been broken and switched off. Hydrogen generation inside of the reactor created its extreme explosive mixes, caused the blasts and fires, destroyed in addition all defense constructions with radioactive leakages in atmosphere and WO. The repeat shocks from next beach earthquakes with not high intensity as the first one in the Ocean didn't allow to construct additional defense from all possible pollution's penetration in environment. The direct discharges of radioactive vapor propagated in atmosphere. The defense capsule's destroyed in the first reactor's counter and melt-down nuclear fuel penetrated into the soil (heavy NPP disaster). May be some underground water channels are located here and the part of such pollution penetrated in the Pacific Ocean by this way. The noticed dramatic scenario have taken place at 3 from 8 FNPP reactors. The nearest suitable electric power source, needed for emergency equipment, is located in 6 km from FNPP. The Japan emergency specialists began to construct electric wires on the utility poles. But we think that the best solution was to put electric cable directly on the oil surface. It allowed to save substantial time.

According to the Russian Medicine Norma the limited irradiation human's organism doses (IHD) levels on every separated radionuclide must not more than 10 MicroSievert in year. At FNPP the irradiation level was up to 10 000 MicroSievert in hour. In the case of NPP exploitation in normal or emergency regimes IHD value is the following function:

$$\text{IHD} = F (\text{RGAD} + \text{LRD}) \quad (2)$$

where RCAD is the value of radio nuclide's gas-aerosol discharges in atmosphere; LRD is the value of liquid radioactive discharges into different water objects. But our method for IHD assessment is available here. Most high irradiation risk levels are especially negative for children and embryos as it creates gene mutation at cells level under speed organism's growth. And today FNPP is constant source of short and long-lived isotopes, that keep its activity now and will be keep during unknown period.

The main problem is the correct assessment RGAD and LRD values and its three-dimension (3D) time variations. The scientists of our Nuclear Safety Institute of Russian Academy of Sciences (IBRAE RAS) have researched some details of FNPP catastrophe in the 10 thematic articles [11] To make the correct categorization of Aqueous Media and Water Bodies by Contamination Radioactive Levels is very important [14].

Japan Government Nuclear Agency classified the FNPP catastrophe as 7-th maximum Global level. Till it was only one time for Chernobyl NPP catastrophe in 1986. The special two step test procedure has been developed in Japan for NPP test on its stability under the intense responses of earthquakes and tsunami. Only after its complete successful passing any NPP may be put into exploitation again.

It is noticed that apart from the technical mistakes in any NPP projecting and during its exploitation, there were some great political mistakes in different countries, that created negative base in future NPP accidents. After atomic industrial energy creation in USSR, at first time our Government considered that all NPPs are presented by itself the same energy objects as hydro or coal thermal stations for energy

production. And it was not necessary to pay the special attention and relation to its exploitation with additional funding and to create new separate thematic Minister Department. The result was the global Chernobyl catastrophe. But under the Chernobyl only the single huge radioactive blast has been happened, that was not located near the Ocean. Today at the FNPP catastrophe we have deal with the constant intense source of environmental wide scale radioactive pollution. It is unknown the temporal final of its activity and it is impossible to assess the total risks and the connected damages. In India when the information about the serious future earthquakes have gotten all NPP reactors have been stopped. Although the similar stopping causes the RGAD and LRD increasing, but it will be not called as any disaster because there is constant monitoring over this technological process and its management.

It is important to notice that the lack of culture in nuclear safety exists at population of most countries. Although Japan population has the high level of culture in respect of different kinds of disasters (for example, to earthquakes), but its population has the great radiophobia for nuclear disasters (result of Hiroshima and Nagasaki atomic bombing in 1945). The information about the future huge earthquake and tsunami in March 11, 2011 has been ignored by the official state organizations and the private energy companies, such as Tepco, that was responsible for normal FNPP exploitation. Today Japan System for Prediction of Environment Emergency Dose Information (SPEEDI) has been modified to WSPEEDI.

Some China specialists consider, that the earthquake on March 11, 2011 has been stimulated by the Japan testing of underground atomic bomb's blast at the Pacific Ocean bottom. We have not information about the methods, how it is possible to differ atomic blast from earthquake at Ocean large depth.

China Mass Media informed, that the huge crater has been created at this place and in result the china ship with 100 men at its board went down. Also they consider that under surface FNPP the secret plant for production of weapon U-235 and plutonium is located. Now agrees with the following fact that FNPP is kept as the constant intensive irradiation source.

Some problems, connected with another Armenian (Metsamor) NPP (ANPP) it is closely located near the main epicenters of last earthquakes with 7-9 balls on Richter scale. For the long-term period of APP exploitation from 1976, after Spitak earthquake in 1989 (6.8 Richter scale) APP has been conserved. In in the whole country has been appeared. Then in 1995 after the total energy absence ANPP has been put into exploitation again. It contains two VVER-400 and V230 (376 MW) nuclear reactors, that produce about 40% of the total country's electricity. After the recent ANPP its active life has been prolonged on 12 years till 2026 year. But the Armenian ecological situation is constantly worse with the huge amounts of highly active, medium-active and low-active wastes has been accumulated and kept in the corresponding storages without the needed keepconditions, located near Araks river, that flows into Kura river and then in Caspian Sea. factor, that at its seismic dangerous territory are located the huge storages of the radioactive wastes. That is why some US specialists call that some Armenian regions are to "black swamp" or "black quicksand."

We should like to do some remarks to the future building of one from the three NPP in Kazakhstan Republic (KR), named as Kurchatov (NPP KNPP) is planed to construct at Eastern Kazakhstan (EK) region near Kurchatov sity, located at Nuclear Semipalatinsk Test Polygon (STP) territory (Fig.2). Today KR occupies the first place in the world on U – extractions. The thematic EK thematic consideration as the the territory of global ecological risk is presented in [8, 9]. Early EK region was not seismic dangerous one. But after about 500 nuclear blasts, produced in 1949-1990 years, it became the global risk zone with the appearance of natural earthquakes in addition the negative great manmade radioactive pollution as the result of STP intense exploitation. Now STP has been closed for nuclear weapon tests.

The large hydro electric stations (HES) have been built on EK Irtysh river, the largest river of the country, with its sizeable artificial reservoirs appeared after the HES building (Fig.2). The huge water masses, accumulated in the new sizeable artificial reservoirs began to press on the surface of the ground, where many Altai high mountains massifs are located. This pressure were not desirable for our Earth at all. The Earth expresses its protest to the people for their manmade constructions in the form of

stimulated new intense earthquakes. In result early non seismic region has been transformed in seismic dangerous one.

At EK territory the numerous multiple mines for extracting metals and minerals, as well as a number of industrial enterprises and their tailing dumps, including uranium, are located in the cities and their suburbs along the Irtysh River. It originates in China, further flows via the lands of Kazakhstan and Russia, including such large cities as East-Kazakhstan capital Ust-Kamenogorsk (UK), Semipalatinsk, Pavlodar, Omsk, and Tobolsk, and after its confluence with the Ob River it flows into the Arctic Ocean (Fig.2) The largest Bukhtarma HES with the 100 m height of dam has the most sizeable reservoir, the basin length is above 300 km and the depth - up to 100 m. The other UK HES with the 42 m height of dam with its huge reservoir is located in 15 km from the city.

The next Shulba HES (1) is built in 180 km from UK. Errors in the design of these HESs have caused a number of different accidents. UK (330,000 inhabitants) is one of the most contaminated towns in the world/ It locates in the narrow Irtysh mountain valley, that oversaturated by different enterprises. Ulba Metallurgical Plant produces enriched U for NPP, Be, Ta and their products. Operating UMP wastes storage, located in city center, has accumulated ~100 thousand tons of wastes, contained U, Th and their decay products. Its size is 400* 220 m² with the depth of contamination > 5 m. The level of gamma-radiation at its surface reaches 360 μR/h and increases with depth up to 1000 -6000 μR/h.

Many other operating UK large plants, such as Lead -Zinc, Titan-Magnezium, Ceramic, worked on Be base, plants, power capacitors plant, nonmetalliferous group of enterprises and Silk Cloth enterprise, use in their technologies the different poisonous and toxins, while their wastes are also located in city boundaries. In Irtysh river basin, where > 40% of HES energy in Kazakhstan is produced, the large active non-ferrous pits, precious and rare-earths metals pits with their dump nations are also located.

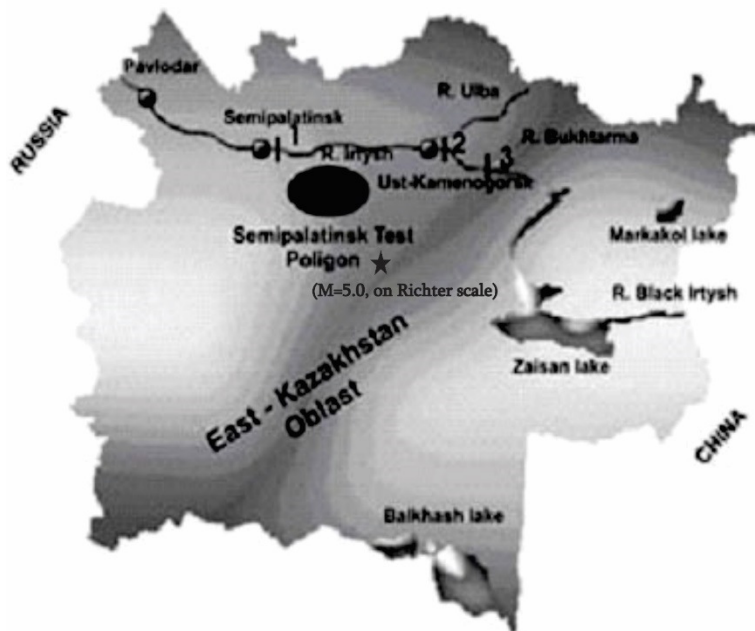


Figure 2. The scheme of Irtysh river flow on the territory of Kazakhstan Republic. 1 – Shulba HES, 2 - Ust-Kamenogorsk HES, 3 - Bukhtarma HES. Future Kurchatov NPP will be located at Semipalatinsk Test Polygon. ★ - Epicenter of the last earthquake on March 16, 2016 (M= 5.0 on Richter Scale)

Risks of the possible ecologic catastrophes are increased, because 2 HES are placed at upriver. We consider that the huge water masses in the manmade reservoirs press strongly on the bottom of mountain surfaces, disturb and deform their initial natural states. These factors resulted to the increasing of the frequency and intensity of the strong earthquakes, included catastrophic ones, that already happened not

only near the city (in 1990), but also in Altai mountains in Russia (in 2003, 2005 years). The last earthquake (M= 5.0 on Richter Scale) was on March 16, 2016 near STP. Such earthquakes may cause the damages of HES dams, where in addition part of them are in non-satisfactory states, especially UK HES dam, operated >50 years. Any HES with its huge water reservoir as the any NPP are very attractive for the possible controlled terrorist acts, including with using of explosive. According to some primary assessments, in result the huge break-through damming wave with its front height ~30 m will destroy the city and its environs. All enterprises, their products and hazard impurities in the storages then will be carried out down Irtysh to many cities and after Irtysh - Ob rivers junction spread over the large territories, including Arctic Ocean through Kara Sea. It results to abrupt worsening of water quality in all cities: UK, Semipalatinsk, Pavlodar, Omsk, Tobolsk and in many inhabited localities. Irtysh-Karaganda manmade channel supplies water to Kazakhstan central regions, such as Karaganda, Kazakhstan capital Astana city and its regions.

The available downstream STP, where are buried more than 18,000 tons of radioactive waste of the total activity of 1.300.000 Ci, significantly aggravates the situation. Radionuclides of the total activity over 10.000.000 Ci were accumulated during nuclear tests in the underground wells, located within the 60 km far from Irtysh. U-235 and Eu-152 are registered as available on the territory of above 300 sq. km.

EK HES are very attractive for realization of directed terrorist acts with using of explosives. It is sufficient to destroy the Bukhtarma HES gate of upper floodgate from 3 ones, that used for passing of ships. And then the huge water mass will realize the global catastrophe with a lot of victims and great pollution including the Arctic and World Oceans. The Earth population prefer to live in regions with comfortable conditions for living in spite of high risks level. For example US California state region with intensive destroyed earthquakes and 8 US NPP constantly operate.

We shortly notice the thematic situation with the building of new NPP in Siberia near Seversk city in Tomsk region. Here the unique Siberian NPP (SNPP) may be called as the second NPP in USSR at present the enterprise is diversifying its economic activities, providing foreign companies broad opportunities for collaboration. SNPP in its initial form was established in 1949 as a unified complex with nuclear cycle, whose main task was production of nuclear weapon components from fissile materials – namely, highly enriched uranium and plutonium. First batch of enriched uranium-235 was produced in 1953. Since the 1960's SNPP has been gradually converting to civil production and serving as an example of how such plant can successfully transition from former defense enterprises to exclusively peaceful manufacturing. Nearly all technologies of Russian nuclear industry are applied at SNPP. Such a diversification is one of the reasons that the company was able to successfully overcome periods of economic instability in Russia and develop new products and services for the international market in the early 1990's. The main little local plants, that entered in SNPP, use the unique closed nuclear cycle, from nuclear energy utilization for power generation to reprocessing and storage of nuclear wastes. After the signing of the 1991 US-Russian Agreement on Utilization of Military Uranium, the Combine became actively engaged in realization of the HEU-LEU Program (“Megatons to Megawatts”, conversion of highly enriched uranium to lowly enriched form to be then used as fuel in civil nuclear industry). Apart from nuclear industry related activities, SNPP conducts continuous product diversification and introduction of new up-to-date productions. In 2005 SNPP jointly with several other Tomsk organizations established the Scientific and Industrial Center for Research and Utilization of Nuclear Energy. US companies actively take part in investment and technical reconstruction processes conducted on SNPP. Under the intergovernmental agreement between the US and Russia dated 1997, oriented to decommissioning of plutonium producing reactors, the US Department of Energy initiated the wide-scale project of SNPP heating and power station reconstruction as an alternative to heat and power produced by the reactors of SNPP Reactor Plant, which should be decommissioned by 2008. Utilization of mixed oxides of uranium and plutonium (MOX fuel) in specially design reactors is considered one of the promising directions for further development of nuclear industry, let alone the challenge of peaceful utilization of the stock of military plutonium.

Utilization of mixed oxides of uranium and plutonium (MOX fuel) in specially design reactors is considered one of the promising directions for further development of nuclear industry. Today it is under

the building on the base of Brest - 300 reactor. Its main design features are the following: It is an evolutionary design with high level of reference; Consideration of safety requirements, including EUR, IAEA (INSAG inclusive); Broad application of passive systems; Using of advanced active safety systems; Low sensitivity to human errors; Complies with modern customer requirements: 60-year service life of the reactor plant equipment;

CONCLUSION

Today it is clear that risk assessments at any NPP and another objects of atomic energy production are presented the great complex problem that has a wide spectrum of objective and subjective reasons. Only under exploitations these objects in regular non disaster regimes it is possible to assess some possible risks and damages. This situation is constantly worsened. It is connected with the intensive growth of natural and manmade catastrophes and increasing of its power, damages and consequences. Also international terrorism attacks are thickened and have more hard consequences with mass victims. We have to develop and apply high technologies for the successful struggle against terrorism [13], including the modern space techniques [14, 15]. Till today the possible nuclear terrorist acts with great global wide scale non reversible damages don't show itself. But world civilization have to be face with new serious treats, that to save and keep itself.

One of the authors of this article Alexander Valyaev was the single participant from Russia at the NATO Advance Training Course Integrated Emergency Management for Mass Casualty Emergencies", that has taken place in Florence, Italia at October 25-30, 2011. The participants from Israel and UK indicated that their countries consider the case, happened in London on 23 November 2006, the poisoning of the UK citizen A. Litvinenko by Russian A. Logovoi with using of Po -210 as the first act of radiological (the branch of nuclear one) terrorism/ But we should like to notice, that this information has not any satisfactory arguments.

The recent clearly expressed fact has confirmed that the Islam State tries to use it its criminal purposes the extreme dangerous nuclear terrorism The security officer at the Belgian NPP has been found murdered with his work pass stolen in the result of recent terror attacks in Brussels.

REFERENCES

1. A.N.Valyaev, G.M. Aleksanyan, et. al, Managing risks to water resources in mountain regions from natural and man-made disasters" 2011, in Proc. of NATO Advanced Research Workshop (ARW):"Stimulus for Human and Societal Dynamics in the Prevention of Catastrophes: NATO Science for Pearce and Security Series. E: Human and Societal Dynamics"-vol. 80, pp. 172-188,IOS Press –Amsterdam – Berlin – Tokyo –Washington, D.C.
2. A.N.Valyaev, G.M.Aleksanyan., et.al,"Risks to aquatic ecosystems in mountains regions and its possible managment" Ibidem, pp. 191-206.
3. R.S. Minasyan, G.M. Aleksanyan., A.N. Valyaev, et. al, Large Artificial Water Reservoirs and Dams as Critical Risk Objects in Armenia, 2011, in Proc. of the NATO Advanced Research Workshop: "Stimulus for Human and Societal Dynamics in the Prevention of Catastrophes: NATO Science for Pearce and Security Series. E: Human and Societal Dynamics" –vol. 80, pp.131-138, IOS Press – Amsterdam – Berlin – Tokyo –Washington, D.C.
- 4..G.M. Aleksanyan, A.N .Valyaev, K I. Pyuskyulyan, Several approaches to the solution of water contamination problems in transboundary rivers, crossing the territory of Armenia, 2006, in NATO Science Series: Proc. of NATO ARW: "Nuclear Risk in Central Asia", Kazakhstan, Almaty, June 20-22, Publ. House: Springer Science +Business Media B.V. 2008, Netherlands, pp. 201-211.
5. A.N. Valyaev, G.M. Aleksanyan, et.al, Prediction, Prevention and Management of Natural and Manmade Catastrophes at Mountain Risk Water Objects, 2013, in Materials of Intern. Conf. "MOUNTAINHAZARDS 2013"Natural Hazards, Climate Change and Water in Mountain Areas" Bishkek, Kyrgyzstan, 16-18 September, pp.112-118.

6. A.N. Valyaev, A. L. Krylov, V.N. Semenov, G.M. Aleksanyan, A.A. Valyaev, Irradiation doses at nuclear power plants at normal and emergency situations”, 2012 in Proc. of NATO ARW: “Correlation Between Human Factors and the Prevention of Disasters” pp. 40-57..IOS Press –Amsterdam – Berlin – Tokyo –Washington, D.C.
7. A.N. Valyaev, A. L. Krylov., V.N.Semenov, D.V Nikolisky 2011 “Prediction of irradiation doses for population under implementation of Russian Federal Program:” Development of Russian atomic energy industrial complex on 2007-2020 years”. in Proc. of NATO ARW: “Stimulus for Human and Societal Dynamics in the Prevention of Catastrophes: NATO Science for Peace and Security Series. E: Human and Societal Dynamics” –vol. 80, pp.172-188, IOS Press –Amsterdam – Berlin – Tokyo –Washington, D.C.
8. A.N. Valyaev, S.V. Kazakov, A.A. H. D. Passell et. al. 2007 “Assessments of Risks and Possible Ecological and Economic Damages from Large-Scale Natural and Man-Induced Catastrophes in Ecology-Hazard Regions of Central Asia and the Caucasus.” pp. 281-299in NATO Science for Peace and Security Series -C: Environmental Security, Proc. of NATO ARW: “Prevention, Detection and Response to Nuclear and Radiological Threat”, Yerevan, Armenia.
9. Valyaev A.N., Passell.H. D., Solodukhin V.P., Alexanyan G.M., et.al.,2011, ”Geo- chemical and Radiological Risks in dangerous regions of Central Asia and Caucasus:, in Proceeding of NATO ARW: “Stimulus for Human and Societal Dynamics in the Prevention of Catastrophes: NATO Science for Peace and Security Series. E: Human and Societal Dynamics” –vol. 80, pp.194-203. IOS Press – Amsterdam – Berlin – Tokyo –Washington, D.C., Edited by A. Avagyan, D. L. Barry, W. G. Goldewey, D.W.G. Reimer.
10. A.N. Valyaev, G.M Aleksanyan, et.al. 2014 “Integrated Emergency Management and Risks for Mass Casualty Emergencies”. Proc. of the 7th Chaotic Modeling and Simulation Intern. Conf. Lisbon, Portugal, 7 - 10 June. pp. 507-522.
11. “Proc. of Nuclear Safety Institute of Russian Academy of Sciences, issue 13: Accident at ”Fukushima -1 NPP: Response Experience and Lessons. Moscow: Nauka 2013, 246 p. ISBN 978-5-02-038468 (bound) (in Russian),
12. Kazakov S.V., Utkin S.S., Linge I.I., Valyaev A.N. 2006 “Categorization of Aqueous Media and Water Bodies by Contamination Radioactive Levels.” in Proc. of Intern. Conf. “Radioactivity after Nuclear Explosions and Accidents”, v.3, pp. 402-407, (in Russian) December 5-6, Moscow, Publ. House: St. Peterburg, GIDROMETIZDAT,.
13. Valyaev A.N. and Yanushkevich V.A. 2003, “Using of Acoustic Techniques for Detection of Explosives in Gas, Liquid and Solid Mediums” NATO Science Series II “Detection of Bulk Explosives: Advanced Techniques against Terrorism” (Mathematics, Physics and Chemistry), vol. 138, pp. 175 – 183, Kluwer Academic Publishers, Netherlands. Proc. of NATO ARW, June 16-21, St. Petersburg, Russia.
14. Valyaev A.N., Kazakov S.V., Aitmatov I.T., Aitmatova D.T. “ Problems of Ecologic Safety under Displacement of Rock Stones, controlled from Space, at Ecological Dangerous Regions of Tien-Shyan Mountains” in Proc. the First Intern. Conf. ”Earth from Space- the Most effective Solutions” (in Russian), 2003. <http://www.transparentworld.ru/conference/presentations/operative.htm>
[tyan_shyan_prsnt.zip](http://www.transparentworld.ru/conference/presentations/operative.htm).
15. Valyaev A.N., Kazakov S.V. Stepanets O.V. et. al. “Using of Space Technologies for Monitoring of Large River’s Basins and Prediction of Large-Scale Natural and Man- Induced Catastrophes in Ecology-Hazard Regions of Central Asia and Caucasus” in Proc. the Second Intern. Conf. ”Earth from Space- the Most Effective Solutions” Section “Space Monitoring in Problems of Management of Territories”; Moscow, 2005 <http://www.transparentworld.ru/conference>

THE ELBE ESTUARY: BALANCE BETWEEN A HIGH FREQUENTED WATERWAY AND THE PROVISION OF ESS

*Carolin Schmidt-Wygasch**, Uwe Schröder and Elmar Fuchs

(Federal Institute of Hydrology, Koblenz, Germany)

Rainer Marggraf and Uta Sauer

(University of Goettingen, Goettingen, Germany)

Jan Barkmann

(Darmstadt University of Applied Sciences, Darmstadt, Germany)

The tidal River Elbe, Northern Germany, serves as an important international waterway feeding the port of Hamburg and thus indicates its function as a significant economic lifeline for that region. At the same time the estuarine riverscape holds valuable nature protected by national and European legislation. In the last centuries the estuary has been impacted by manmade alterations, e.g. by ongoing river training measures.

Several environmental directives like the Water Framework Directive (WFD European Commission 2000) and the national Federal Water Act (2009) have assigned a legal duty to the Water and Shipping Administration (WSV) not to focus only the safety and ease of navigation but also to be responsible for the enhancement of near-natural structures in and nearby the river. The new orientation towards more ecological maintenance and improvement, e.g. pristine river banks and an improved structural diversity, will lead to changes in existing ecosystem services (ESS).

Currently, the database for ESS of waterways is insufficient regarding their benefit, tradeoffs due to maintenance as well as the implementation in cost-benefit-analyses (CBA). To improve this situation our survey focuses on the development and establishment of the ecosystem service approach in water management. Key issues are the assumptions that the reconstruction of artificial bank protections leads to several benefits in terms of the ecosystem services concept and may have advantages even in monetary terms. Improving nature conservation and nature experience for the local residents of the Elbe region are two of them.

Here, we want to present and discuss our steps to assess and determine the public opinion and preferences to certain (cultural) ESS related to river banks. In a questionnaire we ask for attitudes and valuation of varying ESS provided from different bank forms (riprap vs. near natural). As long as the flood protection is ensured, three-quarters of the residents prefer near-natural river banks. An additional choice experiment (CE) determines the willingness to pay (WTP) for three main attributes, which were worked out through previous questionings. For changes within the realms of aesthetic concerns, protection of endangered species as well as natural bank development, we revealed an impressive WTP.

The results made an exemplary cost-benefit analysis (CBA) possible on a small potential bank restoration project promoting specific ESS. We could demonstrate that the primary investment costs facing a high societal benefit. For the first time important (cultural) ESS could be monetized on river banks of the tidal River Elbe. Moreover, the present results provide evidence that the evaluation of the social value of water management, or rather a river bank restoration on the basis of socio-economic methods is possible.

The research results shall find their way into the operational water management and maintenance of federal waterways. Mostly socio-economic factors are easier to communicate to decision makers than often abstract environmental issues and in consequence they could be more relevant for decision taking. The consequent implementation of the ecosystem services approach will help us to achieve a sustainable development of waterways, and on this way a higher transparency, and acceptance.

NOVEL TAXA ARE DOMINANT IN MANGROVE SWAMP OF NIGER DELTA, NIGERIA

Chika Christiana Nwankwo and Gideon Chijioke Okpokwasili
(University of Port Harcourt, Port Harcourt, Rivers State, Nigeria)

Taxonomic study has greatly progressed by the use of a high throughput technology. Metagenomics provides insights into microbial diversity which is not possible using traditional technique. Three georeferenced crude oil spilled soils and three pristine soils with no history of crude oil pollution in the mangrove swamp of Bodo West in Gokana and Bille in Degema locations of Niger Delta, Nigeria were studied. Roche 454 Metagenomic sequencer was used to produce all data sets. Bioinformatics, mathematical and statistical models were used to analyze data sets. DNA sequencing was performed by Next Generation Sequencing Technique to determine the nucleotide sequences of all microorganisms present in the soil sample using Genome sequencer 454 sequences or illumina were compared to sequences obtained from genebank by BLASTX Analysis using CLO bio software. Microbial compositions were estimated. A total of 20 phyla and 36 classes were studied in both polluted and unpolluted sites of study. It was observed that some nucleotide sequences showed no significant similarity and were classified as the potential No hits most of which belonged to the Unknown Phylum, it was dominant phylum in the polluted soils of study with abundance of 49.86% and second dominant in the unpolluted soil with abundance of 27.5%. In these study sites, the Unknown phylum had higher relative abundance when compared to *Proteobacteria* phylum. Frequency occurrence of this phylum at study sites was 91.7%. They were more abundant in the subsection of study sites for both polluted and unpolluted soils. Three non referenced bacteria isolated from mineral salt medium, showed these microbes were able to grow in the laboratory and can utilize hydrocarbons as energy source. Gram reaction revealed they are Gram positive rods. DNA extraction, PCR amplification and sequencing revealed isolates of base pair lengths, 784, 732 and 627 may be potential novel as no significant similarity was found when blast at NCBI website. Specific primers for amplification of alkM, Ppalk B and ndoB genes for hydrocarbon degradation were used for functional gene analysis on the isolates. Result showed 100% amplification of hydrocarbon degrading genes. The means value of the potential novel isolates showed that they were higher in the polluted soil when compared to the unpolluted soil. There was no significant difference between polluted and unpolluted soils as p was 0.224. Agglomerative Hierarchical Clustering method showed 70% similarity between *Gamma proteobacteria* and *No hit* class in the polluted soil, while 55% similarity was observed in the unpolluted soil. Seventy eight percent (78%) similarity was observed between the No hits and *Acidobacteria* in the unpolluted soil, other interactions exist between No hits and other classes of microorganisms. Pearsons correlation, Principal Component Analysis and Canonical Correspondence Analysis reveal the ecological interactions at polluted and unpolluted sites, variations among sites as well as influence of environmental variables on the potential novel isolates. Phylogenic trees constructed using neighborhood joining method showed evolution of novel microorganisms. Nucleotide sequences of some potential novel isolates have been submitted to the gene bank with Accession nos KT899789 to KT899790. This molecular study has revealed potential new isolates that can bioremediate crude oil polluted soil.

PHYLOGENIC DIVERSITY OF MICROORGANISMS IN THE MANGROVE SWAMP UNDER CRUDE OIL PERTURBATION

Nwankwo Chika Christiana and Okpokwasili Gideon Chijioke
(University of Port Harcourt, Port Harcourt, Rivers State, Nigeria)

Microorganisms in the environment have molecular evolution. This study is aimed at using metagenomics tool to assess DNA sequences of microbial compositions in phyla. Phylogenetic study or evolution modeling has given novel insights into microbial composition and potential organisms which are important in bioremediation of crude oil polluted swamp. Soil samples were taken from Cawthorne Channel 11, Bodo West and Bille communities in Niger Delta region of Nigeria. Phylogenetic analysis and estimates were analyzed using sequencer software package (version 4.J) and compared to sequences with NCBI database using Basic Local Alignment Search Tool (BLAST). All phylogenetic affiliations with any bacteria were imported and aligned. Construction of trees were done by neighborhood joining methods using Nucleotide substitution models; trees were rooted with unrooted sequences and 100 replicates were used for bootstrap analysis. Microbial diversity was characterized by 16S rRNA sequences into Operational Taxonomic Units. Specie richness and diversity index using Simpsons diversity index showed no significant difference in diversity between the polluted and unpolluted soil as p is 0.72. while specise richness was higher in polluted soil but showed no significant difference between polluted and unpolluted soils p is 0.20. Fifteen (15) phyla were studied in the unpolluted soil while 13 phyla were studied in the polluted soil, At relative abundance greater than 2%, seven phyla were studied in the polluted soils they are Unknown phylum 49.86%, Proteobacteria 21.5%, Actinobacteria 9.87%, Firmicutes 9.5%, Chloroflexi 3.56%, Ascomycota 2.0% and Bacteroidetes/Chlorobi 1.8%, while a total of six phyla were studied in the unpolluted soils:

Firmicutes>Unknown>Actinobacter>Proteobacteria>Acidobacter>Verucomicrobia. Similarly, Bodo West with 3week crude spill showed the presence of five phyla Actinobacteria >Unknown>Proteobacteria>Chloroflexi > Bacteroidetes. Bille site with 14 week spill showed the presence of seven Phyla in the order of abundance: Unknown> Proteobacteria>Firmicutes> Ascomycota> Bacteroidetes> Acidobacter. Cawthorne Channel with 50week old spill had four phyla in the order of abundance: Proeobacteria> Firmicutes>Unknown>Actinobacter. Sphingobacteria, Chlorobi and Chloroflexi showed significant difference between polluted and unpolluted soils. Variations in phylogenetic diversity was observed among polluted study sites as well as between polluted and unpolluted soils. Cluster analysis using Unweighted Pair Group with Average linkages (UPGMA) and Agglomerative Hierarchical clustering were used to construct dendograms and establish similarity between variables and observe changes in sites. Study has shown that crude oil affects phylogenetic diversity and the knowledge of phylum diversity in a polluted soil is important in bioremediation processes.

STRESS FACTORS TO FISH HABITAT IN URBAN RIVERS

Yuta Yamauchi, Tetsuya Nakata, and Yutaka Sakakibara
(Waseda University, Shinjuku, Tokyo, Japan)

To assess crucial stress factors to life cycle of fish, Life Cycle Risk Assessment (LCRA) was applied to urban rivers in Tokyo. In LCRA, life cycle was divided into 3 life-stages; fry fish, adult fish, and spawning. In addition, the following eight stress factors were considered; depletion of dissolved oxygen (DO), water temperature, disappearance of habitats, shortage of depth in movement, disappearance of evacuation areas, disappearance of spawning areas, existence of obstacles, and shortage of food. In our former study, fish species in rivers in suburban and rural areas could be reasonably well predicted by the LCRA.

Comparisons of LCRA and observed results in urban rivers suggested there are additional stress factors specific in the rivers, because most discrepancies indicated that LCRA predicted the survival while no corresponding fish were observed. Therefore, main focus was put on the additional stress factors including predation by large aquatic species such as carps and red-eared slider turtles, the existence of estrogen (17alpha-ethinylestradiol; EE2), and washout by flooding. And their effects to fish habitats were studied theoretically and experimentally.

As a result, it was demonstrated that predominant feeds found in carps were waterweeds and bloodworms while those of red-eared slider turtles were crayfishes and waterweeds, indicating the predation by large aquatic species is not a crucial stress factor. Concentrations of EE2 ranged from 0.06 to 1.5 (ng/L), suggesting EE2 is also not a crucial stress factor, due to much lower concentration levels in comparison with threshold value in the literature. On the other hand, it was found that flow rates in flooding were reduced below fish swimming speeds (0.05~1.5m/s) by obstacles in rivers. Moreover, spawning periods of most fish whose survivals were not predicted by the LCRA are in May and June. This period is rainy season and large fluctuations in river water are observed. Therefore, it is considered that the additional stress factor would be attributable to the fluctuations.

The Impact of Alternative Measures of Riverbank Fixation on Climate Change and Water Quality

*Lars Symmank** (German Federal Institute of Hydrology, Koblenz, Germany)

Katharina Raupach (University of Goettingen, Goettingen, Germany)

Mathias Scholz and Christiane Schulz-Zunkel (Helmholtz Centre for Environmental Research-UFZ,
Leipzig, Germany)

The majority of riparian zones and floodplains in Europe and North America are heavily modified due to anthropogenic impacts during the last centuries. The need for renaturation is high but rarely compatible with economic interests such as shipping and agriculture. Alternative riverbank fixations, like the replacement of riprap by reedbeds or soft wood can serve as one compromise between ecology and economy on waterways in areas with high human activities. Originally made for enhancement of biodiversity these measures involve a high potential for additional ecosystem services. We here present a first approach to estimate selected ecosystem functions in a case study of alternative riverbank fixations at the river Weser in north-west Germany. In the most cases site specific parameters needed for direct recording of ecosystem functions can only be obtained intricately. Therefore we estimate carbon fixation by biomass equations and nutrient retention by proxies derived from field investigations and published measurements. Our results show distinct additional benefits of riverbank renaturations far beyond the mere increase of biodiversity. The study illustrates the impact of even small-scale measures on climate change and water quality through measurable reductions of nutrients and carbon fixation.

STATE TRANSITIONS AND FEEDBACK MECHANISMS DURING ECOSYSTEM DEVELOPMENT IN THE CONSTRUCTED CATCHMENT 'CHICKEN CREEK'

Wolfgang Schaaf, Christoph Hinz, Werner Gerwin and Markus K. Zaplata
(Brandenburg University of Technology Cottbus-Senftenberg, Cottbus, Germany)
Reinhard F. Huettl
(GFZ German Research Centre for Geosciences, Potsdam, Germany)

Landscapes and ecosystems are complex systems with many feedback mechanisms acting between the various abiotic and biotic components. The knowledge about these interacting processes is mainly derived from mature ecosystems. The initial development of ecosystem complexity may involve state transitions following catastrophic shifts, disturbances or transgression of thresholds.

To study the early development of an ecosystem and the role of feedback mechanisms at the landscape scale, we used a 10-yr time series of hydrological, meteorological, biological, geomorphological and soil data from the catchment 'Chicken Creek' in the mining area of Lusatia, Germany (Gerwin et al. 2009). The world's largest constructed catchment has a hillslope-shaped 6 ha size with defined boundary conditions and well-documented inner structures. The dominating substrate above an underlying 1-2 m clay layer is Pleistocene sandy material representing mainly the lower C horizon of the former landscape. The site was left to unrestricted development since 2005 and was intensively monitored (Elmer et al. 2013, Schaaf et al. 2013).

The data showed a very rapid development of the site with an increasing complexity and heterogeneity. In the first years, stochastic signals like the initial substrate conditions and external drivers like extreme weather events were the most important factors resulting in abiotic/abiotic feedback mechanisms shaping the morphology of the site and creating site diversity. Initial abiotic feedback mechanisms between water and substrate were soon followed by abiotic/biotic feedbacks between biological soil crusts, invading vegetation, geomorphology and hydrology resulting in state transitions in catchment functioning.

The scientific value of sites like Chicken Creek with known boundary conditions and structure information could help to disentangle feedback mechanisms between hydrologic, pedogenic, biological and geomorphological processes as well as a more integrative view of succession and its drivers during the transition from initial, less complex systems to more mature ecosystems. In addition, restoration in general as well as ecological engineering could benefit from this enhanced understanding.

ECOSYSTEM ASSESSMENT AND RESTORATION

Elvis Obeng Boateng

(Czech University of Life Sciences, Environmental Faculty, Sudhol, Prague, Czech Republic)

INTRODUCTION. Ecological restoration is the process of assisting the recovery of an ecosystem that has been degraded, damaged or destroyed. Many of the world's ecosystems have undergone significant degradation with negative impacts on biological diversity and peoples' livelihoods. Ecological restoration can be a primary component of conservation and sustainable development programmes throughout the world.

OBJECTIVES. Given that many people now depend on what have become degraded ecosystems to sustain their livelihoods, ecological restoration needs to address four elements. These elements are critical to successful ecosystem management. Ecological restoration should:

- Improve biodiversity conservation
- Improve human livelihoods
- Empower local people
- Improve ecosystem productivity

METHODS. Ecological restoration is a well-established practice in biodiversity conservation and ecosystem management. The principles, and the Attributes of Restoration Progress below, are consistent with both the scope and intent of the Convention on Biological Diversity's Principles for the Ecosystem Approach.

HUMAN SYSTEMS

- Ensuring all stakeholders are fully aware of the full range of possible alternatives, opportunities, costs and benefits offered by restoration.
- Empowering all stakeholders, especially disenfranchised resource users.
- Engaging all relevant sectors of society and disciplines, including the displaced and powerless, in planning, implementation and monitoring.
- Considering all forms of historical and current information, including scientific and indigenous and local knowledge, innovations and practices.
- Providing short-term benefits leading to the acceptance of longer-term objectives.
- Providing for the accrual of ecosystem goods and services

ECOSYSTEM

- Incorporating biological and environmental spatial variation into the design.
- Emphasizing process repair over structural replacement.
- Allowing sufficient time for self-generating processes to resume.
- Treating the causes rather than the symptoms of degradation.
- Include monitoring protocols to allow for adaptive management.

Although recent evidence indicates that restoration can be successful in increasing both biodiversity and ecosystem services, it should not be assumed that restoring biodiversity will inevitably enhance ecosystem services, or vice versa. Biodiversity and different ecosystem services might display contrasting trajectories during restoration, leading to conflicts and trade-offs. Restoration actions focusing on a particular ecosystem service could lead to negative impacts on biodiversity or provision of other services, which will need to be considered during the planning process. Resolution of conflicts in delivery of different services and biodiversity will probably require a participatory process to land-use planning.

LAND SURFACE TEMPERATURE VARIATION AND LAND COVER CHANGES BASED ON SATELLITE IMAGERY DATA

Anh Kim Nguyen^{1,2,3}, Yuei-An Liou^{3,4,5*}, and Ming-Hsu Li¹

¹The Graduate Institute of Hydrological and Oceanic Sciences, National Central University, Taoyuan City 32001, Taiwan

²Institute of Geography, Vietnam Academy of Science and Technology, 18 Hoang Quoc Viet Rd., Cau Giay District, Hanoi Viet Nam

³Taiwan Group on Earth Observations, Hsinchu, Taiwan

⁴Center for Space and Remote Sensing Research, National Central University, Taoyuan City 32001, Taiwan

⁵Taiwan Geographic Information System Center, Taipei, Taiwan

ABSTRACT: Urban area is a complex eco-environment involving a variety of anthropogenic activities. Its sustainable development is affected by many factors, such as topographical appearance, hydro-meteorological environment, and social economics. Due to urban sprawl and less vegetation, urban areas often exhibit higher thermal signatures than less disturbed rural areas. Thermal signatures represent the thermal status resulting from energy balance at land-air interface. In this study, Land Surface Temperatures (LSTs) are retrieved from Landsat TM, ETM, and OLI & TIRS (Thematic Mapper, Enhanced Thematic Mapper, and Operational Land Imager & Thermal Infrared Sensor, respectively) and serve as basis to derive ecological thermal index for assessing ecological dynamics in years 1989, 2003, and 2014. The Thua Thien - Hue Province, Vietnam, is chosen as a study area because it is a coastal province and has been experiencing with natural disaster, deforestation, and rapid urbanization. Its LST is found to increase by 0.7 °C and 1.5 °C for the 1989-2003 and 2003-2014 periods, respectively. Thermal environment index maps are utilized to categorize ecological conditions into six levels (*excellent*, *good*, *normal*, *bad*, *worse*, and *worst*). To demonstrate urban development a major contributor to thermal anomaly, correlation between LST and Normalized Difference Build-up Index (NDBI) is analysed. The correlation is found to be positive as expected with coefficient values 0.87, 0.89, and 0.84 for 1989, 2003, and 2014, respectively. In contrast, LST-Normalized Difference Vegetation Index (NDVI) is found negatively correlated with corresponding coefficient values -0.81, -0.81, and -0.76, indicating that vegetation reduces thermal intensity. In addition, areas associated with *excellent*, *good*, and *normal* thermal environmental levels are decreased over the same period of time frames 1989-2003 and 2003-2014.

Keywords: Ecological thermal indices; Eco-environment; Thua Thien-Hue Province; Landsat data

INTRODUCTION

Eco-environment has been greatly impacted by anthropogenic processes, such as transformation of land use patterns, urban sprawl, and de-vegetation, so that urban areas often present significantly higher thermal signatures than less disturbed rural areas. Thermal environment is considered as an important aspect of the eco-environment because it represents the status of energy balance through space-time interaction and interdependence association with city micro climate, and urban ecology (Miller and Small., 2003). It has been acknowledged that urban heat island occurred mainly in Land Surface Temperature (LST), which is governed by surface heat fluxes and affected by removal of vegetation, soil, water and their replacement with common urban materials like concrete, metal and asphalt.

The Thua Thien - Hue Province has been experiencing urbanization at a rapidly rate in both population and physical size in the recent decades so that it is selected as our study area where the urban use, agricultural practice, and aquaculture activities have inevitably invaded into natural zones. These changes lead to an increasing burden on the eco-environment (Nguyen et al., 2016) by bringing water, soil, and air pollution. Unfortunately, these outcomes are enhanced by natural disasters including annual floods, landslides, and storms in the Thua Thien - Hue Province (Thanh and De Smedt, 2011; Tran et al., 2007). Thus, it is critical to monitor the land surface dynamics, in particular urban development and its effects on the urban thermal anomaly. However, uneven distribution and limitation of in situ-measurement data often cause a barrier for long-term environmental monitoring across the region. The series of Landsat satellites provide free of charge data, which stimulate various natural and man-made disaster studies and resources monitoring, and support the evaluation of magnitude, dynamics, and spatial distribution of land surface parameters and eco-environmental vulnerability using satellite-derived variables (Nguyen et al., 2014, 2016; Liou et al., 2015; Liu and Zhang, 2011; Chen et al., 2006).

This study aims to identify the trend of LST derived from Landsat TM/ETM+, and OLI thermal infrared bands and examines the influences of land cover changes patterns and its association with LST in the Thua Thien - Hue Province of different time frames from 1989 to 2003 and from 2003 to 2014. The correlation coefficients of LST and Normalize Difference Built-up Index (NDBI), and Normalize Difference Vegetation Index (NDVI) are quantified. Thermal field variance indices are computed and classified into six levels including *excellent*, *good*, *normal*, *bad*, *worse*, and *worst* as a basis for the whole framework of the current eco-environmental study.

MATERIALS AND METHODS

The Study Site Description. The Thua Thien - Hue Province covers an area of 5,054 km² in the north central coastal region of Vietnam with coordinates of 15° 59' -16° 48' N and 106° 25' -107° 51' E, comprising two basins of four rivers and Hue city as the provincial capital (**Figure 1**). Due to its location in the tropical monsoon basin, the average annual temperature ranges from 21° C to 26° C. The highest temperature (approximately 41.3 ° C) normally occurs in June, July, and August, while the lowest temperature (12 ° C) occurs in November, December, and January. The average relative humidity is around 84-85%. Annual average precipitation may reach 2,500-3,500 mm in the plains and 3,000-4,500 mm in the mountains. Impressively in some years, precipitation may be much higher and reaches more than 5,000 mm in the mountains (Tong et al., 2012). In recent years, meteorological observation records, which are collected from Institute of Meteorology and Hydrology of Vietnam, also depicted that there have been significant changes in precipitation patterns in all three stations (A Luoi, Nam Dong, and Hue) of the Thua Thien - Hue Province (increase of precipitation during the rainy seasons from August to December, lessen extent from April to May, and decrease in precipitation during the drier June to July period). This trend implies that there will be very likely more floods and droughts in the future in The Thua Thien - Hue Province (UNDP, 2003; MoNRE, 2003; Tran et al., 2007).

Data Used. The Thua Thien - Hue Province has 3 meteorological stations, Hue, A Luoi, and Nam Dong (**Figure 1**). To evaluate land cover changes, satellite images of two seasons are collected including Landsat 5 TM images (acquired on 08 May 1989; 03 December 1990), Landsat 7 ETM+ images (acquired on 21 April 2003; 06 November 2000), and Landsat 8 OLI & TIRS images (acquired on 27 April 2014; 04 October 2014). Those images acquired in summer months are used to examine the LST and land cover changes with supporting seasonal vegetation features by using those images acquired in winter months.

Image Processing. To analyze the trend of LST, several steps are performed and can be described in six steps: (i) Atmospheric correction is performed for all bands by using Fast Line-of-Sight Atmospheric Analysis of Spectral Hypercubes (FLAASH) (Waner and Chen, 2001) and following the atmospheric correction, the images are geo-referenced to UTM projection, zone 48 north; (ii) Digital numbers (DNs) of

band 6 are converted to spectral radiance and then brightness temperatures are computed; (iii) Land emissivity is estimated based on NDVI method (Valor and Caselles, 1996; Sobrino et al., 2004) and brightness temperatures are converted to LST (Artis and Carnahan, 1982); (iv) Visible bands of images (Landsat 5 TM image acquired on 08 May 1989; Landsat 7 ETM+ image acquired on 21 April 2003; and Landsat 8 OLI & TIRS image acquired on 27 April 2014) are selected to composite to be a single image and land cover classification was performed with Support Vector Machine method; (v) Thermal field variance index is calculated based on LST by using equation (1) (Liu and Zhang, 2011).

$$TFVI = \frac{T_s}{T_s - T_{mean}} \quad (1)$$

where TFVI is the thermal field variance index; T_s is the LST of certain pixel in C degree; and T_{mean} is the mean LST of the whole study area in C degree. To classify thermal field variance index into different levels, histograms are used to reveal the statistical distribution of calculated thermal field variance values from grid cells; and (vi) Calculation of NDBI and NDVI to investigate the relationship between LST and NDBI and NDVI.

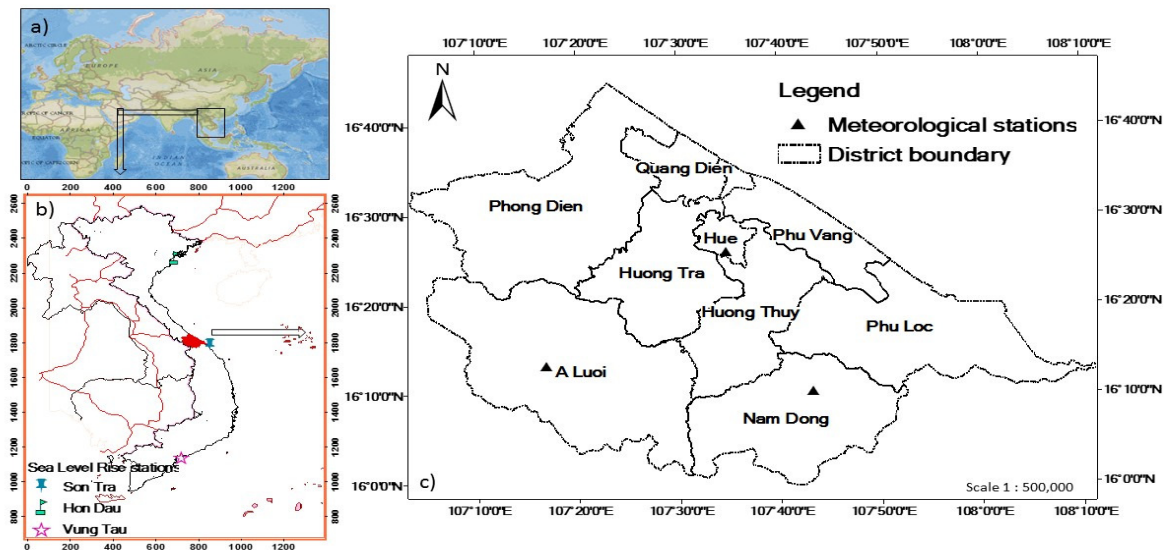


Figure 1. The map shows Asia (a); Vietnam and sea level rise stations (b); and Thua Thien - Hue Province (c).

RESULTS AND DISCUSSION

Trend of LST in the Thua Thien - Hue Province. The LST in urban and rural areas are investigated by estimating mean and standard deviation for each district in the Thua Thien - Hue Province (Table 1). The LSTs in 1989, 2003, and 2014 are shown in Figure 2. There was an increasing trend in LST in both urban and rural areas (mean LST was increased by 0.7 °C and 1.5 °C between the 1989-2003 period and 2003-2014 period, respectively), The difference in the mean LST between urban and rural areas fluctuated from 0.9 °C to 2.9 °C. Figure 2 shows the evolving patterns of LST from urban to rural areas in 1989, 2003, and 2014, and indicates each district has a different spatial-temporal pattern of LST. Annual air temperature from in situ-measurement at 3 stations show a good agreement with an increasing trend of LST derived from thermal bands of Landsat sensors (Figure 3). The measured air temperature increased around at 0.5 °C, 1.0 °C, and 0.9 °C at the Hue, A Luoi, and Nam Dong stations throughout the period from 1989 to 2014. However, the difference of LST from 1989 to 2014 is higher due to the time of satellite passing at around 11 AM and LST varies in different land cover types, so that the difference of LST temperature is higher as compared with that of monthly and annually measured air temperatures.

Trends of Land Cover Changes. Figure 4 shows the increase in the physical size of the development land parallel with expansion of LST over decades (Figure 2). There was a dramatic increase in developed land and decrease in agricultural land and forest land. Developed land had greatest changes during different time period, from 166.12 Km² in 1989, 256 Km² in 2003, to 530.93 Km² in 2014. There was a significant decrease in agricultural land from 357.25 Km² in 1989, 228.94 Km² in 2003, to 240.88 Km² in 2014. Changes in developed land mainly occurred in urban and surrounding areas where cropland was replaced by concrete (buildings, roads, etc.) and the reduction of forest land appeared mainly in rural and mountainous areas where a larger natural forest area was gradually replaced by planted forest and cropland and building. At the regional scale, the increase of developed land, and decrease of crop land, and wood land implies that more people live in the major cities.

Table 1. Changes in LST of 9 districts over decades.

No	District names	Area (Km ²)	08 May 1989		21 April 2003		27 April 2014	
			Mean	Std	Mean	Std	Mean	Std
1	Hue (urban)	71.9	25.7	1.4	26.5	1.6	27.6	2.1
2	Phu Vang (urban)	277.2	24.9	2.2	26.5	2.7	26.7	3.5
3	Quang Dien (urban)	162.7	25.1	2.7	26.1	3.0	26.1	3.4
4	Phu Loc	705.8	24.1	1.8	25.8	2.5	27.7	2.8
5	Huong Tra	518.2	24.7	1.3	24.8	1.4	26.4	1.9
6	Huong Thuy	455.9	24.6	1.7	25.3	2.0	27.3	2.0
7	A Luoi	1105.7	22.5	1.2	22.9	1.1	24.4	1.7
8	Nam Dong	643.7	22.8	1.1	24.0	1.4	26.6	2.3
9	Phong Dien	947.1	24.8	2.6	24.3	3.1	26.4	3.2

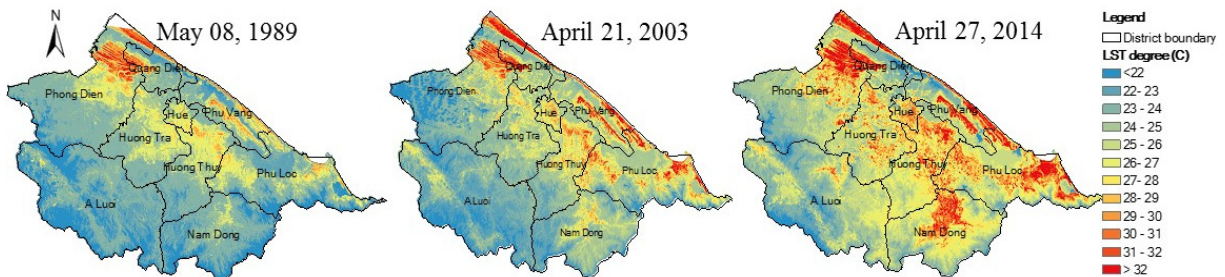


Figure 2. Spatial-temporal LST distribution over the Thua Thien - Hue Province derived from thermal bands Landsat sensors (Mean LSTs and Standard deviations (STDs) are 23.9 (STD 2.1); 24.6 (STD 2.4); and 26.1 (STD 2.7) for 1989, 2003, and 2014, respectively).

Relationship between LST Variation and Land Cover Changes. The sampling points are randomly taken from the Thua Thien - Hue Province. LST, NDBI, and NDVI values are extracted from the raster data to compute correlation coefficient among them. The LST-NDBI correlation coefficient (0.87, 0.89, and 0.84 for 1989, 2003, and 2014, respectively) indicates a positive influence of build-up land on urban temperature, implying that the build-up land can strengthen the thermal environment in the Thua Thien - Hue Province.

In contrast, negative LST-NDVI correlation (-0.81, -0.81, -0.76 in the same period) demonstrates that vegetation can weaken the thermal environment.

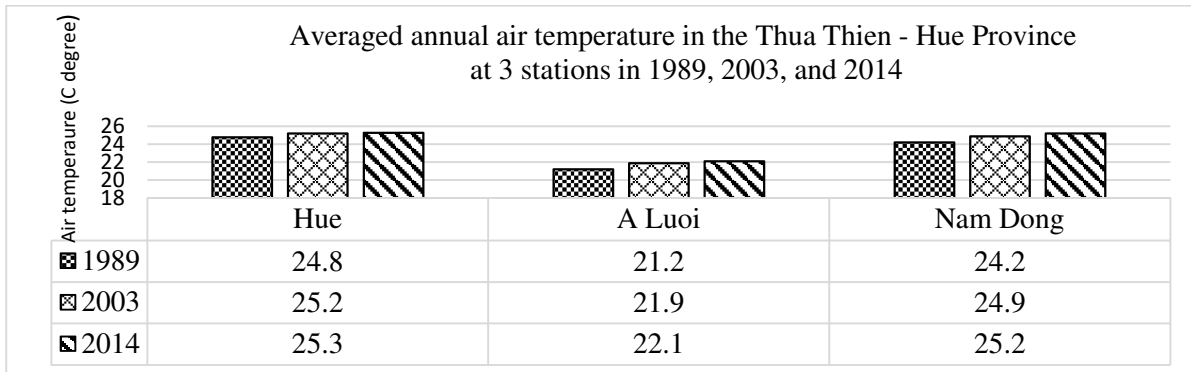


Figure 3. Annual measured air temperature at 3 stations (Hue, A Luoi, and Nam Dong).

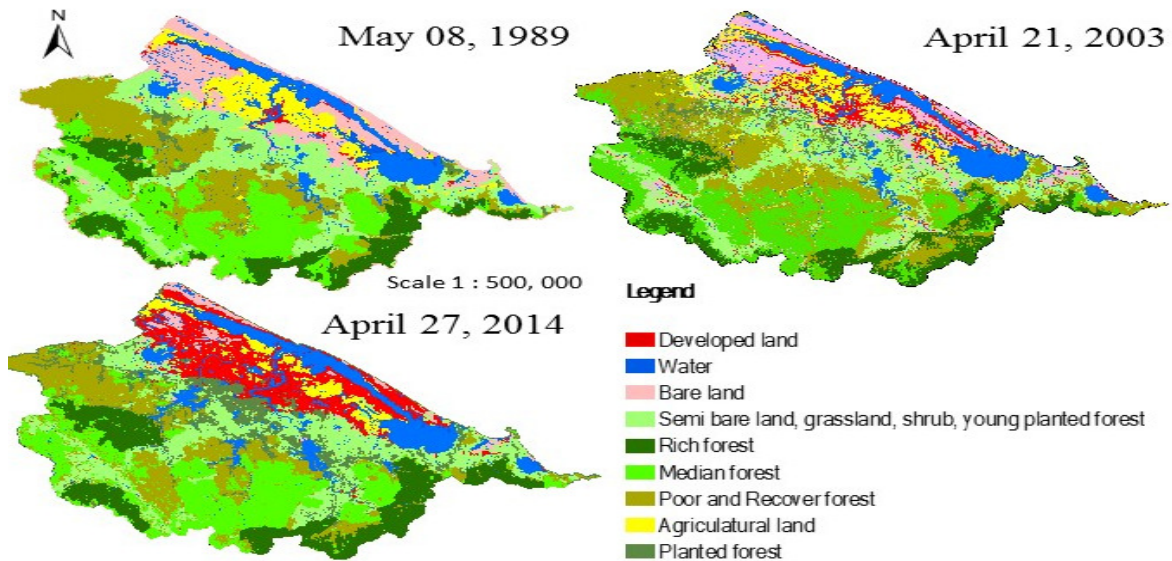


Figure 4. Dynamic of land cover from 1989 to 2014 derived from Landsat images (classification accuracy, Kappa coefficients are 0.84, 0.89, and 0.88 for 1989, 2003, and 2014, respectively).

Thermal field variance index evaluation of the Thua Thien Hue Province. Thermal environment index maps for 1989, 2003, and 2014 are constructed to categorize the ecological condition of the provincial area into six different levels (*excellent*, *good*, *normal*, *bad*, *worse*, and *worst*), which are shown to occupy, respectively, 77.87%, 12.68%, 1.37%, 1.30%, 2.20%, and 4.57% of the entire region of interest in 1989; 62.47%, 3.95%, 8.93%, 4.49%, 4.49%, and 13.68% in 2003; and 58.27%, 3.21%, 11.09%, 5.92%, 3.75%, and 17.75% in 2014 (**Figure 5**).

In general, from 1989 to 2003, and 2014 the areal percentage of *bad*, *worse*, and *worst* thermal environment levels was increased and the spatial distribution was from the low to high elevation belt parallel with time. Compared with the census data acquired in the same period of time, it is obvious that the *bad*, *worse*, and *worst* thermal environmental levels appeared mainly in the urban areas where social-economic activities have been intensified and the increasing trend of *bad*, *worse*, and *worst* thermal environment

levels was in accordance with the urban population growth (about 237,800, 343,800, and 549,800 inhabitants in 1989, 2003, and 2014, respectively).

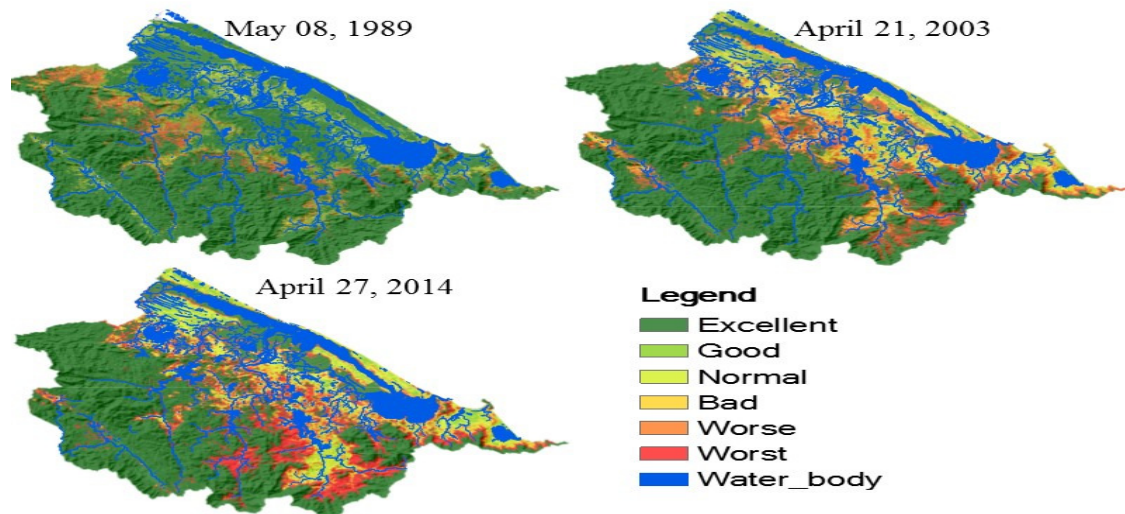


Figure 5. Thermal field variance index classification in the Thua Thien - Hue Province.

CONCLUSIONS

LST is found to increase by 0.7 °C and 1.5 °C for the 1989-2003 and 2003-2014 periods, respectively. Measured air temperature data in the same period also shows an increasing trend and good agreement with LST. However, the difference of LST is higher due to the time of satellite passing at around 11 AM. LST varies in different land cover types so that LST is higher as compared with monthly and annually measured air temperatures. On the contrary, the *excellent*, *good*, and *normal* levels of thermal ecological environment were decreased over the same period of time. Results indicate that land use changes have great influences on urban thermal environment. The time series maps of categorization for ecological thermal indices in the Thua Thien - Hue Province can be used for future urban planning and further eco-environmental quality assessment.

ACKNOWLEDGEMENTS

This research was financially supported by National Central University, Taiwan through the NCU International Student Scholarship. We would like to thank data support from United States Geological Survey (USGS). We also appreciate the financial support of the Ministry of Science and Technology (MOST) of Taiwan under the codes 104-2111-M-008-004 and 104-2221-E-008 -067.

REFERENCES

- Artis D.A, Carnahan WH., 1982. Survey of emissivity variability in thermography of urban areas. *Remote Sens. Environ.* 12, 313-329.
- Chen, X.-L., Zhao, H.-M., Li, P.-X., Yin, Z.-Y., 2006. Remote sensing image-based analysis of the relationship between urban heat island and land use/cover changes. *Remote Sens. Environ.* 104 (2), 133-146.
- Liu, L., Zhang, Y., 2011. Urban heat island analysis using the Landsat TM data and ASTER data: a case study in Hong Kong. *Remote Sens.* 3 (12), 1535-1552.
- Liou, Y.A., Nguyen, A.K., Li, M.H., and Lin, C.Y. 2015. Landsat 8 operational land imager derived variables for environmental risk assessment in Taoyuan, *IGARSS*, July 26-31, Milan, Italy, DOI: 10.1109/IGARSS.2015.7325904.

- Nguyen, A.K., V. Phonekeo, V. C. My, N. D, Duong, and P. T Dat. 2014. Environmental hazard mapping using GIS and AHP - a case study of Dong Trieu District in Quang Ninh Province, Vietnam. IOP Conf. Ser.: *Earth Environ. Sci.* 18 012045.
- Nguyen, A.K., Y.A. Liou, M.H. Li, and T.A. Tran. 2016. Zoning eco-environmental vulnerability for environmental management and protection, *Ecol. Indic.* Vol 69, Pages 100–117. SCI. doi:10.1016/j.ecolind.2016.03.026. IF: 3.444.
- Sobrino, J.A., Jimenez-Munoz, J.C., Paolini, L., 2004. Land surface temperature retrieval from Landsat TM 5. *Remote Sens. Environ.* 90, 434–440.
- MoNRE, 2003. Vietnam Initial National Communication under the United Nations Framework Convention on Climate Change. *MoNRE*, Hanoi, Vietnam.
- Thanh, L.N., De Smedt, F., 2011. Application of an analytical hierarchical process approach for landslide susceptibility mapping in A Luoi district, Thua Thien – Hue Province, Vietnam. *Environ. Earth Sci.* 66 (7), 1739–1752.
- Tran, P., Marincioni, F., Shaw, R., Sarti, M., Van An, L., 2007. Flood risk management in Central Viet Nam: challenges and potentials. *Nat. Hazards* 46 (1), 119–138.
- Tong, T.M.T., Shaw, R., Takeuchi, Y., 2012. Climate disaster resilience of the education sector in Thua Thien – Hue Province, Central Vietnam. *Nat. Hazards* 63 (2), 685–709.
- UNDP, 2003. Reducing Disaster Risk, A Challenging for Development Valor, E., Caselles, V., 1996. Mapping land surface emissivity from NDVI: application to European, African, and South American areas. *Remote Sens. Environ.* 57, 167–184 (18).
- Waner, T., Chen, X., 2001. Normalization of Landsat thermal imagery for the effects of solar heating and topography. *Int. J. Remote Sens.* 22, 773–788.

**CAUSES OF DAMPNES IN RESIDENTIAL BUILDING WALLS IN JOS METROPOLIS,
PLATEAU STATE, NIGERIA**

Kalada Itelima

(Kalite Associates, Jos, Plateau State, Nigeria)

Jos Plateau is located on the North Central region of Nigeria. It is relatively undulating plain bounded by mountainous ridges. The prevailing climatic situation of the study area hinges upon alternate seasons of hot and cold weather conditions interspersed with an average period of about 6 months of rainfall, with July being the peak period. Dampness is the wetting of structural elements through moisture rise by capillary action. Dampness is one of the most serious structural defects in walls of buildings. Dampness in walls spoils paints and interior decorations, encourages the growth of bacteria and moulds, hampers aesthetics, and poses a threat to health of occupants through providing breeding conditions for mosquitoes. Dampness undermines structural integrity of wall elements, reduces thermal insulation property of building of building materials as well as affects the comfort not the occupants. Dampness causes damages to both structural and building materials and reconstruction efforts can be enormous. This study aimed at investigating the causes of dampness in the walls of some of residential buildings within Jos metropolis, Plateau State, Nigeria. The causes were diagnosed through tests, physical inspections and oral interviews. Oral interviews were held with the occupants of 500 randomly selected buildings in the study area. Fifty construction sites were also randomly selected for detailed study of the constructional practices and material adopted in building constructions within the study area. Results identified that about 80% of the houses investigated had damping defects at various degrees. The results also showed that rising damp through defective damp-proof membranes and efflorescence on walling unit serve as the major causes of dampness in residential building walls. Appropriate recommendations were made as preventive and remedial measures to the problem.

WETLANDS

RESTORATION OF A TROPICAL WETLAND THROUGH LOW-COST TECHNOLOGY

Shadananan Nair

(Nansen Environmental Research Centre – India, Kochi, Kerala, India)

Thought the wetlands play a crucial role in maintaining food and water securities and providing rural employment, environmental degradation pose a serious threat to many of them in the developing world, inviting serious shortage of reliable water and health issues. However, water quality in many of them could be improved using low-cost, environment friendly and locally available technologies, if there is proper awareness and support from local people and local administration. Present study is an example of such a success story in a tropical wetland region (eastern Kuttanad) in central Kerala in south India. Thousands of people living in the region depended on the wetland for sanitary purposes, irrigation, transportation, fishing and duck farming. Open domestic wells in the area once provided freshwater for domestic use, except during non-rainy months because of salinity intrusion from the backwater area. But, in recent decades, the region became so polluted that people have to either travel for more than a Kilometre to fetch water or to pay for it for home delivery, in a region that receives more than three times global mean rainfall. Public water supply is unreliable and the quality is poor. The wetland is highly polluted from the direct outflow of domestic waste, effluent from the local industries, outflow of contaminated water from rice fields, bathing of cattle, washing of vehicles etc. Amount of dissolved oxygen became so low that organisms such as fish and frog disappeared from most of the region. These wetlands have become inhospitable to several species of migratory birds and fish. Vectors grew and spread fast in the water, inviting serious health issues. Diseases like Chikun Guinea, Japan Encephalitis, Dengue Fever, Diarrhoea and jaundice became common. People still abstract the same water for non-cooking purpose, as there are no other alternatives. Skin diseases affect those who directly use the water for bathing. Failure in the major project in the region to control flooding and salinity intrusion in rice fields worsened the water quality, as natural flushing was obstructed. Major reason for the deterioration of water quality now is the stagnation of water. Analysis of water sample from the sixteen selected locations showed that quality is much below safety limits and serious health hazards could be expected at any time. However, experiments in the test plots in the canals joining the region with local technology using locally available material like charcoal and lime shell, and locally made cheap aerators prove that condition can be made better without much financial expenditure. Deepening and cleaning of the canals and planting of local herbs for shore protection made a lot of changes. Awareness programmes attracted local population and many of the safety information provided were new to them. This has helped to change their way of life and they show care in disposing solid material into the wetland. If the method adopted in the test plot is extended to the entire area, life in the surroundings can be brought back to earlier conditions. There should be a system for liquid waste treatment and a proper drainage system and collection facility for solid waste. Rooftop water harvesting can solve the shortage of reliable water, as the rainfall in the area is more than 300cm. This is to be done with the assistance from the local government. But, there are new challenges like industrial development associated with economic expansion, rapid rise in population, encroachment into wetlands for real estate business etc that in turn may deteriorate the wetland environment. Climate change may affect the runoff in rivers joining the wetland that may affect the water quality and water level. The proposed scheme of water diversion under national river linking project also may reduce the runoff into the wetland. Proper awareness to the public and students on the environmental issues as part of an adaptation strategy is required to overcome the crisis.

**SPATIAL DISTRIBUTION OF WETLAND VEGETATION AND ITS ECOLOGICAL
FUNCTION ON RIPARIAN ZONE OF RIVERSCAPE**

Lixin Wang

(Inner Mongolia University, Hohhot, Inner Mongolia, China)

Riparian zone is the interface or ecological ecotone between river system and adjacent terrace terrestrial ecosystems, which is an important part of the riverscape, while wetland plants and their communities on riparian zone play essential roles in maintaining ecological functions and values. The focus on riparian zone will associate Riverscape Ecology which is one of hot area of current ecological research with Wetland Ecology. Selected the riparian zones of the typical inland rivers - Wulagai River and the Xilin River in the grasslands of Inner Mongolia, China as the main object of study, with the survey of wetland plant biodiversity and plant communities, the measure of the physical and chemical characterizations of soil, the analysis of micro-topography of riparian zones, and the mapping of riparian vegetations, the formation and maintenance mechanism for the spatial distribution pattern of riparian vegetations at different scales was illustrated. In addition, based on a comparative study between the enclosed conservation plots and grazing degradation plots, the degradation characterization of wetland on riparian zone by the human disturbances was also analyzed.

On the watershed scale, the wetland vegetation on riparian zone along the longitudinal direction presents wooded swamp, shrub swamp, wet meadow, herbaceous swamp and herbaceous saline meadow, from the river source to the end of river, which is forming the spatial distribution pattern named riparian sourceward banded zonation. The Elevation, Temperature (annual mean temperature, insolation duration) and moisture (annual precipitation) are the main environmental factors affecting the formation and maintenance of this pattern. On the river reaches scale, along the lateral direction vegetation presents aquatic plant communities, shoreline pioneer plant clusters, wet meadow communities and saline meadow communities, from river water column to terrace, which is forming the spatial distribution pattern named riparian shoreward banded zonation. The Micro-topography, spatial heterogeneity of physical and chemical characteristics of soil, the biological adaptation and inter-specific competition of wetland plants determine this pattern together.

Selectivity feed on plants and grazing trampling of livestock makes the change of dominant species in the wetland communities, the reduction of spatial heterogeneity, and also the gradually transition of the hygrophyte to the xerophytic on riparian zone. The grazing on riparian zone also leads to significantly reduction of the aboveground and belowground biomass. The obvious phenomenon of "miniaturization" occurred in the wetland plants because of grazing, that to say, the plant height, inter-node length and leaf length growing shorter. The results can provide a theoretical basis for the rational development, protection and management of wetland in the grassland of Northern China.

IMPACT OF URBAN SPRAWLING ON EAST KOLKATA WETLAND AND ON THE ECOSYSTEM FUNCTIONING OF SUNDARBANS MANGROVE ECOSYSTEM, INDIA

Susanta Kumar Chakraborty and Poulami Sanyal

(Department of Zoology, Vidyasagar University, Midnapore (West)-721102, West Bengal, India)

Nandan Bhattacharyya

(UGC Academic Staff College, Jadavpur University (Salt Lake Campus), Kolkata –700098)

Ratnadip Roy and Sumana Bandhopadhyay

(Department of Geography, University of Calcutta, 35, BC. Road, Kolkata-700019)

Kolkata, the largest metropolis of India represents a vivid example of unplanned and uncontrolled type of urbanisation which is marked by severe overcrowding, illegal settlements, loss of biodiversity, destruction of wetlands, poor drainage and pollution of water regime. Eastern side of Kolkata, once dominated by marshes, tidal creeks, mangrove swamps and wetlands had been modified substantially by the colonial power and later on by the uncontrolled forces of urbanization.

East Kolkata wetland is a unique ecosystem that sustains world's largest natural water recycling model and is being considered as the oldest practice of integrated bio-resource management model. The unplanned and uncontrolled mode of urbanisation in and around Kolkata metropolitan has posed severe threats to this very sensitive, vulnerable and biologically productive wetland, the area of which has been reduced drastically (more than 60%) during last few decades as revealed by the analysis of remote sensing satellite imageries. Such analytical tools have also been used side by side ground truth monitoring to delineate the types of wetlands along with their water quality parameters.

Sundarbans Biosphere Reserve of India, being a largest mangrove blocks of the world, is located within 30-40 km away from this wetland area and was once connected with each other through a number of rivulets, creeks and tidal channels. All these aquatic networks have been filled up and blocked because of natural siltation and other anthropogenic activities, leading to the reduction of freshwater drainage and thereby salinity invasion to Sundarbans mangrove estuarine complex.

In this context, the present paper has attempted to discuss urban sprawling and its the impact on the biodiversity and ecology of East Kolkata wetland (a Ramsar site) and thereby to Sundarbans mangrove estuarine complex (a World's Heritage site) in order to suggest the strategies for the conservation of biodiversity and mitigation on environmental perturbation.

BEHAVIOR OF ANTIBIOTICS WITH CORRESPONDING RESISTANCE GENES IN MICROBIAL FUEL CELL WETLAND

Shuai Zhang and Hailiang Song
(Southeast University, Nanjing, Jiangsu, China)

ABSTRACT: Pollution by antibiotics and antibiotic resistance genes (ARGs) has become a major health concern. A microbial fuel cell wetland (CW-MFC) is a new installation to simultaneously treat the wastewater and produce energy. The objective of this study was to access the removal efficiency of tetracycline (TC) and sulfamethoxazole (SMX) and development of TC and SMX resistance genes (*sull*, *sullII*, *sullIII*, *tetA*, *tetC*, *tetO* and *tetW*) in the CW-MFCs. At the same time, electricity was produced during the co-metabolism of antibiotics and glucose. The results indicated that CW-MFCs could significantly reduce the concentration of TC and SMX in wastewater, and the removal efficiency were in the range of 92.3-94.6% and 95.0-97.5%, respectively. The removal efficiency of SMX was significantly higher than that of TC ($p < 0.05$). The satisfactory chemical oxygen demand (COD) removal rates were also obtained. The highest power density was 0.0578 W/m² under the external resistance of 1000 Ω . The relative abundances of target ARGs showed obvious increases compared to the initial levels in the soils ($p < 0.05$).

Key words: Microbial Fuel Cell Wetland; tetracycline; sulfamethoxazole; antibiotic resistance genes

INTRODUCTION

Antibiotics are commonly served as medicine in the treatment of human and animal diseases¹. China leads the world in antibiotic production capacity, approximately 210,000 t of antibiotics manufactured annually, of which 85% is utilized in animal agriculture and medicine². However, majority of applied antibiotics taken by humans and livestock cannot be completely metabolized and are discharged directly into the environment with feces and urine^{3,4}. Excreted antibiotics can then enter river environments through a variety of pathways, including point discharges from wastewater treatment plants (WWTPs), animal feeding operations (AFOs), and fish hatcheries or via nonpoint sources⁵. It is well known that even low concentrations of antibiotics give rise to a significant risk to environmental security and human health⁶. Overuse and misuse of antibiotics pose the occurrence and spread of antibiotic resistant bacteria (ARB) and resistance genes (ARGs), which raises a major health concern. In addition, antibiotics promotes ARGs transfer between nonpathogenic and pathogenic bacteria by vertical gene transfer (VGT) and horizontal gene transfer (HGT)^{3,4,7}. Therefore, Antibiotics, ARB and ARGs are regarded as the three worldwide public health problems by the World Health Organization^{3,8}. Tail water of WWTPs, aquaculture wastewater and agricultural non-point source pollution are the major important sources of pollution to spread ARB and ARG to environment.

A microbial fuel cell wetland (CW-MFC) system is a new device that embeds the MFC into the constructed wetland (CW) to treat the wastewater and produce bio electricity. The first CW-MFC technology was developed via placing the electrodes in the stratified aerobic and anaerobic conditions of the CW⁹. Research suggested that wetland plants can promote the cathode performance of MFCs¹⁰. In addition, CW-MFC was easier to build and operate than traditional MFCs^{11,12}.

Fang et al. (2013) developed a CW-MFC system and obtained high decolorization rate of azo dye while producing a voltage output of 610 mV¹³. Zhao et al. (2013) achieved a power density of 9.4 mW/m² while treating wastewater by using CW-MFCs. Liu et al. (2013) developed a CW-MFC to convert solar energy into electricity by utilizing root exudates of *Ipomoea aquatica*¹⁴. Fang et al (2015) tested CW-MFCs for azo dye removal efficiency and power density¹⁵. Doherty et al. (2015) explored the effects of electrode spacing and flow direction of wastewater in CW-MFCs for investigating the potential to integrate microbial

fuel cells (MFCs) into constructed wetlands (CWs) for simultaneously power generation and wastewater treatment¹⁶.

However, these published works mostly focused on dye and nutrient in municipal and domestic wastewater, the potential and risks of this CW-MFC technology application on the removal of trace antibiotics from domestic sewage received less concern. There are several questions needed to be further clarified. For example, will the CW-MFC have high effective removal of antibiotics during the treatment process? The removal mechanism of antibiotics remains less clear. The influences of antibiotics on nutrients removal and the fate of ARGs in the CW-MFC need to be understood.

In this study, we proposed CW-MFCs to treat domestic sewage containing tetracycline (TC) and sulfamethoxazole (SMX) for eight months. LC-MS was used to determine the concentrations of TC and SMX in the water. The removal efficiencies of CW-MFCs on chemical oxygen demand (COD) were also monitored. In addition, tetracycline resistance genes (*tet* genes) and sulfonamides resistance (*sul*) genes in media and water samples were quantified by real time PCR. Five *tet* genes (*tetA*, *tetC*, *tetO*, *tetQ* and *tetW*) were chosen as representatives of three tetracycline resistance mechanisms because of their frequent occurrence in livestock manure and wastewater treatment lagoon^{3, 4, 17-19}. Three *sul* genes (*sulI*, *sulII*, *sulIII*) were chosen as representatives of sulfonamides resistance mechanisms for their frequent report^{17, 19-21}.

The main objectives of this work were: (1) to study the removal efficiencies of CW-MFC on TC, SMX and COD from the domestic sewage; (2) to discuss the possible removal mechanism of TC, SMX and ARGs; (3) to assess the risks based on TC and SMX accumulation in media and its effect on electricity production and ARGs development.

MATERIALS AND METHODS

Experimental Design of CW-MFCs. The CW-MFC constituted by polyacrylic plastic chamber (the internal diameter is 20 cm and the height is 55 cm) containing four layers from the top to the bottom (Fig. 1). The cathode (3 cm high) the anode (8 cm high) and of the CW-MFC were made by stainless steel mesh and activated carbon. The middle layer (28 cm high) and the bottom layer (17 cm high) were filled with soil and gravel (mass ratio of soil/gravel =1:1). Activated carbon (GAC) has been widely used as CW-MFC electrode material for its efficient electrical conductivity. Stainless steel mesh to strengthen the electron transfer was buried into the electrodes. The same *Oenanthe javanica* was transplanted into each cathode layer. The sampling ports were arranged to collect samples at an interval of 10 cm throughout the installation. The anode and cathode were externally connected by a titanium wire (diameter of 1.5 mm) of 1000 Ω resistance¹⁵.

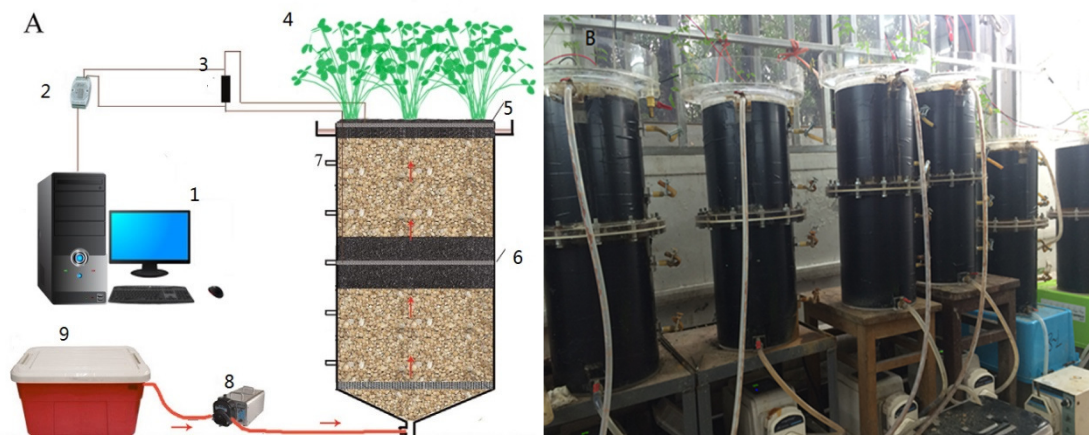


Figure 1. The structure of the CW-MFC (A: 1 computer; 2 data acquisition module; 3 resistance; 4 *Oenanthe javanica*; 5 cathode; 6 anode; 7 sampling points; 8 peristaltic pump; 9 tank, B :The photograph of CW-MFC).

Inoculation and Operation of CW-MFCs. The anaerobic sludge (MLSS: 60 g/L) from the South City Municipal Wastewater Treatment Plant of Nanjing, China. The nutrient solution contained glucose (0.225 g/L), KH₂PO₄ (0.004 g/L), NH₄Cl (0.020 g/L), NaCl (0.15g/L) and 0.20mL trace essential elements solution(contained per liter: 15 g MgSO₄•7H₂O, 2.2 g MnSO₄•H₂O, 5 mg ZnCl₂, 2 g ZnSO₄•7H₂O, 15 g CaCl₂, 1 g FeSO₄, 0.24 g CoCl₂•6H₂O, 10 mg FeCl₃•6H₂O, 2 mg NiCl₂•6H₂O, 0.4 mg Na₂MoO₄•2H₂O and 1 mg CuCl₂•2H₂O,) ²².

After the inoculations were completed, the nutrient solution was fed continuously into the CW-MFCs using peristaltic pumps (BT100-1L, Baoding Longer Precision Pump Co., Ltd., China). The concentrations of TC and SMX in the CW-MFCs (CW-MFC1, CW-MFC2 and CW-MFC3) were 200, 500 and 800 µg/L respectively. The hydraulic retention time was 20h. The whole experiments were took place in the dark at 28±2°C. The experiment had been conducted for eight months from Apr 2015 to Nov 2015. All the cycles were repeated 3 times and error bars were used to represent standard errors of each parallel experiment.

Quantification of Antibiotics and COD Removal. Effluents were collected triple at three sampling periods, Jul 2015, Sep 2015. The antibiotics in the effluents and GAC were detected by LC-MS system (LCQAD-60000, Thermo Fisher Scientific, Waltham, MA, USA). Water samples were filtered through 0.45-µm fiber filters, and extracted using Oasis HLB (6 mL, Waters, USA) extraction cartridges (Huang et al., 2013). Antibiotics analysis in the samples was based on the published method ^{4, 5, 19, 23}. The concentrations of antibiotics were based on external calibration curves, and the correlation coefficients (R²) exceeded 0.996. Concentrations of chemical oxygen demands (COD) in the effluents were measured according to American standard methods (APHA method 5220).

DNA Extraction and ARGs Analysis. Soil of anode, middle layer and cathode were collected triple at Jun 2015. Genomic DNA was extracted by using Power Soil DNA isolation kit (MoBio, Carlsbad, CA, USA) according to the manufacturer's instructions. DNA concentration and quality were examined by UV-9100 spectrophotometer (Lab Tech Ltd, Beijing, China) and gel electrophoresis. Eight tet genes (*tetA*, *tetC*, *tetO*, *tetQ*, *tetW*, *sulII*, *sulIII* and *sulIII*) were quantified using CFX Connect Real-Time PCR System (Bio-Rad, Shanghai, China) and SYBR Green qPCR mix (Bio-Rad, Shanghai, China). Primer sequences targeting these genes and PCR protocol were based on the previous methods ^{4, 17, 19, 24}. Each reaction was conducted in 25 µL on 0.1ml qPCR strip tubes kit(Thermo Fisher Scientific, Taiwan) containing 12 µL SYBR Green qPCR Mix (Bio-Rad, Shanghai, China), Primiers (forward and reverse primers, 0.6 µL each (10 µM)), 0.8 µL DNA templates and 11 µL ddH₂O¹⁹. All PCR reactions were conducted in triplicate. Plasmids carrying with target ARGs were created (Sangon Biotech, Shanghai, China) to make standard curves, and correlation coefficients (R²) were higher than 0.990.

Instrumentation and Analyses. A data acquisition module (DAM-3057, Art Technology Co. Ltd., China) were used to monitor the voltage (V) data. The volumetric power density (P_v, W/m²) is measured by the effective volume of the anode chamber (m²) for the electrons used to power generation was generated in anode¹⁵.

The bioelectricity production of CW-MFC was estimated by the power density curve and polarization curve. A variable resistor with a range of 5 Ω to 50,000 Ω was employed in this study to evaluate the power density and polarization curve. The polarization curve was judged by the current of different external circuit resistance and the electrode potential. The internal resistance (R_i) was measured by the linear region of the polarization curve.

Statistical Analysis. The averages and standard deviations of all data were calculated by Microsoft Excel 2010. Statistical analyses were carried out using SPSS Version 19.0. Analysis of variance and the Student–Newman–Keuls test (p< 0.05) were used to compare treatment means.

RESULTS AND DISCUSSION

Effect of Antibiotics on COD Removal. Table. 1 shows the average COD removal efficiencies of the study period in CW-MFCs. Their cathode COD removal rates were 98.8%, 98.9±2.8% and 97.9% under the different influent conditions where antibiotics were both 400, 1000 and 1600µg/L in CW-MFCs respectively. Their anode COD removal efficiencies were 39.7%, 34.1% and 28.1 under different concentrains of TC and SMX respectively. The COD elimination rate tread for CW-MFCs were cathode > Middle layer > anode. The CW-MFCs remained stable at high level of COD removal efficiencies (97.9-98.9%) under the stress of TC and SMX in this study, for it involving adsorption, water electrolysis, microbial degradation and electro oxidation processes ^{25, 26}. The COD removal efficiencies were not inhibited by high concentrations of antibiotics (1600µg/L) in CW-MFCs.

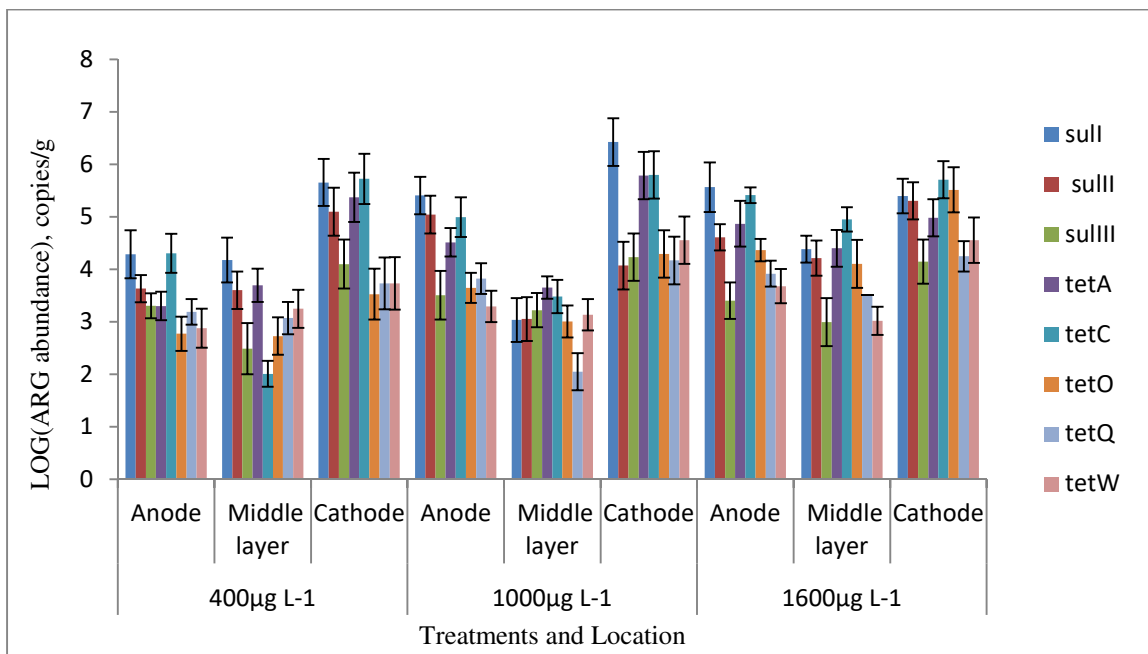


Figure 2. Log 10 the absolute abundances of *tet* and *sul* genes in CW-MFCs

Table 1. Effects of antibiotics (TC and SMX were 200, 500 and 800µg/L respectively) on COD removal in CW-MFCs

Concentrations of antibiotics (µ g/ L)	COD removal rate (%)		
	Anode	Middle layer	Cathode
400	39.7±6.3	78.1±6.2	98.8±3.2
1000	34.1±5.4	73.9±3.2	98.9±2.8
1600	28.1±5.41	61.7±2.6	97.9±4.9

Removal Efficiencies of TC and SMX in CW-MFCs. The target antibiotics concentrations in the influent and effluent of three CW-MFCs are shown in Table. 2. During an operation period of more than eight months, the average effluent concentrations were 14.01, 30.8 and 54.4µg/L for TC, 8.3, 15.0 and 32.4 µg/L for SMX where antibiotics were both 400, 1000 and 1600µg/L in CW-MFCs respectively. The effluent concentrations of TC were notably higher than that of SMX in all CW-MFCs. In terms of mass removal rate (Table. 2), the average mass removal efficiencies were 93.0, 93.9 and 93.2% for TC, and 95.9, 97.0

and 95.4% for SMX, respectively. Similar to the target antibiotics content in effluent, SMX showed better removal efficiency in all CW-MFCs compared to TC. However, comparisons of removal efficiencies of TC and SMX were not considered of statistically significant differences ($P < 0.05$) at different influent concentrations of antibiotics in the three CW-MFCs. CW-MFCs offered the high removal efficiencies for both TC and SMX. Among various types of CWs are most frequently used for pharmaceutical removal⁴. Previous studies demonstrated that CWs were excellent for antibiotics removal^{4, 17, 27}. When using microcosm VSSF-CWs to treat pig farm wastewater containing 100 mg/L of TC, removal efficiencies of 94% was achieved²⁸. So far there are few reports of CW-MFCs application on the removal of antibiotics and ARGs from wastewater. In this study, the proposed CW-MFCs obtained comparable antibiotics removal efficiencies, even though there were higher antibiotics concentrations (1600 $\mu\text{g/L}$) in the influent of CW-MFC3. It is difficult to clarify which pathway contributes to TC and SMX decomposition mostly in such complicated systems. However, in this experiment, organics in the wastewater are used as a renewable resource to feed electrogenic bacteria, and electric energy was produced¹⁵. In addition, the instruments were in total darkness during this period. A series of biological and physicochemical processes, including substrate absorption, microbial degradation, plant uptake, hydrolysis and electric, may involve in antibiotics removal in CW-MFCs^{4, 29, 30}.

Table 2. Concentrations of antibiotics (TC and SMX were 200, 500 and 800 $\mu\text{g/L}$ respectively) in the effluent water of CW-MFCs (mean \pm SD, n=3)

Concentrations antibiotics in influent($\mu\text{g/L}$)	Jul.2015				Sep.2015			
	Concentrations of effluent($\mu\text{g/L}$)		Removal (%)		Concentrations of effluent($\mu\text{g/L}$)		Removal (%)	
	TC	SMX	TC	SMX	TC	SMX	SMX	TC
400	12.63 \pm 2.43	7.2 \pm 1.2	93.7	96.4	15.4 \pm 1.5	94 \pm 0.8	92.3	95.3
1000	27.1 \pm 4.81	12.5 \pm 2.7	94.6	97.5	34.5 \pm 5.5	17.5 \pm 2.9	93.1	96.5
1600	49.6 \pm 6.6	27.2 \pm 3.8	93.8	96.6	59.2 \pm 6.8	37.6 \pm 3.2	92.6	95.0

Typical *tet* and *sul* Genes in Soil Sample. In order to estimate the fate of ARGs in CW-MFCs, we analyzed the total absolute abundances of five *tet* and three *sul* genes in the soil of anode layer, middle layer and cathode layer on day 45 (Fig. 2). All five *tet* and three *sul* genes were detected in soil, and the absolute abundances of the genes with their log units ranged from 0 to 6.42. Previous studies have reported similar absolute abundances of *tet* and *sul* genes in CWs^{4, 17}. Under the conditions of 1000 $\mu\text{g/L}$ and 1600 $\mu\text{g/L}$ antibiotics, the absolute abundances of *tet* and *sul* genes, except for *sulIII* ($p < 0.05$), in anode layer were significantly higher than those under the condition of 400 $\mu\text{g/L}$ antibiotics. It is noteworthy to agree with previous observation that the higher influent TCs concentration in CWs was selected for more copy numbers of *tet* genes in the effluent⁴. The absolute abundances of *tet* and *sul* genes in cathode layer were no significant difference compared with the different influent concentrations of TC and SMX. The absolute abundances of *tet* and *sul* genes are not influenced by different influent concentrations of antibiotic, which is accounted for the obtained comparable antibiotics removal efficiencies (Table. 2). The absolute abundances of *tet* and *sul* genes trend for CW-MFCs were cathode layer \geq anode layer > Middle layer. The high absolute abundances of ARGs in surface soils can also be attributed to its widely-distributed host bacteria³¹.

Effects of Antibiotics on Electricity Production. To explore the performance of MFC under three different concentrations of antibiotics, testing of current densities around 400 hours were performed. Power densities of the 400 and 1000 $\mu\text{g/L}$ almost constantly remained at 30 mA/m^2 . Although the distinctions among three installations were not remarkable, the 1600 $\mu\text{g/L}$ antibiotics illustrated comparative lower values, which was around 25 mA/m^2 . With identical external resistance and electrode area, current densities

substantially reflected the voltage evolutions. Voltage, determining the performance in thermodynamics, was produced by the redox reaction in air-cathode and microbial catalysis in anode^{32, 33}. The increase of antibiotic from 400 to 1000 $\mu\text{g/L}$ did not bring a drop of current density or voltage, which arose from a resistant of microbial to antibiotic. Comparing with lower concentration, the 1600 $\mu\text{g/L}$ antibiotic in the installations impedes the biological activity by antibiotics. Further study was conducted to identify the performance on power output.

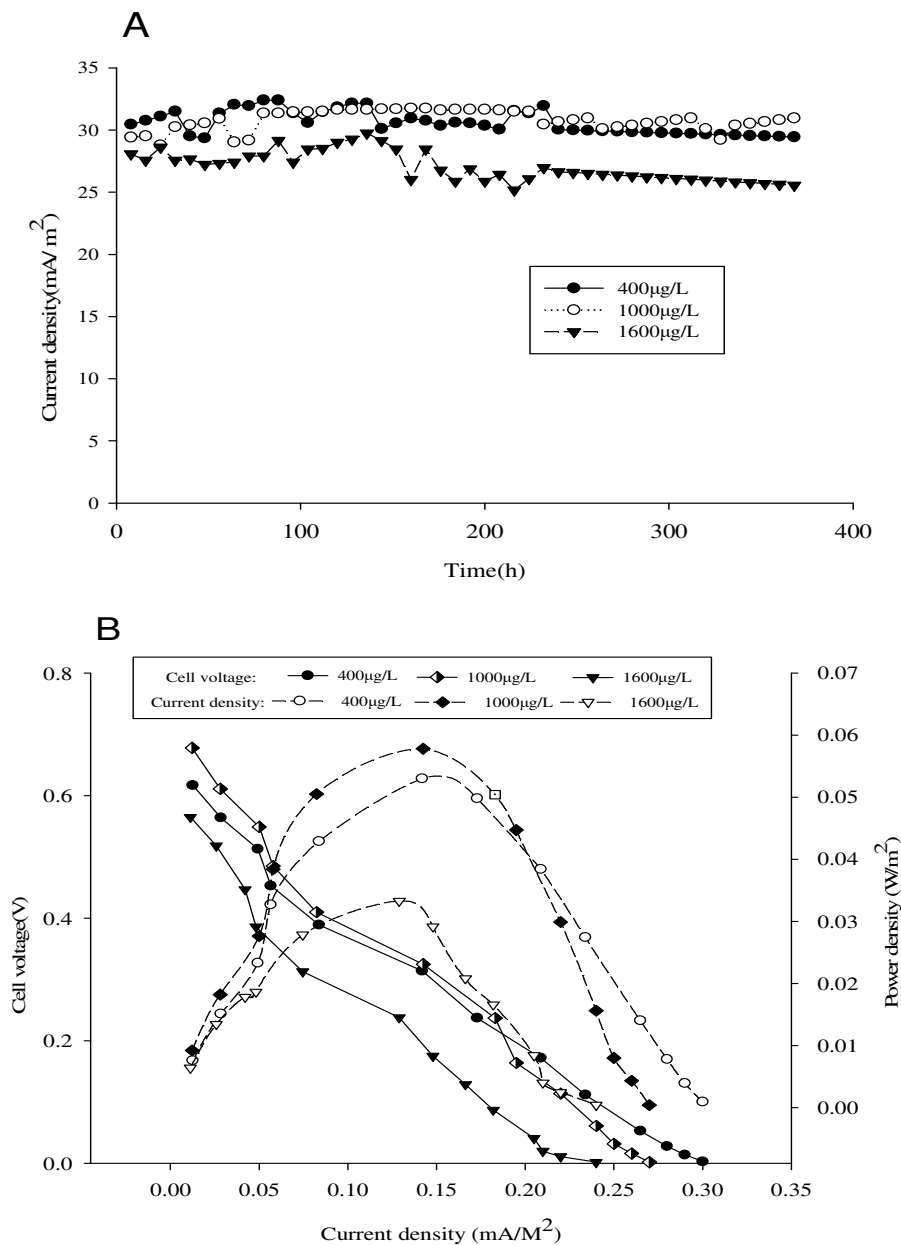


Figure 3 (A, B). Electricity research of CW-MFCs under different concentrations of antibiotics (TC and SMX were 200, 500 and 800 $\mu\text{g/L}$ respectively): (A) current density; (B) polarization and power density curves

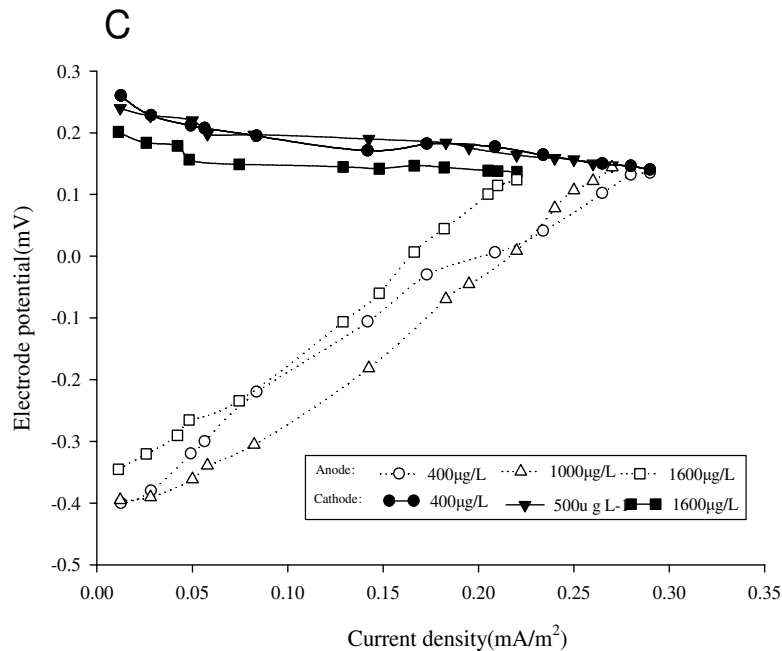


Figure 3 (C). Electricity research of CW-MFCs under different concentrations of antibiotics (TC and SMX were 200, 500 and 800 µg/L respectively): (C) electrode potential

Polarization curves portrayed here visualized the variation in different external resistance. Vertex of cell voltages of the 400 and 1000 µg/L antibiotic (0.62V, 0.68V) was in 0.15 mA /m², however, the 1600 µg/L antibiotics voltage (0.41V) was in 0.13mA/m². An apparent deviation of power density between the 1600 µg/L and Lower concentrations reflected that higher concentration actually brought lower output of power. Notably, three parts namely polarization loss, ohmic loss and diffusion loss in polarization curves almost held analogous slope^{32, 34}, which could be the results of diffusion loss acting as predominant part in this big system³⁵. Furthermore, details about electrode polarization were described below. Anode polarization profiles with identical large slopes were detected by changing their currents in large scope. However, reverse situation happened in all cathodes which maintained voltage at around 0.2V. Performance in all cathodes proved that oxygen reduction reversibility in cathodes was well enough to support big current output. Therefore, the novel structure with huge surface activated carbon and oxygen filling plants in cathodes enhanced the electrochemical reaction³⁶⁻³⁸.

Anodes playing a role as electron output by electric activated bacteria had bad polarization in all installations maybe because of weak electron production capacitance in anaerobic conduction competing with other strains. Small system with intensive electrode potential inducing often owes better performance in anode^{39, 40}.

CONCLUSIONS

This study clearly demonstrated the good performance of CW-MFCs on the wastewater containing TC and SMX based on three aspects: 97.9-98.9% for COD removal efficiencies, 93.7-97.5% for TC and SMX removal efficiencies, 0.0578 W /m² for the highest power density, respectively. Five *tet* and three *sul* genes were detected in soli, and the absolute abundances of the genes with their log units ranged from 0 to 6.42. This study employed gene quantification to study the fate of *tet* and *sul* genes in CW-MFCs. Further study to better understand the fate of potential pathogens caring *tet* and *sul* genes is warranted. It is also needed to investigate the relative abundances of *tet* and *sul* genes in CW-MFCs.

ACKNOWLEDGMENTS

We thank the Provincial Natural Science Foundation of Jiangsu, China (SBK2014020483) for financial support.

REFERENCES

1. Bouki, C.; Venieri, D.; Diamadopoulos, E., Detection and fate of antibiotic resistant bacteria in wastewater treatment plants: A review. *Ecotoxicology and Environmental Safety* **2013**, *91*, 1-9.
2. Luo, Y.; Xu, L.; Rysz, M.; Wang, Y.; Zhang, H.; Alvarez, P. J., Occurrence and transport of tetracycline, sulfonamide, quinolone, and macrolide antibiotics in the Haihe River Basin, China. *Environ Sci Technol* **2011**, *45*, (5), 1827-33.
3. Li, B.; Zhang, X.; Guo, F.; Wu, W.; Zhang, T., Characterization of tetracycline resistant bacterial community in saline activated sludge using batch stress incubation with high-throughput sequencing analysis. *Water Res* **2013**, *47*, (13), 4207-16.
4. Huang, X.; Liu, C.; Li, K.; Su, J.; Zhu, G.; Liu, L., Performance of vertical up-flow constructed wetlands on swine wastewater containing tetracyclines and tet genes. *Water Res* **2015**, *70*, 109-17.
5. Storteboom, H.; Arabi, M.; Davis, J. G.; Crimi, B.; Pruden, A., Identification of antibiotic-resistance-gene molecular signatures suitable as tracers of pristine river, urban, and agricultural sources. *Environ Sci Technol* **2010**, *44*, (6), 1947-53.
6. Kümmerer, K., Antibiotics in the aquatic environment – A review – Part I. *Chemosphere* **2009**, *75*, (4), 417-434.
7. Martinez, J. L., Environmental pollution by antibiotics and by antibiotic resistance determinants. *Environmental pollution* **2009**, *157*, (11), 2893-2902.
8. Davies, J.; Davies, D., Origins and evolution of antibiotic resistance. *Microbiology and molecular biology reviews : MMBR* **2010**, *74*, (3), 417-33.
9. Yadav, A. In *Design and development of novel constructed wetland cum microbial fuel cell for electricity production and wastewater treatment*, Proceedings of 12th International Conference on Wetland Systems for Water Pollution Control (IWA), 2010; 2010.
10. Villaseñor, J.; Capilla, P.; Rodrigo, M. A.; Cañizares, P.; Fernández, F. J., Operation of a horizontal subsurface flow constructed wetland – Microbial fuel cell treating wastewater under different organic loading rates. *Water Res.* **2013**, *47*, (17), 6731-6738.
11. Patil, S. A.; Surakasi, V. P.; Koul, S.; Ijmulwar, S.; Vivek, A.; Shouche, Y. S.; Kapadnis, B. P., Electricity generation using chocolate industry wastewater and its treatment in activated sludge based microbial fuel cell and analysis of developed microbial community in the anode chamber. *Bioresour Technol* **2009**, *100*, (21), 5132-9.
12. Higgins, S. R.; Lau, C.; Atanassov, P.; Minter, S. D.; Cooney, M. J., Hybrid Biofuel Cell: Microbial Fuel Cell with an Enzymatic Air-Breathing Cathode. *ACS Catalysis* **2011**, *1*, (9), 994-997.
13. Fang, Z.; Song, H. L.; Cang, N.; Li, X. N., Performance of microbial fuel cell coupled constructed wetland system for decolorization of azo dye and bioelectricity generation. *Bioresour. Technol.* **2013**, *144*, 165-171.
14. Liu, S. T.; Song, H. L.; Wei, S. Z.; Yang, F.; Li, X. N., Bio-cathode materials evaluation and configuration optimization for power output of vertical subsurface flow constructed wetland - Microbial fuel cell systems. *Bioresour. Technol.* **2014**, *166*, 575-583.
15. Fang, Z.; Song, H. L.; Cang, N.; Li, X. N., Electricity production from Azo dye wastewater using a microbial fuel cell coupled constructed wetland operating under different operating conditions. *Biosens. Bioelectron.* **2015**, *68*, 135-141.
16. Doherty, L.; Zhao, Y. Q.; Zhao, X. H.; Wang, W. K., Nutrient and organics removal from swine slurry with simultaneous electricity generation in an alum sludge-based constructed wetland Incorporating microbial fuel cell technology. *Chem. Eng. J.* **2015**, *266*, 74-81.

17. Liu, L.; Liu, Y. H.; Wang, Z.; Liu, C. X.; Huang, X.; Zhu, G. F., Behavior of tetracycline and sulfamethazine with corresponding resistance genes from swine wastewater in pilot-scale constructed wetlands. *J Hazard Mater* **2014**, *278*, 304-10.
18. Barkovskii, A. L.; Bridges, C., Persistence and Profiles of Tetracycline Resistance Genes in Swine Farms and Impact of Operational Practices on Their Occurrence in Farms' Vicinities. *Water, Air, & Soil Pollution* **2011**, *223*, (1), 49-62.
19. Wu, D.; Huang, Z. T.; Yang, K.; Graham, D.; Xie, B., Relationships between Antibiotics and Antibiotic Resistance Gene Levels in Municipal Solid Waste Leachates in Shanghai, China. *Environ. Sci. Technol.* **2015**, *49*, (7), 4122-4128.
20. Naquin, A.; Shrestha, A.; Sherpa, M.; Nathaniel, R.; Boopathy, R., Presence of antibiotic resistance genes in a sewage treatment plant in Thibodaux, Louisiana, USA. *Bioresour. Technol.* **2015**, *188*, 79-83.
21. Dan, A.; Yang, Y.; Dai, Y. N.; Chen, C. X.; Wang, S. Y.; Tao, R., Removal and factors influencing removal of sulfonamides and trimethoprim from domestic sewage in constructed wetlands. *Bioresour Technol* **2013**, *146*, 363-70.
22. Cao, X.; Song, H. L.; Yu, C. Y.; Li, X. N., Simultaneous degradation of toxic refractory organic pesticide and bioelectricity generation using a soil microbial fuel cell. *Bioresour Technol* **2015**, *189*, 87-93.
23. Liu, L.; Liu, C.; Zheng, J.; Huang, X.; Wang, Z.; Liu, Y.; Zhu, G., Elimination of veterinary antibiotics and antibiotic resistance genes from swine wastewater in the vertical flow constructed wetlands. *Chemosphere* **2013**, *91*, (8), 1088-93.
24. Rodriguez-Mozaz, S.; Chamorro, S.; Marti, E.; Huerta, B.; Gros, M.; Sanchez-Melsio, A.; Borrego, C. M.; Barcelo, D.; Balcazar, J. L., Occurrence of antibiotics and antibiotic resistance genes in hospital and urban wastewaters and their impact on the receiving river. *Water Res.* **2015**, *69*, 234-242.
25. Ramamurthy, S. S.; Chen, Y. H.; Kamesh, K. M.; Nageswara, R. G.; Mitra, S.; Chelli, J., COLL 233-Carbon nanotube-zirconium dioxide hybrid for defluoridation of water. *Abstr. Pap. Am. Chem. Soc.* **2009**, *238*, 1.
26. Nageswara Rao, N.; Rohit, M.; Nitin, G.; Parameswaran, P. N.; Astik, J. K., Kinetics of electrooxidation of landfill leachate in a three-dimensional carbon bed electrochemical reactor. *Chemosphere* **2009**, *76*, (9), 1206-12.
27. Zhang, W.; Huang, M. H.; Qi, F. F.; Sun, P. Z.; Van Ginkel, S. W., Effect of trace tetracycline concentrations on the structure of a microbial community and the development of tetracycline resistance genes in sequencing batch reactors. *Bioresour. Technol.* **2013**, *150*, 9-14.
28. Carvalho, P. N.; Araujo, J. L.; Mucha, A. P.; Basto, M. C.; Almeida, C. M., Potential of constructed wetlands microcosms for the removal of veterinary pharmaceuticals from livestock wastewater. *Bioresour Technol* **2013**, *134*, 412-6.
29. Dordio, A. V.; Carvalho, A. J., Organic xenobiotics removal in constructed wetlands, with emphasis on the importance of the support matrix. *J Hazard Mater* **2013**, *252-253*, 272-92.
30. Hijosa-Valsero, M.; Fink, G.; Schlusener, M. P.; Sidrach-Cardona, R.; Martin-Villacorta, J.; Ternes, T.; Becares, E., Removal of antibiotics from urban wastewater by constructed wetland optimization. *Chemosphere* **2011**, *83*, (5), 713-9.
31. Chen, H.; Zhang, M., Effects of advanced treatment systems on the removal of antibiotic resistance genes in wastewater treatment plants from Hangzhou, China. *Environ Sci Technol* **2013**, *47*, (15), 8157-63.
32. Rabaey, K.; Verstraete, W., Microbial fuel cells: novel biotechnology for energy generation. *TRENDS in Biotechnology* **2005**, *23*, (6), 291-298.
33. Liu, H.; Logan, B. E., Electricity generation using an air-cathode single chamber microbial fuel cell in the presence and absence of a proton exchange membrane. *Environmental science & technology* **2004**, *38*, (14), 4040-4046.

34. Rabaey, K., *Bioelectrochemical systems: from extracellular electron transfer to biotechnological application*. IWA publishing: 2010.
35. Feng, Y.; Lee, H.; Wang, X.; Liu, Y.; He, W., Continuous electricity generation by a graphite granule baffled air–cathode microbial fuel cell. *Bioresource technology* **2010**, *101*, (2), 632-638.
36. Fang, Z.; Song, H.-L.; Cang, N.; Li, X.-N., Performance of microbial fuel cell coupled constructed wetland system for decolorization of azo dye and bioelectricity generation. *Bioresource technology* **2013**, *144*, 165-171.
37. Zhao, Y.; Collum, S.; Phelan, M.; Goodbody, T.; Doherty, L.; Hu, Y., Preliminary investigation of constructed wetland incorporating microbial fuel cell: batch and continuous flow trials. *Chemical Engineering Journal* **2013**, *229*, 364-370.
38. Villasenor, J.; Capilla, P.; Rodrigo, M.; Canizares, P.; Fernandez, F., Operation of a horizontal subsurface flow constructed wetland–microbial fuel cell treating wastewater under different organic loading rates. *Water research* **2013**, *47*, (17), 6731-6738.
39. Torres, C. I.; Kato Marcus, A.; Rittmann, B. E., Proton transport inside the biofilm limits electrical current generation by anode-respiring bacteria. *Biotechnology and Bioengineering* **2008**, *100*, (5), 872-881.
40. Torres, C. I.; Marcus, A. K.; Rittmann, B. E., Kinetics of consumption of fermentation products by anode-respiring bacteria. *Applied microbiology and biotechnology* **2007**, *77*, (3), 689-697.

SEDIMENTS

**THE ELBE ESTUARY (GERMANY): RESISTANCE OF THE SEDIMENTS TO
HYDRODYNAMIC FORCES ON MICROSCALE**

Nina Stoppe and Thomas Neugebauer and Rainer Horn
(Kiel University, Kiel, Germany)

Elmar Fuchs and Uwe Schröder and *Carolyn Schmidt-Wygasch*
(Federal Institute of Hydrology, Koblenz, Germany)

The tidal River Elbe, Northern Germany, serves as an important international waterway feeding the port of Hamburg and thus indicates its function as a significant economic lifeline for that region. At the same time the estuarine riverscape holds valuable nature protected by national and European legislation. In the last centuries the estuary has been impacted by manmade alterations, e.g. by ongoing river training measures. Several national and European environmental directives like the Water Framework Directive demand for a new orientation towards renaturalisation of banks and an improved structural diversity.

However, at the moment there are still many loose ends to tie up. One of the main questions is: Which river reaches can be restored without hampering bank stability, flood protection, and navigation? To identify suitable stretches we need a sound understanding on the dynamic interaction between soils and sediments of the riverbank and vegetation development. Tidal hydrodynamics and hydrodynamic stress are of essential importance, especially to depict and estimate the soil resilience against it.

This survey focuses on soil structure and intrinsic particle-to-particle resistance capacity of the riverine sediment-soil complex. Physicochemical properties and classical soil mechanical methods were combined with rheological measurements, a methodological approach not being applied to soils usually. The latter evaluates the microstructure describing the soil's viscoelastic deformation behavior (Integral Z). A significant result is that water content and texture are the most important factors influencing the microstructural stiffness on the particle-to-particle level. This means, that e.g., increasing soil desiccation results in a more advanced stabilization by inter-particulate menisci forces. This effect decreases with coarser grain sizes. To evaluate the interrelated effect of physicochemical properties and microstructural stiffness, statistical analyses were carried out. In this context especially soil organic matter, calcium concentration, and pedogenic iron oxides show a stabilizing response in terms of soil microstructure, and sodium vice versa. Additionally, the multivariate statistics produced so called pedotransfer functions, which allow predicting Integral Z by a specific set of easy-to-get predictor variables in non-investigated soils. This mechanism gives access to interpolate from local point data to non-examined bank areas.

Present results provide an estimation on the relative stability of the River Elbe banks mirrored by values of the rheologic target parameter Integral Z. Potential suitable stretches for bank restoration and thus a near-natural bank development can be identified. To be able to give a more precise and reliable advice to ecological engineering managers in terms of bank restructuring further site related investigations have to be carried out to precisely quantify the soil stability of pristine river banks towards hydrodynamic pressure.

DEVELOPMENT AND EVALUATION OF NEW INDICES FOR SEDIMENT-ASSOCIATED CONTAMINANTS

Nsikak U. Benson^{*}, Adebusayo E. Adedapo, Omowunmi H. Fred-Ahmadu and Akan B. Williams
(Covenant University, Ota, Nigeria)
Abaas A. Olajire
(Ladoke Akintola University of Technology, Ogbomoso, Nigeria)

New indices (modified hazard quotient, *mHQ* and ecological contamination index, ECI) are developed for evaluating sediment-associated heavy metals contamination. In evaluating the proposed indices, the concentration and chemical fractionation of five heavy metals (Cd, Cr, Cu, Ni and Pb) determined in benthic sediments from five tropical ecosystems off the Bight of Bonny were used to assess the degree of contamination and estimate the extent of anthropogenic inputs from industrial activities into these ecosystems. The analysis shows that the mean concentrations (mg/kg, dw) of Cd, Cr, Cu, Ni and Pb vary from 4.33 – 5.67, 11.12 – 28.52, 30.26 – 43.72, 2.02 – 2.60 and 162.0 – 190.37, respectively. An important observation is that the mean metal levels during the wet and dry seasons did not show significant variability at all sites. The spatial distribution and severity of sediment-associated contamination by heavy metals based on the developed indices (*mHQ* and ECI) are in the descending sequence: Cd>Pb>Cu>Cr>Ni. Hence, the observed trend is in good agreement with existing pollution indices. Contamination severity index, mean hazard quotients and modified risk assessment code are also used to identify the pollution hotspots, which reflect medium risk contamination ecological systems. Aquatic pollution indicators (potential contamination index, ECI, hazard quotients, and *mHQ*) reveal significant anthropogenic contamination of Cd and Pb in the sediments, while Cr, Cu and Ni show relatively low degree of contamination. PCI generally follows the sequence Cd>Pb>Cu>Cr>Ni. Principal component analysis (PCA) and factor analysis indicate that heavy metals in the benthic sediments originate mostly from anthropogenic sources.

**GEOCHEMICAL SPECIATION AND RISK ASSESSMENT OF TRACE METALS IN
SEDIMENTS FROM COASTAL ECOSYSTEMS OFF EQUATORIAL ATLANTIC OCEAN**

Nsikak. Benson, Winifred Anake, Akan Williams, Oyeronke Akintokun, Adebunayo Adedapo
(Covenant University, Ogun State, Nigeria)
Essien D. Udosen
(University of Uyo, Akwa Ibom State, Nigeria)
Abaas A. Olajire
(Ladoke Akintola University of Technology, Ogbomosho, Nigeria)

The concentrations of Cd, Cr, Cu, Ni and Pb in estuarine benthic sediments were determined through multistep speciation scheme to evaluate their spatio-temporal distributions, selective fraction magnitude, degree of contamination and potential ecological risks. The results indicated that the metal fractionation percentages in the residual, oxidizable and reducible fractions are the most significant, while the exchangeable and carbonates bound trace metals are relatively low. High mobility and bioavailability was indicated for Cu, Cr and Ni, while Cd and Pb in sediments present low bioavailability for biota. Contamination factor (CF_m), degree of contamination (DC), modified degree of contamination (mCd), geoaccumulation index (I_{geo}), risk assessment code (RAC), and potential ecological risk index (PERI) were used to assess trace metals sedimentary pollution. The results indicate a prevalent moderate to high contamination of most trace metals analyzed. The contamination ranking of trace metals based on percent contribution to DC was Cd>Pb>Cu>Cr>Ni. RAC values indicate medium risk for Cd and Ni at all studied sites during the wet and dry seasons. Cd and Pb show moderate and very high individual metal potential ecological risk, respectively, while multi-elemental potential ecological risk indices (R_{IS}) indicate very high ecological risk in all the ecosystems.

**MILLING CONDITIONS EFFECT ON CONTAMINATED SEDIMENTS TREATMENT BY
POZZOLANIC MATERIALS**

Rabah Hamzaoui, Othman Bouchenafa, Abdelkrim Bennabi, Johan Colin

(Université Paris-Est, Institut de Recherche en Constructibilité, ESTP, 28 avenue du Président Wilson,
94234 Cachan, France)

Mechanosynthesis is one of the methods that allows obtaining a nanocrystalline state. It is an intensive energy process of mechanical grinding for the preparation of alloyed powders or composites in powder form. It involves a repeated fracturing and rewelding of particles, leading to size reduction and particle shape change. Planetary high-energy ball mill is machine, which contain vials mounted on a planar disc. With the rotation of the disc, the vials move in a circular and opposite direction compared to the disc rotation. The raw Materials (solid, liquid or gas with or without adjuvant) are introduced in vials with balls in order to obtain final product after milling [1-2]. In the context of sustainable development, new regulations on recycling of contaminated soil in the construction sector, leading researchers to research new techniques to value these wastes and to reuse them. The technique of solidification / stabilization (SS) can be used for treating soils or sediments contaminated, for transforming into controlled performance and quality materials suitable for further use, such as recycling in construction materials or paving materials. The objective of this research is to propose method of treatment based on the use of pozzolanic materials structurally modified by grinding (zeolites, fly ash,) and can be considered as an alternative to conventional methods of treatment with hydraulic binders.

SURFACE WATER AND SEDIMENT QUALITY ASSESSMENT IN THE GBARAN-UBIE INTEGRATED OIL & GAS PROJECT, NIGER DELTA, NIGERIA

Seiyaboh, E.I. and Gijo, A.H (Niger Delta University, Wilberforce Island, Bayelsa State, Nigeria)
Sikoki, F.D (University of Port Harcourt, Port Harcourt, Rivers State, Nigeria)

Surface water and sediment quality in the Gbaran – Ubie integrated Oil & Gas Project situated in the Niger Delta region of Nigeria was investigated. The physico-chemical characteristics of surface water and sediment samples collected from the project site were analyzed. Samples were collected from three (3) locations around the project site. The results obtained indicated significant differences ($P < 0.05$) between the studied stations. Water samples analyzed were slightly acidic with pH values ranging from 6.63 - 6.78. Conductivity values of 86.87 - 122.60 $\mu\text{h mos cm}^{-1}$, TDS values of 43.20 - 60.00 mg/l, Cl^- values of 28.00 - 62.60 mg/l, TH values of 23.00 – 34.67 mg/l, Ca values of 15.74 – 22.40 mg/l, Mg values of 4.29 – 6.51 mg/l, Na values of 8.64 – 9.67 mg/l, K values of 3.31 – 4.00 mg/l and Fe values of 0.170 – 0.207 mg/l were significantly higher than those recorded in other studies. Sediments in the study area were slightly acidic ranging from 6.65 - 6.85; acidic sediment can have an adverse effect on fisheries distribution and other benthic organisms. NO_3^- values of 2.76 – 3.75 mg/g, PO_4^{3-} values of 12.69 – 18.61 mg/g, TN values 4.53 – 5.39 mg/g, TOC values of 4.35 – 6.65 mg/g, THC values of 4.92 – 5.44 mg/g, Ca values of 5.73 – 5.77 mg/g, Mg values of 6.36 – 7.85 mg/g, Na values of 4.74 – 5.94 mg/g, K values of 4.84 – 5.54 mg/g, Zn values of 4.57 – 6.29 mg/g, Fe values of 1.66 – 1.85 mg/g, Mn values of 2.54 – 2.83 mg/g, Cd values of 1.23 – 1.55mg/g, and Pb values of 0.04 – 0.44 mg/g were significantly higher than those recorded in other studies. These results were indicative of the influence of activities within the Gbaran-Ubie integrated Oil & Gas Project on surface water and sediment quality.

DISTRIBUTION OF ORGANOCHLORINE PESTICIDE RESIDUES IN EPIPELIC AND BENTHIC SEDIMENTS FROM LAGOS LAGOON, NIGERIA

Akan Williams^{1*}, Nsikak Benson¹ and Egbenya Shaibu-Imodagbe²

¹Department of Chemistry, Covenant University, Canaanland, Ota, Ogun State, Nigeria.

²Samaru College of Agriculture, Ahmadu Bello University, Zaria, Nigeria

*akan.williams@covenantuniversity.edu.ng

ABSTRACT: Epipellic and benthic sediment samples were collected from Agboyi Creek, Oworonshoki, Ajara, Ogogoro and Tarkwa Bay in Lagos Lagoon and analyzed for organochlorine pesticide (OCP) residues using a gas chromatograph coupled with electron capture detector (GC-ECD). Sampling was conducted 4 times at the sites during the dry season months of December 2008, February 2009 and the wet season months of May, September 2009 to study the effects of seasonal variation on the samples. Sediment samples were subjected to cold extraction and clean-up. OCP residues were detected in all the samples though the levels did not show any particular pattern between the epipellic and benthic sediment during the dry and wet seasons. Detection limits of the OCPs ranged between 1.43 ng/g and 10.29 ng/g, indicating the sensitivity of the gas chromatograph at the operating conditions. The residue levels were higher in the lagoon than in the creek while a higher concentration of the residues was observed during the dry season due to reduced dilution effect. The mean recoveries of the residues ranged between 90.14 and 98.15% hence validating the methodology used in the study. Levels of OCPs residues in the sediment were within permissible residue limits.

Keywords: Cold extraction, dry season, gas chromatograph, seasonal variation, wet season

INTRODUCTION

Persistent organic pollutants (POPs) are toxic chemicals that persist in the environment and biomagnify in the food chain. Organochlorines such as chlorinated pesticides and polychlorinated biphenyls (PCBs) represent important groups of POPs, which have caused worldwide concern as toxic environmental contaminants (Covacia et al. 2005). Efforts at minimizing and eventually phasing out POPs globally gave rise to the Stockholm Convention in 2001. Residues and metabolites of many POPs are very stable, with long half-lives in the environment (UNEP 2002). The manufacture and use of organochlorine pesticides (OCPs) have been banned or restricted in developed countries. Although these bans and restrictions were enacted during the 1970s and 1980s, some developing countries are still using OCPs for agricultural and public health purposes because of their low cost and versatility in controlling various pests (Xue et al. 2006). Again, they are being used in most developing countries, including Nigeria, due to a lack of appropriate regulatory control and management of the production, trade and use of these chemicals (Darko and Acquah 2007). There is also a paucity of data on the use of pesticides in the country, a reflection of the lack of a mechanism and planning programme in place for chemicals management as well as a low level of understanding of the environmental and public health hazards of pesticide use (Osibanjo et al. 2002).

Pesticides are chemicals used to kill or control pests. They are classified according to their chemical class or intended use. OCPs are basically insecticides composed primarily of carbon, hydrogen and chlorine and are found in the environment as a result of human activities. The use of OCPs takes many forms, ranging from pellet application in field crops to sprays for seed coating and grain storage. OCP residues enter aquatic environments through effluent release, discharges of domestic sewage and industrial wastewater, atmospheric deposition, runoff from agricultural fields, leaching, equipment washing, disposal of empty containers and direct dumping of wastes into the water systems (Yang et al. 2005). Lagoons, seas, rivers

and lakes are depositories of most effluent discharges, leachates and run-offs from activities on land. The distribution of various chlorinated hydrocarbons in the marine and estuarine environment depends on residues of persistent organochlorine pesticide physicochemical properties of the eco-system as well as the partition coefficients of individual chlorinated hydrocarbons (Sarkar et al. 1997). OCPs could distribute among the components of the ecosystem, such as water and sediments. Pesticides can be bio-concentrated through biogeochemical processes and can be scavenged from the water through sorption on to suspended material before they get deposited to the bottom substrate. Different pesticides pose varying degrees and types of risk to water quality.

Sediment is one of the principal reservoirs of environmental pesticides, representing a source from which residues can be released to the atmosphere, groundwater and living organisms (Xue et al. 2006). Sediment serves as a sink from which water and biota are continuously polluted. Thus, the quality of sediment is essential in assessing the pollution status of the ecosystem (Doong et al. 2002). Persistence of these organic pollutants in sediment is possible due to their low solubility and tendency to associate with suspended particulate matter. As a result of their low water solubility, OCPs have a strong affinity for particulate matter. They are hydrophobic compounds that tend to adsorb to suspended particulate matter and benthic sediments in aquatic ecosystems. Indirect exposure to contaminated sediments takes place when fishes feed on benthic invertebrates that are ingesting particulate matter. Direct exposure through the sediment takes place by the release of contaminated particulate matter into the water column by both natural and anthropogenic processes.

The discharge of rivers into lagoons is the main transport pathway of pesticide residues. The Nigerian coastal belt has estuaries and lagoons as a transition zone between it and the numerous rivers and creeks flowing southwards into the Atlantic Ocean. Nigeria has a variety of industrial establishments producing different industrial wastes and effluents. Industrial establishments in Lagos account for over 60% of all industries in Nigeria. The proliferation of urban settlements and slums in Lagos has also led to increased human pressure and the generation of domestic effluents, which eventually find their way into the Lagos Lagoon. The lagoon, therefore, receives a complex mixture of domestic and industrial wastes and has served as the ultimate sink for the disposal of sewage. Some of the symptoms of pesticides poisoning include irritation, dizziness, tremour, tonic and chronic convulsion (Williams et al. 2013).

Organochlorine pesticide pollutant levels are usually monitored in inorganic ecosystem compartments such as water, air and sediment. Monitoring in inorganic compartments has the advantage of producing an immediate, geographically localized measure of contamination. The continuous monitoring of the pollution status of Lagos Lagoon is imperative as it is a major pelagic column in Nigeria. This study was undertaken to determine the organochlorine pesticide residues in epipelagic and benthic sediments from Lagos Lagoon, Lagos, Nigeria.

MATERIALS AND METHODS

Study Area. The study area for this investigation is the Lagos Lagoon, which lies between latitude 6° 24' - 6° 34' N and longitude 3° 23' - 4° 33' E in the western part of Nigeria. The map of the lagoon is shown in Figure 1. The lagoon consists of three main segments namely Lagos Harbour, Metropolitan End and Epe Division. It empties into the Atlantic Ocean via Lagos Harbour and is drained by Ogun, Agboyi, Majidun and Aye Rivers. The lagoon is shallow, with an average depth of about 1.5 m.

Sampling Strategy. Sampling was conducted between December 2008 and September 2009 during the dry and wet seasons to study the effects of seasonal variations on the samples. Field investigations were carried out four times at the designated sites during the dry season months of December 2008 and February 2009 and the wet season months of May and September 2009. The five sampling sites were Agboyi Creek (AGR), Oworonshoki (OWS), Ajara (AJR), Ogogoro (OGG) and Tarkwa Bay (TBY). The Agboyi Creek is one of the water bodies that drain the Lagos Lagoon and was used as the control site in this study. At Agboyi Creek, samples were collected at the zone where it empties into the lagoon while at Tarkwa Bay

sampling was carried out where the lagoon discharges into the Atlantic Ocean. Sampling locations were identified with a hand-held Garmin-GPSMAP 76S-type global positioning system.

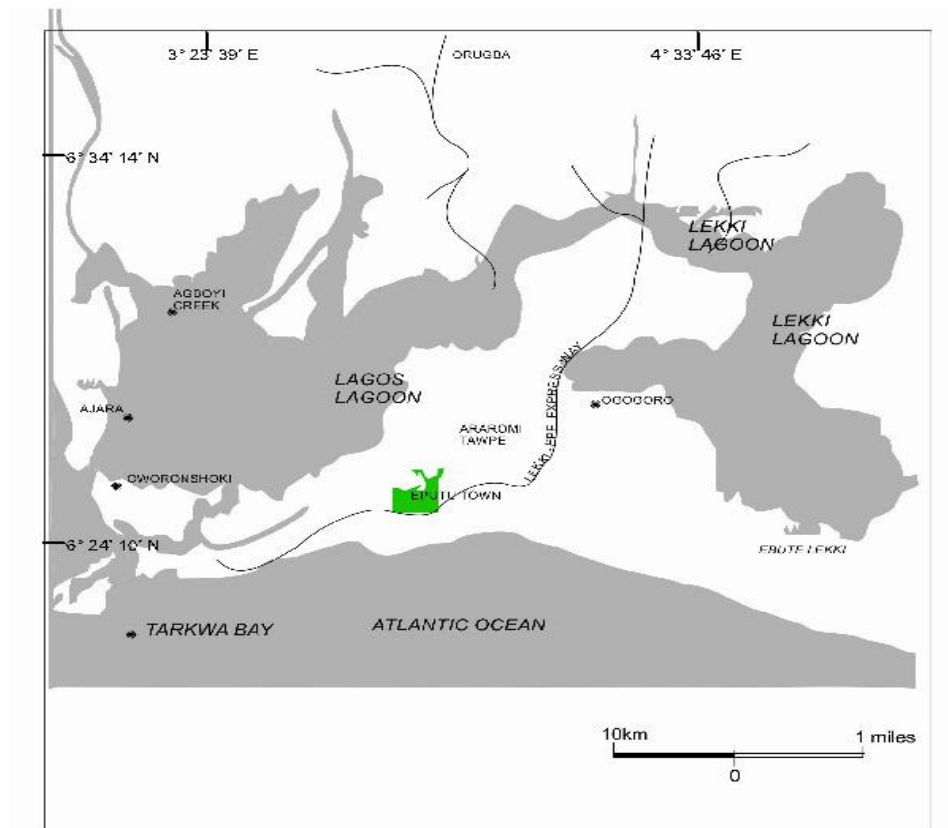


Figure 1. Map of Lagos Lagoon showing the sampling points
Source: Author's field survey (<http://maps.google.ca/maps>)

Collection of Sediment Samples. Epipellic (intertidal) sediments were obtained by using a short core sampler to scoop the top 1 to 5 cm of the sediments at five sites with the following coordinates: Agboyi Creek (31 N 0545069, UTM 0727598), Oworonshoki (31 N 0545159, UTM 0725638), Ajara (31 N 0545136, UTM 0727884), Oogogoro (31 N 0543288, UTM 0710820) and Tarkwa Bay (31 N 0543893, UTM 0707630). Benthic (subtidal) sediment samples were obtained at Agboyi Creek (31 N 0545254, UTM 0726974), Oworonshoki (31 N 05450361, UTM 0725474), Ajara (31 N 0545098, UTM 0727826), Oogogoro (31 N 0543330, UTM 0710845) and Tarkwa Bay (31 N 0543889, UTM 0707582) with the aid of a Shipek grab sampler. Benthic sediments were collected by lowering the grab sampler into the water bed and raising it aboard after a few minutes. Three grab sediment samples were collected at each site and mixed together to form composite samples and subsequently wrapped in labelled aluminium foil. A total of twenty epipellic and twenty benthic composite sediments were collected for OCPs determination. After collection, the sediment samples were stored in ice-packed coolers to preserve the integrity of the samples. Sediment samples were refrigerated in the laboratory at 4 °C to inactivate microbes. Pebbles, shells and vegetable matter were manually removed.

Evaluation of Sediment Particle Sizes. The hydrometer method was used to evaluate the particle sizes of the sediments. 50 g of the air dried sediment was ground and introduced into a plastic beaker. 400 cm³ deionized water and 100 cm³ sodium hexametaphosphate solution were added to the beaker. The mixture was agitated with a stir-rod and emptied into a blender where it was blended for about 30 seconds until the sediment could not be physically broken apart any further. The contents of the blender were poured into a 1000 cm³ graduated cylinder and deionized water was added to the graduated cylinder up to the 1000 cm³ mark. The opening of the graduated cylinder was completely covered and inverted a few times to fully suspend the sediment particles. A bouyoucos hydrometer was gently added to the sediment suspension and reading was taken 40 seconds after the cylinder inversions ended. The hydrometer was removed and cleaned. The temperature of the suspension was recorded and the hydrometer reading was corrected. The introduction of the bouyoucos hydrometer was repeated two hours later. The proportion of sand, silt and clay was determined by simple proportion from the hydrometer readings and the original mass of the sediments. The sediments were separated into the following sizes: % sand (0.20 -2.00 mm), % silt (0.02-0.20 mm) and % clay (<0.02 mm) (Brady and Weil 2007).

Extraction of Sediment Samples for Determination of Organochlorine Pesticide Residues. 5 g of wet sediment was homogenized with 5 g of anhydrous granulated Na₂SO₄ using a mortar and a pestle. Cold solvent extraction (Steinwandter 1992) was carried out using 50 cm³ HPLC grade petroleum ether/acetone (1:1 v/v) mixture in a 250 cm³ reagent bottle containing the homogenized sediment sample. The mixture was well shaken and the stopper was removed continuously to release the gas built up in the reagent bottle. The mixture was allowed to stand for 30 minutes and then filtered with a filter paper into a glass container (US EPA 2002).

Pre-concentration of extracts. The solvent extracts were concentrated to 1 cm³ using a rotary evaporator.

Clean-up of extracts. Column chromatography was employed (US EPA Method 3630B) to clean-up the extracts (US EPA 1996). The glass separating column (20 cm) was packed with activated silica gel (90% < 45 μm) and washed down with n-hexane to remove any dirt. The extracts were demosturized over 1 g of anhydrous granulated Na₂SO₄ and separated into two eluted fractions using mixtures of dichloromethane, hexane and acetonitrile as eluting solvents. For the first fraction, 30 cm³ of a dichloromethane/hexane (20/80) mixture was used, while 30 cm³ of a dichloromethane/hexane/acetonitrile (50/49.5/0.5) mixture was used for the second fraction in order to ensure that the polar acetonitrile eluted any remaining residue. The fractions were combined, concentrated to 1 cm³ using a rotary evaporator and subsequently analysed for organochlorines.

Analytical Methods. Analysis of OCP is summarized as follows.

Identification and determination of OCP residues by gas chromatography. A gas chromatograph equipped with an electron capture detector (GC-ECD) was used for the analyses of the OCPs residues. The cleaned-up extracts were dried and re-dissolved in 1.0 cm³ of analar grade isooctane for injection into the gas chromatograph (Pandit et al. 2002). Blank runs were made for background correction and performance of the system. Organochlorine Pesticides II EPA Method 8081A {Mix AB # 3, cat. #32415 (ea.)} (US EPA 1996) was employed for the analyses. The detection and determination of the residues were performed by injecting 1 μL of the 1.0 cm³ purified extract into the injection port of a gas chromatograph with a ⁶³Ni electron capture detector (GC-μECD Agilent Technology 7890A) equipped with the ChemStation software. The chromatographic conditions are given in Table 1. The purge activation time was 30 s and the run time was 17 mins. Identification of pesticide residues was accomplished using reference standards and relative retention time techniques, while the concentration of the residues was determined by comparing the peak heights of the samples with the corresponding peak heights of the reference standards of known concentrations. The stock solution of the OCP standards was purchased from Restek Corporation, USA. It contained 1000 ppm in n-hexane and was serially diluted to obtain the desired

concentrations of 10 ng/mL, 20 ng/mL and 40 ng/mL. All the extracts from the sediment samples were analysed for alpha-BHC, beta-BHC, lindane, delta-BHC, heptachlor, heptachlor-epoxide (B), aldrin, dieldrin, endrin, endrin aldehyde, endrin ketone, cis-chlordane, trans-chlordane, endosulfan 1, endosulfan 11, endosulfan sulphate, methoxychlor, p,p'-DDE, p,p'-DDD and p,p'-DDT. The concentrations (ww) of the OCP residues were calculated directly by the gas chromatograph after inputting the weight of the samples and blank corrections effected.

Table 1: Operating conditions of the gas chromatograph

Detector	Electron capture
Column	DB-5 fused silica capillary column (30 m length × 0.32 mm i.d. × 0.25 µm film thickness)
Carrier gas	HP – 5 5% Phenyl methyl siloxan
Carrier gas pressure	Helium (99.9992) flowing at 20 mL/min
Make-up gas	10.744 psi
Injector temperature	Nitrogen (99.9995%)
Injection	250 °C
Detector temperature	1 µL Splitless
Temperature programme	300 °C
	Initial temp 50 °C at a rate of 25 °C/min to 100 °C (held for 1 min), then at a rate of 5 °C/min to 300 °C

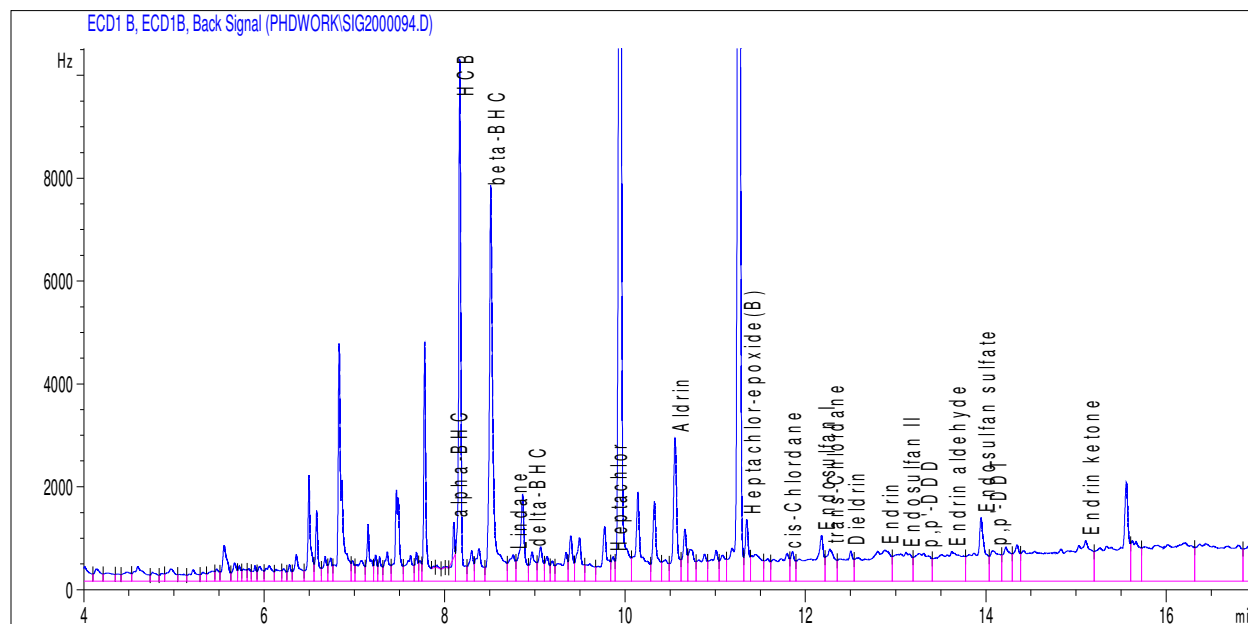


Figure 2. Chromatogram of organochlorine pesticide residues in epipellic sediment during the dry season in Agboyi Creek

Quality assurance. Before analysis was performed, standards were run to check for the column performance, peak height, resolution and the detection limit. The correlation coefficients of calibration curves of OCPs were all higher than 0.998. The quality assurance measures included strict cleaning procedures, procedural blank, recovery of spiked standards and monitoring of detector response.

Recovery study. Recovery studies were undertaken to evaluate the efficiency of the extraction procedure used. The recovery of organochlorines was carried out in replicate and was determined by spiking

the previously analysed samples with the pesticide standard. The recovery values expressed in percentages were calculated from the chromatograms.

$$\% \text{ Recovery} = \frac{CS_2 - CS_1}{CS} \times 100$$

where, CS₁ = concentration of pesticide residues in the sample
 CS₂ = concentration of pesticide residues in the spiked sample
 CS = concentration of added pesticide

Table 2: Mean values of properties of epipellic sediment during the dry and wet seasons

Parameter	Agboyi Creek		Oworonshoki		Ajara		Ogogoro		Tarkwa Bay	
	Dry season	Wet season	Dry season	Wet season	Dry season	Wet season	Dry season	Wet seas	Dry season	Wet season
Colour	Black	Grey	Black	Black	Brown	Black	Black	Brown	Black	Brown
% Sand	58.00±0.12	58.00±0.09	5.00±0.06	5.00±0.18	10.00±0.11	5.00±0.18	80.00±0.14	5.00±0.1	60.00±0.10	60.00±0.16
% Silt	4.00±0.08	4.00±0.06	55.00±0.10	55.00±0.14	50.00±0.08	20.00±0.12	15.00±0.07	60.00±0.	5.00±0.15	5.00±0.08
% Clay	38.00±0.09	38.00±0.03	40.00±0.06	40.00±0.10	40.00±0.12	75.00±0.15	5.00±0.10	35.00±0.	35.00±0.06	35.00±0.13

Table 3: Mean values of properties of benthic sediment during the dry and wet seasons

Parameter	Agboyi Creek		Oworonshoki		Ajara		Ogogoro		Tarkwa Bay	
	Dry season	Wet season	Dry season	Wet season	Dry season	Wet season	Dry season	Vet season	Dry season	Wet season
Colour	Black	Black	Black	Black	Brown	Black	Black	Brown	Black	Brown
% Sand	3.00±0.10	3.00±0.02	5.00±0.05	5.00±0.11	8.50±0.09	5.00±0.03	5.00±0.09	5.00±0.0	60.00±0.13	60.00±0.08
% Silt	90.00±0.06	90.00±0.04	25.00±0.08	90.00±0.12	85.00±0.10	15.00±0.07	90.00±0.06	90.00±0.	5.00±0.10	5.00±0.02
% Clay	7.00±0.04	7.00±0.06	70.00±0.09	5.00±0.14	6.50±0.12	80.00±0.07	5.00±0.02	5.00±0.0	35.00±0.10	35.00±0.12

Determination of limit of detection (LOD). The limits of detection of the organochlorine pesticide residues were determined by replicate chromatographic runs (6 times) of the least concentration of the OCP standards (10 ng/mL) and then multiplying the standard deviation obtained by 3.

Analyses of data. A total of 20 OCPs were detected and determined at various sample locations for both dry and wet seasons. Concentrations of OCP residues were calculated individually and as the sum of their isomeric forms. The mean was calculated from triplicate determinations.

RESULTS

The results of the analyses and other related data are presented in Figure 2 and Tables 2 - 5. The mean physicochemical properties of epipellic and benthic sediments at the five sites during the dry and wet seasons are shown in Tables 2 and 3 while the mean concentrations of organochlorine pesticide residues in epipellic and benthic sediments at the sites are presented in Tables 4 and 5. The mean recoveries of the residues in sediment ranged between 90.14 and 98.15%. These recovery values validate the methodology used in this study. The limits of detection ranged between 1.43 ng/g and 10.29 ng/g, indicating the sensitivity of the gas chromatograph at the operating conditions. The calibration curves of the analysed pesticides present a good regression line ($r > 0.999$) in the range of explored concentrations.

DISCUSSION

The sediments were admixtures of sand, silt and clay. An increase in the % silt in the sediments largely resulted in increasing levels of total organochlorine pesticide residues in the sediments. The persistence of OCPs in sediment is due to their tendency to associate with particulate matter.

Table 4: Mean concentrations (ng/g) of organochlorine pesticide residues in epipellic and benthic sediments during the dry season

OCPs	Agboyi Creek		Oworonshoki		Ajara		Ogogoro		Tarkwa Bay	
	AGR-SS	AGR-BS	OWS-SS	OWS-BS	AJR-SS	AJR-BS	OGG-SS	OGG-BS	TBY-SS	TBY-BS
Alpha-BHC	2.3±1.5	11.9±7.2	7.7±2.2	2.1±1.4	10.1±2.4	4.9±2.3	1.3±0.1	81.2±2.4	17.2±2.5	2.1±1.1
Beta-BHC	178.9±5.1	60.7±4.5	34.2±3.4	21.9±3.2	13.9±4.5	28.5±3.7	0.7±0.1	203.3±5.8	102.0±4.3	12.1±3.2
Lindane	8.2±1.6	24.7±2.3	28.4±1.8	15.6±6.8	10.1±2.1	11.6±2.2	3.6±1.6	56.1±8.3	45.7±8.2	4.9±2.2
Delta-BHC	9.1±3.2	111.2±4.1	37.5±8.6	9.5±2.3	16.1±3.3	20.3±9.4	0.7±0.2	1382.9±5.8	11.7±1.1	0.8±1.4
ΣBHC	198.5±11.4	208.5±18.1	107.8±16.0	49.1±13.7	50.2±12.3	65.3±17.6	5.3±2.0	1723.5±22.3	176.6±16.1	19.9±7.9
Heptachlor	5.6±2.4	44.9±5.6	33.1±5.1	22.8±8.2	9.8±4.2	24.9±3.3	92.5±5.9	278.3±9.9	119.3±5.4	91.8±7.2
Heptachlor -epoxide (B)	11.6±2.8	403.6±9.3	40.4±3.7	38.4±3.1	24.2±5.2	37.4±2.1	2.6±0.2	13681.1±4.3	15.4±8.3	2.2±2.1
Aldrin	27.3±6.3	14.8±4.2	27.9±1.6	4.0±1.3	40.0±2.3	36.8±6.1	6.5±0.4	210.8±5.9	31.6±1.2	12.6±2.5
Dieldrin	17.5±7.6	37.2±7.5	22.2±6.4	3.6±4.2	22.7±3.4	13.9±1.8	0.9±0.1	74.1±3.3	27.4±2.3	2.8±1.2
Endrin	73.8±2.1	139.5±2.3	25.3±3.2	15.1±3.3	120.8±4.6	16.9±4.2	11.8±8.6	170.7±2.2	ND	10.7±3.3
Endrin aldehyde	135.2±6.5	536.2±7.4	202.6±9.6	27.5±4.1	140.3±9.4	113.8±7.3	1.4±1.5	225.8±8.3	143.5±2.4	6.1±2.1
Endrin ketone	442.4±8.2	ND	403.6±3.8	21.5±8.5	79.4±5.6	451.2±2.9	0	294.6±3.5	238.6±8.3	14.5±2.2
Cis-Chlordane	18.4±3.4	28.4±2.5	35.6±2.3	19.4±3.3	23.2±3.5	25.7±4.1	0.6±0.3	76.5±6.4	60.1±5.2	2.8±4.2
Trans-Chlordane	16.1±8.1	90.8±6.2	29.8±2.1	20.1±3.7	31.3±5.2	68.3±7.8	0.5±0.7	63.1±5.5	45.5±3.3	7.7±5.3
Endosulfan 1	30.2±2.0	37.7±3.6	26.9±5.3	14.3±1.2	13.3±9.1	26.7±2.7	0.6±0.3	71.8±9.2	62.9±4.5	2.0±5.2
Endosulfan 11	30.1±4.5	55.3±6.3	39.7±3.6	5.6±2.1	44.7±3.5	16.4±4.4	0.9±0.2	123.3±2.8	260.9±5.8	2.2±4.19
Endosulfan sulphate	71.5±9.1	53.6±4.2	40.5±5.4	8.1±1.9	77.2±5.4	48.2±7.2	2.4±1.1	305.9±8.3	252.6±9.7	10.7±7.4
Methoxychlor	ND	146.7±8.2	22.4±8.5	2.8±3.8	47.4±8.3	43.6±3.6	0	58.7±2.5	84.7±3.4	7.9±8.2
p,p'-DDE	ND	43.1±5.6	44.2±2.5	5.2±5.4	20.9±2.6	39.4±8.2	1.2±0.3	ND	20.6±6.2	ND
p,p'-DDD	31.7±5.6	52.3±8.2	64.9±7.6	8.4±6.4	49.7±3.1	33.2±3.3	2.9±5.2	72.7±3.6	ND	4.6±3.1
p,p'-DDT	26.9±3.8	44.5±2.4	88.9±3.4	11.8±2.5	21.3±1.9	85.3±5.5	2.9±2.4	89.8±8.3	113.2±8.2	7.4±7.3
ΣDDT	58.6±9.4	139.9±16.2	198.0±13.5	25.4±14.3	91.9±7.6	157.9±17.0	7.0±7.9	162.5±11.9	133.8±14.4	12.0±10.4
ΣOCPs	1138.9±83.8	1939.1±101.6	1254.8±90.1	271.±76.7	811.64±89.6	1139±92.1	127±29.2	17521.6±64.3	1646±90.3	195±74.1

AGR-SS = epipellic sediment at Agboyi Creek; AGR-BS = benthic sediment at Agboyi Creek; OWS-SS = epipellic sediment at Oworonshoki; OWS-BS = benthic sediment at Oworonshoki; AJR-SS = epipellic sediment at Ajara; AJR-BS = benthic sediment at Ajara; OGG-SS = epipellic sediment at Ogogoro; OGG-BS = benthic sediment at Ogogoro; TBY-SS = epipellic sediment at Tarkwa Bay; TBY-BS = benthic sediment at Tarkwa Bay.

Sediments with higher percentages of silt accumulated higher concentrations of organochlorine pesticide residues. Methoxychlor and p,p'-DDE were not detected in the epipellic sediment of Agboyi Creek during the dry season. Endrin ketone was not also detected in its benthic sediment. p,p'-DDE was not detected at the benthic sediment of Ogogoro and Tarkwa Bay. Endrin and p,p'-DDD were not detected in epipellic sediment at Tarkwa Bay. During the wet season, p,p'-DDE, aldrin and trans-chlordane, endrin and p,p'-DDD were not detected at Oworonshoki, Ajara and Ogogoro respectively. OCP levels did not show any particular pattern between the epipellic and benthic sediment and during the dry and wet seasons. ΣBHC ranged between 5.27 ng/g in epipellic sediment of Ogogoro and 1723.56 ng/g in its benthic sediment during the dry season. ΣDDT ranged between 4.5 ng/g in benthic sediment of Tarkwa Bay and 378.62 ng/g in epipellic sediment of Oworonshoki during the wet season. Heptachlor-epoxide (B) gave striking levels of 13681.10 ng/g and 13562.80 ng/g at the benthic sediment of Ogogoro and Ajara sites respectively. Total OCPs ranged between 35.97 ng/g and 17513.80 ng/g in the benthic sediments of Tarkwa Bay and Ogogoro respectively.

There is also increasing interest in South America on organic pollutants from the coastal marine environment. Menone et al. (2001) studied the occurrence and distribution of persistent organochlorine compounds in sediments in the Mar Chiquita, Argentina coastal lagoon watershed. Heptachlor epoxide, DDT and its metabolites, and % HCH were the predominant OCPs in sediments. OCPs in sediment from the coastal marine environment of Mumbai, India have been analysed to assess their distribution in various environmental compartments (Pandit et al. 2002). HCH isomers, DDT and its metabolites were the predominantly identified compounds in all the samples. The residue levels of OCPs in this study are similar

to results of earlier studies carried out on sediment at the Lagos Lagoon. Adeboyejo et al. (2011) recorded OCP levels in the sediment that ranged between 0.4 - 43.5 ng/g. In another study by Clarke et al. (2013) endosulfan I had the lowest concentration of OCP while endosulfan II had the highest mean concentration which ranged between 29.67 – 525.55 ng/g. The beta-BHC in the sediment ranged between 33.76 - 436.11 ng/g during the dry and wet seasons, respectively. The OCP levels in this study were within the permissible limits (FAO/WHO 2005; USEPA 2006).

Table 5: Mean concentrations (ng/g) of organochlorine pesticide residues in epipelagic and benthic sediments during the wet season

OCPs	Agboyi Creek		Oworonshoki		Ajara		Ogogoro		Tarkwa Bay	
	AGR-SS	AGR-BS	OWS-SS	OWS-BS	AJR-SS	AJR-BS	OGG-SS	OGG-BS	TBY-SS	TBY-BS
Alpha-BHC	11.1±3.5	28.7±9.4	19.7±6.3	91.4±2.2	12.2±4.4	52.5±8.2	1.3±4.1	159.6±6.3	29.9±3.2	2.1±3.1
Beta-BHC	74.3±2.8	49.7±2.3	52.8±4.5	82.4±6.9	86.4±3.5	97.3±3.5	6.7±2.2	36.8±3.6	16.6±4.3	6.0±2.2
Lindane	25.4±8.3	83.3±4.4	51.4±2.4	13.2±8.5	26.9±8.6	83.1±4.4	3.5±8.5	32.3±2.5	26.9±2.4	0.5±0.8
Delta-BHC	96.3±5.2	20.9±2.3	56.5±5.2	11.2±2.2	21.1±2.3	44.1±6.2	2.2±3.2	9.2±7.3	19.4±2.2	0.6±0.2
ΣBHC	207.1±19.8	182.6±18.4	170.4±18.4	198.2±19.8	146.6±18.8	277.0±22.3	13.7±20.0	237.9±19.7	92.8±12.1	9.2±6.3
Heptachlor	49.5±4.2	125.6±8.5	99.7±9.4	70.3±4.3	60.2±5.3	194.6±4.5	580.9±9.2	45.1±3.2	556.5±5.5	13.2±5.2
Heptachlor										
-epoxide (B)	440.3±8.5	19.0±1.4	97.9±2.2	10.4±2.2	49.3±4.6	13562.8±2.5	1.0±5.5	40.7±8.3	49.0±6.3	0.7±1.2
Aldrin	24.2±2.2	43.6±2.1	44.7±4.4	26.2±7.4	29.5±9.2	ND	3.3±6.2	29.4±5.2	80.4±3.8	2.2±1.3
Dieldrin	33.0±8.5	38.9±7.5	64.8±7.3	36.7±2.3	37.6±4.5	2.0±6.1	0.7±2.5	12.5±3.1	48.8±2.4	0.6±0.2
Endrin	103.0±9.9	137.8±2.4	55.6±8.8	132.8±9.8	24.1±3.3	1.0±4.6	0.9±0.8	ND	49.6±8.5	0.8±0.2
Endrin aldehyde	334.1±4.3	101.8±8.5	226.6±4.1	198.8±4.7	419.3±8.7	1.1±3.8	1.3±0.6	118.2±5.6	375.4±5.5	0.6±0.1
Endrin ketone	426.8±2.8	691.7±5.8	657.8±3.8	148.2±8.3	438.9±2.2	0	0	332.4±8.7	420.6±3.6	0
Cis-Chlordane	61.1±3.3	53.7±3.2	75.2±2.5	23.9±1.1	52.7±2.4	3.0±2.3	0.5±0.3	67.3±5.3	76.6±6.5	0.6±1.2
Trans-Chlordane	34.7±7.2	40.8±2.3	141.7±8.4	25.0±3.2	89.9±4.6	ND	0.5±0.4	50.3±9.4	80.5±2.4	1.2±2.1
Endosulfan 1	39.4±2.1	69.5±3.2	64.8±5.3	44.2±2.2	40.4±3.7	3.8±2.3	0.9±0.9	46.4±7.3	32.6±9.4	0.6±1.4
Endosulfan 11	76.9±8.5	139.7±8.7	30.4±9.2	87.6±6.4	22.2±8.4	1.1±1.4	0.9±0.4	282.9±6.6	102.9±6.5	0.8±3.6
Endosulfan sulphate	78.2±2.4	114.9±5.4	135.4±4.9	151.8±2.2	97.6±9.8	6.9±1.6	1.5±0.4	105.3±3.3	178.6±9.6	2.7±7.3
Methoxychlor	20.1±5.3	74.2±4.2	84.9±7.5	170.2±6.6	61.9±2.5	0	0	61.3±3.2	141.6±5.4	0
p,p'-DDE	41.2±2.5	66.3±8.2	103.7±5.4	ND	49.5±5.4	1.0±1.4	0.7±0.2	54.7±9.4	32.2±3.6	0.8±3.4
p,p'-DDD	52.6±7.2	10.4±4.3	108.7±6.3	41.0±3.2	47.3±3.6	2.1±2.3	2.9±0.3	ND	93.1±2.3	2.9±4.1
p,p'-DDT	104.9±3.3	102.3±8.4	168.2±8.2	58.6±9.4	63.6±6.3	2.1±3.2	1.0±0.9	83.6±5.5	101.8±5.7	0.8±5.2
ΣDDT	198.7±13	279.0±20.9	380.6±19.9	99.6±12.6	160.4±15.3	5.2±6.9	4.6±1.4	138.3±14.9	227.1±11.6	4.5±12.7
ΣOCPs	2121±89.3	2102±102.5	2328±112.1	1418±93.1	1722±100.3	14054±38.3	608±48.6	1562±89.8	2503±111.1	136±42.8

CONCLUSION

Results of the OCP analyses showed that a total of twenty pesticide residues were detected in the samples. The organochlorine pesticide residues were detected in all the samples though the frequency of detection of a few of the residues was less than 100%. The residue levels were higher in the Lagos Lagoon than in Agboyi Creek while a higher concentration of the residues was generally observed during the dry season.

REFERENCES

- Adeboyejo OA, Clarke EO, Olarinmoye MO. 2011. Organochlorine pesticide residues in water, sediments, fin and shell-fish samples from Lagos Lagoon complex, Nigeria. *Researcher* 3: 38-45.
- Brady NC, Weil RR. 2007. *The nature and properties of soil*. Pearson International Edition.

- Clarke EO, Aderinola OJ, Adeboyejo OA. 2013. Persistent organochlorine pesticides in water, sediment, fin fish (*Sarotherodon galilaeus*) and shell fishes, (*Callinectes pallidus* and *Macrobrachium macrobrachium*) samples from Ologe Lagoon, Lagos, Nigeria. *American Journal of Research Communication* 1:122-135.
- Covacia A, Gheorghheba A, Voorspoelsa S, Maervoeta J, Redekere ES, Blustc R, Schepensa P. 2005. Polybrominated diphenyl ethers, polychlorinated biphenyls and organochlorine pesticides in sediment cores from the western Scheldt River (Belgium): analytical aspects and depth profiles. *Environment International* 31: 367-375.
- Darko G, Acquaaah SO. 2007. Levels of organochlorine pesticides residues in meat. *International Journal of Environmental Science and Technology* 4: 521-524.
- Doong RA, Peng CK, Sun YC, Liao PL. 2002. Composition and distribution of organochlorine pesticide residues in surface sediments from Wu-Shi river estuary, Taiwan. *Marine Pollution Bulletin* 45: 246-253.
- Food and Agriculture Organization (FAO) /World Health Organization (WHO). 2005. *Residues in food*. Report of joint FAO/WHO food standards programme. Rome, Italy. 2B: 61-81.
- Menone ML, Aizpún de Moreno JE, Moreno VJ, Lanfranchi AL, Metcalfe TL, Metcalfe CD. 2001. Organochlorine pesticides and PCBs in a Southern Atlantic coastal lagoon watershed, Argentina. *Archives of Environmental Contamination and Toxicology* 40: 355-362.
- Osibanjo O, Bashin N, Onyoyo H, Bouwman H, Yive R, Okond'Ohoka J. 2002. UNEP/GEF regionally based assessment of persistent toxic substances, Sub-Saharan Africa regional report. Available at: <http://www.chem.unep.ch/pts/gr/Global-Report.pdf>.
- Pandit GG, Sahu SK, Sadasivan, S. 2002. Distribution of HCH and DDT in the coastal marine Environment of Mumbai, India. *Journal of Environmental Monitoring* 4: 431-434.
- Sarkar A, Nagarajan R, Chaphadkar S, Pal S, Singbal SY. 1997. Contamination of organochlorine pesticides in sediments from the Arabian sea along the west coast of India. *Water Research* 31: 195-200.
- Steinwandter H. 1992. Development of microextraction methods in residue analysis. In: *Emerging Strategies for Pesticide Analysis* (Eds T. Cairns, J. Sherma). 3-50. CRC. Boca Raton, FL.
- United Nations Environment Programme (UNEP). 2002. Sub-Saharan Africa, regionally based assessment of persistent toxic substances. United Nations Environment Programme, Chemicals (UNEP Chemicals), Geneva, Switzerland. Available at: <http://www.chem.unep.ch/Pts/regreports/ssafrika.pdf>.
- US Environmental Protection Agency (US EPA). 2006. Guidance for assessing chemical contaminant data for use in fish advisories. 2: Risk Assessment and fish consumption limits. Available at: <http://www.epa.gov/ost/fishadvice/volum2/index.html>.
- US Environmental Protection Agency (US EPA). 2002. Method 3570, Revision C. Microscale solvent extraction (MSE), Washington, DC, USA. p 9.
- US Environmental Protection Agency (US EPA). 1996. Method 3630, Revision B. Silica gel Cleanup. SW-846 Manual. Washington, DC, USA.
- US Environmental Protection Agency (US EPA). 1996. Method 8081A. Organochlorine pesticides by gas chromatography. Washington, DC, USA.
- Williams A, Ayejuyo O, Unyimadu J. 2013. Distribution of chlorinated pesticides in shellfishes from Lagos Lagoon, Nigeria. *Journal of Marine and Biological Oceanography* 2: 1. DOI: <http://dx.doi.org/10.4172/2324-8661.1000106>.
- Xue N, Zhang D, Xu X. 2006. Organochlorinated pesticide multiresidues in surface sediments from Beijing Guanting reservoir. *Water Research* 40: 183-194.
- Yang R, Ji G, Zhoe Q, Yaun C, Shi J. 2005. Occurrence and distribution of organochlorine pesticides (HCH and DDT) in sediments collected from East China sea. *Environment International* 31: 799-804.

**DEVELOPMENT AND TESTING OF NEXT GENERATION SORBENT POLYMER
EXTRACTION AND REMEDIATION FROM SEDIMENTS (SPEARS) TECHNOLOGY**

Robert DeVor* (Vencore, Kennedy Space Center, FL, USA)
Phillip Maloney (Easi, Kennedy Space Center, FL, USA)
Jacqueline Quinn (NASA, Kennedy Space Center, FL, USA)

Ongoing research at NASA's Kennedy Space Center has shown the capability of a passive, polymer-based absorption system to be effective for the removal and treatment of sediment systems contaminated with polychlorinated biphenyls (PCBs). This technology, which has been termed **Sorbent Polymer Extraction and Remediation from Sediments (SPEARS)**, utilizes a low-cost, hollow polymer filled with an environmentally friendly solvent to enhance hydrophobic, PCB molecule absorption into the SPEARS units. A recently completed, seven-month field study showed that SPEARS removed 75% of the PCBS (by mass) from contaminated sediments during this period. Longer exposure periods were not considered due to cost and time limitations, however, because the technology is driven by concentration gradients, there is strong evidence that higher removal rates could have been achieved. A next-generation design is currently being developed for use at a larger, longer-term site, with the intent of leaving the SPEARS system in place for as long as 12 to 18 months. Additional studies are currently underway to determine the effectiveness of SPEARS for the remediation of additional hydrophobic contaminants such as chlordane and pyrene (preliminary results will be presented).

**GLOBAL WARMING
AND
CLIMATE CHANGE**

FOREST FIRE A GLOBAL SCENARIO IDENTIFICATION AND SUSTAINABLE MANAGEMENT USING GEO INFORMATION TECHNOLOGY

JOSE T. M*, SUBIN K. JOSE*, G .MADHU**

*Christ College (autonomous), Irinjalakuda, Thrissur Kerala, jthekkan@gmail.com, josesubin@gmail.com

** School of Engineering, Cochin University of Science and Technology, Kalamaserry , Ernakulam.
Email. gmadhu@cusat.ac.in.

ABSTRACT: A forest fire event is influenced by ecological, human and climatic conditions. Forest fire directly cause biodiversity loss, forest degradation and climate change. It has direct ecological, economic and social impact. Fire prone area Modeling is done to have the most effective system of fire management and at the same time to reduce its deleterious effect on ecosystems, communities and landscapes. Geospatial techniques are proving to be powerful tools to assess the forest fire risks and the management. The present study deals with identification of fire prone area and there management in Shendurney wildlife sanctuary, the mega biodiversity hot spot in Western Ghats region, using GIS and Remote sensing techniques. Large extents of forests are affected by fire in every year in this region. Two types of data are used in the study i.e. spatial and non spatial data. Spatial data mainly includes Remote Sensing data, forest block, GPS field data, settlement boundaries, road/trek path network and the most important existing water bodies in that area where the non-spatial data pertains to meteorological data on temperature, rainfall . The parameters in consideration for the analysis are vegetation type, forest fragmentation, vicinity to settlement, distance from road, slope, aspect, temperature, amount of litter and rainfall. All these parameters have direct/indirect influence on the occurrence of fire and were integrated using GIS. A multi parametric weighted index model has been adopted to derive the ‘fire-risk’ zone/ fire prone area map. The final output shows forest fire risk area map of Shendurney wildlife Sanctuary in four categories such as very high risk, high risk, moderate risk and low risk. Based on this final output, the study attempted to give insight in the use of RS and GIS for sustainable fire management. For that, various spatial analysis have been carried out like identification of suitable sites for construction of check dams to ensure water availability in combating fires and for locating fire watch towers for better fire management. The present study effectively proved system for sustainable forest fire management.

Keywords: Forest fire, GIS, Shendurney, Remote Sensing, Wildlife Sanctuary

INTRODUCTION

Fire is a natural factor that has shaped the Earth’s vegetation throughout its natural history. Fire disturbance is a major factor driving patterns of vegetation structure and composition in natural ecosystem (Whelan, 1995). Fire is clearly a global issue, affecting almost all climates and vegetation functional groups (Randerson *et al.*, 2006) Forest fire or wildland fire has become intense and more frequent in the last few decades all over the world, and is a critical issue in the biosphere–atmosphere interface (Crutzen and Andreae, 1990; Penner *et al.*, 1992; Cochrane ,2003). It has a profound effect on atmospheric chemistry, biogeochemical cycling and ecosystem structure (Schimel and Baker, 2002). Human activities can influence natural fire regimes by increasing fires in forests that would seldom burn under natural conditions (Goldammer, 2003).

In India the tropical moist and dry deciduous forests, which are frequently affected by forest fire, are extensive and account for 64% of the total forest area (Forest Survey of India, 2003). Over the past few decades, forest fires in India have received increasing attention because of the wide range of ecological, economic, social, and political impacts. Fire plays an important role in the creation and maintenance of landscape structure, composition, function, and ecological integrity (Covington and Moore, 1994; Goldammer ,1999; Morgan *et al.*, 2001) and can influence the rates and processes of ecological succession and encroachment. At the local scale, fire can stimulate soil microbial processes and combust vegetation ultimately altering the structure and composition of both soils and vegetation (Goldammer, 1999). Also, at

the regional and global scales, combustion of forest and grassland vegetation releases large volumes of radiatively active gases, pyrogenic aerosols, and other chemically active species that significantly influence Earth's radiative budget and atmospheric chemistry (Andreae and Merlet, 2001), impacting air quality (Hardy *et al.*, 2001) and raise concern about risks to human health (Brauer, 1999).

Forest fire research can be considered as one of the most appropriate areas, where Geographic Information System (GIS) approach can be effectively applied. GIS can take definite advantage of the computer's capability in processing, storage and retrieval of immense data. The use of the GIS approach facilitates in integrating several variables in order to establish and focus on the problem. At the same time, it makes it possible to update or retrieve spatial information in different ways included in the database, to develop various models (Yanar and Akyurek, 2006). Geographical Information systems (GIS) are applied as tools to achieve an operational forest fire management system. With GIS models, new understanding of the fire danger situation in a management area can be gained. As an important factor of a risk analysis the damage potential that arises from fires starting at a certain point in the landscape can be estimated. (Rawat *et al.*, 1999). Earth-observing satellite sensors have been used since the 1970s to detect these changes, to quantify the burnt areas and to determine the composition and distribution of byproducts after fire (Robinson, 1991; Fuller, 2000).

The more complex and accurate fire models require spatial information that is furnished by remote sensing and Geographic Information Systems (GIS). The integration of remote sensing with GIS will be helpful for the spatial identification and management of forest fire (Bonazountas *et al.*, 2005). The integration of field data with remote sensing data is needed for the current and accurate fire risk mapping. GIS technology can serve as a vital technological core for the development of an integrated operational system in the case of forest fire crisis management. GIS with multicriteria decision making system will be helpful for the accurate prediction of different environmental phenomenon like landslide, drought and forest fire etc. (Tansey, 2004).

MATERIAL AND METHODS

Since the study is aimed to create a GIS based methodology, both spatial and attribute data of the various thematic layers, available in the form of maps and published report were collected from the various sources. Primary data was collected using various techniques to fill any data gaps. The present study is carried out using GIS based multicriteria decision making methodology in conjunction with fuzzy logic, in a participatory decision-making framework to rank and prioritize the causative factors of fire risk in the study area. We used topographic, vegetation, climatic, social and field level parameters for evaluating the fire risk in the study area. These data were arranged in raster-based maps for further analysis. Spatial data were collected from Survey of India (SOI) Topographic map sheets of 1:25,000 and 1:50000 scale and Indian Remote sensing Satellite (IRS) satellite image. The SOI maps became the source for a number of basic thematic layers like contour, drainage, settlements, roads / trek paths and water body. IRS-1C LISS-III digital image acquired on 12 April 2009 was used to prepare the land cover map. Visual interpretation of the standard False Colour Composite (FCC) with 4-3-2 RGB combination as well as digital classification of the image using ERDAS 9.1 image processing software was used for the preparation of land cover map. The classified image is field verified and found to be accurate. Details regarding trek path, settlement boundary and fire lines inside the sanctuary were collected during field visit. Data regarding fire occurrences during the last few years in study area were collected from the forest department and field visit. Temperature and humidity data was collected from the forest department meteorological stations, Indian Meteorological Department (IMD) station and also from Kerala State Electricity Board (KSEB) meteorological stations. An exhaustive field trip was carried out during the different time period of the study. Field level data collection and mapping was carried out using toposheet as reference. The real world co-ordinates were collected using GPS. The various data collected were processed and put into the Arc GIS software package.

In this study, we used Saaty's (2000) analytical hierarchy process, a MCDM (Multi Criteria Decision Making) methodology in conjunction with fuzzy logic, in a participatory decision-making framework to rank and prioritize the causative factors of fire risk in the study area. Our methodology consisted of four different components: (1) hierarchical structure development of fire risk criteria, (2) weights determination at different levels of hierarchy using linguistic variables and fuzzy sets, (3) assigning criteria weights in GIS, and (4) fire risk quantification using decision rule.

The location of existing fire watchtower was collected from the field with the help of GPS. The collected data is transferred in to GIS platform and analyse the visibility from each watch tower is analysed by using digital elevation model derived from the contour with the help of visibility analysis in Arc GIS. Based on the visibility analysis of existing watchtower suitable site for the construction of new watch tower is located. The criteria used for the identification of new watch tower is based on the invisibility from existing watchtower and the area that come under high fire risk area. Existing watchtower locations collected by the help of GPS during field study. The collected GPS location of existing watchtower location along with elevation data is plotted in Arc GIS. Visibility of existing watchtower is examined with help of spatial analyst extension in Arc GIS. For the identification of suitable check dam location flow accumulation flow direction was measured by using spatial analyst .The area with high flow accumulation and that are come under high fire risk area check dam location was identified. The base layer used for the preparation of flow direction and flow accumulation is elevation data and drainage data. The tool used for the flow accumulation analysis is the spatial analyst extension in hydrological analysis tool.

RESULT AND DISCUSSION

The forest fire risk area map of Shendurney wildlife sanctuary is shown in Figure 1 and the fire risk area calculation is shown in Table 1. The fire risk area map is classified in to four classes, it includes low, medium, high and very high. In Shendurney wildlife sanctuary low fire risk area belongs to 41.7 Km², medium 53.1, high 64.5 Km², very high 11.7 Km².

Table 1. Forest fire risk area – shendurney wildlife sanctuary

Forest fire risk area – shendurney wildlife sanctuary		
Fire risk class	Area (Km ²)	Area Percentage
Low	41.7	24.38
Medium	53.1	31.05
High	64.5	37.71
Very high	11.7	6.86

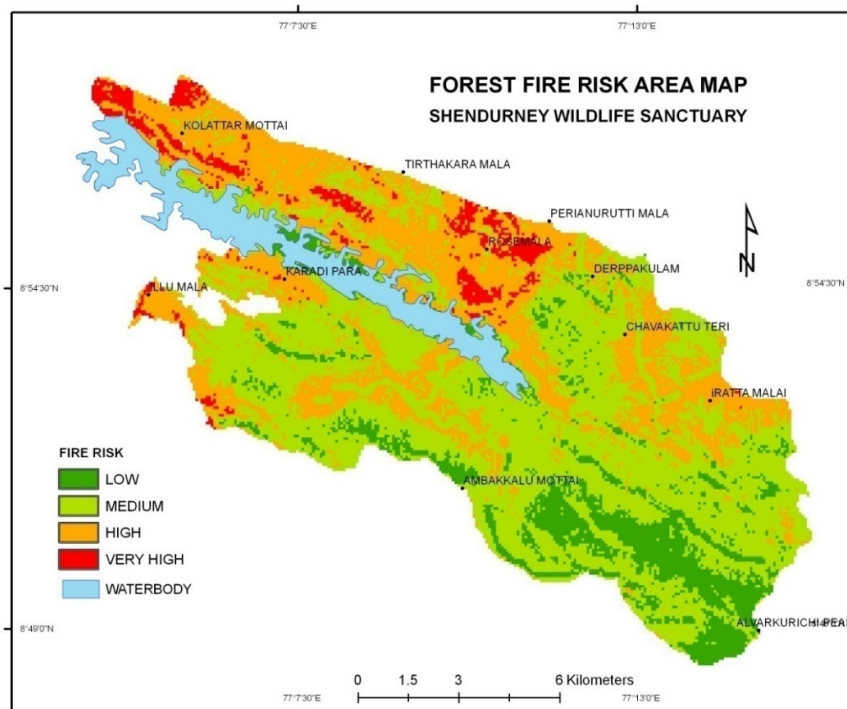


Figure 1. Forest Fire Risk Area Map of Shendurney Wildlife Sanctuary

The visibility from existing watch tower is analysed and shown in Figure 2 and based on the visibility analysis new location for watch tower is proposed. The suitable site for new fire watchtower for Shendurney is shown in Figure 3. The location for new watch tower is near to fire prone area and has high visibility. The suitable site for checkdam location of Shendurney wildlife sanctuary is shown in Figure 4. The check dam location is near to fire prone area and has high flow accumulation.

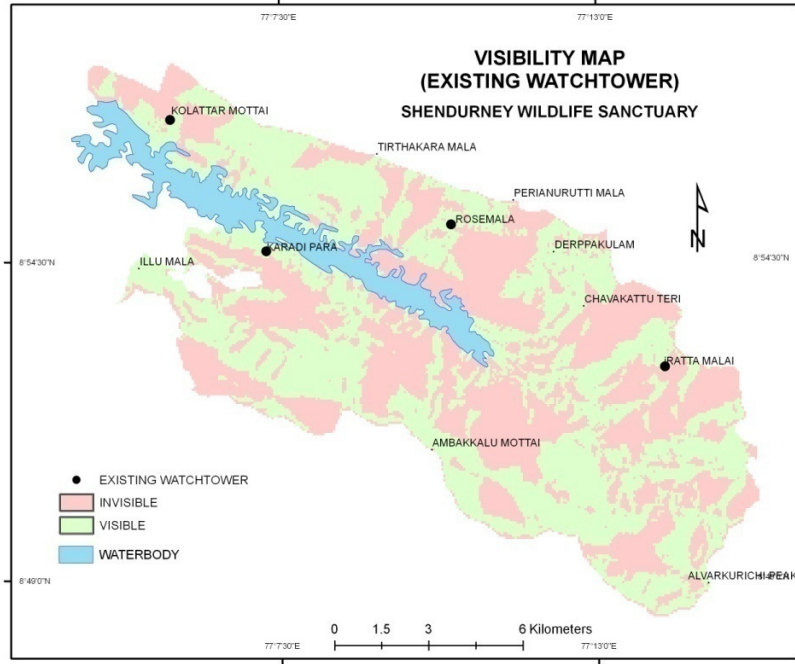


Figure 2. Visibility Map (Existing Watchtower) for Shendurney

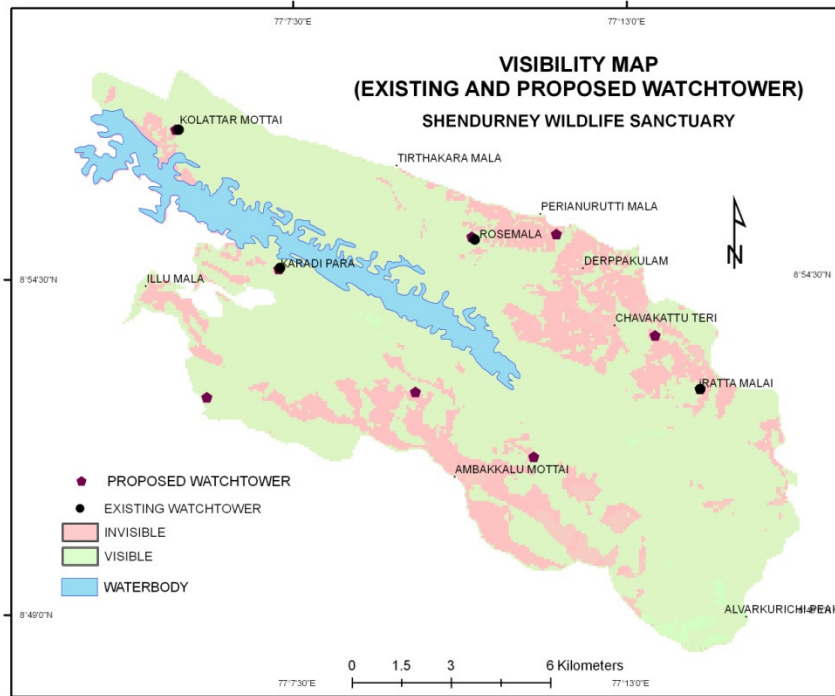


Figure 3. Visibility Map for Existing and Proposed Watchtowers

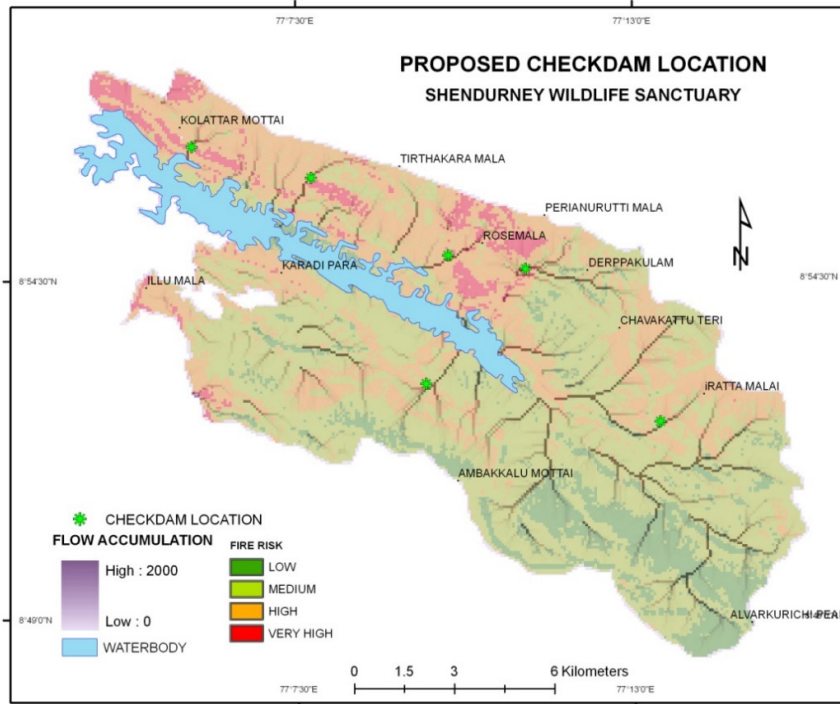


Figure 4. Proposed Checkdam Location for Shendurney

Forest fires controlled or uncontrolled have profound impacts on the physical environment including: landcover, landuse, biodiversity, climate change and forest ecosystem. They also have enormous implication on human health and on the socio-economic system of affected countries. Economic cost is hard to quantify but an estimate by the economy and environment can be provided. Most pronounced consequence of forest fires causes their potential effects on climate change. (Abhineet *et al.*, 1996). The normal fire season in India is from the month of February to May. India witnessed the most severe forest fires in the recent time during the summer.

According to the IFFN (2002) the ecological and socio-economic consequences of wild land fires in India include - Loss of timber, loss of bio-diversity, loss of wildlife habitat, global warming, soil erosion, loss of fuelwood and fodder, damage to water and other natural resources, loss of natural regeneration. Estimated average tangible annual loss due to forest fires in country is Rs.440 crore (US\$ 64.70 millions approximately). The vulnerability of the Indian forests to fire varies from place to place depending upon the type of vegetation and the climate.

Lightning and rubbing of dry plant parts in wind is an important source of natural fires which have influenced dry vegetation (Phillips, 1965; Komarek, 1968). Lightning fires have been observed and reported in the deciduous and semi-deciduous forest biomes as well as occasionally in the rain forest. Today the contribution of natural forest to the overall tropical wildland fire scene is becoming negligible. Most tropical fires are set intentionally by humans and are related to several main causative agents (Goldammer, 1996). Deforestation activities (conversion of forest to other land uses, e.g. agricultural lands, pastures, exploitation of other natural resources); traditional, but expanding slash-and-burn agriculture; grazing land management (fires set by graziers, mainly in open forests with distinct grass strata; use of non-wood forest products (use of fire to facilitate harvest or improve yield of plants, fruits, and other forest products, predominantly in deciduous and semi-deciduous forests); wildland/residential interface fires (fires from settlements, e.g. from cooking, torches, camp fires etc.); other traditional fire uses (in the wake of religious, ethnic and folk traditions; tribal warfare) and socio-economic and political conflicts over questions of land property and land use rights. Forest fire as an agent of regional land cover change and in modifying atmospheric chemistry.

The study attempted to give insight in the use of RS and GIS for fire management. Spatial modelling and analysis have been done in GIS environment for identification of areas prone to fire risk and

subsequently response routes were suggested for extinguishing forest fires (Porwal *et al.*, 1997). Some of the necessary components contributing to the fire behavior viz., fuel (vegetation types), topography (slope and aspect etc.) and the causes of fire (i.e., roads and settlements) have been given due weightages. The above results clearly suggest highly dynamic and spatial nature of fire events in the study area. To manage growing forest fires and associated fire hazards, as well as prioritize prescription efforts, it is essential to improve our understanding of the causative factors of fires. Earlier research relating to forest fire risk involved identifying the potentially contributing variables and integrating them into a mathematical expression, i.e., an index. In creating such an index, most of the earlier researchers focused on using meteorological data alone (Goncalves and Lourenco, 1990) or vegetation parameters (Hernandez-Leal *et al.*, 2006). Predicting the nature of “fires” may not be easy through using such indices alone. The fuzzy based GIS model attempted in our study takes a different approach, compensating MCDM through codifying the expert knowledge for forest fire risk variables and combining it with the human biophysical dimension. Most importantly, several of the causative factors of fire have inherent fuzzy characteristics.

Although humans had introduced fire in the forests of the Western Ghats at least 3500 years ago (Gadgil and Chandran, 1988), increased fragmentation of forests and continued demand on forest resources has contributed to detrimental changes in the spatial and temporal characteristics of the present fire regime (Kodandapani *et al.*, 2004). Human disturbances such as logging, grazing, and harvesting of NTFP could be responsible for altering forest fuel characteristics and maintaining these spatial patterns (Goldammer, 1988). The large number as well as the size of fires in the dry deciduous forests can be explained due to the fuel characteristics especially grass fuels with compact arrangement of fuel particles in the fuelbed (Agee, 2000), continuity in fuels (Miller and Urban, 2000), increased mean maximum daily temperature, and enhanced drying solar radiation during the fire season (Stott, 2000). Forest fires are rare in undisturbed moist deciduous forests, however past disturbance histories such as logging have now rendered the disturbed moist deciduous susceptible to fires (Woods, 1989). Once disturbed, the understorey of these forests are invaded by grass species, rendering the forests vulnerable to forest fires (Suresh *et al.*, 1996; Freifelder *et al.*, 1998).

In addition forest fires could actually be having a net beneficial effect on the species diversity, composition, structure, and regeneration. The low fuel loads and also the low productivity (Mishra, 1983) in these ecosystems could result in patchy, low intensity fires (Oesterheld *et al.*, 1999). These fires could actually be recycling nutrients back into the soil, mitigating invasive species, reducing flammability of vegetation, and promoting regeneration of seedlings and saplings (Goldammer, 1988).

REFERENCES

- Abhineet, J., Shirish, A., Ravan, R.K., Singh, K.K., Das and Roy ,P.S. (1996). Forest fire risk modelling using Remote Sensing and Geographic Information System . *Current Science*, 70(10): 928-933.
- Agee, J.K. (2000). *Wilderness fire science: a state-of-knowledge review*. In: USDA Forest Service Proceedings RMRS-P-15-VOL-5.
- Andreae, M. O. and Merlet, P. (2001). Emission of trace gases and aerosols from biomass burning. *Global Biogeochemical Cycles*, 15, 955–966. doi:10.1029/ 2000GB001382.
- Bonazountas, M., Kallidromitou, D., Kassomenos, P. A. and Passas, N. (2005). Fire risk analysis. *Human and Ecological Risk Assessment*, 11, 617–626. doi:10.1080/ 10807030590949717.
- Brauer, M. (1999). Health impacts of biomass air pollution. In K. T. Goh, D. Schwela, J. G. Goldammer, and O. Simpson (Edt.), *Health guidelines for vegetation fire events—background papers* (pp. 189–254). Singapore: WHO.
- Cochrane, M.A. (2003). Fire science for rainforests. *Nature*, 421:913–919.
- Covington, W. W. and Moore, M. M. (1994). South-western ponderosa pine forest structure: Changes since Euro-American settlement. *Journal of Forestry*, 92, 39–47.
- Crutzen, P.J. and Andreae, M.O.. (1990). Biomass burning in the tropics: impact on atmospheric chemistry and biogeochemical cycles. *Science*, 250:1669–1678.
- Forest Survey of India. (2003). *State of forest report 2003*. Ministry of Environment and Forests, Available from <http://www.fsi.nic.in/sfr2003.html> Accessed 20 Nov, 2007
- Fuller, D.O. (2000). Satellite remote sensing of biomass burning with optical and thermal sensors. *Programme in physical geography*, 24:543–561

- Gadgil, M. and Chandran, M.D.S. (1988). *On the history of Uttara Kannada forest*. In: Dargavel, J., Dixon, K., Semple, N. (Eds.), *Changing Tropical Forests*. Centre for Resource and Environmental Studies, Canberra, pp. 47–58.
- Goldammer, J. (2003). Fire ecology of the recent anthropocene. *In: Proceedings of the 2nd International Wildland Fire Ecology and Fire Management Congress*, Orlando, Florida.
- Goldammer, J. G. (1999). Forests on fire. *Science*, 284, 1782–1783.
- Goncalves, Z. J. and Lourenco, L. (1990). Meteorological index of forest fire risk in the Portuguesemainland territory. *In Proceedings of the international conference on forest fire research* (B07, pp. 1–14). Coimbra.
- Hardy, C. C., Ottmar, R. D., Peterson, J. L., Core, J. E. and Seamon, P. (Eds.) (2001). *Smoke management guide for prescribed and wild land fire: 2001 edition PMS 964 420-2*. NFES 1279.
- Hernandez-Leal, P. A., Arbelo, M. and Gonzalez-Calvo, A. (2006). Fire risk assessment using satellite data. *Advances in Space Research*, 37, 741–746. doi:10.1016/j.asr.2004.12.053.
- IFFN (International Forest Fire News) (2002). Fire Situation In India. *International Forest Fire News*, 26: 23-27.
- Kodandapani, N., Cochrane, M.A. and Sukumar, R. (2004). Conservation threat of increasing fire frequencies in the Western Ghats, India. *Conservation Biology* 18 (6), 1553–1561.
- Komarek, E.V. (1968). Lightning and lightning fires as ecological forces. *International Proceedings of Annual Tall Timbers Fire Ecology conference*. 8. Tall Timbers Research Station. Tallahassee, Florida, USA.. 169-197.
- Miller, C. and Urban, D.L. (2000). Connectivity of forest fuels and surface fire regimes. *Landscape Ecology*, 15, 145–154.
- Mishra, R. (1983). *Indian Savannas*. In: Bourliere, F. (Ed.), *Tropical Savannas*. pp. 151–166.
- Morgan, P., Hardy, C. C., Swetnam, T., Rollins, M. G., and Long, L. G. (2001). Mapping fire regimes across time and space: Understanding coarse and fine-scale fire patterns. *International Journal of Wildland Fire*, 10, 329–342. doi:10.1071/WF01032.
- Oesterheld, M., Loreti, J., Semmartin, M., and Paruelo, J.M. (1999). *Grazing, fire, and climatic effects on primary productivity of grasslands and savannas*. In: Walker, L.R. (Ed.), *Ecosystems of Disturbed Ground*. Elsevier, Amsterdam, pp. 287–306.
- Penner, J.E., Dickinson, R.E., O'Neill, C.A. (1992). Effects of aerosol from biomass burning on the global radiation budget. *Science*, 256:1432–1434.
- Phillips, J. (1965). Fire as master and servant : its influence in the bioclimatic regions of Trans- Variations Saharat Africa. *International Proceedings of Annual Tall Timbers Fire Ecology conference*.. 4. Tall Timbers Research Station. Tallahassee, Florida, USA. pp. 7-109.
- Porwal, M.C., Meir, M.J.C., Hussin, Y.A. and Roy, P.S. (1997). *Spatial Modelling for fire risk zonation using Remote Sensing and GIS*. Paper presented in ISPRS Commission VII Working Group II Workshop on Application of Remote Sensing and GIS for Sustainable Development, Hyderabad, 1997.
- Randerson, J.T., Liu, H., Flanner, M.G., Chambers, S.D., Jin, Y., Hess, P.G., Pfister, G., Mack, M.C., Treseder, K.K. and Welp, L.R. (2006). The impact of boreal forest fire on climate warming. *Science*, 314:1130–1132.
- Schimmel, D. and Baker, D. (2002). Carbon cycle: the wildfire factor. *Nature*, 420:29–30.
- Suresh, H.S., Dattaraja, H.S. and Sukumar, R. (1996). The flora of Mudumalai wildlife sanctuary, Tamil Nadu, southern India. *Indian Forester*, 507–519.
- Tansey, K., Gregoire, J. M., Binaghi, L. E. (2004). A global inventory of burned areas at 1 km resolution for the year 2000 derived from SPOT vegetation data. *Climatic Change*, 67, 345–377. doi:10.1007/s10584-004-2800-3.
- Whelan, J. (1995). *The Ecology of Fire*. Cambridge University Press.
- Woods, P. (1989). Effects of logging drought and fire on structure and composition of tropical forests in Sabah, Malaysia. *Biotropica*, 21, 290–298.
- Yanar, T. A. and Akyurek, A. (2006). The enhancement of the cell-based GIS analyses with fuzzy processing capabilities. *Information Sciences*, 176, 1067–1085. doi:10.1016/j.ins.2005.02.006.

REDUCING GLOBAL WARMING IN AFRICA THROUGH TRADITIONAL AFRICAN ARCHITECTURE: CHALLENGES AND THE WAY FORWARD

Iwuagwu, Ben Ugochukwu. Dept of Architecture, Abia State Polytechnic, Nigeria
Ikechukwu onyegiri. Dept of Architecture, Imo State University, Nigeria
Iwuagwu, Ben Chioma M. Dept of Statistics, Abia State Polytechnic, Nigeria

ABSTRACT: Africa is already a continent under pressure from climate stresses and is highly vulnerable to the impacts of climate change. Many areas in Africa are recognized as having climates that are among the most variable in the world on seasonal and decadal time scales. Rising fossil fuel burning, construction, deconstruction, transportation, general land use changes etcetera have emitted, and are continuing to emit, increasing quantities of greenhouse gases into the Earth's atmosphere. These greenhouse gases include carbon dioxide (CO₂), methane (CH₄) and nitrogen dioxide (N₂O), and a rise in these gases has caused a rise in the amount of heat from the sun withheld in the Earth's atmosphere. This increase in heat has led to the greenhouse effect, resulting in climate change. In 2012, 70 percent of major global droughts occurred in Africa. Kenya, Somalia, Sudan, Malawi, Angola, Chad and Ethiopia were particularly hit hard, and more than 16 million people in those countries were affected. In the same year, floods claimed 363 lives in Nigeria and 65 lives in Niger. In 2013, heavy rains continued with major flooding in Sudan, South Sudan, Mali, South Africa, Zimbabwe, Botswana and Mozambique. The macro-economic impact of these episodes of extreme drought and flooding is significant. It has been ascertained that construction industry alone consumes over 40 percent of energy in Africa leading to global warming and climate change, this paper therefore clamours for reduction in energy consumption in the construction industry and endorse traditional African architecture that is more sustainable and ozone friendly in reducing global warming in Africa and the world at large. This paper employs an extensive literature review and applies techniques which are common in content analysis. A thorough literature reviews was conducted to identify challenges of reducing global warming in Africa through traditional African architecture and conclude by recommending the way forward.

INTRODUCTION

Global warming is an increase in the average temperature of the Earth's atmosphere, especially a sustained increase great enough to cause changes in the global climate. Global warming is synonymous with Enhanced green house effect, implying an increase in the amount of green house gases in the earth's atmosphere, leading to entrapment of more and more solar radiations, and thus increasing the overall temperature of the earth. Global warming is the 'talk of the town' in Africa today, especially with its detrimental effects already being brought to limelight by the recurring events of massive floods, and droughts throughout Africa. The average global temperatures are higher than they have ever been during the past millennium, and the levels of CO₂ in the atmosphere have crossed all previous records. The recent trends of increasing global temperatures and incidences of extreme climate events in Africa, mainly droughts and floods, are likely to continue. According to the most recent report of the Intergovernmental Panel on Climate Change (2007), Africa is likely to warm at a faster rate than the global average during this century. According to the same report, Africa is also the continent that is least likely to be able to cope with climate change. In the East African region, average temperatures have increased by about 0.5 0C over the last century, in some other African countries, there is evidence that average temperatures have increased by as much as 1.4 0C since the 1960s (McSweeney, 'et al'. 2008). Looking further ahead, up to 4.30C change in average temperatures by the 2080s is possible according to Hepworth & Goulden (2008). A temperature rise of that magnitude would have disastrous consequences for Africa.

Climate change poses a significant and unique challenge to Africa because so much of its economy depends so much on a climate-sensitive natural resource base like rain-fed and subsistence agriculture. Dependence on such resources exposes the continent to the risks of reduction in agricultural production, municipal water supply for home use and sanitation services, industrial water use and hydroelectric power generation. While it has not yet been precisely determined how much of the recent warming was caused by

human activities, the consensus among climate scientists is that most of the warming over the past 50 years was probably caused by human-produced greenhouse gases. When fossil fuels are burned to produce energy they release gases – in particular carbon dioxide (CO²) – which build up in the earth's atmosphere. These gases act like a greenhouse, trapping more and more of the sun's light and heat as more fossil fuels are burned. In Africa, fossil fuels are being used at an increasing rate to generate electricity, provide fuel for transport, and heat people's homes. This means more 'greenhouse gases'. The rapidly increasing levels of greenhouse gases in the atmosphere are causing global temperatures to rise at a rate that is unprecedented in modern human history. They are also causing changes in weather patterns, altering rainfall and the timing of the seasons. At the same time as coal, oil and gas is being taken out of the ground and used for heating, electricity and transport, the world's forests are disappearing. Deforestation is also a major contributor to climate change, because trees absorb CO², the most important greenhouse gas.

Global warming has also been motivated by some other human activities like construction. Construction use more than 40 percent of world energy as a result of the high embodied energy materials use in conventional construction, especially in building construction. Using materials like steel, granite, etc that has higher embodied energy in conventional building construction contribute to global warming. It is the recommendation of this paper that in the bid to reduce global warming in Africa, that traditional building materials, like earth, wood, bamboo etcetera which have low embodied energy should be used in building construction.

METHODOLOGY

This paper employs an extensive literature review and applies techniques which are common in content analysis. A thorough literature reviews was conducted to identify the effects of global warming in African, challenges of traditional African architecture and the way forward for traditional African architecture and their building materials in reducing global warming. The broad based, thorough and extensive reviews process aims at examining, synthesizing and recording all issues discussed by various authors in books, journals and other scholarly works. The effect of global warming in Africa and how it could be reduced using traditional African architecture becomes the focus of this paper.

EFFECTS OF GLOBAL WARMING

Global warming has resulted in the warming of the oceans, rising of the sea levels, melting of glaciers, and diminished snow cover in the Northern Hemisphere. The recent catastrophic climatic events like the massive floods in Pakistan India and Nigeria, the Hurricane Katrina in the United States, the prolonged droughts in Australia, China, Pakistan, India, Uganda and Texas, are all the results of increased temperatures due to global warming. During the 21st century, climatic disasters occurred five times as frequently and killed or affected seventy times as many people. Between 2000 and 2004, an average of 26 climatic disasters was reported each year. Thus, the immense geological changes will continue their destruction unabated if steps to mitigate global warming are not taken.

Some of the most obvious impacts of global warming on human communities will be due to the rise in sea level that occurs mainly because ocean water expands as it is heated. Melting of ice on glaciers and polar ice caps adds to the rise. The projected total rise is estimated to be up to one metre this century and the rise will continue for many centuries. The extremely unusual high temperatures in central Europe during the summer of 2003 led to the deaths of over 20,000 people. A warmer world will lead to more evaporation of water from the surface, more water vapour in the atmosphere and more precipitation on average. On average, floods and droughts are the most damaging of the world's disasters. Between 1975 and 2002, due to flooding from rainfall over 200,000 lives were lost and 2.2 billion affected, and due to drought over half a million lives were lost and 1.3 billion affected (Jonkman, 2005). Recent estimates are that by 2050 over 10% of the world's land area will be so affected According to Houghton (2011) extreme droughts will tend to be longer, measured in years rather than months, again leading to many millions of displaced people.

Climate change poses a significant and unique challenge to Africa because so much of its economy depends so much on a climate-sensitive natural resource base like rain-fed and subsistence agriculture. In 2012, 70 percent of major global droughts occurred in Africa. Kenya, Somalia, Sudan, Malawi, Angola, Chad and Ethiopia were particularly hit hard, and more than 16 million people in those countries were affected. In the same year, floods claimed 363 lives in Nigeria and 65 lives in Niger. In 2013, heavy rains continued with major flooding in Sudan, South Sudan, Mali, South Africa, Zimbabwe, Botswana and

Mozambique. The macro-economic impact of these episodes of extreme drought and flooding is significant. Having ascertained that building industry alone consumes over 40 percent of energy in Africa leading to global warming and climate change, it has been also ascertained that global warming and its effects can be reduced especially in Africa through traditional African architecture. According to Iwuagwu and Azubuine (2015) Africa's traditional architecture made certain that its use of the resources neither diminished their availability, nor adversely affected the ecological balance upon which it relied on as an agrarian society. African traditional architecture is essentially sustainable and had evolved culturally to suit the people. Usually, earth, timber, straw, stone/rock and thatch were constructed together with the simplest of tools and methods to build simple, livable dwellings. Although globalization according to Opaluwa, "et al". (2012) has relegated them as being 'primitive'. But a present interpretation of sustainability has given them a new status as likely technologies for the contemporary world.

AN XRAY OF SELECTED TRADITIONAL AFRICAN BUILDING MATERIALS

Straw/Thatch Architecture. In contrast to some other materials which are not easily renewed, straw/thatch is a by-product of grown plants hence, a cultivated material. Large quantities of this material could be sourced from the immediate surrounding as the villagers cultivate much of the straw as cereals in their farms which in turn provide them a building material. Straw has in most case being used with adobe bricks or masonry walls or singularly. Even today nomad tribes within Africa still use this form of construction. Straw construction uses matted or baled straw from wheat, oats, barley, rye, rice and others as walls or covered by earthen or lime stucco. Straw bale are traditionally a waste product; it is the dry plant material or stalk left in the field after a plant has matured and harvested.

Adobe Architecture. the cultural practice of the rural people indicates that adobe surely has been one of the most common and abundantly obtainable materials that influenced and sustained the rural villages in Africa. Local earth technologies of Africa have spanned from the employment of raw-earth, to refined earth brick. Generally employed was wattle-and-daub earth technology; a method that uses solid wooden post frame which is first made then filled with adobe balls to create a wall. Most often, the African builders construct the walls of their building layer by layer using the mud bricks and a slurry mixture of earth as the mortar. Once the wall dries up and binds into a monolithic structure, a dense mud plastic plaster strengthen with various additives depending on the people's culture (cow dung, goat dung, beaten straw, animal hair, animal skin fat) will be spread on by hands to smoothen the facade. The materials having being gotten from the environment certainly made it a highly sustainable practice that utilised small amount of energy and did not generate any greenhouse gas or harmful waste. As soon as it is plastered and properly covered with overhanging roofs, these earth buildings were structurally firm, environmentally sound and could exist for years as long as the day to day maintenance was adhered to.

Bamboo. Bamboo is one of the oldest traditional building materials used by mankind. When you're considering potential building materials for home construction as a society we tend to focus on two or three commonly utilized and widely accepted building materials: wood, stone or concrete. Uses for bamboo can also include building construction, both in exterior and interior design elements. Unlike wood, bamboo (a member of the grass family) regenerates very quickly. It is, in-fact, one of the fastest growing plants in the world, with the fastest growth rate reaching 100cm in a 24-hr period (Farrelly, 1984). In contrast to tree harvesting, there is simply no comparison to the replenishment rate of growing bamboo. Bamboo can be harvested every three to six years for construction purposes (depending on the species); whereas trees range from 25 years (for softwoods) to 50 years (for hardwoods). Major Advantages of Bamboo include: Strength and Durability; Affordability.

ADVANTAGES OF TRADITIONAL AFRICAN BUILDING MATERIALS

Availability. Traditional African building materials are abundant in nature. These materials include earth, stone, thatch, coconut fibre etc. for example earth building technology involves the use of laterite and loamy soil that exist in abundant supply in all part of the continent. Earth has been used by our fathers and fore-fathers to erect buildings, sometimes up to two storeys high without addition of any other reinforcing materials and most of them are still standing till date.

Affordability. The major reason for high cost of imported building materials in Africa includes high cost of importation and general inflation. Because of high cost of these imported building materials,

the low income earners find it difficult to construct their own houses or even rent a decent house. The availability of these local building materials makes the price affordable and gives the low income earners the opportunity to construct their own houses.

Energy Efficient. Environmental protective measures ensure reduction of operational energy in construction. Studies according to Iwuagwu and Azubuine (2015) reveal that the building sectors consume more than one third of the world's energy, and contribute to global warming. A typical traditional building of earth emits fewer greenhouse gases, consumes less energy, and maintains a high level of internal thermal comfort, regardless of prevailing solar radiation outside (Iwuagwu and Azubuine, 2015).

Ozone Friendly. The built environment contributes ultimately to global warming by its high rates of greenhouse gases emission through energy use (for cooling, heating, and lighting) and construction. Local building materials projects a possibility of total reduction to a near zero carbon emission of buildings. Local building materials are eco-friendly, climate responsive and organic protective measures to safeguard and as well minimize environmental impact. The thermal insulation, energy saving, etcetera of local building materials reduces negative environmental impact. The proximity of materials saves cost and reduces pollution by fuel burning through transportation.

Reusability. Reusability is a function of the age and durability of a material. Very durable materials may have many useful years of service left when the building in which they are installed is decommissioned, and may be easily extracted and reinstalled in a new site. Windows and doors, even brick can be successfully reused. Timber from old barns has become fashionable as a reclaimed material for new construction.

Biodegradability. The biodegradability of a material refers to its potential to naturally decompose when discarded. Organic materials can return to the earth rapidly, while others, like steel, take a long time. An important consideration is whether the material in question will produce hazardous materials as it decomposes, either alone or in combination with other substances. Traditional African building materials exhibit this characteristic, example include, earth, thatch, bamboo, timber etcetera.

CHALLENGES OF TRADITIONAL AFRICAN ARCHITECTURE AND THEIR BUILDING MATERIALS

Acceptability. The future of any Architecture depends on the extent to which it is acceptable to the people for whom it is intended. The notion that buildings of traditional materials are substandard is the main obstacle to the development of an authentic African Architecture that is truly indigenous to the people. Perhaps issue of acceptability has brought destruction of traditional values and their replacement with alien ones.

Durability/ Low Strength. The highest problem of houses built with traditional African building materials was the low strength of the houses, implying that the locally available materials have strength that is below expectation when compared with strength of the houses built with conventional materials such as cement, concrete, steel, among others. The strength of every house is important because it determines the durability and security of the house. This is consistent with the view of Venkatarama and Prasanna (2009) that one of the drawbacks for using earth alone as a material for construction is its durability which is strongly related to its compressive strength. Riza et al. (2011) further explained that most soil in their natural condition lack the strength, stability and durability required for building construction. The above indicates that the local materials for building houses lack the desired strength and improvement of their strength properties would be beneficial to the users.

Building Tall. The nature and strength of these traditional building materials make it impossible for building tall. They encourage low rise buildings leading to over use of land. Millions of acres of land in Africa have buildings constructed on them. For instance, spread of buildings require the construction of new roads, drainage, utility poles, and other infrastructure, which lead to, habitat destruction, land disturbance and erosion, environmental pollution, global warming among other.

Deforestation: the building materials sources in Africa contribute to prevailing problem of deforestation on the continent. When timber for construction is harvested, in many cases, replacement trees are not planted, if replanted, the rate of replacement is far lower than the rate of consumption.

Civilization. Local and indigenous cultures have practiced sustainable resource use due to their practical experience and human dependency on earth's life support systems. Traditional communities integrated buildings into the natural environment in terms of adequate use of cost effective and easily

assessable local building material for construction and maintenance. However, importation and the use of imported building materials has put the African traditional and sustainable way of building and construction processes in danger, thus relegating our architecture

Frequent Maintenance. Frequent maintenance of houses built with local materials especially earth, is another challenge facing African architecture. According to Rumana (2007) there is high maintenance requirement of earthen plinth and walls which are often plastered, especially during the wet season. This is due to the low strength of the materials that make it a requirement for the frequent maintenance in order to keep the building in good condition for use. If the houses built with local materials are not maintained regularly, they will deteriorate in some few years after their construction due to their vulnerability to weather such as rain and storm.

THE WAY FORWARD FOR TRADITIONAL AFRICAN ARCHITECTURE AND THEIR BUILDING MATERIALS

Re-engineering of traditional African building materials. Traditional African building materials should be re-engineered to suit the present need of building materials. Like the compressed earth block (CEB), this is an emerging alternative to adobe blocks and wattle and daub construction. Compressed earth blocks are a creative, re-engineering of the adobe brick. Unlike the native adobe block, which is a mixture of soil, water and distinct cultural additives moulded to desired shape with the hand, the compressed earth block is supplemented in very small amounts (in most cases less than 10%) with either cement or lime component in its blending process. The blend is not worked to achieve a plastic state, but simply blended until the cement/lime and soil are thoroughly mixed. Afterwards, the mixture either machine pressed or placed in a mould and compacted with a high level of pressure applied through a hand- operated machine. After aeration, the CEBs gain a high compressive strength appropriate generally for three floors constructions but higher potentials can also be attained for up to five floors constructions [Maini, 1999]. CEB construction is more durable than wattle and daub, and is also accepted as a more refined construction method than wattle and daub.

Combination with modern building materials. there should be combination of conventional building materials with traditional African building materials to add to their strength and durability. One of the disadvantages is strength, but that notwithstanding, in high rise buildings CEB could be used for the walling system not minding the height of the building while the conventional materials would be used for the foundation, reinforcement etcetera.

Government encouragement. government should encourage the use of local building materials by using them in government projects all over Africa. Traditional African building materials should be included in building code of various countries in Africa, as building materials. In every construction there should be a little destruction, efforts should be made to plant more trees and make sure natural resources are not being used more than it generate. As our natural resources are quickly depleting and our homes and vehicles are damaging our planet more than ever, it's time for a change. We should detach ourselves from the notion that local building materials are low-grade material. Considering the depletion of the ozone layer, high energy consumption by buildings we will realize that local building materials are not only the past, but the future of our society and one should take into consideration the benefits that they offer.

CONCLUSION

In general, the use of local materials needs to be supported and reinforced to produce sufficient quantities of materials of adequate quality to withstand the effects of climatic conditions which range from humid rainy seasons to extremely hot dry seasons. The submission of this paper is that with the use of traditional African building materials, we could achieve a huge reduction in global warming in Africa and save human and the environment. it is therefore necessary to promote the construction with traditional African materials and combine its potentials with modern technology so as to produce a new generation of buildings that are cheap, environmentally friendly and require no mechanical air-conditioning during hot days and nights.

REFERENCES

Farrelly, D. 1984. *The Book of Bamboo*. Sierra Club Books.

- Hepworth, N. & M. Goulden. 2008. "Climate Change in Uganda: Understanding the Implications and Appraising the Response". Scoping Mission for DFID Uganda.
- Houghton, J. R. 2011. "Global Warming, Climate Change and Sustainability: Challenge to Scientists, Policy Makers and Christians". JRI Briefing Paper No 14
- Intergovernmental Panel on Climate Change. 2007. "A Report of Working Group I of the Intergovernmental Panel on Climate Change: Summary for policymakers; Royal Society. (2010). Climate change: A summary of the science. <http://royalsociety.org/climate-change-summary-of-science/>
- Iwuagwu, B.U & C. E. Azubuine. 2015. *Global Warming Versus Green Architecture: African Experience*. Proceedings of International Conference on IT, Architecture and Mechanical Engineering (ICITAME'2015) May, 2015
- Jonkman, S. N. (2005). *Natural Hazards* 34, 151-175
- Maini S. 1999. "Seminar on earth architecture at Alliance Françoise De Colombo". Auroville Building Center, India
- McSweeney, C., M. New and G. Lizcano. 2008. "UNDP Climate Change Country Profiles: Uganda". New York: UNDP.
- Opaluwa E, P. Obi and O. C. Osasona. 2012. *Sustainability in traditional African architecture: a springboard for sustainable urban cities*. Proceedings of sustainable Futures: Architecture and Urbanism in the Global. South Kampala, Uganda, June 2012
- Rumana, R. 2007. "Traditional House of Bangladesh: Typology of House According to Materials and Location". Virtual Conference on Sustainable Architectural Design and Urban Planning AsiaSustainabilityNet.upc.edu, September 2007
- Riza, F. V., I. A. Rahman & A. M. A. Zaidi. 2011. "Preliminary Study of Compressed Stabilized Earth Brick (CSEB)". *Australian Journal of Basic and Applied Sciences*, 5(9) 6-12
- Venkatarama, R. B. V., & K. P. Prasanna. 2009. "Embodied energy in cement stabilised rammed earth walls". *Energy and Buildings*, 42(3) 380-385.

ENHANCEMENT OF WASTEWATER FACILITIES FOR LONG TERM GLOBAL CLIMATE CHANGES

Amirthaganth Amithalingam (Parsons Brinckerhoff Inc., Seattle, Washington, USA)
D. S. Mahamah (Saint Martin's University, Lacey, Washington, USA)

Most scientists and climate science practitioners agree that the global weather patterns are changing. In fact the general agreement is that the earth is warming at about 0.15°F per decade (USEPA). Although there is much disagreement on the causes, many believe gas emissions such CO₂ and other greenhouse gases are the culprit. The EPA indicates that the three major causes of global warming are: greenhouse effect, variation in the sun energy, and changes in reflectivity of earth surface and atmosphere. The effects of an increase in global temperature include, a rise in sea levels, changes in the amount and pattern of precipitation, expansion of subtropical deserts, threat to food security and more frequent occurrence of extreme weather events including heat waves, droughts and heavy rainfall. The operation and in particular performance of wastewater treatment plants (WWTPs) are temperature dependent. Effects of the temperature on the entire wastewater treatment process (production to treatment) can be identified as follows:

- Increased overflows- Results in more untreated sewer overflows, thus more raw sewage will be mixed with receiving bodies of water.
- Increased flooding of Treatment plants -With increased storms comes increased flooding which can be harmful to infrastructure since most WWTPs are in low, coastal areas.
- Effect on microbiology of treatment systems -Increased temperature in effluent has delicate effect on ecosystems which could affect the system negatively. In addition, biological speciation is temperature dependent and as such different bacterial populations dominate at different temperatures.

Suggested enhancement methodologies to the WWT Facilities so as to overcome impacts of long term climate change are include; utilizing Best Management Practices (BMP's), highly efficient flood management plan, bypass systems in case of emergency, backup power systems, and the continuous monitoring of influent characteristics so as to alter treatment methodologies accordingly etc. Impacts due to climate are not preventable but mitigated through BMP's and other efficient methodologies.

**AN INTEGRATED ASSESSMENT OF LOW CARBON EMISSION SCENARIOS PROPOSED
IN CLIMATE POLICY**

Sascha Hokamp and *Mohammad Mohammadi Khabbazan*

(Center for Earth System Research and Sustainability, University of Hamburg, Hamburg, Germany)

In 2015 the Conference of the Parties held in Paris, France, has discussed, among other things, climate policy proposals to decarbonize the global economy before the end of the 21st century. Eventually, on this challenging task the Conference of the Parties found no consensus view but nevertheless the final agreement of Paris calls for enhanced scientific investigation of low carbon emission scenarios. We pick up this call and address how carbon emission cuts in accordance to recent climate policy proposals may allow for holding the increase of global mean temperature below 2° Celsius. To tackle this research question, we employ the socio-economic integrated assessment Model of INvestment and endogenous technological Development (MIND), which has a sophisticated energy sector module. Further, we make use of a climate module consisting of three layers: Atmosphere, Upper Ocean, and Lower Ocean; a kind of climate modelling that is frequently used in the Dynamic Integrated model of Climate and the Economy (DICE) by William D. Nordhaus. We perform, within our stylized integrated assessment model, a cost effectiveness analysis with constraints on anthropogenic carbon emissions (instead of constraints on the increase of global mean temperature). We find that carbon emission cuts from 2100 onwards to annually 0.5 Giga tons Carbon lead to a stronger increase of global mean temperature in the short-term than the business as usual scenario without any changes of climate policy. In line with the literature this contra intuitive outcome can be explained by the vanishing cooling effect of sulfur dioxide. However, considering extremely low carbon emission scenarios we find that zero emissions from 2060 become feasible if the investments for renewable energy production peak in 2020, reach a plateau from 2040 to 2050, and decline thereafter. This finding seems to be driven by the depreciation rate of installed capacity devoted to renewable energy production. Hence, decarbonizing the global economy and meeting the 2° Celsius target could be possible before the end of the 21st century; but urgent action is necessary since the time window is closing for low carbon emission scenarios recently proposed in climate policy.

LEAPFROGGING CARBON CAPTURE SEQUESTRATION

Adel J. Al-Khalifah

(Saudi Electricity Company, EOA-Generation Technical Support Dept. Dammam, Saudi Arabia)

There are many barriers and knowledge gaps regarding the development of carbon dioxide capture and storage (CCS). For instances, when it comes to costs, life-cycle effects, and storage capacity. In spite of these barriers and need for further science studies, the scientists are generally very hopeful regarding CCS development. The purpose of this work is focus on two key aspects: First is the function and potential of CCS and secondly are uncertainties. The optimism among the CCS experts is tentatively explained. The explanatory flexibility of CCS is claimed to be an essential clarification for the optimism. CCS is promoted from a wide variety of perspectives, including team spirit, peace, bridge to a sustainable energy system, sustaining the modern lifestyle and compatibility with the fossil fuel lock-in. Awareness of the uncertainties and potential over-optimism is warranted within policy and decision making as they often rely on scientific forecasts and experts' judgements. Concerning economic barriers, governments should urgently consider methods to assist stakeholders to significantly drive down the cost of CCS deployment, since it is the stakeholders who will be making the majority of the financial investments. Also governments should review institutional regulatory policies to identify how the barriers to CCS deployment may be reduced. Finally, international collaboration should be a key component of any CO₂ emissions reductions strategy.

AEROBIC AND NITRITE-DEPENDENT METHANE OXIDIZERS IN THE ZOIGE WETLAND OF THE TIBETAN PLATEAU

Anzhou Ma, Guoqiang Zhuang, Mengmeng Cui

(Research Center for Eco-Environmental Sciences, Chinese Academy of Sciences, Beijing, China)

Methane (CH₄) plays an important role in global warming. However, most CH₄ is consumed by the methane oxidizers before its emission into the atmosphere. To investigate the impacts of CH₄ on global warming, it is important to understand the methane oxidizers in wetlands, the largest source habitat of atmospheric CH₄. In this study, we used quantitative PCR and functional gene-targeted 454 pyrosequencing to elucidate the abundance and diversity of aerobic methanotrophs and nitrite-dependent methane oxidizers (N-DAMO) in the Zoige Wetland, which is located on the Tibetan Plateau and is the largest alpine wetland in the world. Our results demonstrated type I methanotrophs were the primary aerobic methanotrophs, and *Methylobacter* comprised approximately 50% of the community. Type II methanotrophs, represented by the genus *Methylocystis*, were also detected, and the presence of N-DAMO bacteria in the Zoige Wetland was confirmed by the quantification and pyrosequencing analyses of N-DAMO 16S rRNA and *pmoA* genes. Moreover, *pmoA* ranged from 10⁷ to 10⁸ copies•g⁻¹ of fresh soil, and the 16S rRNA gene of the NC10 phylum ranged between 10⁴ and 10⁵ copies•g⁻¹ of fresh soil. The results suggest the aerobic methanotrophs and N-DAMO communities together affect CH₄ cycle at the Zoige Wetland.

ENERGY CONSERVATION HELPS IN MITIGATION OF ADVERSE EFFECTS OF CLIMATE CHANGE

Mehboob Alam Khan

(Energy Conservation Department, K-Electric, Karachi, Pakistan)

Energy generation plays a vital role in development of any country but at the same time it also enhances the emission levels if Energy is produced through Oil, Gas or other similar resources in which carbon is emitted.

In order to reduce carbon emissions the ultimate approach is to switch towards renewable and green Energy generation resources but shifting of peak demands requires sufficient amount of time and investments, as a low hanging fruit and workable solution to get **win win** situation is to opt for Energy Conservation methodologies by which we can easy reduce the load demand as well as Generation burden hence resulting in reduced carbon emissions which is the key element of Climate change.

This Paper explains how and by what measure we can reduce the demand of Electricity hence reducing carbon emissions to achieve an overall goal of mitigating adverse effects of Climate change and Global warming.

METALS

SPATIAL AND TEMPORAL DISTRIBUTION OF HEAVY METALS IN COASTAL RED SEA SEDIMENTS

Bandar Almur and Andrew Quicksall (Southern Methodist University, TX, USA)
Ahmed Al-Ansari (King Abdul-Aziz University, Saudi Arabia)

ABSTRACT: Jeddah is the most industrialized city on the west coast of Saudi Arabia. In this study, the spatial and temporal distributions of heavy metals were obtained from near-coast Red Sea sediment cores in close proximity to Jeddah. Six elements (Cr, Cu, Mn, Zn, Pb, and Fe) from three impacted locations (Prince Naif Street, the Downtown area, and Al-Khumrah) and an upstream reference site (Salman Gulf) were analyzed via heavy acid digestion and inductively coupled plasma-mass spectrometry (ICP-MS). The average concentrations of Cr, Cu, Mn, Zn, Pb, and Fe in core sediments of all sites were 245.96, 251.82, 478.45, 623.09, 362.75, and 8506.13 mg/kg, respectively. The depth-resolved results showed that highest concentrations of Mn, Cu, and Pb were found in the top 15 cm of the core profile distributions compared to other depth sub-samples. Heavy metal concentrations in core sediments seem to be increasing toward the area of the downtown and higher in the recent years. This indicates that this area has suffered from heavy metal pollution compare to other locations in the Red Sea. Heavy metal contamination due to anthropogenic activity should be taken into account to protect the Red Sea during future growth.

INTRODUCTION

Heavy metal contamination in sediments is a major environmental concern due to potential remobilization, bioaccumulation in fauna and flora and large mammal toxicity upon consumption of such biota (Nemati et al. 2011). Sediments are the primary sink of heavy metals in the aquatic environment due to their chemical-physical properties, such as particle characteristics, and processes including precipitation and sorption/desorption (Rath et al. 2009; Fukue et al. 2006). Determination of heavy metal concentrations in core sediments can provide important information about the current and the background levels of contamination. Furthermore, it may provide historical evidence of the anthropogenic effect in the aquatic environment (Chatterjee et al. 2007; Al-Najjar et al. 2011; Tang et al. 2010). Sediment cores can provide chronologies of contaminant concentrations and a record of the changes in concentrations of chemical indicators in the environment over time (Conrad et al. 2007; Li et al. 2012).

Here, Jeddah, Saudi Arabia is the area of study and the most industrialized city in the west coast of Saudi Arabia on the Red Sea. The coastal area of western Saudi Arabia has been subjected to pollution stress from land-based activities due to rapid increase in industrialization for several decades. The problem is greatly magnified by the production of numerous toxic chemicals that are harmful in trace concentrations (Badr et al. 2009; Usman et al. 2013; Ghandour et al. 2014). The study of depth-resolved heavy metals in coastal sediments is needed to provide useful information on human activities in the Jeddah area of the Red Sea. In the present study, four Red Sea sediment cores were collected near major industrialized areas in Jeddah, Saudi Arabia. Heavy metals were measured to investigate their spatial and temporal distribution pattern in the Red Sea. The results of this study fills the gap of research in the region and serve as a baseline for future studies in the Red Sea area. The aim of this study was to (i) assess of the spatial and temporal distribution of Cr, Cu, Mn, Zn, Pb, and Fe in the sediments of the coastal area of Jeddah; (ii) identify the origin of heavy metal pollutants in the sediment cores.

MATERIAL AND METHODS

Four Red Sea sediment cores were collected offshore of Jeddah in January 2015. Sites were chosen to cover the coastal area, which known to be affected by land-based activities. The four different sites were selected from three impacted locations (Prince Naif Street, the Downtown area, and Al-Khumrah) and an upstream reference site (Salman Gulf). Figure 1 shows a location of the study area and sampling sites. Each sampling location was determined using a GPS and located between 21° 51' 52" N and 39° 9' 26" E. Sediment cores were collected by scuba divers, using PVC tubes of 75 cm long and 5 cm in diameter. The cores were kept in an icebox at 4°C until delivered to the laboratory for analysis. After core samples were obtained at selected locations across the study area, samples were stored frozen at -20°C for 24 hours. Sediments were recovered from the PVC tubes and sliced at 2 cm interval. Each layer was homogeneously mixed and stored in plastic vials, labeled, and stored frozen at -20°C until shipping to U.S.A.



FIGURE1. Map of four sampling location in the west coast of Saudi Arabia on the Red Sea.

Sediment samples were prepared according to US EPA 3050B method to determine the total heavy metals for Cr, Cu, Mn, Zn, Pb, and Fe in core sediments. Briefly, samples were dried in an oven at 105°C and ground into a powder using a mortar and pestle. Nitric acid (70% HNO₃) and hydrofluoric acid (HF) were used for the total metal analyzes. Approximately 0.20 grams of the sediment samples were digested in heavy acid with 3:1 mixture of HNO₃ and HF acid. Nine ml of HNO₃ and three ml of HF were added to the sediment samples inside a fume hood. Sediment samples plus HNO₃ and HF acid were digested at 100°C on a hot plate until dryness. The solutions were allowed to cool to room temperature. The metal determinations were performed on ICP-MS in collision cell mode with kinetic energy dispersion (CCT-KED). For Quality Control (QC) and Quality Assurance (QA), blanks and replicates (about 10 % of the total number of samples) were analyzed to check precision under the same procedures mentioned above. A multi-element standard was used with a range from 0.5 to 75 ppb. The calibration curves were based on

elements standard solution were obtained. A blank (5% HNO₃) was analyzed every 10 samples. The final concentration of each metal was reported in mg/kg dry weight.

RESULTS AND DISCUSSION

Heavy metal concentration variations at different depths for sediment cores are shown in Figure 2. Heavy metal distributions at four different locations with depths between 0 and 50 cm were evaluated throughout this study. Generally, heavy metals concentrations increase stratigraphically through the cores with a constant decrease from the top to lower level of the sediment cores. The highest concentration of heavy metals in the upper-most segments of the sediment cores compared to lower depth sub-samples for most of metals suggests increases in metals delivery to sediments in recent years (Figure 2). These high concentrations likely correspond to an increase in anthropogenic pollutant inputs from urbanization and industrialization. In this study, the results show that the average total concentrations as follows: Mn 478.45, Cr 245.96, Cu 251.82, Zn 623.09, Pb 362.75, and Fe 8506.13 mg/kg. The highest concentrations of all heavy metals were found at the downtown area.

Several authors have investigated the levels of heavy metal pollution in the marine environment of the Red Sea, especially near Jeddah (Badr et al. 2009; Al-Najjar et al. 2011; Pan et al. 2011; Usman et al. 2013; Ghandour et al. 2014). Concentrations of Mn, Zn, Cu, and Cd in sediments of Jeddah were studied by different scientist (Badr et al. 2009; Ghandour et al. 2014). In fact, most of the studies that have been carried out on the marine environment of the Red Sea have been concentrated in the central and northern parts of the coastal waters of Jeddah (Badr et al. 2009; Ghandour et al. 2014). In general, the higher concentrations of Mn in core sediments in the present study areas were similar to those found in Red Sea sediments by Hilal et al. (1988) and Ghandour et al (2014) in sediment composition of an arid coastal environment. In comparison with other studies in the Red Sea, little information on Fe concentration has been reported. In the present study, the higher concentrations of Fe were similar to Badr et al. (2009) results in Salman Gulf and Al-Khumrah areas and less than the world average concentration (48,000 mg/kg) (Venkatraman et al. 2015).

Zn is a natural abundant element and can present in marine environment via human activities, such as food wastes, antifouling paints, and manufacturing of pesticides (Badr et al. 2009). The results of Zn were similar to Pan et al. (2011) and Badr et al. (2009) and they indicate that the high concentration of Zn might be due to recently anthropogenic activities in this area. Levels of Zn concentration in Salman Gulf, Prince Naif Street, and the Downtown areas were high from 15 cm to the surface area and significantly high in Salman Gulf in the same vertical distribution as shown in Figure 2. The higher concentrations start from the top 15 cm to the surface area indicate of being influenced from human activities from hidden non-point sources occur in the recent years or could be natural occur due to the high carbonate present in this area as ZnCO₃ (Othmani et al. 2015).

Linear regression analysis showed the strong positive correlation in some area between Mn and Cr and Fe (Naif Street, and the Downtown) and not correlation in other area (Salman Gulf and Al-Khumrah). The strong significant positive correlation are found in the Downtown area among Mn and Fe ($r^2= 0.94$ $p < 0.05$), Cr and Fe ($r^2= 0.6$ $p < 0.05$) and Cr with Mn ($r^2= 0.54$ $p < 0.05$) (Table 1). Pattan et al. (1995) found that Cr, a redox sensitive metal, was precipitated with Mn-Fe oxide. The correlation analysis indicates that Cr, Mn, and Fe have a significant positive correlation and could indicate of a redox condition in the Downtown area. Fe and Mn oxides have been recognized as playing a significant role in controlling the location of heavy metal pollution in sediments (Gasparatos 2012).

Usman et al. (2013) studied the heavy metal contamination in mangroves from the coastal of the Red Sea. Their result revealed that Cu and Cr were highly bio-accumulative in mangroves (*A. marine.*) from the coastal of the Red Sea. In this study, the results of Cu indicate that Cu were following the same vertical profile of Mn and Pb, which was higher in the recent years (top 15 cm to the surface area) with a highly significant increase in the downtown area (Figure 2). The higher concentrations of Cu and organic matter in the Downtown area indicate of complexes of Cu with organic matter (Sun & Puettmann 2000; Tribovillard et al. 2006). The average concentrations of Cu were 251.82 mg/kg while sediments having a

higher concentration than 60 mg/kg is classified as contaminated via the US EPA (Ingersoll and Nelson 1989). The major source of Cu in the marine environment due to antifouling paints, which is most boaters use it and content high copper concentration (CuO ~ 75%) (Srinivasan and Swain 2007). Copper also easily enters into the marine environmental through industrial discharge containing CuSO₄, which is used in metal plating and fishing operations (Srinivasan and Swain 2007).

TABLE 1. Correlation coefficient matrix (r^2) for heavy metal concentrations in four core sediments (n=180) from coastal Red Sea (P<0.05).

Salman Gulf (Core1)						
	Cr	Mn	Fe	Cu	Zn	Pb
Cr	1.00					
Mn	0.57	1.00				
Fe	0.33	0.29	1.00			
Cu	0.43	0.69	0.21	1.00		
Zn	0.40	0.67	0.24	0.41	1.00	
Pb	0.07	0.24	0.0	0.19	0.02	1.00
Prince Naif Street (Core2)						
	Cr	Mn	Fe	Cu	Zn	Pb
Cr	1.00					
Mn	0.70	1.00				
Fe	0.63	0.83	1.00			
Cu	0.49	0.48	0.27	1.00		
Zn	0.00	0.00	0.00	0.01	1.00	
Pb	0.46	0.22	0.12	0.56	0.00	1.00
The Downtown (Core 3)						
	Cr	Mn	Fe	Cu	Zn	Pb
Cr	1.00					
Mn	0.54	1.00				
Fe	0.60	0.94	1.00			
Cu	0.19	0.74	0.69	1.00		
Zn	0.29	0.73	0.69	0.73	1.00	
Pb	0.31	0.60	0.50	0.48	0.54	1.00
Al-Khumrah (Core 4)						
	Cr	Mn	Fe	Cu	Zn	Pb
Cr	1.00					
Mn	0.53	1.00				
Fe	0.21	0.24	1.00			
Cu	0.09	0.36	0.11	1.00		
Zn	0.13	0.44	0.06	0.06	1.00	
Pb	0.66	0.78	0.23	0.27	0.33	1.00

Mean concentrations of lead in the studied sediment profiles showed high values in all cores (362.75 mg/kg). Othmani et al. (2015) reported that Pb is strongly complex with CaCO_3 , which acts as a strong absorbent for Pb and can complex as PbCO_3 . This is attributed to several sources such as boat exhaust systems, spilling of oil, the discharge of sewage effluents, and atmospheric input of Pb (Abo-Hilal et al. 1987). The high level of Pb in Red Sea may due to the use of gasoline as a possible reason contamination (Usman et al. 2013). Other authors assign to Pb contamination of marine sediments to boat exhaust emissions, leakage of oil from mechanized boats and sewage effluents (Badr et al. 2009).

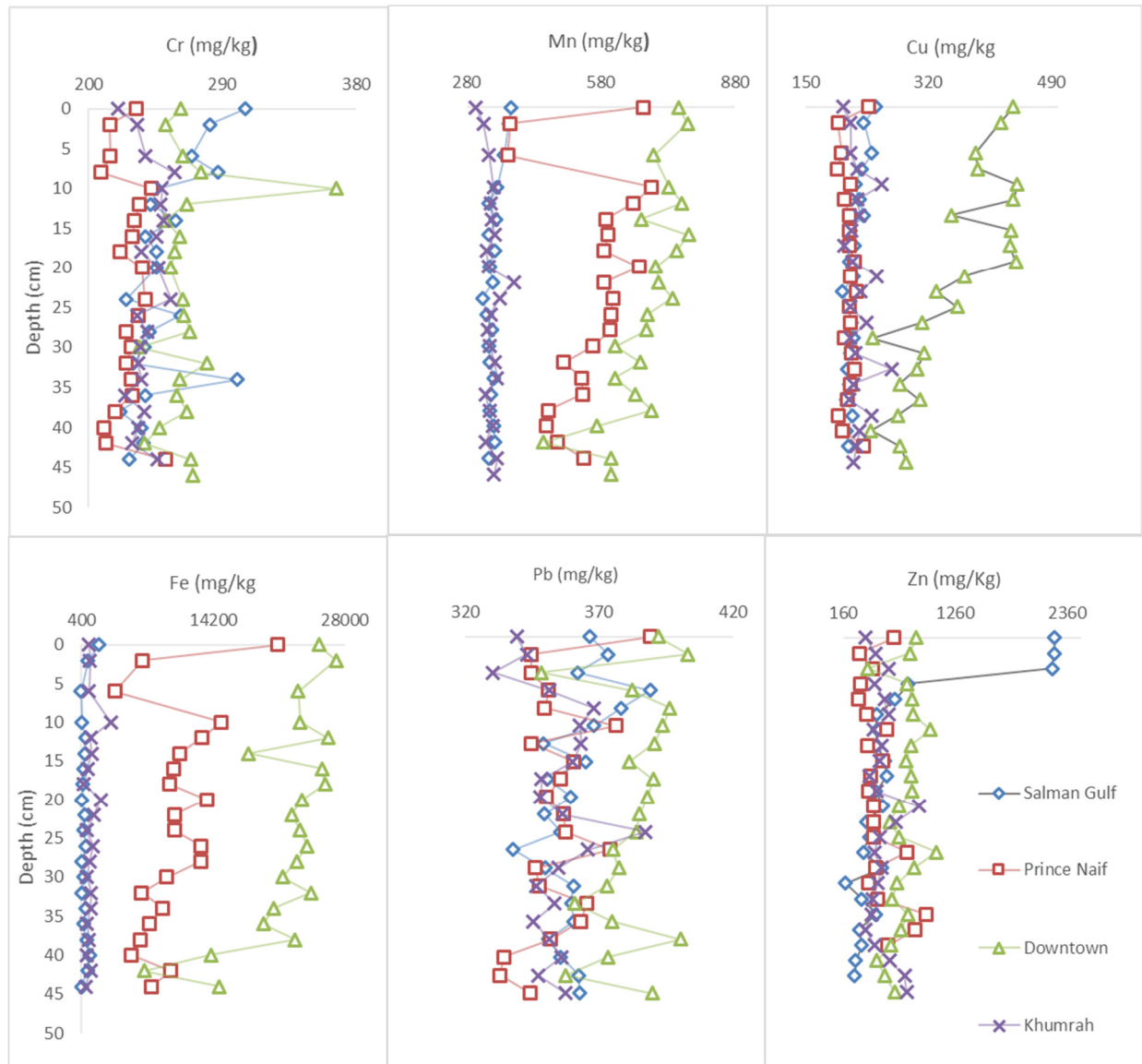


FIGURE 2. Vertical distribution of heavy metal concentrations in different depth of four core sediments on the Red Sea offshore Jeddah coast.

Generally, in the Red Sea, the average concentration of Mn, Cu, and Pb in all sediments followed the order: The Downtown > Prince Naif Street > Salman Gulf > Al-Khumrah. The influence of anthropogenic activities, such as fertilizers and sewage wastes are the primary metals sources on the marine

environment (Qiu et al. 2011; Varol 2011). Shang et al. (2015) results indicate that the significant positive correlation among Cu, Mn, Fe, and Zn. The sources of heavy metals in the considered areas are mainly natural as well as anthropogenic through the impact of oil refinery wastes, untreated sewage effluents, and cement plants, which had been increased over the past years. The significantly positive correlations at the Downtown area of Fe ($r^2 = 0.94$ $p < 0.05$), Cu ($r^2 = 0.74$ $p < 0.05$), Zn ($r^2 = 0.73$ $p < 0.05$) and Pb ($r^2 = 0.60$ $p < 0.05$) with Mn (Table 1) showed that heavy metal pollutants were most likely derived from same source of contamination. Given the association of Mn, Cu, and Pb and copper's use as an indicator of organic complexes (Sun & Puettmann 2000; Tribouvillard et al. 2006), Pb and Mn are, therefore, likely being delivered to the seafloor as organic matter complexes. Recognizing the speciation of these metals during and post delivery may play a key role in potential mitigation and/or treatment.

CONCLUSION

Heavy metal concentrations in four sediments cores from the Red Sea near Jeddah were analyzed. The results showed high heavy metal concentrations of Mn, Cu, and Pb. Based on the heavy metal concentrations, this study indicates that the heavy metals in the core sediments were much higher in the top 15 cm. Generally, the results of heavy metal concentrations suggest that some area may be strongly impacted by anthropogenic sources with major contamination of Mn, Cu, and Pb. Future research would include isotopic data for sediment age dating by measuring the gamma emitting isotope. Sediments samples will be analyzing to measure radioactive ^{210}Pb to assign an absolute age and sedimentation rates on Red Sea sediments.

ACKNOWLEDGEMENTS

This research was financially supported by King Abdul-Aziz University, Jeddah, Saudi Arabia.

REFERENCES

- Al-Najjar, T., Rasheed, M., Ababneh, Z., Ababneh, A., & Al-Omarey, H. (2011). Heavy metals pollution in sediment cores from the Gulf of Aqaba, Red Sea. *Natural Science*, 03(09), 775-782.
- Badr, N. B., El-Fiky, A. A., Mostafa, A. R., & Al-Mur, B. A. (2009). Metal pollution records in core sediments of some Red Sea coastal areas, Kingdom of Saudi Arabia. *Environ Monit Assess*, 155(1-4), 509-526.
- Chatterjee, M., Silva Filho, E. V., Sarkar, S. K., Sella, S. M., Bhattacharya, A., Satpathy, K. K., et al. (2007). Distribution and possible source of trace elements in the sediment cores of a tropical macrotidal estuary and their ecotoxicological significance. *Environ Int*, 33(3), 346-356.
- Conrad, C. F., Fugate, D., Daus, J., Chisholm-Brause, C. J., & Kuehl, S. A. (2007). Assessment of the historical trace metal contamination of sediments in the Elizabeth River, Virginia. *Mar Pollut Bull*, 54(4), 385-395.
- Fukue, M., Yanai, M., Sato, Y., Fujikawa, T., Furukawa, Y., & Tani, S. (2006). Background values for evaluation of heavy metal contamination in sediments. *J Hazard Mater*, 136(1), 111-119.
- Gasparatos, D. (2012). Sequestration of heavy metals from soil with Fe-Mn concretions and nodules. *Environmental Chemistry Letters*, 11(1), 1-9.
- Ghandour, I. M., Basaham, A. S., Al-Washmi, H. A., & Masuda, H. (2014). Natural and anthropogenic controls on sediment composition of an arid coastal environment: Sharm Obhur, Red Sea, Saudi Arabia. *Environ Monit Assess*, 186(3), 1465-1484.
- Ingersoll, C. G. & Nelson, M. K. (1989). Testing sediment toxicity with *Hyallorella azteca* (Amphipoda) and *Chironomus riparius* (Diptera). ASTM STP 13th Symposium on Aquatic Toxicology Risk Assessment, Atlanta, Georgia, 43.
- Nemati, K., Abu Bakar, N. K., Abas, M. R., & Sobhanzadeh, E. (2011). Speciation of heavy metals by modified BCR sequential extraction procedure in different depths of sediments from Sungai Buloh, Selangor, Malaysia. *J Hazard Mater*, 192(1), 402-410.

- Othmani, M. A., Souissi, F., Duraes, N., Abdelkader, M., & da Silva, E. F. (2015). Assessment of metal pollution in a former mining area in the NW Tunisia: spatial distribution and fraction of Cd, Pb and Zn in soil. *Environ Monit Assess*, 187(8), 523.
- Pan, K., Lee, O. O., Qian, P. Y., & Wang, W. X. (2011). Sponges and sediments as monitoring tools of metal contamination in the eastern coast of the Red Sea, Saudi Arabia. *Mar Pollut Bull*, 62(5), 1140-1146.
- Pattan, J. N. Rao Ch, M. Higgs, N. C. Colley, S. & Parthiban, G. (1995). Distribution of major, trace and rare-earth elements in surface sediments of the Wharton Basin, Indian Ocean. *Chemical Geology*, 121, 201-215.
- Qiu, Y. W., Yu, K. F., Zhang, G., & Wang, W. X. (2011). Accumulation and partitioning of seven trace metals in mangroves and sediment cores from three estuarine wetlands of Hainan Island, China. *J Hazard Mater*, 190(1-3), 631-638.
- Rath, P., Panda, U. C., Bhatta, D., & Sahu, K. C. (2009). Use of sequential leaching, mineralogy, morphology and multivariate statistical technique for quantifying metal pollution in highly polluted aquatic sediments--a case study: Brahmani and Nandira Rivers, India. *J Hazard Mater*, 163(2-3), 632-644.
- Srinivasan, M., & Swain., G. (2007). Managing the Use of Copper-Based Antifouling Paints. *Environ Manage* 39:423-441.
- Sun, Y., & Puettmann, W. (2000). The role of organic matter during copper enrichment in kupferschiefer from the Sangerhausen Basin, Germany. *Organic Geochemistry* 31 (11), 1143-1161.
- Tang, W., Shan, B., Zhang, H., & Mao, Z. (2010). Heavy metal sources and associated risk in response to agricultural intensification in the estuarine sediments of Chaohu Lake Valley, East China. *J Hazard Mater*, 176(1-3), 945-951.
- Tribovillard, N., Algeo, T.J., Lyons, T., Riboulleau, A. (2006). Trace metals as paleoredox and paleoproductivity proxies; an update. *Chemical Geology* 232 (1-2), 12-32.
- Usman, A. R., Alkredaa, R. S., & Al-Wabel, M. I. (2013). Heavy metal contamination in sediments and mangroves from the coast of Red Sea: *Avicennia marina* as potential metal bioaccumulator. *Ecotoxicol Environ Saf*, 97, 263-270.
- U.S. Environmental Protection Agency. (1995). Test Methods for Evaluating Solid Waste. Vol. IA: Laboratory Manual Physical/Chemical Methods, SW 846 U.S. Gov. Print. Office. Washington, DC.

**VERTICAL DISTRIBUTION AND CHEMICAL BEHAVIOR OF URANIUM IN THE
TAILINGS MATERIAL OF SCHNECKENSTEIN (GERMANY)**

Taoufik Naamoun

(University of Sfax, Faculty of Sciences, Route de Soukra Km 3,5; P.B. 1171, Sfax, 3000, Tunisia)

Broder Merkel

(TU Bergakademie Freiberg, Gustav-Zeuner-Str. 12 . D-09596 Freiberg, Germany)

The purpose of this study was to investigate the spatial distribution of uranium and its mobility. In this work, the total concentration of uranium was determined by means of gamma and alpha spectrometry. The study of uranium mobility in selected samples from different intervals was made by the application of a seven steps sequential extraction procedure. Also hydrochemical investigation was carried out. The distribution of uranium species and saturation indices were calculated by means of the hydrochemical model PHREEQC. Results showed that uranium content ranges from 185 Bq/kg in the heap material to 6193 Bq/kg in the processed material. Also the data analysis shows the high uranium contents in most analysed water samples. Moreover, the PHREEQC model indicates the change of the tailing sediments with depth from aerobic to post aerobic or anaerobic conditions. Moreover, it illustrates the presence of uranium mostly (90%) in its high soluble form $\text{UO}_2(\text{CO}_3)_3^{4-}$. This is in agreement with the results of the selective extraction procedure which proves the association of important amounts of its contents with the carbonate phase (until 24%). Furthermore, as between 30 and 80 % of the non residual uranium is in association with the nodular hydrogenous fraction, the decrease of the Eh values in the study areas enhance its solubility.

SYNERGETIC EFFECTS OF Cd²⁺ AND Cu²⁺ ON CHLOROPHYLL FLUORESCENCE OF MICROCYSTIS Aeruginosa

Cui Jiansheng, Song Yanyan

(Hebei University of Science and Technology, Shijiazhuang, Hebei, China)

Microcystis aeruginosa as testing plant was selected to investigate the effects of Cd²⁺ Cu²⁺ to its chlorophyll fluorescence property under temperature (25°C), humidity (75%RH) and photoperiod (2000-3000 lux). The separated and combined effects of different concentrations Cd²⁺ and Cu²⁺ on chlorophyll fluorescence intensity of *Microcystis aeruginosa* were investigated. The experiment took the Cu²⁺ (0.2 mg/L) as the invariant, and Cd²⁺ (0.1 mg/L, 0.4 mg/L, 0.6 mg/L, 0.2 mg/L) as the variable. The heavy metals were added to the *Microcystis aeruginosa* which was in logarithmic phase growth. Determine the chlorophyll fluorescence intensity at the same time and observe the changes, taking 96 h as a cycle. Results showed that chlorophyll fluorescence intensity were significantly upregulated by exposure to lower concentrations of Cd²⁺ (< 0.5 mg/L), and the changing trends is of time-dependence at higher exposure concentration. When the exposure concentration of Cd²⁺ were 0.2 mg/L and 0.6 mg/L at 96 h, the inhibition ratio of chlorophyll fluorescence intensity were 0.36% and 30.48%, respectively. A similar trend of the fluorescence intensity were observed by exposure to Cu²⁺ (0.2 mg/L). When its exposure time was 96 h, the inhibition ratio of chlorophyll fluorescence intensity was 25.58%. Compared to the exposure of Cu²⁺, the tolerance of *Microcystis aeruginosa* was stronger when exposure to Cd²⁺, demonstrating the stronger toxicity of Cu²⁺ to the fluorescence intensity of *Microcystis aeruginosa*. The chlorophyll fluorescence intensity and exposure concentration was both time-dependent and concentration-dependent by exposure to Cd²⁺ and Cu²⁺, simultaneously. After 96 h exposure time, the inhibition ratio of chlorophyll fluorescence intensity was 48.83% when the exposure concentration of Cd²⁺ and Cu²⁺ were both 0.2 mg/L, the toxicity of which was much higher than that when single heavy metals was exposed. Moreover, when the exposure concentration of Cd²⁺ and Cu²⁺ were 0.6 mg/L and 0.2 mg/L, respectively, the inhibition ratio of chlorophyll fluorescence intensity was up to 58.14%. All these results confirm the significant synergetic effects of Cd²⁺ and Cu²⁺ stress on chlorophyll.

CHARACTERISTICS OF HEAVY METAL POLLUTION FROM ANTIMONY MINING, ORE DRESSING AND SMELTING PROCESS IN CHINA

Mengchang He

(State Key Laboratory of Water Environmental Simulation, School of Environment, Beijing Normal University, Beijing 100875, China)

China has the most abundant antimony (Sb) resources of any country in the world, and was the highest producer of Sb, with approximately 84.0% of the world's share. Antimony mining and smelting industries produced huge amounts of wastes, and release large quantities of Sb, As and other heavy metals into the environment. In general, the Sb and As pollution from the metallurgical area is very severe, and has resulted in significant environmental problems. In recent years, more than Sb pollution accident occurred in China. The Chinese government strengthens the prevention and control of heavy metal pollution from Sb nonferrous industry, and issued the "Emission standards of pollutants for stannum, antimony and mercury industries" (GB30770-2014).

In this study, the waste waters, solid wastes and dusts from main Sb mining, ore-dressing and smelting enterprises in China were sampled. The Sb, As and other heavy metals were determined. The leaching characteristics of heavy metals in the Sb-bearing waste rock and ores were also studied. High concentrations of Sb and As were found in the mine water inrush and mineral processing wastewater. The tailings reservoir overflow also has high Sb and As concentration. The mining and smelting activities produced huge quantities of Sb-bearing waste rock and tailings. These solid wastes released high concentration of Sb and As due to the dissolution and weathering. The release percentage of Sb and As from three ores are different. The various solid wastes from smelting processes, which included water-quenched slag, arsenic-alkali residue, desulfurized slag and blast furnace dust, were enriched in a variety of heavy metals and metalloids. And more specifically the As and Sb levels in arsenic-alkali residue are up to 8.6×10^4 and 3.16×10^5 mg/kg, respectively. The smelting activities also cause serious Sb and As pollution in the soil profiles around the Sb metallurgical area. The highest degree of Sb was found in the uppermost layers of the profiles (<40 cm).

CITRIC ACID ENHANCED METALS IN REED SEEDLINGS IN ACID MINE DRAINAGE SOLUTIONS

Lin Guo (Texas A&M University-Commerce, TX, USA)
Teresa J. Cutright (The University of Akron, OH, USA)

ABSTRACT: Acid mine drainage (AMD) with low pH and high levels of heavy metals affects many regions in the worlds. Wetland plant *Phragmites australis* (common reed) is widely used to treat AMD contaminated sites. This study investigated the effects of different levels (low 0.34 g/L, middle 17.86 g/L and high 33.62 g/L) of chelator citric acid (CA) on metal (i.e. Fe, Al and Mn) accumulation in reeds cultured in AMD contaminated solution for 12 weeks. The results indicated that CA increased Fe and Mn accumulation in both belowground and above ground tissues of reeds. The more CA was added, the more Fe and Mn were accumulated in plants. However, the Al accumulation in reeds was not affected by CA. After 12 weeks, 0.18 ± 0.01 mg Mn/g, 56.78 ± 7.63 mg Fe/g, and 0.60 ± 0.01 mg Al/g were accumulated in roots; while 0.06 ± 0.01 mg Mn/g; 6.38 ± 0.06 mg Fe/g; and 0.19 ± 0.01 mg Al/g were sequestered in stems of reeds treated with 33.62 g/L CA. Further research is needed to study the application of CA to enhance the phytoremediation efficiency of AMD contaminated field.

INTRODUCTION

Acid mine drainage (AMD) is a serious environmental issue (Whitehead and Prior, 2005). AMD is produced when sulfide minerals which were initially under anoxic conditions are exposed to oxygen and water during mine activity (Akcil and Kodals, 2006). AMD can severely contaminate soils, affect water quality and pollute ecological environments due to its low pH and high concentrations of toxic elements (Peppas et al., 2000).

Wetland plants species that can survive under atrocious conditions (i.e. low pH and low levels of nutrients, high concentrations of metal concentrations), such as common reed *Phragmites australis* and cattail *Typha latifolia* are commonly used to treat AMD contaminated sites (Stoltz and Greger, 2006; Batty and Younger, 2004). However, a main disadvantage of phytoremediation is that its efficiency is affected by the mobility of metals. To overcome this limitation, chelators are applied to contaminated environment, to enhance metal bioavailability and subsequent increase accumulation by plants (Garbisu and Alkorta, 2001). The main mechanism is that chelator can react with metals to form metal-chelate complexes, thus prevent the precipitation of metals and maintain their availability for plant uptake (Marques et al., 2009). Several chelating agents, such as Ethylenediaminetetraacetic acid (EDTA) and citric acid (CA) have been studied and applied to increase the bioavailability of heavy metals and enhance the metals accumulation in plants. However, most of the research focused on heavy metals contaminated soil. Little was known whether chelator CA can be effective in increasing phytoremediation efficiency from heavy metal contaminated water. Even less is known about the effect of CA on metal accumulation in plants from AMD contaminated solutions with low pH. This study will address the knowledge gap by investigating the effects of different levels of CA on metal (i.e. Fe, Al and Mn) accumulation in reeds cultured in AMD contaminated solution for 12 weeks.

MATERIALS AND METHODS

Plant Sources. Rhizomes of *P. australis* were randomly collected from an AMD-contaminated site located in Beaver Township, North Lima, Ohio, USA. After cleaning with distilled (DI) water, rhizomes were

transferred into commercial potting soil. After 30 days, new seedlings from the wild rhizomes with similar biomass were used to initiate the seedling (i.e., young reeds) hydroponic experiments.

Hydroponic Solutions. The control group only contained nutrient materials, 0.250 g N (NH_4NO_3), 0.060 g Mg ($\text{MgSO}_4 \cdot 7\text{H}_2\text{O}$), 0.109 g P (KH_2PO_4), and 0.207 g K (KH_2PO_4 and K_2SO_4) per liter DI water (Guo and Cutright 2014). The treatment solution contained nutrients, synthetic AMD and different levels of CA (control 0 g/L, low 0.34 g/L, middle 17.86 g/L and high 33.62 g/L). The metal concentrations used in synthetic AMD were based on the characteristics of AMD described by Senko et al. (2008) and the metal levels of the actual AMD contaminated site (Sivaram. 2010). Synthetic AMD contained 42.94 g Fe ($\text{FeSO}_4 \cdot 7\text{H}_2\text{O}$), 0.27g Al ($\text{Al}_2(\text{SO}_4)_3 \cdot 16\text{H}_2\text{O}$), 0.05 g Mn ($\text{MnSO}_4 \cdot \text{H}_2\text{O}$), 1.24 g Ca ($\text{CaSO}_4 \cdot 2\text{H}_2\text{O}$), 0.59 g Mg ($\text{MgSO}_4 \cdot 7\text{H}_2\text{O}$), and 0.28 g Na (Na_2SO_4) per liter of DI water. The pH was adjusted to 3.5 with H_2SO_4 (Senko et al. 2008). The dosages of CA were selected based on previous research (Mihalík et al. 2010) and the concentrations of metals in solution. Reeds were cultured in each hydroponic solution for 12 weeks and then harvested for analysis.

Plant Digestion. Upon harvesting, the roots of reeds were gently washed with DI water. Next, reeds were further separated into roots, rhizomes, stems, and leaves and air dried. One gram of dried tissue sections were digested as described in Cutright et al. (2010). The solutions were analyzed by inductively coupled plasma mass spectrometry (Perkin-Elmer Plasma 400 Spectrophotometer ICP-MS). All experiments were conducted in triplicate.

Statistically Analysis. The metals uptake in reeds were analyzed with one-ANOVA using the Minitab statistical package (Minitab 16). Differences between specific CA levels were identified by the Tukey test at 5 % probability

RESULTS AND DISCUSSIONS

Mn Accumulation. As indicated in Figure 1, CA enhanced the Mn accumulation and translocation in all the tissues of reeds ($p < 0.05$). For instance, after 12 weeks, the rhizomes in high level of citric acid (HC) contained 0.17 ± 0.01 mg/g Mn which was also significantly higher ($p < 0.05$) than that in the rhizomes grown in solutions without citric acid (NC) for the same period (0.10 ± 0.01 mg/g Mn).

According to the results of Najeeb et al. (2009), significant enhancement in Mn accumulation and translocation in *J. effusus* plants cultured in Mn hydroponic solution was recorded under the application of CA. The elevated Mn translocation caused by chelator may related to the activation of ATPase in the plasma membrane which can produce and then increase the translocation of both essential and non-essential metals (Najeeb et al., 2009; Williams et al., 2000). It was also reported that CA can enhance metal mobility by formation of metal-chelator complex or change of binding sites (Wang et al., 2009). Furthermore, CA may alleviate the toxic effects of Mn to plants which enable to increase the accumulation of Mn in plants (Najeeb et al., 2009).

Fe Accumulation. As shown in Figure 2, CA also played an important role in increasing the accumulation of Fe in both underground and above ground tissues of reeds during all the growth period ($p < 0.05$). After 12 weeks, the Fe levels in roots of reeds grown in solution with middle levels of CA (MC) and low levels of CA (LC) for were 33.31 ± 3.03 mg/g Fe, 47.72 ± 1.57 mg/g Fe, respectively. CA also increased the Fe amounts in the aboveground tissues of reeds. For instance, the leaves of reeds grown in solution HC for 12 weeks contained 3.47 ± 0.01 mg/g Fe. It was significantly higher ($p < 0.05$) than the Fe concentrations in leaves of reeds grown in solution LC for the same time period (2.05 ± 0.01 mg/g). Citrate can maintain Fe in a soluble form by forming of stable plant-available organic- Fe^{3+} complexes at low pH value (< 6.8) (Jones et al., 1998), thus enhance Fe accumulation in plants.

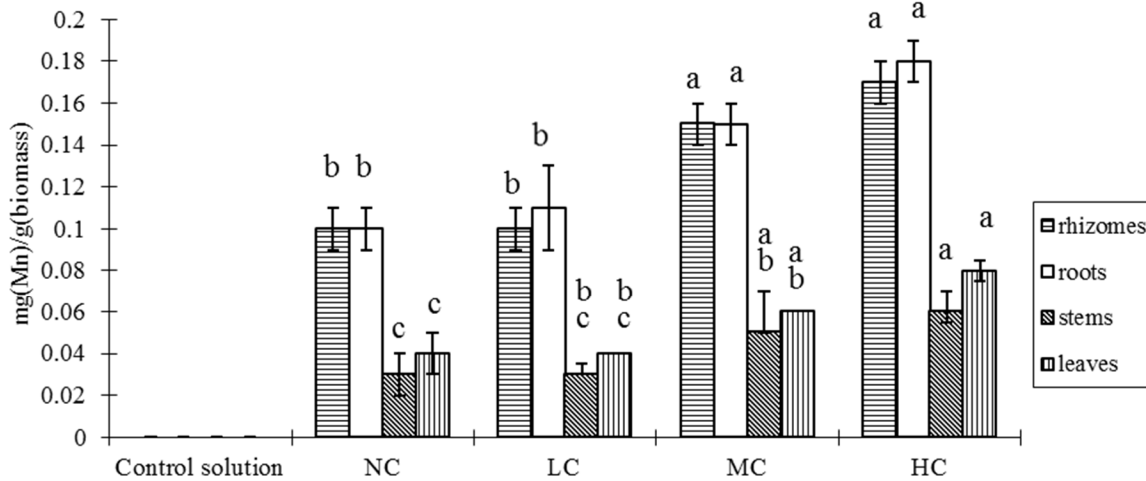


FIGURE 1. Mn concentration in the organs of reeds cultured in solution for 12 weeks. Error bars represent the standard deviation of triplicate samples. Different letters on the same plant organ indicate a significant difference at $p < 0.05$.

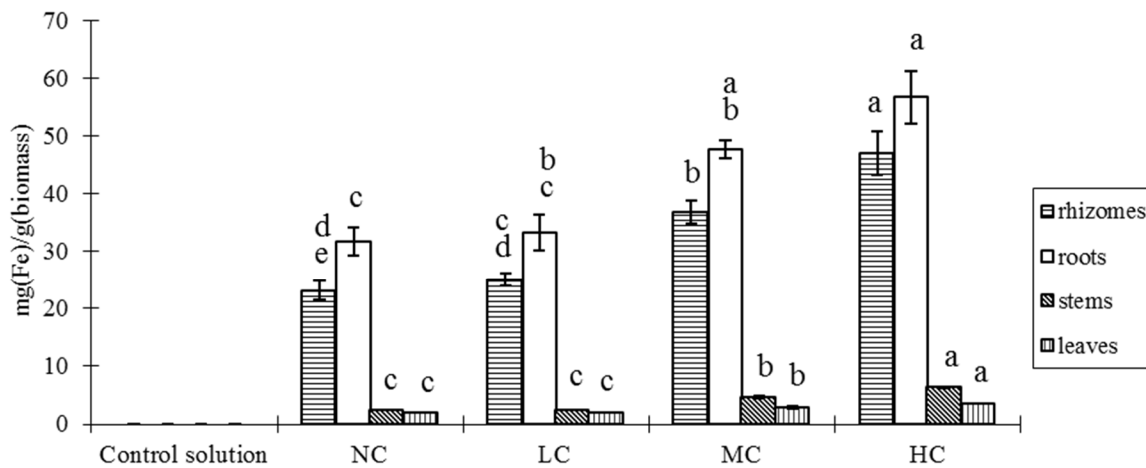


FIGURE 2 Fe concentration in the organs of reeds cultured in solution for 12 weeks. Error bars represent the standard deviation of triplicate samples. Different letters on the same plant organ indicate a significant difference at $p < 0.05$.

Al Accumulation. However, CA also did not significantly elevated ($p > 0.05$) the uptake of Al in different tissues of reeds (Figure 3). It was reported that the extent of complexation between metals and organic acid was related to the type of organic acid involved, the concentration of metals and the pH of solution, etc. (Jones, 1996). Since CA had higher affinity for Fe and Mn (Morel and Hering, 1994), and the Fe concentrations were higher than Al in solutions, most CA reacted with Fe and Mn. No citrate-Al complex were formed. That may be the main reason why CA can no improve the Al uptake in reeds.

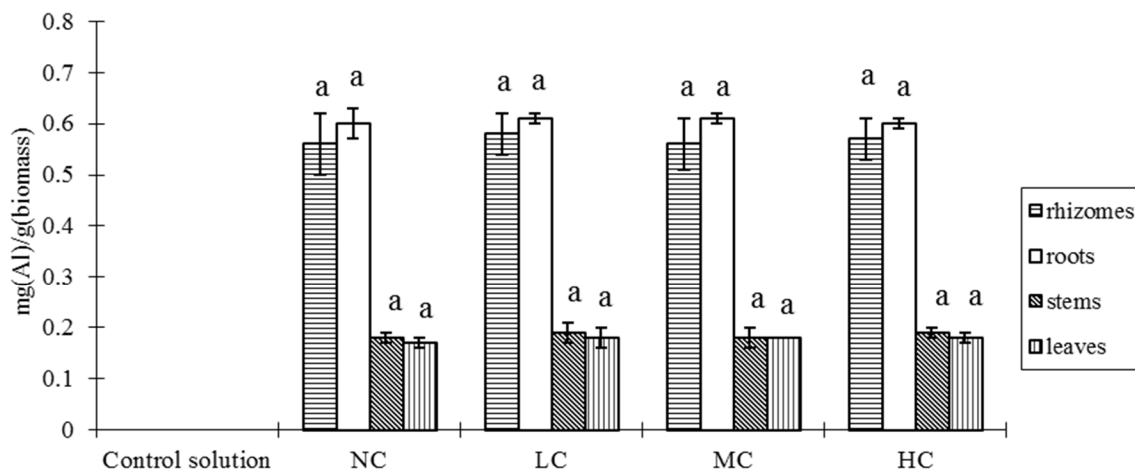


FIGURE 3 Al concentration in the organs of reeds cultured in solution for 12 weeks. Error bars represent the standard deviation of triplicate samples. Different letters on the same plant organ indicate a significant difference at $p < 0.05$.

CONCLUSIONS

The effectiveness of CA to increase the metal accumulation in was related to the concentrations of metals and CA in solution. The more CA added, the more Fe and Mn uptake in reeds. However, CA did not have important effect ($p > 0.05$) on Al accumulation in reeds, since most of CA reacted with Fe and Mn which had higher affinity with CA. Thus no citrate-Al complex was formed. It is recommended that CA in conjunction with reeds to remediate AMD contaminated sites. However, a thorough site characterization should be conducted to assess the type and concentrations of metals at the site. Second, the suitable mounts of CA needed should be determined depending on the levels of metals at sites. In future, more research on the molecular genetics and physiology alternation in reeds caused by heavy metals and CA may be needed.

ACKNOWLEDGEMENTS

The work was partially supported by the Office of Research and Sponsored Programs and Faculty Development Grants of Texas A&M University-Commerce.

REFERENCES

- Akcil, A., and Koldas, S. 2006. "Acid Mine Drainage (AMD): causes, treatment and case studies." *J. Clean. Prod.* 14 (12): 1139-1145.
- Batty, L. C., and Younger, P. L. 2004. "Growth of *Phragmites australis* (Cav.) Trin ex. Steudel in mine water treatment wetlands: effects of metal and nutrient uptake." *Environ. Pollut.* 132(1): 85-93.
- Cutright, T. J., Gunda, N. and Kurt, F. 2010. "Simultaneous hyperaccumulation of multiple metals by *helianthus annuus* grown in a contaminated sandy-loam soil." *Int. J. Phytoremediation.* 12(6):562-73.
- Garbisu, C. and Alkorta, I. 2001. "Phytoextraction: a cost effective plant-based technology for the removal of metals from the environment." *Bioresour. Technol.* 77(3): 229-236.
- Guo L., Ott D. W. and Cutright T. J. 2014. "Accumulation and histological location of heavy metals in *Phragmites australis* grown in acid mine drainage contaminated soil with or without citric acid." *Environ Exp Bot.* 105:46-54.

- Jones, D. L., Darah, P. R. and Kochian, L. V. 1996. "Critical evaluation of organic acid mediated iron dissolution in the rhizosphere and its potential role in root iron uptake." *Plant Soil*. 180(1): 57-66.
- Jones, D., 1998. "Organic acids in the rhizosphere -a critical review." *Plant Soil*. 205(1): 25-44.
- Marques, A. P. G. C., Oliveira, R. S., Samardjieva, K. A., Pissarra, J., Rangel, A. O. S. S. and Castro, P. M. L., 2007. "EDDS and EDTA-enhanced zinc accumulation by *Solanum nigrum* inoculated with arbuscular mycorrhizal fungi grown in contaminated soil." *Chemosphere*. 70(6): 1002-1014.
- Mihalík, J., Tlustoš, P. and Szaková, J. 2010. "Comparison of willow and sunflower for uranium phytoextraction induced by citric acid." *J. Radioanal. Nucl. Chem*. 285(2): 279-285.
- Morel, F. M. M. and Hering, J. G., (Ed.), 1993. "Principles and applications of aquatic chemistry." John Wiley and Sons, INC.
- Najeeb, U., Xu, L., Ali, S., Jilani, G., Gong, H. J., Shen, W. Q. and Zhou W. J. 2009. "Citric acid enhances the phytoextraction of manganese and plant growth by alleviating the ultrastructural damages in *Juncus effusus* L." *J. Hazard Mater*. 170(2): 1156-1163.
- Peppas A., Komnitsas K. and Halikia I. 2000. "Use of organic covers for acid mine drainage control." *Miner. Eng*. 13(5): 563-574.
- Wang, H., Jia, Y., Wang, S., Zhu, H. and Wu, X. 2009. "Bioavailability of cadmium adsorbed on various oxides minerals to wetland plant species *Phragmites australis*." *J. Hazard. Mater*. 167(1-3) 641-646.
- Whitehead, P. G. and Prior, H. 2005. "Bioremediation of acid mine drainage: an introduction to the Wheal Jane wetlands project." *Sci. Total Environ*. 338(1-2): 15-21.
- Williams, L. E., Pittman, J. K. and Hall, J. L. 2000. "Emerging mechanisms for heavy metal transport in plants, Biochim." *Biophys. Acta*. 1465(1-2):104-126.
- Senko, J. M., Wanjugi, P., Lucas, M., Bruns, M. A. and Burgos, W. D. 2008. "Characterization of Fe(II) oxidizing bacterial communities at two acidic Appalachian coal mine drainage impacted sites." *Int. Soc. Microb. Ecol*. 2(11): 1134-1145.
- Sivaram, S., 2010. Assessment of bioremediation efficiency of indigenous bacteria and plants at an abandoned acid mine drainage. M.S. Thesis, The University of Akron, Akron, OH.
- Stoltz, E. and Greger, M. 2005. "Effects of different wetland plant species on fresh unweathered sulphidic mine tailings." *Plant Soil* 276(1): 251-261.

SILVER RECOVERY: SILVER ION TOXICITY

Syed Sabir and Mansour Ibrahim Alhazza

(Chemical Engineering Department, King Saud University, P.O. Box 800, Riyadh-11421, Saudi Arabia,
E-mail: sabirsyed2k@yahoo.com)

ABSTRACT: Although we traditionally think of silver as ‘second best’ after gold, having high electrical, thermal conductivity, malleability and ductility are some of the characteristics that assign silver as an extremely relevant and valuable metal. Owing to these properties, silver is widely used in industrial activities including the production of mirrors, photographic films, batteries and electronic devices. Moreover, silver compounds are used as disinfectant agent on food and pharmaceutical industries due to its anti-bacteria properties. The extensive number of industrial applications increases the amount of silver concentration in spent sources, requiring a recovery before being discharged into the environment. However, there is a hot debate on the source of silver ion toxicity, because Ag^+ are biologically active and readily interacts with proteins, amino acid residues, free anions and receptors on mammalian, eukaryotic cell membranes, absorbed in the human body and enters the systemic circulation as a protein complex to be eliminated by the liver, kidneys degeneration and respiratory disorders and also highly toxic to bacteria at low concentrations (ng l^{-1}) and cause several negative health effects when disposed in large concentrations e.g. argyria or argyrosis, a disease related to skin pigmentation. Furthermore the high economic value of silver and toxicity result in the demand of recovery that both remove the metal from diverse spent sources and recover silver, in order to avoid the ecosystem contamination and bring economic advantages to the process, a critical comparison of existing technologies is analyzed for both economic viability and environmental impact was made in this presentation.

Keywords: Hydrometallurgy; Silver; Recovery; Spent Sources; Ion-toxicity

INTRODUCTION

Globally, the silver market saw rising record demand in 2015, with increasing usage of electronic equipment, photovoltaic sectors, jewelry, coin and bar posting new highs, helping to boost total silver demand to 1.17 billion ounces, instead last year and silver mine production growth slowed to 2% in 2015 and reached a record 886.7 million ounces and the overall slowdown in mine production last year is expected to continue (World Silver Survey, 2016). While we traditionally think of silver as 'second best' after gold, as distributions of medals still reflects today, pure silver holds three world records: the low contact resistance and electrical conductivity (used for audio cables, electric power switches and circuit breakers), which makes it a popular option in electronics and the highest brilliance (which lead to mirrors and optical applications) of all elements under standard conditions, and the best thermal conductivity of all metals (Syed and Mansour, 2016).

In recent year's extraction and recovery of silver was carried out either by hydrometallurgical or bio-metallurgical routes. Leaching represents the first step of the hydrometallurgical route and the recovery of silver by different techniques including cementation, chemical precipitation, adsorption, bio-sorption, electro-coagulation, electro-winning, ion-exchange and solvent-extraction etc. are very important cost-effective silver recovery and extraction process from various silver containing sources. In this book, the evaluation of lucrative and nature- friendly technologies to recover silver from primary and secondary spent sources was made (Syed, 2016).

With the growth of all these industries, the recovery and removal of silver have been intensely studied because of his present market demand poses an acute problem of recovery of silver from spent

sources by new economically efficient and environmentally clean technologies (Gromov et al., 2004). Meanwhile, the phenomenal increase in the regulations against environmental pollution of silver ion toxicity for the marine, microbial, invertebrate and vertebrate community (including humans) through chains and have caused numerous diseases and disorders (Yang et al., 2012). Since it has become of great concern to recover and remove monovalent silver ions (Ag^+) from industrial effluents and spent sources, up to ppm level (De et al., 2010). Moreover, a great interest in silver recovery for both environmental toxicity and economic point of view (Lee et al., 2005; Park and Fray, 2009).

TABLE 1 Silver recovery agents from leaching solutions*

Recovery agents	Efficiency (%)
<i>Cementation</i>	
Zn from nitric acid	100
Cu from sulphuric acid	99.2
Mn from thiocyanate	99
Zn powder	93
Magnesium from cyanide solutions	99
Iron waste	99.8
<i>Chemical Reduction</i>	
Hydrogen peroxide	95
NaCl+ KOH +H ₂ O ₂	87.30
Potassium borohydride	98
Sodium dithionite	99
Cellulose (CMK)	84.25
Hydrogen reduction	99.8
Hydrazine hydrate	87
Sodium hydroxide	95.94
<i>Electro-winning</i>	
Pulsed electric field (PEF) and static cylinder electrodes (SCE)	99
Rotating cylinder electrode reactor (RCE)	90
Titanium and vitreous carbon cathodes	95
<i>Ion flotation</i>	
Dodecylamine	100
<i>Solvent extraction</i>	
Calixarene tetramide (LBC) and thio-analogue (THIO)	99
<i>Ion exchange resins</i>	
PSGA resin	100
VDP-1, VDP-2, N-0	100
Macro-porous anion exchanger AV-17-10P	90
IRA-68 (weak base)	98

*(Syed, 2016).

RESOURCES RECYCLING PROCESS: THE DAWN

Silver containing materials arise from diverse sources, such as manganese silver ore, refractory antimony ore, silver sulfide concentrates, lead–zinc sulfide concentrates, mining wastewater, spent photography/radiography films, electronic and electrical materials, waste jewelry, silver wares, brazing alloys, catalyst, batteries, dental amalgam, orthopedic materials, spent bleach-fixing photographic/radiographic solution, electroplating solution and metallurgical processing-solution are available in many forms. Processing of such sources is, therefore complicated. However, the basic processing technology is shown in Figure 1. The pretreatment process involves washing, crushing, physical separation and incineration depending on the nature of materials and the metal obtained is of low purity. In the recovery process, such low purity metals are converted into crude silver by repeated leaching, adsorption or chemical reduction or cementation. Crude silver is subjected to the refining process to improve their purity to over 99.9% (Syed, 2016).

SILVER RECOVERY ACCESSIBLE TECHNIQUES

Various technologies were applied for silver recovery from variety of silver containing sources, such as chemical reduction, precipitation, metallic replacement or cementation, adsorption, bio-sorbents, ion exchange, ion flotation, electro-deposition or electro-wining and solvent extraction Etc. Silver recovery agents from leachents are presented in Table 1.

HYDRO-TECHNOLOGIES

Manuella et al., (2016) used, thermally modified bentonite clay (Verde-lodo) for batch adsorption of silver from aqueous solution. The adsorption rate was evaluated by Mass Transfer in External Film model, showed agreements between experimental and calculated data and the process is mainly controlled by external transport. Langmuir model showed best correlation coefficient and Relative Standard Deviation results and the maximum adsorption capacities for Verde-lodo clay was 61.48 mg g^{-1} , the result indicated that, clay is an effective adsorbent for silver recovery from aqueous sources.

Pablo et al., (2016) described two methods for extraction and concentration of silver from waste crystalline silicon photovoltaic modules. In the first method, the modules were milled, sieved and leached in 64% nitric acid solution with 99% sodium chloride; the silver concentration yield was 94%. In the second method, photovoltaic modules were milled, sieved, subjected to pyrolysis at $500 \text{ }^{\circ}\text{C}$ and leached in 64% nitric acid solution with 99% sodium chloride; the silver concentration yield was 92%. The first method is preferred as it consumes less energy and presents a higher yield of silver. This study shows that the use of pyrolysis does not assist in the extraction of silver, as the yield was similar for both methods with and without pyrolysis. Figure 1 shows silver recovery process diagram.

Choong, (2015) used immobilized crab shell beads to recover silver from industrial wastewater and the highest silver removal efficiency was 83%, achieved from 4.0 g of crab shell beads. The Langmuir isotherm model showed significant fit to the equilibrium adsorption data and maximum adsorption capacity of 2.951 mg/g of silver ions was achieved at the pH 6.0 and 95% of silver was recovered from adsorbed beads using 1.0 M of HNO_3 solution. Therefore, these crab shell beads sufficiently used to remove silver in batch and continuous process.

Sami et al., (2015) used polyamine functional resin WP-1 for silver recovery from concentrated base metal chloride solutions, using batch equilibrium experiments. However, HCl was found to be the best choice for washing impurities, exclusively Cu, from the bed after the loading step. Tetrasodium salt of EDTA was found suitable especially for selective desorption of Pb from the loaded bed. Furthermore, thiosulfate and thiourea were used in silver elution from the WP-1 bed; nonetheless thiourea was preferred because of the trivial affinity of thiosulfate towards the resin. With this developed process, 72% pure silver was recovered. Subsequently, silver recovery yield depends purely on loading step length, and even 100% recovery was achieved from this process.

Meng et al. (2015) studied selective adsorption of Ag^+ using ion-imprinted O-carboxymethyl chitosan (ITG-OCMC) beads grafted with thiourea–glutaraldehyde from a bimetallic aqueous solution.

However, results indicated that high degree of carboxymethylation and low level of crosslinking was helped to achieve higher uptake of Ag^+ and the maximum uptake of Ag^+ was 156.32 mg g^{-1} at 40°C with an initial Ag^+ concentration of 160.5 mg L^{-1} and the biosorbent dosage of 1.0 g L^{-1} . Furthermore, Langmuir isotherm and Lagergren's pseudo-second-order kinetic was used to describe the sorption process of Ag^+ . Consequently, FT-IR and XPS analyses confirmed that selective adsorption of Ag^+ was on the surfaces of ITG-OCMC beads by chelation through $>\text{C}=\text{S}$, amine, carboxyl and hydroxyl groups.

Extraction And Concentration

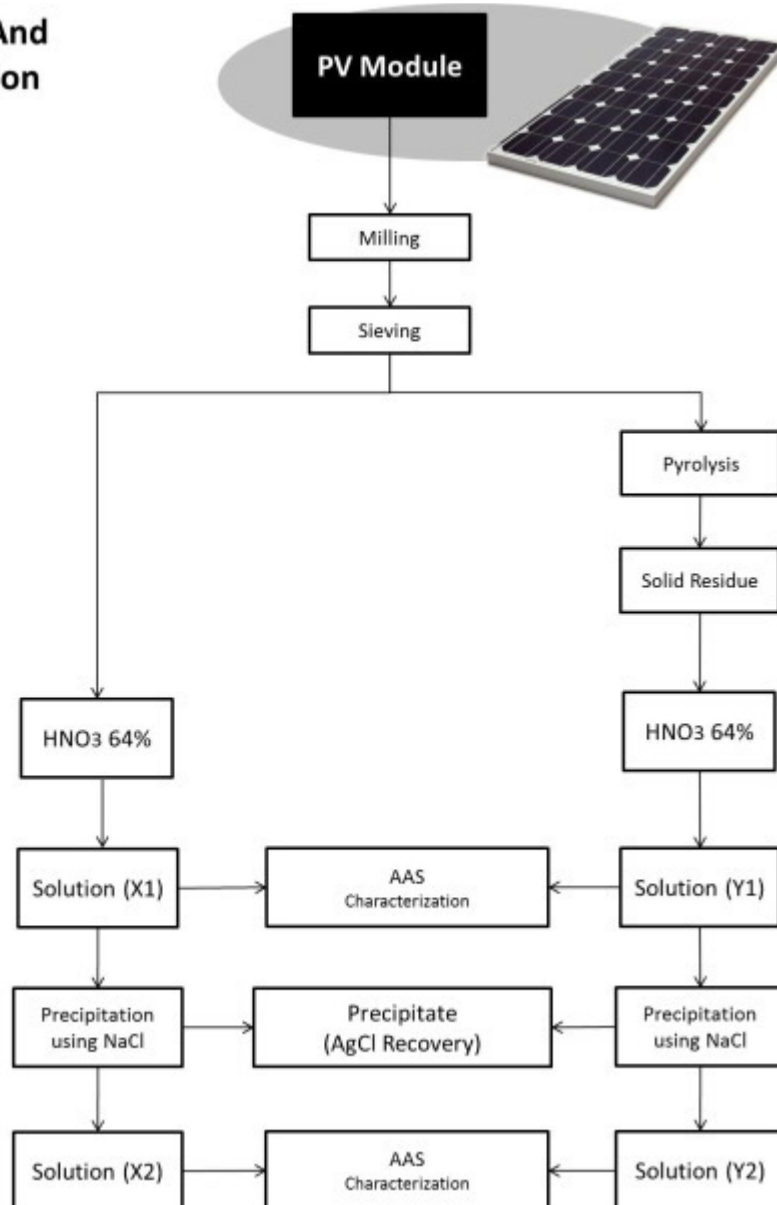


FIGURE 1. shows a process diagram of silver recovery from spent silicon photovoltaic modules.

Walaikorn and Thanut (2015) prepared chitosan/bamboo charcoal composite beads from blending chitosan and bamboo charcoal and used for silver ion adsorption. However, the maximum Ag^+ removal was at pH 6, adsorbent dosage (0.4 g/L), interaction time (180 min), and Ag^+ removal was 100%. The adsorption isotherm of chitosan/bamboo charcoal composite beads fitted well Langmuir model and the maximum adsorption was 52.91 mg/g .

Gholamreza, (2014) recovered silver ions from aqueous solution using natural Halloysite nanotubes (HNTs) and silver ions adsorption was influenced by silver ion concentration, temperature, pH, interaction time and adsorbent dose. However, adsorption increased with increasing initial silver ion concentration, pH and temperature. Pseudo-first order, pseudo-second-order and intra particle diffusion models were used to appraise the rate parameters. The adsorption followed pseudo-second-order kinetic model with correlation coefficients above 0.999. The experimental isotherm data were analyzed using the Langmuir, Freundlich and Temkin equations. The Langmuir isotherm model showed significant fit to the equilibrium adsorption data and the maximum adsorption capacity of 109.79 mg g^{-1} (99.8% removal) of Ag^+ was achieved.

Ulisses et al., (2014) reported electrochemical recovery of silver from discarded X-ray photographic films by employing recyclable super paramagnetic carbon particles (Cmag). However, this exhibits a high affinity for Ag^+ ions in aqueous solution and is capable of capturing a large amount of this element because of great surface area and external magnet. Furthermore, this also provides an efficient way of transporting and concentrating the silver ions at the electrode surface. By this way electro-deposition was carried out directly from the electrode. The adsorption process at the magnetic carbon particles proceeds according to the Langmuir model, exhibiting an adsorption of 61.5 mg of silver per gram of Cmag. Consequently, complete setup for this process was shown in Figure 2.

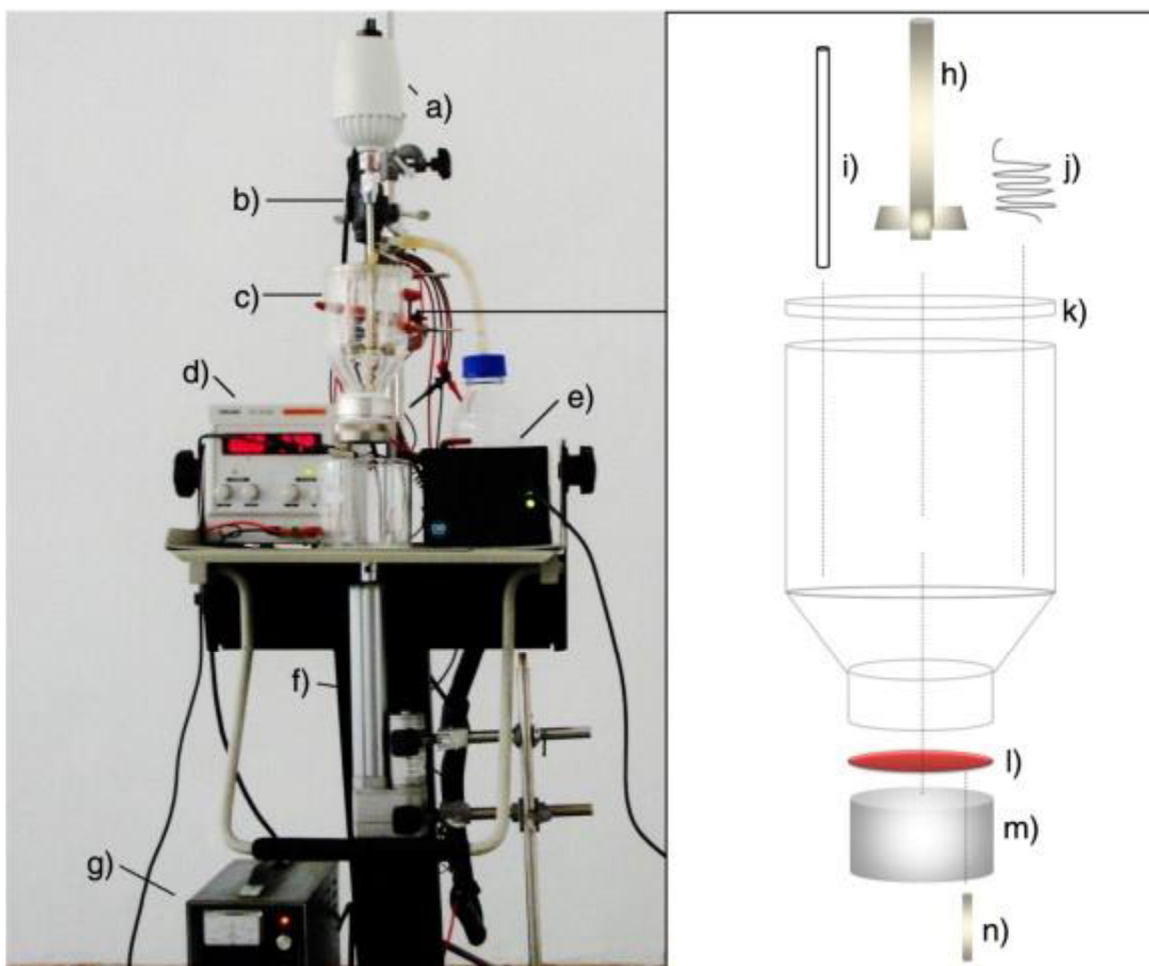


FIGURE 2. Complete setup of this process

BIOSORPTION

Bio-sorption is the term given to the passive sorption and/or complexation of silver ions by biomass. The mechanisms of bio-sorption are generally based on physico-chemical interactions in silver ions and the functional groups present on the cell surface, such as electrostatic interactions. This is because of the fact that the properties of certain types of inactive or dead microbial biomass materials allow them to bind and concentrate silver ions from industrial effluents and aqueous solutions. These types of biomasses are relatively inexpensive and available in large quantities. Bio-sorption is a metabolism independent process that takes place in the cell wall, and the mechanism responsible for the metal uptake differ according to the biomass type. Bio-sorption is as promising technology for the recovery of silver from their silver containing sources (Syed, 2016). Table 2 presents various bio-sorbent for silver recovery from leaching solution.

TABLE 2 Silver recovery bio-sorbent

Bio-sorbents	Efficiency (%)
<i>Persimmon tannin gel</i>	100
<i>Cellobiose and cellulose</i>	Unknown
<i>Aspergillus versicolor protease</i>	Unknown
<i>Chitosan/amine and chitosan/azole resins</i>	Unknown
<i>Valonia tannin (VT)</i>	97
<i>Aeromonas punctata</i>	Unknown
<i>Magnetospirillum gryphiswaldense</i>	Unknown
<i>Bacillus cereus biomass</i>	Unknown
<i>Corynebacterium glutamicum</i>	Unknown
<i>Pleurotus platypus</i>	Unknown
<i>Molecular-imprinted biosorbent</i>	Unknown
<i>Chemically modified chitosan resin</i>	Unknown
<i>Bisthiourea (BS) resin</i>	95
<i>Chitin</i>	Unknown
<i>Cladosporium cladosporioides</i>	70
<i>Enzyme of Bacillus subtilis ATCC 6633</i>	Unknown
<i>Myxococcus xanthus Biomass</i>	Unknown
<i>Aspergillus niger</i>	100
<i>Saccharomyces cerevisiae</i>	Unknown
<i>Neurospora crassa</i>	Unknown
<i>Alga Chlorella vulgaris (211/11b)</i>	97.5

BIO-HYDROTECHNOLOGIES

Yufeng et al., (2015) explicated biosorbents from brewer fermentation industry waste yeast to adsorb silver from aqueous solution. However, the FTIR result of waste yeast showed that the ion exchange, chelating and reduction were the main binding mechanisms between the silver ions and the binding sites on the surface of the biomass. Furthermore, TEM, XRD and XPS results suggested that silver nanoparticles were deposited on the surface of yeast. Subsequently, the kinetic experiments revealed that sorption equilibrium was reached within 60 min, and 93 % Ag⁺ removal efficiency was achieved when the initial concentration of Ag (I) was below 100 mg/L. Thermodynamic parameters of the adsorption process (ΔG , ΔH and ΔS) identified that the adsorption was spontaneous and exothermic.

Mostafa et al., (2014) prepared magnetic cellulose xanthate sorbents and used for silver adsorption from acidic medium, the maximum adsorption capacity within 5 min was 166 mg g⁻¹. Moreover, the reusability of the sorbent was investigated by elution the adsorbed ions with 3.0 mL of 0.4 mol/L Na₂S₂O₃ solution. It was found that the recovery was (90–97%) after 3 cycles of sorption and desorption.

Manju et al., (2013) purported a new approach of silver recovery from waste mobile printed circuit boards (PCBs) by acidothiourea leaching followed by selective adsorption on low-cost biomass of

agricultural waste. It was found that smaller particle size PCBs (53- 75 μm) yielded higher amounts of silver leached into the solution. Nonetheless, silver leaching was achieved in 0.5 M TU in 0.01 MH_2SO_4 at 60 $^\circ\text{C}$, under this condition, an average of 6.8 mg/g of silver was extracted from PCBs. Kinetic studies revealed that the complete leaching of silver was achieved in below 2 h. *Persimmon tannin extract* cross-linked with sulfuric acid was found to be a promising material for complete recovery of silver from the leached liquor. Furthermore, this adsorbent not lone adsorbed the dissolved silver selectively, but also reduced the adsorbed cationic species of silver to metallic silver. The proposed flow sheet is shown in Figure 3.

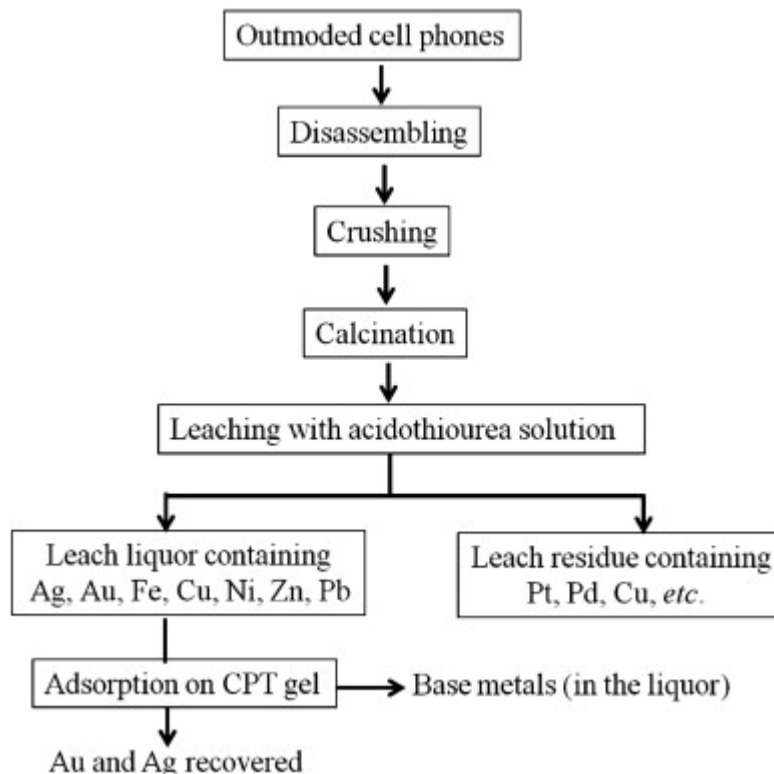


FIGURE 3. Flow sheet of precious metal leaching from spent mobile PCBs and recovery by adsorption (Manju et al., 2013).

SILVER LOSSES TO THE ENVIRONMENT

In the world, maximum silver losses occur in mining industries, photographic processing and electroplating industries. Etc. But, the maximum loss occurs in mining and smelting facilities, fuel-fired power plants, manufacturing products and through waste disposal. The photographic utilize of silver was 30% this drive not account for much loss. However, direct discharge of silver containing effluent to rivers cause the silver deposition in the sediments of rivers and coastal areas of Oceans (Syed, 2005). The silver ions influence be accumulated in organisms (including human) through the food chain, and then should harm to their body. Recently, it is found that Ag^+ exposure caused an inhibition of active Na^+ and Cl^- uptake, resulting in ion regulatory failure by inhibition of branchial Na^+ -ATPase and K^+ -ATPase in crayfish and daphnids. Henceforth, for economic as well as increasingly serious environmental problem, the active removal and recovery of Ag^+ has become a vigorous task (Hongyan et al., 2009).

Evaluation of silver recovery from primary and secondary spent sources and comparisons of eco-friendly and economically viable technologies are presented in Table 3.

TABLE 3 Nature-friendly and economical viable silver recovery technologies

Techniques	Efficiency (%)
Recovery of gold and silver from spent mobile phones by means of acidothiourea leaching followed by adsorption using biosorbent prepared from persimmon tannin	100
Preparation of a novel chelating resin containing amidoxime–guanidine group and its recovery properties for silver ions in aqueous solution	100
E-waste management through silver recovery from scrap of plasma TV monitors	100
A novel recovery technology of trace precious metals from waste water by combining agglomeration and adsorption	100
An <i>Aspergillus niger</i> strain accumulated gold and silver from solution containing high cyanide concentrations. Our results show that <i>A. niger</i> is of potential use for the removal of metals and/or the recovery of valuable metals from cyanide-containing solutions.	100
Recovery of silver from wastewater coupled with power generation using a microbial fuel cell	99.91
Preparation of fine silver powder from silver phosphate by direct electro-reduction	99.8
Silver(I) Sorption by Silica Gels Chemically Modified with Mercaptopropyl or Dipropyl Disulfide Groups	99.9
Adsorption and desorption behavior of silver ions onto valonia tannin resin	99.6
Silver recovery and chemical oxygen demand (COD) removal from waste fixer solutions	99.55
Kinetic Aspects of Gold and Silver Recovery in Cementation with Zinc Powder and Electro-coagulation Iron Process	99.5
Recovery of high-purity silver directly from dilute effluents by an emulsion liquid membrane-crystallization process	99.24
An optimization study on the cementation of silver with copper in nitrate solutions by Taguchi design	99.2
A Novel Silver Recovery Method from Waste Photographic Films with NaOH Stripping	99
Study of silver precipitation in thiosulphate solutions using sodium dithionite. Application to an industrial effluent	99
A Novel Technique for Silver Extraction from Silver Sulphide Ore	99
Electrochemical recovery of silver from waste aqueous Ag(I)/Ag(II) redox mediator solution used in mediated electro oxidation process	99
Electrochemical reclamation of silver from silver-plating wastewater using static cylinder electrodes and a pulsed electric field	99
Solvent extraction of silver from nitric acid solutions by calix[4]arene amide derivatives	99
Powerful adsorption of silver(I) on thiol-functionalized polysilsesquioxane microspheres	99
Extraction of silver from spent silver oxide-zinc button cells by using <i>Acidithiobacillus ferrooxidans</i> culture supernatant	98
A method to recover silver from waste X-ray films with spent fixing bath	98
Clean technology for the recovery of silver from processed radiographic films	97
Recovery of silver from X-ray film processing effluents by hydrogen peroxide treatment	95
Recovery of silver from silver(I)-containing solutions in bioelectrochemical reactors	95

SILVER IONS TOXICITY

There is a hot debate on the source of silver ion toxicity, because Ag^+ are biologically active and readily interacts with proteins, amino acid residues, free anions and receptors on mammalian, eukaryotic cell membranes, absorbed in the human body and enters the systemic circulation as a protein complex to be eliminated by the liver and kidneys and also highly toxic to bacteria at low concentrations (ng l^{-1}) (Lansdown, 2006; Katharina, 2011). However, silver ion absorbed in a range of 0.4–18% in mammals with a human value of 18%. Based on determination in animals, silver seems to be dispersed to all of the organs investigated, with the maximum levels being observed in the intestine and stomach. Consequently, prolonged exposure to silver may cause the silver deposition in the body, resulting in irreversible blue–grey discoloration of skin, eyes and hair caused by deposition of silver-protein complex or metabolized product (silver sulfide or silver selenide) in tissues, i.e. argyria or argyrosis (Su-juan et al., 2013). Excretion occurs via the bile and urine and following dose dependent animal toxicity findings have been described: death, weight loss, hypoactivity, altered neurotransmitter levels, altered liver enzymes, altered blood values, expanded hearts and immunological effects. Silver is precipitated in bone where Ag^+ displaces Ca^{++} from hydroxyapatite with the potential risk of osteoporosis, but the extent of this problem is not known (Alan, 2010). Considerable proof exists suggesting that the effects induced by particulate silver are interceded via silver ions that are discharged from the particle surface (Niels and Henrik, 2014). Also, ionic silver is a toxic element of the marine microbial and invertebrate community (Ratte, 1999; Tappin et al., 2010), mainly by disabling the enzymes Na/K adenosine triphosphatase and carbonic anhydrase in animals (Morgan et al., 2004; Bielmyer et al., 2007), and interacting with thiol groups in enzymes and proteins of micro-organisms (McDonnell and Russell, 1999). Silver is strongly bio-accumulated by several marine phytoplankton, macro-algae and invertebrates (Fisher et al., 1984; Bryan, 1984), and it is known that the degree of silver accumulation by organisms is dependent on chemical speciation. The monovalent silver ion (Ag^+) is believed to be the utmost toxic silver species in aquatic systems and it has been shown that silver toxicity in freshwater phytoplankton is directly allied to intracellular accumulation (Campbell, 1995; Lee et al., 2005). The monovalent silver ion is the main dissolved species in fresh waters, experimental data have shown that in rivers and estuaries dissolved silver associated with colloidal macromolecular organic matter is a significant or dominant fraction of the total dissolved silver pool (Wen et al., 1997).

Ivana et al., (2014) studied the toxicity mechanisms of nano and ionic forms of silver on human hepatoblastoma (HepG2) cells. The results indicated that silver ions and citrate-coated AgNPs decreased cell viability in a dose-dependent manner. The IC50 rates of silver ions and citrate-coated AgNPs were 0.5 and 50 mg L^{-1} , respectively. The LDH leakage and inhibition of albumin synthesis, along with reduced ALT activity, indicated that treatment with either AgNP or Ag^+ ions resulted in membrane damage and decreased the cell function of human liver cells. Rating of oxidative stress markers demonstrating depletion of GSH, increased ROS production, and increased the SOD activity, indicated that oxidative stress contribute to the toxicity effects of nano and ionic forms of silver. The noticed toxic effect of AgNP on HepG2 cells was substantially weaker than that induced by ionic silver, while the uptake of nano and ionic forms of silver by HepG2 cells was same.

Fabianne et al., (2014) investigated the toxicity of silver nanoparticles (AgNP) and AgNO_3 on *Pseudokirchneriella subcapitata*, *Daphnia magna* and *Danio rerio* as model organisms to by assessing different biological endpoints and exposure periods. Organisms were periled following specific and standardized protocols for each species/endpoints, with modifications when necessary. In each test media, AgNP was characterized by Transmission Electron Microscopy (TEM) and experiments were executed by Dynamic Light Scattering to investigate the aggregation and the agglomeration behavior of AgNP under different chemical composition and test period. TEM images of AgNP in the different test media indicated dissimilar pattern of agglomeration, with some agglomerates inside an organic layer, some loosely

associated particles and the presence of some individual particles. The perniciousness of both AgNO₃ and AgNP differ significantly based on the test species: no differences in toxicity for algae, a small difference for zebrafish and a major difference in toxicity for *Daphnia magna*.

Shaokun et al., (2013) appraised the cytotoxicity of Ag ions and silver chloride colloids on red blood cells and human mesenchymal stem cells (hMSCs). Subsequently, adverse effects of silver chloride on red blood cells and hMSC were viewed by SEM and LIVE/DEAD viability staining, respectively. A different tested chemical form of silver showed that, AgCl was identified to be the tiniest cytotoxic. Furthermore, a decline in the cytotoxicity of AgCl at significantly higher concentrations was observed. We attributed the reduced cytotoxicity to aggregated AgCl that limited the bioavailability of free Ag⁺ ions; furthermore, molecular level studies are required to understand the mode of cytotoxic mechanisms.

Takamitsu et al., (2013) exposed human bronchial epithelial cells (BEAS-2B) to AgNO₃ and investigated uptake and intracellular distribution of Ag, expression of metallothionein (MT), generation of reactive oxygen species (ROS), and changes in mitochondrial respiration. The culture medium concentration of Ag decreased with time and stabilized at 12 h. Furthermore, the concentration of Ag and MT in the soluble cellular fraction increased in 3 h and then decreased, indicating that cytosolic Ag relocated to the insoluble fraction of the cells. The levels of mRNAs for the major human MT isoforms MT-I and MT-II paralleled with the protein levels of Ag-MT. Subsequently, the intensity of fluorescence derived from ROS was elevated in the mitochondrial region in 24 h. Ag decreased mitochondrial oxygen consumption in a dose dependent manner and the activity of mitochondrial complex I-IV enzymes was significantly inhibited due to exposure. However, in a separate experiment, hydrogen peroxide at concentrations of 0.001% (equivalent to the concentration of H₂O₂ in Ag-exposed cells) removed Ag from MT. These results suggested MT was decomposed by cytosolic H₂O₂, and Ag released from MT relocated to insoluble cellular fractions and inhibited the electron chain transfer of mitochondrial complexes, which eventually led to cell damage.

Christina et al., (2012) studied the toxic effect of silver ions and silver nanoparticles towards bacteria and human cells and generally ascribed to a higher toxicity towards prokaryotic cells than towards mammalian cells. Furthermore, comparative studies with both silver ions (silver acetate) and polyvinylpyrrolidone (PVP)-stabilized silver nanoparticles (70 nm) showed the toxic effect of silver occurs in a similar concentration range for *Escherichia coli*, *Staphylococcus aureus*, human mesenchymal stem cells (hMSCs), and peripheral blood mononuclear cells (PBMCs), i.e. 0.5 to 5 ppm for silver ions and 12.5 to 50 ppm for silver nanoparticles. However, toxicity of silver ions and silver nanoparticles was different due to the presence of salts and biomolecules like proteins. The effective toxic concentration of silver towards bacteria and human cells is almost the same. Studied the toxic effect of silver ions and silver nanoparticles towards bacteria and human cells and generally ascribed to a higher toxicity towards prokaryotic cells than towards mammalian cells. Furthermore, comparative studies with both silver ions (silver acetate) and polyvinylpyrrolidone (PVP)-stabilized silver nanoparticles (70 nm) showed the toxic effect of silver occurs in a similar concentration range for *Escherichia coli*, *Staphylococcus aureus*, human mesenchymal stem cells (hMSCs), and peripheral blood mononuclear cells (PBMCs), i.e. 0.5 to 5 ppm for silver ions and 12.5 to 50 ppm for silver nanoparticles. However, toxicity of silver ions and silver nanoparticles was different due to the presence of salts and biomolecules like proteins. The effective toxic concentration of silver towards bacteria and human cells is almost the same.

CONCLUSIONS

This article presents promising techniques for recovery of silver from various sources that are important subject not solitary from the point of energetic economic and high demand but also from waste treatment management and toxicity of silver ion. Subsequently, an evaluation of lucrative and nature friendly technologies to recover silver from primary and secondary spent sources and the toxicity of silver ion was made in this paper.

ACKNOWLEDGEMENTS

Support for this research by College of Engineering, Research Center and The Deanship of Scientific Research, King Saud University, is gratefully acknowledged.

REFERENCES

- Alan D. T, Jose L. B, Charlotte B. B, Hywel E E. , Matthew D. P., Eric P. A. 2010. "Dissolved silver in European estuarine and coastal waters". *Water Research*, 44: 4204–4216.
- Alan, B. G. L. 2010. "The Toxicology of Silver" Silver in Health Care: Antimicrobial Effects and Safety in Use", RSC Publication (DOI:10.1039/9781849731799)
- Bryan, G.W., 1984. Pollution due to heavy metals and their compounds. In: Kinne, O. (Ed.), *Marine Ecology*, volume 5, part 3. John Wiley & Sons Ltd, Chichester, pp. 1289–1431.
- Campbell, P.G.C., 1995. Interactions between trace metals and aquatic organisms: a critique of the free-ion activity model. In: Tessier, A., Turner, D.R. (Eds.), *Metal Speciation and Bioavailability on Aquatic Systems*. John Wiley & Son, Chichester, pp. 45–102.
- Choong, J. 2015. "Adsorption behavior of silver ions from industrial wastewater onto immobilized crab shell beads", *Journal of Industrial and Engineering Chemistry*, 32:195–200.
- Christina G., Dieter B., Alexander P., Jörg D., Bettina S., Matthias E., Manfred K. 2012. "The toxic effect of silver ions and silver nanoparticles towards bacteria and human cells occurs in the same concentration range". *RSC Advances*, 2: 6981–6987.
- De, R. Q., Santoro, R., Proost, J., 2010." Kinetic transitions during Ag and Cu electrorecovery on reticulated vitreous carbon electrodes in flow-by mode". *Chemical Engineering Journal*, 162: 273–277.
- Fabianne, R., Julián, A. G., Kerstin, J., Alison, C., Martin, H., Cameron, T., Amadeu, M.V.M. S., Susana, L., 2014. "Silver nanoparticles and silver nitrate induce high toxicity to *Pseudokirchneriella subcapitata*, *Daphnia magna* and *Danio rerio*". *Science of The Total Environment*, 466–467: 232–241.
- Fisher, N.S., Bohe´, M., Teyssie´, J.L., 1984. "Accumulation and toxicity of Cd, Zn, Ag, and Hg in four marine phytoplankters". *Marine Ecology Progress Series*, 18: 201–213.
- Gholamreza, K. 2014. "High removal capacity of silver ions from aqueous solution onto ch Halloysite nanotubes". *Applied Clay Science*, 90: 159–164.
- Gromov, O. G., Kuz' min, A. P., Kunshina, G. B., Lokshin, E. P., Kalinnikov, V. T., 2004. "Electrochemical recovery of silver from secondary raw materials". *Russian Journal of Applied Chemistry*, 77(1): 62–66.
- Hongyan, H., Haijia, S., Tianwei, T., 2009. "Adsorption of Ag⁺ by a surface molecular-imprinted biosorbent". *Chemical Engineering Journal*, 150: 139–144.
- Ivana V. V., Irena Ž., Roberta P., Ivan P., Maja D. S., Marija Č.,Walter G. 2014. "Comparison of in vitro toxicity of silver ions and silver nanoparticles on human hepatoma cells". *Environmental Toxicology*, 31: 679 – 692
- Katharina, M.F. 2011. "Give silver a shine". *Nature Chemistry*, 3: 178.
- Lansdown, A.B. 2006. "Silver in health care: antimicrobial effects and safety in use". *Current Problems in Dermatology*, 33: 17–34.
- Lee, D.Y., Fortin, C., Campbell, P.G.C., 2005. "Contrasting effects of chloride on the toxicity of silver to two green algae, *Pseudokirchneriella subcapitata* and *Chlamydomonas reinhardtii*". *Aquatic Toxicology*, 75:127–135.
- Manju, G, Birendra, B.A, Hidetaka, K., Keisuke, O., Katsutoshi, I., Shafiq, A., 2013. "Recovery of gold and silver from spent mobile phones by means of acidothiourea leaching followed by adsorption using biosorbent prepared from persimmon tannin". *Hydrometallurgy* 133: 84–93.
- Manuella, L. C., F. D Ambrosio, S. N. Eric and G.A.V. Melissa. 2016. "Adsorption of silver from aqueous solution onto pre-treated bentonite clay: complete batch system evaluation". *Journal of Cleaner Production*, 112: 1112–1121.
- McDonnell, G., Russell, A.D., 1999. "Antiseptics and disinfectants: activity, action, and resistance". *Clinical Microbiology Reviews*, 12: 147–179.

- Meng, Z., Yan Z., Robert, H. 2015. "Selective adsorption of Ag⁺ by ion-imprinted O-carboxymethyl chitosan beads grafted with thiourea–glutaraldehyde". *Chemical Engineering Journal*, 264: 56–65.
- Morgan, T.P., Grosell, M., Gilmour, M., Playle, R.C., Wood, C.M., 2004. "Time course analysis of the mechanism by which silver inhibits active Na⁺ and Cl⁻ uptake in gills of rainbow trout". *American Journal of Physiology-Regulative Integrative and Comparative Physiology*, 287: R234–R242.
- Mostafa, H. B., Mehrnoosh, B., Simin, M., Farzaneh, S., Hassan, A. 2014. "Synthesis, characterization, and silver adsorption property of magnetic cellulose xanthate from acidic solution: prepared by one step and biogenic approach". *Industrial & Engineering Chemistry Research*, 53 (39): 14904–14912.
- Niels H., Henrik R. L. 2014. "Oral toxicity of silver ions, silver nanoparticles and colloidal silver – A review". *Regulatory Toxicology and Pharmacology*, 68:1–7.
- Pablo D., S. Javimczik, M. Benevit, H. Veit and A. M. Bernardes. 2016. "Recycling WEEE: Extraction and concentration of silver from waste crystalline silicon photovoltaic modules", *Waste Management* (<http://dx.doi.org/10.1016/j.wasman.2016.03.016>).
- Park, Y.J., Fray, D.J., 2009. "Recovery of high purity precious metals from printed circuit boards". *Journal of Hazardous Materials*, 164: 1152–1158.
- Ratte, H.T., 1999. "Bioaccumulation and toxicity of silver compounds: a review". *Environmental Toxicology and Chemistry*, 18: 89–108.
- Sami, V., Mikko T., Mika H., Tuomo S., 2015. "Ion exchange recovery of silver from concentrated base metal chloride solutions". *Hydrometallurgy* 152: 100–106.
- Shaokun, Z., Chan, D., Zaizhi, W., Xinguang, H., Kun, Z., Lihong, L., 2013. "Reduced cytotoxicity of silver ions to mammalian cells at high concentration due to the formation of silver chloride". *Toxicology in Vitro*, 27: 739–744.
- Su-juan, Y., Yong-guang Y., Jing-fu L. 2013. "Silver nanoparticles in the environment". *Environmental Science: Processes & Impacts*, 15, 78–92.
- Syed, S. 2016. "Silver recovery aqueous techniques from diverse sources: Hydrometallurgy in recycling". *Waste Management*, 50: 234–256.
- Syed, S., M. I Alhazza .2016. "Silvery Hydrometallurgy: Recovery and Recycling", *King Saud University Press, K.S.A* (Under Publishing) Pages 103
- Syed, S., 2005. "A critical review on the recovery of silver from photographic processing waste". *Journal of Saudi Chemical Society*, 9: 243–252.
- Takamitsu, M., Yuta, A., Noriyuki S., Seishiro H. 2013. "Mitochondrial electron transport is inhibited by disappearance of metallothionein in human bronchial epithelial cells following exposure to silver nitrate". *Toxicology*, 305: 20– 29.
- Ulisses, C., Alceu, T. S., George, W. C., Sergio, H. T., Araki, K., Henrique, E. 2014. "Silver recovery using electrochemically active magnetite coated carbon particles". *Hydrometallurgy* 147–148: 241–245.
- Walaikorn, N., Thanut, J. 2015. "Removal of silver (I) from aqueous solutions by chitosan/bamboo charcoal composite beads". *Journal of Cleaner Production*, 87: 850–855.
- Wen, L.-S., Santschi, P.H., Gill, G.A., Paternostro, C.L., Lehman, R.D., 1997. "Colloidal and particulate silver in river and estuarine waters of Texas". *Environmental Science and Technology*, 31: 723–731.
- World Silver Survey, 2016. GFMS Limited/The Silver Institute. <http://www.silverinstitute.org>.
- Yang, W., Xiaojie, M., Yanfeng, L., Xiaoli, L., Liuqing, Y., Lei, J., Yin, H., 2012. "Preparation of a novel chelating resin containing amidoxime–guanidine group and its recovery properties for silver ions in aqueous solution". *Chemical Engineering Journal*, 209: 394–400.
- Yufeng, Z., Dongfang, W., Hezhen X., Sung W. W., Longzhe C., Guiping W. 2015. "Adsorption of Ag (I) from aqueous solution by waste yeast: kinetic, equilibrium and mechanism studies". *Bioprocess Biosystem Engineering*, 38: 69–77.

REMOVAL OF Hg(II) BY ENCAPSULATED THIOPHOSPHINIC EXTRACTANTS

Janette Alba, Ricardo Navarro, Imelda Saucedo, (University of Guanajuato, Guanajuato, Mexico)
Eric Guibal (Ecole des Mines d'Ales, France)

The recovery of metal ions from wastewater or from effluents from metal processing has become an important challenge for the last decade due to the increasingly restricting regulations concerning water discharge to the environment (toxic elements). Mercury is an emblematic example of these metals that are concerned by the recovery regulations due to its high toxic effect (cumulative and highly toxic effect on human and animal beings, as dramatically illustrated by Minamata drama), therefore is proposed to carry out the removal of mercury by microencapsulation of extractants (EIRs), Cyanex 301 and Cyanex 302 (thiosubstituted organophosphinic acid extractants) have been successfully immobilized in alginate using matrix type encapsulation with distribution of the extractant as multi-nuclear micron-size drops. A novel process consists in the immobilization of the extractant as a single drop coated by a biopolymer layer (mononuclear type encapsulation). E-390 Encapsulator (Büchi, Switzerland) equipped with single nozzle and concentric nozzles was used for the preparation of the different materials. The objective of this study is to compare the two modes of encapsulation (i.e., matrix type versus mononuclear type) in the process of removal and recovery of Hg(II).

The study begins with the characterization of composite materials (optical microphotographs, SEM observations and SEM-EDX characterization of Hg(II) interactions with EIRs). The next step investigates the effect of HCl concentration on Hg(II) sorption for Cyanex 301 and Cyanex 302 mononuclear capsules in order to select the optimum pH for further sorption studies. Sorption isotherms and uptake kinetics are then compared for different lots of EIRs: changing the mode of immobilization, the loading of the extractant (varying the dilution of the extractant in kerosene), and the size of sorbent particles. Finally, the desorption properties (and the recycling of the material) are carried out.

Cyanex 301-based EIR is less sensitive to HCl concentration than Cyanex 302-based EIR in terms of Hg(II) sorption. Mononuclear encapsulation shows faster uptake kinetics but lower sorption capacities (in relation with lower capacity to immobilize the extractants, based on stability issues). On the other hand, matrix-type immobilization increases sorption capacity and improves the quantities of extractant that can be immobilized. The extractant loading should be optimized taking into account both the rational use of reactive groups and the accessibility to these sites: indeed, an excess of extractant may impact the accessibility and availability of reactive functions due to aggregation phenomena and viscosity effect. Metal desorption can be performed using 1 M thiourea solution (in 1 M HCl solution). The fabricated materials have good properties to carry out the removal of Hg(II).

TECHNOLOGIES FOR REDUCING UPTAKE AND TRANSPORT OF HEAVY METALS INTO RICE GRAIN

Yongchao Liang and Tingqiang Li

(College of Environmental & Resource Sciences, Zhejiang University, Hangzhou, 310058, China)

Alin Song, Zhaojun Li, and Fenliang Fan

(Institute of Agricultural Resources and Regional Planning, CAS, Beijing 100081, China)

Xionghui Ji

(Institute of Soil and Fertilizer, Hunan Academy of Agricultural Sciences, Changsha 410125, China)

Contamination of heavy metals in soil is a worldwide environmental problem. Over last decades increasing amounts of heavy metals have been released by geological activities or anthropogenic impacts and industrialization such as 1) combustion of fossil fuels, 2) mining, 3) smelting activities, 4) release of wastes and sewage water, and 5) repeated use of organic manures, chemical fertilizers (especially rock phosphate) and pesticides that contain heavy metals. Currently, approximately 20 M ha arable land is subjected to contamination of heavy metals in China, which poses high risks of food safety and human health. Specifically, uptake and transport of heavy metals into rice grain has received more and more attention recently in China. To solve this problem, some alternative *in situ* measures and/or strategies should be taken in addition of phytoremediation. Here we report some cost-effective and environmentally-friendly technologies that are proven to be highly effective in reducing accumulation of heavy metals in rice grain: 1) forming iron plaque on root surfaces via field water management and hence reducing root-to-shoot transport of heavy metals, 2) immobilizing heavy metals and hence reducing their uptake and transport via chemical amendments (fertilization or soil conditioning), and 3) reducing heavy metals uptake by using low-accumulating rice varieties. Large-scale field trials show that these “low-tech” but knowledge-intensive technologies are extremely effective in reducing accumulation of heavy metals in rice grain, and hence the environmental and food safety risks in heavy-metal-contaminated soils.

LEVELS OF HEAVY METALS IN ORGANS OF *Oreochromis Niloticus* FROM GREAT KWA RIVER, SOUTH-EAST NIGERIA

Philomena Asuquo and Lynda-Uta Okon (University of Calabar, Calabar, Nigeria)

Juliet Yakubu (Federal University Wukari, Wukari, Nigeria)

Levels of heavy metals such as Cu, Pb, Cd, Hg and Zn in the gills, offals and muscles of *Oreochromis niloticus* from Great Kwa River were observed for twelve months with the aim of evaluating the ecological risk of elevated levels of heavy metals in tissues of aquatic organisms. Results of chemical analysis with Atomic Spectrophotometry (AAS) showed that copper ranged from 0.92-1.511 $\mu\text{g/g}$ ($1.21\pm 0.24 \mu\text{g/g}$) in the muscles, 2.12-2.854 $\mu\text{g/g}$ ($2.42\pm 0.27 \mu\text{g/g}$) in offal and 1.99-3.225 $\mu\text{g/g}$ ($2.48\pm 0.55 \mu\text{g/g}$) in the gills showing the trend: gills>offal>muscle. Lead ranged from 1.88-2.25 $\mu\text{g/g}$ ($2.00\pm 0.14 \mu\text{g/g}$) in the muscles, 3.21-5.14 $\mu\text{g/g}$ ($3.71\pm 0.74 \mu\text{g/g}$) in offal and 8.32-11.09 $\mu\text{g/g}$ ($9.49\pm 0.98 \mu\text{g/g}$) in the gills showing the trend: gills>offal> muscle. Cadmium ranged from 1.78-3.26 $\mu\text{g/g}$ ($2.55\pm 0.62 \mu\text{g/g}$) in the muscles, 5.23-7.17 $\mu\text{g/g}$ ($6.07\pm 0.76 \mu\text{g/g}$) in offal and 5.63-7.66 $\mu\text{g/g}$ ($6.39\pm 0.82 \mu\text{g/g}$) in the gills showing the trend: gills>offal>muscle. Mercury ranged from 3.98-5.06 $\mu\text{g/g}$ with mean value of 4.36 $\pm 0.42 \mu\text{g/g}$ in the muscles, 18.4-35.17 $\mu\text{g/g}$ ($28.72\pm 5.67 \mu\text{g/g}$) in offal and 21.9-30.41 $\mu\text{g/g}$ ($25.78\pm 2.97 \mu\text{g/g}$) in the gills of *O. niloticus* showing the trend: offal>gills>muscle. The results showed a significant variance ($P<0.05$) between levels of heavy metals in muscles, offal and gills of *O. niloticus* due to different accumulating potentials of the organs. Based on these findings, the levels of heavy metals in organs of *O. niloticus* were within the stipulated limits. However, the present study recommends that precautionary measures need to be maintained in order to avoid possible elevated levels in the future.

EFFECT OF SELECTED HEAVY METALS ON THE GERMINATION AND EARLY SEEDLING GROWTH OF *Jatropha curcas* (Linnaeus)

*Ogunbanjo O.R., Akintola O.O. and Awotoye O.O.

(Federal College of Forestry, Ibadan, Nigeria)

*Email: aolunike@yahoo.com

ABSTRACT: Heavy metal contamination of agricultural soil has become a critical ecological concern. Over the past years there has been increasing interest in the use of live plants and other natural materials to remediate contaminated soils and water. Phytoremediation of this polluted soil with non-edible plants like *Jatropha curcas* offers an environment-friendly and cost-effective method for remediating polluted soil. This study thus investigated the effect of varying concentration of heavy metals on seed germination and seedling growth of *Jatropha curcas*.

Heavy metals used in this study were nitrate salts of copper (Cu), zinc Zn and lead Pb. Solutions of the salt of each of the metals were prepared using distilled water at concentrations of 0(control), 10, 20, 30 and 40mg/l. The experiment consisted of a total of 45 pots with ten seeds planted per pot and each containing 600g of sterilized and washed river sand thoroughly spiked with the prepared solutions. Seed germination and seedling growth were monitored for three weeks. Data assessed included the mean seed germination (%), mean root length (cm) and mean shoot length (cm) of the *Jatropha curcas* seedlings. All data obtained were analyzed using descriptive statistics and analysis of variance (ANOVA) using ASSITAT version 7.7 package.

The exposure of *Jatropha curcas* seeds to heavy metal salts increased the seed germination at 10mg/l but further increase in heavy metal concentration resulted in a decrease in *Jatropha curcas* seed germination. Germination index (GI) values of *Jatropha curcas* seed sown in soil spiked with zinc, lead and copper nitrates were 91-94, 88-82 and 47-87 respectively. It was observed that the GI values of *Jatropha curcas* at 20, 30 and 40 (mg/l) in Pb spiked soil were lower than 80% recommended value for phytotoxic free and mature compost. Heavy metals (Zn, Cu and Pb) concentration at 10mg/l promoted *Jatropha curcas* root length by 101%, 102% and 131% respectively relative to the root length in control experiment. It was noticed that Cu²⁺ values reduced the shoot length when compared with the control at 20 and 40mg/l while Zn²⁺ and Pb²⁺ increased the shoot length *Jatropha curcas* even at higher concentration. Results also showed that Zn was the only metal that significantly increased the seed germination at the concentrations used in this study (p<0.05) while shoot length reduced significantly for seedlings in Cu²⁺.spiked soils at concentration higher than 10mg/l.

Thus, the study showed that *Jatropha curcas* can germinate and grow efficiently at any zinc concentration assessed in this study; and may be grown directly in the soils that are moderately contaminated with copper and lead. Further studies need to be conducted in order to establish the maximum amount of zinc that the plants may tolerate and its ability to germinate and grow in media containing mixtures of these metals.

INTRODUCTION

Heavy metal refers to any metallic element that has a relatively high density compared to water. These metals sometimes exist as natural components of the Earth's crust that cannot be degraded or destroyed but remain indefinitely in the environment (Raskin and Ensly, 2000). Heavy metals such as iron,

copper, manganese and zinc are essential to maintain the metabolism of the human body and can serve as nutrients for plant growth while lead, mercury and cadmium have no known biological functions (Antosiewicz, 1992; Hawkes, 1997 ; Xiong, 1998; Nedelkoska and Doran, 2000 and Nicholls and Tarun, 2003).

Lead, cadmium and mercury are common contaminants in soil and at high concentrations; they may cause metabolic disorders and growth inhibition for most plant species which often lead to death (Kabata-Pendias and Pendias, 1989; Wang *et al.*,2003 and Tripathi, 2007). Soils may become contaminated by the accumulation of heavy metals.

Soil contamination is a very important environmental issue which had been attracting considerable public attention over the last few decades. Heavy metal contamination of agricultural soil had become a critical ecological concern due to it's numerous adverse ecological effects. Heavy metals are released into the environment mainly by anthropogenic means such as mining and smelting, oil spills, domestic, agricultural and industrial activities (Zubillaga and Lavada, 2008).

Physico-chemicals processes such as ion-exchange, precipitation, reverse osmosis, evaporation and chemical reduction had been used to remediate heavy metal contaminated soils but had been found to be very expensive and toxic to the environment; (Lasat, 2002 and Schnoor and McCutcheon, 2003). Over the past years there had been increasing interest in the use of live plants and other natural materials to remediate contaminated soils and water. Phytoremediation technology is aimed at providing an innovative, economical and environmentally-friendly approach to removing toxic metals from hazardous waste sites. This method makes use of metal-accumulating plants to remove heavy metals and other compounds from heavily contaminated environmental soil or water.

Plants to be used for effective phytoremediation should be non-edible, able to accumulate, degrade or volatilize the contaminants. They should also grow quickly in a range of different conditions and lend themselves to easy harvesting. Numerous plant species such as water hyacinths (*Eichhornia crassipes*), poplar trees (*Papulus spp*), forage kochia (*Kochia spp*), alfalfa (*Medicago sativa*), Kentucky bluegrass (*Poa pratensis*), coontail (*Ceratophyllum demersvm L.*) etc. had been identified and tested for their traits in the uptake and accumulation of different heavy metals.(Pandey, 2012)

Jatropha curcas L. commonly known as physic nut belong to the family Euphorbiaceae. It is a multipurpose small tree or large shrub and is found throughout the tropical region. *Jatropha curcas L.* is a vigorous, drought and pest-tolerant plant unpalatable to animals. It is used in Nigeria principally as a hedge plant for protecting cropland from the cattle, sheep and goats *Jatropha* is popularized as unique candidate among renewable energy plants due to its peculiar features like drought tolerance , rapid growth, and easy propagation, higher oil content than other oil crops , small gestation period, wide range of environmental adaptation,. It is regarded as a potential biofuel crop with high economic value to biodiesel and can also be used as anti-cancer medicine, pesticide, cosmetics, and for the treatment of various diseases (Jamil *et al.*, 2009; Li *et al.*, 2010a; Yadav *et al.* 2010).

Phytoremediation of polluted soil with non edible plant like *Jatropha curcas L.* offers an environment- friendly and cost effective method for remediating polluted soil. This study thus investigated the effect of varying concentration of heavy metals on seed germination and seedling growths of *Jatropha curcas L.*

MATERIAL AND METHODS

The experiment was carried out at Federal College of Forestry, Ibadan Nigeria. The river sand used in was air dried and sieved to remove all pebbles and particles that might disturb the proper germination of the seed. The air dried river sand was analyzed in the laboratory to determine the physiochemical parameters and heavy metal contents using appropriate standard instrumentation methods. The soil used had a pH of 6.5, organic carbon -0.65%, total nitrogen- 0.65mg/kg, Zinc- 0.85mg/kg, lead- 0.35mg/kg, Copper - 0.15 mg/kg, iron -13.42 mg/kg and manganese- 8.53 mg/kg. Heavy metals salts used to spike the soil were nitrate salts of copper (Cu), zinc (Zn) and lead (Pb). Solution of salt of each of the metals were prepared using distilled water at concentrations of 0, 10, 20, 30, 40mg/l. the experiment consisted of a total of 45 pots with

ten seeds planted per pot and each containing of 600g sterilized and washed river sand thoroughly spiked with the prepared solutions. Seed germination and seedling growth were properly monitored for three weeks. Data assessed include the mean seed germination (%), mean root length (cm) and mean shoot length (cm) of the *Jatropha curcas L.* seedlings. Seed germination percentage, germination index and root elongation were calculated using the formula given by Zucconi et al (1991) as follows.

$$\text{Seed Germination (\%)} = \frac{\text{No of seeds germinated in sowing medium}}{\text{No of seeds sown}} \times 100$$

$$\text{Root elongation (\%)} = \frac{\text{Mean root length in spiked medium}}{\text{Mean root length in control}} \times 100$$

$$\text{Germination Index} = \frac{\text{Seed germination} \times 100}{\text{Root elongation}}$$

All data obtained were analyzed using descriptive statistics and analysis of variance (ANOVA) using ASSITAT version 7.7 package.

RESULTS AND DISCUSSION

Effects of Heavy Metals on Seed Germination. Results obtained from the experiment revealed that germination percentage of *Jatropha curcas L.* was highest at 10mg/l (figure. 1). However at concentration above 10mg/l of Zn, Cu and Pb, there was a reductions in the seed germination. It can be inferred that seed germination of *Jatropha curcas L.* was reduced with increasing heavy metal concentration except for zinc that did not record a significant reduction in seed germination. even at a concentration of 40mg/l ($p < 5\%$) in this study. This is in line with the findings of Claire *et al* (1991) in a study using nickel and other heavy metals on cabbage, lettuce, miller, radish, turnip and wheat and Aydinal and Marinova (2009) in the study of heavy metals on the growth of Alfalfa plant where they observed significant reduction on the effect of other heavy metals on seed germination with the exception of Zn even at higher concentration. The insignificant reduction of the seed germination to the exposure of Zn levels in the soil may be attributed to its nutritive importance to plant growth. Also the reduction in the seed germination of *Jatropha curcas L.* exposed to Cu may be attributed to the fact that Cu becomes more soluble in acidic soils. Therefore, Cu uptake by the plant would be more in acidic soil and as a result a higher reduction in the growth will occur (Marcel, 2006). As an essential micronutrient and constituent of many enzymes, at higher concentrations it creates toxicity to plants, humans and microorganisms (Perk, 2006). Lead (Pb) is one of the most common inorganic pollutants in the soils (Alkorta *et al.*, 2004). The normal levels of Pb in soils is in the range of 0.85 to 65.8 % (Zarcinas, 2003). It is potentially toxic even at low concentrations and at concentration above 400 mg/kg, the soil is considered hazardous to human health (USEPA, 2001).

Germination index (GI) values of *Jatropha curcas L.* sown in spiked soils vary between 107-118%, 54-88% and 98-99% for zinc, lead and copper nitrates respectively (table 1). Zucconi *et al.*, (1981) stated that a GI value of more than 80% is an indication of phototoxic-free and mature sowing media and this is also in line with the findings of Tiquia and Tam (1998). However, in this study only spiked soils of lead concentration higher than 10mg/l recorded GI that were lower than the suggested value which may be attributed to the release of toxic concentration of lead nitrates. This implies that Pb concentrations above 10mg/l become phototoxic to the studied plant. Generally, it was observed that, the higher the concentration of the heavy metal in sowing media, the lower the germination index value. The reduction in *Jatropha curcas L.* seed germination and increase in the GI values of Zn spiked soils may be due to it's uptake by plant as an essential micronutrient. Zn and Cu are both essential for man, plants and animals but at high

concentration can be toxic. In addition, zinc plays an important role in many biochemical functions in the plants (Fox and Guerimot, 1998).

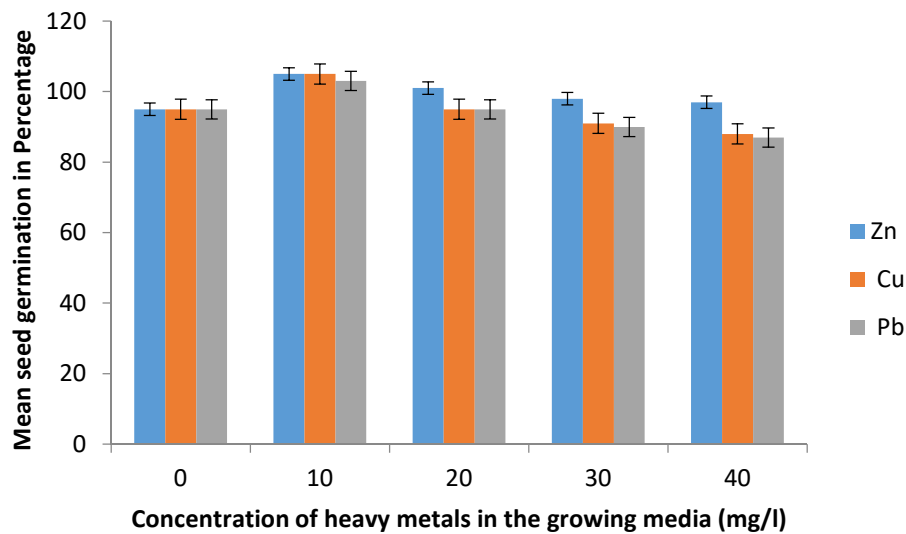


Fig. 1. Seed Germination after Two Weeks of Exposure to Heavy Metals

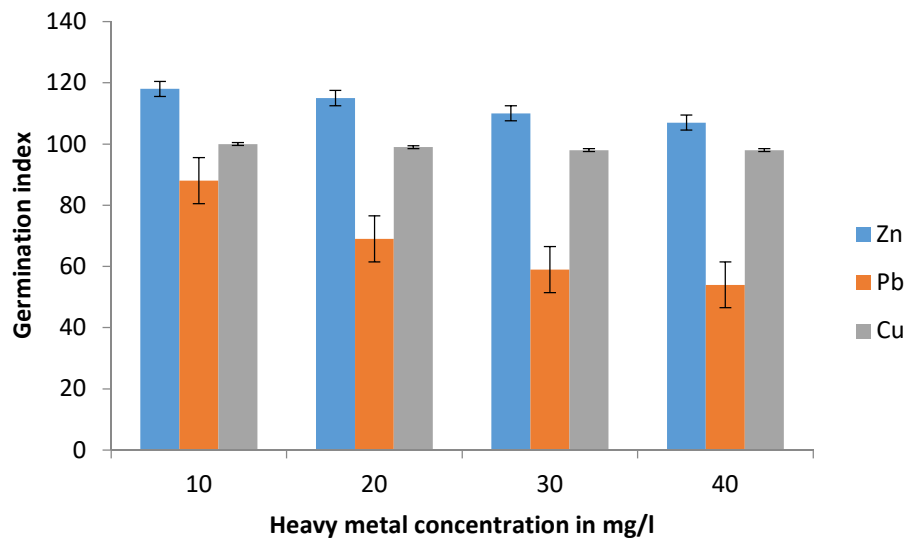


Fig. 2. Germination Index after Weeks of Exposure to Heavy Metals

Effects of Heavy Metals on shoot and Root Growth. The shoot growth of *Jatropha curcas L.* were affected by exposure to heavy metals. It was observed that the effect on the shoot growth was different when compared with the root growth (Figures 3 and 4). Copper at 20, 30 and 40mg/l reduced the shoot length of experimental plant when compared with the control while the doses of Zn²⁺ and Pb²⁺ increase the shoot length. However, there is significant reduction in shoot length at concentration higher than 10mg/l of Cu²⁺ as shown in the control experiment (P<5%) and this agreed with the findings of Once *et al* (2000) where he stated that heavy metal (Cd) reduces the chlorophyll in wheat while Chatterjee and Chatterjee

(2000) found that Cu^{2+} and Cr^{2+} significantly decreased the water potential and Fe^{2+} concentration in cauliflower.

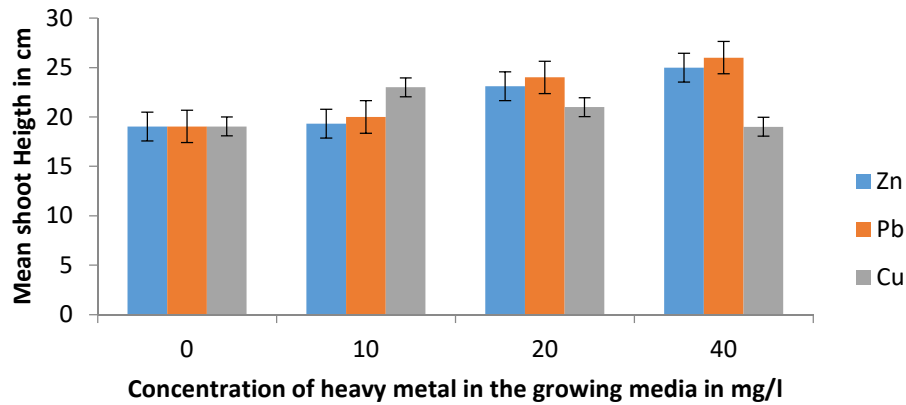


Fig. 3. Shoot Length after Weeks of Exposure to Heavy Metal

The root length of *Jatropha curcas L.* were affected by the exposure to heavy metals. It can be deduced from data obtained that at 10mg/l concentration of Zn and Cu salts, there was no significant effect (Fig.4). The Zn, Pb and Cu at 20, 30 and 40mg/l promote root growth giving a mean root length percentage of 101-135%, 105-137% and 100-121% respectively. This agreed with the findings of Once *et al.* (2000); and Aydina and Marinova (2009) where similar results were obtained on cadmium effect in wheat seedlings and effects of cadmium, copper, chromium, nickel and zinc on the germination and growth of Alfalfa plant respectively. The root lengths increased with increasing concentration of Pb and this may be attributed to the toxicity of Pb which promotes the root growth. The high root length values of all the metals at various concentrations when compared to control had depicted the adaptation ability of the plants to accumulate heavy metals from contaminated soil.

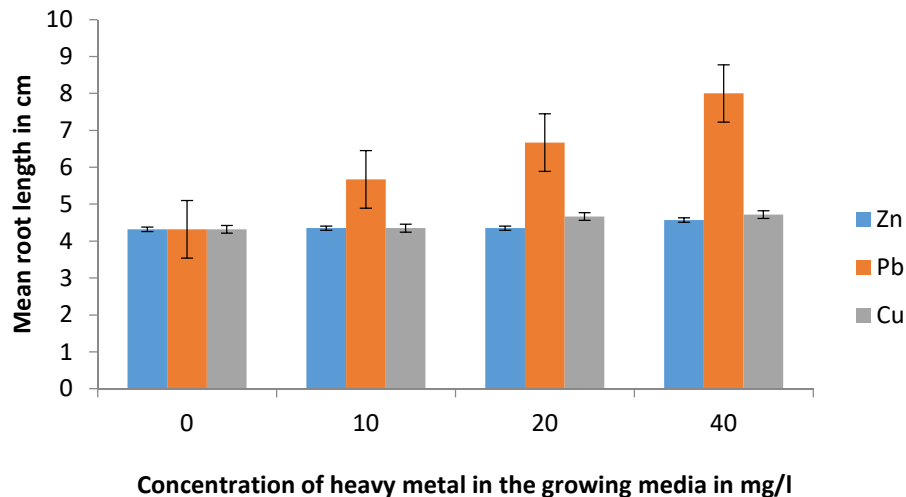


Fig. 4. Root Length after Weeks of Exposure to Heavy Metal

Generally, the significant effect of the heavy metals on the root and shoot growth could be attributed to the accumulation of heavy metals in plant which largely occur in the roots and to a slighter extent in leaves and stems. Plant roots promote the degradation of toxic organic material and act as a medium for soil microorganism to accelerate the biodegradation rates of organic pollutant (Palmroth *et al*, 2002 and Luhach and Chauthry, 2012). Thus, *J. curcas* plant has the ability to nurture well in soil with high levels of heavy metals (Macnair, 1987 and Baker, 1987).

CONCLUSION

This study had shown that exposure of *Jatropha curcas L.* seeds to Cu^{2+} and Pb^{2+} concentrations have significantly affected the seed germination but slightly affected by Zn^{2+} . The root and shoot growth are stimulated at higher levels up to 20mg/l of Zn^{2+} , Cu^{2+} and Pb^{2+} . However, *Jatropha curcas L.* was able to germinate and grow efficiently at any zinc concentration assessed in this study.

Further studies need to be done in order to establish the maximum amount of zinc that the plants may tolerate and its ability to germinate and grow in media containing mixtures of these metals.

REFERENCES

- Alkorta, I., Hernandez-Allica, J., Becerril, J.M., Amezaga, I., Aibizu, I., Onaindia, M., Garbisu, S., (2004): Chelate-enhanced phytoremediation of soils polluted with heavy metals. *Rev. Environ. Sc. Biotechnol.* 3, 55-70.
- Antosiewicz, D. M. (1992). Adaptation of plants to an environment polluted with heavy metals. *Acta Societatis Botanico rum Poloniae.* 61:2811-919.
- Aydinalp, C. and Marinova, S. (2009). The effects of heavy metals on seed germination and plant growth on alfalfa plant (*Medicago sativa*). *Bulg. Journ. Agric. Sci.*, 1547-350.
- Baker, A.J.M. (1987). Metal tolerance, *New Phytol.*, 106: 93-111
- Chatterjee, J. and Chatterjee, C. (2000). Phytotoxicity of cobalt, chromium, and copper in cauliflower. *Environ. Pollution*, 109: 69-74.
- Claire , L.C. ,Adriano, D.C., Sajwan, K.S., Abel, S.L., Thoma, D.P. and Driver, J.T. (1991). Effects of selected trace metals on germinating seeds of six plant species. *Water Air and Soil Pollution* 59: 231-240.
- Fox T.L., Guerimot, M.L., (1998). Molecular biology of cationtransport in plants. *Annual Review of Plant Physiology and Plant Molecular Biology* 49, 669–696.
- Hawkes J.S. (1997): Heavy Metals, *J. Chem. Educ.* 74(11): 1374.
- Jamil, S., P.C. Abhilash, N. Singh and P.N. Sharma, (2009). *Jatropha curcas*: a potential crop for phytoremediation of coal fly ash. *J. Hazard. Mater.*, 172: 269–275
- Kabata-Pendias, A. and Pendias, H., (1989). Trace elements in the Soil and Plants. "CRC Press, Boca Raton, FL.
- Lasat, M.M. (2002). Phytoextraction of toxic metals: A review of biological mechanisms. *J. Environ. Qual.*, 31:109-120
- Li, X., Hou, S., Su, M., Yang, M., Shen, S., Jiang, G., Qi, D., Chen, S. and Liu, G. (2010). Major energy plants and their potential for bioenergy development in China. *Environ. Manage.*, 46: 579–589.
- Luhach, J. and Chauthry, S. (2012). Phytoremediation of heavy metals: Mechanism of tolerance in plants and advancements in techniques" *Proc: Conference on Strategies for mitigation of Environmental Degradation and Climate Change.* 83-89.
- Macnair, M.R., (1987). Heavy metal tolerance in plants: A model evolutionary system, *Trends Ecol. Evolut.*, 2: 354-359.
- Marcel, V.D.P (2006). Soil and water contamination from molecular to catchment scale. London Lewis publishers.
- Nedelkoska, T.V. and Doran, P. M. (2000). Characteristics of heavy metal uptake by plant species with potential for phytoremediation and phytomining. *Mineral Engineering* 13:549-61.

- Nicholls A, and Tarun M. (2003). Effects of lead and copper exposure on growth of an invasive weed, *Lythrum salicaria* L. (Purple Loosestrife). *The Ohio J Science* 103: 129-133.
- Oncel, I., Y. Kele and A. S. Ustun. (2000). Interactive Effects of Temperature and Heavy Metal Stress on the Growth and Some Biochemical Compounds in Wheat Seedlings. *Environmental Pollution*. 107: 315-320.
- Palmroth, M.R.T., Pitchel, J., and Puhakka, J.A. (2002). Phytoremediation of subarctic soil contaminated with diesel fuel. *Bioresour. Technol.* 84: 221-228.
- Pandey V.C, Singh K., Singh J.Sc, Akhilesh Kumar A, Singh B., Rana P., Singh R.P. (2012): *Jatropha curcas*: A potential biofuel plant for sustainable environmental development. *Renewable and Sustainable Energy Reviews* 16: 2870– 2883
- Perk, M.V.D (2006). Soil and water contamination from molecular to catchment scale. Taylor and Francis group. London pp 89-135
- Raskin, I. and Ensley, B.D. (2000). Phytoremediation of toxic metals: Using plants to clean up the environment. John Wiley & Sons, New York.
- Schnoor, J.L. and McCutcheon, S.C. (2003). Phytoremediation Transformation and Control of Contaminants,”Wiley-Interscience Inc, USA.
- Tiquia S.M. and Tam N.F.Y.(2000): Co-composting of spent pig litter and sludge with forced-aeration. *Bioresource Technology* 72 1±7
- Tripathi, L., Tripathi, J.N., Tushemereirwe, W.K. and Bandyopadhyay, R. (2007) Development of a semi-selective medium for isolation of *Xanthomonas campestris* pv. *musacearum* from banana plants. *Eur. J. Plant Pathol.* 117:177-186.
- USEPA, (2001). Risk assessment guidance for super fund volume 111-part A, process for conducting probabilistic risk assessment. Washington DC.
- Wang, Q.R., Cui, Y.S., Liu, X.M., Dong, Y.T. and Christine, P. , (2003). Soil contamination and plant uptake of heavy metals at polluted sites in China. *J. Environ. Sci. Health*, 38, 5: 823-838.
- Xiong, Z.T. (1998). Lead uptake and effects on seed germination and plant growth of a Pb accumulator, *Brassica perkinensis* Rupr. *Bulg. of Environ Contamination and Toxicology* 60:285-91
- Yadav, S.K., Juwarkar, A.A. , Kumar, G.P. , Thawale, P.R., Singh, S.K. and Chakrabarti, T. (2009): Bioaccumulation and phyto-translocation of arsenic, chromium and zinc by *Jatropha curcas* L.: impact of dairy sludge and biofertilizer. *Bioresour. Technol.*, 100: 4616–4622
- Zarcinas B.A¹, Ishak C.F, McLaughlin M.J, Cozens G.(2004): Heavy metals in soils and crops in Southeast Asia. 1. Peninsular Malaysia. *Environ Geochem Health*.26(4):343-57.
- Zubillaga, M.S. and R.S. Lavado, (2008): Accumulation and movement of four potentially toxic elements in soils throughout five years, during and after biosolid application. *Am. J. Environ. Sci.*, 4: 576-582.
- Zucconi, F.; M. Forte A. M and M. de Bertoldi (1981): Biological evaluation of compost maturity. *BioCycle*, 22(2): 27–29.

**STUDIES ON EFFECT OF MIXED CROPPING TECHNIQUE ON THE PHYTOEXTRACTION
POTENTIAL OF VEGETABLES OVER HYPERACCUMULATORS**

Sidi.S¹, *Tank Shantilal K²*

(1. Research Scholar, Dept. of Biosciences, V N South Gujarat university, Surat- 395007 India; 2. Dept. of Biosciences, VNSouth Gujarat U,niversity, Surat – 395007 India)

Accumulation of heavy metals by plants may depend on plant species and soil properties. Long-term consumption of vegetables grown with sewage water near the railway tracks can lead to the early onset of Parkinson's disease, neuron degeneration, hearing and vision impairment, and gastro-intestinal infection. The sewage water contains industrial effluents, which enter the plants through the soil. The uptake of heavy metals in cereals and vegetables is likely to be higher and accumulation of these toxic metals in human body has created growing concern in the recent days. Mixed cropping technique in the present study was tried to seek for the possibility of growing sturdy field crops like *Helianthus annuus* and *Brassica juncea* along with garden vegetables like spinach and *Amaranthus viridus* to ensure decrease metal uptake by edible garden vegetable. The technique was proven to be unreliable as it rather triggered the efficiency of *Spinacea oleracea* and *Amarathus viridus* considerably rendering it unsuitable for mixed cropping as it would lead to unhealthy crop.

PERSISTENT ORGANIC POLLUTANTS

BIOLOGICAL AND INSTRUMENTAL ANALYSIS OF EMERGING CONTAMINANTS OF CONCERN: IN SINGLE AND MULTIPLE PROFILING.

Momoh A. Yakubu, Nina Brinkley, Syntia Kwende, Sara Munyu, Chioma Ihemadu, Fatemeh Bidabadi, Bhavin Rena, Joan Tran, Naga Naidu, Gloria Okome
(Texas Southern University, Houston, TX, USA)

Emerging Contaminants of Concern- can be described in several ways. Chemicals are being discovered in water/environments that previously had not been detected or were being detected at significantly very low levels. They were hitherto viewed as being incapable of causing harm or that they may be significantly different than expected. Advances in chemical analysis, biochemical assay development and technology have made it possible to detect chemicals that were hard to detect and evaluate for toxicity. These advances made it possible to establish the cellular and molecular mechanisms of their toxic reactions thereby raising the possibilities of injury. However, challenges remains as this information cannot be used to predict toxic effects in risk assessment evaluation of individual organism. With legislative aided effective reduction in emissions of conventional and priority pollutants from their sources in most developed countries, focus has shifted to compounds present in trace concentrations and that have only recently been thought of as pollutants. Some of these chemicals can interfere with the endocrine system of a wide range of organisms -these endocrine-disrupting chemicals (EDCs); have been the focus of much scientific attention in recent years. The interaction of multiple agents with the host's endocrine system could result in a wide spectrum of potential adverse health effects and much scientific uncertainty remains regarding the risks from these emerging pollutants. Most of the controversy surrounding the association between emerging environmental contaminants (EEC)/ EDCs and the various health endpoints is probably related to the lack of convincing evidence; the strength or weight of evidence and the association. For human health endpoints considered, concern arises from the little or lack of evidence that environmental levels of weakly active compounds elicit similar effects, either with hormonally active Pharmaceuticals or risk factors related to endogenous hormone levels. With high frequency of occurrence and/or coming from diverse sources of pollutants, they are now becoming a major concern due to their potential adverse effects on human health and environment. Despite their low concentrations within the environment and seemingly low biological activities individually – possibility exist for interactions of these diverse chemicals at low level concentrations, multiple interactions-interfacing with sensitive biochemical and hormonal pathways. These possibilities could lead to untoward and devastating consequences on human development and health - these *scenarios* are alarming. The major sources of these emerging contaminants are found in our waters -derived particularly from biopharmaceuticals, personal care products, agricultural and household used products especially multiple pesticides etc. We have over these years developed methods for biological and instrumental analysis of these contaminants as single entities or in multiple mixtures in our environmental resources, leachates into our water sources and foods as well as their effects on biological functions. Survey and analytical results (instrumental and biological) of studies of these emerging contaminants of concern will be presented with associated major health implications discussed.

ANALYSIS OF NONYLPHENOL COMPOUNDS IN AQUATIC ENVIRONMENT USING GAS CHROMATOGRAPHY-MASS SPECTROMETRY

Seçil Ömeroğlu (Middle East Technical University, Tukey)
Fadime Kara Murdoch (Selçuk University, Tukey)
Faika Dilek Sanin (Middle East Technical University, Tukey)

Nonylphenol compounds are a group of organic chemicals (nonylphenol-NP, nonylphenol polyethoxylates-NPnEO and nonylphenoxy polyethoxy acetic acid-NPnEC) that are found in various industrial and commercial formulations. They are toxic and carcinogenic but beyond these, they tend to mimic hormones and interfere with the proper functioning of the endocrine system. For this reason, NP compounds are called as “endocrine disrupting chemicals” (EDCs).

Due to their surface active properties, these compounds are known to be excellent detergents, surface cleaners and lubricants that are widely used in everyday life. Although most of the countries banned their use in domestic formulations, these compounds are still present in personal care products such as shampoos, anti-wrinkle creams and deodorants. Since they have widespread use, they eventually end up in the wastewater treatment systems and environment. Most of the NP compounds are not fully degraded treatment plants, therefore, it is inevitable that they reach surface waters, sediments, etc. Many of the research showed their presence in environmental systems at a range of concentrations. Although these concentrations do not seem high, their effects are severe since NPnEOs start to degrade and form metabolites that are more toxic and persistent.

Once discharged into the receiving bodies, majority of the NP compounds remain in the water body. Unfortunately, due to their concentrations and complex matrix of the environmental systems, it is very difficult to detect these compounds in aquatic environment. Therefore, the aim of this study is to analyze the research on the measurement of NP compounds in aquatic environment and development of a rapid and reliable method to detect NP, NPnEOs and NPnECs in water systems using gas chromatography-mass spectrometry (GC-MS).

PHOTOLYTIC AND PHOTOCATALYTIC DECOMPOSITION OF PHARMACEUTICALS IN WATER BY ULTRAVIOLET LIGHT-EMITTING DIODE

Burhanuddin Khuzema Zaveri and Hyeok Choi (The University of Texas at Arlington, TX, USA)
Mohammad Reza Eskandarian and Mostafa Fazli (Semnan University, Semnan, Iran)
Mohammad Hossein Rasoulifard (University of Zanjan, Zanjan, Iran)

ABSTRACT: Pharmaceutical residues in the environment and their potential toxic effects have been recognized as one of the most emerging research areas in environmental chemistry. Among many treatment technologies for pharmaceuticals, ultraviolet (UV)-based oxidation has gained popularity as it has capability to decompose a broad range of refractory chemicals. As an alternative UV source to problematic conventional mercury lamps, light-emitting diode (LED), so-called UV-LED, has gained attraction. UV-LED shows many advantages such as high efficiency, low power consumption, long lifetime, no disposal problem, no warming-up time, and compactness. Although over the last decade and half several research has been done on decomposition of pharmaceutical products using heterogeneous photocatalysis and photolysis very little importance has been given to the parameters like wavelength of light, intensity of light. Analysis of SMX showed that considerable photolytic decomposition was obtained using UVC while UVA and UVC were very effective for photocatalytic decomposition process. From high intensity to low intensity brought down the degradation from 90% to 0%, thus showing its significance.

INTRODUCTION

The occurrence of pharmaceuticals and their metabolites and transformation products in the environment is becoming a matter of concern because these compounds, which may have adverse effects on living organisms, are extensively and increasingly used in human and veterinary medicine and are released continuously into the environment (Xekoukoulotakis, N.P., C. Drosoua, and C. Breboua, et al, 2011). Many PPCPs have been classified as emerging chemicals of concern (ECCs) and endocrine disrupting compounds, meanwhile, some industries continue to emphasize the benefits of such PPCPs in their products. Most antibiotics are often partially metabolized in the organism (i.e. less than 30%) and they are excreted as the parent substance or as metabolites into wastewaters at concentrations ranging from ng/L to g/L (Kümmerer, K., 2009). Most pharmaceuticals are known to be bio recalcitrant under aerobic conditions because their function is to remove microorganisms from body, thus escaping intact from conventional wastewater treatment plants. In response to the growing concerns about the presence of potentially toxic PPCPs and other ECCs in water resources, advanced oxidation processes (AOPs) have been widely studied and proposed to be effective for the complete degradation of such contaminants. AOPs involve the generation of transitional reactive free radicals, particularly hydroxyl radicals (HRs, $\cdot\text{OH}$) and sulfate radicals (SRs, $\text{SO}_4^{\cdot-}$), which are stronger oxidizing species than conventional oxidants (Anipsitakis and Dionysiou, 2004; Son et al., 2003). Among the different advanced oxidation processes (AOP's), heterogeneous photo catalysis has emerged as a promising process for wastewater treatment, because it is a versatile and inexpensive (eliminating use of chemicals, UV radiation from sunlight, LED powered with solar radiation) technique to be applied to the treatment of different organic pollutants. When a semiconductor is illuminated with photons, whose energy is equal to or higher than the energy corresponding to the band-gap of the semiconductor, there is absorption of these photons and consequently some electrons (e^-) may jump from the valence to the conduction band. Simultaneously, a photo-hole is generated in the valance band (h^+). The electron/hole pairs migrate to the surface of the catalyst, where they

can whether recombine and dissipate the input energy as heat, or react with the molecules object of degradation (Abella'n M.N., and B. Bayarri, 2007).

Ultraviolet disinfection of water has a long and well proven history. UV light has long been accepted as an effective germicidal treatment and has been installed in many major public drinking water and wastewater treatment plants. Recent developments to use UV as a means removing contaminants that cannot be removed by traditional biological process has led several research on Photocatalysis and photolysis degradation. Minimal research focuses towards the effect of UV wavelength and light intensity on overall process and problems associated with disposal of traditional UV lamps. LEDs offer potential advantages over conventional UV lamps such as a better adequacy in converting electricity into light (high quantum yields), lower power requirements, compactness and robustness, no warm-up time, no disposal problems, and potential for long lifetimes.

Our research has explored the degradation of sulfamethoxazole under UV LED. Three different UV LED (UVA, UVB and UVC) that emit light under various UV wavelengt to compare the degradation variation based on wavelength. The light source is placed at different heights and the intensity of light falling on the reactor is measured and degradation percentage of target contaminant is monitored.

MATERIALS AND METHODS

Chemicals. Sulfamethoxazole (SMX) is obtained in salt form from Sigma Aldrich and are used as obtained. The chemicals used for analytical analysis acetonitrile was obtained from Sigma Aldrich and is used as received The Degussa P25 titanium dioxide is used as a catalyst for Photocatalytic experiments. 0.75 mg/L of TiO₂ was added to the solution which was decided based on some experiments and literature review. Most experiments revealed that an increase in catalyst loading above 1 mg/L did not show any significant increase in degradation.

Experimental Setup. The UVA and UVB lamps were purchased from International Light Technologies while UVC was obtained from Crystal Light. UV-LEDs and cooling system were attached using a clamp above the reactor. The solution were prepared using DI water in order to eliminate effects of any ions on the experiment. The solution was continuously agitated using a magnetic stirring bar. Current and voltage was adjusted by a DC power supply with galvanostatic operational options. Three reactor vessels with definite shape and size were considered for every wavelength experiments analysis. In order to measure different light intensities the clamp was fixed at different heights and measured using PD300RM-UV obtained from Ophir photonics.

Analysis of Samples. Samples were drawn at time intervals 10, 20, 30, 60, 120 and 180 minutes and filtered through 0.45 µm membranes. SMX concentration was monitored with a reversed-phase high performance liquid chromatography (1200 series, Agilent) equipped with a quaternary pump, C18 column, and ultraviolet (UV) detector. A mixture of water and acetonitrile was used as the mobile phase at water:acetonitrile ratio of 60:40% v/v with a flow rate of 1 ml/min for SMX. The UV detector was operated at a wavelength of 265 nm for SMX, which was pre-determined using a UV-visible spectrophotometer (UV 2550, Shimadzu).

RESULTS AND DISCUSSION

The effectiveness of degradation of organic pollutants by photocatalytic process depends up on the wavelength of the emitted radiation which relates to the adsorption wavelength of target molecule, the intensity of radiation, catalyst loading, which are responsible for generation of hydroxyl radicals. The photolysis degradation depends upon the UV adsorption range of target molecule. The UV-LED has lower intensity compared to traditional mercury lamps and can be applied only if competitive degradation is observed. The figure 1 and 2 below show the degradation achieved from different wavelengths (UVA, UVB and UVC) for SMX under photolysis and photocatalysis condition respectively.

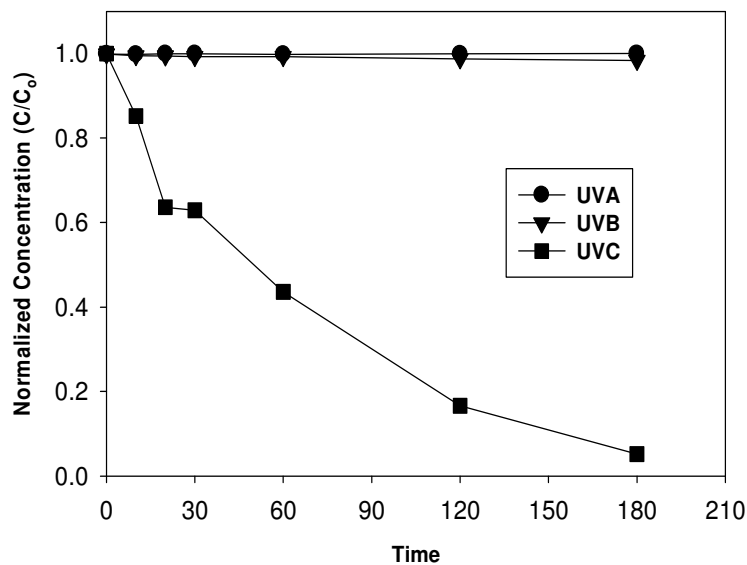


FIGURE 1. Effect of Wavelength on Photolytic Degradation of SMX. [SMX]₀= 20 mg/L and TiO₂= 0.75 mg/L

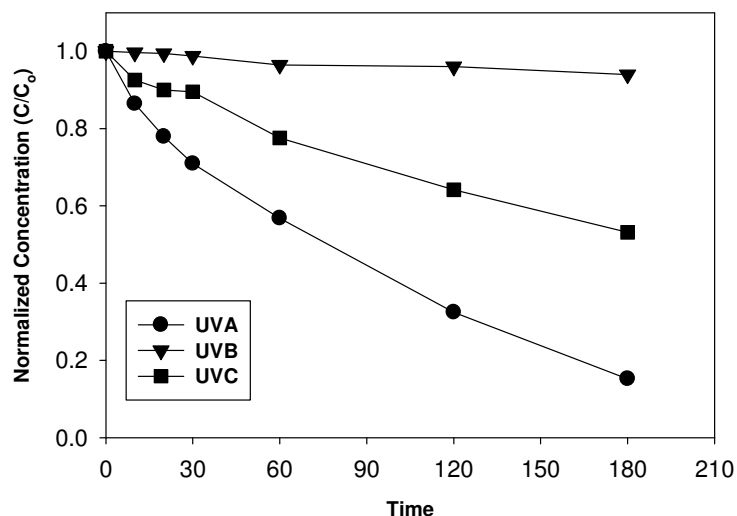


FIGURE 2. Effect of Wavelength on Photocatalytic Degradation of SMX. [SMX]₀= 20 mg/L and TiO₂= 0.75 mg/L

From figure 1 and 2 it can be seen that UVC performs better in both photolytic and photocatalytic process of degradation. Although UVA has its wavelength in the range of 315 nm to 400 nm which is far away from the adsorption radiation of SMX its high intensity (8.6 mW/cm²) produces sufficient radicals to bring almost 90% degradation of SMX during photocatalytic process.

UVB which has its wavelength in the range of 280 nm to 315 nm does not show any sufficient degradation of SMX. The adsorption wavelength of SMX is far away from the range of UVB and also the

high intensity of UVB is very low (0.1 mW/cm²) and hence not a significant degradation like in case of UVA is observed in photocatalytic process.

UVC photolysis brings about 95% and 50% degradation of SMX in photolysis and photocatalysis process respectively. The peak adsorption wavelength of SMX coincides with peak wavelength of UVC lamps and hence a high degradation is observed in photolysis process in comparison to photocatalytic process where both target molecule and TiO₂ particles compete for the radiation thereby reducing the degradation percentage.

TABLE 1. Effect of Intensity on Photolysis and Photocatalytic Degradation of SMX. [SMX]₀= 20 mg/L and TiO₂= 0.75 mg/L

SMX Degradation Observed at 180 Minutes						
	UVA		UVB		UVC	
	Photolysis	Photocatalysis	Photolysis	Photocatalysis	Photolysis	Photocatalysis
High Intensity	0%	90%	0%	10%	95%	50%
Low Intensity	0%	35%	0%	0%	0%	0%

The irradiance is a proportional to driving current and its position in a reactor. When the UV lamps are placed closed to the reactor increase of the incident photon quantity in this irradiance interval enhances the chance of photon absorption which leads to electron-hole formation and thus photo catalytic degradation. It is reported that at high irradiance values, electron-hole recombination dominates and therefore reaction rate decreases and is not anymore related to irradiance linearly but to the square root of the irradiance (Jamalia.A, and R.Vanraes, 2013).

CONCLUSION

UVA and UVC performed better in comparison to UVB, which is most likely because of high intensity of both the lamps in comparison to UVB. A negligible amount of irradiance was measured at the bottom of the reactor which implies a non-optimal distribution of light. To improve further the performance of the reactor, it is necessary to design a structure with more uniform light distribution. Other benefits that can be expected by using UV LED, is the small bulb size enables more optimized reactor design to be developed that should reduce dose requirements further extending the opportunity that LED bulbs provide. Looking further into the future the continued development will drive down the energy associated with the use of AOP making the overall technology a more viable alternative especially in places where current systems are struggling to meet treatment needs such as the removal recalcitrant micro-pollutants such as pharmaceuticals. However, for these predictions to happen, several parameters need to improve especially the intensity in order to give UV LED/TiO₂ AOPs a chance of implementation at larger scale.

ACKNOWLEDGEMENTS

Dr. Choi appreciates the financial support of the University of Texas at Arlington in form of startup fund to initiate this study.

REFERNCES

- Jamalia.A., and R.Vanraes. 2013. "A Batch LED Reactor For The Photocatalytic Degradation Of Phenol." *Chemical Engineering and Processing:Process Intensification*. 71: 43-50.
- Kümmerer,K. 2009. "Antibiotics in the Aquatic Environment". *Chemosphere* 75: 417-434.

- Abella'n, M.N., and B. Bayarri. 2007. "Photocatalytic Degradation Of Sulfamethoxazole In Aqueous Suspension Of TiO₂". *Science Direct, Applied Catalysis B: Environmental* 74: 233-241.
- Xekoukoulotakisa,N.,P., C.Drosoua, C.Breboua, and E.Chatzisyneona. (2011). "Kinetics of UV-A/TiO₂ Photocatalytic Degradation And Mineralization Of The Antibiotic Sulfamethoxazole In Aqueous Matrices". *Catalysis Today* 161: 163-168.
- Anipsitakis, G. P., and D. D. Dionysiou. 2003. "Degradation of organic contaminants in water with sulfate radicals generated by the conjunction of peroxymonosulfate with cobalt." *Environ. Sci. Technol.* 37(20):4790-4797.

IN-SITU DECOMPOSITION OF BIOLOGICAL TOXINS ON NITROGEN-DOPED NANOSTRUCTURED TiO₂ FILMS UNDER SOLAR RADIATION

Hesam Zamankhan Malayeri and Hyeok Choi
(The University of Texas at Arlington, Arlington, TX, USA)

ABSTRACT: Contamination of water resources with natural and anthropogenic chemicals has been a huge concern worldwide, considering growing population and economy. Particularly, increasing occurrence of harmful algal blooms (HABs) alarms water and health authorities and general public. Most seriously, some algae produce and release lethal biological toxins such as microcystins (MCs). MCs are among the most powerful natural poisons. The presence of MCs in drinking water sources has raised major concern. As a result, the goal of this study is to decompose MCs, if feasible, on-site and in real-time with minimal efforts, less chemicals, and low energy inputs. To achieve the goal, we introduced TiO₂ photocatalysis for the generation of hydroxyl radicals which are responsible for the decomposition of MCs. High efficiency nitrogen-doped nanostructured TiO₂ photocatalysts, which can be activated under visible light, were developed to utilize solar radiation as a sole energy source for TiO₂ activation and radical generation. Considering on-site applications, TiO₂ was firmly immobilized onto a substrate and characterized with nanoporous, transparent, and ultrathin properties which are beneficial to photocatalytic reactivity, light utilization, and mechanical stability. Results so far showed that the TiO₂ film has high potential to decompose biological toxins under solar radiation within a reasonable time.

INTRODUCTION

The increasing occurrence of harmful algal blooms (HABs) in water resources worldwide is alarming the environmental and health authorities because of their potential to release biological toxins (Vazquez et al., 2011). Of particular interest are microcystins (MCs) produced during cyanobacterial HABs (Mohamed et al., 2003). MCs are among the most powerful natural poisons. Exposure to MCs can affect the number and diversity of wild animal populations, cause bioaccumulation of toxins in the tissues of fish and shellfish, and indirectly affect other organisms through the food chain and eventually humans (Palikova, et al., 2011). Compared to particulate algae which are easily removed by conventional processes, biological toxins dissolved in water are not easy to remove and thus they are not the focus of the treatment processes. Consequently, removal of biological toxins in water resources is important, if feasible, on-site and in real-time with minimal efforts, less chemicals, and low energy inputs. The on-site treatment strategy also provides a systematic tool to protect living creatures and ecosystem in HAB sites.

Progress in chemical oxidation has resulted in advanced oxidation technologies (AOTs), one of the most powerful water treatment processes (Nfodzo, et al., 2013). AOTs are based on generation of hydroxyl radicals and sulfate radicals with high oxidation potentials. Particularly, TiO₂ photocatalysis has been highlighted as one of the most promising and green AOTs due to its effectiveness to generate hydroxyl radicals (Choi, et al., 2010). For the generation of hydroxyl radicals from TiO₂, ultraviolet (UV) radiation which provides high photon energy above the band gap of TiO₂ is required. This greatly inhibits the utilization of solar radiation as a sustainable energy source for the TiO₂ activation because only 4% of the incoming solar energy onto the earth's surface is in UV range. To utilize visible light in solar radiation for TiO₂ activation, dye-sensitized or metal ion-doped TiO₂ has been developed and the TiO₂ has shown promising results for the degradation of chlorinated compounds and nitrogen oxides (Bae and Choi, 2003).

Introduction of anionic dopants, especially nitrogen, to TiO₂ also makes it possible to reduce the TiO₂ band gap and thus to activate TiO₂ under visible light.

In addition to the intrinsic photocatalytic activity of TiO₂, which is directly related with its crystal properties, the structural properties of porous TiO₂ catalysts, such as their surface area, porosity, and pore size and distribution, are also of importance because of their potential role in enhancing the light absorbance of TiO₂ catalysts and the accessibility of reactants to the active catalytic sites (Zakersalehi et al., 2013). One of the methods to fabricate highly porous materials with desired pore structure and size for target-specific applications is to use amphiphilic organic molecules such as surfactants and block copolymers as pore directing agents when TiO₂ is formed from its molecular precursor in a sol-gel process. In particular, we used a nitrogen-containing surfactant in the sol-gel method, which is expected to produce N-doped porous TiO₂.

Moreover, sol stability and film homogeneity are also important. Conventional approaches immobilize already-synthesized (or commercially-available) TiO₂ particles onto a substrate and thus result in a non-uniform and instable thick film. In this study, TiO₂ precursor sol was directly deposited onto a borosilicate glass via dip-coating technique (Choi, et al., 2006). After coating, the glass substrate coated with the TiO₂ precursor sol was precisely heat-treated using a programmable furnace. Binding of the TiO₂ precursor to the glass surface at high temperatures, uniform and ultrathin nature, and nanocrystalline TiO₂ are believed to significantly enhance the mechanical stability of the TiO₂ film. Transparency is also another important factor, which is related with light penetration through the TiO₂/glass composite and thus overall photocatalytic reactivity. As a result, this study was focused on developing an innovative integrated material processing method to synthesize nanocrystalline N-doped TiO₂ with a controlled porous structure and to fabricate a robust, transparent, and ultrathin TiO₂ film. Preliminary results demonstrated successful decomposition of MCs on the high efficiency visible light-activated TiO₂ under visible light.

MATERIALS AND METHODS

TiO₂ Sol Synthesis. Two different nitrogen containing surfactants, diethanolamine (DEA), and benzyltrimethylammonium chloride (BTAC) purchased from Aldrich were used. First each surfactant was dissolved in isopropanol (i-PrOH, Fisher) and then acidic acid (Fisher) was added to the solution for the esterification reaction with i-PrOH (Choi, et al., 2006). Finally, titanium tetraisopropoxide (TTIP, Aldrich) was added under vigorous stirring. The molar ratio of surfactant/i-PrOH/acetic acid/TTIP was 1:45:6:1. Control TiO₂ was also prepared with the surfactants.

TiO₂ Thin Film Formation. A borosilicate glass substrate with an effective surface area of 10 cm² was used to immobilize TiO₂. The substrate was dip-coated with the sol using a PTL-MM01 (MTI Corporation) dip-coating device at a withdrawal rate of 15 cm/min. After coating, the films were dried at room temperature for 1 h and then put into furnace (Paragon HT-22-D, Thermcraft). The heat-treatment temperature was increased at a ramp rate of 60 °C/h to 100 °C and maintained at this temperature for 1 h. Then the temperature was increased again to 500 °C, maintained at this temperature for 2 h, and then cooled down naturally. The dip-coating and calcination process was repeated five times.

Photocatalytic Activity. In order to quickly check whether the film works under visible light, first we tested decomposition of methylene blue (MB) as a model organic dye. Two 15W fluorescent lamps (Philips) were used at the intensity of 2.1 mW/cm² and mounted with a UV block filter (UV420, Bower) to cut the spectral range below 420nm. The initial concentration of MB was 5 mg/l and the volume of the solution was 10 ml. In order to measure dark adsorption, the solution was kept in dark condition for 30 min and then irradiation began and continued for 4 hours. After that, we switched target chemical to decompose from MB to MC-LR (Cayman Chemicals). The initial concentration of MC-LR was 1 mg/l.

Analysis of Samples. Water samples were drawn at each sampling intervals. Concentration of MB was measured using a UV–Vis spectrophotometer (UV-2550, Shimadzu) at adsorption peak of 664 nm. Concentration of MC-LR was monitored with a reversed-phase high performance liquid chromatography (1200 series, Agilent) equipped with a quaternary pump, C18 column, and ultraviolet (UV) detector. A mixture of trifluoroacetic acid (TFA, Sigma-Aldrich) and acetonitrile was used as a mobile phase at TFA:acetonitrile ratio of 80:20% v/v with a flow rate of 1 ml/min. The UV detector was operated at a wavelength of 238 nm.

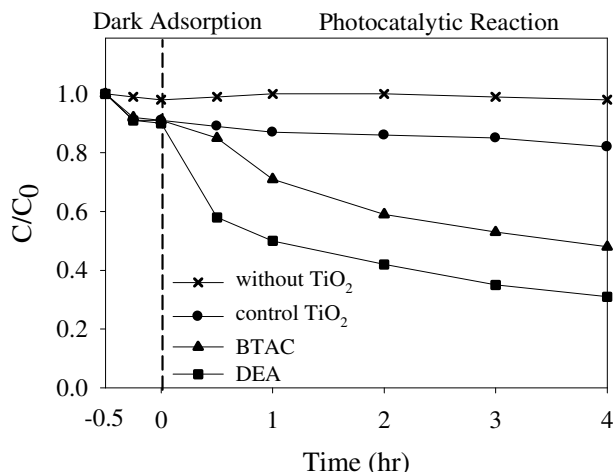


FIGURE 1. Photocatalytic decomposition of MB by different TiO₂ thin films under visible light of > 420 nm

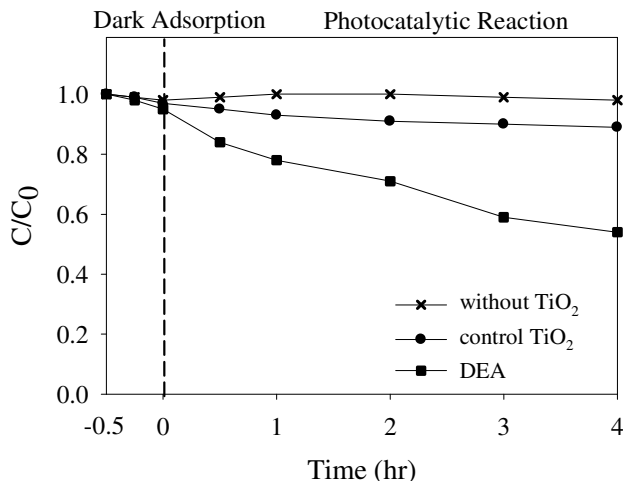


FIGURE 2. Photocatalytic decomposition of MC-LR by TiO₂ thin films under visible light of > 420 nm

RESULTS AND DISCUSSION

Photocatalytic activity of different TiO₂ thin films was measured in terms of MB decomposition, as shown in Figure 1. As expected, there was no removal (adsorption) in the dark condition in the absence of TiO₂. All three TiO₂ materials showed around 10% adsorption of MB in the aqueous solution. Under visible light, there was no photolysis of MB in the absence of TiO₂. Control TiO₂ which was made without the surfactants showed negligible photocatalytic decomposition of MB under visible light. However, N-

doped TiO₂ thin films made of BTAC and DEA showed significant decomposition. In particular TiO₂ made of DEA achieved around 70% removal of MB after 4 hours. The result implied the surfactant BTAC and DEA are effective to improve the physicochemical properties of TiO₂ for visible light activation (Vaiano et al. 2015).

Since TiO₂ made of DEA showed the highest reactivity with MB under visible light, we tested the TiO₂ for the decomposition of MC-LR, as shown in Figure 2. As expected, there was no photolysis of MC-LR by visible light because MC-LR is a strong chemical and control TiO₂ made without the surfactants did not show any reactivity under visible light. TiO₂ made with DEA showed successful decomposition of MC-LR at around 40% after 4 hours.

CONCLUSION

This study was focused on developing an innovative integrated material processing method to synthesize nanocrystalline N-doped TiO₂ with a controlled porous structure and to fabricate a robust, transparent, and ultrathin TiO₂ film. Preliminary results demonstrated successful decomposition of MC-LR on the high efficiency visible light-activated TiO₂. Our research effort was to develop a new sustainable approach to decompose MCs, if feasible, on-site and in real-time with minimal efforts, less chemicals, and low energy inputs, is under progress. The effort includes characterization of the materials for explaining the high reactivity under visible light, control of calcination temperature for manipulating porous structure and nitrogen content, utilization of many other N-containing surfactants, and test of the materials under solar radiation. This study implies high potential for utilizing solar radiation as a sole energy source for the on-site treatment of MCs by using the TiO₂ photocatalytic system.

ACKNOWLEDGEMENTS

This research was supported by the Texas Higher Education Coordinating Board through the Norman Hackerman Advanced Research Program Fund (THECB13311).

REFERENCES

- Bae, E., and W. Choi. 2003. "Highly enhanced photoreductive degradation of perchlorinated compounds on dye- sensitized metal/TiO₂ under visible light." *Environ. Sci. Technol.*, 37(1), 147-152.
- Choi, H., S. R. Al-Abed, D. D. Dionysiou, E. Stathatos, and P. Lianos. 2010. "TiO₂-based advanced oxidation nanotechnologies for water purification and reuse" in: *Sustainability Science and Engineering, Volume 2: Sustainable Water for the Future* (Eds. Isabel I. Escobar and Andrea I. Schafer, ISSN 1871-2711), pp. 229–254, Elsevier Science, Netherlands.
- Choi, H., E. Stathatos, and D. D. Dionysiou. 2006. "Synthesis of Nanocrystalline Photocatalytic TiO₂ Thin Films and Particles Using Sol-Gel Method Modified with Nonionic Surfactants." *Thin Solid Films*, 510(1-2):107-114.
- Mohamed, Z. A., W. W. Carmichael, and A. A. Hussein. 2003. "Estimation of microcystins in the freshwater fish *Oreochromis niloticus* in an Egyptian fish farm containing a *Microcystis* bloom." *Environ. Toxicol.* 18(2):137-141.
- Nfodzo, P., D. D. Dionysiou, and H. Choi. 2013. "Water Supply and Treatment." in: *Encyclopedia of Environmetrics Second Edition* (Eds. Abdel H. El-Shaarawi and Walter W. Piegorsch), pp. 1712-1726, John Wiley & Sons, Chichester, UK.
- Palikova, M., J. Mares, R. Kopp, J. Hlavkova, S. Navratil, O. Adamovsky, L. Chmelar, and L. Blaha. 2011. "Accumulation of Microcystins in Nile Tilapia, *Oreochromis niloticus* L. and Effects of a Complex Cyanobacterial Bloom on the Dietetic Quality of Muscles." *Bulletin Environ. Contam. Toxicol.* 87: 26-30.

- Vaiano, V., O.Sacco, D. Sannino, and P. Ciambelli. 2015. "Nanostructured N-doped TiO₂ coated on glass spheres for the photocatalytic removal of organic dyes under UV or visible light irradiation." *Applied Catalysis B: Environmental*, 170:153-161.
- Vazquez, E. J. N., I. G. Lizarrage, C. J. B. Schmit, A. C. Tapia, D. J. L. Cortes, F. E. H. Sandoval, A. H. Tapia, and J. J. B. Guzman. 2011. "Impact of harmful algal blooms on wild and cultured animals in the Gulf of California." *J. Environ. Biol.* 32: 413-423.
- Zakersalehi, A., M. Nadagouda, and H. Choi. 2013. "Suppressing NOM access to controlled porous TiO₂ particles enhances the decomposition of target water contaminants." *Catalysis Communications*, 41:79-82.

DECHLORINATION OF DDT AND ITS PRODUCTS USING PALLADIZED BACTERIAL CELLULOSE IN A REACTOR

Vyjayanthi Jeevan Prakash and *Sumathi Suresh** (Centre for Environmental Science and Engineering, Indian Institute of Technology Bombay, Powai, Mumbai, India, e-mail: *sumathis@iitb.ac.in)

ABSTRACT: A rotating catalytic contact reactor comprising of zerovalent palladium immobilized on bacterial cellulose was used in the present investigation in both batch and continuous modes for the dechlorination of DDT, DDD and DDE. Treatment of aqueous solution of 72 mg L⁻¹ DDT, 99 mg L⁻¹ DDD and 100 mg L⁻¹ DDE solubilised in 0.05% (v/v) biosurfactant resulted in greater than 99% removal by dechlorination within 30 minutes of reaction when the reactor was operated in batch mode using molecular hydrogen as the reductant.. Approximately 10 L of 72 mg L⁻¹ DDT solution could be treated with 90% efficiency when the reactor was operated in continuous flow mode with a hydraulic retention time (HRT) of 1 hour in the presence of hydrogen. GC-MS analysis confirmed the formation of completely dechlorinated hydrocarbon skeletons of DDT, DDD and DDE, namely, diphenylethane and diphenylethylene, as the end products, thereby implying the removal of all alkyl and aryl chlorine atoms during the course of reductive reaction. The foregoing results thus provide a successful demonstration of the dechlorination efficiency of the catalytic system towards the target compounds studied.

INTRODUCTION

DDT (1,1,1-trichloro-2,2-bis (4-chlorophenyl) ethane), DDD (1-chloro-4-[2,2-dichloro-1-(4-chlorophenyl)ethyl]benzene), DDE (1,1-bis-(4-chlorophenyl)-2,2-dichloroethene) are toxic and highly stable hydrophobic compounds that are known to bioaccumulate and biomagnify along the food chains. The US Environmental Protection Agency as well as the Stockholm Convention on persistent organic pollutants classified DDT, DDD and DDE as priority pollutants (Gryglewicz and Piechocki, 2010). Although use of DDT was banned worldwide in 1972, it continues to persist in soil, sediments and ground water bodies. Thus development of effective treatment technologies for the removal of DDT and its products is critical to the restoration of environment.

It is acknowledged that DDT, DDD and DDE are susceptible to reductive dehalogenation reactions that lead to detoxified products that are vulnerable to biodegradative processes. Based on this premise reductive degradation technologies based on the application of monometallic (such as Fe⁰, Mg⁰ and Pd⁰) and bimetallic systems (examples include Fe⁰/Pd⁰, Mg⁰/Pd⁰) have been developed for the degradation of recalcitrant chlorinated compounds. Anodic corrosion of the base metals such as Fe⁰, Mg⁰ can supply electrons for the direct dehalogenation of target compounds. However such reactions are slow and often result in the accumulation of partially dechlorinated products. Therefore combination of the base metal with an efficient catalytic metal such as Pd⁰ is desirable for complete dehalogenation of pollutants. Palladium-based catalysts in association with molecular hydrogen (H₂) gas have been also applied for aqueous-phase destruction of halogenated organic compounds in groundwater at ambient pressure and temperature (Mekhaev et al., 2011; Jujjuri and Keane, 2010). These studies cite several key advantages of Pd which are: (i) effective for a wide range of contaminants (ii) presents high rates of reaction and efficiency (iii) requires mild reaction conditions and iv) generation of fewer toxic end products that require minimal follow-up treatment. Molecular hydrogen has been reported to dissociate to form atomic hydrogen (called hydride) at room temperature at the surface of the hydrogenation catalyst Pd to form highly reactive Pd hydride which has a low reduction potential (-2.2V). However, commercial applications of palladium have been impeded due to the fact that it is an expensive catalyst and its recovery after the reduction reaction is

very poor. This problem can be overcome by immobilizing the catalyst onto suitable support materials which enhances its reusability which is the goal of the present investigations. The overall goal of our research project was to explore the possibility of using metallic palladium that has been immobilized irreversibly on bacterial cellulose (palladized bacterial cellulose) as a versatile and novel bio-inorganic catalyst to mediate the reductive dechlorination of 3 persistent organochlorinated pesticides, namely, DDT, DDD and DDE, in a reactor. The specific objectives of our research project were to (1) design and develop a rotating catalytic contact reactor, which uses palladium immobilized on bacterial cellulose for the treatment of water spiked with DDT, DDD and DDE; (2) study the kinetics of removal of DDT, DDD and DDE in the reactor operated in batch mode; (3) to study the efficiency of removal of DDT in reactor operated in continuous flow mode; and 4) identify the end products formed as a result of reductive removal of the target compounds. Extracellular cellulose synthesized by bacteria offers the following attractive features as a biogenic support matrix: a) ability to precipitate noble metals such as palladium, gold and silver and immobilize the metal particles within its cellulose network (Evans *et al.*, 2003) b) can be grown to any desirable size and shape and applied in reactors c) Can be prepared in situ from a wide range of biodegradable substrates and d) easily biodegradable.

MATERIALS AND METHODS

Design and Operation of Rotating Catalytic Contact Reactor (RCCR): The design characteristics used for development of the reactor used for the present study were adapted from Patel and Suresh (2008). The schematic diagram of the RCCR is shown in Figure 1.

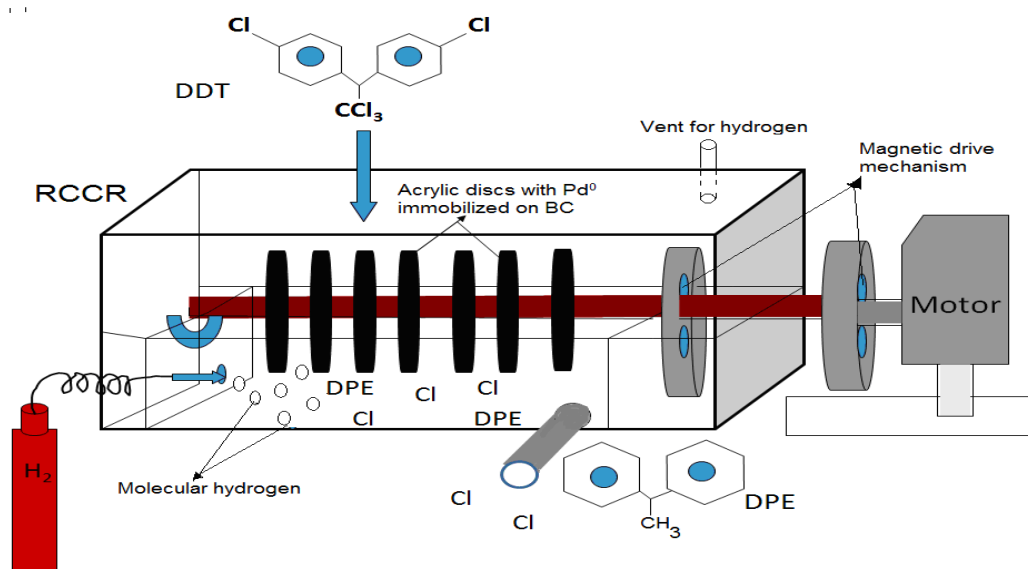


FIGURE 1. Schematic diagram of the rotating catalytic contact reactor (RCCR).

The rectangular reactor consisted of 7 circular discs of 100 mm diameter providing a total surface area of 1142 cm². The discs were mounted on a horizontal shaft, which was rotated using a magnetic drive mechanism. Effective liquid volume of the reactor was ~650 ml while the speed of rotation was 8 RPM for all experiments. The top of the reactor was covered with a tight lid (although no precaution was taken to keep the reactor free of oxygen). Molecular hydrogen was bubbled into the liquid phase of the reactor at a flow rate of 40 ml min⁻¹ and 0.1 kg cm⁻² pressure. Continuous purging of hydrogen was required as hydrogen is a reactant and is required for the reductive dehalogenation reactions. Rotation of discs in RCCR facilitated exposure of immobilized palladium alternately to the liquid phase containing the substrate solution and the gaseous phase containing molecular hydrogen to perform effective reduction. The reactor was provided

with a vent for hydrogen to prevent explosive conditions and maintained under atmospheric pressure and room temperature (28°C - 30°C).

Production of Bacterial Cellulose in the Laboratory and Its Palladization: Microbial culture capable of producing cellulose was prepared in the laboratory as per the conventional method followed in Philippines (Thampan, 1981) with modifications as suggested by Patel and Suresh (2008). Three cups of orange fibre pulp was mixed with 6 cups of water and 3 cups of sugar and left undisturbed in a wide-mouthed plastic container covered by a thin cloth. A thin layer of soft, white, jelly like film (bacterial cellulose) of ~2 mm thickness was observed after 12-15 days. Cellulose-producing bacteria have been reported to adhere to cellulose deposits and grow actively at the cellulose-air interface (Seráfica *et al.*, 2002). Hence cellulose films were scraped and used as the source of bacterial inoculum for production of cellulose in RCCR.

Development of Bacterial Cellulose Film and Immobilization of Metallic Palladium: The medium for growth of bacterial cellulose-producing culture consisted of 65 g L⁻¹ of sucrose and 25 g L⁻¹ of acetic acid added to 650 ml of filtered mature coconut water. The resulting medium was autoclaved and then introduced into the reactor and inoculated with bacterial cellulose deposits. The discs were rotated at slow speed for even deposition of bacterial cellulose until a film thickness of ~2 mm was attained. Pre-treatment and palladization of BC was conducted according to the protocol described by Evans *et al.*, (2003). As a first step, discs were immersed for 24 hours in 1% NaOH to kill bacterial cells adhering onto the cellulose following which they were washed thrice with water and then equilibrated in 0.5 M sodium acetate solution (pH of 5) for 2 h. Finally bacterial cellulose immobilized on the rotating discs was incubated in 650 ml of 5 mM K₂PdCl₆ solution prepared in 50 mM sodium acetate solution (at 90°C, pH 4.5) until all the discs turned black due to the deposition of zerovalent palladium (3 hours). The palladized discs were subsequently washed in water to remove any residual salt of palladium or unbound Pd⁰.

Kinetics of Dechlorination of DDT, DDD and DDE Using RCCR in Batch Mode: Kinetic studies were conducted in batch mode by introducing 650 ml of DDT (72 mg L⁻¹) or DDD (99 mg L⁻¹) or DDE (100 mg L⁻¹) solubilised in 0.05 % of JBR biosurfactant into the reactor. The order of reaction and rate constant values were computed. Removal could be influenced by both non-reactive sorption (adsorption of target molecules onto BC matrix) and reactive sorption followed by dechlorination. Hence, the effects of both these factors on the extent of removal were determined. Aliquots (3 ml) were collected at chosen time points, extracted thrice with cyclohexane and 0.2 µl of the pooled extracts were analyzed by GC-ECD. Dechlorination was also performed using Tween 80, a commercially available chemical, as the solubilising agent for DDT.

Dechlorination of DDT Using RCCR in Continuous Flow Mode: DDT (72 mg L⁻¹) was passed through the reactor in the presence of hydrogen. Constant inflow and outflow rates were maintained using a dual channel “Masterflex” (Cole-Parmer) peristaltic pump. The effluent was pooled continuously and analyzed for residual DDT concentrations using GC-ECD. Because complete mixing of the liquid phase occurred in the reactor, the relationship between the concentration of target substrate, DDT in the reactor (or the effluent) to that in the reactor inlet (under steady state conditions) can be given by equation 1 as given below.

$$C_e = \frac{C_0}{1 + k\theta} \quad (1)$$

where, C_e and C_0 are the concentrations of DDT (mg L⁻¹) in the reactor/effluent and inlet to the reactor, respectively, θ = hydraulic retention time (min) and k = first order reaction rate constant (min⁻¹).

Gas Chromatography with Electron Capture Detector (GC-ECD) and Gas Chromatography-mass Spectroscopic (GC-MS) Analyses: Extracted samples were analyzed using an Agilent model 6890 gas chromatographic instrument equipped with Ni⁶³ electron capture detector (ECD). HP-5 capillary column of 0.32 mm ID, 0.25 μm film thickness and 30 m length was used. Injection was made in splitless mode using nitrogen as the carrier gas. The following temperature programme was used: the initial oven temperature of 150°C with hold time of 4 min, ramped at 6°C min⁻¹ up to final temperature of 290°C held for 4 min. Detector temperature was set at 300°C. Residual concentrations of DDT, DDD and DDE were quantified from peak areas obtained through automated integration. GC-MS analyses of extracted samples were performed using Perkin Elmer GC system (model Clarus 500) interfaced with a mass detector or Agilent Technologies 7890A GC system coupled with 5975C mass detector. An Elite 5MS (methyl polysiloxane) column of 0.25 mm ID, 0.25 μm thickness and 30 m length was used with helium as the carrier gas (flow rate 1.0 ml min⁻¹). The column temperature was ramped as follows: initial temperature of 100°C with hold time of 1 min, ramped at 8°C min⁻¹ to final temperature of 290°C held for 10 min. The ion trap was operated at 70 eV with a scan range of m/z from 30 to 500. A sample of 2.0 μl was injected in splitless mode. Intermediates and end products were identified by comparing the mass spectral data with the existing Wiley library data base.

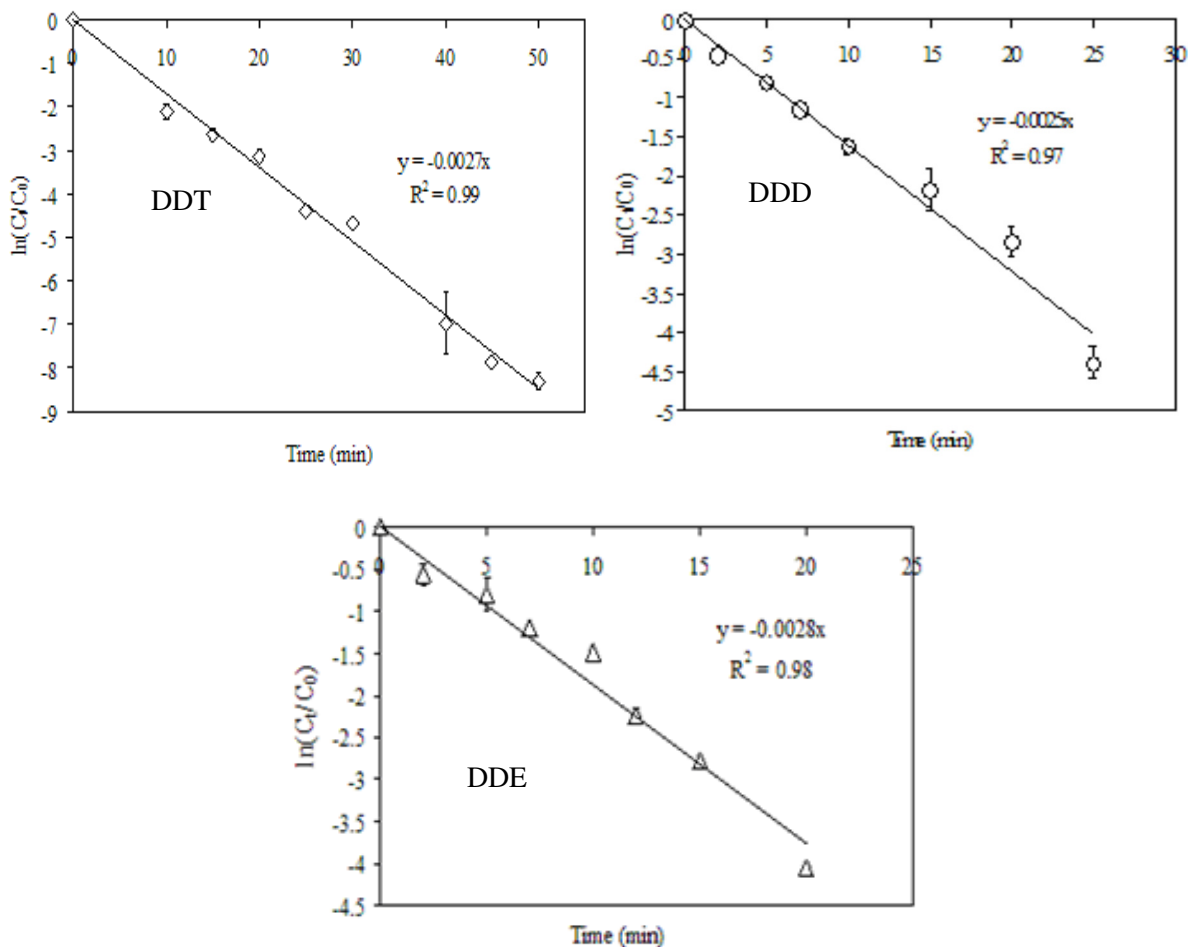


FIGURE 2. First order kinetic plots for the removal of DDT, DDD and DDE in RCCR operated in batch mode using 0.05% (v/v) biosurfactant and H₂ as the reductant.

RESULTS AND DISCUSSION

Removal of DDT, DDD and DDE Using RCCR in Batch Mode: Figure 2 compares first order kinetic plots for the removal of DDT, DDD and DDE in RCCR. It may be noted that sorption contributed to approximately 35%, 28% and 21% removal (data not shown) while reaction in the presence of hydrogen caused >99% dechlorination of all three compounds. The observed first order rate constants were computed to be 0.0027, 0.0025 and 0.0028 $\text{min}^{-1} \text{mg}^{-1} \text{Pd}^0$ for DDT, DDD and DDE respectively. pH of the treated solutions turned acidic probably due to the release of chloride ions. Partially dechlorinated intermediates such as DDD, DDE and DDMS could not be detected by GC-ECD probably due to high rate of dechlorination of sorbed target molecules and their partially dechlorinated intermediates. Removal of DDT solubilized in 0.05% Tween 80 also followed pseudo first order kinetics with comparable first order rate constant of 0.0029 $\text{min}^{-1} \text{mg}^{-1} \text{Pd}^0$ (plot not shown).

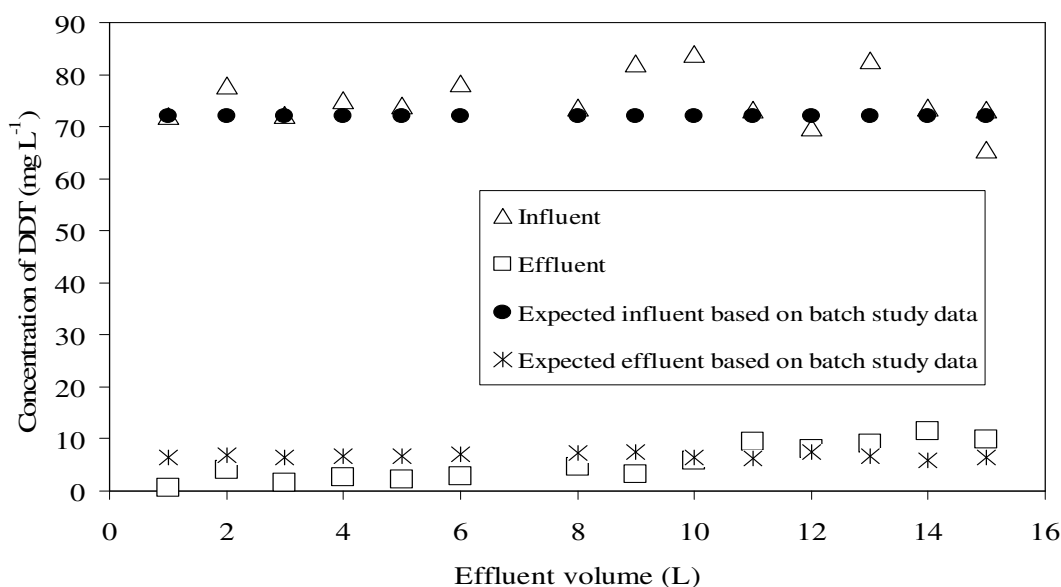


FIGURE3. Removal of DDT in RCCR operated under continuous flow mode using H₂ as the reductant. Experimental condition □ bio surfactant = 0.05% (v/v); RPM = 8; Pd⁰ content = 63 mg g⁻¹ dry weight of BC; hydraulic retention time = 1 h; flow rate = 10.83 ml min⁻¹.

Removal of DDT Using RCCR in Continuous Flow Mode: By substituting the first order rate constant value of 0.17 min^{-1} (0.0027 $\text{min}^{-1} \text{mg}^{-1} \text{Pd}^0$) and setting θ at 1 h, the expected outlet DDT concentration was calculated to be 6.5 mg L^{-1} giving a predicted efficiency of approximately 94% for the removal of 72 mg L^{-1} DDT solution. It can be observed from Figure 3 that the concentrations of DDT in the effluent (obtained experimentally) closely matched with that of computed value (until the pooled volume of effluent reached 10 L). Intermediates or end-products of reaction in the reactor might be responsible for the deterioration of catalytic efficiency above this

Identification of End Products of DDT, DDD and DDE Dechlorination in RCCR Treated Water by GC-MS Analyses: The identity of intermediates and end products formed following 50, 20 and 20 minutes of reaction of DDT, DDD and DDE in RCCR, respectively, were determined by GC-MS. The total ion chromatogram and the corresponding fragmentation pattern after reaction of 72 mg L^{-1} DDT are shown in Figures 4 (a) and 4 (b) respectively. Weiss and LaPierre (1980) reported that DDT and DDD yield a base

peak of 235 while DDE gives a base peak of 246 in the corresponding mass spectra. Figure 4 (a) reveals the presence of a dominant ion eluting at 8.6 min. Based on the molecular ion fragmentation of this peak as seen in Figure 4 (b), the product was identified as 1,1-diphenylethane (DPE), characterized by m/e of 182. A base peak of m/e 167 is expected to be formed due to the elimination of $-CH_3$ from DPE and presence of the above peak as seen in Figure 4 (b), provided further confirmatory evidence for the formation of this product. Formation of DPE is expected to occur by the successive or sequential removal of 3 alkyl and 2 aryl chlorine atoms from DDT. Based on the GC-MS analyses the product obtained after reductive dechlorination of DDD and DDE in RCCR were determined to be 1,1-diphenylethylene, which is the expected chlorine-free carbon backbone of DDD or DDE (MS data not shown). Complete dechlorination of DDT to form DPE and DDD and DDE to form diphenylethylene by zerovalent palladium immobilized on various supports using hydrogen as the reducing agent have been previously reported (Hashimoto *et al.*, 2010).

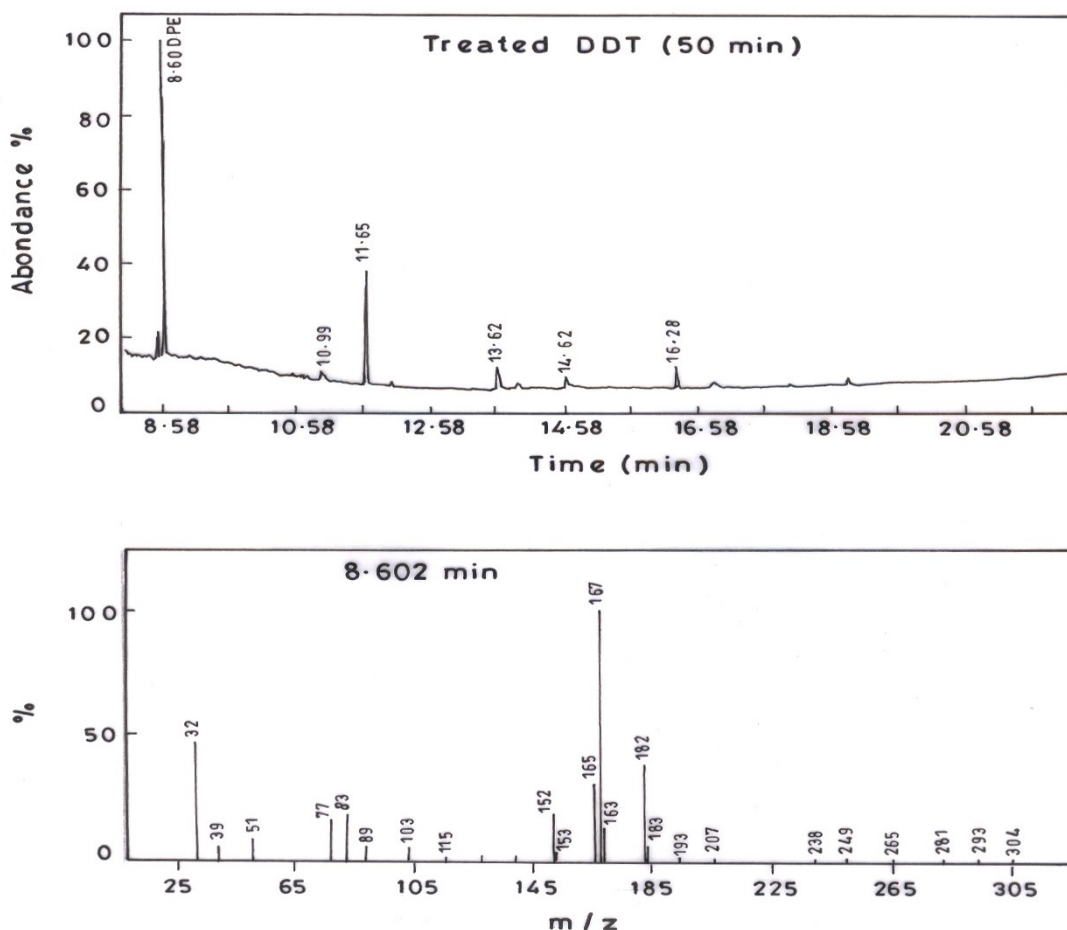


FIGURE 4. (a) Total ion chromatogram of DDT (72 mg L^{-1}) following 50 min of reaction with palladized bacterial cellulose and hydrogen in RCCR (b) fragmentation pattern of the product ion eluting at 8.6 min.

CONCLUSIONS

Results obtained through this investigation demonstrate the catalytic efficiency of zerovalent palladium immobilized on the biogenic support matrix, bacterial cellulose. Complete dechlorination of

DDT, DDD and DDE could be achieved in RCCR under batch and continuous flow modes. Reusability of the expensive catalyst, Pd⁰ immobilized on bacterial cellulose is expected to lower the cost of the technology. Due to the extremely small particle size, large surface area and high *in situ* reactivity, RCCR may be applied for remediation of ground and surface water bodies.

ACKNOWLEDGEMENTS

The authors thank DST and CSIR, Government of India, for providing financial support. The authors acknowledge IIT Bombay for providing infrastructural facilities to execute the project and services provided by Sophisticated Analytical Instrument Facilities, IIT-Bombay for GC-MS analyses.

REFERENCES

- Gryglewicz, S. and W. Piechocki. 2010. "Conversion Pathways of DDT and its Derivatives During Catalytic Hydrodechlorination". *Pol. J. Environ. Stud.*, 19(4): 715–721.
- Mekhaev, A.V., M. G. Pervova, O. P. Taran, I. L. Simakova, V. N. Parmon, M. A. Samorukova, V. P. Boyarskiy, T. E. Zhesko, V. I. Saloutin, and Y. G. Yatluk. 2011. "Liquid-Phase Dechlorination of Toxic Man-made Products Using Nanodispersed Palladium Catalysts Sibunit". *Chemistry for Sustainable Development*. 19: 173–180.
- Hashimoto, N., T. Hara, S. Shimazu, Y. Takahashi, T. Mitsudome, T. Mizugaki, K. Jitsukawa, and K. Kaneda. 2010. "Complete Hydrodechlorination of DDT and its Derivatives Using Hydroxyapatite-Supported Pd Nanoparticles Catalyst". *Chem. Lett.* 39: 49–51.
- Patel, U.D. and S. Suresh. 2008. "Complete Dechlorination of Pentachlorophenol Using Palladized Bacterial Cellulose in a Rotating Catalyst Contact Reactor". *J. Colloid Interf. Sci.*, 319: 462–469.
- Serafica, G., R. Mormino and H. Bungay. 2002. "Inclusion of Solid Particles in Bacterial Cellulose". *Appl. Microbiol. Biotechnol.*, 58(6): 756–760.
- Jujjuri, S. and M. A. Keane. 2010. "Catalytic Hydrodechlorination at Low Hydrogen Partial Pressures: Activity and Selectivity Response". *Chem. Eng. J.* 157: 121–130
- Evans, B. R., H. M. O'Neill, V. P. Malyvanh, I. Lee and J. Woodward. 2003. "Palladium-Bacterial Cellulose Membranes for Fuel Cells". *Biosens. Bioelectron.* 18(7): 917–923.
- Weiss, A. H., and R. B. Lapierre. 1980. "Gas Chromatographic/Mass Spectroscopic Analysis of Partially Dechlorinated 1,1-Diphenylethane and Ethylene". *Environ. Int.* 3: 353–357.
- Thampan, P. K. 1981. *Handbook on Coconut Palm*. Oxford & IBH Publishing, New Delhi, India

THE POTENTIAL OF SPORE FORMING BACTERIA IN HEAVY OIL SPILL CLEAN UP

Biji Shibulal, Saif Al-Bahry, Yahya Al-Wahaibi, Abdulkadir Elshafie, Ali Al-Bemani, Sanket J
(Sultan Qaboos University, Muscat, Sultanate of Oman)

The Sultanate of Oman, located in the Southeast of Arabian Peninsula is seriously threatened by oil pollution as Oman is one of the major oil producing countries in the Middle East and about 30-40% of the oil produced is passed along the Oman Coast. Oil spills may occur due to drilling rigs, routine shipping, run-offs and dumping or human negligence and have severe ecological and economic consequences. Clean-up and remediation of heavy crude oil is a challenge. Bacteria isolated from heavy oil contaminated environment are accustomed to heavy oil and could be much effective in its bioremediation. The objectives of the study were to isolate heavy crude oil degrading spore forming bacteria and to study their responses to heavy oil spills. A total of 42 different spore forming bacteria were isolated and confirmed as heavy oil biodegrading ones. The bacterial isolates were primarily representatives of genera *Bacillus* and *Paenibacillus*. Two different isolates which showed maximum growth at high concentrations of heavy crude oil (7% w/v, API 6^0) in Bushnell Haas media (BHM) were selected for the study. The isolates were identified by 16S rDNA sequencing as *Bacillus licheniformis* strain BG2 (KP119098) and *Bacillus subtilis* strain BS2 (KP119102) and their nucleotide sequences were submitted to NCBI GenBank, USA. Degradation efficiency was measured using Gas Chromatography–Mass Spectrometry (GC–MS). The heavy crude oil, degraded for a period of one week, was compared with those of a naturally biodegraded oil and the effect of these bacteria on biodegradation of heavy crude oil was studied. The GC-MS analysis showed a significant effect of these organisms in the biodegradation on heavy crude oil on the ninth day of incubation ($T_{stat} \geq T_{critical}$, $P \leq 0.05$). The results showed that the overall reduction of total heavy crude oil 58% and 62% for BG2 and BS2 respectively compared to that of the control. It can be concluded these strains can be used as an effective eco-friendly candidate for heavy oil spill clean-up can be introduced to a spill in order to hasten biodegradation.

SEPARATION OF POLYBROMINATED DIPHENYL ETHERS IN FISH FOR COMPOUND-SPECIFIC STABLE CARBON ISOTOPE ANALYSIS

Yanhong Zeng*, Xiaojun Luo, and Bixian Mai

(Guangzhou Institute of Geochemistry, Chinese Academy of Sciences, Guangzhou, 510640, China)

Polybrominated diphenyl ethers (PBDEs) are a group of brominated flame retardants, which have been added to a large variety of commercial products. Due to their widespread industrial use, PBDEs have been detected as a ubiquitous pollutants in the environment. Moreover, studies reported that PBDEs can bioaccumulate and undergo biotransformation in wildlife and humans. Debromination occurring in biota is a confounding factor to evaluate bioaccumulation behaviour of individual PBDE congener. It is very important to understand whether a specific PBDE congener in organism is an accumulated contaminant or the debromination product of the higher brominated congeners. Compound specific isotope analysis (CSIA) using gas chromatography in combination with isotope ratio mass spectrometry (GC-IRMS) is a suitable tool to study such issues.

Purification and isotope analysis method were developed to accurately measure the stable carbon isotope ratio of PBDEs with three to six substituted bromine atoms in fish samples. Pooled fish samples were treated with concentrated sulfuric acid, separated using a complex silica gel column, and finally purified with an alumina/silica gel column using a proper elution solvent. The purities of extracts were verified by gas chromatography and mass spectrometry in the full scan mode. The average recoveries of all compounds across the purification method were between 60% and 110%, with the exception of BDE-154. The stable carbon isotopic compositions of PBDEs can be measured with a standard deviation of less than 0.5‰. No significant isotopic fraction was found during the purification of the main PBDE congeners. A significant change in the stable carbon isotope ratio of BDE-47 was observed in fish carcasses compared to the original isotopic signatures, implying that PBDE stable carbon isotopic compositions can be used to trace the biotransformation of PBDEs in biota.

MODELING

DESIGN OPTIMIZATION OF GAS-TO-LIQUID BIOSLUDGE MANAGEMENT SYSTEMS

Rana Abbass, Emad Imam (The American University in Cairo, Cairo, Egypt) and Udeogu Ongwusogh (Qatar Shell Research and Technology Center, Doha, Qatar)

ABSTRACT: The optimum management system of biosludge varies according to the type of the biosludge, applicable environmental legislations as well as site and climate conditions. Biosludge generated from plants treating wastewater of Gas-To-Liquid (GTL) plants was used for experimental investigation of its treatability characteristics. Lab results characterized the biosludge to have an organic content of more than 80% of its dry solids content. Aerobic digestion (AD) of the GTL biosludge achieved solid content reduction values of as high as 70% in 9 weeks with corresponding decay constant of 0.0145day^{-1} . An optimization design model was developed for the management of GTL biosludge. The optimum design obtained by the model excluded the use of the Aerobic Digester (AD) and comprised of the centrifuge, drying beds (DB) and landfill disposal resulting in a unit cost of \$7.26/ton. To meet the EPA requirement, the design required 21 days in the AD and 8 days in the DB with a unit cost of \$9.97/ton. Applying the design model to domestic and refinery biosludge that have higher decay constants has resulted in management costs of \$6.01/ton and \$4.55/ton, respectively.

INTRODUCTION

Biosludge is the end product of biological, physical or chemical wastewater treatment plants (WWTPs) (Guyer, 2011). As environmental awareness spreads across industries and cultures, environmental regulations have constrained how WWTPs deal with biosludge waste. Moreover, biosludge treatment demands a considerable percentage of any WWTP's costs. Such regulations require the proper design and installation of a functional and feasible biosludge treatment system as part of any WWTPs while taking into consideration environmental and operational constraints. It is also imperative to treat the produced biosludge to achieve volume reduction and stabilization to be suitable for safe disposal or reuse in accordance with environmental legislation.

The U.S. Environmental Protection Agency (EPA) has proposed certain techniques to achieve volume reduction and stabilization known as Processes to Significantly Reduce Pathogens (PSRPs) (U.S. EPA, 2003). Such processes include aerobic digestion (AD) where biosludge is agitated with oxygen for a certain residence time at the prevailing temperature to achieve stabilization of the organic content (U.S. EPA, 2003). Other methods include air-drying, composting and lime stabilization (U.S. EPA, 2003). As for anaerobic digestion, biosludge is treated in the absence of air at high temperatures to produce stabilized biosludge and biogas (U.S. EPA, 2003).

Once sludge is left to separate, it is mostly highly putrescible organic matter hence; a stabilization treatment technique is inevitable to produce inert biosludge fit for reuse or disposal (Appels et al., 2008). Volume reduction follows digestion and includes dewatering using centrifuge units and drying beds (DB) (Appels et al., 2008).

Biosludge composition differs widely depending on the type of wastewater and the treatment train dictating different treatment processes. The optimum biosludge management system should also account for the applicable environmental legislations as well as site and climate conditions. Therefore, there is no standard solution to treat biosludge. Engineers usually follow certain technical design codes to decide on and size the suitable treatment units to treat the biosludge at hand. These codes disregard the effect of external factors like for example cost and availability of land, variations in ambient temperature from one

season to another and other site-specific conditions. Design codes are resorted to due to a lack of models that assist the designer to decide on the optimal line-up for the treatment of a certain biosludge composition.

Literature on optimizing biosludge management systems in general is limited. However optimization studies were carried out. Tang et al. developed a model to prioritize sludge treatment alternatives to select the optimum process for a situation (Tang et al., 1997). The model focused on developing countries where the trade-off between cost and effectiveness must consider socio-cultural and environmental conditions (Tang et al., 1997). Linear programming models have been developed to optimize the design of sludge treatment processes at the lowest cost but were soon found to be inadequate for optimization of these processes as they have a more dynamic nature (Tang et al., 1997). An Analytic Hierarchy Process (AHP) was used owing to its ability to take into account environmental and social aspects (Tang et al., 1997). Parameters considered included land size, location and cost, economic factors, climatic conditions, sludge nature and age, local construction skills and community support (Tang et al., 1997). However, the AHP is not quantitative enough to obtain the optimum design of the sludge management system. On the other hand, Bertanza et al. emphasized the importance of optimizing the dewatering stage in the biosludge management system (Bertanza et al., 2014). They carried out an experimental methodology to evaluate the technical and financial performance of dewatering devices that can be used as a Decision Support System (DSS) (Bertanza et al., 2014). The limitation of this study lies in its focus on only one treatment stage however; this choice was made due to the high volume reduction potential achieved through dewatering coupled with sludge's poor dewatering qualities.

This study focuses on the design of an optimum management system for biosludge generated from plants treating wastewater of Gas-To-Liquid (GTL) plants, which is important in many areas, such as the Gulf region, with high land cost, warm arid climate and a lack of sludge re-use markets. Therefore, a tailored management system is needed for such conditions, which is likely to be different from the conventional sludge management systems. This research hence, consists of two parts: (i) experimental investigation of the characteristics of GTL biosludge and its aerobic treatability, and (ii) developing a design model to obtain the optimum design of a GTL biosludge management system.

MATERIALS AND METHODS

Experimental Work. The treatment of GTL biosludge using aerobic digestion was simulated in a lab experiment to derive the GTL decay constant. Samples were collected from the GTL WWTP on a weekly basis for lab analysis. The lab set-up was an aerobic digester batch set-up, which is also referred to as a die-out design where aerobic bacteria are put in a non-limiting environment given that the supply of oxygen is in excess allowing for maximum oxidation rate of Volatile Suspended Solids (VSS) (Bhargava & Datar, 1988). Furthermore, other performance critical parameters like pH and temperature are kept within optimal range to eliminate their effect. The used lab scale reactors were equipped with an aerator, a mixer, pH, temperature and Dissolved Oxygen (DO) probes. Nine batch experiments were run over the course of 12 weeks in three phases. Both influent biosludge and final biosludge samples were characterized and analyzed. Samples were extracted from the reactor at predefined Sludge Retention Times (SRTs), on a weekly basis. To study the performance of a batch reactor, chosen response variables were tested and monitored including the digestion rate of aerobic bacteria which is tested through monitoring the reduction rate in solid content especially VSS through monitoring Volatile Solids (VS) destruction and Chemical Oxygen Demand (COD) concentrations (Rao & Baral, 2011).

Aerobic digestion causes stabilization and volume reduction owing to the process of endogenous metabolism being its core activity (Wang & Shamma, 2009). Endogenous metabolism is a function of the active fraction of the bacterial population in biosludge (Wang & Shamma, 2009). Hence a drop in solids during aerobic digestion will only be due to a decrease in the active biomass or in other words the organic content in the digester. GTL biosludge was analyzed for solid content distribution showing that the VSS content is more than 80% of the Total Suspended Solid (TSS). This proves that aerobic digestion is an

optimal treatment technique for GTL biosludge stabilization and volume reduction, since it acts on the VSS content.

The main aim of running those experiments is to derive the GTL biosludge specific decay constant to be fed into the optimization model. To derive k_d , the change in solids content can be represented by a first order biochemical reaction represented by equation 1 (Bhargava & Datar, 1988):

$$\frac{dX}{dt} = -k_d X \quad (1)$$

Where;

dX/dt = rate of change of solids per unit of time, mg/L/d; k_d = reaction rate constant, d^{-1} ;
 X = concentration of solids content remaining at time t in the aerobic digester, mg/L; and
 t = time, d

Rearranging equation 1 and integrating both sides results in equation 2 (Park et al., 1997), which is used to estimate k_d .

$$-\ln\left(\frac{X_t}{X_o}\right) = k_d t \quad (2)$$

Where;

X_t = cell mass at time t (mgVSS/L); and X_o = initial cell mass (mgVSS/L).

The resulting GTL biosludge plot has produced a k_d value of 0.0145 at 20°C. The higher the value of k_d , the faster the decay rate indicating a higher organic constant. This is evident by the high value of decay constants for shrimp processing, dairy products and municipal waste biosludge, which range between 0.02 and 0.5 day^{-1} (Mardani et al., 2011). While on the other hand, industrial, tannery and textile biosludge samples yielded considerably lower decay constant values in the range of 0.012 day^{-1} indicating lower organic content (Ramdani et al., 2012).

The Optimization Model. The model aims at simulating a biosludge management system through tracking the changes in biosludge content as it flows from one treatment unit to the other. The model consists of three sub-models; first, the simulation sub-model, which is used to track the daily water and solids content of the inflow biosludge through the AD, centrifuge and DB. It also predicts the daily final sludge amounts collected from the DB and transported to the landfill (LF) for disposal.

The AD stage is responsible for the reduction in solid content although the flow rate Q_1 entering and leaving the reactor stays the same, as shown in Figure 1. The percentage drop in solids (D) is calculated as shown in equation 3 where S_1 and S_2 are solid concentrations in and out of the digester while $k_{d(T)}$ is the decay constant at a specified temperature (T) and (t) is the residence time measured in days.

$$D (\%) = \frac{S_2 - S_1}{S_1} \times 100 \quad (3)$$

where $S_2 = S_1 e^{-k_{d(T)} t}$

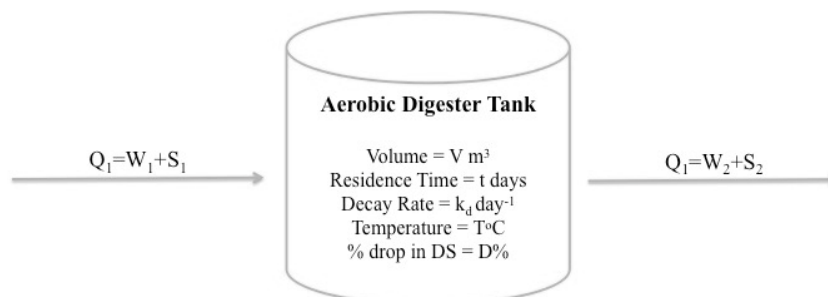


FIGURE 1. Flow and Mass Diagram of the AD

The centrifuge is then modeled as it receives an inflow of biosludge Q_1 to produce two streams, a water stream known as centrate W_R and a biosludge stream Q_2 known as sludge cake. The sludge cake is made-up of water content W_3 and solid content S_2 , which is equal to the influent solids concentration since the centrifuge does not affect the solid content. The centrifuge accepts a range of influent solid concentrations chosen based on the range of concentrations produced by the AD. It then produces an effluent with a predefined solid content percentage P_c chosen as a specification of the procured dewatering unit. P_c and S_2 are used to calculate Q_2 and consequently W_3 and W_R are found. Equations 4, 5 and 6 quantify the centrifuge operation.

$$Q_2 = \frac{S_2 \times 100}{P_c \%} \quad (4)$$

$$W_3 = Q_2 - S_2 \quad (5)$$

$$W_R = W_2 - W_3 \quad (6)$$

Drying beds (DB) receive biosludge with a certain water content W_3 and a solid content of S_2 where they do not affect the solid content. Volume reduction achieved in the drying beds is done through the loss of moisture content, which is owed to two processes, water drainage W_s through seepage into the leaching system and water evaporation W_E . Drying beds operations is illustrated in figure 2.

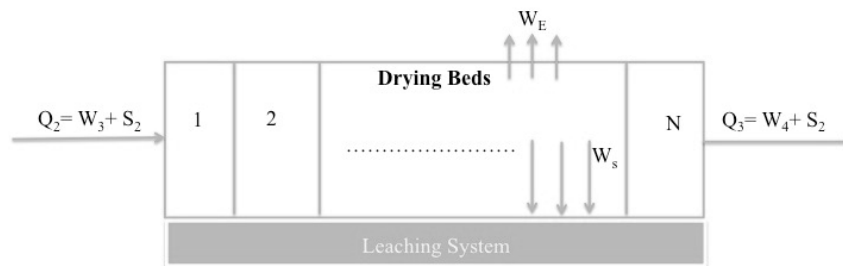


FIGURE 2. Flow and Mass Balance of Drying Beds

The second sub-model is the design sub-model, which is used to size the AD, the centrifuge, and DB based on selected values for sludge residence times. The AD is designed based on the design volume flow rate of the inflow biosludge Q_1 and its Dry Solids (DS) contents. According to the design; Q_1 in m^3/d , the volume (V) of the AD in m^3 , should ensure a design residence time (t) in days, as per equation 7. AD should be equipped with an efficient aeration system where the DO concentration in excess of $2mg/L$ must be maintained (U.S. EPA, 2003). The aeration system of the AD is comprised of an air blower, a piping system and air diffusing equipment, which need to be appropriately sized to ensure proper aeration. Equation 8 empirically relates the blower power P_w in horsepower (hp) to the airflow rate in standard cubic feet per minute (SCFM). To calculate the number of diffusers needed to uniformly spread the airflow from the blower across the volume of the tank, the blower airflow rate is divided by the airflow rate per diffuser disc, which typically ranges between 0.5 and 4.5 SCFM and is chosen as 3 SCFM for this model (Xylem, Inc., 2012).

$$Volume V (m^3) = Flow rate Q_1 (m^3/d) \times Residence Time t (d) \quad (7)$$

$$Blower Power P_w (hp) = 0.0517 \times Air Flow Rate (SCFM) + 0.8849 \quad (8)$$

The sizing of the centrifuge or its power rating depends on the volumetric flow rate of biosludge into the centrifuge unit. Furthermore, the centrifuge is set to achieve a certain degree of dryness given a certain range of DS content of influent sludge.

Drying beds are paved shallow basins, equipped with leaching systems and divided into equally sized beds where the daily batch of biosludge is moved from one bed to the other to allow for proper aeration, increase evaporation and prevent the release of odors. The length of each cell can then be estimated using equation 9 (Guyer, 2011). The number of beds is equal to the number of days the biosludge will stay in the DB. This is a decision made by the designer based on the percent dryness that needs to be achieved to meet landfill requirements, environmental standards and economic constraints.

$$\begin{aligned} \text{Area of one bed} &= \frac{\text{Volume of a daily batch of biosludge}}{\text{Sludge layer thickness}} \\ &= \text{Length of bed} \times \text{Width of bed} \end{aligned} \quad (9)$$

This design sub-model generates alternatives where each alternative is a combination of different values of the design variables. Two main design variables are varied to identify the optimum design: residence time in the AD and time spent in the DB. The residence time in the AD sets tank volume yielding a different digestion rate and solids concentration of the AD effluent.

The third sub-model is the cost and optimization sub-model, which estimates the costs for each design alternative. The minimum cost alternative is chosen as the optimal treatment line-up recommendation. The minimum cost is a trade-off between the cost of biosludge being aerated for a longer time and the drying and disposal cost savings achieved by smaller volumes of produced biosludge.

To quantify the optimization process, it is imperative to realize the investments made for each scenario. Hence, cost functions that vary according to the treatment units sizing options were developed to derive the unit cost of handling one ton of biosludge over an annual average performance. Cost functions were divided into capital expenses (CAPEX) and operational expenses (OPEX). The Cost Recovery Factor (CRF) formula was used to find the annual CAPEX for each cost item where CRF is multiplied by the CAPEX to give the annual cost which is then used to find the cost per day. CAPEX items included the cost of land, material and construction costs of the AD tank, the cost of the blower and its diffusers and the cost of a centrifuge. The OPEX costs included operation and maintenance cost of digestion, dewatering and handling the sludge at the drying beds as well as its transportation and disposal in the landfill (LF). The CAPEX and OPEX per ton figures are summed to give a numeric value that reflects the performance of each alternative.

The sludge flow rates and composition and their treatment are simulated on a daily basis over a typical year to account for the effect of changes in the sludge and the variable climatic conditions since simulating the effects of external variations are expected to affect performance and costs. Also, running the model over one year allows the designer to monitor the variations in performance and cost and vary the design accordingly, which allows flexibility in design choices that result in the optimal system design.

RESULTS AND DISCUSSION

Varying the residence time in the AD tank, keeping other variables constant yields treatment alternatives with different unit costs. The chosen point is preferably the minimal cost point unless other environmental legislations dictate the validity of one alternative over the other. Increasing the residence time of the AD stage affects the volume of dry solid content going through the centrifuge and the drying beds and ultimately disposed of in the landfill. An increase in residence time reflects as a reduction in cost of dewatering, drying and disposal. However, it also translates into an increase in costs due to the need for larger AD tank and aeration equipment. After choosing the optimal AD residence time, the designer keeps it constant and starts varying the time biosludge is left in the DBs. Increasing the time in the DB reduces the final volume of the disposed biosludge, which in turn reduces the costs of trucking and landfill

occupation. However, the longer the time a biosludge batch is left in the DB, the higher the capital costs. Consequently, the minimum cost point is chosen such that the maximum dryness is achieved with minimal increase in cost. Finding the minimum cost point achieved by each variable suggests the optimal design configuration for the treatment line-up.

The optimization model was tested using different applications to obtain the optimal treatment line-up. The main application used for this study is GTL biosludge.

The first two applications test the optimum management system of GTL biosludge under different constraints. In the first case, no constraints were imposed on the management system. The optimum system suggested the exclusion of the AD from the line-up and retaining the centrifuge, and the DBs for duration of 8 days. The unit cost for sludge management was \$7.26/ton including transportation and disposal to LF of 22.18 tons of biosludge. The second case, the sludge management was to meet the EPA requirement of limiting the final sludge to 20 tons. The design retained the AD with a residence time of 21 days plus 8 days in the DBs with a unit cost of \$9.97/ton.

Applying the design model to domestic and refinery biosludge that have higher decay constants has resulted in a drop in the amounts and costs of biosludge produced to 16.8 tons/d of sewage sludge costing \$6.01/ton and 10.21 tons/d of refinery sludge costing \$4.55/ton.

CONCLUSIONS

Experimental investigations show that the biosludge generated from plants treating wastewater produced from GTL plants has an organic content of more than 80% of its dry solids, which suggests the feasibility of its treatment through digestion techniques whether aerobically or anaerobically. The optimization model, the design sub-model can be used for initial sizing and conceptual design. On the other hand, the simulation sub-model can track the solids content, sludge volumetric flow rates, volumes, amount of polymers in the centrifuge, airflow and power requirements for the aeration system as well as drainage water and evaporated water from the drying beds. The estimates can be a good base to predict the capital and operation cost of the various treatment units.

ACKNOWLEDGEMENTS

Support for this research by the American University in Cairo Environmental Engineering Department and the Qatar Shell Research and Technology Center is gratefully acknowledged.

REFERENCES

- Appels, Lise, Jan Baeyens, Jan Degreeve, and Raf Dewil. 2008. "Principles and Potential of the Anaerobic Digestion of Waste-Activated Sludge." *Progress in Energy and Combustion Science* 34 (6): 755–81.
- Bertanza, Giorgio, Matteo Papa, Matteo Canato, Maria Cristina Collivignarelli, and Roberta Pedrazzani. 2014. "How Can Sludge Dewatering Devices Be Assessed? Development of a New DSS and Its Application to Real Case Studies." *Journal of Environmental Management* 137 (May): 86–92.
- Bhargava, Devendra, and Madhav Datar. 1988. "Progress and Kinetics of Aerobic Digestion of Secondary Sludges." *Water Research* 22 (1): 37–47.
- Guyer, J. Paul. 2011. *Introduction to Sludge Handling, Treatment and Disposal*. NY, USA: CED Engineering.com.
- Mardani, Sh., A. Mirbagheri, M.M. Amin, and M. Ghasemian. 2011. "Determination of Biokinetic Coefficients for Activated Biosludge Processes on Municipal Wastewater." *Iran Journal of Environmental Health Science* 8 (1): 25–34.
- Park, Jae Kwang, Jenchie Wang, and Gerald Novotny. 1997. "Wastewater Characterization for Evaluation of Biological Phosphorus Removal- Biological Kinetic Parameter Estimation." *Ecology and Natural Resources Collection*, 14–23.
- Ramdani, Abdellah, Peter Dold, Alain Gadbois, Stéphane Déléris, Dwight Houweling, and Yves Comeau. 2012. "Biodegradation of the Endogenous Residue of Activated Sludge in a Membrane Bioreactor with

- Continuous or on-off Aeration.” *Water Research* 46 (9): 2837–50.
- Rao, P. Venkateswara, and Saroj S. Baral. 2011. “Experimental Design of Mixture for the Anaerobic Co-Digestion of Sewage Biosludge.” *Chemical Engineering Journal* 172: 977–86.
- Tang, S. L., C. L. Wong, M Phil, and K. V. Ellis. 1997. “An Optimization Model for the Selection of Wastewater and Sludge Treatment Alternatives.” *Water and Environment Journal* 11 (1): 11–23.
- U.S. EPA. 2003b. “Control of Pathogens and Vector Attraction in Sewage Sludge: Under 40 CFR Part 503.” Guidance. Environmental Regulations and Technology. Cincinnati, OH 45268: U.S. Environmental Protection Agency.
- Wang, Lawrence K., and Nazih K. Shamma. 2009. “Aerobic Digestion.” In *Handbook of Environmental Engineering*, 8:635–69. Totowa, NJ, USA: Springer.
- Xylem, Inc. 2012. “Aeration Products for Energy-Efficient Biological Treatment.” Product Report. Charlotte: Sanitaire.

PROBING THE WATER QUALITY TRANSFORMATION OF UNDERGROUND CAVERNS IN A TROPICAL REGION USING ELCOM-CAEDYM MODEL

Ming Chen, Jian Li, and *Xiaosheng Qin* (School of Civil and Environmental Engineering, Nanyang Technological University, Singapore)

ABSTRACT: This study aims to preliminarily model the water quality variations in an underground cavern environment using the coupled hydrodynamic and ecological model ELCOM-CAEDYM. The water quality transformation in terms of nitrogen and chlorophyll-*a* under both light and dark environment was analyzed. The ecological part of the model (i.e. CAEDYM) was calibrated and verified by experimental data. It was found that the chlorophyll-*a* concentration (phytoplankton biomass) decreased under the dark and light conditions with the decreasing rate being faster in a dark environment. The ammonia concentrations under both dark and light conditions increased rapidly first and then declined to an equilibrium state. The trend for the nitrite concentrations differed under these two conditions. Nitrite concentrations under the light condition only slightly fluctuated during the entire experiment, while they varied significantly under a dark environment. Nitrate concentrations generally increased with time except for the initial stage under both conditions. The modeling results demonstrated that ELCOM-CAEDYM could reasonably reproduce the experimental observations. Different scenarios for hypothetical design were also run for ascertaining the critical factors controlling the water quality in an underground cavern.

INTRODUCTION

Water shortage is a global problem today due to uneven distribution of water resources and fast economic and population growth. In 2006, it was reported that about one third of the world population (about two billions) was suffering from water scarcity (Oki and Kanae 2006). Unfortunately, the situation for water shortage is getting worse due to climate change and human-induced activities. In the past decades, Singapore has been developing at an accelerating rate, leading to an increasing water demand. Although Singapore receives considerable rainfall throughout the year, she has limited land to collect and store rainwater. The use of underground caverns has proved to be an effective technology to mitigate water resources shortage (Broch 2007; Zhao and Bergh-Christensen 1996). Due to enclosed and dark environment in underground caverns, water quality may deteriorate, rendering the water unsuitable for human usage. Thus, research is needed to investigate and predict how water quality changes during the storage in underground caverns.

Light is an important factor associated with many processes in an aquatic ecosystem. There is evidence that light controls the concentrations of dissolved inorganic phosphorus and dissolved total phosphorus at the water-sediment interface in Taihu, China (Jiang et al. 2008). It was reported that light intensity was related to nitrogen cycling rates in lake Maracaibo, Venezuela (Gardner et al. 1998). Many other researchers also investigated the light effects on various aspects of aquatic ecologic systems (Spears et al. 2008; Dalai et al. 2014; Bhuvaneshwari et al. 2015). Generally, an open environment allows oxygen to enter the water, while enclosed environment limits the normal air exchange between water and air interface. Although the underground reservoir may still be subject to intermittent episodes of inflows with certain nutrient and pathogenic loads, the absence of solar radiation would lead to severe limitations on algal dynamics, nutrient uptake and cycling. Previously, few efforts have been made in exploring water quality variations in underground caverns (Trolle et al. 2012). In this study, a preliminary modeling study

is to be carried out for exploring the water quality changes in an underground cavern environment, with the aid of experimental test.

MATERIALS AND METHODS

Bench-scale Experiment. Singapore is a tropical country, with a total land area around 700 km² and population about 5 million. The annual rainfall is around 2,400 mm and mean daily temperature varies generally from 23-32°C (Gin et al. 2011). To better understand the mechanisms of the ecological processes in an underground environment in such a region and also to support verification of numerical modelling, a bench-scale experimental test was conducted. A local lake near Nanyang Technological University (NTU), Singapore, was selected for water sampling. The nitrification level in this lake is found higher than the general Singapore raw water and is useful for our experimental purpose. Two stainless-steel water tanks with one having light and the other without light were prepared to store the water samples. FIGURE 1a shows the dimension (40cm×30cm×20cm) and configuration of the water tanks. The tank with light input has its top open to sunlight to ensure phytoplankton photosynthesis, and the one without light was covered to mimic the underground environment. Both tanks have connection pipes to atmosphere and are not completely sealed, which is similar to real cavern condition. The experimental test started from September 9th, 2015 to October 27th, 2015. The analyzed parameters include dissolve oxygen (DO), pH, temperature, total carbon (TC), inorganic carbon (IC), ammonia, nitrate, nitrite and Chl-*a*. The experimental instruments used for the measurement of these parameters are: DO: YSI 5000 DO meter; pH: pH meter (Mettler toledo); Temperature: YSI 5000 DO meter; TC and IC: TOC Analyzer (Shimadzu); Ammonia: Ammonia TNTplus, ULR; Nitrate: Nitrate TNTplus vial test, LR; Nitrite: Nitrite TNTplus, LR; Chl-*a*: UV-vis Spectrophotometer (UVmini-1240, Shimadzu).

Ecological Modeling. The ELCOM-CAEDYM model was used to simulate the water quality deterioration in an underground cavern environment. The CAEDYM module was customized to reproduce the water quality changes in the experimental water tanks. The configuration and preprocessing of the model mainly include water-tank meshing, bathymetry processing, boundary/initial condition setup, and parameter estimation. The metrological factors were considered major driving forces influencing the water quality in the water tank as there was no inflow into the water tank and the water body was always static. The solar radiation and air temperature used in the modelling process was assumed following the Sine function as they varied diurnally. The air temperature was set to 29 °C considering no major changes for the studied period. The model used the actual size of the water tanks to study water quality changes with and without light input (see FIGURE 1a). The settling of the particle nutrients and phytoplankton cells may cause limited vertical distribution of concentration; in areal direction, it is assumed spatially uniform due to the small size of the system. The mesh size used in the ecological modeling was 0.02 m with grid numbers 20×15×10, which was deemed sufficiently dense for capturing the chemical/biological reactions in the tank.

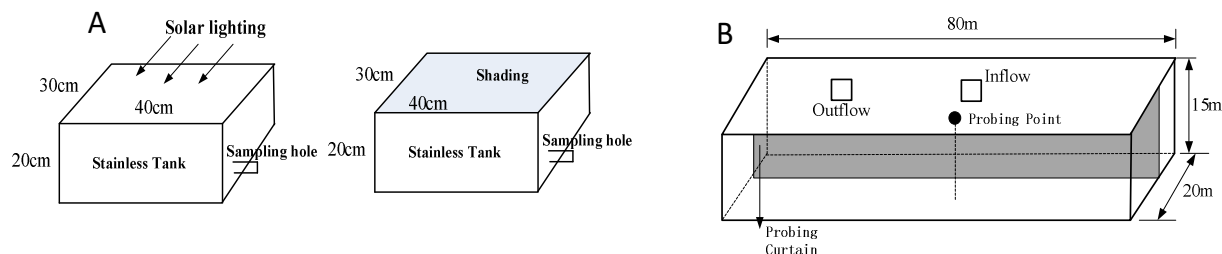


FIGURE 1. (a) Water tank configuration and (b) hypothetical underground water cavern.

A number of water quality variables including ammonia (NH₄), nitrate (NO₃), dissolved oxygen (DO), water temperature, pH, TC, and Chl-*a* concentration were measured. The phosphate (PO₄)

concentration was below the detection limit of our equipment and its initial concentration in the model was provided from the related literature on Singapore reservoir water quality. The initial concentrations of NH₄, NO₃, DO, water temperature, pH, TC, and Chl-*a* were set based on the laboratory measurement data listed in TABLE 1. The initial concentrations of nutrients and Chl-*a* were higher in the light condition than those without light as some reactions may already have started before the first measurement on September 9th, 2015.

Modelling a Hypothetical Underground Water Cavern. The modelling of a hypothetical underground water cavern was carried out assuming frequent inflows into the cavern. This was to simulate the water input from surface catchment under high storm events. Also, the hydrodynamic cycling would affect the internal water quality changing process. As shown in FIGURE 1b, the modeling case was designed as a rectangular tank with dimensions of 80 m long, 20 m wide and 15 m high. The total volume of the modelling case is 24,000 m³. One inflow point and one outflow point were setup in the middle of the left and right sections, respectively. The wall was assumed to be a concrete wall which means no light could penetrate into the tank. The size of the case was referred to two real projects including one pilot underground oil cavern built in Bukit Timah granite bedrock in Singapore (Zhao and Bergh-Christensen 1996) and one underground water storage cavern built in Trondheim, Norway (Broch 2007).

TABLE 1. The initial condition of water quality variables in modeling

Variables	Without Light	With Light	Unit	Value obtained from
DO	5.20	5.80	mg/L	Measured
Water temperature	28.0	28.0	°C	Measured
pH	8.03	8.06	-	Measured
NH ₄	0.037	0.041	mg/L	Measured
NO ₃	0.095	0.151	mg/L	Measured
PO ₄	0.01	0.01	mg/L	Reference (Low et al. 2010)
ON	1.10	1.10	mg/L	Reference (Low et al. 2010)
OP	0.05	0.05	mg/L	Reference (Low et al. 2010)
Chl- <i>a</i>	54.91	115.77	µg/L	Measured

The factors influencing the water quality changing process in the studied underground water storage tank include the inflow/outflow rates, the discharging frequency and duration, and the pollutant loads. The nutrients and Chl-*a* concentration of the inflow water will be studied through scenario analysis. But some other influencing factors such as the chemicals from the concrete wall, the suspended particulate matter and microorganisms were not considered in this study.

The initial conditions of DO, water temperature, nutrients and Chl-*a* concentrations were the same in all the scenarios of modeling studies, which aims to compare the effect of different boundary conditions on the underground water quality changing process. The total Chl-*a* concentration was the sum of the phytoplankton groups. Three kinds of algae including Cyanobacteria, Nodularia and Freshwater Diatoms were chosen according to the literature related to the reservoirs in Singapore (Low et al. 2010), and the ratio of the above algae was set as 2:2:1. The simulation period was set to 60 days for all scenarios.

In total, 4 cases were modelled to examine the effects of different boundary conditions on the water quality changing process in the hypothetical underground water storage cavern. Case-1 was used as a standard benchmark case and other cases will be used for comparison. All the boundary conditions used in the scenarios are listed in TABLE 2. The nutrient concentrations including both nitrogen and phosphorous increased in Case-2. The inflow Chl-*a* concentration was 10 times higher in Case-3, and the inflow frequency and duration all decreased by half in Case-4. It should be noted that the general Chl-*a* concentration in Singapore raw water is usually lower than 100 µg/L; we set it at a higher value for theoretical analysis only.

RESULTS AND DISCUSSION

Changes in Water Quality. Water sampling was performed continuously from these two water tanks for water quality analyses over about two months. It was found that DO concentrations exhibited a similar trend under the two types of conditions (FIGURE 2). Their mean DO concentrations were at similar levels (5.76 mg/L for no light and 5.78 mg/L for light conditions, respectively). We did not observe significantly different patterns for TC, IC and pH concentrations between water samples under light and dark conditions. However, the curves for Chl-*a* concentrations were notably different under these two conditions, although all of them showed a generally decreasing tendency. The declining trend in Chl-*a* concentration under the dark condition was faster than that under the light one. Temporal plots of ammonia, nitrate and nitrite were shown in FIGURE 2. The mean ammonia, nitrate and nitrite concentrations were 0.053, 0.540 and 0.036 mg/L for the dark condition, respectively, and 0.045, 0.515 and 0.022 mg/L for the light condition, respectively. There was a similar trend for the ammonia concentrations under the dark and light conditions. Both observed ammonia concentrations increased rapidly within the first week, and then quickly declined. After about 10 days, they would reach an almost equilibrium state. It is noted that, the trend for the nitrite concentrations was largely inconsistent under these two conditions. Nitrite concentrations under the light condition only slightly fluctuated during the entire experiment, while they varied significantly under the dark condition. Nitrate concentrations generally increased with time except for the initial stage under both conditions. But the increasing rate was obviously higher for the tank with dark condition.

TABLE 2. Scenarios modeling boundary conditions

Variables	Case-1	Case-2	Case-3	Case-4	Unit
Discharge	5.0	5.0	5.0	5.0	m ³ /s
Frequency	1	1	1	2	/10days
Duration	6	6	6	3	hours
Temperature	29.0	29.0	29.0	29.0	°C
DO	8.0	8.0	8.0	8.0	mg/L
NH ₄	0.06	0.20	0.06	0.06	mg/L
NO ₃	0.15	1.50	0.15	0.15	mg/L
PO ₄	0.01	0.02	0.01	0.01	mg/L
ON	0.60	3.0	0.60	0.60	mg/L
OP	0.02	0.02	0.02	0.02	mg/L
Chl- <i>a</i>	91.5	91.5	915	91.5	µg/L

Modeling Results for Lab Water Tanks. CAEDYM model was used to simulate the changing process of water quality variables to repeat the lab test results. The variation of nitrogen nutrient components has been given a priority for analysis. The phosphate (PO₄) concentration was very low and limited the phytoplankton growth in the reservoir of Singapore (Gin et al. 2011), so it was not analyzed. The concentrations of ammonia would decrease gradually in the simulated period (30 days) because ammonia would transform into nitrate through the nitrification process and also the phytoplankton cells adsorption. From FIGURE 2a, the simulated ammonia concentration changed following a similar trend with observed one regardless of with light or without light. From FIGURE 2b, the nitrate concentration would consistently increase from 0.1 to about 1.0 mg/L until the end of simulation period. The Chl-*a* concentration dropped from an initial high concentration to nearly zero due to the death of phytoplankton cells (FIGURE 2c).

Nevertheless, the total nitrogen in the water tank shows only a slight decrease which means the total mass of nitrogen was kept in equilibrium. The simulated nitrogen nutrients and Chl-*a* concentrations are in a good agreement with the observed data. It seems that the relatively weak solar lighting in the laboratory would not significantly affect the chemical reaction and phytoplankton dynamics; the adapted

CAEDYM could well reproduce the ecological process in the dark environment. Generally, both the simulated results and measured data indicate that (i) the phytoplankton would die because of the limiting factors from phosphorous nutrients and organic carbon, (ii) the nitrate concentration, that are transformed from the initial organic nitrogen, would rise and keep at a high level, and (iii) the transformation rates of ammonia and nitrate under the dark environment are somewhat higher than those under the light one, but the decay rate of Chl-*a* is somewhat lower under the light condition than under the dark one. The observed DO concentration decreased before the 10th day and then increased due to re-aeration from the atmosphere (FIGURE 2d). Interestingly, the trends for DO concentrations under light and dark conditions were very close, as shown in FIGURE 2d. The simulated DO concentration agrees with the observed data well to a large extent.

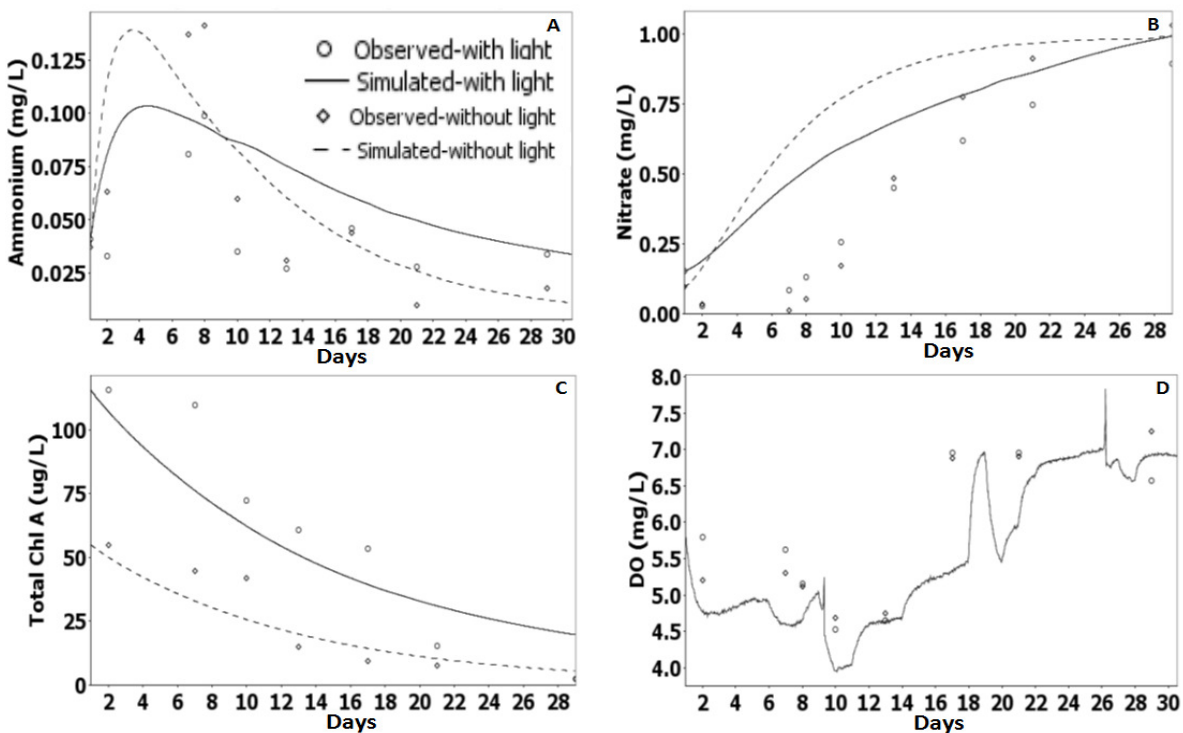


FIGURE 2. Dynamic trend of the measured variables (a: Ammonia, b: Nitrate, c: Chl-a, and d: DO).

Modelling Results for the Hypothetical Underground Cavern. Based on the parameter setting for the lab model under no light condition, we conducted a modeling study for the hypothetical underground cavern. It should be noted that, there are multiple possibilities of results under different scenarios (e.g., DO concentration, inflow patterns, pollutant loadings, location of probing profile). Herein, only one scenario was presented (as shown in FIGURE 3). The NH_4 concentration variations were affected by the boundary conditions, as demonstrated from FIGURE 3a where the NH_4 concentrations of Cases 2, 3 and 4 were different from those of benchmark Case 1. The increase of NH_4 concentrations in the inflow water had a significant impact on those in the underground cavern. From FIGURE 3b, with a high Chl-*a* concentration, the frequency and duration of inflow had a minor effect on the nitrate concentrations. However, these nitrate concentrations would largely increase when the nitrate concentrations in the inflow water increase as reflected by Case 2. The Chl-*a* concentration would decrease gradually in all the simulation periods when no inflow was presented (FIGURE 3c). The presence of inflow would increase the Chl-*a* concentrations. The TN concentrations were higher in Case-2 and Case-3 with higher inflow nutrients and Chl-*a*

concentrations than in Case-1 and Case-4, where the inflow boundary conditions related to N and Chl-*a* would affect the TN concentration more obviously than other factors (FIGURE 3d). This study only gives a projection of possible water quality changes under a hypothetical cavern case, with the main purpose of demonstrating the capability of ELCOM-CAEDY. The results may vary significantly under different settings of operating modes or physical characteristics of the cavern.

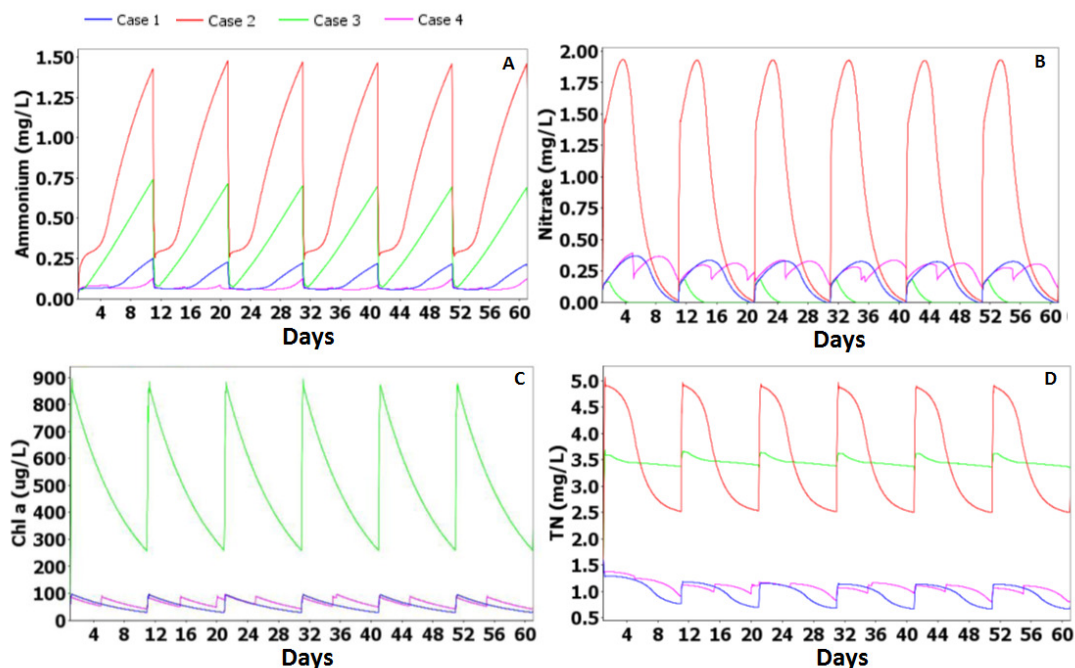


FIGURE 3. Variations of water quality variables at the probing point.

CONCLUSIONS

This study conducted a preliminary modeling study on the water quality variations in dark and light environment using the coupled hydrodynamic and ecological model (i.e. ELCOM-CAEDYM). The experimental data was used for model validation. Different varying trends for Chl-*a*, ammonia, nitrite, and nitrate concentrations were found in the experiment and they could be well reproduced by the applied model. Some scenarios for a larger scale system were run for ascertaining the critical factors controlling the water quality in an underground cavern environment.

ACKNOWLEDGEMENTS

This material is based on research/work supported by the Land and Liveability National Innovation Challenge under L2 NIC Award No. L2NICCFP1-2013-3 (WBS no.: M4061545.D63).

REFERENCES

- Bhuvaneshwari, M., et al. 2015. "Cytotoxicity of ZnO NPs towards fresh water algae *Scenedesmus obliquus* at low exposure ..., visible and dark conditions." *Aquat Toxicol*, 162: 29-38.
- Broch, E. 2007. "Use of the Underground in the City of Trondheim, Norway." 11th ACUUS Conference: Underground Space: Expanding the Frontiers, Sep. 10-13 2007, Athens - Greece.
- Dalai, S., et al. 2014. "Studies on interfacial interactions of TiO₂ nanoparticles with bacterial cells under light and dark conditions." *B Mater Sci*, 37(3): 371-381.

- Gardner, W. S., et al. 1998. "Nitrogen cycling rates and light effects in tropical Lake Maracaibo, Venezuela." *Limnol Oceanogr*, 43(8): 1814-1825.
- Gin, K. Y.-H., et al. 2011. "Comparison of nutrient limitation in freshwater and estuarine reservoirs in tropical urban Singapore." *J Environ Eng*, 137(10): 913-919.
- Jiang, X., et al. 2008. "Effects of biological activity, light, temperature and oxygen on phosphorus release processes ... of Taihu Lake, China." *Water Res*, 42(8): 2251-2259.
- Low, E., et al. 2010. "Top-down control of phytoplankton by zooplankton in tropical reservoirs in Singapore." *Raffles B Zool*, 58(2): 311-322.
- Oki, T., and Kanae, S. 2006. "Global hydrological cycles and world water resources." *Science*, 313(5790): 1068-1072.
- Sanudin, N., et al. 2014. "Feeding Activity and Growth Performance of Shrimp Post Larvae *Litopenaeus vannamei* Under Light and Dark Condition." *J Agr Sci-Cambridge*, 6(11): 103-109.
- Spears, B. M., et al. 2008. "Effects of light on sediment nutrient flux and water column nutrient stoichiometry in a shallow lake." *Water Res*, 42(4): 977-986.
- Trolle, D., et al. 2012. "A community-based framework for aquatic ecosystem models." *Hydrobiologia*, 683(1): 25-34.
- Zhao, J., and Bergh-Christensen, J. 1996. "Construction and utilization of rock caverns in Singapore Part D: Two proposed cavern schemes." *Tunn Undergr Sp Tech*, 11(1): 85-91.

DEPTH FILTRATION THROUGH POROUS MEDIA

Hooman Fallah*

(Department of Petroleum Engineering, Islamic Azad University, Firoozabad Branch, Firoozabad, Iran)

*Email address: hooman.fallah@gmail.com⁸⁸

ABSTRACT: Porous medium occurs in numerous processes of environmental, chemical, petroleum and civil engineering. Several investigations have been done in order to understand the mechanisms of the transport of particulate suspension flow through porous medium. Transport of particulate suspensions and colloids in porous media is accompanied by particle capture and consequent permeability decline. In general, deep bed filtration studies have been conducted to analyse the mechanism involved in the processes of capturing and retaining particles occurs throughout the entire depth of the filter and not just on the filter surface. In this work, the steady-state transport equation is presented and the solution to the complete advective-dispersion equation for particulate suspension flow has been derived for the case of a constant filter coefficient. This model includes transport parameters which are particle advective velocity and particle longitudinal dispersion coefficient. This theoretical investigation of the transport of particles flowing in porous media is limited to flows with low Reynolds number (linear and laminar flow) and high Peclet number.

Keywords: Porous Media, Particle Advective Velocity, Longitudinal Dispersion Coefficient, Filter Coefficient

INTRODUCTION

Transport through porous medium occurs in numerous processes of environmental, chemical, petroleum and civil engineering. Transport of particulate suspensions and colloids in porous media is accompanied by particle capture and consequent permeability decline. It occurs in oil reservoirs during sea or produced water injection, drilling fluid invasion causing formation damage, filtration of completion fluid, fines migration during production of heavy oils in low consolidated reservoirs resulting in productivity. Prediction of particle propagation and retention by mathematical modeling is an essential stage during planning and design of above-mentioned industrial processes. It helps in design of injected water treatment, in particle sizing of drilling and completion fluids, in sizing the gravel pack and designing the sand screens. In general, deep bed filtration studies have been conducted to analyse the mechanism involved in the processes of capturing and retaining particles occurs throughout the entire depth of the filter and not just on the filter surface [1].

In this work, the steady-state transport equation is presented and the solution to the complete advective-dispersion equation for particulate suspension flow has been derived for the case of a constant filter coefficient. This model includes transport parameters which are particle advective velocity, particle longitudinal dispersion coefficient and filter coefficient. The numerical model needs to be developed for general case of a transition filter coefficient. The individual parameters are analysed according to dimensional analysis argument. Here, a particle mass transport equation is developed which includes the transport parameters, advective velocity and longitudinal dispersion coefficient. A solution to the complete advective-dispersion equation for particle transport was derived for the case of constant filter coefficient. The individual parameters are analysed according to dimensional analysis argument.

In order to develop the theories understanding of the basics of flow in porous media is needed advective fluid velocity and longitudinal dispersion coefficient. This theoretical investigation of the

transport parameters of particles flowing in porous media is limited to flows with low Reynolds number (linear and laminar flow) and high Peclet number (advection dominates diffusion). The theoretical development used dimensionless numbers to define the transport parameters and incorporated them into an advective-dispersion equation describing particle transport.

ADVECTIVE VELOCITY

The averaged particle velocity in the porous media, has been found to be either the same or slightly higher than that of the carrier fluid [2]. This deviation is caused by the particle's size. The expected difference can be determined by analyzing the velocity profiles of both the fluid and the particles in a pore [3]. The model has been formulated for a capillary tube which has a constant rate with the following assumption: No interactions between the particles and the wall, suspension is well-mixed with a constant concentration across the cross section. There is no transverse flow.

$$U_S = U_O \left\{ 1 - \left(\frac{r}{r_o} \right)^2 \right\} \quad (1)$$

$$(0 < r < r_o)$$

$$U_P = U_O \left\{ 1 - \left\{ \frac{r}{r_o} \right\}^2 - \gamma \left\{ \frac{a_p}{r_o} \right\}^2 \right\} (0 < r < r_o - a_p)$$

As the particle travels through a tube, Brownian motion and shear action will cause the particle to travel across the entire cross-section of the tube except that the center-line of the particle will be excluded from the immediate region of the wall due to its radial dimension.

After the particle has traveled far enough longitudinally through the tube, the particle will have spent equal amounts of time in all radial position across the capillary tube [4].

Integration of the velocity profile over the range of possible radii shown in Eq. (1) for both the particle and fluid yields the higher average velocity for the particle than that for the carrier fluid.

The average fluid velocity, V_S , in a capillary tube is:

$$V_S = \frac{U_O}{2} \quad (2)$$

The average velocity of a particle, V_P , in a capillary tube is:

$$V_P = U_O \left(1 - \frac{1}{2} \left\{ 1 - \frac{a_p}{r_o} \right\}^2 - \gamma \left\{ \frac{a_p}{r_o} \right\}^2 \right) \quad (3)$$

By inspecting Eq. (2) and (3), the particles are expected to have a larger average velocity than the carrier fluid velocity. This enhanced velocity of the particle can be expressed as a fractional difference between the two average velocities:

$$\Delta V = \frac{V_P - V_S}{V_S} = 2 \frac{a_p}{r_o} - \frac{7}{3} \left(\frac{a_p}{r_o} \right)^2 \quad (4)$$

This equation shows that as the radius of the particle increase, the difference between the average particle velocity and the average fluid interstitial velocity also increase. This increase is not unbounded but reaches a maximum ΔV value for $\frac{a_p}{r_o} = \frac{3}{7}$; as $\frac{a_p}{r_o} > \frac{3}{7}$ the velocity difference decrease.

In physical sense, the pore radius can be estimated to approximately equal to one-fifth of media grain diameter ($r_o = \frac{1}{5} d_g$); therefore the largest possible particle to be able to fit through the porous bed has a radius to this pore radius ($a_p = r_o$).

For a particle with $a_p = r_o$, the particles have been shown to collect on the bed surface in a cake [4].

These references show that the onset of deep bed filtration occurs for a particle radius a_p less than one-twentieth of the media grain diameter ($a_p < \frac{1}{20} d_g$). Particles with the radii larger than this will not

transport into the bed, but will collect on the surface. By letting $d_g = 5r_o$, the largest particle which will transport has a radius equal to one-fourth of the pore radius ($a_p \leq \frac{1}{4}r_o$).

LONGITUDINAL DISPERSION COEFFICIENT

An important element of any dispersion model is the representation of the geometry of the porous medium. Houseworth [5] has thoroughly reviewed such longitudinal dispersion model for solute tracers.

Instead of modeling the internal structure of a porous medium, dimensional analysis is used to analyze the problem. In this study, the effect of mechanisms is expected to scale with the pertinent transport variables.

The pertinent variables for solute dispersion are:

$$D_L = \text{longitudinal dispersion coefficient} ;$$

$$D = \text{free fluid molecular diffusion coefficient of solute} ;$$

$$V_S = \text{fluid interstitial velocity} ;$$

$$\text{and } d_g = \text{media grain diameter (L)}.$$

From the Buckingham pi theorem, the following pairs of groups are formed:

$$\frac{D_L}{V_S \cdot d_g} = F \left[\frac{V_S \cdot d_g}{D} \right], \text{ or alternatively,}$$

$$2. \frac{D_L}{D} = F \left[\frac{V_S \cdot d_g}{D} \right] \quad (5)$$

$$\text{where: } Pe = \text{Peclet number} = \frac{V_S \cdot d_g}{D}$$

Experimental data for solute longitudinal dispersion in uniform media show good correlation with these dimensionless groups [5], [6].

When the Peclet number is greater than 1, the two groups can be reduced to one:

$$\frac{D_L}{V_S \cdot d_g} \approx \text{Constant} \quad (6)$$

$$\text{Where: } Pe_D = \text{dynamic Peclet number} = \frac{V_S \cdot d_g}{D_L}$$

An order to magnitude approximation for the longitudinal dispersion coefficient for solutes can be made with:

$$D_L = V_S \cdot d_g \quad (7)$$

Particle longitudinal dispersion is expected to be similar to that of solutes.

Currently, no particle breakthroughs have been performed by others from which particle longitudinal dispersion coefficient be determined.

TRANSPORT OF FLUID THROUGH POROUS MEDIUM

In this part, the steady-state transport equation is presented and the solution to the complete advective-dispersion equation for particulate suspension flow has been derived for the case of a constant filter coefficient. This model includes transport parameters which are particle advective velocity and particle longitudinal dispersion coefficient [7].

These parameters have been defined by dimensional analysis using the pertinent variables of the porous media system.

Particle Advective Velocity. The result of the size exclusion for particles flowing in capillary tube can be written as equation (3) where $\gamma = \frac{2}{3}$. By using the equations (2) and (4) we will have:

$$V^* = 1 + \Delta V \quad (8)$$

$$\text{where: } V^* = \frac{V_P}{V_S} \quad (9)$$

As the particle size increase, the difference between particle velocity and fluid velocity increase.

Particle Longitudinal Dispersion Coefficient. The previous stated method uses a single velocity and length scale and does not model the internal structure of porous medium. In modeling particle dispersion, the following variable substitutions are used:

$$D \rightarrow D_P$$

$$V \rightarrow V_P$$

$$D_L \rightarrow D_{LP}$$

where: D_{LP} = particle dispersion coefficient ;

D_P = particle molecular diffusion coefficient ;

V_P = particle velocity ;

d_g = media grain diameter (L); and

d_p = particle diameter (L).

Particle size variable can be removed by using the particle properties as shown, provided $\frac{d_p}{d_g} \ll 1$. also the effect of particle size is included in the enhanced advective velocity for the particles.

This analysis shows that particle and solute longitudinal dispersion are similar. When the particle Peclet number ($Pe_p = \frac{V_P d_g}{D_P}$) is greater than 10, the two groups can be reduced to one :

$$\frac{D_{LP}}{V_P d_g} = \text{constant} \quad (10)$$

where: $Pe_p = \frac{V_P d_g}{D_P}$ = particle dynamic Peclet number.

An order of magnitude approximation for the longitudinal dispersion coefficient for particles can be made with:

$$D_{LP} = V_P d_g \quad (11)$$

As mentioned before, the dimensional argument for defining the longitudinal dispersion coefficient is only valid when $Pe_p \gg 1$. For uniform media, this restriction is seen to be $Pe_p > 10$ [5].

Flow conditions are simultaneously limited to the linear, laminar regime for which the Reynolds

number must be less than 10.

Steady-State Transport in Porous Medium Equation and Solution. Particle removal or filtration occurs as a particle suspension flows through a porous medium due to the interaction of the advecting particles and grains of the medium. Iwasaki [8] is credited with being the first to express filtration a first-order decay of particle concentration with distance:

$$\frac{\partial C}{\partial x} = -\lambda C \quad (12)$$

$$1. C(x = 0) = C_0 \quad (13)$$

And a solution in dimensional terms:

$$C = C_0 \exp[-\lambda x] \quad (14)$$

Or, in dimensionless terms:

$$C^* = \exp[-\lambda^* x^*] \quad (15)$$

$$\text{where: } C^* = \frac{C}{C_0};$$

$$C_0 = C(x = 0);$$

$$\lambda^* = \lambda d_g;$$

$$x^* = \frac{x}{d_g};$$

A complete equation of steady-state filtration can be formulated by using the general steady-state advection-dispersion equation of transport for particle concentration with a sink term to describe particle removal due to filtration:

$$0 = D_{LP} \frac{\partial^2 C}{\partial x^2} - V_p \frac{\partial C}{\partial x} - V_p \lambda C \quad (16)$$

The following semi-infinite medium boundary conditions are:

$$C(x = 0) = C_0;$$

$$\lim_{x \rightarrow \infty} C(x) = 0. \quad (17)$$

The solution which is shown in dimensional terms is derived in appendix:

$$C(x) = C_0 \exp[\alpha x] \quad (18)$$

$$\text{where: } \alpha = \frac{1}{2} \frac{V_p}{D_{LP}} \left(1 - \sqrt{1 + 4\lambda \frac{D_{LP}}{V_p}} \right)$$

In dimensionless terms the transport equation becomes:

$$0 = \frac{\partial^2 C^*}{\partial x^{*2}} - Pe_{Dp} \frac{\partial C^*}{\partial x^*} - Pe_{Dp} \lambda^* C^* \quad (19)$$

With the same boundary conditions:

$$C^*(x^* = 0) = 1 \quad \lim_{x^* \rightarrow \infty} C^*(x^*) = 0 \quad (20)$$

And a solution in dimensionless terms:

$$C^* = \exp[\alpha^* x^*] \quad (21)$$

$$\alpha^* = \alpha d_g = \frac{1}{2} Pe_{DP} \left(1 - \sqrt{1 + \frac{4\lambda^*}{Pe_{DP}}} \right) \quad (22)$$

CONCLUSION

In this work, a mass balance particle transport equation which includes filtration has been developed. This model includes transport parameters which are particle advective velocity, particle longitudinal dispersion coefficient and filter coefficient. The steady-state transport equation is presented and the solution to the complete advective-dispersion equation for particulate suspension flow has been derived for the case of a constant filter coefficient.

This work recommends to be investigated by particle longitudinal dispersion calculation from experimental data. Besides, the numerical model needs to be developed for general case of a transition filter coefficient.

APPENDIX

A.1 Solution Derivation

Consider the one-dimensional steady-state particle advective-dispersion equation which includes the removal term to account for filtration effects:

$$0 = D_{LP} \frac{\partial^2 C}{\partial x^2} - V_p \frac{\partial C}{\partial x} - \lambda V_p C \quad (A.1)$$

where: C = concentration ;
 x = longitudinal distance (L);
 D_{LP} = longitudinal dispersion coefficient for particles;
 V_p = average particle interstitial velocity ; and
 λ = filter coefficient (L^{-1}).

With the following boundary conditions:

$$\begin{aligned} 1. C(x = 0) &= C_0; \text{ and} \\ 2. \lim_{x \rightarrow \infty} C(x) &= 0. \end{aligned} \quad (A.1.1)$$

For convenience, the x-variable is allowed to range from negative to positive infinity ($-\infty < x < \infty$), although the equations are only applied for $x > 0$. this avoids difficulty at $x=0$, because small dispersion is allowed. In dimensionless form, the transport equation becomes:

$$0 = D_{LP} \frac{\partial^2 C^*}{\partial x^{*2}} - Pe_{DP} \frac{\partial C^*}{\partial x^*} - \lambda^* Pe_{DP} C^* \quad (A.2)$$

where: $C^* = \frac{C}{C_0}$;
 $C_0 = C(X = 0)$;
 d_g = media grain diameter;
 $x^* = \frac{x}{d_g}$;
 $Pe_{DP} = \frac{V_p d_g}{D_{LP}}$; and $\lambda^* = \lambda d_g$.

With the same boundary conditions:

$$\begin{aligned} 1. C^*(x^* = 0) &= 1; \text{ and} \\ 2. \lim_{x^* \rightarrow \infty} C^*(x^*) &= 0. \end{aligned} \quad (A.2.1)$$

In order to derive a solution, try the following as a solution:

$$C^*(x^*) = \exp[\alpha^* x^*] \quad (A.3)$$

Check the equation (A.3) by substituting into Eq. (A.2), this results in second-degree polynomial in term of α^* , and two roots of this polynomial are:

$$\alpha_1^* = \frac{1}{2} Pe_{DP} \left(1 - \sqrt{1 + \frac{4\lambda^*}{Pe_{DP}}} \right); \alpha_2^* = \frac{1}{2} Pe_{DP} \left(1 + \sqrt{1 + \frac{4\lambda^*}{Pe_{DP}}} \right)$$

Using these two roots, Eq. (A.3) becomes:

$$C^*(x^*) = A \exp[\alpha_1^* x^*] + B \exp[\alpha_2^* x^*] \quad (A.4)$$

The constants of this equation can be determined by applying the boundary conditions:

1. $C^*(x^* = 0) = 1 = A + B$; and
 2. $C^*(x^* \rightarrow \infty) = 0 = (A)(0) + (B)(+\infty)$
- $\therefore A = 1$ and $B = 0$.

By substituting these constants into equation (A.4), the solution to equation (A.2) becomes:

$$C^*(x^*) = \exp \left[\frac{1}{2} Pe_{DP} \left(1 - \sqrt{1 + \frac{4\lambda^*}{Pe_{DP}}} \right) x^* \right] \quad (A.5)$$

A.2 Solution Approximation

Consider an approximation for Eq. (A.5) by simplifying α^* :

$$\alpha_1^* = \frac{1}{2} Pe_{DP} \left(1 - \sqrt{1 + \frac{4\lambda^*}{Pe_{DP}}} \right) \quad (A.6)$$

Perform a Taylor series expansion of the radical portion of α^* of Eq. (A.6) by considering a function $f(x)$:

$$f(x) = \sqrt{1+x}$$

where: $x = \frac{4\lambda^*}{Pe_{DP}}$.

The Taylor series approximation is:

$$\sqrt{1+x} = 1 + \frac{1}{2}x - \frac{1}{8}x^2 + \frac{1}{16}x^3 - \frac{5}{128}x^4 \dots$$

Since this series is an alternating series, the truncation error must be less than the first truncated term (absolute values). Substituting the first two terms of the series into Eq. (A.6) for the radical portion of x^* yields:

$$x^* \cong \frac{1}{2} Pe_{DP} \left(1 - \left\{ 1 + \frac{2\lambda^*}{Pe_{DP}} \right\} \right) = -\lambda^* \quad (A.7)$$

Substituting the approximation for α^* , Eq. (A.7), into the exact steady-state equation:

$$C^* = \exp[-\lambda^* x^*] \quad (A.8)$$

Using Eq. (A.8), λ^* can be directly calculated from concentration and position measurements. Also, Eq. (A.8) is the same result that would have been derived by ignoring the dispersion term originally.

A.3 Approximate Versus Exact Solution

The error using the approximate solution can be determined from the relative error of the two solutions, Eq. (A.3) and (A.8):

$$\Delta C^* = \frac{C_a^* - C_e^*}{C_e^*} = \frac{\exp[-\lambda^* x^*] - \exp[\alpha^* x^*]}{\exp[\alpha^* x^*]} \quad (A.9)$$

where: C_a^* = approximate solution; and C_e^* = exact solution.

Eq. (A.9) can be simplified as follows:

$$\Delta C^* = \exp[-x^*(\lambda^* + \alpha^*)] - 1 \quad (A.10)$$

The Taylor series expansion for Eq. (A.10) is:

$$\exp[-x^*(\lambda^* + \alpha^*)] = 1 - x^*(\lambda^* + \alpha^*) + \dots \quad (A.11)$$

So, the approximate value for α^* can be determined using the Taylor series for α^* found in section A.2:

$$\alpha_1^* = \frac{1}{2} Pe_{DP} (1 - \sqrt{1+x}) = -\frac{1}{2} Pe_{DP} \left(\frac{1}{2}x - \frac{1}{8}x^2 \dots \right) \leq -\frac{1}{4} Pe_{DP}x + \frac{1}{16} Pe_{DP}x^2$$

Substitute for x:

$$\alpha^* \leq -\lambda^* + \frac{\lambda^{*2}}{Pe_{DP}} \quad (A.12)$$

Add λ^* to Eq. (A.12) in order to determine the argument of the exponential term of Eq. (A.10) so that Eq. (A.11) can be evaluated:

$$\alpha^* + \lambda^* \leq \frac{\lambda^{*2}}{Pe_{DP}} \quad (A.13)$$

Substitute this approximation into the series expansion expression, Eq. (A.11), of the exponential term in Eq. (A.10):

$$|\Delta C^*| \leq |1 - x^*(\lambda^* + \alpha^*) - 1| \leq \frac{\lambda^{*2}x^*}{Pe_{DP}} \quad (A.14)$$

The absolute value of the error is the absolute value of ΔC^* of Eq. (A.14):

$$\therefore |Error| = |\Delta C^*| \leq \frac{\lambda^{*2}x^*}{Pe_{DP}} \quad (A.15)$$

Nomenclature

- d_g = media grain diameter (L)
- d_p = particle diameter (L)
- c = suspended particle concentration in carrier fluid
- σ = particle retained concentration
- k_{det} = detachment rate coefficient
- U = flow velocity
- U_S = fluid velocity
- U_P = particle velocity
- U_O = fluid centerline velocity
- r = radial distance
- r_o = capillary radius
- a_p = particle radius
- p = dynamic pressure
- x = longitudinal distance
- DL = longitudinal dispersion coefficient (L·T⁻¹)
- D = free fluid molecular dispersion coefficient of solute (L²·T⁻¹)
- VS = fluid interstitial velocity (L·T⁻¹)
- Pe = Peclet number = $SgV.dDL$
- PeD = dynamic Pec let number = $SgV.dDL$
- C = particle concentration (M·L⁻³)
- X = longitudinal position (L)
- λ = filter coefficient (L⁻¹)
- WS = particle settling velocity

V_S = fluid interstitial velocity

ρ_p, ρ_f = densities of particle and fluid, respectively

g = gravitational acceleration

H = Hamaker constant (ergs)

NG = gravitational group = ηG

DLP = particle longitudinal dispersion coefficient ($L^2 \cdot T^{-1}$)

DP = particle molecular diffusion coefficient in a free fluid ($L^2 \cdot T^{-1}$)

VP = particle velocity ($L \cdot T^{-1}$)

REFERENCES

- R. Farajzadeh, "An Experimental Investigation into Internal Filtration and External Cake Build Up," *MSc. thesis*, Delft University of Technology (2004).
- C.G. Enfield., G. Bengtsson., "Macromolecular Transport of Hydrophobic Contaminants in Aqueous Environments", *Ground Water*, Vol.26, No.1, 1988, pp. 64-70.
- E. A. DiMarzio., C. M. Guttman, "Separation By Flow", *Macromolecules*, Vol. 3, No. 2, 1970, pp. 131-146.
- J.P. Herzig, , D.M. Leclerc, P. Le Goff, "Flow of suspension through porous media –application to deep filtration" *J. Ind. Eng. Chem.* 65(5), 8-35 (1970).
- J.E. Houseworth, "Longitudinal Dispersion in Nonuniform, Isotropic Porous Media," Ph.D. Thesis, W.M. Keck *Laboratory of Hydraulics and Water Resources, California Institute of Technology*, Report No. KH-R-45, (1984).
- Foppen, J.W.A., Schijven, J.F "Evaluation of data from the literature on the transport and survival of *Escherichia coli* in aquifers under saturated conditions," *J. Water Res.* 40,401-426 (2006).
- J.F. Schijven, S.M. Hassanizadeh, "Removal of viruses by soil passage: overview of modeling processes, and parameters," *Crit. Rev. Environ. Sci. Technol.* 30(1), 49-127 (2000).
- T. Iwasaki, "Some notes on sand filtration," *Water Works Ass.* 1591-1602, 1937.

ENVIRONMENTAL QUALITY AND FOREIGN TRADE IN TURKEY: A CO-INTEGRATION ANALYSIS WITH A STRUCTURAL BREAK

Nilgün Çil*

(Istanbul University, Istanbul, Turkey)

ABSTRACT: This paper explores the existence of a long run relationship between environmental quality and foreign trade indicators for Turkey over the period from 1974 to 2011. For this purpose, we use carbon dioxide emission as an environmental quality indicator and export, foreign direct investment, GDP per capita as explanatory variables. In our empirical analysis, we use Perron (1997) unit root test and Gregory-Hansen (1996) co-integration test. Both tests allow for a structural break. The obtained results indicate that there is evidence of co-integration between carbon dioxide emission, export, foreign direct investment and GDP for Turkey.

INTRODUCTION

Carbon dioxide emission is one of the major factors causing global warming, climate change and environmental pollution and is also an important indicator of environmental destruction. The increase in the carbon dioxide emission which is emitted into the atmosphere by the use of fossil fuels such as gasoline, coal and natural gas, increases the temperature of the earth's surface. So, it is critical to understand the relationship between carbon dioxide emission and its determiners.

In environmental economics literature, the relationship between environmental destruction and income is called the environmental Kuznets curve (EKC) hypothesis. According to this hypothesis, environmental pollution increases as a country develops, but after a turning point, begins to decrease as income increases. This hypothesis derives its name from the study of Kuznets (1955) who proposed a similar relationship between income inequality and economic growth. Since the seminal work of Grossman and Krueger (1991), several studies have examined the relationship between pollution and economic growth for different countries, using various methodologies. Some of these studies support the environmental Kuznets curve hypothesis (see Galeotti et al. (2006), Millimet et al. (2003)) and some others fail to find evidence for environmental Kuznets curve hypothesis (see Dinda et al. (2000), Perman and Stern (2003)).

In recent years, economists argue that foreign trade affects the environment, both locally and globally. Expanding trade from domestic market to international market not only increases market share of each country but also rising competition among the nations and improve efficiency of utilizing scarce resources. But on the other hand, environmental economists claim that the costs of spreading trade to international markets are depleting natural resources and rising pollution emissions that ultimately deteriorates environmental quality [Antweiler et al. (2001), Copeland and Taylor (2001), Chaudhuri and Pfaff (2002)].

Since there is not enough empirical research that investigates the relationship between environmental quality and foreign trade indicators, this paper empirically examines the long-run relationship among carbon dioxide emission (as an environmental quality indicator), export, foreign direct investment and GDP per capita for Turkey over the period 1974-2011. During this period, many internal and external developments take place in Turkish economy. In other words, the Turkish economy was influenced by both international developments (e.g. the oil crises of 1973 to 1974 and Asia Crisis of 1996) and national developments including the structural transformation and transition to a free market economy after 1980, capital account liberalization in 1989 along with the economic crises in 1994, 2000 and 2001.

Especially within the framework of the structural transformation program of 1980, the rapid industrialization breakthrough in Turkey caused an increase in the amount of greenhouse gas emitted into the atmosphere as it increased the demand for energy. In the 2007 report of the United Nations, Turkey was announced to be the country with the most dramatically increasing emission of gases that cause the greenhouse effect with a ratio of 74.4% for the period between 1990 and 2004. The reasons for the dramatic increase are listed as emissions due to the energy sector and industrial sector and use of fossil fuels. After these internal and external developments, it is very important to take into account existence of structural breaks in our empirical analysis. As argued by many authors before, conventional unit root and co-integration tests lose power when existing structural break(s) are not taken into consideration. From this point of view, we investigate the unit root properties of the mentioned series by using Perron (1997) unit root test, which takes into account one structural break. After obtaining necessary conditions, we explore long run relationship by using Gregory-Hansen (1996) co-integration test with a structural break.

The balance of the paper is organized as follows: The next section presents the materials and methods, the third section gives results and discussions. Finally, the last section concludes.

MATERIALS AND METHODS

This paper examines the long run relationship between carbon dioxide emission, export, foreign direct investment and GDP by considering existence of structural breaks. We explore the unit root properties of the series by using Perron (1997) unit root test, which takes into account one structural break. We also use Gregory-Hansen (1996) co-integration test with a structural break for long run relationship between these series.

Perron(1997) Unit Root Test. Nelson and Plosser (1982) argue that almost all macroeconomic time series have a unit root. The presence or absence of unit root helps to identify some features of the underlying data generating process of a time series. The commonly used unit root method to test unit root properties of a time series is Augmented Dickey Fuller (ADF) test. But, Perron (1989) claims that standard ADF tests are biased towards the non rejection of the null hypothesis in the presence of a structural break. Following this argument, Perron (1989) develops a modified Dickey-Fuller unit root test, which includes a dummy variable for one known or exogenous structural break. This test allows for a structural break under both the null and alternative hypothesis. The test equations take into account the existence of three different kinds of structural breaks: a break in the intercept, a break in the trend and a break in both intercept and trend. The equation that takes into account an exogenous structural break in both intercept and trend can be seen below:

$$y_t = \alpha_0 + \alpha_1 DU_t + d(DTB)_t + \gamma DT_t + \beta t + \rho y_{t-1} + \sum_{i=1}^p \phi_i \Delta y_{t-i} + e_t \quad (1)$$

where DU_t represents a change in the intercept; DT_t represents a change in the trend and TB is the break date.

However, this procedure is criticized on including structural break as exogeneous. Then, Perron(1997) develops one endogeneous structural break version of this unit root test. In this version, the first model allows only a change in the intercept under both the null and alternative hypotheses and the unit root test is performed using the t- statistic for testing $\alpha = 1$ in the following regression:

$$y_t = \mu + \theta DU_t + \delta (DTB)_t + \beta t + \alpha y_{t-1} + \sum_{i=1}^k c_i \Delta y_{t-i} + e_t \quad (2)$$

where $DU_t = 1(t > TB)$ and $(DTB)_t = 1(t = TB + 1)$ with $1(\cdot)$ the indicator function. Under the second model, both a change in the intercept and trend are allowed at time TB . The test is performed using the t-statistic for the null hypothesis that $\alpha = 1$ in the regression:

$$y_t = \mu + \theta DU_t + \gamma DT_t + \delta (DTB)_t + \beta t + \alpha y_{t-1} + \sum_{i=1}^k c_i \Delta y_{t-i} + e_t \quad (3)$$

with $DT_t = 1(t > TB)t$. Under the third model, a change in the trend is allowed but both segments of the trend function are joined at the time of break. The other detailed information on the test can be seen in the original paper of Perron (1997).

Gregory-Hansen (1996) Co-integration Test. Since the standard co-integration methods lose power in the existence of structural breaks, we apply Gregory-Hansen (1996) co-integration test in order to investigate the long run relationship between environmental quality and foreign trade indicators for Turkey by allowing structural break. The importance of Gregory-Hansen (1996) test lies in the fact that conventional co-integration tests are biased towards non-rejection of the null of no co-integration when there exists any structural break(s) in the co-integrating relationship. Gregory and Hansen (1996) suggest three models for a possible endogenous structural break in the co-integrated relation. They use modified Augmented Dickey Fuller, Z_a and Z_t tests in order to test the null of no co-integration against the alternative of co-integration with an unknown regime shift. The first model considers level shift (Model C), where the second one considers level shift and trend (Model C/T). The last model is the regime shift model (Model C/S), which has the following form:

$$y_{1t} = \mu_1 + \mu_2 \varphi_{1\tau} + \alpha_1^T y_{2t} + \alpha_2^T y_{2t} \varphi_{1\tau} + e_t \quad (4)$$

In Model 4, μ_1 denotes the intercept before the regime shift where μ_2 represents the change in intercept at the time of the regime shift. Similarly, α_1 shows the slope coefficients before the regime shift and α_2 is the change in the slope coefficients after the shift. They suggest to apply Augmented Dickey Fuller (ADF) unit root test and Z_a and Z_t tests of Phillips (1987) to the residuals (e_t). Since the true dates of the breakpoints are not known, we estimate the Model 4 for all the possible breakpoints and determine the dates of the structural breaks via selecting the dates, which give the minimum test statistics. The test statistics are defined as follows:

$$ADF^- = \inf_{\tau \in T} ADF(\tau) \quad Z_T^- = \inf_{\tau \in T} Z_t(\tau) \quad Z_\alpha^- = \inf_{\tau \in T} Z_\alpha(\tau)$$

where $T = (0.15n, 0.85n)$ shows the sample area which we search for the breakpoints. Critical values are available in Gregory and Hansen (1996).

RESULTS AND DISCUSSION

This paper uses annual data on the carbon dioxide emission (metric tons per capita) as an environmental quality indicator, export of goods and services (US \$), foreign direct investment net inflows (US \$) and GDP per capita (US \$) for Turkey over the 1974-2011 period. The data are obtained from World Development Indicators website. Before the analysis, we take the natural logarithms of the series. The labels for the natural logarithms of the carbon dioxide emission, the natural logarithms of the export, the natural logarithms of the foreign direct investment and the natural logarithms of the GDP per capita are LCO2,

LEX, LFDI and LGDP respectively. Before testing for cointegration, the unit root properties of the series are explored by using Perron (1997) unit root test with a structural break. The results can be seen in Table 1.

The results in the table show that we failed to reject the null hypothesis of unit root for all the series. After insuring that the series are difference stationary, it is possible to apply cointegration test. For this purpose, we apply Gregory and Hansen (1996) cointegration test with a structural break. The results for the full break model are reported in Table 2.

TABLE 1: Perron(1997) unit root test results

Series	Test Statistic	Time of break
LCO2	-4.013	1984
LEX	-4.378	1980
LFDI	-5.055	2004
LGDP	-3.524	1983

Note: The critical values are -6.32, -5.59 and -5.29 for 1%, 5% and 10% significance levels, respectively.

TABLE 2: Gregory Hansen (1996) cointegration test results

Test Statistic	Lag length (k)	Time of break
-6.188 ^b	0	1991

Note: ^b indicates statistically significance at 5% significance level. The used critical values are -6.51 and -6.00 for 1% and 5% significance levels, respectively.

The results of Gregory and Hansen (1996) cointegration test indicate that there exists a long-run relationship with a structural break among the variables and the break in 1991 is statistically significant. The test results reveal that the structural break in 1991 can be refer to the financial liberalization period in Turkey. It means that financial liberalization affected the relationship between carbon dioxide emission, export, foreign direct investment and GDP per capita for Turkey.

CONCLUSIONS

In this paper, an attempt has been made to investigate the long run relationship between carbon dioxide emission, export, foreign direct investment and GDP for Turkey over the period 1974-2011. For this aim, we use Perron (1997) unit root test and Gregory-Hansen(1996) co-integration test in our empirical analysis. These tests allow for existence of one structural break. According to obtained results, it is found that there is a long run relationship between carbon dioxide emission, export, foreign direct investment and GDP for Turkey with the structural break in 1991. This break can be refer to the financial liberalization period of Turkey.

ACKNOWLEDGEMENTS

This research is supported by Scientific Research Projects Unit of Istanbul University.

REFERENCES

- Antweiler, W., B. Copeland, and M. S. Taylor. 2001. "Is Free Trade Good for the Environment?." *American Economic Review*. 91: 877-908.
- Chaudhuri, S., and A. Pfaff. 2002. "Economic Growth and the Environment: What Can We Learn from Household Data?." *Columbia University Discussion Paper Series*. No: 0102-51.

- Copeland, B. R., and M. S. Taylor. 2001. "International Trade and the Environment: A Framework for Analysis." *National Bureau of Economic Research Working Paper*. No: 8540.
- Dinda, S., D. Coondoo, and M. Pal. 2000. "Air Quality and Economic Growth: An Empirical Study." *Ecological Economics*. 34: 409-423.
- Galeotti, M., A. Lanza, and F. Pauli. 2006. "Reassessing the Environmental Kuznets Curve for CO2 Emissions: A Robustness Exercise." *Ecological Economics*. 57: 152-163.
- Gregory, A. W., and B. E. Hansen. 1996. "Residual-Based Tests for Cointegration in Models with Regime Shifts." *Journal of Econometrics*. 70: 99-126.
- Grossman, G., and A. Krueger. 1991. "Environmental Impacts of a North American Free Trade Agreement." *National Bureau of Economics Research Working Paper*. 3194, NBER, Cambridge.
- Kuznets, S. 1955. "Economic Growth and Income Inequality." *American Economic Review*. 45: 1-28.
- Millimet, D.L., J.A. List, and T. Stengos. 2003. "The Environmental Kuznets Curve: Real Progress or Misspecified Models?." *Review of Economics and Statistics*. 85: 1038-1047.
- Nelson, C.R., and C.I. Plosser. 1982. "Trends and Random Walks in Macroeconomic Time Series." *Journal of Monterey Economics*. 10: 139-162.
- Perman, R., and D.I. Stern. 2003. "Evidence from Panel Unit Root and Cointegration Tests that Environmental Kuznets Curve does not Exist." *The Australian Journal of Agricultural and Resource Economics*. 47: 325-347.
- Perron, P. 1989. "The Great Crash, the Oil Price Shock and the Unit Root Hypothesis." *Econometrica*. 57: 1361-1401.
- Perron, P. 1997. "Further Evidence on Breaking Trend Functions in Macroeconomic Variables." *Journal of Econometrics*. 80: 355-385.
- Phillips, P. C. B. 1987. "Time Series Regression with a Unit Root." *Econometrica*. 55: 277-301.

ENVIRONMENTAL KUZNETS CURVE HYPOTHESIS AND STRUCTURAL BREAKS: EVIDENCE FROM TURKEY

Burcu Kiran

(Istanbul University, Istanbul, Turkey)

ABSTRACT: This paper tests the environmental Kuznets curve hypothesis which means an inverted U-shape relationship between various indicators of environment degradation and income per capita for Turkey over the period 1960-2011. In our empirical analysis, we use Narayan and Popp(2010) unit root test which is flexible enough to allow for at most two structural breaks in the level and trend, and also Hatemi-J(2008) cointegration test which calculates three residual based test statistics for cointegration by taking into account two possible regime shifts. The results reveal that there is evidence of cointegration between carbon dioxide emission, energy consumption and income with two structural breaks. Hence, the environmental Kuznets curve hypothesis is valid for Turkey.

INTRODUCTION

The Kuznets curve which implies an inverted U-shaped curve relationship between per capita income and income inequality is first suggested by Kuznets(1955). According to Kuznets(1955), there is a changing relationship between per capita income and income inequality. As per capita income increases, income inequality also increases at first and then starts declining after a turning point. Following Kuznets curve, the same inverted U-shaped relationship is found between environmental degradation and income per capita. This relationship developed and tested by Grossman and Krueger(1991) is known as the Environmental Kuznets Curve hypothesis. This hypothesis indicates that as per capita income grows, environmental impact increases, reaches a peak and then declines. In other words, pollution levels increase as a country develops, but begin to decrease as the rising incomes pass beyond a turning point (Odhiambo, 2012).

Grossman and Krueger(1995) point out that there are three accesses for economic growth to affect environmental degradation, namely scale effect, composition effect and technique effect. Scale effect occurs as pollution increases with the size of the economy. Panayotou(2003) states, when the production of an economy shifted mainly from agriculture to industry, pollution intensity increases. Therefore, it could be argued that scale effect will do harm to environment. However, composition and technique effects will improve environment. When the industrial structure enhances further, from energy-intensive heavy industry to service and technology-intensive industries, pollution falls as income grows. This is known as the composition effect. Actually, technique effect goes with the composition effect. Technical progress makes it possible to replace the heavily polluting technology with cleaner technology.

The aim of this paper is to test environmental Kuznets curve hypothesis by investigating the long term relationship between carbon dioxide emission (an indicator of environment degradation), energy consumption and income for Turkey over the period from 1960 to 2011. Although numerous studies exist in the literature based on this hypothesis, there are some reasons for choosing Turkey in our analysis. Lise(2006) and Lise and Montfort(2007) report these reasons in a multi-dimensional perspective. The first reason is that Turkey is a candidate for becoming an European Union (EU) member in the near future. So, Turkey has strict environmental obligations to fulfill in order to qualify for full membership. According to the Commission of the European Communities, the EU aims at reducing environmental pollutants 30% below the 1990 levels by 2020. Hereafter, it is expected that Turkey will be under strong pressure from the EU to comply with the Union's regulations on environmental policy (Halicioğlu, 2009). The second reason

to find Turkey as an interesting country is that Turkey has a strategic position as a gas and oil transportation country. And also, Turkey is listed as an Annex 1 country and has not yet set a greenhouse gas emissions reduction target. The last reason is that the Turkish economy has a boom-bust structure in the recent past. According to the 2006 report of World Energy Council Turkish National Committee, Turkey's contribution to carbon dioxide emissions is quite low; in 2003 per capita carbon dioxide emissions were at 2.87 tons, much lower than the OECD average of 11.08 tons and also its share in total OECD emissions was 1.59% and in world emissions was 0.81%. But, in recent years, there is a rapid increase in the carbon dioxide emissions of Turkey. In 2008, carbon dioxide emission was the leading greenhouse gas with the ratio of 81.1%. The results of greenhouse gas emissions inventory show that total greenhouse gas emissions in Turkey are 401.9 million tons on a carbon equivalent basis in 2010 and 81.23% of these emissions is carbon dioxide.

There are limited number of empirical studies which test the environmental Kuznets curve hypothesis for Turkey and their results are mixed based on different time periods, different variables and different methodologies [Lise(2006), Akbostancı et al.(2009), Halıçioğlu(2009), Soytas and Sarı (2009), Öztürk and Acaravcı(2010), Omay(2013), Yavuz(2014)]. The contribution of our paper to the literature is that, specifically, we test the validity of the environmental Kuznets curve hypothesis by using Narayan and Popp (2010) unit root test and Hatemi-J (2008) cointegration test in the same analysis. Both tests take into account existence of two structural breaks. Narayan and Popp (2010) unit root test is flexible enough to allow for at most two structural breaks in the level and trend. And also, Hatemi-J (2008) cointegration test calculates three residual based test statistics by taking into account two possible regime shifts. It is clear that taking into account the structural breaks is necessary because the long run relationship between carbon dioxide emission, energy consumption and income might change and the shifts can occur in the cointegrating vector. Hatemi-J (2008) mentions about many reasons to expect structural changes in the relationship between the series such as economic crises, technological shocks, changes in the economic actor' preferences and behaviour accordingly, policy and regime changes, and organizational and institutional evolution.

The rest of the paper is constructed as follows: The next section presents the materials and methods, the third section reports results and discussions. Finally, the last section concludes the paper.

MATERIALS AND METHODS

This paper intends to test environmental Kuznets curve hypothesis by taking into account existence of two structural breaks in the relationship between carbon dioxide emission, energy consumption and income. For unit root properties of the series, we use recently developed Narayan and Popp (2010) unit root test which can identify two structural breaks in the level and trend. For long run relationship between the series, we apply Hatemi-J (2008) cointegration test which considers two possible regime shifts.

Narayan and Popp (2010) Unit Root Test. Perron(1989) argues that the exclusion of structural breaks while modeling the unit root often leads to accepting the false null hypothesis. Since this argument, many authors addressed this issue by identifying structural breaks endogenously and exogenously. However, Popp(2008) noticed that spurious regression arises from different interpretations of test parameters under the null and alternative hypothesis, because of the parameters affect the selection of the break date. This problem is solved by Narayan and Popp(2010). Following Schmidt and Philips (1992), they developed an ADF type test for the case of innovational outlier (IO) where the data generating process is constructed as an unobserved component model. Narayan and Popp(2010) take into account the following data generating process of a time series y_t :

$$y_t = d_t + u_t \quad (1)$$

$$u_t = \rho u_{t-1} + \varepsilon_t \quad (2)$$

$$\varepsilon_t = \psi^*(L)e_t = A^*(L)^{-1}B(L)e_t \quad ; \quad e_t \square iid(0, \sigma_e^2). \quad (3)$$

Here, y_t has two components; d_t and u_t . d_t is deterministic component and u_t is a stochastic component. $A^*(L)$ and $B(L)$ are the lag polynomials. It is assumed that the roots of these lag polynomials which are of order p and q , respectively, lie outside the unit circle.

In the construction of this test, two different specifications both for trending data are considered: One specification allows for two breaks in the level (denoted M1) and the other specification allows for two breaks in level and trend (denoted M2). These model specifications (M1 and M2) differ in deterministic component d_t . For M1, d_t is defined as follows:

$$d_t^{M1} = \alpha + \beta t + \psi^*(L)(\theta_1 DU'_{1,t} + \theta_2 DU'_{2,t}) \quad (4)$$

And also d_t which is defined for M2 can be seen in below:

$$d_t^{M2} = \alpha + \beta t + \psi^*(L)(\theta_1 DU'_{1,t} + \theta_2 DU'_{2,t} + \gamma_1 DT'_{1,t} + \gamma_2 DT'_{2,t}) \quad (5)$$

In both specifications, $DU'_{i,t}$ and $DT'_{i,t}$ are defined as follows, respectively:

$$\begin{aligned} DU'_{i,t} &= 1(t > T'_{B,i}) \quad ; \quad i=1,2 \\ DT'_{i,t} &= 1(t > T'_{B,i})(t - T'_{B,i}) \quad ; \quad i=1,2. \end{aligned} \quad (6)$$

Here $T'_{B,i}$, $i=1,2$ describe the true break dates, θ_i and γ_i parameters indicate the magnitude of the level and trend breaks, respectively. The inclusion of ψ^* in corresponding equations enables breaks to occur slowly over time. Specifically, it is assumed that the series responds to shocks to the trend function the way it reacts to shocks to the innovation process e_t (Vogelsang and Perron, 1998). This process is known as IO model. In order to test unit root hypothesis for M1 and M2, the IO-type test regression can be derived by merging the structural model (1)-(5). Narayan and Popp(2010) use t-statistics in order to test the null hypothesis of a unit root ($H_0 : \rho = 1$) against the alternative hypothesis ($H_1 : \rho < 1$).

Hatemi-J (2008) Cointegration Test. According to Gregory and Hansen (1996), the cointegration tests which do not take into account the presence of structural changes or regimes shifts, have low power. Following this argument, they introduce a new cointegration test procedure, which allows for an endogenously determined break in the cointegrating relationship. Their test includes three alternative forms of structural break: level shift (Model C), level shift with trend (Model C/T) and regime shift (Model C/S). The model with regime shift (Model C/S) can be constructed as follows:

$$Y_t = \alpha_0 + \alpha_1 D_t + \beta_0 X_t + \beta_1 (D_t * X_t) + u_t \quad (7)$$

where D_t is a dummy variable equal to 0 if $t \leq \tau$ and 1 if $t > \tau$. Here, the unknown parameter τ denotes the timing of the change, α_1 denotes the change in the intercept coefficient at the time of the shift and β_1 represents the change in the slope of the cointegrating equation. Given that the timing of structural break is unknown a priori, Gregory and Hansen (1996) propose a suite of tests: the commonly used ADF test statistic and the extensions of the Z_t and Z_α test statistics of Phillips (1987). By calculating these statistics, the null hypothesis of no cointegration is tested against the alternative of cointegration with structural break. The Equation (7) is generalized by Hatemi-J (2008) for two structural breaks in the cointegrating

relationship. The equation which takes into account the possibility of two structural breaks can be seen in below:

$$Y_t = \alpha_0 + \alpha_1 D_{1t} + \alpha_2 D_{2t} + \beta_0 X_t + \beta_1 (D_{1t} * X_t) + \beta_2 (D_{2t} * X_t) + e_t \quad (8)$$

where D_{1t} and D_{2t} are dummy variables constructed as follows:

$$D_{1t} = \begin{cases} 0 & \text{if } t \leq \tau_1 \\ 1 & \text{if } t > \tau_1 \end{cases} \quad \text{and} \quad D_{2t} = \begin{cases} 0 & \text{if } t \leq \tau_2 \\ 1 & \text{if } t > \tau_2 \end{cases}.$$

Here, τ_1 signifies the period before the first break and τ_2 signifies the period before the second break. In order to test the null hypothesis of no cointegration, ADF, Z_t and Z_α test statistics are calculated. The critical values can be found in the original paper of Hatemi-J (2008).

RESULTS AND DISCUSSION

To test the validity of the environmental Kuznets curve hypothesis for Turkey, we use the following linear logarithmic quadratic model construction:

$$\ln CO_{2t} = \beta_0 + \beta_1 \ln EC_t + \beta_2 \ln GDP_t + \beta_3 \ln GDP_t^2 + e_t$$

Here, $\ln CO_2$ refers to the natural logarithm of the carbon dioxide emission per capita (metric tons) which is an indicator of environment degradation, $\ln EC$ is the natural logarithm of the energy consumption per capita (kilograms of oil equivalent), $\ln GDP$ represents natural logarithm of the gross domestic product per capita (with constant prices), $\ln GDP^2$ is the natural logarithm of the square of gross domestic product per capita. We use annual data over the period 1960-2011 obtained from World Development Indicators database of World Bank. As a first step, we neglect existence of possible structural breaks and start our analysis by investigating unit root properties of the series with conventional Augmented Dickey Fuller (ADF) and Philips and Perron (PP) unit root tests. The test results are tabulated in Table 1.

TABLE 1. The results of ADF and PP unit root tests

Series	ADF		PP	
	Level	First difference	Level	First difference
$\ln CO_2$	-2.6190	-7.0409 ^a	-2.6677	-7.0422 ^a
$\ln EC$	-2.3923	-6.8914 ^a	-2.4461	-6.8899 ^a
$\ln GDP$	-2.9317	-7.1164 ^a	-3.0356	-7.1214 ^a
$\ln GDP^2$	-2.8572	-7.0914 ^a	-2.9908	-7.0969 ^a

Note: ^a indicates rejection of the unit root null hypothesis at the 1% significance level.

According to the obtained results, ADF and PP unit root tests show that all the series in the analysis are nonstationary in level but stationary after first differencing. In other words, these results give evidence to support that the integration order of the series can be considered as one ($I(1)$) for all series. Since Perron (1989) argues that ignoring a structural break can lead to false acceptance of the unit root null hypothesis, we extend our unit root analysis with structural breaks. For this purpose, we use a new unit root test proposed by Narayan and Popp (2010). This test is flexible enough to allow for at most two structural breaks in the level and trend of the series. The results based on M1 (breaks in level only) and M2 (breaks in level and trend) are reported in Table 2.

The results in Table 2 imply that the null of unit root hypothesis cannot be rejected for all $\ln CO_2$, $\ln EC$, $\ln GDP$ and $\ln GDP^2$ series. These results are consistent with ADF and PP unit root tests. The implication of this evidence is that validity of the environmental Kuznets curve hypothesis can be tested by using cointegration methods. Conventional cointegration methods are biased towards accepting the null of

no cointegration and if there is structural breaks in the relationship, these standard tests may produce spurious cointegration results. By considering that the long run relationship between mentioned $\ln CO_2$, $\ln EC$, $\ln GDP$ and $\ln GDP^2$ series might change and the shifts can occur in their cointegrating vector, instead of conventional cointegration tests, we apply Hatemi-J (2008) cointegration test in the presence of two unknown structural breaks. The results can be seen in Table 3.

TABLE 2. The results of Narayan and Popp (2010) unit root test with two structural breaks

Series	M1			M2		
	Test statistic	TB1	TB2	Test statistic	TB1	TB2
$\ln CO_2$	-2.238	1977	2000	-4.065	1977	2000
$\ln EC$	-2.488	1978	2000	-4.156	1978	2000
$\ln GDP$	-3.839	1979	2000	-4.622	1979	2000
$\ln GDP^2$	-3.974	1979	2000	-4.129	1979	2000
Critical values for unit root test						
Model M1 (Breaks in level only)						
1%		5%		10%		
-5.259		-4.514		-4.143		
Model M2 (Breaks in level and trend)						
1%		5%		10%		
-5.949		-5.181		-4.789		

Note: The critical values for endogenous two breaks are from Narayan and Popp (2010).

TABLE 3. The results of Hatemi-J (2008) cointegration test with two unknown structural breaks

Test statistics	Statistic value	τ_1	τ_2
ADF^*	-8.079 ^a	1972	1984
Z_t^*	-8.370 ^a	1979	1993
Z_α^*	-57.383	1972	1984

Note: ^a indicates statistically significance at the 1% significance level. The critical values for ADF^* , Z_t and Z_α test statistics are collected from Hatemi-J (2008). These are -7.833, -7.352 and -7.118 for ADF^* and Z_t statistics; -118.577, -104.860 and -97.749 for Z_α statistic at the 1%, 5% and 10% significance levels, respectively.

The results indicate that ADF^* and Z_t^* statistics give evidence in favour of the existence of long run relationship between carbon dioxide emission, energy consumption and GDP series with two structural breaks. The meaning of this result is that environmental Kuznets curve hypothesis is valid for Turkey. When the attention is given to the identified structural breaks, it is seen that the results are mixed. At a glance, the first break points to the 1972 while the second break points to the 1984 for ADF^* and Z_α^* statistics. These break points refer to the oil crisis of 1973 and structural transformation reforms which opened up the Turkish economy to international forces after 1980s, respectively. According to the Z_t^* statistic, we identify the first break in 1979 and the second break in 1993. These break points are consistent with the important economic events of Turkish economy. The break in 1979 refers to the period which there is an increase in

energy consumption and carbon dioxide emissions due to the growth in the industrial sector and the break in 1993 provides apparent evidence for 1994 economic crisis.

CONCLUSIONS

In this paper, the environmental Kuznets curve hypothesis is tested by investigating the long run relationship between carbon dioxide emission, energy consumption and income for Turkey over the period from 1960 to 2011. For this purpose, we employ Narayan and Popp(2010) unit root and Hatemi-J(2008) cointegration tests. Both tests take into account the existence of two structural breaks. The obtained results indicate that there is evidence of cointegration between carbon dioxide emission, energy consumption and income with two structural breaks, hence the validity of the environmental Kuznets curve hypothesis for Turkey. It is also seen that the identified structural breaks point to the important economic events of Turkish economy such as oil crisis, structural transformation reforms, carbon dioxide emission increases and economic crisis.

ACKNOWLEDGEMENTS

This research is supported by Scientific Research Projects Unit of Istanbul University.

REFERENCES

- Akbostancı, E., S. Türüt-Aşık, S., and G. İ. Tunç. 2009. "The Relationship between Income and Environment in Turkey: Is There an Environmental Kuznets Curve?." *Energy Policy*. 37(3): 861-867.
- Gregory, A. W., and B. E. Hansen. 1996. "Residual-Based Tests for Cointegration in Models with Regime Shifts." *Journal of Econometrics*. 70: 99-126.
- Grossman, G., and A. Krueger. 1991. "Environmental Impacts of a North American Free Trade Agreement." *National Bureau of Economics Research Working Paper*. 3194, NBER, Cambridge.
- Grossman, G., and A. Krueger. 1995. "Economic Growth and the Environment." *Quarterly Journal of Economics*. 110(2): 353-377.
- Halıcıoğlu, F. 2009. "An Econometric Study of CO₂ Emissions, Energy Consumption, Income and Foreign Trade in Turkey." *Energy Policy*. 37(3): 1156-1164.
- Hatemi-J, A. 2008. "Tests for Cointegration with Two Unknown Regime Shifts with An Application to Financial Market Integration." *Empirical Economics*. 35(3): 497-505.
- Kuznets, S. 1955. "Economic Growth and Income Inequality." *American Economic Review*. 45: 1-28.
- Lise, W. 2006. "Decomposition of CO₂ Emissions over 1980-2003." *Energy Policy*. 34: 1841-1852.
- Lise, W., K. V. Monfort. 2007. "Energy Consumption and GDP in Turkey: Is There a Cointegration Relationship?." *Energy Economics*. 29: 1166-1178.
- Narayan, P. K., and S. Popp. 2010. "A New Unit Root Test with Two Structural Breaks in Level and Slope at Unknown Time." *Journal of Applied Statistics*. 37: 1425-1438.
- Odhiambo, N. M., 2012. "Economic Growth and Carbon Emissions in South Africa: An Empirical Investigation." *Journal of Applied Business Research*. 28(1): 37-46.
- Omay, R. E. 2013. "The Relationship between Environment and Income: Regression Spline Approach." *International Journal of Energy Economics and Policy*. 3: 52-61.
- Ozturk, I., and A. Acaravcı. 2010. "CO₂ Emissions, Energy Consumption and Economic Growth in Turkey." *Renewable and Sustainable Energy Reviews*. 14(9): 3220-3225.
- Panayotou, T. 2003. "Economic Growth and the Environment. Economic Survey of Europe." 2(2): http://www.unece.org/fileadmin/DAM/ead/pub/032/032_c2.pdf.
- Perron, P. 1989. "The Great Crash, the Oil Price Shock and the Unit Root Hypothesis." *Econometrica*. 57: 1361-1401.
- Phillips, P. C. B. 1987. "Time Series Regression with a Unit Root." *Econometrica*. 55: 277-301.
- Popp, S. 2008. "New Innovational Outlier Unit Root Test with A Break at An Unknown Time." *Journal of Statistical Computation and Simulation*. 78: 1143-1159.

- Schmidt, P., and P. C. B. Phillips. 1992. "LM Test for a Unit Root in the Presence of Deterministic Trends." *Oxford Bulletin of Economics and Statistics*. 54: 257-287.
- Soytas, U., and R. Sari. 2009. "Energy Consumption, Economic Growth and Carbon Emissions: Challenges Faced by An EU Candidate Member." *Ecological Economics*. 68(6): 1667-1675.
- Vogelsang, T., and P. Perron. 1998. "Additional Tests for a Unit Root Allowing for a Break in the Trend Function at an Unknown Time." *International Economic Review*. 39(4): 1073–1100.
- Yavuz, N. Ç. 2014. "CO2 Emission, Energy Consumption and Economic Growth for Turkey: Evidence from a Cointegration Test with a Structural Break." *Energy Sources, Part B: Economics, Planning and Policy*. 9(3): 229-235.

**A LINEAR GENETIC PROGRAMMING APPROACH FOR DISCHARGE FORECASTING.
JONATHAN BARGE AND HATIM SHARIF**

Jonathan Barge and *Hatim Sharif*
(University of Texas at San Antonio, TX, USA)

This study focuses on assessing the ability of Linear Genetic Programming (LGP) to model the rainfall-discharge relationship and forecast next-day discharge. The approach is quite different from more complex modeling environments such as physically based models, conceptual models, and more intricate data-driven techniques such as Artificial Neural Networks (ANNs). The main difference between LGP and most data-driven techniques is that it deals with multiple solutions while optimizing the functional relationships between input variables. Individual models are optimized through the application of crossover and mutation operators, which mimic Darwinian evolutionary processes. Model results indicate that a minimum number of input variables are necessary for deriving highly robust solutions, as the application of LGP as a standalone technique returned strong validation values while using only two days of observed discharge and one day of precipitation information. The potential of LGP was found to be further enhanced when embedded into hybrid model designs. Clustering the input space through Kohonen's Self Organizing Map (SOM) proved to allow LGP to create a better fit to each data cluster. Decomposing the original streamflow time-series into a number of subcomponents through the data Ensemble Empirical Mode Decomposition (EEMD) decomposition technique and utilizing that information as additional input data significantly improved results. Combining all three techniques in an EEMD-SOM-LGP design returned the best performance statistics of any model produced.

CFD MODELLING OF CYLINDRICAL VORTEX FLOW REGULATORS PERFORMANCE - SIMULATION AND EXPERIMENTS

*Patryk Wójtowicz** and Małgorzata Szlachta
(Wrocław University of Technology, Wrocław, Poland)

Vortex flow regulators (also known as hydrodynamic flow regulators) are used in wastewater and storm water collection systems for flow throttling and control. Vortex regulators are not only very efficient energy dissipaters but also effective atomizers, which is beneficial for sewer aeration. Maintaining a proper oxygen balance is important to preserve against putrefaction, odours and concrete sewer corrosion. In this study, we present the experimental and numerical results for the cylindrical type of vortex regulators (CVR).

Laboratory and pilot scale devices were examined in a closed-circuit test rig. For CFD modelling, the commercial solver ANSYS Fluent as well as OpenFOAM were used. We performed testing for a range of different RANS, URANS and LES (Large Eddy Simulation) turbulence models to find that unsteady incompressible two-phase URANS Reynolds Stress Model (RSM) yielded the best results and was less computationally expensive than LES. The application of seven-equation Reynolds stress turbulence model allowed us to take into account the complex hydrodynamics of vortex regulators. Specifically, this model addresses the effects of turbulence anisotropy (Reynolds stresses), streamline curvature, swirl and rotation. To minimize numerical diffusion, we used only hexahedral meshes. To study mesh dependence, we tested meshes from 200k to 1.5 million cells. In most cases, the meshes composed of 500k cells were finally used in simulations. The initial steady solution was obtained with the use of two-equation k-epsilon model. The converged k-epsilon solution was used as boundary conditions for URANS simulations. The important parameters of CFD simulation were as follows: Reynolds stress model for turbulence closure with the enhanced wall functions. Pressure-based (segregated) solver with PRESTO! scheme for pressure interpolation and SIMPLE scheme for pressure-velocity coupling. In the final solution, we used the second order upwind scheme. In order to obtain the converged solution, we applied dynamic simulation control for unsteady RSM simulation (e.g. by adjusting Courant number). Grid adaption was also employed (only with Fluent simulations) – mesh was optimized on the basis of velocity gradients. The CFD simulations were compared with experimental data (pressure and velocity profiles, inlet pressure and flow rate, photo measurements – spray angle, air core diameter, air core offset). All calculations were run in parallel on the Macintosh computer (running Linux openSUSE) with 12 GB RAM and Intel quad-core i7 3.4 GHz.

The comparison of computed pressure profiles with the experiments exhibited a high level of accuracy. The major quantities of interest, such as pressure drop, discharge coefficient and minor loss coefficient were accurately predicted (within 5% of error). The swirl flow features, such as air core diameter and (asymmetrical) shift vectors from the outlet center were well captured in the CFD simulations. The selected Reynolds-stress turbulence model was suitable for simulation of complex vortex flow in hydrodynamic flow regulators.

VULNERABILITY ASSESSMENT OF THE CENTRAL GULF OF MEXICO COAST USING A MULTI-DIMENSIONAL INDEX APPROACH

David E. Dismukes and *Siddhartha Narra*
(Louisiana State University, Baton Rouge, LA, USA)

The coastal communities of the central Gulf of Mexico (GOM) form a highly productive and complicated human, physical, and natural environment that interact in ways unique compared to other coastal areas of the globe. Past studies on understanding coastal resiliency and developing coastal vulnerability indices for this region have mainly focused on climate change and sea-level rise, with more recent research directed towards socio-economic and demographic factors. However, the interactions of climate change with non-climatic drivers of the coastal ecosystem such as economy and infrastructure concentration are often overlooked. To support the development of policies relating to coastal management and climate change, it is vital to integrate all the relevant parameters. This paper presents a relative vulnerability assessment of the Central GOM coast by incorporating climatic, geological, socio-economic, demographic and economic variables in a GIS system. A multi-dimensional Coastal Vulnerability Index (CVI) developed based on these parameters is used to rate coastal segments into different classes based on their relative range of vulnerability. We study the relationship between energy infrastructure and the physical and human aspect of communities to identify and prioritize communities, and the proximate infrastructure most at risk from coastal climate change. Special focus is directed towards the concentration of pipeline and transportation infrastructure in this region when developing these vulnerability indices. Spatial analysis will be a component part of the index-based approach to characterize, organize, and analyze data in order to assess coastal community vulnerability in areas supporting critical energy infrastructure.

PREDICTING THE LONG-TERM LEACHING BEHAVIOR OF COAL ASH DEPOSITS IN MINE SITE: A COLUMN STUDY

Mina Mohebbi*, Farshad Rajabipour, Barry E. Scheetz
(Pennsylvania State University, University Park, PA, USA)

Combustion of coal to generate electricity produced about 116 million tons of coal combustion products (CCPs) in 2013. Approximately, 56% (vol.) of CCPs consists of pulverized coal (PC) fly ash and fluidized bed combustion (FBC) ash. 43% of fly ashes are used for beneficial applications such as concrete construction, soil stabilization, and land reclamation, and the remaining 57% are deposited in landfills or surface impoundments. Reclamation of mine sites with coal ash has been shown to potentially alleviate the negative effects of mining activities on the environment. These effects include disturbance of large areas of land, risk of land subsidence, and risk of contamination of water resources due to acid mine drainage and heavy metal leaching. The alkaline pH of fly ash has been proved to neutralize the acid mine drainage, and consequently precipitate the dissolved elements out of the mine leachate, thereby reducing contamination to water resources. However, the long-term (several decades) leaching of harmful trace elements from coal ash deposits to subsurface aquifers is still not fully understood, and continues to be a major concern.

In this study, CrunchFlow, a quantitative reactive-transport model, is developed to predict the long-term (30 years) leaching risk of elements from a Pennsylvania PC fly ash in a 1D leaching column geometry considering the geochemical conditions of mine sites. This model assists in correct identification of the leaching mechanisms of major (Si, Al, Fe, Ca, K, S), minor (Na, Mg), and trace elements of interest (i.e., As, Mo, B). Simulation considers fly ash mineralogy, host phases for target elements, and environmental/mine conditions (i.e., influent pH and porosity evolution), and predicts leaching by accounting for solubility controlled phase dissolutions as well as delayed release/leaching of elements from ash phases exposed to flowing water for long durations.

The simulation results revealed that dissolution, precipitation of secondary phases, adsorption, and surface complexation are the main mechanisms controlling the leaching of trace elements in long term. The influent water pH was changed from 5.5 (pH of rain water flow) to 8 which shows the alkalinity and neutralization potential of studied fly ash. To evaluate the accuracy of the model, it is applied to leaching column test geometry, and the model results are compared with the experimental data. If successful, this model could be scaled up in future to an actual mine site, and be used to evaluate the risk of groundwater contamination. Such information are crucial to find appropriate mitigation techniques to retain the harmful elements in solid phases and prevent their leaching to underground water resources.

INVESTIGATING, MODELING AND PREDICTION OF TRICLOSAN AND CARBAMAZEPINE IN SURFACE WATERS USING EFDC: CASE STUDY IN THE SHAHE STREAM

Xiao Yuan, Shiyu Li*, Jiatang Hu, Yuying Li, Ziyun Wang
(Guangdong Provincial Key Laboratory of Environmental Pollution Control and Remediation Technology, School of Environmental Science and Engineering, Sun Yat-sen University, Guangzhou 510275, China)

ABSTRACT: The aim of this study was to preliminary attempt to model pharmaceuticals and personal care products (PPCPs) in surface water bodies, and to use EFDC model to forecast. As two kinds of PPCPs, triclosan (TCS) and carbamazepine (CBZ) were generally used in disinfectant or anticonvulsants agent. Hydrolysis, biodegradation and photolysis as the major routes of TCS and CBZ in this study. A central composite design methodology has been investigated to determine the relevant natural parameters (including pH, DO, salinity, temperature, light intensity, humic acid) for their degradation as far as possible in laboratory. Several important impacts on the parameters were discussed. The Shahe Stream has been selected, of which hydrodynamic condition was extremely simple and pollution sources were very specific, in order to reduce the difficulty of simulation under natural conditions. Then, the fate and behavior of TCS and CBZ during the stream were investigated using a 2D numerical flow and transport model with EFDC. Results showed that the predicted values of the model were basically higher than the measured values, and the prediction deviation between 23%-52% of TCS, 23%-37% of CBZ. It proved that PPCPs can be simulated by using the numerical model in simple water, but must pay attention to the process of PPCPs about adsorption and desorption between water and sediment.

Keywords: triclosan, carbamazepine, pharmaceuticals and personal care products (PPCPs), modeling, surface waters

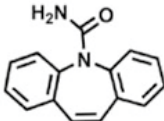
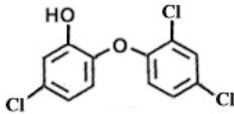
INTRODUCTION

Active ingredients in pharmaceuticals, personal care products are collectively referred to as PPCPs, including not just prescription drugs and biological agents, but also commonly used diagnostic reagent, nutrition, perfumes, and skin care, shampoo hair care, oral health and so on (Daughton and Ternes, 1999). The presence of PPCPs in surface waters has been frequently reported in the literature (Yoon *et al.*, 2010; Ortiz de Garcia *et al.*, 2013; Carmona *et al.*, 2014). China is a large country with high production and consumption of PPCPs owe to its economic development and population growth, which may result in serious pollution by PPCPs (Peng *et al.*, 2014; Wu *et al.*, 2014; Wang *et al.*, 2015). The technology for prediction and monitoring of PPCPs in different areas of China is urgent.

PPCPs selected in this study are triclosan (TCS) and carbamazepine (CBZ) (Table. 1). Triclosan [5-chloro-2-(2,4-dichlorophenoxy)phenol] is a broad spectrum antibacterial agent used in cosmetics, household cleaning products, toys, medical devices, plastic materials, textiles, and kitchen utensils (Bedoux *et al.*, 2012). TCS is used in great quantities in the daily chemical products, along with the wastewater discharge into the natural environment, the concentration of TCS about the related test was 0.01 ug/L to 10 ug/L. Xu reported that the concentration of TCS was 0.030 ug/L to 0.100 ug/L in the Victoria harbor of Hongkong, and 0.025 ug/L to 0.035 ug/L in the Pearl River (Xu *et al.*, 2007). Just one year later, another study pointed out that the concentration of TCS was reached 0.035 ug/L to 1.023 ug/L in the same area (Peng *et al.*, 2008). Furthermore, the concentrations of TCS was detected higher in the sewage treatment plant, such as Wu investigated that the average concentration of TCS were 0.1585 ug/L, 0.0225 ng/L in the

primary treatment effluent and the secondary treatment effluent of the sewage treatment plant in Shenzhen city (Wu *et al.*, 2007). Another target, carbamazepine [5H-dibenzo[b,f]azepine-5-carboxamide] is an antiepileptic drug belongs to anticonvulsants that commonly used in control certain types of seizures by reducing abnormal electrical activity in the brain (Mohapatra *et al.*, 2014). It was the most frequently detected pharmaceutical residue in water bodies (Zhang *et al.*, 2008), and related to the growth rate of microorganisms and to effluent concentrations as a possible anthropogenic marker and sewage markers in the aquatic environment (Clara *et al.*, 2004; Kuroda *et al.*, 2012). Based on the significant correlations between PPCPs, it can also as the chemical indicators for predicting the overall PPCPs contamination (Wang *et al.*, 2015). In Pearl River, the concentrations of carbamazepine in surface water were lower than those in USA and European countries (Yang *et al.*, 2013), but it was still detected with a detection frequency of 81% and median concentration of 15.6 ng/L, and the maximum concentration of carbamazepine (43.1 ng/L) was also found in the Shijing River which was tributaries of Pearl River (Zhao *et al.*, 2010).

Table 1. Physicochemical properties of the target compounds

Common Name	Carbamazepine ^a	Triclosan ^a
Therapeutic groups	Psychiatrics-antiepileptics	Disinfectants
Abbreviation	CBZ	TCS
Chemical Formula	C ₁₅ H ₁₂ N ₂ O	C ₁₂ H ₇ Cl ₃ O ₂
Chemical Structure		
CAS No. ^b	298-46-4	3380-34-5
Mol. Mass (g mol ⁻¹)	236.27	289.54
Solubility (mg/L) ^c	17.7	10
pK _a	7/13.9	4.5/8.1
LogK _{ow}	2.47	4.80/5.34

^a (Kosma *et al.*, 2014); ^b (Deo, 2014); ^c (Stackelberg *et al.*, 2007).

Although there are a lot of reports about the concentration and distribution of TCS and CBZ, and their degradation mechanism, processing technology in the laboratory research, but the data collected in such studies rarely provide quantitative information on the various processes that determine the fate of the compound in the natural environment. To our knowledge, almost no information on which water quality model about the fate of TCS and CBZ in surface water is available in the literature.

MATERIALS AND METHODS

Chemicals and Reagents. Standards of TCS (99.0%), CBZ (99.5%), ¹³C₃-caffeine and simatone were purchased from Dr. Ehrenstorfer (Augsburg, Germany). Stock solutions of the standards were prepared by dissolving each compound in methanol or ultrapure water. The solvents, HPLC-grade methanol, water (Lichrosolv), HPLC-grade phosphoric acid and formic acid 98% were provided by Merck (Darmstadt, Germany). Sulfuric acid, sodium hydroxide, sodium chloride, humic acid (fulvic acid, 90%), disodium ethylenediamine tetraacetate (Na₂EDTA) were all purchased from Aladdin (Los Angeles, USA).

Sampling Site and Sample Collection. Sampling sites (S1-S6) were located in the upstream of the Shahe Stream (Fig. 1). The Shahe Stream is located in the center of Guangzhou city, which is the provincial capital of Guangdong province in China. It's discharged into the Pearl River which flows through the Pearl River Delta and finally merges into the South China Sea via the Pearl River Estuary. The Pearl River is the third largest river of China. A wastewater treatment plant (WTP) is located in the upstream of Shahe Stream, the

plant facilities used half buried type structure, using biological membrane technology to deal with the sewage near the living area. Its tail water through the pipe into the Shahe Stream.

After field survey and measurement, the pollution sources is single the this area. At the same time, due to the regional water mainly comes from the WTP and the stream was artificial built and hardening. Therefore, the study can effectively reduce the difficulty of the simulation by further simplifying the hydrodynamic conditions. This choice can not only try to avoid some unpredictable influence to achieve the purpose of this study, but also provide good foundation for deeper research in the future.

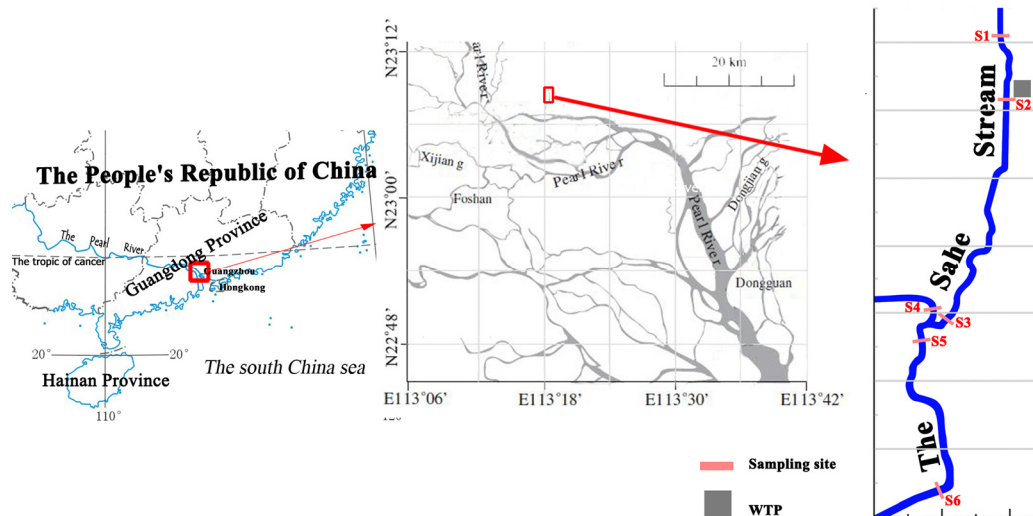


Fig. 1. Location of the sampling sites

Sampling was respectively performed on March, 2014. All sampling sites were sampled during both the level period (Peng *et al.*, 2008). All of the samples was taken at the middle of each cross-section, 0.5 m from the water surface.

Grab water samples (1 L) were collected in clean polypropylene bottles, from the middle of the river width at ca. 30 cm depth (Carmona *et al.*, 2014). Before sample collection, each bottle was thoroughly pre-rinsed with ultrapure water in the laboratory and then, rinsed with sample water three times prior to sample collection.

All water samples analyzed in this study were previously filtered with a 0.45 μm cellulose nitrate membranes of 47 mm by CNW (Düsseldorf, Germany) in the laboratory. Then, samples were adjusted pH to 2.5 with concentrated sulfuric acid to suppress microbial activity and kept in their original package at 4 $^{\circ}\text{C}$ until the analysis that was always performed within two days.

Sample Preparation and Extraction. Typical concentrations of antibiotics in the environmental water samples were less than 1 $\mu\text{g/L}$ (Boyd *et al.*, 2003; Richardson *et al.*, 2005), so Solid-phase extraction (SPE) methods should be using to cleanup and preconcentration at the beginning of the pretreatment procedures. Procedures for preparation of water samples for instrumental analysis were described in detail previously (Yang *et al.*, 2013).

A 500 mL sample was extracted using SPE cartridges (Strata C18-E cartridges, 3mL 500mg; Phenomenex, Los Angeles, USA) on a 16-position vacuum system (Supelco). Briefly, 60 mg SPE cartridges were conditioned with 6 mL of methanol, 1 mL acidified methanol (0.1 % formic acid in methanol, v/v), followed by 2 \times 6 mL of HPLC-grade water at a flow rate of 2 mL min^{-1} . Samples were spiked with 10 mL 5 g L^{-1} Na_2EDTA and 50 μL 500 $\mu\text{g L}^{-1}$ $^{13}\text{C}_3$ -caffeine and loaded on the cartridges at 5 mL min^{-1} . After extraction, the cartridges rinsed with 2 \times 6 mL of HPLC-grade water, dried under vacuum for 5 min, to remove excess of water, and eluted with 4 \times 2 mL of acidified methanol. The extracts were then evaporated

and reduced to -50 μL under a gentle nitrogen stream, reconstituted with 250 μL of methanol-water (10:90, v/v). Then, the extracts were added and mixed ten microliters of internal standards (2.5 mg L^{-1} simatone). Addition of internal standards in the final extract compensates possible matrix effect, but does not compensate any of the possible procedure losses (Petrovic *et al.*, 2014). Finally, the extracts were filtered with 0.45 μm syringe filters into 2 mL amber autosampler vials containing 250 μL inserts.

The Degradation Experiments. The migration and degradation process of PPCPs is mainly divided into the biodegradation, photolysis, hydrolysis, the adsorption and desorption in surface water (Pal *et al.*, 2010). Among them, photolysis is the main chemical way except adsorption process which PPCPs degrade in surface water, the reaction is mainly influenced by light intensity, pH, dissolved oxygen and chloride ions (Onesios *et al.*, 2009; Batchu *et al.*, 2013). Besides photolysis reactions, hydrolysis and microbial degradation is also an important way, including microbial response affected by pH, temperature, illumination, dissolved oxygen, nutrient, microbial species and quantity, the hydrolysis reaction is mainly influenced by pH, temperature, organic carbon and dissolved oxygen (Luo *et al.*, 2011). In consideration, the degradation experiment combined with three reaction process (biodegradation, photolysis, hydrolysis), and each factor in surface water bodies actual values range, by central composite experiment method. Central Composite Design (CCD) is the most frequently used five level fractional factorial designs for the construction of second-order response surface model. One of the advantages of CCD is the possibility to explore the whole of the experimental region (Daghrir *et al.*, 2014). Each reaction process set as eight factors five levels. The experiment would serve initial concentration PPCPs (C_0), pH, temperature (Temp), light intensity (LH), time (T), and salinity, humic acid (AH), and the concentration of dissolved oxygen (DO) as variable factors (Table. 2).

Table 2. Experimental Parameters.

Name	Units	-1	+1	$-\alpha$	$+\alpha$
Initial concentration (C_0)	$\mu\text{g/L}$	192.61	807.39	0.00	1000.00
Time (T) ^a	h	23.11	96.89	0.00	120.00
Temperature (Temp)	$^{\circ}\text{C}$	10.93	33.07	4.00	40.00
pH		6.39	7.61	6.00	8.00
DO	mg/L	1.73	7.27	0.00	9.00
Salinity ^b	‰	3.09	12.92	0.01	16.00
Humic acid (AH)	mg/L	5.79	24.23	0.02	30.00
Light intensities (LH) ^c	lux	282.43	817.57	100.00	1000.00

^a The value of the time (T) were 18.24, 71.76, 0, 90 min in the photolysis reaction process,

^b The value of the salinity expressed by the concentration of sodium chloride.

^c The value of the Light intensities (LH) were zero in the biodegradation reaction process and hydrolysis reaction process.

Before the degradation experiment, the raw water which used by the degradation experiments sampled from the Shahe Stream had been filled by membrane filter (0.45 μm) to remove the impurities in the water. Moreover, the raw water would be filled by membrane filter (0.22 μm) to filter sterilization in photolysis and hydrolysis experiments. An rotary photochemical reactor (BL-GHX-V, Bilon, Shaha, China) (Fig. 2) and a solar-simulated light source (350 W xenon lamp with 290 nm filter, $\lambda > 290 \text{ nm}$) were used to perform the degradation experiment. in a dark-room (Ma *et al.*, 2014). For controlling and maintaining the temperature, the constant temperature condensate tank drove the recirculated water to flow around the quartz tube.

Instrumental Analysis And Quality Control. Target chemicals were determined using a high-performance liquid chromatography system (1100 LC, Agilent, Santa Clara, USA), which consisted of two G1312A Binary HPLC pumps and a diode array detector. The gradient separation and the conditions in HPLC were done at an ZORBAX SB-C18 column (4.6×150 mm, 5µm, Agilent, Santa Clara, USA) was maintained at 30 °C, with injection volumes of 20µL and the mobile phase flow rate was 1 mL min⁻¹. The mobile phase comprised the mobile phase A was ultrapure water with HPLC-grade phosphoric acid (pH = 3.0) and the B was methanol. The gradient elution was set as follows: started at 40 % B, 0–2-min linear gradient to 45 % B, 2–10-min linear gradient to 80 % B, then the eluent was brought up to 90 % B and maintained for 10 min.

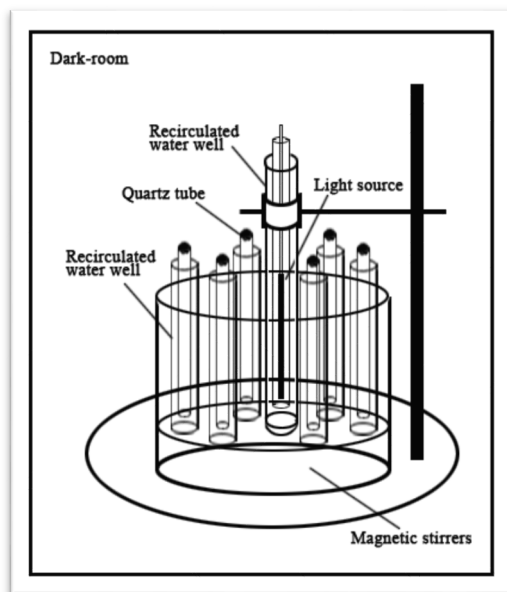


Fig. 2. Rotary photochemical reactor

The PPCPs with a signal-to-noise ratio more than 3 were considered as detectable ones. The average recovery ratios of CBZ, TCS, ¹³C₃-caffeine were 98.15 %, 85.30 %, 97.75 % with, respectively, the relative standard deviations were all less than 3 %, suggesting that the extraction procedure and instrumental analysis method for PPCPs in sampling was reliable. Furthermore, it should be pointed out here that this study used ¹³C₃-caffeine just to assure of the PPCPs extraction protocol, not to quantify other compounds (Chen *et al.*, 2013).

The Degradation Modeling. In this study, a two-dimensional numerical model, Environment Fluid Dynamics Code (EFDC), was applied in the modeling and prediction of the TCS and CBZ in the target area. The EFDC was originally developed by Virginia Institute of Marine Science as authorized by US EPA (Jeong *et al.*, 2010). It solves finite-differenced forms of the hydrostatic Navier-Stokes equations which uses stretched or sigma vertical coordinates and Cartesian or curvilinear orthogonal horizontal coordinates to represent the physical characteristics of a water body (Sucsy and Morris, 2001).

The reach area used for simulation which summing up to a length of 3 km by an orthogonal curvilinear grid. The model grids consist of 264 × 782 cells in the horizontal direction, and the horizontal grid spacing ranged from 1.59 to 6.33 m. The water depth in each grid ranges from 0.51 m to 1.13 m. In the vertical direction, one layer was employed, i.e. horizontal two-dimensional model (Wu and Xu, 2011). The hydrodynamic and mass transportation calculation time steps were both set as 86400 seconds.

After the generalization of the area, a set of input files including initial concentrations and boundary conditions need to be configured to drive the EFDC model. In order to simplify the hydrodynamic model, The boundary conditions such as inflows and the initial concentrations of the water quality factors were setup in efdc.inp file. This study set the drainage of WTP and the only tributary to constant flow. On the premise of no precipitation, the terms of source and convergence of the flow could keep the balance by measured in this area.

RESULT AND DISCUSSION

Occurrence of TCS and CBZ in Effluent and Surface Waters. The two PPCPs, TCS and CBZ were detected in most of samples from the Shahe Steam, the tributary of the Shahe Stream as well as the effluents from the WTP. The concentration of TCS and CBZ descended which was accompanied by the flow direction as a whole. Finally, the concentrations of TCS and TCC in the downstream of the Shahe Stream (S6) were below the detection limits (LOD: 50 ng/L for both compounds). Table. 3 shows concentrations of TCS and CBZ in surface water samples. Values of target compounds ranged from less than 64.38ng/L to 5.45ug/L. Maximum concentrations were measured in the tributary (S4).The WTP was another source of TCS and CBZ in Shahe Stream, the WTP couldn't dispose all of PPCPs in spite of its process had used the membrane filtration treatment technology(Yang *et al.*, 2011), on the contrary, some studies show that CBZ in all cities mainly originated from WTP effluents(Wang *et al.*, 2015). In all sampling site, the concentration of CBZ was much higher than TCS. There are maybe two reasons to explain this phenomenon: The one was that Jingxi Southern Hospital and a medical university were located in the upstream of the tributary. Medical wastewater contains many CBZ which become the main source in Shahe Stream. The other one was that the degradation rate of TCS is far higher than that of CBZ.

Table 3. TCS and CBZ (ug/L) in surface water samples.

	S1	S2	S3	S4	S5	S6
Conc.TCS (ng/L)	290.70	428.51	161.50	411.06	64.28	ND ^a
Conc.CBZ (ng/L)	1348.45	3862.52	4117.79	5454.64	9963.00	3312.24
Temperature (°C)	25.0	25.8	25.5	25.5	25.5	25.1
DO	2.78	2.35	7.37	ND ^a	6.34	8.07

^a ND, not determined, below the limit of detection

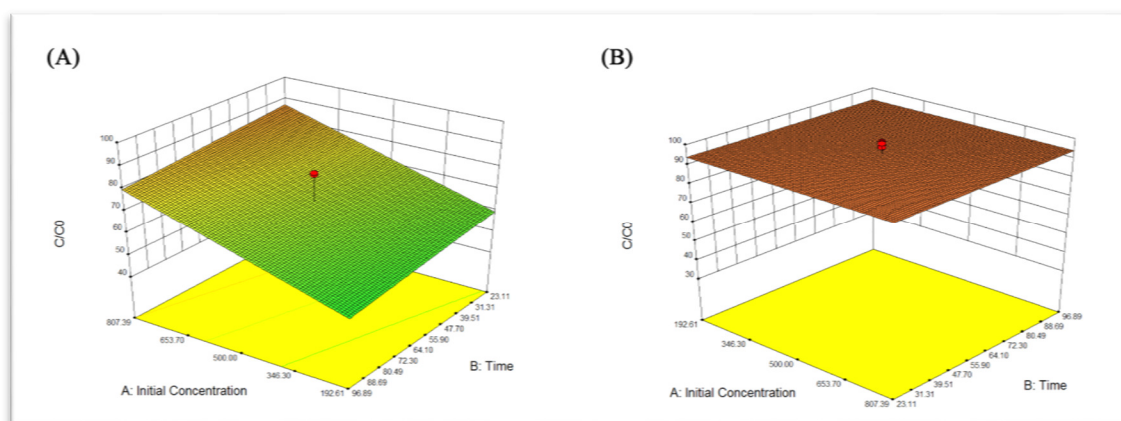


Fig. 3. Hydrolysis of CBZ (A) and TCS (B), as a function of time and a ratio about residual concentration (C) to initial concentration (C0). Other conditions: 22.00°C temperature, 7.00 pH, 4.50mg/L DO, 8.01 Salinity, 15.01mg/L Humic acid.

Hydrolysis, Biodegradation and Photolysis. All statistical analyses were conducted by Design Expert 8 for Windows (Stat-Ease Inc., Minneapolis, USA). The software can set of quadratic polynomial curve, establishing the mathematical model, drawing the response surface.

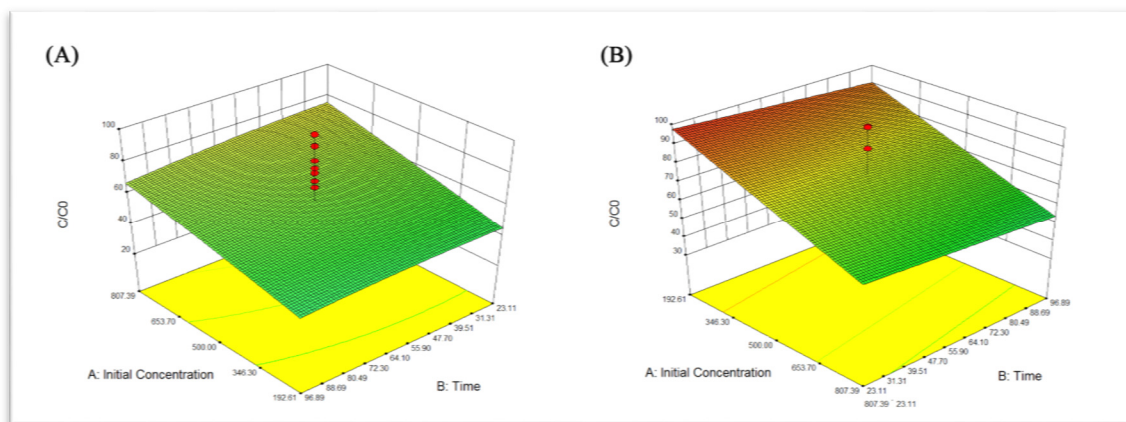


Fig. 4. Biodegradation of CBZ (A) and TCS (B), as a function of time and a ratio about residual concentration (C) to initial concentration (C₀). Other conditions: 22.00°C temperature, 7.00 pH, 4.50mg/L DO, 8.01 Salinity, 15.01mg/L Humic acid.

Hydrolysis. The Hydrolysis of PPCPs mainly electrophilic group of nucleophilic reagent and molecular reaction, and replace a leaving group. Usually, the hydrolysis of organic matter in water is first order reaction. In the process of hydrolysis, pH took the main effect, and temperature also had important influence to hydrolysis. Other factors, like DO, salinity, humic acid, light intensity hadn't find that obvious effects on PPCPs' hydrolysis. Moreover, from Fig. 3 we can find that the initial concentration maybe influences the hydrolysis rate of CBZ but TCS doesn't. Along with the time, the hydrolysis rate of CBZ was falling. Due to the very low Henry's law constant (pK_a) and the resistance against strong bases, we can expect that hydrolysis can be neglected for CBZ and TCS (Tixier *et al.*, 2003). In this study, we also confirmed this view. In the hydrolysis experiment, The hydrolysis of TCS was fewer than 10%, and the hydrolysis of CBZ was negatively correlated with initial concentration, the higher the concentration of CBZ, the less its hydrolysis. Combining with the Shahe Stream, we could also think that the hydrolysis reaction of CBZ was very small in the total degradation process.

Biodegradation. Biodegradation of PPCPs has been extensively studied in wastewater treatment systems (Onesios *et al.*, 2009; Mohapatra *et al.*, 2014; Durán-Álvarez *et al.*, 2015), but the degradation of them are very difficult to determine under natural conditions. From Fig 4, we can find that the initial concentrations can influence the biodegradation rates of CBZ and TCS. During the period of experiment, the concentrations of CBZ and TCS failed to reach half of the initial concentrations, namely the half-life time of biodegradation. Although CBZ and TCS were all biodegradable during the test, but the biodegradation rate of TCS was far less than CBZ could be seen clearly.

Biodegradation conforms to the first-order degradation equation as Eq. (1):

$$C_t = C_0 \cdot e^{-k_b t} \quad (1)$$

where C₀ and C_t are the concentrations of the target pollutants at time 0 and t, respectively; k_b is the first order biodegradation rate constant, and t is the experimental time (in days for biodegradation experiments).

From Fig. 5, although DO, pH and Salinity has influenced to the CBZ biodegradation certainly, but the temperature effect on the biodegradation rate plays a main role. The most suitable temperature for biodegradation of CBZ are between 25-19°C. When the temperature is less than 19°C or over 25°C, it doesn't favor the bacteria growth. So we used the Arrhenius function, Eq. (2):

$$k_b = k_{b20} \cdot \theta^{(T-20)} \quad (2)$$

where k_{b20} is the first order biodegradation rate constant when the temperature is 20°C, T is the water temperature in the reaction (°C), and θ is the temperature correction factor. The k_{b20} of CBZ is obtained by solving that is approximately equal to $1.5443E-2 \text{ d}^{-1}$, and θ is 1.0002; And the k_{b20} of TCS is approximately equal to $1.5397E-2 \text{ d}^{-1}$, and θ is 0.0087.

According to related research, the biodegradation half-life time of CBZ was between 3000 ~ 5600 h in two rivers, because these rivers may contain different microbes, so there will be quite different of the biodegradation rate in different rivers(Kimura *et al.*, 2014). And half-life time was determined by using Eq. (3):

$$t_{1/2} = \frac{\ln 2}{k_b} \quad (3)$$

where $t_{1/2}$ is the half-life time for each compound under the experimental conditions (days), so the half-life times of CBZ and TCS were 43 ± 2 days for CBZ and 45 ± 1 days for TCS..

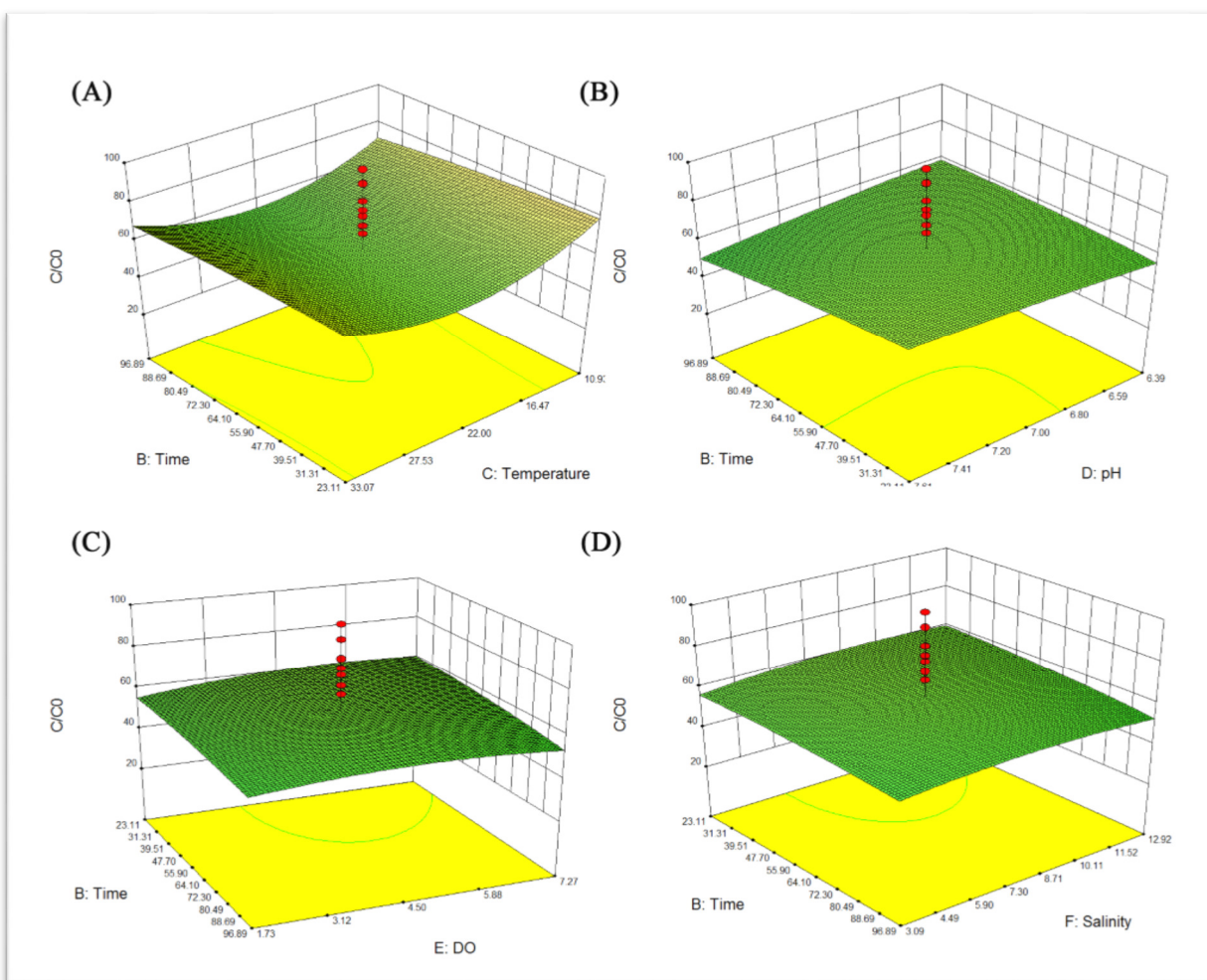


Fig. 5. The parameters effect on biodegradation of CBZ, as a function of time and a ratio about residual concentration (C) to initial concentration (C0). Other conditions: 22.00°C temperature, 7.00 pH, 4.50mg/L DO, 8.01 Salinity, 15.01mg/L Humic acid.

Photolysis. Photolysis reactions can be divided into direct photolysis, indirect photolysis and photosensitivity photolysis. In the literature(Fabbri *et al.*, 2015), the important photochemical parameters

are available (direct photolysis determined by the quantum yields and indirect photolysis involves reactive transients). Moreover, photolysis reactions via direct photolysis is expected to be an important degradation pathway, compared to other processes such as sorption or biological degradation, in the environmental fate of TCS (Bianco *et al.*, 2014). Direct photolysis is determined by the amount of the chemical when quantum yield, as well as photolysis absorption wavelength (Aranami and Readman, 2007; Dann and Hontela, 2011). Indirect photolysis, reactive transients such as reaction rate constants with $\cdot\text{OH}$, CO_3^- and the triplet states of chromophoric dissolved organic matter, $^3\text{CDOM}^*$ (Bianco *et al.*, 2014). In this case, we can see the photolysis of CBZ and TCS happened quickly under the condition of laboratory. Due to the low initial concentrations of the reactants, the difference of the photolysis rates between CBZ and TCS is extremely small, so we think that both of them were mainly indirect photolysis.

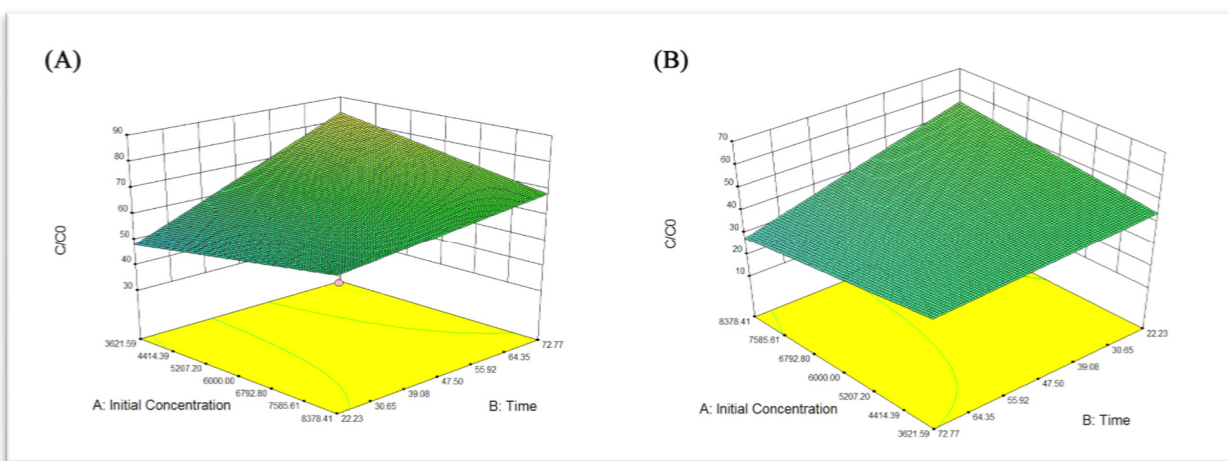


Fig. 6. Photolysis of CBZ (A) and TCS (B), as a function of time and a ratio about residual concentration (C) to initial concentration (C0). Other conditions: 22.00 °C temperature, 7.00 pH, 4.50mg/L DO, 8.01 Salinity, 15.01mg/L Humic acid.

From Fig. 7, we can see that all parameters had effect on photolysis of TCS. For molecules of acid and alkali solution from the group of antibiotics, pH can significantly affect the photochemical reaction (De Laurentiis *et al.*, 2014), TCS degraded more easily under the condition of alkaline because this condition promoted the reaction between humic acid and TCS. DO and humic acid provided active oxygen reactants, however, because of their photoionization, competitive relationship between them and TCS which can inhibit the photolysis of TCS. Salinity had important influence to the photolysis. When the low concentration of salinity could promote the photosensitivity of TCS. However, when the salinity was increased to a certain extent, the chloride ions released that would be inhibit the indirect photolysis of TCS. Worth noting is that temperature showed a negative correlation with the photolysis of TCS, raising the temperature is not good for photolysis of TCS in this study, and the reason is not clear now.

The photolysis also conforms to the first-order degradation equation as Eq. (1), but there are too many factors affecting photolysis rate. In order to simplify the photolysis rate of various factors of influence, we used the Design-Expert software to process the data and use the Quadratic equation for fitting to get the Eq. (4) for CBZ and Eq. (5) for TCS:

$$\begin{aligned}
 C_{\text{CBZ}} = & -5641.03 + 0.439686A + 0.266565B - 31.1352C + 1603.668D + 99.64726E - 6.31369F + 5.263092G - 6.657635312H - \\
 & 0.00029848AB + 0.002879818AC - 0.063961331AD + 0.004627611AE + 0.001724795AF + 0.001317929AG + 9.02243E-07AH + 0.122107505BC - \\
 & 1.720424763BD + 0.304967623BE + 0.078051509BF - \\
 & 0.286997603BG + 0.008100496BH + 0.16302462CD + 0.89250154CE + 0.125101639CF + 0.684069113CG - 0.002023905CH - \\
 & 26.32559608DE + 1.567497878DF - \\
 & 2.644672393DG + 0.428268019DH + 0.291545646EF + 0.755724953EG + 0.100098074EH + 0.199106181FG + 0.025159551FH + 0.037131861GH - \\
 & 4.76803E-06A^2 + 0.138897604B^2 + 0.062492738C^2 - 85.53735285D^2 - 1.837417777E^2 - 1.737470199F^2 - 0.286250728G^2 + 0.002851302H^2 \quad (4)
 \end{aligned}$$

$$C_{TCS} = 4.38 + 0.65A - 2.03B + 3.37C + 0.17D - 1.65E + 3.03F + 2.97G - 1.80H - 0.84AB + 2.90AC - 2.27AD - 3.18AE - 2.95AF - 0.16AG + 4.28AH - 9.26BC - 5.95BD - 0.20BE + 0.34BF - 2.26BG - 4.17BH + 3.94CD + 6.55CE + 6.9C2F + 7.13CG - 3.97CH - 4.60DE + 2.12DF + 1.42DG + 7.49DH + 4.34EF + 0.19EG + 3.60EH + 1.09FG + 10.30FH + 9.92GH - 0.73A^2 + 0.17B^2 - 2.04C^2 - 0.65D^2 + 0.27E^2 + 1.20F^2 - 2.60G^2 + 11.05H^2 - 2.16ACE - 6.62ACF - 7.14ACH - 6.61ADE - 6.89ADF - 0.48ADH - 1.23AEG + 1.72AFG - 3.08AGH - 6.54BCE - 1.19BCF + 3.12BCH + 5.82BDE + 2.64BDF - 8.95BDH + 5.49BEG - 0.25CDE + 2.15CDF - 1.70CDH + 6.23CEF + 4.04CEG \quad (5)$$

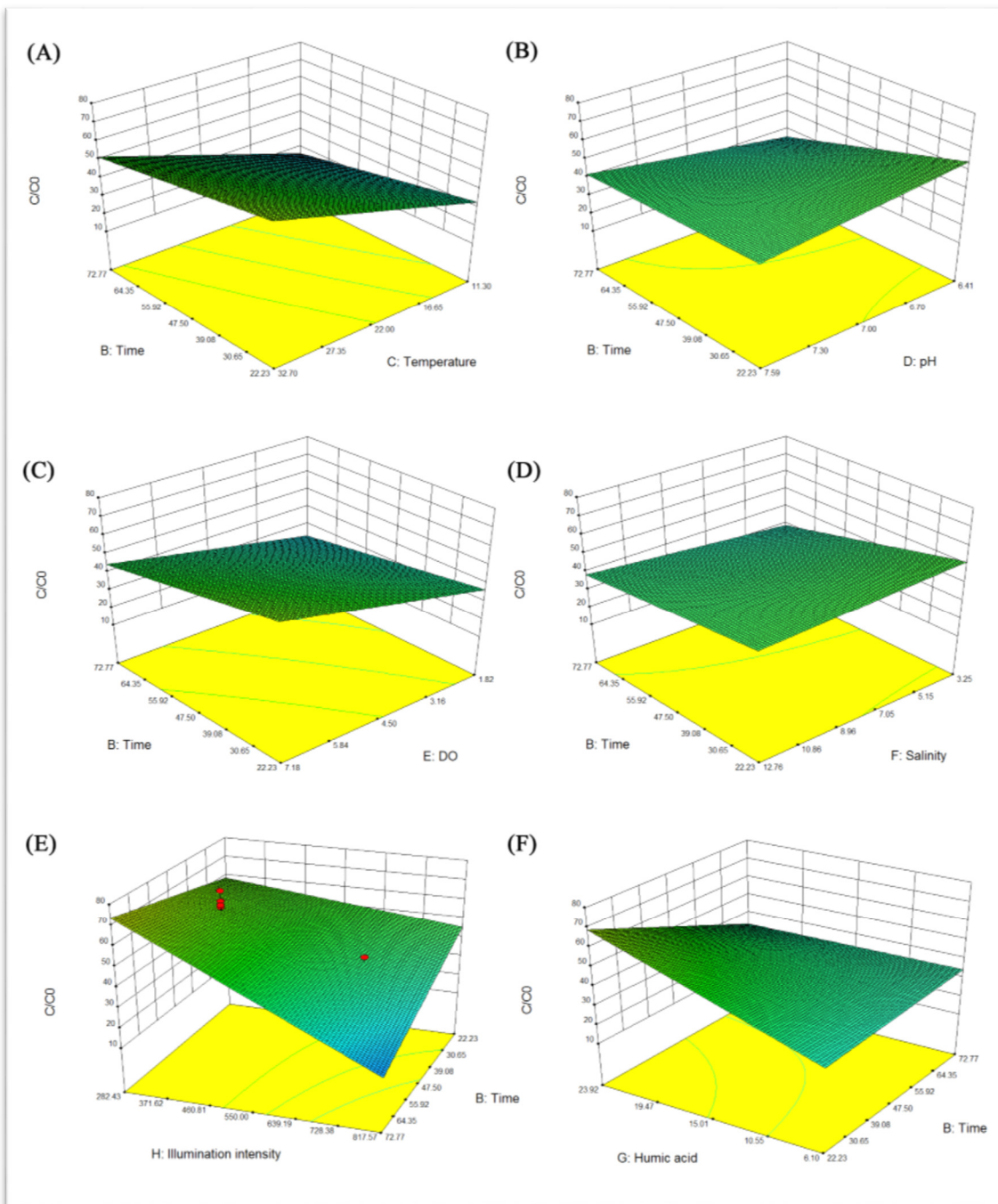


Fig. 7. The parameters effect on photolysis of TCS, as a function of time and a ratio about residual concentration (C) to initial concentration (C0). Other conditions: 22.00°C temperature, 7.00 pH, 4.50mg/L DO, 8.01 Salinity, 15.01mg/L Humic acid.

A, B, C, D, E, F, G, H means the initial concentrations of the pollutions(mg/L), the reaction time (min), water temperature (°C), pH, DO (mg/L), salinity (‰), humic acid (mg/L), light intensity (Lux), respectively.

These equations of the F values were 2.99 and 4.38, the p values were 0.003 and 0.002, it shows that the model is significant. Then, we use the corresponding data with samplings in the above equations, get the corresponding C_{CBZ} and C_{TCS} . Finally, the photolysis rate constant had been solved with Eq. (1), the k_p is the first order photolysis rate constant, the k_p of CBZ is 0.1081 d^{-1} , and the k_p of TCS is $5.9322\text{E-}2 \text{ d}^{-1}$.

Modeling the Targets in Surface Waters. EFDC model was calibrated with sequential trials by modifying hydrodynamic and water quality parameters. Water balance showed good agreement between simulation and daily observation at the Shahe Stream. This stream has special terrain and the boundary condition which is simplified to its hydrodynamic conditions, so we set the Shahe Stream as one-dimensional unsteady flow. The highest water level and lowest water level were initialized at 5.80 m and 8.96 m and steadily fell to 5.36 m and 11.2 m.

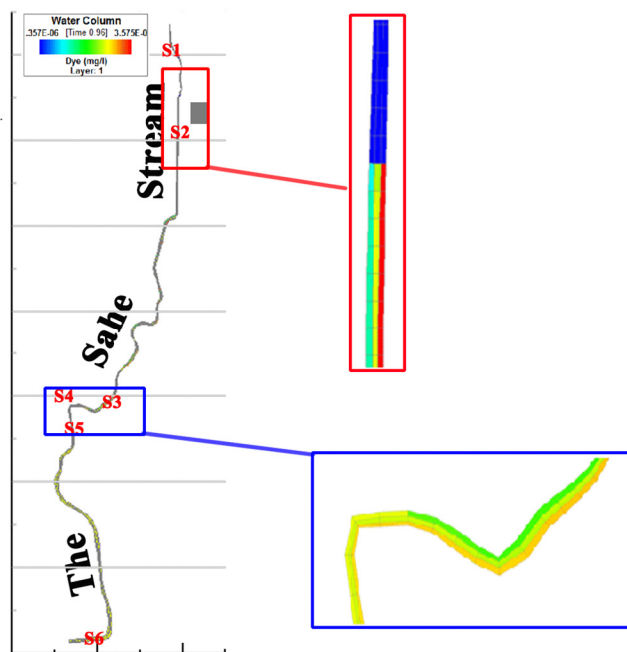


Fig. 8. CBZ in simulation by EFDC

Due to the bottom of the river are the rocks, the study ignored the adsorption and desorption. And the hydrolysis of CBZ and TCS were relatively weak, so the degradation of equation, Eq. (6) is:

$$C_t = C_0 \cdot e^{-kt} = C_0 \cdot e^{-k_b t} + C_0 \cdot e^{-k_p t} \quad (6)$$

The degradation rate constant k was 0.6324 d^{-1} for CBZ and 0.6560 d^{-1} for TCS. Using the Dye module by EFDC, CBZ and TCS were simulated respectively. The time of simulation is the same day at sampling. The relative deviation (RD) of water level simulation was calculated at 23%-52% of TCS, 23%-37% of CBZ indicating good fittings.

CONCLUSIONS

CBZ and TCS undergo hydrolysis, biodegradation and photolysis in surface water. Under the condition of the same nature and the low concentrations of pollutants, degradation of CBZ and TCS are given priority to photolysis since hydrolysis of both types is relatively weak.

To our knowledge, this is the first report of modeling of CBZ and TCS with the degradation mechanism in the surface water. It demonstrates that PPCPs can be modeled and predicted in natural

environment. However, the adsorption and desorption of PPCPs in water-sediment has not been considered because special at the bottom of the Shahe Stream, and failing to consider more water quality parameters. Moreover, the degradation rate of CBZ and TCS in EFDC model was globally set as constant, which is unreasonable as degradation rate is a dynamic coefficient varied across the Shahe Stream. So degradation rate value set as a constant maybe suitable in the Shahe Stream only. The dynamic degradation rate coefficient and the adsorption and desorption of PPCPs in water-sediment should be further investigated around the Shahe Stream in the next step and more studies should be conducted.

ACKNOWLEDGMENTS

This study was financially supported by “Monitoring, prediction and control technology of Pharmaceutical and personal care products (PPCPs) in the surface water and drinking water system” funded by the major cultivation program of Sun Yat-sen university. Authors thank Jia Huang, Hanjie Yang and Dehong Liu for their help during sampling collection and modeling.

REFERENCES

- Aranami, K. and J.W. Readman, 2007. Photolytic degradation of triclosan in freshwater and seawater. *Chemosphere*, 66(6): 1052-1056. Available from <http://www.ncbi.nlm.nih.gov/pubmed/16930676>. DOI 10.1016/j.chemosphere.2006.07.010.
- Batchu, S.R., V.R. Panditi, K.E. O'Shea and P.R. Gardinali, 2013. Photodegradation of antibiotics under simulated solar radiation: Implications for their environmental fate. *Science of the Total Environment*, 470-471C: 299-310. Available from <http://www.ncbi.nlm.nih.gov/pubmed/24144935>. DOI 10.1016/j.scitotenv.2013.09.057.
- Bedoux, G., B. Roig, O. Thomas, V. Dupont and B. Le Bot, 2012. Occurrence and toxicity of antimicrobial triclosan and by-products in the environment. *Environmental Science and Pollution Research*, 19(4): 1044-1065. Available from <http://www.ncbi.nlm.nih.gov/pubmed/22057832>. DOI 10.1007/s11356-011-0632-z.
- Bianco, A., D. Fabbri, M. Minella, M. Brigante, G. Mailhot, V. Maurino, C. Minero and D. Vione, 2014. New insights into the environmental photochemistry of 5-chloro-2-(2,4-dichlorophenoxy)phenol (triclosan): Reconsidering the importance of indirect photoreactions. *Water research*. Available from <http://www.ncbi.nlm.nih.gov/pubmed/25179274>. DOI 10.1016/j.watres.2014.07.036.
- Boyd, G.R., H. Reemtsma, D.A. Grimm and S. Mitra, 2003. Pharmaceuticals and personal care products (ppcps) in surface and treated waters of louisiana, USA and ontario, canada. *Science of the Total Environment*, 311(1-3): 135-149. DOI 10.1016/s0048-9697(03)00138-4.
- Carmona, E., V. Andreu and Y. Pico, 2014. Occurrence of acidic pharmaceuticals and personal care products in turia river basin: From waste to drinking water. *Science of the Total Environment*, 484: 53-63. Available from <http://www.ncbi.nlm.nih.gov/pubmed/24686145>. DOI 10.1016/j.scitotenv.2014.02.085.
- Chen, Y.S., S. Yu, Y.W. Hong, Q.Y. Lin and H.B. Li, 2013. Pharmaceutical residues in tidal surface sediments of three rivers in southeastern china at detectable and measurable levels. *Environmental Science and Pollution Research*, 20(12): 8391-8403. Available from <http://www.ncbi.nlm.nih.gov/pubmed/23764981>. DOI 10.1007/s11356-013-1871-y.
- Clara, M., B. Strenn and N. Kreuzinger, 2004. Carbamazepine as a possible anthropogenic marker in the aquatic environment: Investigations on the behaviour of carbamazepine in wastewater treatment and during groundwater infiltration. *Water research*, 38(4): 947-954. Available from <http://www.ncbi.nlm.nih.gov/pubmed/14769414>. DOI 10.1016/j.watres.2003.10.058.
- Daghrir, R., A. Dimboukou-Mpira, B. Seyhi and P. Drogui, 2014. Photosonochemical degradation of butylparaben: Optimization, toxicity and kinetic studies. *Science of the Total Environment*, 490: 223-234.

- Available from <http://www.ncbi.nlm.nih.gov/pubmed/24858220>. DOI 10.1016/j.scitotenv.2014.05.006.
- Dann, A.B. and A. Hontela, 2011. Triclosan: Environmental exposure, toxicity and mechanisms of action. *Journal of Applied Toxicology*, 31(4): 285-311. Available from <http://www.ncbi.nlm.nih.gov/pubmed/21462230>. DOI 10.1002/jat.1660.
- Daughton, C.G. and T.A. Ternes, 1999. Pharmaceuticals and personal care products in the environment: Agents of subtle change? *Environmental Health Perspectives*, 109(Suppl 6): 907-938.
- De Laurentiis, E., C. Prasse, T.A. Ternes, M. Minella, V. Maurino, C. Minero, M. Sarakha, M. Brigante and D. Vione, 2014. Assessing the photochemical transformation pathways of acetaminophen relevant to surface waters: Transformation kinetics, intermediates, and modelling. *Water research*, 53: 235-248. Available from <http://www.ncbi.nlm.nih.gov/pubmed/24525071>. DOI 10.1016/j.watres.2014.01.016.
- Deo, R.P., 2014. Pharmaceuticals in the surface water of the USA: A review. *Current Environmental Health Reports*, 1(2): 113-122. DOI 10.1007/s40572-014-0015-y.
- Durán-Álvarez, J.C., B. Prado, D. González, Y. Sánchez and B. Jiménez-Cisneros, 2015. Environmental fate of naproxen, carbamazepine and triclosan in wastewater, surface water and wastewater irrigated soil — results of laboratory scale experiments. *Science of The Total Environment*, 538: 350-362. Available from <http://www.sciencedirect.com/science/article/pii/S0048969715305313>. DOI <http://dx.doi.org/10.1016/j.scitotenv.2015.08.028>.
- Fabbri, D., M. Minella, V. Maurino, C. Minero and D. Vione, 2015. Photochemical transformation of phenylurea herbicides in surface waters: A model assessment of persistence, and implications for the possible generation of hazardous intermediates. *Chemosphere*, 119(0): 601-607. Available from <http://www.sciencedirect.com/science/article/pii/S0045653514008959>. DOI <http://dx.doi.org/10.1016/j.chemosphere.2014.07.034>.
- Jeong, S., K. Yeon, Y. Hur and K. Oh, 2010. Salinity intrusion characteristics analysis using efdc model in the downstream of geum river. *Journal of Environmental Sciences*, 22(6): 934-939. Available from <http://www.sciencedirect.com/science/article/pii/S1001074209602011>. DOI [http://dx.doi.org/10.1016/S1001-0742\(09\)60201-1](http://dx.doi.org/10.1016/S1001-0742(09)60201-1).
- Kimura, K., Y. Kameda, H. Yamamoto, N. Nakada, I. Tamura, M. Miyazaki and S. Masunaga, 2014. Occurrence of preservatives and antimicrobials in japanese rivers. *Chemosphere*, 107: 393-399. Available from <http://www.ncbi.nlm.nih.gov/pubmed/24556546>. DOI 10.1016/j.chemosphere.2014.01.008.
- Kosma, C.I., D.A. Lambropoulou and T.A. Albanis, 2014. Investigation of ppcps in wastewater treatment plants in greece: Occurrence, removal and environmental risk assessment. *Science of the Total Environment*, 466-467: 421-438. Available from <http://www.ncbi.nlm.nih.gov/pubmed/23933429>. DOI 10.1016/j.scitotenv.2013.07.044.
- Kuroda, K., M. Murakami, K. Oguma, Y. Muramatsu, H. Takada and S. Takizawa, 2012. Assessment of groundwater pollution in tokyo using ppcps as sewage markers. *Environmental science & technology*, 46(3): 1455-1464. Available from <http://dx.doi.org/10.1021/es202059g>. DOI 10.1021/es202059g.
- Luo, Y., L. Xu, M. Rysz, Y. Wang, H. Zhang and P.J. Alvarez, 2011. Occurrence and transport of tetracycline, sulfonamide, quinolone, and macrolide antibiotics in the haihe river basin, china. *Environmental science & technology*, 45(5): 1827-1833. Available from <http://www.ncbi.nlm.nih.gov/pubmed/21309601>. DOI 10.1021/es104009s.
- Ma, D., G. Liu, W. Lv, K. Yao, X. Zhang and H. Xiao, 2014. Photodegradation of naproxen in water under simulated solar radiation: Mechanism, kinetics, and toxicity variation. *Environmental Science and Pollution Research*, 21(13): 7797-7804. Available from <http://www.ncbi.nlm.nih.gov/pubmed/24638836>. DOI 10.1007/s11356-014-2721-2.
- Mohapatra, D.P., S.K. Brar, R.D. Tyagi, P. Picard and R.Y. Surampalli, 2014. Analysis and advanced oxidation treatment of a persistent pharmaceutical compound in wastewater and wastewater sludge-carbamazepine. *Science of the Total Environment*, 470-471: 58-75. Available from <http://www.ncbi.nlm.nih.gov/pubmed/24140682>. DOI 10.1016/j.scitotenv.2013.09.034.

- Onesios, K.M., J.T. Yu and E.J. Bouwer, 2009. Biodegradation and removal of pharmaceuticals and personal care products in treatment systems: A review. *Biodegradation*, 20(4): 441-466. Available from <http://www.ncbi.nlm.nih.gov/pubmed/19112598>. DOI 10.1007/s10532-008-9237-8.
- Ortiz de Garcia, S., G. Pinto Pinto, P. Garcia Encina and R. Irusta Mata, 2013. Consumption and occurrence of pharmaceutical and personal care products in the aquatic environment in Spain. *Science of the Total Environment*, 444: 451-465. Available from <http://www.ncbi.nlm.nih.gov/pubmed/23287535>. DOI 10.1016/j.scitotenv.2012.11.057.
- Pal, A., K.Y. Gin, A.Y. Lin and M. Reinhard, 2010. Impacts of emerging organic contaminants on freshwater resources: Review of recent occurrences, sources, fate and effects. *Science of the Total Environment*, 408(24): 6062-6069. Available from <http://www.ncbi.nlm.nih.gov/pubmed/20934204>. DOI 10.1016/j.scitotenv.2010.09.026.
- Peng, X., C. Wang, K. Zhang, Z. Wang, Q. Huang, Y. Yu and W. Ou, 2014. Profile and behavior of antiviral drugs in aquatic environments of the Pearl River Delta, China. *Science of the Total Environment*, 466-467: 755-761. Available from <http://www.ncbi.nlm.nih.gov/pubmed/23973541>. DOI 10.1016/j.scitotenv.2013.07.062.
- Peng, X., Y. Yu, C. Tang, J. Tan, Q. Huang and Z. Wang, 2008. Occurrence of steroid estrogens, endocrine-disrupting phenols, and acid pharmaceutical residues in urban riverine water of the Pearl River Delta, South China. *Science of the Total Environment*, 397(1-3): 158-166. Available from <http://www.ncbi.nlm.nih.gov/pubmed/18407320>. DOI 10.1016/j.scitotenv.2008.02.059.
- Petrovic, M., B. Skrbic, J. Zivancev, L. Ferrando-Climent and D. Barcelo, 2014. Determination of 81 pharmaceutical drugs by high performance liquid chromatography coupled to mass spectrometry with hybrid triple quadrupole-linear ion trap in different types of water in Serbia. *Science of the Total Environment*, 468-469: 415-428. Available from <http://www.ncbi.nlm.nih.gov/pubmed/24055661>. DOI 10.1016/j.scitotenv.2013.08.079.
- Richardson, B.J., P.K. Lam and M. Martin, 2005. Emerging chemicals of concern: Pharmaceuticals and personal care products (PPCPs) in Asia, with particular reference to Southern China. *Marine Pollution Bulletin*, 50(9): 913-920. Available from <http://www.ncbi.nlm.nih.gov/pubmed/16038943>. DOI 10.1016/j.marpolbul.2005.06.034.
- Stackelberg, P.E., J. Gibs, E.T. Furlong, M.T. Meyer, S.D. Zaugg and R.L. Lippincott, 2007. Efficiency of conventional drinking-water-treatment processes in removal of pharmaceuticals and other organic compounds. *Science of the Total Environment*, 377(2-3): 255-272. Available from <http://www.ncbi.nlm.nih.gov/pubmed/17363035>. DOI 10.1016/j.scitotenv.2007.01.095.
- Sucsy, P.V. and F.W. Morris, 2001. Salinity intrusion in the St. Johns River, Florida. *ML Spaulding* (ed.), ASCE, pp: 120-139.
- Tixier, C., H.P. Singer, S. Oellers and S.R. Müller, 2003. Occurrence and fate of carbamazepine, clofibric acid, diclofenac, ibuprofen, ketoprofen, and naproxen in surface waters. *Environmental Science & Technology*, 37(6): 1061-1068.
- Wang, Z., X.-H. Zhang, Y. Huang and H. Wang, 2015. Comprehensive evaluation of pharmaceuticals and personal care products (PPCPs) in typical highly urbanized regions across China. *Environmental Pollution*, 204: 223-232. Available from <http://www.sciencedirect.com/science/article/pii/S0269749115002109>. DOI <http://dx.doi.org/10.1016/j.envpol.2015.04.021>.
- Wu, C., X. Huang, J.D. Witter, A.L. Spongberg, K. Wang, D. Wang and J. Liu, 2014. Occurrence of pharmaceuticals and personal care products and associated environmental risks in the central and lower Yangtze River, China. *Ecotoxicology and Environmental Safety*, 106: 19-26. Available from <http://www.ncbi.nlm.nih.gov/pubmed/24836873>. DOI 10.1016/j.ecoenv.2014.04.029.
- Wu, G. and Z. Xu, 2011. Prediction of algal blooming using EFD model: Case study in the Daoxiang Lake. *Ecological Modelling*, 222(6): 1245-1252. Available from <http://www.sciencedirect.com/science/article/pii/S0304380011000020>. DOI <http://dx.doi.org/10.1016/j.ecolmodel.2010.12.021>.

- Wu, J.-L., N.P. Lam, D. Martens, A. Kettrup and Z. Cai, 2007. Triclosan determination in water related to wastewater treatment. *Talanta*, 72(5): 1650-1654. Available from <http://www.sciencedirect.com/science/article/pii/S0039914007002135>. DOI <http://dx.doi.org/10.1016/j.talanta.2007.03.024>.
- Xu, W.H., G. Zhang, S.C. Zou, X.D. Li and Y.C. Liu, 2007. Determination of selected antibiotics in the victoria harbour and the pearl river, south china using high-performance liquid chromatography-electrospray ionization tandem mass spectrometry. *Environmental pollution*, 145(3): 672-679. Available from <http://www.ncbi.nlm.nih.gov/pubmed/16996177>. DOI 10.1016/j.envpol.2006.05.038.
- Yang, X., F. Chen, F. Meng, Y. Xie, H. Chen, K. Young, W. Luo, T. Ye and W. Fu, 2013. Occurrence and fate of ppcps and correlations with water quality parameters in urban riverine waters of the pearl river delta, south china. *Environmental Science and Pollution Research*, 20(8): 5864-5875. Available from <http://www.ncbi.nlm.nih.gov/pubmed/23608973>. DOI 10.1007/s11356-013-1641-x.
- Yang, X., R.C. Flowers, H.S. Weinberg and P.C. Singer, 2011. Occurrence and removal of pharmaceuticals and personal care products (ppcps) in an advanced wastewater reclamation plant. *Water research*, 45(16): 5218-5228. Available from <http://www.ncbi.nlm.nih.gov/pubmed/21864879>. DOI 10.1016/j.watres.2011.07.026.
- Yoon, Y., J. Ryu, J. Oh, B.G. Choi and S.A. Snyder, 2010. Occurrence of endocrine disrupting compounds, pharmaceuticals, and personal care products in the han river (seoul, south korea). *Science of the Total Environment*, 408(3): 636-643. Available from <http://www.ncbi.nlm.nih.gov/pubmed/19900699>. DOI 10.1016/j.scitotenv.2009.10.049.
- Zhang, Y., S.-U. Geißen and C. Gal, 2008. Carbamazepine and diclofenac: Removal in wastewater treatment plants and occurrence in water bodies. *Chemosphere*, 73(8): 1151-1161. Available from <http://www.sciencedirect.com/science/article/pii/S004565350800996X>. DOI <http://dx.doi.org/10.1016/j.chemosphere.2008.07.086>.
- Zhao, J.L., G.G. Ying, Y.S. Liu, F. Chen, J.F. Yang, L. Wang, X.B. Yang, J.L. Stauber and M.S. Warne, 2010. Occurrence and a screening-level risk assessment of human pharmaceuticals in the pearl river system, south china. *Environmental Toxicology and Chemistry*, 29(6): 1377-1384. Available from <http://www.ncbi.nlm.nih.gov/pubmed/20821582>. DOI 10.1002/etc.161.

SPACE/TIME GEOSTATISTICAL ESTIMATION OF CHLORIDE ALONG MARYLAND RIVERS USING A COVARIANCE MODEL WITH RIVER DISTANCES

Prahlad Jat, Marc L Serre
(University of North Carolina at Chapel Hill, NC, USA)

Chloride, which is widely used for road deicing, is an emerging pollutant that is causing substantial increases in the salinity of the Nation's ground and surface waters and is threatening our aquatic environment. In this work we use chloride monitoring data collected in Maryland to estimate its concentration along all river miles of three sub basins (Gunpowder-Patapsco, Severn and Patuxent) from 2005 to 2014.

A previous study on Dissolved Oxygen Carbon (DOC) using the Maryland Biological Stream Survey (MBSS) data collected in Maryland in 1996 found that DOC geostatistical estimates obtained using a covariance model based on Euclidean distances are more accurate than estimates obtained using a flow-weighted (weighted asymmetric hydrologic distance) covariance model. However, that study did not report results for a covariance model based on river distances (distances measured along river network), unlike several subsequent studies which proposed and used covariance models based on river distances to study water quality along river networks.

We queried the MBSS database for all chloride measurements from 2005 to 2014 in our study area, which resulted in a dataset of 390 space/time chloride values. Using this dataset we performed a geostatistical analysis using a covariance with an Euclidean or river metric, and we compared their accuracy based on a leave one out cross validation. We found that the R^2 between measured and estimated values was 0.72 when using the river distance, compared to 0.65 when using an Euclidean distance. This work is the first to demonstrate that the river distance covariance model is better than the Euclidean distance covariance model for the geostatistical estimation of chloride in stream waters of three sub basins in Maryland. This finding indicates that processes that are distributed along river networks such as highways (a known source of chloride), and vegetation buffers (a known attenuation factor), are important drivers of the distribution of chloride along rivers. The implication of this finding are that (1) the river covariance model should be used in place of the Euclidean covariance model whenever modeling chloride concentration in these sub basins, and (2) the areas of impaired water identified using the river covariance model are confined along the river branches, which are easier to target for remedial purposes than areas spreading across multiple parallel branches.

A limitation of this work is that the river distance was only used for the covariance model. Our results suggest that the use of river distances should be expanded to other aspect of space/time modeling, such as mean trend modeling or spatial regression.

MODELING OF SPREADING OF SUBMARINE MINE TAILINGS IN A NORWEGIAN FJORD

Øyvind Leikvin¹, **Venkat Kolluru**², Guttorm N. Christensen¹, Magdalena Kempa³, Torulv Tjomsland³
(¹Akvaplan-niva AS, Tromsø, Norway; ²Environmental Resources Management, Inc., Philadelphia, USA;
³Norwegian Institute of Water Research (NIVA), Oslo, Norway)

Four different submarine disposal sites in Repparfjorden situated by the town of Kvalsund, Norway, were assessed for the suitability as dumping ground for the disposal of fine tailings from the beneficiation of ores in Wolf Ridge and Nussir, operated by a confidential client. The area northeast of Fæg fjordholmen is the only one that has a large enough volume of water with low bottom currents that was found appropriate, and thus impacts were assessed through consequence modeling for compliance with the Norwegian and OSPAR environmental regulations. Simulations of the spread of tailings were made with a 3-D hydrodynamic, water quality and sediment transport model called GEMSS. The model was calibrated to available ADCP measurements. The model was then used to evaluate the tailings depositional footprint at the bottom of the fjord and total suspended sediment concentrations (TSS) in the water column. The calibrated model was used to run many different scenarios to find the best possible location for the release of tailings through an outfall pipe. It was found that it was necessary to have a relatively deep discharge point (> 50 meters) to the north of Markoppneset, in order to get the tailings to be deposited within the prescribed fjord bed area. An area of 2.4 km² got more than 10 cm footprint thickness, while an area of 7.4 km² got more than 1 mm thickness. The flocculated tailings deposited mainly on the bottom, while only 2% were suspended in the water column. Though the near-field turbidity due to TSS was very high, the far-field region showed a small increase of turbidity in the water column that is comparable to background values measured in the fjord. The copper content in the tailings was designated with chemical status class V (very bad). The pore water concentrations in the modeled tailings footprint were similarly high in the same chemical status class, as calculated by the equilibrium constants. Ecotoxicological tests showed that the tailings had potentially toxic effects on marine organisms, but it was found a NOEC (no-observable-effect-concentration) of 32% tailings. The natural sedimentation in the fjord will eventually dilute the tailings within a few years after cessation of the deposit.

**GIS, DATABASE,
AND
REMOTE SENSING APPLICATIONS**

ESTIMATION OF CROP COEFFICIENTS USING REMOTE SENSING AND GIS: A CASE STUDY OF KHUSKERA-BHIWARI NEEMRANA INVESTMENT REGION, RAJASTHAN, INDIA

Rohit Goyal, Kuldeep Tiwari, and Priyamitra Munoth
(Malaviya National Institute Of Technology Jaipur, Jaipur, Rajasthan, India)

ABSTRACT: Satellite data based estimation of crop coefficient (K_c) is one of the widely accepted methods for irrigation water management for large and/or inaccessible areas. Similarities between the crop coefficient curve and a satellite-derived vegetation index showed potential for modelling the crop coefficient as a function of the vegetation index. Therefore, in this paper the possibility of directly estimating the crop coefficient from moderate resolution satellite reflectance of crops of Rabi (winter) season has been investigated. Two different approaches, single (K_{c_single}) and dual (K_{c_dual}) crop coefficients have been used and are compared with standard curves from FAO. In present work, NDVI data from MODIS (MOD13Q1) sensor on-board Aqua/Terra satellite has been used to estimate both single and dual crop coefficient at the cell level for agriculture area of the study area. This study is conducted using data of Rabi (winter) season for climate conditions in the Khuskera-Bhiwari Neemrana Investment Region, located in Rajasthan, India. Land-use in around 70% of the study area is agriculture. Major crops grown in this area for Kharif season are Beans (Gwoar) and Millet and for Rabi season Wheat and Mustard. K_c values have been estimated for wheat and mustard crops at 16 days interval. Comparison of these two different approaches with standard curve shows that dual crop coefficient approach is more accurate for the estimation of K_c values.

INTRODUCTION

Knowledge of crop water requirements is an important practical consideration for designing and managing irrigation systems (Mohan and Arumugam 1994; Kashyap and Panda 2001; Dhotre *et al.*, 2015). The water requirement varies widely from crop to crop and also during the period of growth of individual crops. Thus estimation of crop water demand considering the cropping pattern is an area of research, which has attracted the attention of water resources planners and engineers. In India, agriculture accounts for about 85% of total annual groundwater draft. Also it fulfills about 60% irrigation and 80% drinking water requirements (Kushwaha and Goyal, 2016). The crop coefficient (K_c) represents crop specific water use and is essential for accurate estimation of irrigation requirement of different crops in the any area (Tyagi *et al.*, 2000). Crop coefficients are properties of plants used in predicting evapotranspiration (ET). The most basic crop coefficient, K_c , is simply the ratio of ET observed for the crop studied over that observed for the well calibrated reference crop under the same conditions (Wikipedia, 2016). The crop coefficient can be calculated by using FAO-56 approach, which is based on the concepts of combining reference evapotranspiration ET_0 and crop coefficients (K_c). There are two methods used to estimate crop evapotranspiration from remote sensing data: the single and the dual crop coefficients. In the single crop coefficient (K_{c_single}), the effect of crop transpiration and soil evaporation are combined into a single K_c (Kamble *et al.*, 2013). The dual crop coefficient consists of two coefficients: a basal crop coefficient (K_{cb}) and a soil evaporation coefficient (K_e) (Er-Raki *et al.*, 2007). The crop coefficient values have been calculated by both approaches in this paper. MODIS vegetation indices like Normalized Difference Vegetation Index (NDVI) and Enhanced Vegetation Index (EVI) data are widely used for vegetation and crop study (Sharma *et al.*, 2016). NDVI can be used as an indicative parameter for vegetation density (Singhal and Goyal, 2012). Several studies have been specifically dedicated for estimating K_c from vegetation indices (VI). Er-Raki *et al.*, (2007) tested three methods based on the FAO-56 “dual” crop

coefficient approach to estimate actual evapotranspiration (AET) for winter wheat under different irrigation treatments in the semi-arid region. The three methods differ in the calculation of the basal crop coefficient (K_{cb}) and the fraction of soil surface covered by vegetation (f_c). The first approach strictly follows the FAO-56 procedure, with K_{cb} given in the FAO-56 tables and f_c calculated from K_{cb} (No-Calibration method). The second method uses local K_{cb} and f_c values estimated from field measurements (Local-Calibration method) and the last approach used a remotely-sensed vegetation index to estimate K_{cb} and f_c (NDVI-Calibration method). The results showed that there exists a good potential for modeling K_{cb} from NDVI values. Rafn *et al.* (2008) estimated the evapotranspiration parameter K_c or K_{cb} using readily available satellite-derived NDVI values. Results from a case study in Idaho for irrigated agriculture indicated that the NDVI/ K_c method has significant potential to estimate K_c because it is comparably fast, easy, and less costly to apply, and does not require images from the thermal band. Pakhale *et al.* (2010) calculated the irrigation water requirement of wheat crop for Rabi season from 1999 to 2003 in Karnal district of Haryana state, India. Area under wheat cultivation was determined using Landsat ETM+ image by applying Artificial Neural Network (ANN) classification technique. Potential Evapotranspiration and crop coefficient for wheat was used for estimating crop water requirement. Kamble *et al.*, (2013) developed a linear regression model between NDVI and the K_{c_single} from a moderate resolution satellite data (MODIS). They showed the correlation between the NDVI-estimated K_{c_single} and the measured K_{c_single} with an R^2 of 0.91 and 0.90, while the root-mean-square error (RMSE) for K_{c_single} were 0.16 and 0.19, respectively. Development of daily crop coefficients and their seasonal variability have not been studied for major crops under tropical climatic conditions. Thus, the present study was undertaken with the objective of deriving the crop coefficients for major crops using remote sensing data. The objective of this study was to investigate the applicability of time-series MODIS 250m NDVI data to the development of spatially representative K_c .

STUDY AREA

The study area selected for present study is Khushkheda-Bhiwadi-Neemrana Investment Region (KBNIR), located in the Alwar district, Rajasthan state, India (Fig. 1). The study area is situated in North-East of Rajasthan between 27°54'33" N and 28°03'20" North latitudes and 76°24'06" E and 76°35'40" East longitudes covering a geographical area of about 162.4 km². The climate of the KBNIR area is semi-arid and very hot in summer and extremely cold in winter. The maximum temperature of the region has been 48°C and the minimum is up to freezing point. Average annual temperature is 26°C. The average annual rainfall is 588.7 mm. The major crops grown in this area in Rabi (winter) season are wheat and mustard and in Kharif (summer) season are barley and beans.

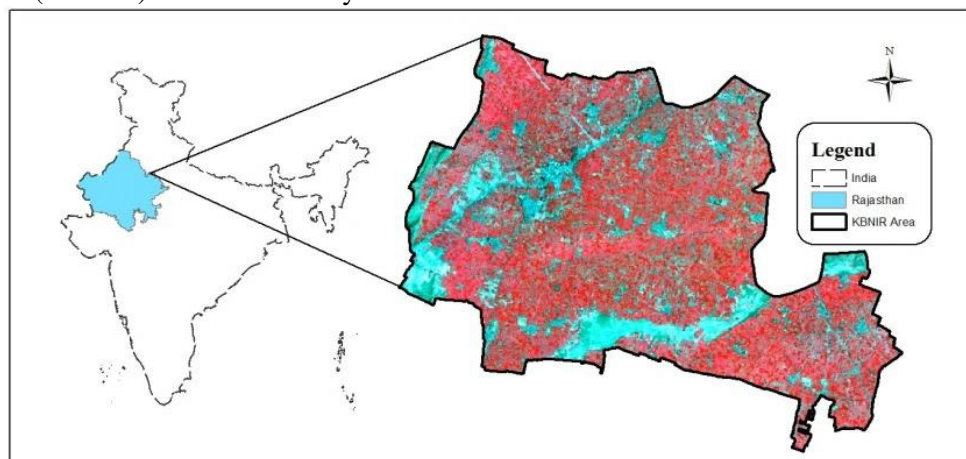


FIGURE 1. Study area (KBNIR) map

METHODOLOGY

The data used for this study includes NDVI images of MOD13Q1 from MODIS sensor on-board Aqua/Terra satellite spanning from 16th Sept. 2014 to 23rd April 2015. The MODIS instrument offers possibilities for large-area crop mapping by providing a daily global coverage of high-quality, intermediate resolution (250 m) data. MOD13Q1 images were downloaded from the National Aeronautic and Space Administration (NASA) Land Process Distributed Active Archive Centre (LP DAAC, 2016) for the study area. The NDVI utilizes reflectance of the canopy in the near-infrared (NIR) and red (R) bands of the spectrum. The value of NDVI ranges theoretically from -1 to +1 but practically from approximately -0.2 to 0.7. This vegetation index is given by:

$$NDVI = \frac{NIR-R}{NIR+R} \quad (1)$$

Where NIR is the reflectance in near infrared band and R is the reflectance in the red band. In this study two modals developed by Er-Raki *et al.*, (2007), which gives the values of dual crop coefficient ($K_{c_dual} = K_{cb} + K_e$) and Kamble *et al.*, (2013), which gives the value of single crop coefficient (K_c) are used. According to Er-Raki *et al.*, (2007) the main plant parameters needed to calculate the dual crop coefficient (K_c) is the values of basal crop coefficient (K_{cb}) at three crop growth stages (initial, mid-season and maturity respectively), the soil evaporation coefficient (K_e) and the height of vegetation (f_c). The detail equations of all these parameters are given below. The K_{cb} can be defined as follows:

$$K_{cb} = 1.07 \times \left[1 - \left(\frac{NDVI_{max} - NDVI}{NDVI_{max} - NDVI_{min}} \right)^{\frac{0.84}{0.54}} \right] \quad (2)$$

Where $NDVI_{min}$ and $NDVI_{max}$ are the minimum and maximum values of the NDVI associated with bare soil and dense vegetation, respectively. The soil evaporation coefficient (K_e) and the height of vegetation (f_c) is given as follows:

$$K_e = 0.25 * (1 - f_c) \quad (3)$$

$$f_c = 1.18 * (NDVI - NDVI_{min}) \quad (4)$$

The equation (3) shows that K_e decreases with the development of crop (As ground cover fraction increase, f_c will increase) and becomes negligible when the crop is well developed and completely covers the soil i.e. at (f_c) = 1

Kamble *et al.* (2012) developed a simple linear regression model to establish a general relationship between a NDVI from a moderate resolution satellite data (MODIS) and the single crop coefficient (K_c), which is given as:

$$K_{c_single} = 1.457 NDVI - 0.1725 \quad (5)$$

The K_c values are calculated for wheat and mustard crops for Rabi (winter) season for particular date of the year based on the phenological cycle of the respective crops, when NDVI values were available.

RESULTS AND DISCUSSIONS

MODIS data is re-projected from the sinusoidal (SIN) projection to the standard UTM projection and resampled to spatial resolution (23.5 m) with the available LULC map created by LISS-III sensors to identify agriculture and non-agriculture area. Before applying the FAO dual approach for each pixel, the images were masked to keep only wheat, mustard and other crops fields. Re-classification method was applied to the 16-days NDVI time series to produce the crop. As vegetation types can be characterized using their seasonal (or phonological) variations in the NDVI time series (Mingwei *et al.*, 2008) so wheat and mustard crops were delineated by examining NDVI temporal profiles from the crop growing season. The crop calendar for Rabi (winter) season is given below in Fig. 2. The mustard crop is sown in September and harvested in March while the wheat crop is sown in October and harvested in April as shown in Fig. 2.

Crop	Sep 14	Oct 14	Nov 14	Dec 14	Jan 15	Feb 15	Mar 15	Apr 15
Wheat								
Mustard								

	Harvest
--	---------

FIGURE 2. Crop calendar of Rabi (winter) season of India.

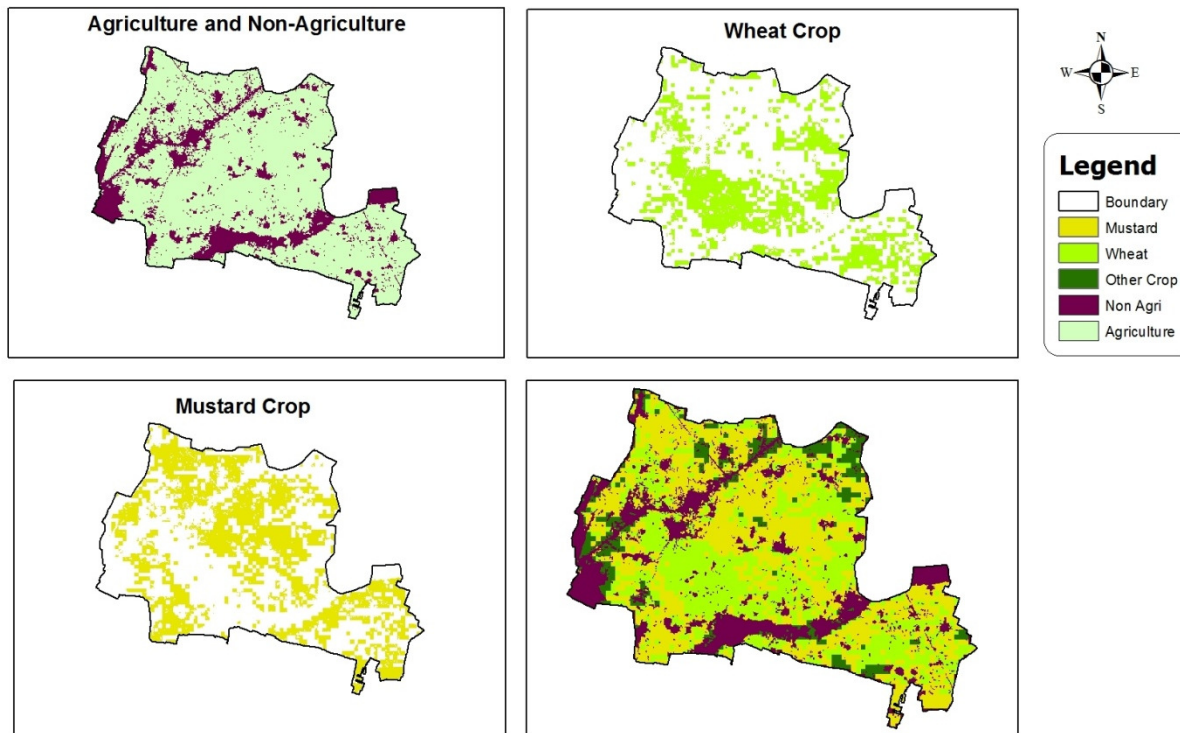


FIGURE 3. Distribution of wheat and mustard in KBNIR area in 2014-15.

A crop classification map was generated using GIS tools as shown in Fig. 3. The area identified for mustard crop was 55%, for wheat crop 39% and for other crops, it was 6%. There was little difference between the crop area estimated by the MODIS data and the statistics already available from Agriculture department, government of Rajasthan.

As mentioned above, both K_c single and dual were derived by using equations 2 to 5. The date wise K_c values of wheat and mustard are listed in table 1.

The crop coefficient (K_c) for a crop varies throughout the growing season, and its full value will not only depend on the crop development stage but also on the sowing date and climatic conditions. The variation in crop coefficient values for wheat crop at various growth stages estimated by different methods and standard value by FAO, are given in Fig. 4. There is a constantly increasing trend in K_{c_dual} and K_{c_single} during the crop development growth stage beginning from 16/10/14 to 18/02/15. The peak value of K_{c_dual} around 1.12 is reached in mid-February while 0.88 for K_{c_single} in the beginning of February. During the development stage good correlation were found between K_{c_dual} and K_{c_FAO} as shown in Fig. 4. The K_{c_dual} declined rapidly to 0.488 and K_{c_single} to 0.196 during the last crop growth stage covering the period from 28/02/15 to 14/04/15. It is observed that K_{c_dual} values are in general 0.35 more than K_{c_single} for wheat crop.

The estimated K_{c_FAO} values of wheat by the FAO method during initial, crop development and reproductive stages are 0.3, 1.15 and 0.3.

TABLE 1: NDVI and K_c values for wheat and mustard crops

Date	Day of Year	Wheat Crop			Mustard Crop		
		NDVI	K_{c_dual}	K_{c_single}	NDVI	K_{c_dual}	K_{c_single}
16-10-2014	289	0.2537	0.6959	0.1971	0.3288	0.6982	0.3065
01-11-2014	305	0.2539	0.6962	0.1975	0.2443	0.6335	0.1835
17-11-2014	321	0.395	0.8443	0.403	0.2589	0.6678	0.2047
03-12-2014	337	0.4813	0.913	0.5287	0.4137	0.8782	0.4302
19-12-2014	353	0.5497	0.954	0.6284	0.4994	0.9344	0.5551
01-01-2015	1	0.6326	1.0453	0.7491	0.6027	1.0392	0.7057
17-01-2015	17	0.6516	1.0949	0.7769	0.6699	1.0869	0.8036
02-02-2015	33	0.726	1.1078	0.8852	0.7076	1.0933	0.8585
18-02-2015	49	0.6925	1.1258	0.8364	0.7281	1.0897	0.8884
06-03-2015	65	0.6616	1.0732	0.7915	0.6632	1.0703	0.7937
22-03-2015	81	0.461	0.7361	0.4992	0.6329	1.059	0.7497
07-04-2015	97	0.2532	0.4882	0.1964	Crop Harvested		
23-04-2015	113	0.2128	0.5884	0.1375			

Similarly, the variation in crop coefficient values for mustard crop at various growth stages can be seen in Fig. 5. The K_{c_dual} and K_{c_single} values increase during the crop development growth stage beginning from October to starting of February. The estimated K_{c_FAO} values of mustard by the FAO method during initial, crop development and reproductive stages are 0.25, 1.28 and 0.3. The average difference in K_{c_dual} and K_{c_single} for mustard crop has also been observed to be approximately 0.35. The K_c value is modified by variation in climate, mean daily wind speeds and variable crop height.

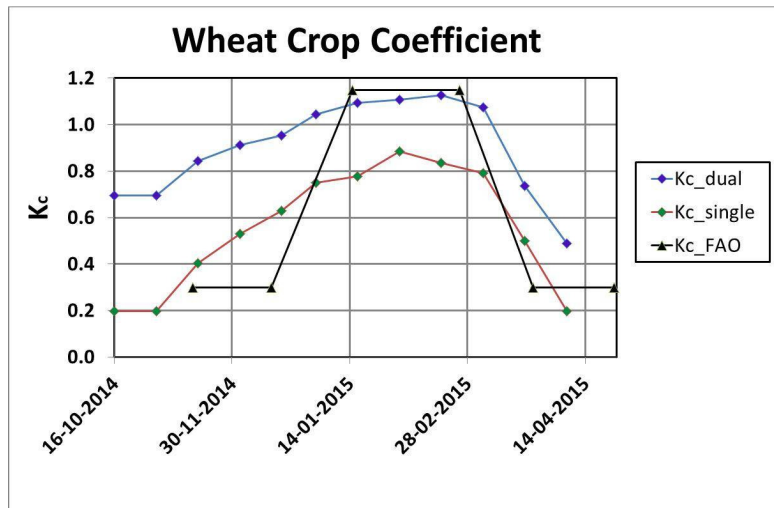


FIGURE 4. K_c curves for wheat crop

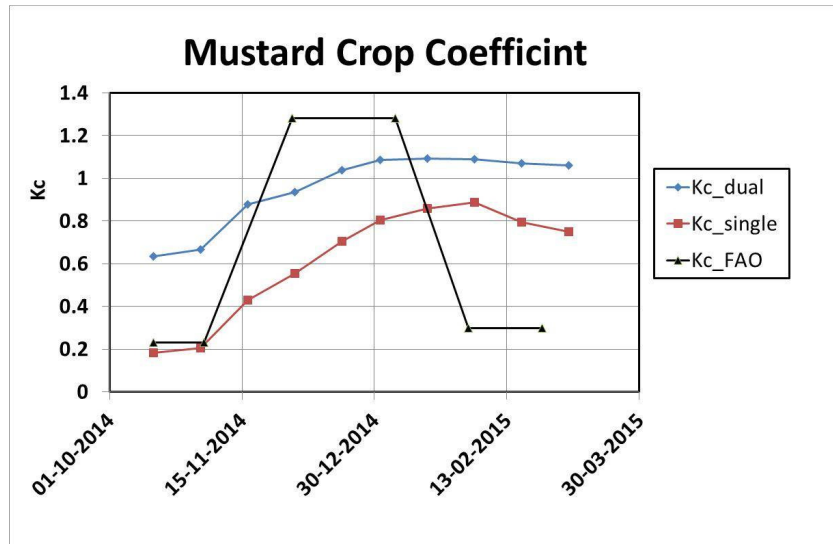


FIGURE 5. K_c curves for mustard crop

CONCLUSIONS

This study has demonstrated that time-series MODIS 250 m NDVI data provide a viable option for regional-scale crop mapping, however small error in estimation may be due to the mixed pixels at the 250 m spatial scale level. The present study shows that Remote Sensing and GIS integrated approach can be used for the estimation of crop coefficients for different crops. For the study area, the K_{c_dual} value varies from 0.6959 to 0.5884 for wheat crop and from 0.6982 to 1.059 for mustard crop while the K_{c_single} value varies from 0.1971 to 0.1375 for wheat crop and 0.3065 to 0.7497 for mustard crop. It is observed that in general K_{c_dual} values are 0.35 more than K_{c_single} values. There is good correlation between K_{c_dual} and K_{c_FAO} for both the crops hence it can be concluded from the study that dual crop coefficient approach is more accurate than the single crop coefficient approach for the estimation of K_c values. The local climatic parameter and soil characterises also effects the variation in K_c values.

REFERENCES

- Chen, J. M., Chen, X., Ju, W. and Geng, X. 2005. "Distributed hydrological model for mapping evapotranspiration using remote sensing inputs". *Journal of Hydrology*. 305:15–39. <http://doi.org/10.1016/j.jhydrol.2004.08.029>
- Tyagi, N. K., Sharma D. K. and S. K. Luthra. 2000. "Evapotranspiration and Crop Coefficients of Wheat and Sorghum." *Journal of Irrigation and Drainage Engineering*. 126 (4): 215–22. doi:10.1061/(ASCE)0733-9437(2000)126:4(215).
- Dhotre, ST, Sharma, G., Goyal, R. and Parikh, SK. 2015. "Soil Moisture Estimating Governing Models – Parameter Estimation- A Review," *Int. J. of Emerging Tech. and Adv. Engg.* 5(2): 165-172. www.ijetae.com
- Er-Raki, S., Chehbouni, A., Guemouria, N., Duchemin, B., Ezzahar, J. and Hadria, R. 2007. "Combining FAO-56 Model and Ground-Based Remote Sensing to Estimate Water Consumptions of Wheat Crops in a Semi-Arid Region." *Agricultural Water Management*. 87 (1): 41–54. doi:10.1016/j.agwat.2006.02.004.

- Er-Raki, S., Chehbouni, A. and Duchemin B. 2010. "Combining Satellite Remote Sensing Data with the FAO-56 Dual Approach for Water Use Mapping in Irrigated Wheat Fields of a Semi-Arid Region." *Remote Sensing*. 2 (1): 375–87. doi:10.3390/rs2010375.
- Gontia, N. K., and Tiwari, K. N. 2010. "Estimation of crop coefficient and evapotranspiration of wheat *Triticum aestivum* in an irrigation command using remote sensing and GIS". *Water Resources Management*. 24(7): 1399–1414. <http://doi.org/10.1007/s11269-009-9505-3>
- Kamble, B., Kilic, A., and Hubbard, K. 2013. "Estimating crop coefficients using remote sensing-based vegetation index". *Remote Sensing*. 5(4): 1588–1602. <http://doi.org/10.3390/rs5041588>
- Kashyap, P. S., and Panda, R. K. 2001. "Evaluation of evapotranspiration estimation methods and development of crop-coefficients for potato crop in a sub-humid region". *Agricultural Water Management*. 50(1): 9–25. [http://doi.org/10.1016/S0378-3774\(0100102-0\)](http://doi.org/10.1016/S0378-3774(0100102-0)).
- Kumar, R., Shankar, V., and Kumar, M. 2011. "Development of Crop Coefficients for Precise Estimation of Evapotranspiration for Mustard in Mid Hill Zone- India Abstract: Mid-season Late-season". *Universal Journal of Environmental Research and Technology*. 1(4): 531–538.
- Kushwaha, K. and Goyal, R. 2016. "Methodology for the Estimation of Groundwater Flux across Simplified Boundary using GIS and Groundwater Levels", *J. of Current Science*. 110 (6): 1050-1058.
- LP DAAC, USGS. 2016. "Vegetation Indices 16-Day L3 Global 250m" URL: https://lpdaac.usgs.gov/dataset_discovery/modis/modis_products_table/mod13q1
- Mohan, S., and Arumugam N. 1994. "Crop Coefficients of Major Crops in South India." *Agricultural Water Management*. 26: 67–80. doi:10.1016/0378-3774(94)90025-6.
- Pakhale, G., Gupta, P., and Nale, J. 2010. Crop and Irrigation Water Requirement Estimation by Remote Sensing and GIS : A Case A Case Study Of Karnal District, Haryana, India. *International Journal of Engineering and Technology*. 2(4): 207-211
- Rafn, Eric B., Bryce Contor, and Daniel P. Ames. 2008. "Evaluation of a Method for Estimating Irrigated Crop-Evapotranspiration Coefficients from Remotely Sensed Data in Idaho." *Journal of Irrigation and Drainage Engineering*. 134 (6): 722–29.
- Sharma G, Zaidi, S and Goyal, R. 2016. "Trend analysis of temporal variations in evi with respect to rainfall of jaipur district". *International Journal of Research in Engineering and Technology*, 05 01
- Singhal, V and Goyal R. 2012. "A methodology based on spatial distribution of parameters for understanding affect of rainfall and vegetation density on groundwater recharge", *European Journal of Sustainable Development*.1 (2): 85
- Wikipedia. 2016. "Crop coefficient", URL: https://en.wikipedia.org/wiki/Crop_coefficient, accessed in April 2016.

GEOSPATIAL MAPPING OF GROUNDWATER QUALITY USING GIS

Prachi Singh and Raj Mohan Singh

(Department of Civil Engineering, MNNIT, Allahabad, India)

ABSTRACT: The groundwater is a highly useful and abundant natural resource. However, groundwater is vulnerable to pollution and depletion, and needs to be managed carefully to avoid serious economic and environmental costs. The contamination of aquifer not only threatens public health and the environment, it also involves large amounts of money in fines, lawsuits, and cleanup costs. Once groundwater is contaminated, it may be difficult and expensive to clean up. Therefore, it is imperative to know the spatial and temporal extent of the pollution so that necessary remedial steps may be taken. In this work the spatial distribution of groundwater quality has been developed for quality parameters such as pH, TDS, EC, Ca, Na and NO₃. These water quality parameters of 22 locations each varying in four seasons from 2005-2007 are shown in GIS framework. Different kriging interpolation techniques are used for spatiotemporal representation of water quality parameters in aerial study area.

INTRODUCTION

Groundwater is the major source of irrigation and drinking water in both urban and rural India. Even in those areas where surface water is abundant, the groundwater is used as practical source of water for public supply, agriculture and industry due to its quality, easy accessibility, reliability and relatively low cost associated with its use. However, groundwater is vulnerable to pollution and depletion, and needs to be managed carefully to avoid serious economic and environmental costs. Contamination of groundwater poses serious threat to people.

The assessment of spatial correlation in hydrochemical variables is an important tool in the analysis of groundwater chemistry. In geostatistical methods, kriging technique is quite popular. The technique is applicable to cases such as determining groundwater level, estimation of hydrochemical distribution of soil properties, and other estimations. Kumar and Remadevi (2006) have compared various variogram models, i.e., spherical, exponential, and Gaussian semivariogram models to fit the experimental semivariograms in identifying the spatial analysis of groundwater levels in small part of Rajasthan area, India. The results indicate that the kriged groundwater levels satisfactorily matched the observed groundwater levels. Ahmadi and Sedghamiz (2007) used ordinary and universal kriging methods in identifying the spatial and temporal analysis of monthly groundwater level fluctuations in the arid region, the Darab Plain, in the south of Iran. Results revealed that the spatial and temporal variations of groundwater level and groundwater level fluctuations were underestimated by 3 and 6 %, respectively. Very low variation and acceptable errors support the unbiased hypothesis of kriging. Shamsudduha (2007) used different interpolation procedures in evaluating the most appropriate prediction method for the estimation of arsenic concentrations in the shallow aquifer in Bangladesh. In this case, ordinary kriging on original arsenic concentrations and their residual values produced better prediction models regarding the cross-validation, mean prediction error, and biasedness analyses.

The role of geographic information system (GIS) software in analyzing spatial distribution of groundwater has been investigated by many authors such as Mehrjardi et al. (2008). Pradhan (2009) studied groundwater potential zonation for basaltic watersheds. Ayazi et al. (2010) investigated disasters and risk reduction in groundwater. Manap et al. (2012) applied the probabilistic based frequency ratio in groundwater potential. El Afly (2012) and Machida et al. (2012) applied an integrated Geostatistics and GIS technique in groundwater. Neshat et al. (2013) estimated groundwater vulnerability to pollution, and Manap et al. (2013) studied prediction of groundwater potential zones.

Present work investigate the application of various spatial models to interpret the spatial distribution of the groundwater quality and to predict the general trend of the spatial distribution of groundwater in the recharge area of Muzaffarnagar district, Uttar Pradesh in Yamuna-Krishni sub-basin. In this study, kriging techniques in the framework of GIS software (ArcGIS Geostatistical Analyst) are used.

DESCRIPTION OF THE STUDY AREA AND DATA COLLECTION

The study area falls in the District of Muzaffarnagar between Longitudes 77°05' and 77°27' E and latitude 29°15' and 29°41' N (Fig.1) and covers an area about 1100 km². It lies in the interfluvies of Ganga and Yamuna rivers in the western most part of the Uttar Pradesh. The Rivers Yamuna and Krishni forms the western and eastern boundaries, respectively. Heavy withdrawal of groundwater has set a declining trend of water table over the decade in the study area.

District Muzaffarnagar is rectangular in shape and it is situated between the district of Saharanpur on the north, Meerut and Baghpat on the south, and is bounded by the Ganga on the east and the Yamuna on the west. The main rivers, the Ganga, the Kali, the Hindon and the Yamuna have played an important role in carving the topography of the district and divide it into four distinct tracts (Nevill, 1903, Varun, 1980) i.e. (i) the Ganga Khadir (ii) upland upto Kali Nadi (iii) the Kali Hindon doab and (iv) the Hindon Yamuna doab. The study area Krishni-Yamuna sub basin is a part of Hindon-Yamuna doab. Out of total water resources of the Yamuna-Krishni sub-basin, only 8.1% is derived from the surface water sources and 91.9% from the groundwater. The Eastern Yamuna Canal and its distributaries are main source of surface water irrigation (CGWB, 2008). Water quality data is available for 22 wells collected in the four different seasons. The observation data for 6 parameters are used for spatiotemporal representation using different kriging techniques.

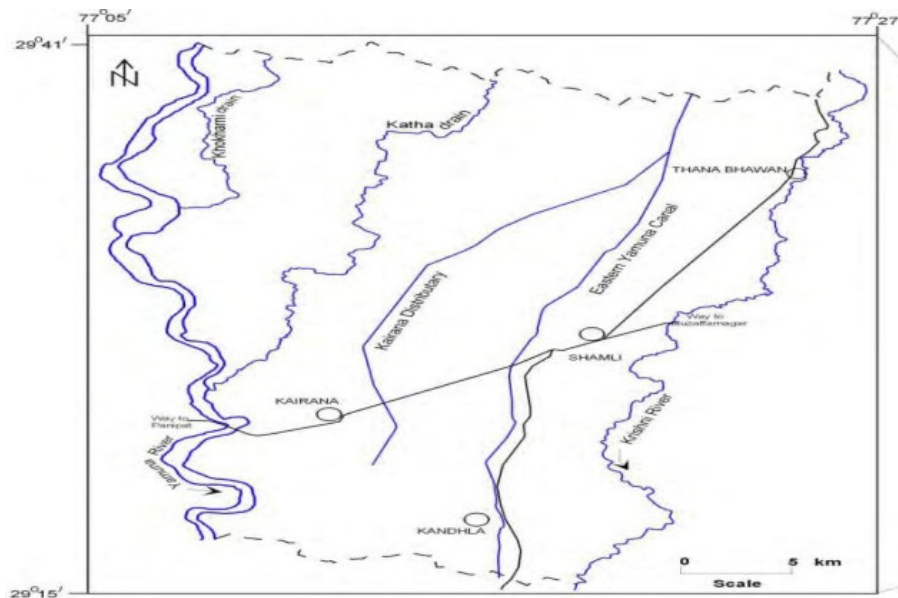


Figure **Error! No text of specified style in document.** Map of the Study Area

METHOD OF SPATFIOTEMPORAL ANALYSIS

Spatial distribution of groundwater chemistry parameters is analyzed using GIS software. In this research, classification of concentration values to identify water quality for drinking water purposes follows the approach by McNeely et al. (1979). Spatiotemporal methodology are developed using the following steps:

1. Preparation of base map.
2. Georeferencing and geometric correction

3. Digitization
4. Assigning attributes to the study area.
5. Interpolation using different ordinary kriging.
6. Representation of different water quality parameter by contour map.

Geostatistical analysis is used to model the spatial distribution of groundwater chemistry. Geostatistics can be regarded as a collection of numerical techniques that deal with the characterization of spatial attributes employing primarily random models in a manner similar to the way in which time series analysis characterizes temporal data (Olea 1999). It deals with spatially autocorrelated data that have a basic structure or spatial patterns which can be manifested in (semi)variogram analysis. (Semi)variogram is a characterization of the spatial correlation of the variables under study. The semivariogram shows the relationship between the lag distance on the horizontal axis and the semivariogram value on the vertical axis. Lag distance is the distance between the measurements of a particular property. From the semivariogram, the spatial correlation of a spatially varying property can be described. The semivariogram value increases from low to high values indicating higher spatial autocorrelation at the small lag distance (Nayanaka et al. 2010). Theoretically, to calculate the semivariogram, the following formula is commonly used:

$$\lambda(h) = \frac{1}{2n(h)} \sum_{i=1}^{n(h)} [Z(x_i) - Z(x_i + h)]^2 \quad (1)$$

Where $\gamma(h)$ is the semivariogram value for the lag distance (h), $n(h)$ is the total number of the variable pairs separated by a lag distance (h), and $Z(x)$ is the value of the variable. Kriging is a technique of making optimal, unbiased estimates of regionalized variables at unsampled locations using the structural properties of the semivariogram and the initial set of data values (David 1977). The general equation of the kriging method has the following form:

$$Z^*(x_0) = \sum_{i=1}^n \lambda_0^i Z(x_i) \quad (2)$$

Where λ_0^i is the weight associated with each data point i ($i = 1, 2, 3, \dots, n$), $Z(x_i)$ is the observed value at point x_i , $Z^*(x_0)$ is the predicted value at point x_0 , and n is the number of sample points. The values of the weights, λ_0^i , are estimated by minimizing the kriging (error) variance (σ^2) given by,

$$\sigma^2 = \frac{1}{n} \sum_{i=1}^n [Z^*(x) - Z(x)]^2 \quad (3)$$

The unbiased condition in kriging method is expressed as

$$E[Z^*(x_i)] = E[Z(x_i)] \quad (4)$$

Where $E[\]$ is the expected value operator.

Eq.4 will lead to the formula of De Marsily (1984), $\sum_{j=1}^n \lambda_0^j = 1$ which means that the sum of the weight should be 1. The kriging system of equations that should be solved are as follows:

$$\sum_{j=1}^n \lambda_0^j \gamma(x_i - x_j) + \mu = \gamma(x_i - x_0) \quad (5)$$

$\sum_{j=1}^n \lambda_0^j = 1$, $i=1, \dots, n$, Where μ is a Lagrange multiplier, and $\gamma(x_i - x_j)$ is the semivariogram between two points x_i and x_j .

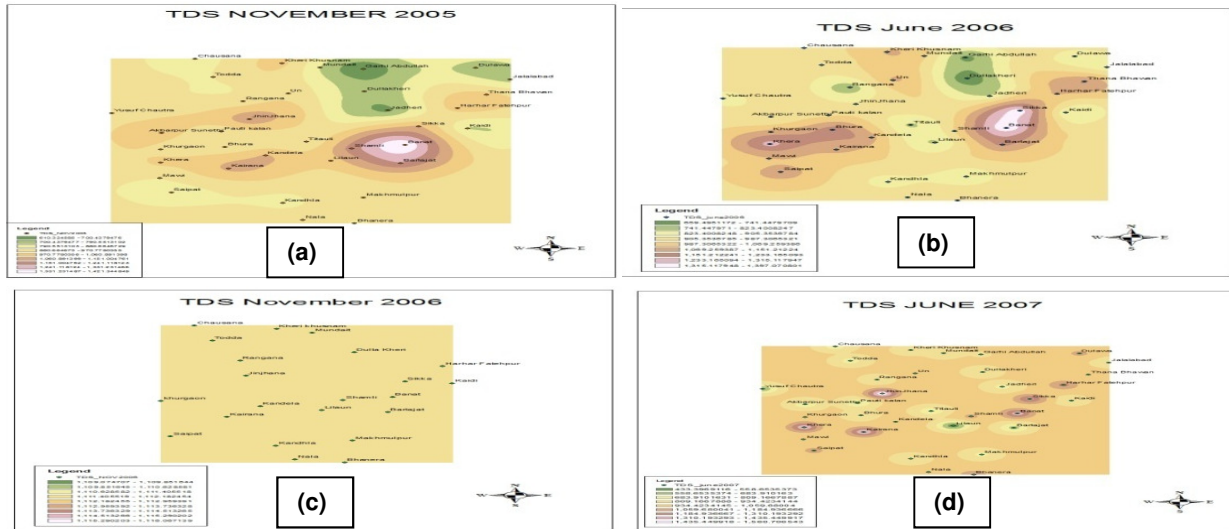


Figure 2. Interpolation of TDS Using Spherical Kriging in (A) Nov 2005, (B) June 2006, (C) Nov. 2006 & (D) June 2007

RESULT AND DISCUSSION

The spatial distribution of TDS for four different seasons and five different kriging are shown on the maps and is presented in Figs. 2 to 7. From the various kriging techniques used in the spatial distribution, it is clear that spherical kriging gives much accurate and clear distribution pattern as compared to other kriging method.

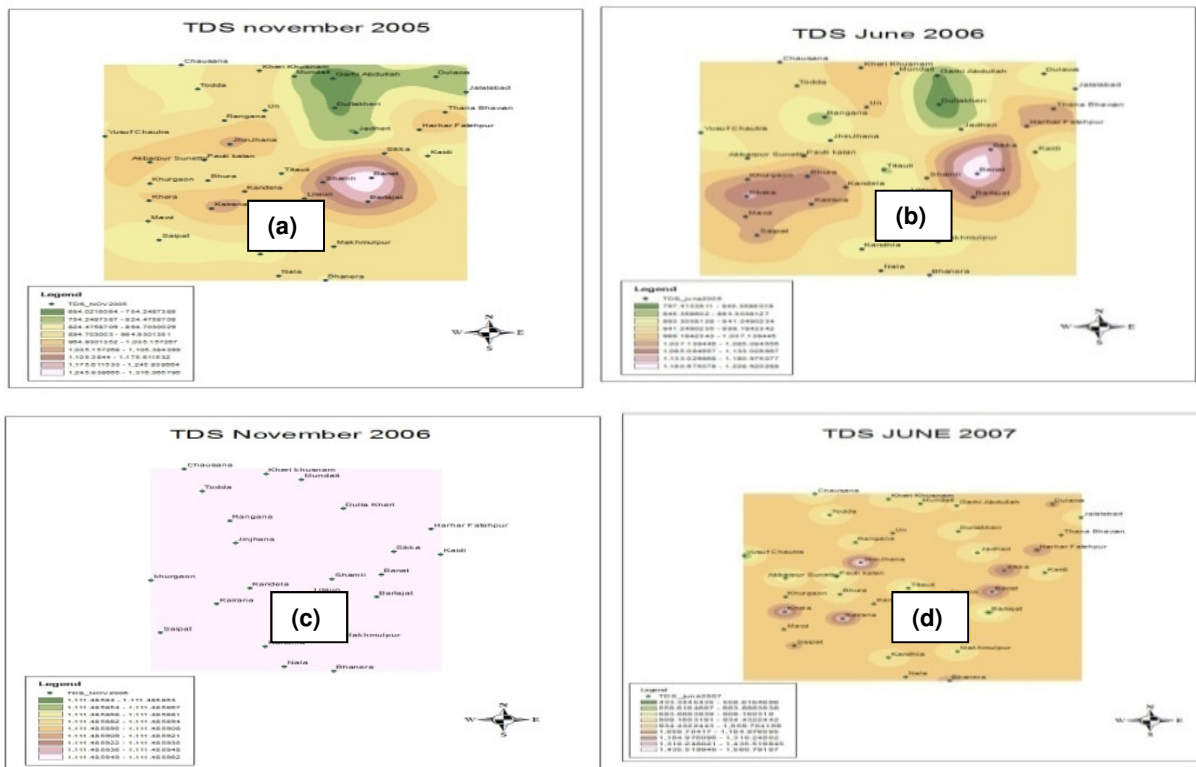


Figure 3. Interpolation of TDS Using Circular Kriging in (A) Nov 2005, (B) June 2006,

(C) Nov. 2006 & (D) June 2007

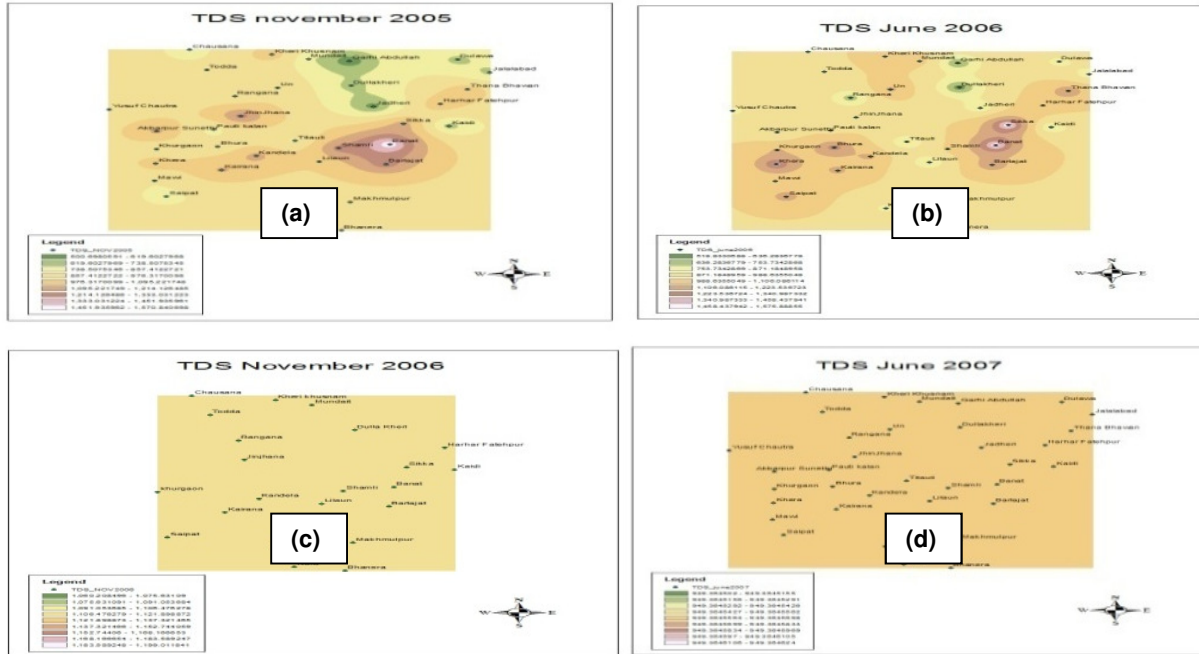


Figure 4. Interpolation of TDS Using Exponential Kriging in (A) Nov 2005, (B) June 2006, (C) Nov. 2006 & (D) June 2007

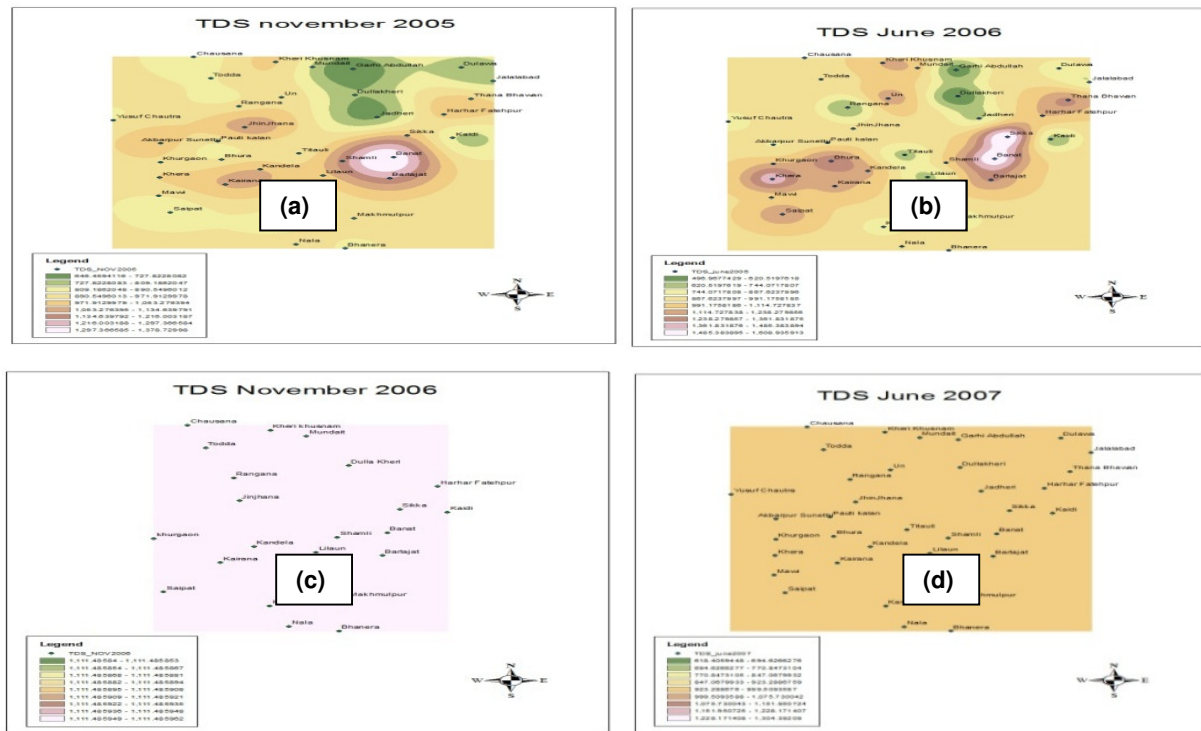


Figure 5. Interpolation of TDS Using Gaussian Kriging in (A) Nov. 2005, (B) June 2006, (C) Nov. 2006 & (D) June 2007

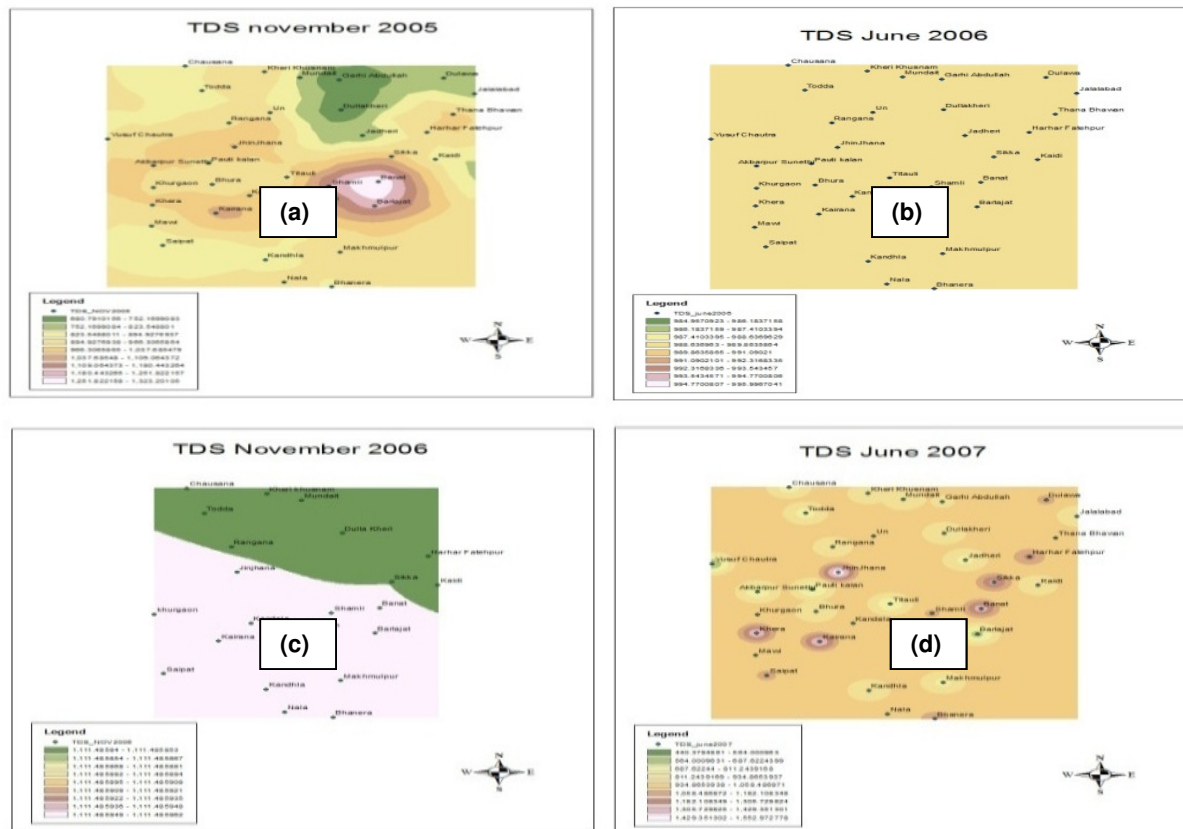


Figure 6. Interpolation of TDS Using Linear Kriging in (A) Nov 2005, (B) June 2006, (C) Nov. 2006 & (D) June 2007

CONCLUSIONS

The spatiotemporal analysis in different kriging method is performed. It was found the results obtained by spherical interpolations are much more precise to actual values in comparison of other kriging interpolations. The maximum values of TDS, EC and Na using different kriging are found at Banat and nearby areas, maximum pH was observed at makhmulpur, maximum NO_3 at harhar fatehpur and khera.

REFERENCES

- Ahmadi S.H., A. Sedghamiz.2007. "Geostatistical analysis of spatial and temporal variations of groundwater level". *Environ Monit Assess.* 129: 277–294. doi: 10.1007/s10661-006-9361-z
- Ayazi M.H., S. Pirasteh,A. K. P. Arvin, B. Pradhan, B. Nikouravan, S. Mansor. 2010. "Disasters and risk reduction in groundwater: Zagros Mountain Southwest Iran using geoinformatics techniques". *Disaster Adv* 3(1): 51–57
- Central Ground Water Board (CGWB).2008. *Groundwater Flow Modelling and Aquifer vulnerability assessment studies in Yamuna–Krishni Sub-basin, Muzaffarnagar District*: Project no 23/36/2004.
- David M. 1977. "Geostatistical ore reserve estimation". Elsevier, Amsterdam
- De Marsily G. 1984. Spatial variability of properties in porous media: a stochastic approach. In: Bear J, Corapcioglu M (eds) *Fundamentals of transport phenomena in porous media*. Martinus Nijho, Dordrecht, pp 721–769

- El Afly M. 2012. Integrated geostatistics and GIS techniques for assessing groundwater contamination in Al Arish area, Sinai, Egypt. *Arab J Geosci* 5(2): 197–215. doi: 10.1007/s12517-010-0153-y
- Kumar V, Remadevi. 2006. “Kriging of groundwater levels—a case study”. *J Spat Hydrol.* 6(1): 81–92.
- Manap M.A., H. Nampak, B. Pradhan, S. Lee, W. N. A. Sulaiman, M.F. Ramli. 2012. Application of probabilistic-based frequency ratio model ingroundwater potential mapping using remote sensing data and GIS. *Arab J Geosci.* doi: 10.1007/s12517-012-0795-z
- Manap M.A., W. N. A. Sulaiman, M. F. Ramli, B. Pradhan, N. Surip. 2013. A knowledge driven GIS modelling technique for prediction of groundwater potential zones at the Upper Langat Basin, Malaysia. *Arab J Geosci* 6(5): pp. 1621–1637
- McNeely R.N., V. P. Nelamnis, L. Dwyer.1979. Water quality source book: a guide to water quality parameter. Inland Waters Directorates, Water Quality Branch, Ottawa
- Mehrjardi R.T., M. Z. Jahromi, S. Mahmodi, A. Heidari. 2008. “Spatial distribution of groundwater quality with geostatistics (case study: Yazd-Ardakan Plain)”. *World Appl Sci J.* 4(1): pp. 9–17
- Nayanaka V.G.D., W. A. U. Vitharana, R. B. Mapa .2010. “Geostatistical analysis of soil properties to support spatial sampling in a paddy growing alfisol”. *Trop Agric Res* 22(1): 34–44. doi: 10.4038/tar.v22i1. 2668
- Neshat A., B. Pradhan, S. Pirasteh, H. Z. M. Shafri .2013. Estimating groundwater vulnerability to pollution using modified DRASTIC model in the Kerman agricultural area. *Iran Environ Earth Sci.* doi: 10.1007/s12665-013-2690-7
- Olea R.A. 1999. *Geostatistics for engineers and earth scientists.* Kluwer Academic, Boston
- Pradhan B .2009. “Ground water potential zonation for basaltic watersheds using satellite remote sensing data and GIS techniques”. *Cent Eur J Geosci* 1(1): pp.120–129. doi: 10.2478/v10085-009-0008-5
- Shamsudduha M .2007. “Spatial variability and prediction modeling of groundwater arsenic distributions in the shallowest alluvial aquifers in Bangladesh”. *J Spat Hydrol.* 7(2):pp. 33–46.

**DEVELOPMENT AND APPLICATION OF THE INTEGRATED WATER DISTRIBUTION
MANAGEMENT SYSTEM**

*Patryk Wójtowicz** (Wrocław University of Technology, Wrocław, Poland)
Andrzej Ziółkowski (Warsaw School of Information Technology, Warsaw, Poland)
Jan Studziński (Systems Research Institute, Warsaw, Poland)

In recent years, a rapid growth of IT, automation and measurement technologies accelerated the implementation of computer aided decision systems in the water sector. We present research and innovation aimed to meet the need for a scalable, automated and robust solution for water utilities that can integrate existing (commercial, in-house and open source) software and hardware solutions into one package, benefiting in a synergetic effect.

We demonstrate the results of tests in two contrasting, both in terms of type and size, case-studies in Poland, facing different short-term and long-term challenges. First was a large-scale main water transportation system of the Upper Silesian Waterworks in Katowice serving to almost 3 million customers. In the other case-study, we implemented ICT system in a typical medium-size municipal water supply of Głubczyce (population of ca. 13 000). These two case-studies provided us with a unique opportunity to test various approaches to calibration as well as automatic hydraulic model updating and validation. The key elements of this system have been examined, namely: GIS, telemetry (AMI and SCADA), hydraulic model as well as tools for multi-criteria optimization and forecasting. We explain the details of our custom semi-automated calibration procedure, where we applied the combination of fuzzy logic and genetic algorithms.

Specific aspects of data collection, model calibration and simulation were discussed. Special focus was also given to the development of the hydraulic model using in-house MOSKAN-W modelling software - EPANET based mobile (Javascript) for two very different water distribution systems. GIS is the central element of integrated system, which was used to manage and process input and output data from the model. In particular, we demonstrate the integration between GIS system and other modules.

**ENVIRONMENTAL ANALYSIS
AND
MEASUREMENTS**

ENVIRONMENTAL IMPLICATIONS OF FOOD AND PLA WASTE MANAGEMENT OPTIONS

Shakira R. Hobbs^a, Jay P. Devkota^a, Prathap Parameswaran^b and Amy E. Landis^a

(^aInstitute of Sustainability, Glenn Department of Civil Engineering, Clemson University Clemson, SC, 29634 USA; ^bDepartment of Civil Engineering, Kansas State University, Manhattan, KS 66506, USA)

ABSTRACT: The study assesses the environmental impacts of anaerobic digesting, composting and landfilling of food and PLA waste via the Environmental Protection Agency's Waste Reduction Model (WARM) and life cycle assessment (LCA) of anaerobic digestion model. WARM contains composting and landfilling food and polylactic acid (PLA) waste, but not anaerobic digestion. Compost, landfill and anaerobic digestion of food and PLA waste data was extracted and assessed from WARM, Ecoinvent and literature to show environmental impacts. Results show landfilling 200 tons of food and PLA waste per year produces the most CO₂ equivalent at 132 tons/yr. Composting resulted in negative emissions for food waste, however PLA does not degrade in industrial composting facilities and are instead sent to landfills. Anaerobically digested food and PLA waste is the best scenario, in terms of reduced carbon emissions, when biogas is used to heat the digester. In contrast, anaerobic digestion requires the most energy, even when biogas is utilized in comparison to landfilling and composting. Although WARM shows energy and carbon impacts from food and PLA waste, it does not show process breakdowns. Results from the study highlight the limitations of WARM and show processes that can be further optimized to reduce environmental impacts.

INTRODUCTION

Sending food to landfills has serious and detrimental environmental impacts. Food waste in landfills breakdown anaerobically and produces a greenhouse gas, methane, 25 times more potent than CO₂ (IPCC, 2007). Although landfills can recover gas, only 20% of landfills are capable of recovering the gas (EPA, 2016a). Food waste can be redirected from landfills to compost and anaerobic digestion facilities to produce nutrient rich soil amendments and produce methane for combine-heat and power.

Recently, handling food waste has become more complicated because it is often 'contaminated' with bioplastic such as PLA. Bioplastic are often used in food packaging and increasingly used to achieve zero-waste efforts and sustainability goals. While PLAs are intended to be composted after use alongside food waste, industrial composting facilities managers report that PLAs do not fully biodegrade in their systems (Meeks et al., 2015; Siracusa et al., 2008). Many composting facilities are rejecting PLAs and sending them to landfills (Hottle et al., 2013). New sustainable solutions are needed to manage both food and PLA waste. PLA and food waste can be sent directly to anaerobic digesters without being cleaned or sorted. These waste management scenarios may be more environmentally friendly and energetically positive when compared to compost facilities and landfills.

The aim of this study was to understand the energy and carbon impacts of composting, landfilling and anaerobically digesting food and PLA waste. WARM (an EPA waste reduction model) has compost and landfill options to estimate energy use and green house gas (GHG) emissions from food and PLA waste. However, there is no model that exists that considers anaerobic digestion of food and PLA waste to estimate energy use and GHG emissions. Therefore, we developed a new anaerobic digestion model based on data from Ecoinvent and literature. This model can be used by designers and practitioners for optimizing processes with an aim for reducing environmental impacts and understanding trade-offs.

METHODS

Goal and Scope Definition. The goal of this LCA was to evaluate and compare three different end-of-life waste management options: compost, landfill and anaerobic digestion in terms of environmental impacts and energy use. The functional unit for the LCA was normalized to 200 tons to reflect the amount of food and PLA waste produced per year (EPA, 2016b; NatureWorks, 2012). 200 tons was used because the capacity of anaerobic digester was 200 tons.

The analysis begins once food and PLA waste is discarded as shown in Figure 1. Other processes outside of the system boundary (dotted line) are also shown in the background and are not considered in the analyses since they do not deal with use-phase or end of life processes. In this analysis, food waste consists of: beef, poultry, grains, bread, fruits and vegetables and dairy products—this also includes uneaten and prepared food from commercial, non-commercial and industrial sources (Buzby et al., 2014). PLAs are often used for food packaging such as forks, cups, lids and thin films, which are also considered in this analysis.

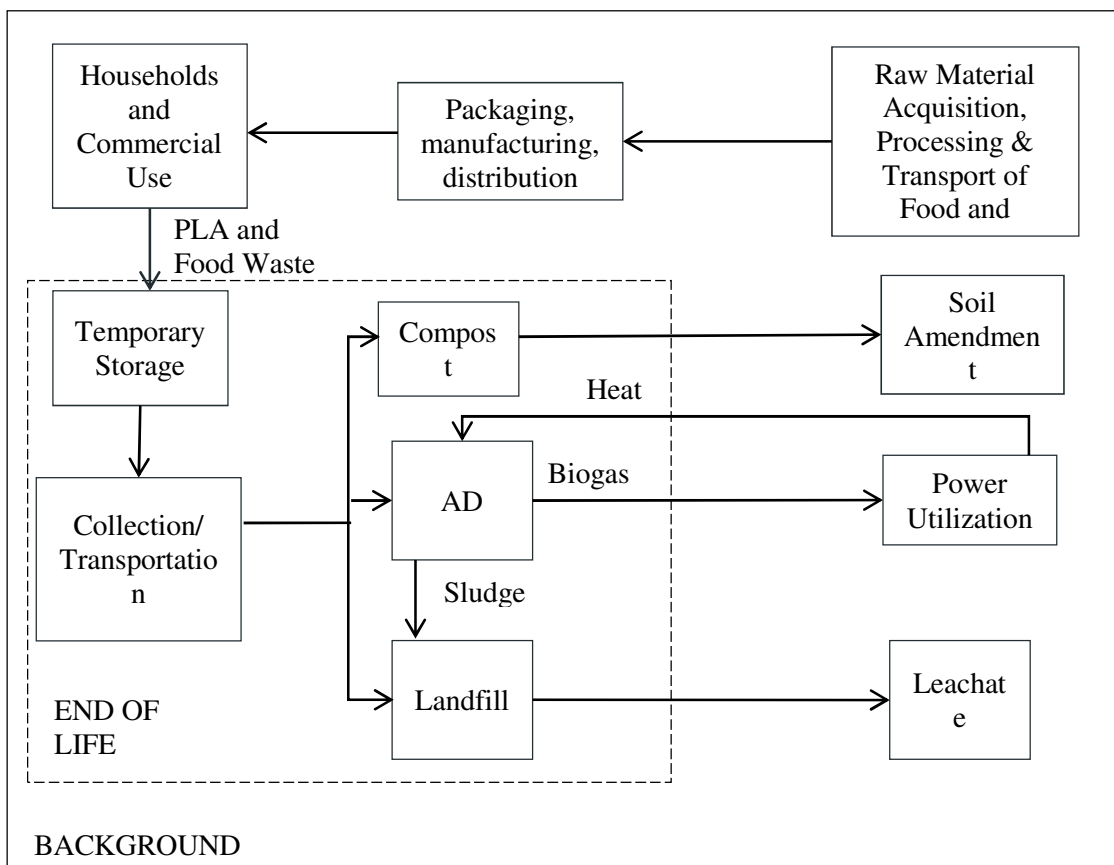


FIGURE 1. Life cycle of food and PLA waste.

WARM an AD LCA Model. Waste Reduction Model (WARM) was created by the EPA to assist waste solid managers in environmental assessment of material types and waste management practices (EPA, 2015). WARM allows users to select material inputs for solid waste management options and compare different treatment options. Results are reported as metric tons of carbon dioxide equivalent (MTCO₂E), metric tons of carbon equivalent (MTCE) and units of energy (million BTU). WARM has waste management options such as: recycling, landfilling, combusting and composting, but does not have anaerobic digestion.

End of life-cycle data was used to create a model for anaerobic digestion that shows the carbon and energy impacts of digesting food and PLA waste. Similar system boundaries, inputs and outputs were used based on WARM. However, WARM gives limited life cycle inventory (LCI) data, which makes it difficult to replicate the model. Therefore, data was collected from WARM, Ecoinvent and from literature. Life Cycle Impact Assessment was completed using the TRACI 2.1 V1.01 impact characterization–Global Warming Potential (GWP) and energy use was calculated.

Scenario 1, the landfilling scenario. This scenario describes the management system for handling food and PLA waste. WARM was used to assess landfilling emission factors, which are made up of:

1. Transportation CO₂ emissions from landfilling equipment;
2. Biogenic carbon stored in the landfill;
3. CO₂ emissions avoided through landfill gas-to-energy projects” (EPA, 2015).

Scenario 2, the composting scenario. WARM was used to assess this scenario and describes the management system for handling food and PLA waste. Compost emission factors are calculated based: 1. “Collecting and transporting the organic materials to the central composting site; 2. Mechanical turning of the compost pile; 3. Non-CO₂ GHG emissions during composing (primarily CH₄ and N₂O); 4. Storage of carbon after compost application to soils.” (EPA, 2015).

Scenario 3, the anaerobic digestion scenario. Anaerobic digestion LCA model was used to assess this scenario and describes the management system for handling food and PLA waste. Data was retrieved from (Ecoinvent, 2010) and (Salter, 2008). Anaerobic digestion factors are calculated based on: 1. Collecting and transporting the organic material to central AD site; 2. Operation of anaerobic digester; 3. CO₂ and Methane emissions avoided through AD gas to energy products or utilization of natural gas; 4. Transportation CO₂ emissions from landfilling equipment.

RESULTS AND DISCUSSION

The results show significant differences in energy use and environmental impacts between the waste management techniques assessed in this study. The results from the study emphasize the importance of showing individual processes rather than impacts from food and PLA waste only.

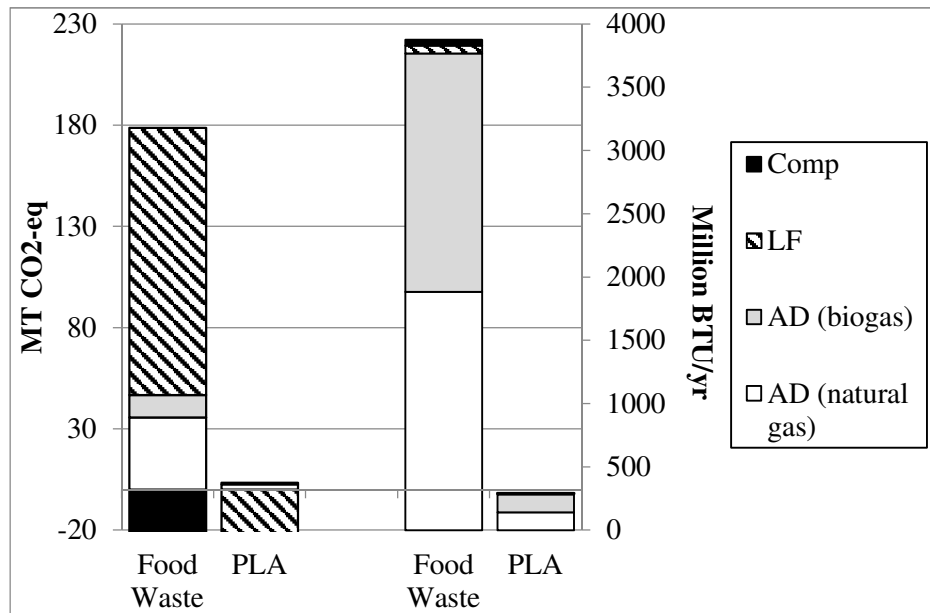


FIGURE 2. Global warming potential and energy use of food and PLA waste compared to four waste management techniques.

Comparison of Four Waste Management Options Results. Results showed anaerobic digestion, utilizing natural gas or biogas, had significantly lower CO₂ emissions than landfilling (Figure 2). Utilizing natural gas to operate the digester instead of biogas results in 26.6 more MT CO₂ eq (Figure 2). The additional surplus of biogas from the anaerobic biogas scenario can be sold or stored for future uses. Therefore, using biogas, produced from anaerobic digestion, to operate anaerobic digester facilities further reduces the global warming potential as opposed to utilizing natural gas. However, there is no significant difference in energy use between utilizing biogas versus natural gas. Furthermore, landfilling and composting food and PLA waste requires significantly less energy to dispose and treat than anaerobic digestion. Landfilling food and PLA waste resulted in significant GWP collectively, 132 MT CO₂ eq. compared to compost at -30 MT CO₂ eq. avoided emissions (Figure 2). Emissions are avoided from food and PLA when composted since WARM considers composting food and PLA waste to biogenic, not anthropogenic like landfilling food waste. However, there is some debate in the literature on whether or not PLA produces anthropogenic or biogenic waste.

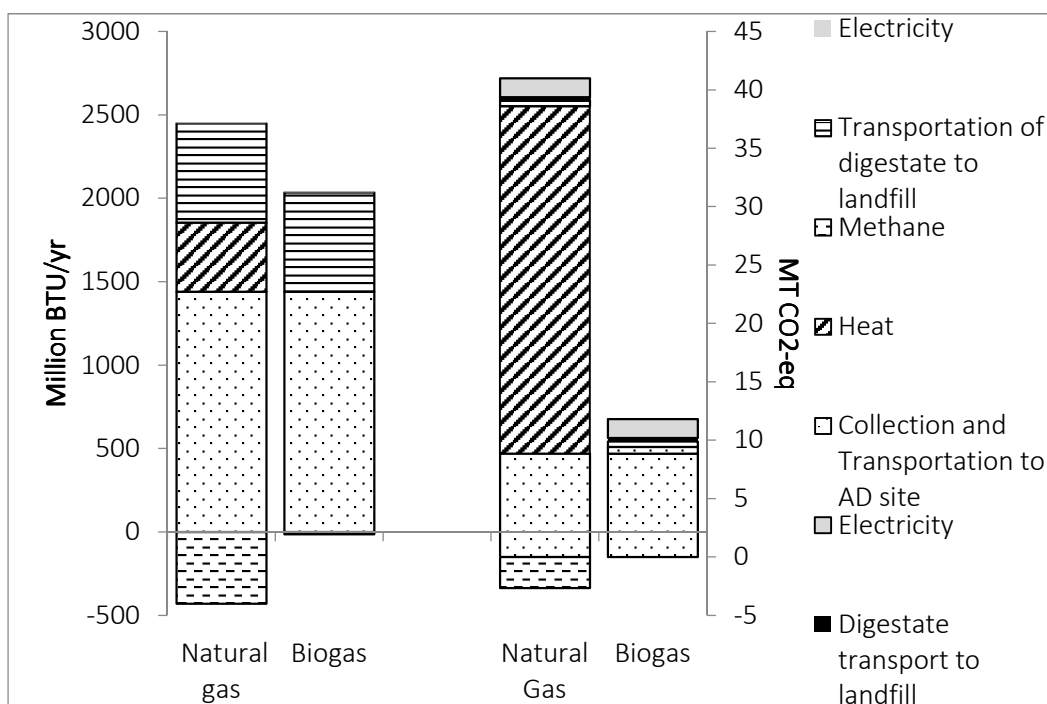


FIGURE 3. Energy use and Global Warming Potential of individual processes of anaerobic digestion utilizing biogas and natural gas

WARM does not distinguish between amorphous and crystalline PLA and states that PLA does not degrade in landfills, but degrade in composting facilities resulting in negative PLA emissions for the waste management option landfill and compost. There is some debate in the literature. For example, crystalline PLA, which are typically forks and cups, do not degrade in landfills (Kolstad et al., 2012), therefore emissions are avoided from PLA in landfill. Furthermore, composting facilities in the US are reporting that PLA does not degrade at the same rate as organic materials, such as food waste, and are rejected and sent to landfills (Hottle et al., 2013). However, amorphous PLA, which are typically thin films, degrade in anaerobic conditions like landfills (Kolstad et al., 2012) and produce methane and carbon dioxide—i.e. GHG. There are experiments, which also show that amorphous and crystalline PLA biodegrade under

thermophilic anaerobic conditions (Krause & Townsend, 2016; Vargas et al., 2009)–same conditions as landfills.

Anaerobic Digestion (Biogas And Natural Gas) Process Results. Collection and transportation of food and PLA waste to anaerobic digestion site, heat, electricity, methane and transportation of digestate to landfill are ancillary processes that are used to create the model. 415 million BTU/yr of natural gas is needed to operate the anaerobic digester with about 430 million BTU/yr produced as a byproduct (Figure 3). Methane produced from the digester can be substituted for natural gas and used to power and operate the anaerobic digester leaving a byproduct of 15 million BTU/yr of methane. Utilizing natural gas as a heating source for the anaerobic digester contributed to 38.4 MT CO₂-eq compared to utilizing biogas at 11.8 MT CO₂ eq. Substituting natural gas for biogas drastically reduces MT CO₂ eq. (Figure 3) and demonstrates the benefits of showing individual processes.

Majority of the energy used in the anaerobic digestion scenario is the collection and transport to the anaerobic digester site at 1440 million BTU/yr (Figure 3). Quantifying and showing individual processes assist in waste management operators' decision-making and provide concise guidance highlight sustainable waste handling techniques.

CONCLUSION

The study assessed the environmental impacts of anaerobic digestion, composting and landfilling of food and bioplastic-PLA waste via WARM and anaerobic digestion LCA model. WARM does not have anaerobic digestion as a waste management option. Therefore, data was extracted and assessed from Ecoinvent, literature and WARM to create a LCA model for anaerobic digestion and to estimate the environmental impacts. Results showed that, landfilling 1 tons of food and PLA waste per year produced the most CO₂ at 0.55MT CO₂ eq. Composting resulted in negative emissions for food waste, however PLAs do not degrade in industrial composting facilities and are instead sent to landfills. Negative emissions from composting were because WARM considered PLA to be biogenic emission, despite literature stating otherwise. Among the waste reduction scenarios considered in the study, anaerobically digesting food and PLA waste was reported as the best scenario, in terms of reducing CO₂ emission, provided that the produced biogas was used to operate the digester. However, anaerobic digestion required the most energy (10 Million BTU/yr) to digest 1 ton of food and PLA waste, even when biogas was utilized. The anaerobic digestion scenarios highlight the importance of showing individual processes. It also assists in identifying individual process that require and emit the most energy and CO₂ that can be further optimized.

ACKNOWLEDGEMENTS

This material is based upon work supported by the National Science Foundation under CBET Grant No. 1066658.

REFERENCES

- Buzby, J. C., Wells, H. F., & Hyman, J. (2014). *The Estimated Amount, Value, and Calories of Postharvest Food Losses at the Retail and Consumer Levels in the United States* Retrieved from Ecoinvent. (2010). *Ecoinvent v2.2 database*. Dübendorf, Switzerland: Swiss Centre for Life Cycle Inventories.
- EPA. (2015). Waste Reduction Model (WARM). from Environmental Protection Agency (EPA)
- EPA. (2016a). Energy Projects and Candidate Landfills. <https://www3.epa.gov/lmop/projects-candidates/index.html>
- EPA. (2016b). Turning Food Waste into Energy at the East Bay Municipal Utility District (EBMUD). *Reducing Food Waste*. <https://www3.epa.gov/region9/waste/features/foodtoenergy/food-waste.html>
- Hottle, T. A., Bilec, M. M., & Landis, A. E. (2013). Sustainability assessments of bio-based polymers. *Polymer Degradation and Stability*, 98(9), 1898-1907.

- IPCC. (2007). *Climate Change 2007-:Synthesis Report*. Retrieved from Geneva, Switzerland: https://www.ipcc.ch/pdf/assessment-report/ar4/syr/ar4_syr_full_report.pdf
- Kolstad, J. J., Vink, E. T. H., Wilde, B. D., & Debeer, L. (2012). Assessment of anaerobic degradation of Ingeo polylactides under accelerated landfill conditions. *Polymer Degradation and Stability*(97), 1131-1141.
- Krause, M. J., & Townsend, T. G. (2016). Life-Cycle Assumptions of Landfilled Polylactic Acid Underpredict Methane Generation. *Environmental Science & Technology Letters*, 3(4), 166-169. doi:10.1021/acs.estlett.6b00068
- Meeks, D., Hottle, T., Bilec, M. M., & Landis, A. E. (2015). Compostable biopolymer use in the real world: Stakeholder interviews to better understand the motivations and realities of use and disposal in the US. *Resources, Conservation and Recycling*, 105, Part A, 134-142.
- NatureWorks. (2012). NatureWorks Broadens INGENEO Product Portfolio with Sulzer Proprietary Production Equipment Retrieved from <http://www.natureworkslc.com/News-and-Events/Press-Releases/2012/09-05-12-Sulzer-equipment-for-increased-Ingeo-production>
- Salter, A. (2008). *Anaerobic Digestion: Overall Energy Balances–Parasitic Inputs & Beneficial Outputs* Paper presented at the Sustainable Organic Resources Partnership - Advances in Biological Processes for Organics and Energy recycling Birmingham
- Siracusa, V., Rocculi, P., Romani, S., & Rosa, M. D. (2008). Biodegradable polymers for food packaging: a review. *Trends in Food Science & Technology*, 19(12), 634-643.
- Vargas, L. F., Welt, B. A., Teixeira, A., Pullammanappallil, P., Balaban, M., & Beatty, C. (2009). Biodegradation of treated polylactic acid (PLA) under anaerobic conditions. *Transactions of the ASABE*, 52(3), 1025-1030.

**DEUTERATED MONITORING COMPOUNDS FOR BETTER ACCURACY AND PRECISION
MEASUREMENT OF GC/MS ENVIRONMENTAL DATA**

C. Appleby

(U.S. Environmental Protection Agency, 1200 Pennsylvania Ave., NW, MC5203P, Washington, DC
20460, USA)

The use of surrogate compounds to measure method performance in Gas Chromatography/Mass Spectroscopy (GC/MS) methods for environmental monitoring is not a new practice. All EPA-approved methods require the use of three to six compounds; however only a few are deuterated analogs of target analytes. Deuterated analogs are more representative of target analytes, thereby providing more information regarding matrix effects while measuring the accuracy and precision. Since 2001, the EPA's Office of Superfund Remediation and Technology Innovation's Contract Laboratory Program (CLP) has required laboratories to add over a dozen deuterated monitoring compounds (DMCs) to each sample, all analogs of target analytes. Developed to improve data quality used in decision-making processes, this approach ultimately reduced the cost to the Superfund Program. This presentation will show, with thousands of data points, how incorporating more DMCs into EPA-approved GC/MS methods has improved data quality and provided cost savings to the Agency, and how it may benefit the entire analytical chemistry community.

**PRETREATMENT METHOD FOR TOTAL ORGANIC CARBON (TOC) ANALYSIS OF
SUSPENDED SOLIDS-CONTAINING WATER SAMPLES**

Han-Saem Lee, So-Hui Kim, and *Hyun-Sang Shin* (Seoul National University of Science & Technology, Seoul, Republic of Korea)

Jin Hur (Sejong University, Seoul, Republic of Korea)

Keun-Heon Lee (HUMAS Co., Ltd. Daejeon, Republic of Korea)

Total organic carbon (TOC), an index of the total amount of organic matters in water, is widely used as a tool to measure the organic pollutant loading of water samples and to manage wastewater treatment plants. However, the samples often contain wide variety of particulate matters depending on the origin, which make it complicated to analyze the accurate and precise determinations of organic carbon. The purpose of this study was to evaluate the effect of pretreatment by ultra-sonication, filtration and dilution on TOC analysis for the samples with high levels of suspended solid (SS) and organics. The SS samples used in this study included sewage sludge, algae and soil particles. Two different methods for the TOC analysis, high temperature catalytic oxidation and wet chemical oxidation with sulfate, were also compared with regard to their TOC response efficiency for the SS samples. The probe-type sonicator was more effective in reducing particle sizes of SS and producing higher TOC response efficiency than bath-type one. Dilution of samples followed by sieving (200~300 μm) produced higher TOC than the dilution after sieving, and the differences were increased as the dilution ratio decreased from 1/50 to 1/200. The results of this study showed that the pretreatment procedures with ultrasonic crushing, dilution and sieving can effectively be applied to analyze TOC for high concentration of suspended solids-containing samples. It also demonstrates that the two different TOC oxidation method yields comparable results at low concentration of suspended solids ($< \sim 20$ mg/L) in water.

EXPERIMENTAL STUDY ON SURFACE FLOW MEASUREMENT USING LARGE SCALE PARTICLE IMAGE VELOCIMETRY TECHNIQUES

Aadhi Naresh¹ and M. Gopal Naik²

(Department of Civil Engineering, Osmania University, Hyderabad, Telangana, India)

¹ayyaure@gmail.com; ²mgnaike@gmail.com

ABSTRACT: The rapidly increasing demands on the water resources around the globe and most of the world make it imperative that they can be determined with high degree of precision as is practicable. Stream flow determinations will require a greatly expanded network of hydrometric stations and high degree efficiency in their operation. The standard methods such as trained hydrographers and rational formulae are competent to make stream flow measurements but there are becoming increasingly scarce. The latest techniques such as ADCV, UHF Doppler Radar, LIF and Large Scale Particle Image Velocimetry (LSPIV) are more intensive use of high-speed computing devices, which are made available. LSPIV technique shoots the target area using a video camera and can obtain the instantaneous flow field to overcome the limit of the measuring equipment based on existing sensors such as LDV and ADV. In this study, LSPIV techniques has been adopted to measure the velocity and discharge of surface flow performed on the tilting flume at Fluid Mechanics Laboratory, University College of Engineering, Osmania University. The LSPIV device consists of an adjustable tripod with a video camera. The digital video camera acquired sequences of images of the surface flow velocities. It is observed from the study that, the velocity of fluid particles are varies from minimum 0.20 m/s to maximum of 0.415 m/s for different discharges. Floating objects like polypropylene particles are used as floating tracers to track the flow direction and their velocities. The average velocity has been calculated with applying the multiplication factor. The simulated flow velocity and discharges using LSPIV have been compared with the actual measurement values calculated through experimental results. Two different types of bed materials such as coarse aggregates Bermuda type grass vegetation are used for flow variations. It is found from the study that, the flow parameters varies within error of $\pm 10\%$. However, the results obtained from LSPIV techniques indicate that the adopted technique is more reasonable and have good agreement with volumetric method results.

Keywords: Stream Flow, Large Scale particle Image Velocimetry.

INTRODUCTION

Open channel shallow flows are defined as largely unidirectional, turbulent shear flows occurring in a confined layer (Jirka, 2001). These confined flows lead to the development of strong large scale two-dimensional turbulent structures mutually interacting with the omnipresent small three-dimensional turbulence scales. The main geometrical scale for these flows is their depth. Shallow flows are omnipresent in various areas of the surrounding landscape and situations. They are typically encountered in small streams, ephemeral rivers, ponds, and river floodplains in the natural environment. Ubiquitous shallow flows in urban landscape are the storm water runoff over impervious surfaces (e.g., pavements and compacted soils) and gutter flows. Given their reduced depth, shallow flows are often associated with low-velocities over the cross section. Documenting flow features in these measurement situations is usually problematic for both traditional methods (e.g., propeller meters) and the newer acoustic-based instruments. The mechanical-based techniques require a minimal water depth to accommodate the instrument measurement volumes (of the order of several centimeters), and they cannot accurately acquire near-zero velocities. The newer acoustic techniques (such as Acoustic Doppler Velocimeter, Acoustic Doppler

Current Profiler) are quasi-non-intrusive but they require immersion of the probe in the water body (Simpson, 2001). The minimum measurement volumes of the acoustic instruments are of typically larger than those of mechanical methods and they also encounter difficulties in capturing low-velocity flows (Church et al., 2012). More promising for measuring velocities in natural-scale shallow flows are image-based techniques, collectively labeled herein as Large-Scale Particle Image Velocimetry (LSPIV). These techniques stem from the Particle Image Velocimetry (PIV) methodology extensively used in laboratory fluid mechanics studies since the mid-1980s (Adrian, 1991). PIV is essentially a non-contact, non-intrusive velocity measurement technique that quantifies the movement of small and light particles moving within illuminated planes transecting the body of a fluid. The particles, polypropylene tracers, are expected to accurately follow the underlying flow and to uniformly “seed” the area to be measured.

Under natural light sources it would adequately illuminate the particles visualizing the flow motion. Images of the illuminated surfaces are captured with cameras using various combinations for the timing of the lighting and camera acquisition rate (Adrian, 1991). Velocities are eventually obtained using pattern-recognition algorithms based on statistical methods that allow to “guess with known confidence” where the image patterns are moving in a series of images recorded at known time intervals. Specifically, the recorded images are divided in small “interrogation areas” that are evaluated using statistical means (auto- or cross-correlations) to extract velocities. The process of interrogation is repeated for all areas of the recording leading to a whole-field velocity distribution over the imaged area. LSPIV is a newer sub-family of the PIV technique and it is applied to moving fluid bodies with the objective to quantify velocities at the free surface. The first attempts to extend the PIV methodology for quantifying the velocity at the free surface was made in Japanese rivers in early 1990s (Fujita and Komura, 1994). Given that the areas subjected to velocity measurements are considerable larger than the laboratory-size PIV measured areas this variation of the technique is labeled “Large-scale” PIV. The technique is subsequently applied in laboratory conditions for quantifying velocity at the free surface in hydraulic models for riverine environment (Muste et al. 2008). Ambient light is typically used for visualizing tracers on the free surface in field or laboratory measurements.

The main distinctions between PIV and LSPIV are the size of the measurement volume and the size and characteristics of the tracers used for visualization of the flow. Since the targeted area for LSPIV velocity measurements is order of magnitudes larger than those measured with conventional PIV, the image recording is usually made from an oblique angle. The flow tracers are also considerable larger for LSPIV compared with the micron-size particle used in the laboratory PIV. Practically, the tracers are not anymore individual particles as in PIV but clusters of particles of larger sizes that collectively form floating patterns at the free surface by the moving water body. The oblique angles used for recording inherently introduce distortion of the physical space images due to geometric perspective. The distortion is removed using few selected points contained in the images in conjunction with a geometrical transformation that relates the camera with real-world coordinates. The result of this transformation is that the LSPIV estimated velocities are provided as vectors with actual magnitudes and orientations everywhere over the imaged area. Although LSPIV has been successfully employed in a variety of field and laboratory conditions, there are substantially few reported measurements acquired with the technique in shallow water bodies. Often time these flows are also slow (at times close to zero velocities) and confined within changing and difficult to access boundaries such as in the floodplain flow situations. The non-intrusive and two-dimensional (2D) nature of the measurements coupled with its capability to instantaneously provide velocity over large areas, makes LSPIV a good candidate for the situation and at times the only one possible measurement solution (Nord et al., 2009). The goals for this study are to illustrate that: a) to measure surface flow velocity using Large Scale Particle Image Velocimetry, b) To compare the accuracy of the PIV measurements and decrease the work that has to be done manually and c) To optimize the certainty for each vector and the fluency of the mean frame, the part of the channel that is photographed should be covered with tracers, for each frame of the series

MATERIALS AND METHODOS

In recent years, methods have been developed for using an LSPIV system to measure discharge in open channel. The USGS procedure for evaluating emerging open-channel discharge measurement technologies (Melcher et al., 2002) adopted. In general, the methods developed in this study follow the steps (Harpold A.A. et al., 2006) as shown in Figure 1 and initially, an appropriate location is selected for optimum installation of the equipment using established guidelines (ISO, 1997; Rantz et al., 1982). The images of 8fps are recorded with Camera (Canon EOS 7D) is mounted on a Vanguard tripod and adjusted to remove erroneous illumination of flow. The effect of an oblique camera angle on LSPIV accuracy is investigated using 0°, 15°, 30°, 45° and 90° oblique angles to get best picture (Harpold A.A. et al., 2006). The channel is first seeded with tracer particles that mimic the fluid movement. Subsequently, successive images of the channel surface are recorded and saved. The image quality is enhanced to improve tracer visibility, and spatial distortion is removed prior to velocity estimation. The surface velocity field is estimated using statistical correspondence methods. A representative open channel velocity field is estimated by correcting the surface velocity to account for a non-uniform vertical velocity profile. After the velocity field is estimated, the channel dimensions and stage measurements are used to estimate discharge with area-velocity methods (e.g., midpoint method).

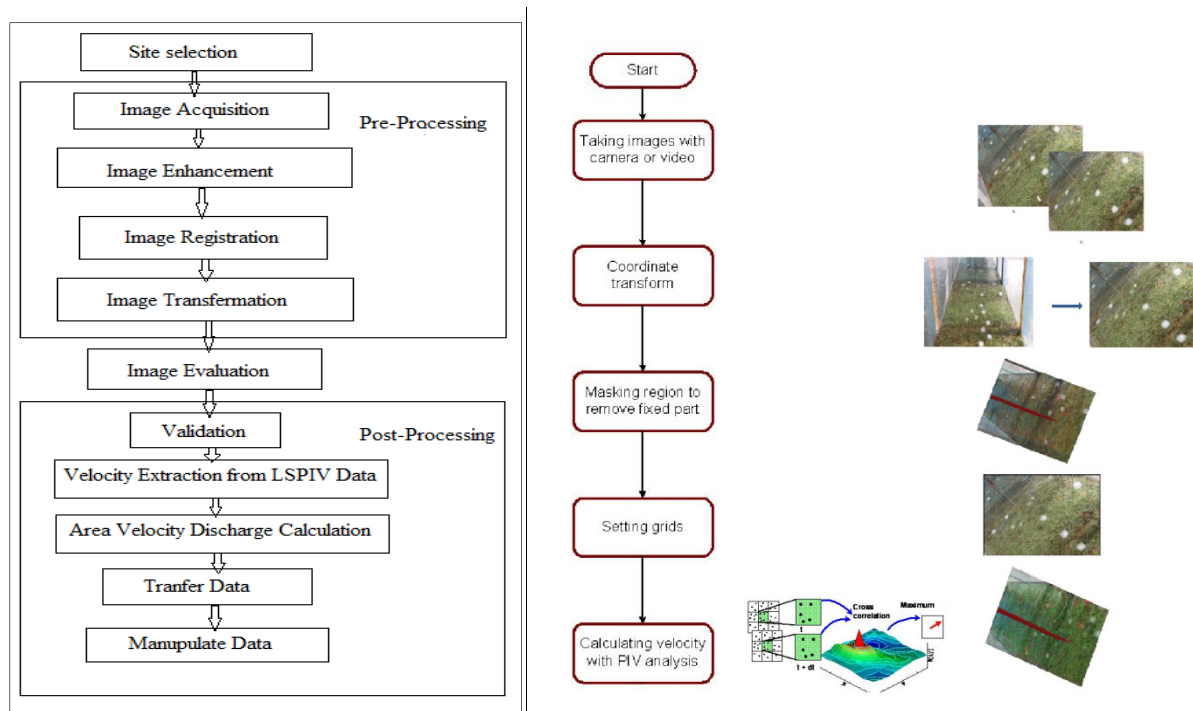


FIGURE 1. Flow Chart of Generalized Steps Involved in LSPIV for Low-Order Stream and LSPIV Measurement Sequence

Pre-Processing. Pre-Processing is must for removing the basic errors obtained in the images. Further, the images are checked with all the errors which going to cause in the post processing. The errors mainly affect the velocity vectors of seeding tracers in the water.

Image Acquisition. Good image acquisition is crucial for obtaining accurate measurements with LSPIV. There are three key components to image acquisition using LSPIV. First, there must be adequate features on the stream or channel surface to capture velocity measurements across the image plane. A homogeneous distribution of particles at a medium seeding density is optimum for image evaluation and the tracers must occupy at least one pixel. Second, the channel must be sufficiently illuminated to create contrast between

the tracers and the water surface. Finally, the camera must be able to capture the image field at the desired frame rate, field of view, and resolution. Appropriate incorporation of all of these components is a prerequisite for the development of a functioning LSPIV system. The image acquisition equipment and procedures used in the laboratory experiments is developed after an extensive review of the literature. The camera used in the study is Canon EOS 7D DSLR camera. This camera is selected because of its high resolution 5184 x 3456, 8 fps continuous shooting speed in image mode, and robustness for outdoor and indoor use. After that a PIVlab tool is used to collect images and the high image capture rate is necessary to capture reasonable pixel displacements for high velocities. An Acer ASPIRE 5733 computer with 4GB RAM, and 2.40 GHz operating speed is used to collect and analyze the data. All forms of PIV analysis using PIVLab must start with importing a series of images.

Image Enhancement. Several aspects of image acquisition can introduce error, such as poor illumination, glare, and shadows. Image enhancement methods can remove some of these errors prior to image evaluation. Image enhancement is performed by altering the pixel values of the recorded image using image-processing software. Typical image enhancement methods used in LSPIV include increasing the signal-to noise ratio, attenuating background noise, and improving the contrast and brightness of the image, DPP (Digital Photo Professional) software is used for Raw Image Processing, Viewing and Editing of images.

Registration and Transformation. In LSPIV laboratory and field applications, the camera is usually at an angle of 90° fixed to the tripod arranged in the channel flow, which introduces spatial distortion. The distortion is corrected through image transformation, which relates the pixels to their physical locations. The transformation can be corrected through implicit parameters of the camera. LSPIV applications, the transformation is explicit, as ground reference points (GRP) are used to numerically optimize the parameters. In the laboratory experiments, registration points are fixed using gauge placed in the flume prior to data collection. Prior to the experiment, the pixel and physical locations of four reference points with respect to flume are found for all the camera angles (0°, 15°, 30°, and 45°). The average dimensions of the pre-processed images are approximately 5184 × 3456 pixels. The images are analyzed to determine tracer displacements using cross-correlation algorithms.

Image Processing Parameters. Several parameters must be specified prior to image evaluation, including the interrogation window size, region of interest (ROI), window-offset scheme, and grid spacing (Adrian, 1991). Optimization of the interrogation window size and location is a principal means of acquiring accurate displacement measurements. The window size must be small enough to preserve the spatial scale of interest (any scale smaller than the window size is lost) and avoid second-order effects (e.g., displacement gradients). The ROI sizes are selected to be four times the maximum displacement in order to deliver minimum displacement error. The ROI sizes varied depending on the size of the image and the average tracer displacement. The laboratory procedure with ROI window size as a first pass, and then a (128, 64) offset window as a second pass. The cross-correlation coefficients and corresponding displacement vectors are calculated at the user-specified grid spacing of 32 pixels. This produced a 12 × 20 or more vector surface velocity field. The image evaluation procedures are used in the laboratory flow analysis. Our image velocimetry algorithm uses the cross- correlation coefficient as a similarity index (Fujita et al., 1998). Cross correlation is computed between an interrogation area (IA) in the first image and interrogation areas located within a search area (SA) in the second image. The pair of particles showing the maximum cross-correlation coefficient is selected as a candidate vector. The cross-correlation coefficient, R_{ab} , is defined as;

$$R_{(a_{ij}, b_{ij})} = \frac{\sum_{\substack{1 \leq i \leq M_i \\ 1 \leq j \leq M_j}} (A - \bar{A}_{ij})(B_{ij} - \bar{B}_{ij})}{\left[\sum_{\substack{1 \leq i \leq M_i \\ 1 \leq j \leq M_j}} (A - \bar{A}_{ij})^2 \sum_{\substack{1 \leq i \leq M_i \\ 1 \leq j \leq M_j}} (B_{ij} - \bar{B}_{ij})^2 \right]^{1/2}} \quad (1)$$

Where M_i and M_j are the respective sizes of the interrogation areas in pixels. $\overline{A_{ij}}$ and $\overline{B_{ij}}$ are the respective distributions of grey-scale intensity in the two images. $\overline{A_{ij}}$ and $\overline{B_{ij}}$ are the mean intensities in that interrogation area used to normalize the intensities. The most probable displacement of the fluid from point in a time interval is the one corresponding to the maximum correlation $R(a_{ij}, b_{ij})$. Our image processing algorithm is similar to the correlation imaging velocimetry of Fincham and Spedding (1997). Both algorithms use a variance normalized correlation, in which each pixel in the IA is equally weighted, such that the background is just as important as the particle images.

Post Processing. Post processing is the analysis window in which all the experimental parameters can be changed to our requirements.

Data Processing. The PIV algorithms are some of the most robust available and well-tested in laboratory settings. After the desired images have been selected for import into PIVLab it is necessary to choose the settings with which the program will analyze the images. It is here that the user is able to setup the interrogation area and the interrogation offset that will determine how PIVLab tracks the particles. It is also possible to setup multiple passes to try to increase the accuracy of the measurements. The multiple pass options work in the exact same way as the initial interrogation window setup. Using ROI can also drastically reduce computation time by eliminating part of the image from the analysis. Image Masks work in the opposite way from ROI. Instead of choosing the area that you wish to analyze, instead you are choosing the area which you chose to ignore.

Vector Validation. This particular set of options allows the user to put local filters on the image to change how PIVLab analyses the data. These filters can remove vectors based on how many standard deviations they are away from the mean or local median.

Image Evaluation Using PIV. Image evaluation techniques use image intensity fields to measure tracer displacements and estimate a surface velocity field. Image evaluation is a critical step in LSPIV, requiring the most specialized techniques. Most LSPIV research has used correspondence techniques to determine particle displacement. Cross-correlation algorithms work well for the velocities and the low seeding densities found in open-channel applications.

Discharge Estimation. The LSPIV velocity measurements are used to calculate discharge using the same area-velocity procedures as other devices (e.g., current meter). In the laboratory, a surface correction factor of 0.95 is used to estimate average velocity from surface velocity. This value is determined from preliminary testing that indicated a parabolic vertical velocity profile. The Plexiglas flume provided minimal resistance, necessitating a smaller correction coefficient. However, at shallower depths, the velocity profile may have changed, which is not reflected in the surface correction coefficient.

EXPERIMENTAL STUDY AND DATA ANALYSIS

An Experiment is conducted on a tilting flume having 12m long, 0.5m wide, and 0.6m depth and a collecting tank with attached pitot tub. The flow is allowed to release from the elevated tank directly connected through pipes and a constant head is maintained by operating the valve. The flow measurements have been taken with various discharges as well as for varying slopes with constant discharges. The actual discharges are calculated through tank measurements. The Concurrent measurements are conducted using LSPIV technique and volumetric method. Measurements are acquired near the flume approximately 10 m long from the inlet of a channel Schematic depicting the experimental setup at Fluid Mechanics laboratory as shown in Figure 3. The LSPIV images are taken using a commercial HD camera shown in Figure 2 (Canon EOS 7D) and fixed to the adjustable tripod. Volumetric method acquires two transects to take readings but LSPIV covering two transects in image. The vector fields at the surface and in the verticals

across the channel are acquired with relatively small amount of effort is less than hour. Continuous images are recorded for different depth of flows to allow for several analyses. Both the techniques are adopted, analyzed manually and the data acquisition software. However the technique requires the tracers to track the flow.

The measured data from a flume with vegetation, coarse aggregate is tabulated in table1 and is used to calculate various flow measurements such as velocity, discharge. The equation is used for the calculation of these values are shown below.

$$V = \frac{C_1 R^{2/3} S^{1/2}}{n} \quad (2)$$

$$Q = A \times V \quad (3)$$



FIGURE2. Canon Eos 7d Professional Camera

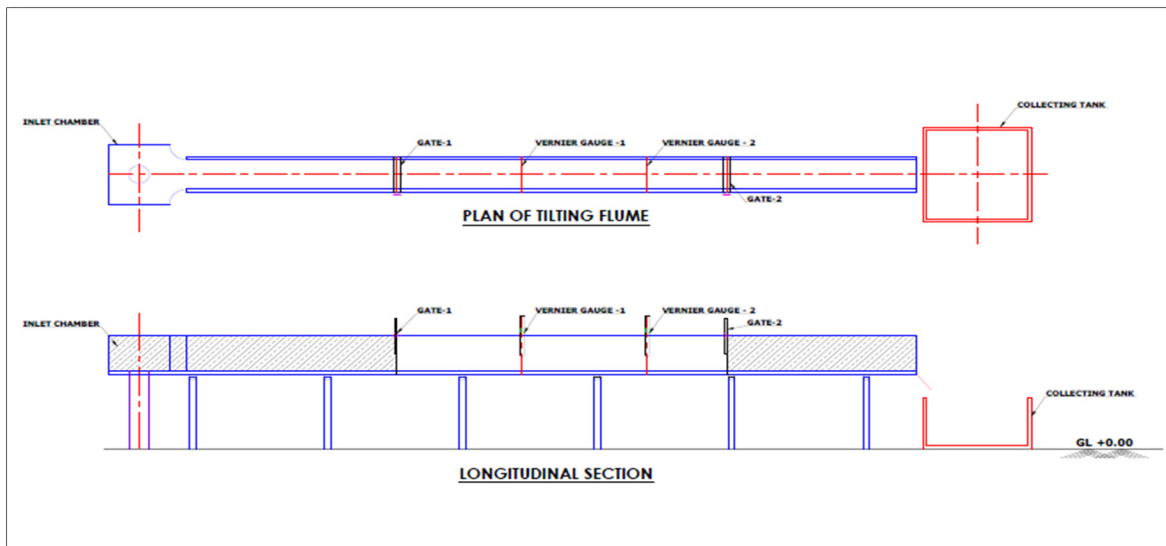


FIGURE 3. Schematic Depicting the Experimental Setup at Fluid Mechanics Laboratory

RESULTS AND DISCUSSIONS

Measuring discharges with traditional methods is time consuming and other errors. Local remote sensing, using imaging systems and appropriate image analysis techniques, could provide a reliable and

cost-effective technique for discharge measurement in some situations. This study examines an image-based non-contact approach in an experiment on the open channel. PIV is used to estimate surface velocities from floating particles that are moving along with the channel flow. Velocity–area methods are then used to estimate discharge at a channel cross section. In most laboratory applications of PIV, flow seeding is needed to assure that there are sufficient flow tracers to compute velocities. This experiment uses artificially introduced seeding particles. Secondly, the ground reference points are required to correlate in the PIVLab with actual measurements.

TABLE 1. Experimental Condition, PIV Surface Velocity and Flume Velocity under Coarse Aggregate.

Date	Water Level(m)	Weather	Recording Local Time	Channel Slope	PIV velocity m/s	Flume Velocity m/s	PIV Discharge m ³ /s x 10 ⁻³	Actual Discharge m ³ /s x 10 ⁻³
2/9/2014	0.053	Sunny	8:04PM	1/1200	0.267	0.258	6.8	6.83
	0.058		8:10 PM		0.268	0.259	7.5	7.51
	0.06		8:14 PM		0.263	0.272	8.03	8.16
6/9/2014	0.06		11:49 AM		0.267	0.278	8.33	8.34
6/9/2014	0.064		11:53 AM		0.297	0.293	9.37	9.37
6/9/2014	0.045	Sunny	12:01 PM	1/600	0.297	0.29	6.25	6.52
	0.052		12:04 PM		0.268	0.263	6.81	6.83
	0.055		12:07 PM		0.283	0.279	7.5	7.67
	0.057		12:10 PM		0.297	0.296	8.33	8.43
6/9/2014	0.06	Sunny	12:18 PM	1/400	0.297	0.311	9.37	9.33
	0.047		12:25 PM		0.291	0.275	6.42	6.46
	0.05		12:28 PM		0.268	0.274	6.81	6.85
	0.052		12:31 PM		0.291	0.286	7.5	7.43
6/9/2014	0.054	Sunny	12:34 PM	1/300	0.297	0.308	8.33	8.31
	0.057		12:37 PM		0.332	0.331	9.37	9.43
	0.045		12:48 PM		0.267	0.273	6.08	6.14
	0.048		12:52 PM		0.297	0.302	7.03	7.24
6/9/2014	0.05	Sunny	12:54 PM	1/240	0.297	0.314	7.75	7.85
	0.053		12:57 PM		0.313	0.317	8.33	8.4
	0.056		12:59 PM		0.332	0.348	9.78	9.74
	0.042		1:05 PM		0.297	0.303	6.25	6.36
6/9/2014	0.046	Sunny	1:08 PM	1/200	0.297	0.306	7.03	7.03
	0.049		1:12 PM		0.2697	0.312	7.5	7.64
	0.05		1:16 PM		0.325	0.337	8.33	8.42
	0.053		1:19 PM		0.335	0.356	9.37	9.43
6/9/2014	0.04	Sunny	1:28 PM	1/171	0.332	0.32	6.25	6.4
	0.044		1:30 PM		0.297	0.311	6.81	6.84
	0.046		1:33 PM		0.332	0.325	7.5	7.47
	0.048		1:36 PM		0.332	0.349	8.33	8.37
6/9/2014	0.05	Sunny	1:39 PM	1/171	0.369	0.377	9.37	9.42
	0.038		3:38 PM		0.335	0.343	6.25	6.51
	0.041		3:42 PM		0.335	0.353	7.25	7.23
	0.044		3:45 PM		0.384	0.387	8.03	8.51
6/9/2014	0.046	Sunny	3:47 PM	1/171	0.38	0.379	8.65	8.71
	0.047		3:51 PM		0.415	0.403	9.37	9.47

LSPIV Velocity Measurements. The velocity vectors measured during the flow release and are performed at different depths for seven slopes. It appeared that the data values are near to the actual velocities but velocity coefficient 0.95 (Tom Vanden Berghe) is used in the laboratory studies for measuring the discharges. In case of flow under vegetation the effect is more in actual measurement. This relatively large variation of flow for the effective height of grass may be explained by the contraction of bed material because of stagnation water.

LSPIV Parameterization and Computations. The image sampling frequency depends on apparent water velocity and is adjusted to obtain pattern displacements of 124 pixels, which is an acceptable compromise to obtain significant displacement of well-correlated patterns. As the view points and velocity magnitudes are different for the varying flows. Image sequences have variable quality, and some of them have sun reflection and shadows. However all the image sequences are used for LSPIV analysis. The LSPIV correlation is performed on squares of gray-scale pixels which are called interrogation areas (IA). The maximum correlation search is restricted to a rectangular domain which is called search area (SA). Surface Velocities of a Channel with Coarse Aggregate and Vegetation as a Bed Material using LSPIV (Slope: 1:1200) are analyzed. Likewise for every slope discharges are measured and tabulated 1 and 2. The comparison of LSPIV surface and discharge measurements with concurrent methods gives a valuable indication of the LSPIV discharge reliability and accuracy. The deviations for both the methods of discharge values an average are -0.075% and +0.094%. The resulting discharge deviation is $\pm 0.05\%$ for vegetation whereas -0.02% is for coarse aggregate.

TABLE 2. Experimental Conditions, PIV Surface Velocity and Flume Velocity under Vegetation.

Date	Water Level(m)	Weather	Recording Local Time	Channel Slope	PIV velocity m/s	Flume Velocity m/s	PIV Discharge x 10^{-3} m ³ /s	Actual Discharge m ³ /s x 10^{-3}
30/08/2014	0.051	Sunny	4:24PM	1/1200	0.249	0.240	6.349	6.12
	0.054		4:28 PM		0.283	0.263	7.641	7.1
	0.058		4:31 PM		0.281	0.270	8.149	7.83
	0.061		4:34 PM		0.281	0.280	8.57	8.54
	0.064		4:37 PM		0.334	0.310	0.01	9.92
30/08/2014	0.047	Sunny	5:46 PM	1/300	0.242	0.265	5.687	6.22
	0.051		6:37 PM		0.222	0.220	5.661	5.61
	0.056		6:40 PM		0.205	0.200	5.74	5.6
	0.058		6:43 PM		0.242	0.240	7.018	6.96
	0.06		6:46 PM		0.268	0.270	8.04	8.1
30/08/2014	0.048	Sunny	7:05 PM	1/240	0.263	0.260	6.312	6.24
30/08/2014	0.052		7:08 PM		0.242	0.262	6.292	6.81
2/9/2014	0.054		12:34 PM		0.335	0.290	9.045	7.83
2/9/2014	0.057		12:37 PM		0.335	0.300	9.547	8.55
2/9/2014	0.059		12:40 PM		0.336	0.320	9.912	9.44
2/9/2014	0.061	Cloudy	2:38 PM	1/600	0.336	0.300	9.912	9.15
	0.065		2:42 PM		0.298	0.310	9.685	0.01
	0.067		2:48 PM		0.297	0.325	9.949	0.01
	0.068		2:52 PM		0.297	0.326	0.010	0.011
	0.071		2:55 PM		0.332	0.328	0.011	0.011
2/9/2014	0.052	Cloudy	5:22 PM	1/400	0.291	0.253	7.566	6.57
	0.056		5:29 PM		0.297	0.255	8.316	7.14
	0.057		5:32 PM		0.297	0.263	8.464	7.49
	0.059		5:35 PM		0.299	0.280	8.82	8.26
	0.062		5:37 PM		0.297	0.310	9.207	9.61
2/9/2014	0.051	Cloudy	12:48 PM	1/200	0.268	0.250	6.834	6.37
	0.052		12:51 PM		0.297	0.280	7.722	7.28
	0.054		12:54 PM		0.297	0.308	8.019	8.31
	0.056		12:57 PM		0.297	0.300	8.316	8.4
	0.058		13:00		0.335	0.326	9.715	9.45
2/9/2014	0.052	Cloudy	1:20 PM	1/171	0.257	0.251	6.682	6.52
	0.054		1:23 PM		0.268	0.265	7.236	7.15
	0.056		1:26 PM		0.267	0.270	7.476	7.56
	0.059		1:28 PM		0.268	0.275	7.906	8.11
	0.061		2:28 PM		0.297	0.310	9.058	9.45

CONCLUSIONS

A new LSPIV technique has been adopted to measure the velocity and discharge of surface flow performed on the tilting flume and it is observed from the study that, the flow velocity varies from minimum 0.20 m/s to maximum of 0.415 m/s for different discharges. It is observed from the Table 1 that, the error in velocity variation is found to be of $\pm 1\%$ when compare with both LSPIV values and the experimental results values when the coarse aggregates used as channel bed materials. It is found from the measurements that, the error in velocity variation is less than 1% when compare with both LSPIV values and the experimental values and the bed material used as Bermuda grass type vegetation. It is concluded based on the results that, the adopted new LSPIV techniques is more suitable for stream flow measurements and have good agreement with volumetric method results. This LSPIV technique is very much useful and reliable for surface flow measurements where there is a difficulty to measure directly. This technique also has advantage for measurement of flow circulation, shear rate and normal strain rate analysis.

REFERENCES

- Adrian, R.J. 1991. Particle-imaging techniques for experimental fluid mechanics. *Annual Review of Fluid Mechanics* 23 (1): 261–304.
- Church, M., Biron, P., Roy A. 2012. *Gravel-bed Rivers: Processes, Tools, Environments*. John Wiley & Son.
- Fincham, A.M., and Spedding, G.R. 1997. “Low cost, high resolution DPIV for measurement of turbulent fluid flow”. *Experiments in Fluids* 23 (1997) 449-462.
- Fujita, I., Komura, S. 1994. “Application of Video Image Analysis for Measurements of River- surface Flows”. *Annual Journal of Hydraulic Engineering*, Japan Society of Civil Engineers, 38: 733-738.
- Fujita, I., Muste, M., Kruger, A. 1998. “Large-Scale Particle Image Velocimetry for flow analysis in Hydraulic Engineering Applications”. *Journal of Hydraulic Research* 36(3), 397-414.
- Harpold, A. A., Mostaghimi, S., Vlachos, P.P., Brannan, K., Dillaha, T. (2006). “Stream Discharge Measurement Using A Large-Scale Particle Image Velocimetry (LSPIV) Prototype.” *American Society of Agricultural and Biological Engineers* Vol. 49(6): 1791–1805.
- ISO 1997. Optimum installation of the equipment using established guidelines.
- Jirka, G.H. 2001. “Large scale flow structures and mixing processes in shallow flows”. *J. Hydraul. Res.*, 39, 567-573.
- Melcher, N. B., Costa, J.E., Haeni, F.P., Cheng, R.T., Thurman, E.M., Buursink, M., Spicer, K.R., Hayes, E., Plant, W.J., C. Keller, and Hayes, K.. 2002. “River discharge measurements by using helicopter-mounted radar.” *Geophysical Res. Letters* 29(22): 411-414.
- Muste, M., Fujita, I., Hauet, A. 2008. “Large-scale particle image velocimetry for measurements in riverine environments”. *Water Resources Research* 44(4):W00D19.
- Nord, G., Esteves, M., Lapetite, J.M., Hauet, A. 2009. “Effect of particle density and inflow concentration of suspended sediment on bedload transport in rill flow”. *Earth Surface Processes and Landforms* 34(2): 253-263.
- Rantz, S.E.1982. “Measurement and Computation of Streamflow”. *Measurement of Stream and Discharge*, vol. 1, Water Supply Paper 2175. US Geological Survey, Washington.
- Simpson, M.R. 2001. *Discharge Measurements Using a Broad-Band Acoustic Doppler Current Profiler*. Open-File Report 01-1, U.S. Geological Survey, Sacramento, CA.
- Tom Vanden Berghe (2013). “Image processing for a LSPIV application on a river”. Thesis Submitted to the ingenieurswetenschappen: bouwkunde.

RADIOSONDE LAUNCH UNDER HIGH SURFACE WIND

Boris S. Yurchak

(EPA, Arlington, VA, USA)

ABSTRACT: Under emergency situation accompanied with hazardous atmospheric releases of pollutants from chemical or nuclear enterprises, the reliability and continuity of the upper-air data flow, which are primarily measured with radiosonde, are of particular importance for mapping the transport of contamination. However, the ability to launch the radiosonde can be strongly impacted by the high surface wind speeds under inclement weather. To increase the speed range of the successful launch, the cone-shaped tower is suggested to be used for launch. Use of the cone-shaped tower will allow for a greater initial height of instrumental box pre-start position as compared with the routine launch method. The tower uses the wind force jointly with the lifting force of the balloon to deliver the instrumental box up to the top of the tower. The installation of the lower part of the tower into the wind shelter secures the operator from contamination and wind impacts and provides the radiosonde launch even in case of very strong wind (i.e., gale, ~ 18–24 m/s). The shelter has a sliding roof with an opening. It is reasonable to convert some of aerological stations, located close to the potentially dangerous enterprises, into proposed secure all-weather facility.

INTRODUCTION

Air pollution dispersion as a result of an accident in potentially dangerous enterprises (PDE) of chemical and nuclear industries is governed by the physical parameters of the Atmospheric Boundary Layer, which are primarily measured with radiosonde (upper-air) sounding. The radiosonde (RS) consists of the balloon filled with a gas lighter than air (hydrogen or helium) and connected with a harness string to the instrumental box consisting of the sensors for meteorological parameters and with the radio transmitter for wirelessly delivering the data to the ground receiver. The balloon filling and other preflight preparation and maintenance procedures are conducted in a shelter (NWS Manual, 2007). The contemporary upper-air (aerological) sounding is carried out up to the moderate surface wind (to 12 m/s) by the operator, usually from the open launching pad located at some distance from the shelter. The RS launching under conditions of the strong surface wind at the speeds of higher than 12 m/s is a complex, physically hard and sometimes even dangerous work for the operator. There is no reliable way to protect the operator from contamination deposition during the launch. The objective of the research presented is to work out a method of RS launching at the wide range of the surface wind speed, which provides safe launch of the instrumental box and ensures the protection of the operator from impacts of strong wind and contamination/debris.

AN EQUATION OF THE SUCCESSFUL LAUNCH

The RS launching at the presence of the wind at the launching pad is provided by the use of some well-known measures briefly considered below using the criteria of the successful launch formulated in (Yurchak, 2013, 2014a):

$$Z_g(t_0) \equiv \frac{z(t_0)}{L} = y + \frac{\pi}{2} \frac{\bar{W}}{\sqrt{gL}} - 2 \sin^2 \frac{\theta}{2} > 0 \quad (1)$$

where $Z_g(t_0)$ is the relative height of RS payload at the moment t_0 ; $t_0 \approx (\pi/2)\sqrt{L/g}$ (L is the length of the harness string, g is the acceleration of gravity) is the time needed for the harness string to take the vertical position after releasing the RS; $z(t_0)$ is the height of the instrumental box above the surface at the vertical position of the harness string at the time moment t_0 ; $y = h/L$, where h is the initial height of the

instrumental box above the surface at the moment of releasing the RS; \bar{W} is the mean speed of the balloon ascent during the time t_0 (equation (20) in (Yurchak, 2013)); θ is the angle of the deviation of the harness string from the vertical at the moment of releasing the RS that depends on surface wind speed (equation (2) in (Yurchak, 2013)). The above equation (inequality) (1) is the theoretical basis for the method presented below.

A CONE TOWER AS THE BASIC ELEMENT TO IMPROVE CONDITION OF RS LAUNCH

As follows from (1), the increase in the initial height of RS release h causes the increasing of the relative height y and, consequently, makes the left part of the inequality greater that mitigates the satisfaction of its condition ($\dots > 0$). This is the primary idea of the proposed technique. It should be noted that known solutions of the problem are based on temporary shortening of the length of the payload harness string (L) with so-called temporarily harness shortening devices (THSD) which brief review has been provided in (Yurchak, 2014a). To put the idea into practice, it is proposed to launch the RS using a cone tower as that schematically shown in Figure 1.

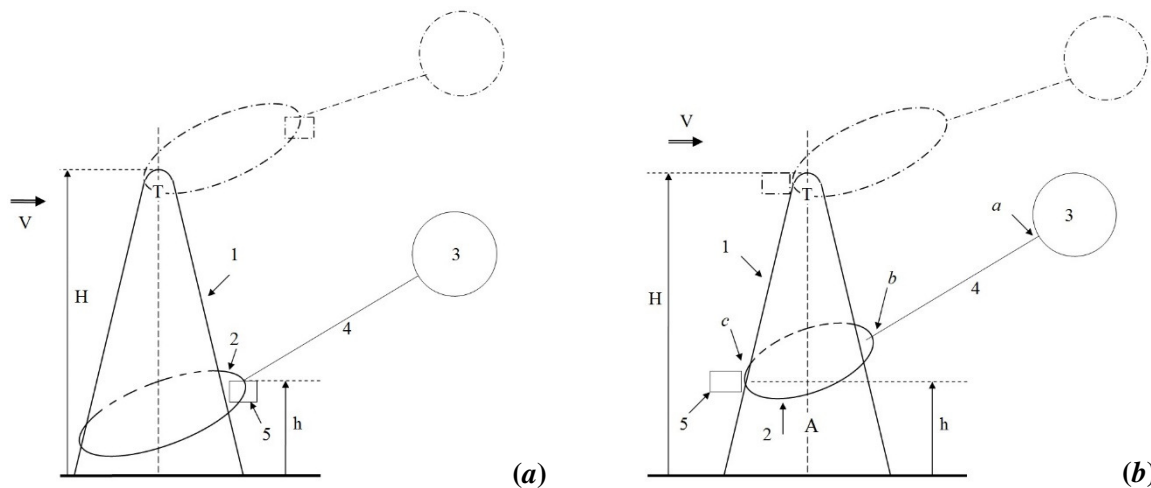


FIGURE 1. A scheme of RS launch using the cone tower. (a) The launching from the leeward side of the tower. (b) The launching from the windward of the tower using the sliding loop as a constituent of the harness string. Designations of the elements are in the text.

An operational principle of the cone tower A is the following: the transportation of the sliding loop 2 (embracing a perimeter of the tower A) is directed along the inclined conic wall 1 with the harness string 4 stretched from the side of the balloon 3 moving under the pressure of the wind force and its own lifting force. Due to the inclination of the lateral wall 1 which lifts the sliding loop 2 and the instrumental box 5 connected with it, to the top of the tower T. The inclined surface of the lateral wall 1 should be smooth in order to minimize the friction with the sliding loop 2. To provide the unimpeded separation of the sliding loop 2, the top T of the tower is rounded. The launch can be carried out at the joining of the instrumental box 5 and the sliding loop 2 both from the lee and windward sides (Figures 1a and 1b, respectively). In the latter case, the sliding loop 2 becomes a constituent of the harness string 4 after the separation from the tower. Other versions of the launching pattern as well as the physical substantiation of the RS harness moving along to the top of the tower are provided in (Yurchak, 2014a, 2014b). The resume of this analysis states the relationship between wind speed and constructive features of the tower to make this moving possible as follows:

$$\cot \left[\theta(V_{\max}) - \frac{\omega(r_T)}{2} \right] \geq k_f \quad (2)$$

where $\theta(V_{\max})$ is the angle of the deviation of the harness string from the vertical at the moment of releasing the RS that depends on surface wind speed V_{\max} (equation (2) in (Yurchak, 2013)); $\omega(r_T) = 2 \cot^{-1}(r_T/H)$ is the vertex angle of the cone tower of base radius r_T and the height H ; k_f is the friction factor of the sliding loop on the surface of the lateral wall of the tower. The smaller the difference between the angle of deviation of the harness string θ and the vertex angle ω , the better is the meeting of inequality (2). Equation (2) helps to find some constructive features of the tower. For example, if one expects $V_{\max}=20$ m/s then $\theta=80^\circ$ (see (2) in (Yurchak, 2013)). If $k_f \leq 0.22$ then $\theta-\omega/2=77.35^\circ$ and it results $\omega=5.3^\circ$. If $H=10-12$ m then $r_T \approx 0.5$ m. It should be noted that even in the case of very high wind speed, when the chord of the balloon is oriented practically horizontally (i.e., $\theta \sim 90^\circ$), the sliding loop 2 has the nonzero component of the driving force which brings the balloon to the upper point of the tower. According to its functional purpose, the cone tower is named a cone launching tower (CLT). The essential property of the CLT is the delivery of the instrumental box to the top of the tower using only the energy of the wind and balloon lift, without using any additional devices and mechanisms. To launch the RS using CLT, the use of THSD is not ruled out from the general point of view. However, a possibility of THSD usage in practice needs additional field testing. If the upper part of the CLT is made of an electromagnetically transparent material, the antennas of the radio equipment including the radar can be installed in the tower for the reception of the telemetry data (Yurchak, 2014b).

SECURE RS LAUNCH USING THE SHELTER

The CLT only is not sufficient for the implementation of the method because it is very difficult for the operator to reach the tower from inflation room and to dock the RS to the sliding loop due to obstructing impact of the strong wind. To resolve the issue, the secure method of the RS launching using the CLT that is partially installed in the room-shelter can be suggested, Figure 2. The launching procedure is as follows. When installing the CLT A in the shelter 6, both halves of the sliding roof 8 are made with half-round notches that adjoin close to the prominent part of the cone tower A in the closed position. This enables carrying out the prestart preparation of the RS in the absolutely wind- and precipitation / contaminant sedimentation-proof room. To provide the unhampered launching of the filled balloon 3 through the open roof 8 along the cone tower A, the second (upper) sliding loop 7 is used, Figure 2a. It is docked with the appendix a (see location of point a in Figure 1b) of the balloon 3. To launch the RS, the roof 8 slides apart and the operator moves the balloon 3 through the open roof 8 gradually releasing the harness string 4. The balloon 3 contacting the edges of the open roof 8 is prevented by the upper sliding loop 7 which does not allow the balloon 3 impacted by the wind to separate from the tower A at the level of the roof 8. When reaching the tower top T, the upper sliding loop 7 slips off (Figure 2b) and the balloon 3 separates from the tower A. After that, the operator releases the instrumental box 5 docked to the lower sliding loop 2 which is transported by this loop to the tower top T along the lateral wall 1 under the influence of the tight harness string 4. The contact of the string 4 with the internal half-rounded edge of the open part of the roof 8 and even its flexure do not affect at all the ability of the instrumental box 5 to reach the tower top T freely and the ability of the lower sliding loop 2 to slip off it subsequently for providing the free flight of the RS, Figure 2c. Other versions of the launching pattern from the shelter using sliding loops as harness string constituents are provided in (Yurchak, 2014a, 2014b). During the RS launching after the opening of the roof 8, the operator remains protected from the direct wind impact and is subjected to the short-term tilt directed (due to the wind impact) precipitation / sedimentation only. If the room-shelter 6 is provided with proper ventilation and heat insulation from auxiliary rooms of the aerological station, the preflight maintaining of the RS can be carried out both at the open and close roof 8 of the shelter 6. It also should be noted when the roof is opened, the difference of wind speed over the shelter and inside the shelter causes

the pressure difference directed (from high to low) out of the shelter. That prevents penetration of the contamination into the shelter and thus is favorable from the point of view of the health protection.

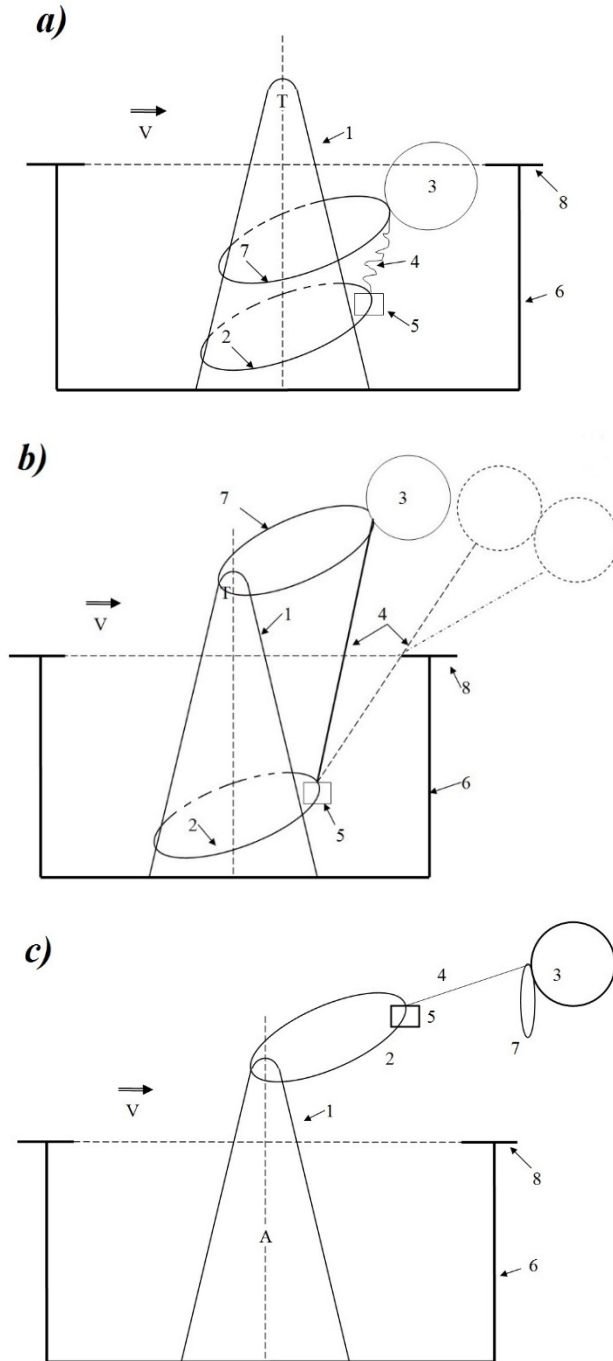


FIGURE 2. Radiosonde launch from the shelter using the cone tower. Designations are in the text.

FIELD MODEL EXPERIMENT

The field model test of the RS launching from the CLT with one and two sliding loops was carried out for the experimental qualitative testing of the feasibility of the proposed technique. The S-78790 signal road cone made of polyvinyl chloride with the height of 70 cm and diameters of base and top equal to 27.5 cm and 5.6 cm, respectively, was used as a cone tower model. The latex balloon having a shape close the ellipse in the inflated state with the major and minor axes of 42 cm and 30 cm, respectively, was used. The strong wind, that causes the deviation of the harness string from the vertical of about 80° , was generated by the industrial vacuum cleaner blowing out. The harness string made of the nylon thread had a length equal to the cone height. The sliding loops were made of the same thread. The instrumental box was imitated by the light cylinder container with diameter of ~ 4.5 cm. As a result of the test, the major principle of the method was corroborated: the balloon moves the sliding loop with the payload fixed to it to the top of the tower using the natural wind force and its own aerostatic lift. It was revealed, additionally, that with using two sliding loops, the sharp upward jerk of the harness string that takes place at the moment of the separation of the upper loop from the tower is reduced. At the same time, the lower loop with the model of the instrumental box reaches the cone top very quickly and moves away from it. It may be assumed this occurrence is due to the disappearance of the friction of the upper loop that, in turn, causes additional acceleration of the lower loop movement along the cone wall. Therefore, this feature is an additional favorable factor for the unhampered launching of the instrumental box from the shelter.

CONCLUSIONS

To extend the range of the surface wind speed that allows for successful radiosonde launch, it is substantiated to use the cone tower; it provides the delivery of radiosonde elements to the desired launching height using the wind energy only. The possibility of the technique is corroborated experimentally by means of the field model testing. To protect the operator against wind, precipitation and contamination from hazardous air-borne pollutants, the cone tower is partly installed in the shelter with the sliding roof. It is shown how the unhampered launching of the radiosonde from the shelter can be done. The radiosonde launch using the cone launching tower within the shelter can be carried out. Not going beyond the area of the aerological station considerably improves the working conditions of aerologists, especially under extreme weather conditions and contaminated environment. To have the reliable and uninterrupted data flow of air physical parameters and to have protected working conditions for personnel of the aerological stations, it is reasonable to convert some of aerological stations, located close to the potentially dangerous enterprises, into proposed secure all-weather facility. The novelties of the method and of the aerological station type have been confirmed by the US patent (Yurchak, 2014b).

REFERENCES

- National Weather Service. 2007. Manual 10-1401. "Operations and Services, Upper Air Program NWSPD 10-14, Radiosonde Observations." Washington, D.C.
- Yurchak, B.S. 2013. "An Assessment of Radiosonde Launch Conditions Affected by the Surface Wind." *Russian Meteorology and Hydrology*, 38(3):159-167.
- Yurchak, B.S. 2014a. "A Technique of Radiosonde Launch under the Surface Wind of High Speed." *Russian Meteorology and Hydrology*, 39(1):38-46.
- Yurchak, B.S. 2014b. "Cone Tower Based Facility and Method for Launching an Atmospheric Sounding Device under Strong Winds." Patent No.: US8,857,759 B2. Date of Patent: Oct. 14, 2014. United States Patent and Trademark Office. Washington, D.C.

**THE CRITICAL PARAMETERS FOR HOW TO ADDRESS OIL/HYDROCARBON
BASED MATERIAL SPILLS**

Steven Pedigo

(OSEI Corp, P.O. Box 515429, Dallas, Texas 75251, USA)¹⁰⁶

The purpose of these actions is to insure a safe for humans, non toxic to marine species clean up that will permanently remove spills from the environment without creating secondary clean up processes trade offs or adverse effects, if possible.

Three basic parameters are main considerations when determining how to clean up an oil/fuel hydrocarbon based material spill. (1) Is the product/process safe for humans? (2) Is the product/process safe for aquatic marine life? (3) Does the product/process permanently remove oil/fuel from the environment in accordance to the US Clean water act, without creating any secondary clean up problems/processes.

There is one Solution that meets these 3 basic criteria, that has been used on over 33,000 spills since 1989, Oil Spill Eater II (OSE II).

The process developed with OSE II emulates mother natures own process, except OSE II speeds the process of converting oil/fuels/hydrocarbon based materials to CO₂ and water in a matter of days to weeks, while mother nature may take 25 to 50 years, allowing the lingering toxicity of the oil I the environment. Oil Spill Eater II the proven, safe for humans, non-toxic to aquatic species, means to permanently remove oil/fuel spills from the environment, without creating any secondary spill problems or clean up processes.

This information is presented to show how and why decisions should be based for spill response and show there is a safe effective means to meet the US Clean Water act, and requirements set forth in other countries.

AN ALTERNATIVE METHOD TO OVERCOME INCONSISTENT CELLULOLYTIC SCREENINGS WHEN USING GRAM'S IODINE

Joshua OHair, Terrance Johnson, Anthony Ejiofor and Suping Zhou
(Tennessee State University, Nashville, TN, USA)

Gram's Iodine is currently used in detection of endoglucanase, a cellulase enzyme which cleaves beta 1-4 glycosidic bonds in carboxymethylcellulose (CMC). However, when a zone of degradation was noticed around non-cellulolytic *Escherichia coli* JM109, Gram's Iodine Assay was further scrutinized. It was during this investigation that a clear ring of degradation around several bacterial colonies was observed in plates containing no cellulose, and on plates containing agar only. However, when agar was removed as a solidifying agent and substituted with phytigel, zones of clearing around all cellulolytic organisms were altered. This led to the conclusion that phytigel should be used as a designated solidifying agent when using the Gram's Iodine Assay for cellulase screening. The use of the improved method can overcome the inconsistency problems for detecting cellulose activity on agar-CMC plates.

LANDSCAPE CHANGES IN LOPÉ NATIONAL PARK, GABON: TO WHAT IS THE EXTENT OF SAVANNAH THICKENING?

Gilbert Gauci

(Environmental Management, University of Stirling, Stirling, Scotland, FK9 4LA, United Kingdom)¹⁰⁸

Savannah thickening and forest encroachment are two phenomena occurring as parallel processes throughout Africa threatening the seasonal use of the habitat by large mammals and the existence of rare specialist and endemic species found in the savannah that are unable to grow in a forest environment. For the past 23 years Lopé National Park, Gabon has been practicing prescribed burning of the savannah in order to slow down the process. Understanding the extent and effects of this process will aid park managers to develop management strategies to tackle conservation threats. The present study aimed at quantifying the extent of savannah thickening in Lopé National Park. A habitat classification was used to classify the change in habitats between open savannah and colonising forest. Using digital photography taken in each cardinal and ordnance direction in October 2008 and February 2016, 10 sites were examined. Using the free software paint.net, a standard grid was overlaid on the photos and each square was assigned a colour according to the habitat classification. The grid technique detected thickening in 6 out of 10 sites, however, thickening was not always detected due to the size of the squares and a qualitative analysis was applied to further describe habitat change. The photo monitoring method is a low-cost method that can be easily replicated. The study concludes with recommendations on how to monitor savannah thickening by making use of citizen science and remote sensing.

**SOCIETY
AND
THE ENVIRONMENT**

PUBLIC PERCEPTION AND ACCEPTANCE OF FERTILIZERS FROM HUMAN URINE AMONG TURKISH CITIZENS HOLDING UNIVERSITY DEGREES

Ayşe D. ALLAR EMEK, Nihan YILDIZ DOĞAN, *Bilsen BELER BAYKAL*
(Istanbul Technical University, Istanbul, Turkey)

ABSTRACT: Human urine is a viable source of fertilizers, through direct use as well as indirect routes. Proper use of this source will contribute to global sustainability, however such practice will not be effective without the acceptance of the final consumers in a target community. Public perception and approval for/acceptance of fertilizers from human urine was investigated in this work among Turkish citizens holding university degrees in two surveys: a generalized one and a more specific one based on the results of the former. The use of human urine as fertilizer received considerable acceptance among citizens with higher education. Indirect use received preference over direct use. Landscape application was more highly accepted in comparison to food stuff. Use in public areas and commons received higher preference as compared to self-use in households. Plants which were cooked received higher acceptance than those which are eaten raw. The level of acceptance decreased with the higher levels of possible urine contact with food stuff. An appreciable acceptance was also observed for industrial plants grown using urine/urine-based fertilizer. Installation of urine diverting toilets (UDT) received acceptance provided that they are supplied free of charge.

INTRODUCTION

Stream segregation is a recent domestic wastewater management approach which claims that domestic wastewater is not a waste to be discarded but a source to be reevaluated. Segregation has to be done at the point of generation and one of the options is Ecological Sanitation (ECOSAN) which suggests separation as yellow/brown/grey water. Of those streams, yellow water is separately collected human urine which is rich in nutrients, with over 80% of nitrogen and 50% of phosphorus in conventional domestic wastewater, but only 1% by volume (Belçer Baykal, 2015). Nutrients are indeed problematic from the perspective of water pollution however; they also constitute the major ingredients of fertilizers. Urine contains macronutrients nitrogen, phosphorus and potassium in a form which is readily available to plants. The idea is to recover nutrients in urine to return them back to soil and to reuse them as fertilizer. This can be done either through direct application of urine onto soil, or through indirect routes, where not the entire urine itself but only nutrients recovered from urine using different processes, are applied onto soil in due course. Direct use of human urine lends concerns including pathogens, pharmaceuticals, hormones and salinity, however, elimination of these drawbacks can be accomplished by processes such as struvite precipitation, ion exchange/adsorption, stripping/absorption. In addition to contributing to sustainability through recovery/recycling/reuse due to this fertilization potential, source separation and ECOSAN is an alternative for conventional water/wastewater management where water pollution can be managed. Urine diverting toilets (UDTs) and urinals help to collect urine separately to make it available for further reuse. Combining the information that the global fertilizer equivalent of human excreta amounts up to about 35% of the global fertilizer consumption, and that one person's urine provides enough fertilization capacity to produce 200 kg of cereals, based on information given by Wach (2007), on an annual basis, with the fact that natural fertilizers are actually excreta of animals, the use of human urine in agriculture seems reasonable.

Several pieces of research work in the literature have provided justification that human urine is an effective source of fertilizers (for example Morgan, 2003; Belçer Baykal et al., 2011a; Kocaturk and Belçer

Baykal, 2012; Andersson, 2015; Ranasinghe et al., 2016). However, putting this proposal into practice on a large scale requires acceptance by the community. Table 1 is prepared to summarize surveys about the acceptance of urine as fertilizer based on those reported in the literature. A survey of those investigations on a general sense shows that typically about half of the respondents have shown acceptance towards the use of urine as fertilizer. As can be seen from the Nigerian case, when given evidence from an actual demonstration field, acceptance by the community seems to increase remarkably. The table also shows that a significant group of farmers were not aware of the fertilizing potential of urine. In a previous survey made with Turkish citizens who were residents of Istanbul, the acceptance for natural fertilizers was 100% while only about half thought synthetic fertilizers were acceptable. There was a considerably higher acceptance for indirect use of human urine as fertilizer after processing as compared to direct use. Landscape plants received a much higher acceptance as compared to food stuff. The use of human urine was more acceptable for plants eaten cooked in comparison to those eaten raw. Self-consumption of plants fertilized with human urine received a slightly lower (3-11%) acceptance than approval of the use of fertilizers (Belar Baykal et al., 2011b).

Table 1. Surveys about the acceptance of urine as fertilizer

Country	Community	Focus	Opinion	Reference
Switzerland	Farmers	Use of fertilizer is a good idea	57% yes	Lienert et al., 2003
Switzerland	Consumers	Will eat vegetables fertilized with urine?	72% yes	Pahl-Wosti et al., 2003
		Preference for urine over artificial fertilizer	80% yes	
Indonesia	Farmers	Use urine and feces based fertilizers?	80% yes	WSP, 2010
		Eager to inform customers about the type of fertilizer used	40% yes	
South Africa	Homedwellers with UDDT*	Currently use fertilizers from toilet pits	2% yes	Okem et al., 2013
		Use own urine as fertilizer	53% yes	
		Use other people's urine as fertilizer	21% yes	
Nigeria	Local community	Use urine as fertilizer (no demonstration)	8% yes	Sridhar et al., 2005
		Use urine as fertilizer (after showing a demonstration field)	80% yes	
		Willingness to build urine diversion toilet (after showing a demonstration field)	95% yes	
Ghana	Farmers	Are not aware of human urine as fertilizer	65% no	Cofie et al., 2011
	Marketers	Accept to sell vegetable fertilized urine	57% yes	
	Consumers	Accept to buy vegetable fertilized with urine	54% yes	
Turkey	Residents of Istanbul	Acceptance of natural fertilizer	100% yes	Belar Baykal et al., 2011b
		Acceptance of synthetic fertilizer	49% yes	
		Direct use of urine as fertilizers	23-55%**	
		Use of fertilizers from urine after processing / indirect use	68-91%**	

* UDDT: Urine diversion dehydration toilet

** for different types of plants: landscape plants, cooked crops, uncooked crops

The aim of this paper is to summarize the results of two preliminary surveys in an attempt to assess the perception and level of acceptance of the use of urine and urine-based fertilizers amongst well educated Turkish citizens. Two sets of questionnaires were done in two consecutive years with respondents holding university degrees. Questionnaires were aimed at finding out public attitude in the segment with higher education towards the utilization of urine as fertilizer for agricultural and landscape purposes as well as for industrial plants, and urine diverting toilets.

MATERIAL AND METHODS

Of the two sets of questionnaires, the first one was directed towards general acceptance of reuse of human urine while the second was focused upon more specific issues taking first one as basis. The first survey had 252 respondents while the second one had 358, a total of 610 respondents, all of which received university education (bachelor degree or higher education). In addition to personal data like age, gender, education, occupation, residence etc., the first questionnaire was directed at assessing (Allar, 2015)

- acceptance of natural and synthetic fertilizers
- approval of using urine directly as fertilizer for specified products
- willingness to self-consume specified products that were fertilized directly using urine
- approval of using processed urine as fertilizer for specified products (i.e. indirect use)
- willingness to self-consume specified products that were fertilized with processed urine (i.e. indirect use)

where the specified products were landscape plants, plants which are consumed after cooking, and plants which are consumed raw.

The second questionnaire explored further (Yildiz-Dogan et al., 2015)

- approval of the use of urine directly/indirectly for different types of plants which included cereals, nuts and fruits which grow on trees, fruits that grow on the ground, which had different chances to be in contact with the urine/urine-based fertilizer applied
- approval of the use of urine directly/indirectly for different types of green areas which included landscape areas, parks, stadiums, home gardens, picnic areas, school gardens
- approval for self-use of industrial plants which included cotton, tobacco/cigarettes, sugar/chocolate, wicker basket fertilized with urine
- motivations/obstacles for using UDTs
- willingness to install and use UDTs

The participants were Turkish citizens who were currently living in Istanbul, in the range of 18-60 years of age, the largest percentage of which was between 20-30. The participants were from different cities of the country, educational backgrounds and occupations. 55% (335 respondents) of the respondents were female, while the rest 45% (275 respondents) were male.

Most of the questions were in multiple-choice format, which requested respondents to choose the most appropriate answer. Additionally, respondents were asked to state any concerns and comments regarding the use of urine as fertilizer. No information about urine-based fertilizers and UDTs were given, so that participants could make decisions based on their existing knowledge on urine, environmental pollution and sustainability.

The surveys were conducted through both face-to-face and internet questionnaires. The analysis of the surveys was based on results as simple head counts and their respective percentages.

RESULTS AND DISCUSSION

Almost all of the participating individuals (98% of the total of 610 respondents) indicated that they would accept the use of natural fertilizers, however, only 22% approved of the use of synthetic fertilizers, a considerably lower percentage as compared to Table 1.

Figure 1, summarizing the outcome of the first survey, shows the approval of using urine and willingness for self-consumption of products that were fertilized with urine directly or indirectly for landscape plants, cooked and raw crops. The approval of using urine and willingness for self-consumption of plants fertilized through indirect use of urine was higher as compared to direct use. This was true for all three groups of plants questioned. The gap between direct and indirect use was less pronounced for landscape use as compared to plants which are eaten either raw or cooked. The approval and willingness for self-consumption was highest for landscape plants and lowest for plants which are consumed raw. With Turkish citizens holding university degrees, the results in terms of approval and willingness for self-consumption of plants grown with urine-based fertilizers were comparable, within $\pm 2\%$. The acceptance

levels for both were 74% for direct use and 86% for indirect use for landscape plants, 45% for direct use and 65% for indirect use for cooked crops, and 31% for direct use and 56% for indirect use for uncooked crops. This is to be compared to 3-11% lower willingness for self-consumption as compared to acceptance observed in the previous study (Belar Baykal et al., 2011b) without any differentiation in terms of educational level. The difference was more obvious when direct and indirect use was compared as well as in terms of different type of plants produced as shown in Figure 1. Indirect use was clearly preferred over direct use and landscape plants received the highest acceptance, followed by cooked crops and finally uncooked crops.

Following the first survey, more detailed questioning was adopted in the second survey. Different types of food groups were chosen to observe how people's attitudes will change with the changing proximity of urine-based fertilizer to the food products including fruits from ground, fruits from trees, nuts, and cereals. Considering the entire set of products, the maximum level of acceptance of direct use was 11% for nuts. Acceptance for indirect use was in the order of cereals, nuts, fruits from trees, fruits from ground, cooked vegetables and non-cooked vegetables and ranged between 36-54% as shown in Figure 2. This was in line with the results of the first survey. As expected, the level of acceptance decreases with the higher levels of possible urine contact with food, i.e. the lowest acceptance was for fruits from the ground which will have the highest probability of contact. Likewise, the level of acceptance for application on uncooked vegetables was lower as compared to cooked ones due to higher possible bacteriological risks associated with the former. Of the total respondents, 32-56% said they would rather have no use of urine-based fertilizers applied to food stuff. Of the products questioned, the highest disapproval was for uncooked vegetables with 56% followed by fruits from ground with 53%. Under all circumstances, indirect use received far more acceptance as compared to direct use and the levels of acceptance were 5-8 times that of direct use.

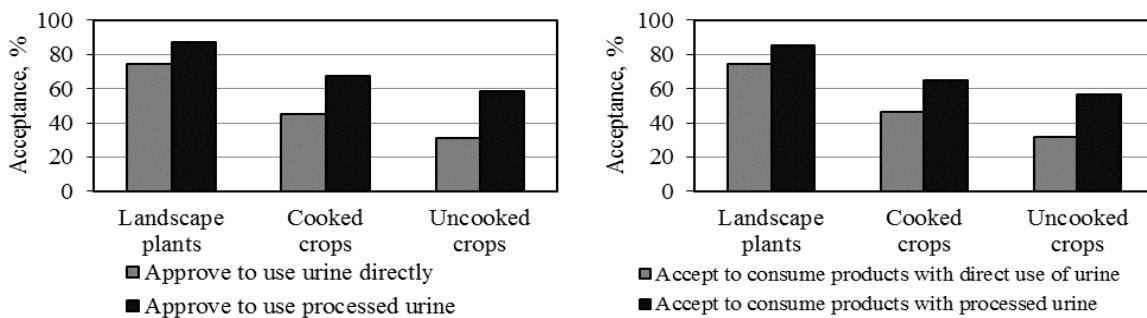


FIGURE 1. Approval of using urine as fertilizer directly or indirectly and willingness to consume products that were fertilized with urine directly or indirectly

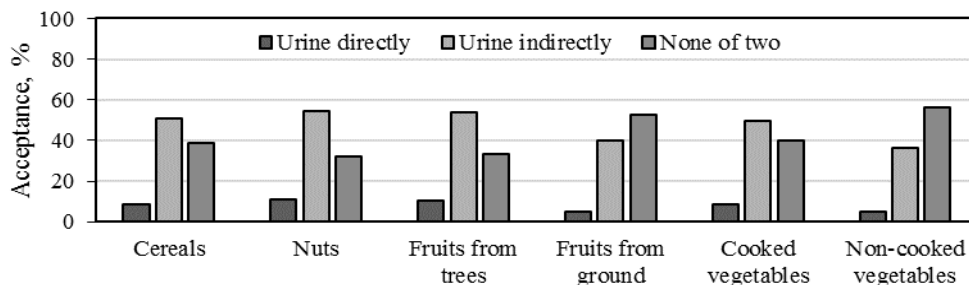


FIGURE 2. Application of human urine for various food types

A more detailed survey was also included in the second part regarding green areas which was detailed as landscape areas, parks, stadiums, home gardens, picnic areas and school gardens. As expected, people were observed to question the use of urine more when the point of use was in closer proximity. As shown in Figure 3, stadiums, parks and landscape areas received higher acceptance for both direct and indirect use as compared to home gardens, picnic areas, school gardens. Once again, under all circumstances, indirect use received far more acceptance as compared to direct use, as in the case of food stuff and the levels of acceptance for indirect use were 2-3 times that of direct application. 19-41% of the respondents indicated that they would prefer not to have any urine-based fertilizers applied.

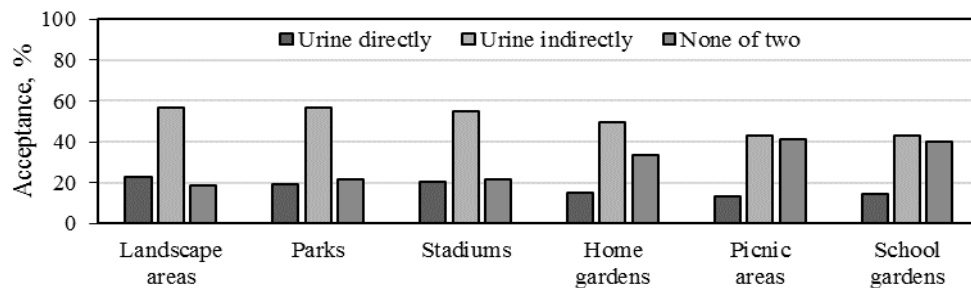


FIGURE 3. Application of human urine in various green areas

Another question in this study was directed towards finding out participants' attitude to wearing a cotton dress manufactured in a farm fertilized with urine/urine-based fertilizer. According to the results, 65% of the respondents answered as 'Yes, I would wear one' while, 34% of all did not find this idea appealing. This high ratio was taken as a starting point for investigating the reuse of human urine for non-edible industrial products as exemplified by cotton, and motivated the investigation of the use of urine for other industrial products. As an attempt to begin this, another small survey was conducted with 107 people to see acceptance towards the use of industrial products fertilized with urine/urine-based fertilizer. The results have revealed that at least 50% of the respondents were willing to use those products including chocolate made of sugar produced with fertilizer of urine origin and cigarettes as shown in Figure 4. The highest acceptance in this group was for wicker basket with 77%. Acceptance for cotton was 62% for this part which was comparable with 65% observed in the main survey.

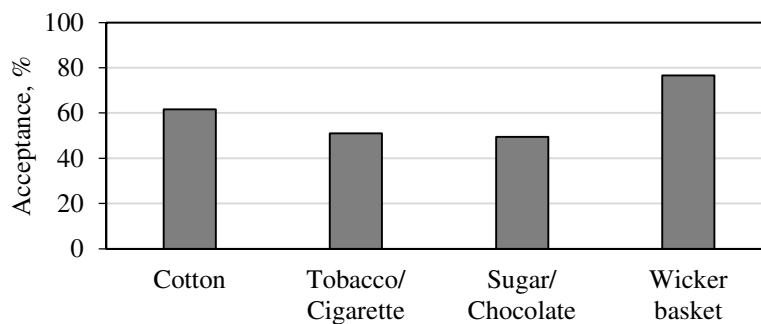


FIGURE 4. Acceptance of the use of human urine for industrial plants/production

Going back to the results of the second survey, 44% of the respondents said they were aware of the fertilization value of human urine. In response to the question 'Do you think urine can be collected separately to make fertilizer out of it?' 82% of the respondents answered as 'Yes' which is considered as a high ratio showing that people think it can be done. Similarly, respondents replied positively with 81% to practice it themselves.

The most interesting point regarding UDTs was the willingness to pay money for these toilets. The idea of paying extra money for the installation of a UDT was rejected by 70% of the participants. However, when the question was asked as ‘Would you allow a UDT to be installed at your home for free?’, acceptance raised to 77% as seen in Figure 5. These numbers illustrate how the financing/funding of this new approach is linked with the acceptance level.

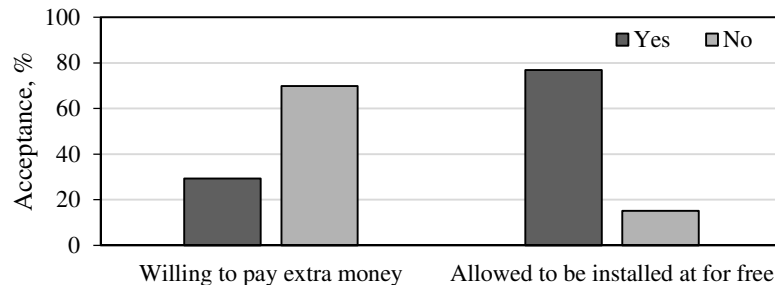


FIGURE 5. Willing to pay money for UDTs

Throughout both parts of the survey, the participants were asked to state their concerns and comments about the use of urine/urine-based fertilizers, too. Those who indicated concern were uncomfortable about the idea of using urine from a psychological point of view. They also had uncertainties about the reliability of utilization including human health aspects, especially pharmaceuticals, and pathogenic safety in terms of the use of urine as fertilizer. Several had expressed other concerns including odor and religious reasons.

CONCLUSION

Results have indicated that as opposed to almost 100% acceptance of natural fertilizers (animal excreta), synthetic fertilizers got the approval of less than 25% of the respondents. The use of human urine as fertilizer received considerable acceptance. Indirect use received an obvious preference over direct use. Landscape application was the most highly accepted one. Use in public areas and commons received higher preference as compared to respondents' own premises. Plants which were cooked received higher acceptance than those which are eaten raw. The level of acceptance decreased with the higher levels of possible urine contact with food stuff. An appreciable acceptance was also observed for industrial plants grown using urine/urine-based fertilizers. Installation of UDTs received quite a high level of acceptance provided that they are supplied free of charge.

Source separation of urine and recovery of nutrients is a promising source of fertilizers. Creating value from this 'waste' by recovering and reusing plant nutrients in urine will lead to a sustainable future through closing the nutrient loop. There is an appreciable amount of acceptance of this approach by highly educated Turkish citizens. This will most probably be enhanced through future public education.

REFERENCES

- Allar, A. D. 2015. *Alternatives for Indirect Use of Urine as Fertilizer through Processing with Clinoptilolite* (İnsan İdrarının Gübre Olarak Dolaylı Kullanımında Klinoptilolitle Muamele ve Alternatifleri). PhD Thesis, Istanbul Technical University, Istanbul, Turkey (in Turkish with extended abstract in English).
- Andersson, E. 2014. "Turning waste into value: using human urine to enrich soils for sustainable food production in Uganda." *J. Clean. Prod.* 96:290-298.
- Beler Baykal, B. 2015. "Stream segregation in household use: A review of grey water as an alternative source of water and yellow water as an alternative source of fertilizers." *Water Quality, Exposure and Health* 7:27-37.

- Belér Baykal, B., A.D. Allar, and S. Bayram. 2011a. "Nitrogen recovery from source-separated human urine using clinoptilolite and preliminary results of its use as fertilizer". *Water Sci. Technol.* 63(4):811-817.
- Belér Baykal, B., A. D. Allar, and E. D. Bozkir. 2011b. "A preliminary survey of the public acceptance of the use of human urine as fertilizer in Turkey." III. International Congress Smallwat11 on Wastewater in Small Communities. Towards the Water Framework Directive (WFD) and the Millennium Development Goals (MDG), April 25-28, Seville, Spain.
- Bonvin C., B. Etter, K. M. Udert, E. Frossard, S. Nanzer, F. Tamburini, and A. Oberson. 2015. "Plant uptake of phosphorus and nitrogen recycled from synthetic source-separated urine." *Ambio* 44(2):217-227.
- Cofie, O., P. Amoah, I. Egyir, N. Adamtey and F. Tettey-lower. 2011. "Demonstration on the use of urine in urban agriculture." SWITCH Sustainable Water Management in the city of the future, Final Report. http://www.switchurbanwater.eu/outputs/pdfs/W5-2_GEN_RPT_D5.2.4_Demonstration_on_the_use_of_urine_in_urban_agriculture.pdf.
- Kocaturk, N.P., and B. Belér Baykal. 2012. "Recovery of plant nutrients from dilute solutions of human urine and preliminary investigations of pot trials". *Clean - Soil, Air, Water* 40(5): 538-544.
- Lienert, J., M. Haller, A. Berner, M. Stauffacher, and T. A. Larsen. 2003. "How farmers in Switzerland perceive fertilizers from recycled anthropogenic nutrients (urine)." *Water Sci. Technol.* 48(1):47-56.
- Morgan, P., 2003. "Experiments using urine and humus derived from ecological toilets as a source of nutrients for growing crops." 3th World Water Forum, March 16-23, <http://aquamor.tripod.com/KYOTO.htm>.
- Okem A. E., S. Xullu, E. Tilley, C. Buckley, and E. Roma. 2013. "Assessing perceptions and willingness to use urine in agriculture: A case study from rural areas of eThekweni municipality, South Africa." *J. Water Sanitation and Hygiene for Development* 3(4): 582-591.
- Pahl-Wosti, C., A. Schönborn, N. Willi, J. Muncke, and T. A. Larsen. 2003. "Investigating consumer attitudes towards the new technology of urine separation." *Water Sci. Technol.* 48(1):57-65.
- Ranasinghe E. S. S., C. L. S. M. Karunaratne, C. K. Beneragama, and B. G. G. Wijesooriya. 2016. "Human urine as a low cost and effective nitrogen fertilizer for bean production." *Procedia Food Science* 6:279-282.
- Sridhar, M. K. C., A. O. Coker, G. O. Adeoye, and I. O. Akinjogbin. 2005. "Urine harvesting and utilization for cultivation of selected crops: trials from Ibadan, South West Nigeria." The 3rd International Ecological Sanitation Conference, 23-26 May, Durban, South Africa. http://conference2005.ecosan.org/papers/sridhar_et_al.pdf.
- Yildiz-Dogan, F. N., M. S. Shihab, F. T. Citak, B. Belér-Baykal, M. E. Pasaoglu, and A. Ozturk, 2015. "A preliminary survey of public willingness and acceptance of segregation and use of human-urine as fertilizer in Turkey." 2nd ICSAE 2015 International Conference on Sustainable Agriculture and Environment, Abstract Book, 116, September 30-October 3, Konya, Turkey. http://www.2ndicsae.org/docs/abstrack_book.pdf.
- Wach, F. G. 2007. "Sustainable water management and Ecological Sanitation." TUBITAK Marmara Research Center Chemistry and Environment Institute, Zer0-M Course on Sustainable Water Management and Technologies, April 16-17, Kocaeli, Turkey.
- WSP 2010. Ecological sanitation, social factors impacting use of EcoSan in rural Indonesia (Researcher Entin Sriani Muslim). Water and Sanitation Program (World Bank). https://www.wsp.org/sites/wsp.org/files/publications/WSP_EcoSan.pdf (accessed on July 24, 2015).

Fragmented Stakeholders: Unaccountable Representatives

Yaw Amo Sarpong; Nelson Owusu Ansah, **Francisca Amoatema**
(Bureau of Integrated Rural Development, KNUST, Ghana)
Emmanuel Marfo
(Forestry Research Institute of Ghana, Ghana)

Democratic representation has gained increased attention globally as a mechanism of promoting good governance and management of the environment and natural resources. Stakeholders are critical players in every democratic representation process. However, little scientific work has been done to assess the nature of stakeholder groups and whether the current model of representation has indeed been an effective mechanism in ensuring grassroots participation in the natural resource sector. This study therefore examined the peculiar challenge of stakeholder organization and participation in the natural resource sector and how that may affect democratic representation. A sample of 30 stakeholder groups who participated in a multi-stakeholder dialogue was selected for the study. The survey results showed that 37% of the stakeholder groups were not organized into any formal grouping. Content analysis and observation done further indicated that the 37% constitute grassroots stakeholder groups who are rarely included in decision-making process in the management of natural resources. Using the democratic representation theory as a lens to investigate the participation approach, it was realized that, the engagement process fails to promote accountability since representatives are unable to solicit views and provide feedback to the larger constituents. It further confirms the notion that participation in the natural resource sector is superficial and a mere rhetoric. The de facto management approach alienates the grassroots from substantive participation in the decision-making process.

SOME REMARKS TO RISK ASSESSMENTS OF NUCLEAR POWER PLANTS (NPP)

*Alexander Valyaev*¹, Gurgun Aleksanyan², Alexey Valyaev³

(¹Nuclear Safety Institute of Russian Academy of Sciences, Moscow, Russia; ²Yerevan State University, Yerevan, Republic of Armenia; ³The University of Sydney, Australia, NSW 2049)

Today NPP using for energy production is constantly increasing in the world with the growth of different threats, for example, caused by directed terrorist attacks. It is necessary to make possible correct assessments of corresponding risks levels in common case and for single NPP from moment of NPP projecting, building and especially during its exploitation. It demands to provide exclusive attention and special conditions under realization of complex integrated emergency NPP management.

We use our universal formula for assessment of the total vector of limited losses under NPP exploitation for the fixed time interval under the following assumptions: (1) at initial state the object is in normal (non accidents) exploitation; (2) the different kinds of accidents may be occurred as noticed $i=2, 3, \dots, m$, where m is the total number of possible accidents ($m=1$ is corresponded to the normal regime); (3) every accident may create the different kinds of losses. (4) realization of i accident creates the loss of j kind with P_{ij} probability,

$$\vec{a}_{lim} = P(1)\vec{a}_{1n} + \sum_{i=2}^m \hat{P}_{ij}\vec{a}_j \quad (1)$$

Here j is the kind of loss with a_j value. Then $j = 1, 2, \dots, n$, where n is the total number of possible kinds of losses; where $P(1)$ is the probability of loss formation under normal exploitation; \vec{a}_{1n} is the vector of limited loss under regular exploitation. $P_{ij}a_j$ coordinate vector value in sum is equal the loss value of j kind under realization of i kind accident. Thus the matrix of loss probabilities is determined. Under absent of accidents \vec{a}_{lim} total vector is determined only the first part of (1) formula.

The correct assessment of loss probability matrix elements is the main global problem. If representative statistic data, obtained for long NPP exploitation period, are present, then some of its elements may be assessed by statistic methods. We have predicted the irradiation doses and corresponded risks for population under implementation of Russian Federal Program: "Development of Russian atomic energy industrial complex on 2007-2020 years at 10 homeland NPP that operated during some last decades. But early some types of NPP disasters were absent at researched NPP. Using of classic methods of expertise assessments is not correct in this case. Some needed data may be obtained from primary virtual computer tests of concrete NPP with imitation of possible disasters. It allows to assess risk values and also to plan the actions for NPP operators and special services under serious NPP disasters or may be to prevent them at all. These problems are under detail consideration in our communication.

COST-RISK ANALYSIS OF SOLAR RADIATION MANAGEMENT

Mohammad Mohammadi Khabbazan, *Elnaz Roshan*, and Hermann Held (Center for Earth System Research and Sustainability (CEN), University of Hamburg, Grindelberg 5, 20144 Hamburg, Germany)

Potential side-effects of solar-radiation management (SRM) should be taken into account before society decides on its implementation as a climate policy option to alleviate anthropogenic global warming. Here we evaluate SRM alongside mitigation considering precipitation change as the so far most prominent side-effect of SRM and probabilistic knowledge about climate sensitivity. To do so, we perform a cost-risk analysis, which trades off expected welfare-loss from mitigation and SRM costs, and the risk from transgressing climate targets. We maximize social welfare for the following three scenarios: temperature-risk-only, precipitation-risk-only, and both-risks. Our simulations show that in the temperature-risk-only scenario, perfect compliance with 2°-temperature target is attained for all numerically represented climate sensitivities while the 2°-compatible precipitation corridor is violated. Our analysis of the precipitation-risk-only scenario displays that precipitation and temperature remain confined to their targets for all and more than half of climate sensitivities, respectively. When both precipitation and temperature risks are activated with equal weights in both-risks scenario, almost 95% and perfect compliance can be achieved for temperature and precipitation targets, respectively. The results suggest that welfare in joint-mitigation-SRM analysis converges to welfare in no-climate-policy option. However, the average welfare-loss from mitigation cost plus climate risk is about 3.6% over the scenarios in a mitigation-only analysis compared to no-climate-policy option.

**IN LIGHT OF INFRASTRUCTURE AND CONSTRUCTION AFFORDABILITY, CAN
SOUTHEAST QUEENSLAND CATER FOR CURRENT POPULATION FORECASTS?**

Kirsty Miller (Undergraduate Student at the Queensland University of Technology, Brisbane,
Queensland, Australia)

David Hood (Queensland University of Technology, Brisbane, Queensland, Australia)

Without a significant increase in development of infrastructure and better housing affordability, the region of Southeast Queensland, Australia, will not be able to cater for current forecasts in population growth. This study investigates the discourse of population growth, the impacts that substantial growth can cause, and looks at solutions to these issues. It is proposed that when humans recognize that we live on a finite planet, with finite resources, we simply cannot provide for infinite population growth.

Most infrastructure in this densely populated region is aged, and plans for restoration do not adequately consider resilience to extreme weather events likely from global warming. Furthermore, due to increasing urbanisation over recent years, there is a high demand for dwellings in the region. This is pushing rental and property prices beyond the reach of most incoming residents. More and more are relying on housing assistance. With increasing population size, these stresses exacerbate. The growth of the region needs to be focused on consolidation with the better assistance from Government through planning and support programs. As urbanization has already resulted in highly populated suburbs it is recognized that current growth management plans often sacrifice the liveability of the region. Opportunities such as utilising biophilic urbanism to relieve the pressures of population growth are discussed. Based on the research in this paper, recommendations are proposed for further research.

**SCIENCE, POLITICAL POLARIZATION, AND HOW HYDRAULIC FRACTURING IS
FRAMED AS ENVIRONMENTALLY SAFE OR RISKY**

Michelle L. Edwards

(Texas Christian University, Fort Worth, TX, USA)

ABSTRACT: Environmental science issues have become increasingly politically polarized in America (McCright and Dunlap 2011). From energy production to global climate change, conflicts originating between political party elites have begun diffusing through the general public. Additionally, social scientists have found an increasing divergence in trust in the scientific community among liberals and conservatives over the past 30 years, with conservatives becoming increasingly less trusting of the scientific community (Gauchat 2012). However, scholars have recently found support for the “contextual thesis” that both liberals and conservatives express distrust in science when it challenges their ideological worldviews (Nisbet et al. 2015). Using semi-structured, in-depth interviews, this study explores societal perceptions of hydraulic fracturing to extract unconventional natural gas resources in the Dallas-Fort Worth region of Texas. Results demonstrated that key informants who have been actively involved in the debate over “frac’ing” in this region – both in support of “frac’ing” and in opposition to it – often rely on scientific arguments to frame the hydraulic fracturing process as either environmentally safe or risky. Similar to the “contextual thesis,” participants often identified scientific findings, or interpreted the absence of findings, in ways that likely fit their ideological worldviews.

INTRODUCTION

The United States continually seeks new sources of energy to support its growing demands. One of these new sources of energy is unconventional natural gas, which, due to recent technological advances, can now be extracted from the ground using hydraulic fracturing or “frac’ing” (or “fracking”). While some have praised frac’ing for its contributions to energy production, others have questioned whether its potential benefits outweigh its potential risks, particularly in terms of its environmental impacts. Some researchers have begun to explore residents’ perceptions toward hydraulic fracturing. This study furthers this research by considering how individuals involved in the debate in the Dallas-Fort Worth region use scientific arguments to frame frac’ing as either environmentally safe or risky.

Increased Use of Hydraulic Fracturing. Though hydraulic fracturing was originally developed in the late 1940s, advances in horizontal drilling techniques and the discovery of large new gas reserves have recently driven a massive increase in this form of natural gas extraction (Ladd 2013). According to the Energy Information Administration (2016), hydraulic fracturing accounts for about two-thirds of U.S. natural gas production. One prominent site for this energy development has been the Barnett Shale field underneath the Dallas-Fort Worth region. Large-scale horizontal drilling began in this region around 2005, with higher productivity areas tapped first (Jackson et al. 2014). By 2011, median initial production rates had actually increased, in part due to companies increasing production through “tailoring their practices to local geology,” as well as increasing the intensity of extraction (Jackson et al. 2014:331-332). Refracturing wells has also contributed to estimated ultimate recovery in the region.

Many individuals have questioned whether the potential economic benefits of this type of energy development outweigh its potential risks. Major concerns expressed about hydraulic fracturing often relate to its potential environmental impacts, including: increased water pollution for groundwater and surface water, decreased water availability, increased air pollution and greenhouse gas emissions, and induced seismicity associated with hydraulic fracturing and wastewater disposal (Jackson et al. 2014).

Public Perceptions of Hydraulic Fracturing. Scholars have also examined the public's perceptions of hydraulic fracturing. In the Barnett Shale region, social scientists focused originally on the perceptions of rural residents in communities experiencing unconventional energy development (Anderson and Theodori 2009; Theodori 2009; Wynveen 2011). These studies highlighted both the perceived positive economic benefits and improved services resulting from this development, as well as the potential concerns residents held about the impacts of frac'ing on public health, community safety, and the environment.

However, as development has expanded, public opinion researchers have also expanded their sampling frames beyond those directly affected by hydraulic fracturing. National surveys of American adults have demonstrated that only a minority of Americans are aware of and have formed an opinion on frac'ing (Boudet et al. 2014), with fairly similar percentages of supporters and opponents (Davis and Fisk 2014). Political views play a key role in predicting Americans' perceptions on frac'ing, with political conservatives more likely to be supporters of frac'ing (Boudet et al. 2014); and Democrats more likely to support greater regulation of frac'ing (Davis and Fisk 2014). Researchers have also found political conservatives to perceive frac'ing as less risky compared to liberals (Choma et al. 2016).

Scholars have also found a negative relationship between support for hydraulic fracturing and how much a person had heard or read about it (Boudet et al. 2014). Those with greater basic objective knowledge about frac'ing also tend to have higher perceptions of risk related to frac'ing than those with less knowledge (Choma et al. 2016). However, Choma et al. found that frac'ing knowledge tended to "strengthen conservatives' belief that fracking does *not* present risks" (2016:113). While these studies are useful for capturing the public's overall support or opposition to hydraulic fracturing, they do not capture how stakeholders with varied views on frac'ing use science to frame their position on risk.

METHODS

Data Collection. In 2015 and 2016, I conducted in-depth interviews with key informants in the Dallas-Fort Worth (DFW) region to gain insight into the public's perceptions of hydraulic fracturing as environmentally risky or safe. I interviewed individuals who represent a wide variety of views including: residents, scientists, community activists, realtors, industry representatives, business owners, and government regulators familiar with frac'ing in the region. As past research has demonstrated, semi-structured in-depth interviews allow a researcher to "explore a topic more deeply" through allowing respondents to "shape the order and structure of the interview" to fit their own experiences (Esterberg 2002:87).

Analysis. Following transcription of the interviews, I analyzed the data using the two-stage coding techniques described by Esterberg (2002). In the first stage, I utilized open coding to analyze each line of the interview for conceptual categories. In the second stage, I sorted the earlier-found information into more clearly defined thematic groups and reanalyzed the interviews using focused coding.

RESULTS

Participants discussed how science impacted perceptions of hydraulic fracturing as environmentally safe or risky along three major themes: 1) hydraulic fracturing as a complex, scientific process, 2) selective interpretation of science and scientists, and 3) absence of scientific information.

Hydraulic Fracturing as a Complex, Scientific Process. Opponents and supporters of hydraulic fracturing described this process as complex and highly technical. For some participants, their confidence in the safety of hydraulic fracturing was rooted in the technical nature of this process. For example, one participant described his experience visiting a frac site:

People watch the movie, for instance, "There Will Be Blood," and they think, "my God, this is just the wild West. You go out, you dig a hole, oil shoots all over the place..." The reality is, I was on a frac site about four years ago, and the thought that actually came to mind to me was that it was boring... I'm standing in the trailer or office building or whatever they call it, and there are a dozen

people sitting there all looking at computer screens and assessing these millions of data points that are coming up. It's a constant assessment of scientific and engineering principles just to frac a single well. The industry's predisposition is to leverage science and facts and data to show how this is safe and show why it is safe.

However, others argued that the technical complexity of the process increases the probability that an unpredicted event could occur, with potentially negative environmental implications. For example, one respondent explained: "There are so many moving parts that I do believe in most cases the hydraulic fracturing event is probably not at fault for any problems, but just the sheer logistics of how many wells are drilled, some things failed." Several of these participants cited scientific studies which have measured error related to different parts of the process of unconventional natural gas extraction, such as cement casing failure rates.

Part of the disagreement among participants as to the amount of risk involved in hydraulic fracturing had to do with how they defined the term "fracking." Some participants expressed concern that "fracking" is a "catch-all term" used to capture the many processes included in unconventional natural gas extraction. For these participants, calling everything "fracking" is problematic for measuring the different risks involved in the various steps of unconventional natural gas extraction, as well as in identifying causes of environmental problems. For example, one participant discussed how "as scientists, we are always very careful to draw a distinction between the actual process of hydro-frac'ing fresh shale to extract the natural gas versus drilling the well and extraction activities, and then the wastewater disposal associated with it, because we need to actually physically, mathematically model each set of processes."

However, other stakeholders argued that disconnecting frac'ing from the other components of unconventional natural gas extraction is misleading. For example, one participant stated:

They're trying to say, "Well, the fracking itself didn't cause that. That was something else." What they're not saying is that something else would never occur if there wasn't fracking. To us, it's all part and parcel of the same operation. When you start clearing a pad site, from that point on everything is what is commonly referred to as "fracking," even though, technically speaking, frac'ing is always about where you fracture the well itself...You don't have wastewater injection if you're not frac'ing to begin with. They're just splitting hairs and trying to use semantics to avoid the reality when they say frac'ing doesn't lead to earthquakes.

By using different definitions of "fracking," participants were able to come to vastly different conclusions regarding whether hydraulic fracturing is safe or risky.

Selective Interpretation of Science and Scientists. In response to questions about how science impacts the public's perceptions of hydraulic fracturing, many participants also discussed how the public selectively interprets science and scientists depending on their predetermined views on this issue. Several stakeholders identified this as a potential explanation for how opponents and supporters of frac'ing could reach very different conclusions using access to the same scientific information.

For example, a number of respondents discussed the various interpretations of the Environmental Protection Agency's (EPA) 2015 report assessing the potential impacts of hydraulic fracturing on drinking water resources. Two major findings presented in the draft form of this report were discussed across a variety of media sources: 1) the EPA did not find evidence of "widespread, systemic impacts on drinking water resources" (Brady 2015), and 2) the EPA found "'specific instances' when fracking 'led to impacts on drinking water resources, including contamination of drinking water wells'" (Banerjee 2015). As one participant explained: "If you were to read Fox News and Huffington Post about that report, you'd get two drastically different takes on it. I think people's preconceived notions are what govern the way they're going to think about it." Participants described how, to really understand the report, the public would need to read past the headlines and understand the "facts [that] are buried" in the report, as well as the limitations to the report's data. From the perspective of an opponent to hydraulic fracturing:

The EPA told several cities and towns, "Do not drink your water. Stop today. Don't shower with it. Don't put your kids anywhere near it." All that is in the EPA report, but the report was politically

corrupted... so the average person in Fort Worth is going to say, "Oh, it's okay to frack. No worries anymore." But that's not necessarily the truth... Also, it's very important to know that the EPA report, even though it's done by the EPA and it took five or six years, it was still a relatively small sample and a lot of that sample was provided by the industry. Someone like me with my perspective, I know enough about the corruption in this industry that it's a tainted report, simple as that. It can't be totally scientific.

Though both supporters and opponents of frac'ing critiqued the credibility of the EPA as the sponsor of this study, they each highlighted separate parts of this study as evidence confirming their claims that hydraulic fracturing is scientifically found to be safe or risky.

A number of participants also described their own experiences working as scientists on issues related to hydraulic fracturing as examples of how the public selectively interprets science. For example, one participant joked that their research project is like a "Rorschach test. Everyone listens to us, but what they hear us saying depends on how they felt about it coming in" and "we get accused of bias from every side." Others expressed similar experiences:

Let's say I went and gave a presentation. Half the room might think I'm a junk scientist, and the other half of the room might think that I'm a great scientist. That's based solely on their predetermined opinion on the issue. None of them are going to look at my CV and read any of the papers we've done. They're not going to know the quality of the work and the quality of the journals we publish in.

Several scientists also pointed to the key role funding plays in predicting how the public is going to perceive one's work. One participant explained, "If you're not affiliated with industry, then you get accused of being biased against it. If you are affiliated with industry, you're biased for it. There are a lot of political ramifications for who gets what type of data and what their results actually mean." Even though participants in this study argued that their "source of funding was never going to change [their] results," they worried about how it would affect perceptions of their work.

Some participants proposed that finding less traditional funding sources, utilizing internal university grants, or personally funding their own research may be some of the few currently viable ways to support scientific work on a controversial topic like this one. However, researchers also argued that the need to pursue nontraditional funding sources "dissuades a lot of researchers from getting into the area." Participants with scientific and non-scientific backgrounds both argued that the contentious nature of this topic made "totally scientific" research more challenging, with several participants citing worries about academic freedom and others discussing the difficulty drawing a line between research and regulatory or court matters. Some participants even described how divisions over this topic affected data collection:

I can tell you that the people that we take samples from run the full gamut. Some will let you take water because they're very much afraid of what's happening to their water. Some are absolutely indifferent. Some will let you come on and take the water because they're absolutely sure that you're not going to find anything... My colleague has had people come and hug him and thank him for doing this work and he's also had guns pulled on him.

Thus, the public's selective interpretation of scientific research and scientists begins before data is even collected and continues long after the publication of results.

Absence of Scientific Information. The third theme that emerged from conversations about hydraulic fracturing risk had to do with how participants discussed the absence of scientific information. Many participants argued that more data are needed to assess the impacts of hydraulic fracturing. For example, one participant discussed their initial reaction to viewing the documentary "Gasland": "In this documentary, they're making some pretty significant statements. [I thought] there must be a lot of data on this issue. We looked... and the truth of the matter was no, there wasn't." Participants posed questions about the entire gas development process such as "exact locations, timing, when things start, how long they go on, volumes of fluids being put down there as well as components of what's in them, what they do with the waste products, where that stuff goes, if there are ever any surface spills." As this participant explained, "There's a million

links in the chain where something could go wrong, and those are the kinds of things we just don't have data on."

A number of participants also noted the difficult nature of assessing causality (e.g., does hydraulic fracturing cause water contamination?) when so much information is missing from scientists' analyses, including baseline data for comparisons, and exact information on chemicals used during hydraulic fracturing operations. Several participants discussed companies' nondisclosure of proprietary information, such as mixtures of chemicals or where faults are located, as contributing to this problem. However, others noted that even when scientists can access proprietary data, for places which companies have determined to be "not that economically viable," companies have "stopped spending millions of dollars collecting the data," and thus, the issue is sometimes not lack of access, but lack of collected data.

While most of the scientists interviewed specifically noted that their goals were to answer research questions and not to prevent energy development, the opponents of frac'ing more explicitly argued that until a sufficient amount of research has been completed, companies should not be allowed to move forward. For example, according to one participant:

We're getting more and more data. Do we need more? Yeah, but we need more data about earthquakes in general. Here's what I think about this. If there is even a sliver of doubt that this is dangerous to the public, shut it down until we know. If we shut it down, we know for certain there will be no danger, but if we keep going, we aren't so certain... I am really worried. Is Fort Worth going to become a toxic dump?... What's going to happen... not tomorrow, not even five to ten years down the line, but twenty-five years down the line?

For this participant, as well as others that expressed the precautionary principle regarding hydraulic fracturing, the financial benefits or "mailbox money" especially did not outweigh the known and unknown *long-term* environmental risks of hydraulic fracturing. One participant said, "That's why we fought this so hard. Because once they get the wells in, it's too late. You can't go back. You can't undrill it... Those wells are going to be fracked for the next fifty years and that means all this mess is going to continue."

In contrast, several participants who viewed frac'ing as less environmentally risky claimed that a sufficient amount of study had already been done. One participant explained:

Typically the people who are advancing the argument... "We don't have enough information on this to move forward" are the people who don't want it to ever occur anyway... It's also, I would say, incredibly misleading to suggest that we don't have enough information on this. Frac'ing started in 1947... We know [it is safe] from over sixty years of experience, and that's not just experience, that's sixty years of data points, of understanding what works, what doesn't, trial and error, figuring these things out... Are we actually asking for more study, or are we trying to advance something else?

From this perspective, the argument of "not enough information" is a strategic one intended to prevent hydraulic fracturing indefinitely and is typically used by individuals who are critical of oil and gas drilling. However, some supporters of hydraulic fracturing did occasionally use the argument of "not enough information" to explain their lack of confidence in studies that have demonstrated negative environmental impacts of hydraulic fracturing. For example, one participant described his critique of a past study of water contamination based on the lack of baseline data: "Ideally, you would've tested those wells twenty years ago, before the drilling started. How do you know those wells weren't [already] contaminated? You don't." Thus, the absence of scientific information is problematic for people who view hydraulic fracturing as risky, as well as those who view it as safe.

CONCLUSIONS

A number of participants likened the debate over hydraulic fracturing in the United States to the debate over climate change, where political polarization has played a key role in explaining different levels of concern, as well as differences in trust in the scientific community (McCright and Dunlap 2011). In a study of perceptions of hydraulic fracturing in Texas, a largely conservative state, one might expect to find participants often expressing their *distrust* in the scientific community. To the contrary, most participants

of this study framed their discussion of risk related to hydraulic fracturing in scientific terms demonstrating the important role science plays in how participants justify their views on hydraulic fracturing as a risky or safe process. This work finds support for the “contextual thesis” which suggests that liberals and conservatives engage in motivated reasoning, where “equally informed citizens may employ scientific evidence in very different ways depending on their ideological orientation” (Nisbet et al. 2015:38). Residents in the Dallas-Fort Worth region seemed to be concerned about scientific perspectives on frac’ing, but in ways that fit their prior viewpoints on this issue.

ACKNOWLEDGMENTS

This research was supported in full by grants from the Texas Christian University Research and Creative Activities Fund and the Junior Faculty Summer Research Program.

REFERENCES

- Anderson, B.J., and G.L. Theodori. 2009. “Local Leaders’ Perceptions of Energy Development in the Barnett Shale.” *Southern Rural Sociology* 24:113-129.
- Banerjee, N. 2015. “Fracking Has Contaminated Drinking Water, EPA Now Concludes.” Retrieved 30 May 2016. (<http://insideclimatenews.org/news/05062015/fracking-has-contaminated-drinking-water-epa-now-concludes>).
- Boudet, H., C. Clarke, D. Bugden, E. Maibach, C. Roser-Renouf, and A. Leiserowitz. 2014. “‘Fracking’ Controversy and Communication: Using National Survey Data to Understand Public Perceptions of Hydraulic Fracturing.” *Energy Policy* 65:57-67.
- Brady, J. 2015. “EPA Finds No Widespread Drinking Water Pollution From Fracking.” Retrieved 30 May 2016. (<http://www.npr.org/sections/thetwo-way/2015/06/04/412047602/epa-finds-no-widespread-drinking-water-pollution-from-fracking>).
- Choma, B.L., Y. Hanoch, and S. Currie. 2016. “Attitudes toward Hydraulic Fracturing: The Opposing Forces of Political Conservatism and Basic Knowledge about Fracking.” *Global Environmental Change* 38:108-117.
- Davis, C. and J.M. Fisk. 2014. “Energy Abundance or Environmental Worries? Analyzing Public Support for Fracking in the United States.” *Review of Policy Research* 31:1-16.
- Energy Information Administration. 2016. “Hydraulically Fractured Wells Provide Two-Thirds of U.S. Natural Gas Production.” Retrieved 30 May 2016. (<http://www.eia.gov/todayinenergy/detail.cfm?id=26112>).
- Esterberg, K.G. 2002. *Qualitative Methods in Social Research*. McGraw Hill, Boston, MA.
- Gauchat, G. 2012. “Politicization of Science in the Public Sphere: A Study of Public Trust in the United States, 1974 to 2010.” *American Sociological Review* 77(2):167-187.
- Jackson, R.B., A. Vengosh, J.W. Carey, R.J. Davies, T.H. Darrah, F. O’Sullivan, and G. Pétron. 2014. “The Environmental Costs and Benefits of Fracking.” *Annual Review of Environment and Resources* 39:327-62.
- Ladd, A.E. 2013. “Stakeholder Perceptions of Socioenvironmental Impacts from Unconventional Natural Gas Development and Hydraulic Fracturing in the Haynesville Shale.” *Journal of Rural Social Sciences* 28:56-89.
- McCright, A.M., and R.E. Dunlap. 2011. “The Politicization of Climate Change and Polarization in the American Public’s Views of Global Warming, 2001-2010.” *The Sociological Quarterly* 52:155-194.
- Nisbet, E.C., K.E. Cooper, and R.K. Garrett. 2015. “The Partisan Brain: How Dissonant Science Messages Lead Conservatives and Liberals to (Dis)Trust Science.” *The ANNALS of the American Academy of Political and Social Science* 658:36-66.
- Theodori, G.L. 2009. “Paradoxical Perceptions of Problems Associated with Unconventional Natural Gas Development.” *Southern Rural Sociology* 24:97-117.

Wyneen, B.J. 2011. "A Thematic Analysis of Local Respondents' Perceptions of Barnett Shale Energy Development." *Journal of Rural Social Sciences* 26:8-31.

IMPLEMENTATION OF ENVIRONMENTAL LAWS AND ETHICS IN INDIA

C.V. Rajeswari

(Government Degree College, Pattikonda, 518380, A.P, India)

Sustainable development can be achieved through effective implementation of Environmental Laws and Ethics. The nature of the of the individual to protect the environment is not only to punish the culprit but also to balance the eco system. Even though in India, evolution of environmental laws and ethics can be dated back to Pre-Vedic age, strict adherence to law has not been achieved till now due to lack of proper awareness among public and also due to lack of punishment for breaking the laws. In this paper environmental legislation in India and loop holes in its implementation are elaborated upon and new laws to be introduced to protect the environment are also focused.

ENVIRONMENTAL EDUCATION AT THE MARITIME EDUCATION TRAINING

Tanzer Satır (Istanbul Technical University (ITU), Tuzla-Istanbul, Turkey)

Neslihan Doğan-Sağlamtimur (Nigde University, Nigde, Turkey)

Environmental education has different definitions. This education refers to organized efforts to teach how natural environments function, particularly, how human beings can manage behavior and ecosystems to live sustainably. It is a multi-disciplinary field integrating disciplines such as biology, chemistry, physics, ecology, earth science, atmospheric science, mathematics, and geography. It is a process that allows individuals to explore environmental issues, engage in problem solving, and take action to improve the environment.

Environmental education is an important part of Maritime Education Training (MET) that provides and educates manpower for maritime industry. Marine pollution is one of the key issues at the maritime sector. Most of the maritime universities and institutes have increased the number of environmental courses. In this study, authors will analyze and compare environmental courses in the maritime universities and institutes in the world. The study's aim is to find ideal environmental education for the MET system.

EDUCATION PROGRAM TO THE ENVIRONMENT: AN ADVOCACY OF A TRAVEL AGENCY IN DAVAO CITY, PHILIPPINES

Ruben A. Neri; Recto B. Campos; *Lilia F. Panchito*; Elisa P. Madrazo (Research and Marketing of Surelite Travel and Tours, Davao City, Philippines 8000; City Environment and Natural Resources, Davao City, Philippines)¹¹⁷

Davao City is situated in the southern most of the Philippines. With a total population of approximately 1.6 million people, the city boasts of its 4 icons; namely: Waling- waling (vanda sanderiana)-Queen of the Orchids; Mt. Apo- the tallest mountain in the Philippines; Philippine Eagle- 2nd biggest raptor in the world; and the Durian- an exotic and King of the fruits. Davao City was judged by Numbeo.com that it is the 4th safest city in the world. That is why tourists from all walks in life do come and visit our place.

Travel and tour, nowadays, is a lucrative business in the tourism industry. People got the chance to visit places and adventures, may it be foreigners or local residents as your market. For having served the industry for a decade, it is the advocacy of Surelite Travel and Tours, Davao City, Philippines to give back to Mother Nature what is due to her. Educating to the students from kinder, elementary, high school and college on what is the importance of the environment to mankind. *Environment* is the complex of physical, chemical, and biotic factors (as climate, soil, and living things) that act upon an organism or an ecological community and ultimately determine its form and survival. (Merriam Dictionary). In short, Environment is the natural world, the place we live in and its surroundings.

Our company visited schools within the city and inform administrators the advocacy of having an educational program to the environment. The administrators are so happy and willing to have this said program. In fact they will integrate it to their school curriculum for the next school year and such succeeding years. They say that some of our youngsters are so busy on their gadgets found in their houses and in school. They do not do household chores when they are hooked in the computers. Students seldom have time to explore their surroundings and be in contact with Nature. Some are alien to other things found in nature. We think it is high time that we give back to Nature what is due to them. Our company formulated different modules to different grade levels and activities done during the trip. It is a different fieldtrip to the students.

As a result, the administrators are so pleased that such an educational program does exist in our city. In fact the city government thru the City Environment and Natural Resources Office is really very much willing to help us in this advocacy. Students have the chance to plant a tree in this trip. Although, the trip is so tedious and tiresome, it is worthwhile to the students and the administrators.

It is high time now that such an advocacy exists in the tourism industry especially that we have our global warming through climate change.

STUDENTS' ATTITUDES TOWARDS THE ENVIRONMENT

Mile Srbinovski, *Veton Latifi* & Zamir Dika
(South-East European University- Tetovo, The Republic of Macedonia)

The objective of this study is to determine the students' attitudes towards the environment. A 13-item, 5-point bipolar Likert – type scale instrument was used. The statements included several environmental parameters: utilization of natural resources, interconnection of components in the biosphere, consequences of the environment pollution, anthropogenic influence, the role of the environmental consciousness for the survival of the Earth, characteristics of nature, environmental balance, etc. The study included 51 students from the South East European University- Republic of Macedonia. All of them have been chosen The Environmental Protection course as free elective. This research was conducted at the beginning of this course.

Results indicate that more students display pro-ecological conceptions and they are aware of the negative impact humankind has on nature. Here we engage in a deep discussion and comparison of the obtained results in relation to the factors which influence students' environmental attitudes in the Republic of Macedonia.

**DOES VIEWING DOCUMENTARY FILMS AFFECT ENVIRONMENTAL PERCEPTIONS
AND BEHAVIORS?**

Henry Janpol (Nova Southeastern University, Ft. Lauderdale, FL., USA)

Rachel Dilts (Walden University, Minneapolis, MN., USA)

This research examined the question of whether viewing of documentary films about the natural or human built environment can exert a measurable influence on people's behaviors and perceptions toward the environment. To explore this question, two different documentary films were viewed by college student subjects. One film emphasized the natural environment, while the other focused on the built environment. Eighty-one subjects were included in the study. Each subject was randomly assigned to one of two conditions (watching a film about dolphins or a bridge building video). Immediately after viewing the film, participants played a computer generated game designed to assess their implicit attitudes about the natural and built environments. Finally, after completion of the computerized assessment instrument, participants took part in a charitable donation activity. They were given an opportunity to make a monetary donation to either one of two causes (helping dolphins or a fund for bridge rejuvenation).

Results yielded significant differences in subjects' environmental perceptions regarding the natural or human-built worlds, as measured by the computer game, depending on which video they had viewed. Significant differences were also found between the two treatment groups on the monetary donation variable. Findings are discussed as well as implications for future research in communication about environmental conservation and documentary films.

**ENVIRONMENTAL PLANNING
AND
MANAGEMENT**

A STUDY ON VULNERABILITY OF ALAHSA GOVERNORATE TO GENERATE URBAN HEAT ISLANDS

Ilham S. M. Elsayed

(King Faisal University, Hufuf, Eastern Province, KSA)

ABSTRACT: The purpose of this study is to investigate Alahsa Governorate status and its vulnerability to generate urban heat islands. Alahsa Governorate is considered as the largest oases in the Arabic Peninsula with the largest conventional oil field in the world that accounts for more than half of the cumulative oil production of Saudi Arabia. Nevertheless, literature reviewed shows that no researches were done for this region concerning urban heat island. The data was collected from authorized bodies who are control weather station networks over Alahsa Governorate, Eastern Province, Saudi Arabia. Although, the number of weather station networks within the region is very limited and the analysis using GIS software and its techniques is difficult and limited, the data analyzed confirms an increase in temperature for more than 2⁰C from year 2004 to year 2014. Such increase is very considerable whenever human health and comfort are the concern. The increase of temperature within one decade confirms the availability of urban heat islands. The study concludes that, Alahsa Governorate is vulnerable to create urban heat islands and more attention should be drawn to strategic planning for this governorate that is developing with a high pace and a considerable increasing levels of urbanization.

INTRODUCTION

Alahsa Governorate is located in the South-eastern corner of Saudi Arabia occupying the southern part of the eastern region between 17-26 latitudes and 48-55 longitudes. Alahsa climate is hot summer, cold wet winters, and mostly cloudy atmosphere, seasonal rains in winter and autumn, and the region is exposed to sand storms from time to time.

Alahsa Governorate covers a vast area of around 530 000 km², representing 68% of the area of the eastern region and 24% of the area of Saudi Arabia. It is considered as the largest oases in the Arabic Peninsula. It is famous of palm cultivation (Mohamed, I. Sharaf. 1996). There are more than 10 thousand hectares of cultivated land for more than two million palms that produces the best and most famous types of dates in Saudi Peninsula.

According to Census 2010, the population of Alahsa province is 1, 063, 112 people. The Saudi citizens counted for 870.577 and 192.535 residents. The Governorate consists of many cities and villages in addition to the most famous empty desert that is called Empty Quarter. Hofuf and Mubarraz cities are the oldest urban centers in this region and most developed areas (Alahsa Municipality, 2015). Hofuf city is considered as the capital city because of its economic role in the region. Its leading economical role importance increased after the discovery of oil in Eastern Province of the Kingdom. Several oil centers are located in Alahsa Governorate, among them the largest oil field in the world that accounts for more than half of the cumulative oil production of Saudi Arabia, which is named Al- Ghawar. It measures 280 by 30 km.

Historical Background. As a result of population growth and continuing migration to both Hofuf and Mubarraz largest and most urban developed cities (Alahsa Municipality, 2015), urban development passed over four stages during the period 1957-2012.

First stage before 1963. This stage is considered as the city origination phase. Water is one of the most important foundations for the emergence of the region and the stability of human. Wherever springs and water wells are located, communities are formed. Hofuf, Mubarraz are famous of their permanent springs and water wells that helps in formalizing the cities and affect the level of urbanization by increasing the rate of migration. Hofuf, Mubarraz were characterized by tribal groupings communities having their own lands and natural resources.

The first phase was characterized as the phase of looking for the best position to stabilize population making use of the presence of wells and springs as a source of permanent water, enough to provide drinking water and Agriculture. The stability of the region was supported by the discovery of oil in 1939 in Eastern region that led to the evolution of national income and creation of municipal system that affects action plans for development and supervision. Figure 1. below shows an aerial view to Hofuf and Mubarraz during first stage of growth before 1963.

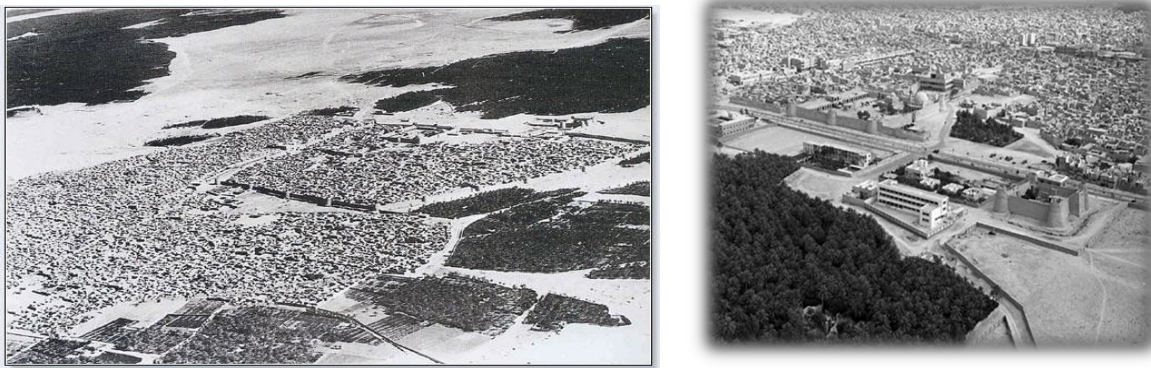


Figure 1. First growth stages for Hofuf and Mubarraz before 1963

Second stage 1963-1973. This stage is considered as growth and configuration phase. The region passed through many urban growth stages during this ten years. Recognized economic and social changes were recorded during this decade. Noted urban growth rates increased with parallel development especially in the development of transport networks. A five-year development programs started with the concurrent trebling increase in oil prices. That directly affected the whole country income and lead to doubling of national incomes. New neighborhoods were built at both Hofuf and Mubarraz towns. Population grown as well as commercial activities increased on main streets in the heart of the metropolis. The expansion of development at that time was in southern and Western directions of the region and its commercial centers. At that stage, major services and Government departments were centered at Hofuf town and a transportation system connected the town with Mubarraz town. Therefore at this stage Hofuf was considered as administrative capital of the surrounding territory.

Third stage 1973-1994. This is stage is considered as the evolution and jump development phase. . As a result of the accumulation of wealth and escalating economic development, a substantial urban growth rates were recorded in Alahsa specifically in Hofuf and Mubarraz. At this period, employment of international labor to implement development and reconstruction operations started. This phase was characterized by urban extension towards the West and South, resulting in the emergence of residential buildings on both sides of the new roads that stretch beyond the capital of Hofuf. Due to the increased migration of nomads, districts were formed as Alrogaigah District. At this stage Hofuf start to take its current form as a capital city.

Fourth stage 1994- 2012. This stage is the recent recorded phase (Alahsa Municipality, 2015). A considerable increase in urban growth in Alhasah Governorate took place; from 7649 to 22869 Acre of built area. While the growth in Hofuf city was from 3730 to 14877 Acre that influenced urban development to present situation. Moreover, the approved expected urban growth is 38000 Acres in 2028 by adding approximately 19000 Acres to Hofuf and Mubarraz City. Figure 2. Below shows urban growth stages and trends in Hofuf and Mubarraz.

MATERIAL AND METHOD

Data collected from authorized bodies, who are controlling weather station network over the area under study, Alahsa Governorate, Eastern Province, Saudi Arabia. The total number of weather station networks within the region is very limited. After a comprehensive and long investigation, the number of weather station that cover Alahsa Governorate are only three weather stations:

Alahsa Meteorological Station. Alahsa Meteorological Station is counted as the main and oldest authorized governmental meteorological station in the region. It works under ministry of Defence and Aviation, presidency of Meteorology and Environmental Protection, National Meteorology and Environmental Center. It is located inside Alahsa Airport premises at 25 17 53 N Latitude and 49 29 11E Longitude, 178.17 m Elevation. The data collected from this station is for 2004 and 2014 over a period of three months that are counted as the hottest months of the year (Mohamed, 1999). Accordingly, the data used are for June, July and August for the two previously mentioned years.

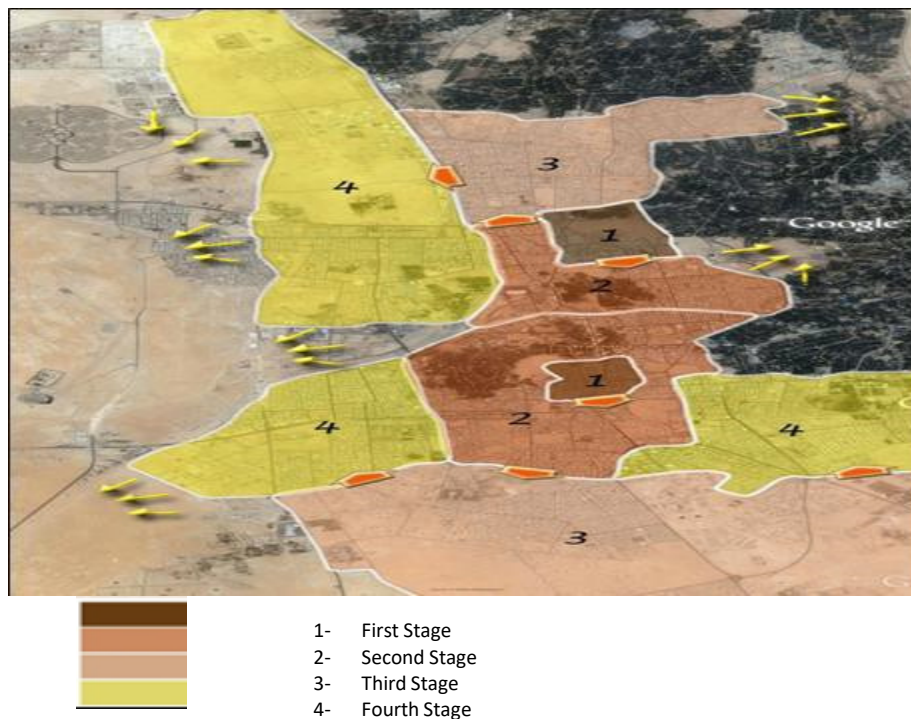


Figure 2. Stages and trends of urban growth in Hofuf and Mubarraz City

Training, Agricultural & Veterinary Research Center (TAVRC) Meteorological Station. The TAVRC Meteorological Station is located inside King Faisal University (25.3401 latitude and 49.5968 longitude) with in the premises of the Training, Agricultural & Veterinary Research Center. The data collected from this station is for less than two years. It is for whole 2013 and almost 2014, as the authorized bodies confirm that, this data is the maximum data that they can provide. According to the purpose of the study, the data

used from this station is confined to year 2014 to match that data collected from Alahsa Meteorological Station. While data for 2013 is excluded from analysis.



Figure 3. The location of Alahsa Airport and King Faisal University Courtesy: Google maps, Saturday, April 30, 2016.

College of Engineering Meteorological Station. The third station is located inside King Faisal University too. It is running in collaboration and control of King Abdulaziz City for Science and Technology at College of Engineering, King Faisal University premises. It is the latest station built before around three years. Although such data is very recent, it will help in comparing the data collected from other station for year 2014. Nevertheless, as authorized body mentioned, data retrieval process is on hold waiting for new password and user names after renewing contract between King Faisal University and King Abdulaziz City. Therefore, it is not included with the data used for this study.

The data collected from the above mentioned stations is used mainly to investigate the temperature pattern over the Governorate. Figure 3. below shows the location of Alahsa Airport and King Faisal university using Google maps on Saturday, April 30, 2016. TAVRC Meteorological Station is located within the most populated well developed urban area in Hofuf city. While Alahsa Meteorological Station is located at the far end of the city in a less populated and less developed area. (Streutker, 2003) defined the urban heat island as the difference in temperature between the urban and rural areas. Accordingly, the research investigates and analysis the temperature measured at TAVRC and Alahsa stations during June, July and August of 2014. Moreover, it investigates on temperature measured at Alahsa station in 2004 and 2014 for months of June, July and August.

RESULTS AND DISCUSSION

TAVRC and Alahsa stations during June, July and August of 2014. Chart 1. Below shows the average maximum temperature measured in degree Celsius at TAVRC and Alahsa station during June, July and August 2014. The difference in maximum temperature between the two stations in the three previously mentioned months is more than 1.5 °C. It reached 2.0 °C during June, 2014. Which confirmed that the city centers are always hotter than suburban areas (Elsayed, 2012).

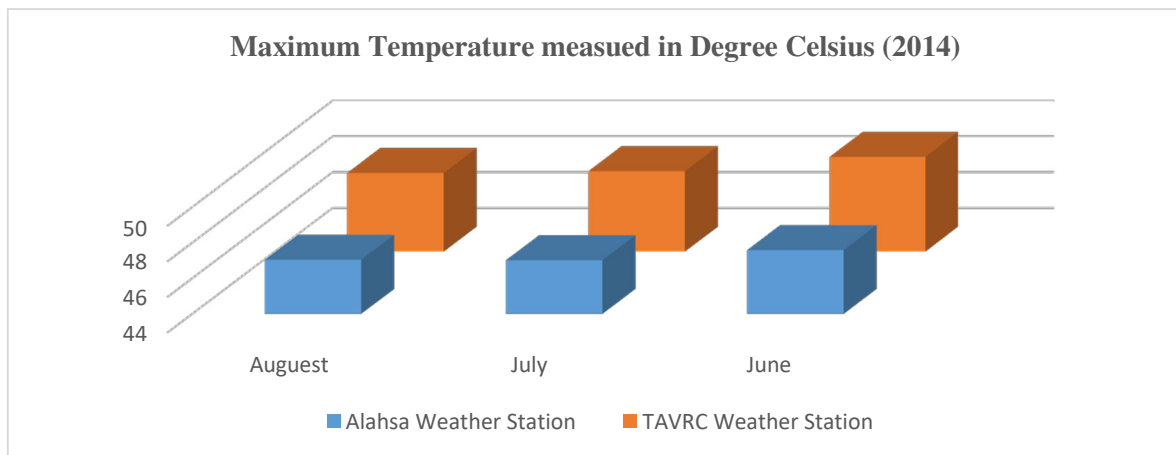


Chart 1. Maximum temperatures at TAVRC and Alahsa station during June, July and August 2014

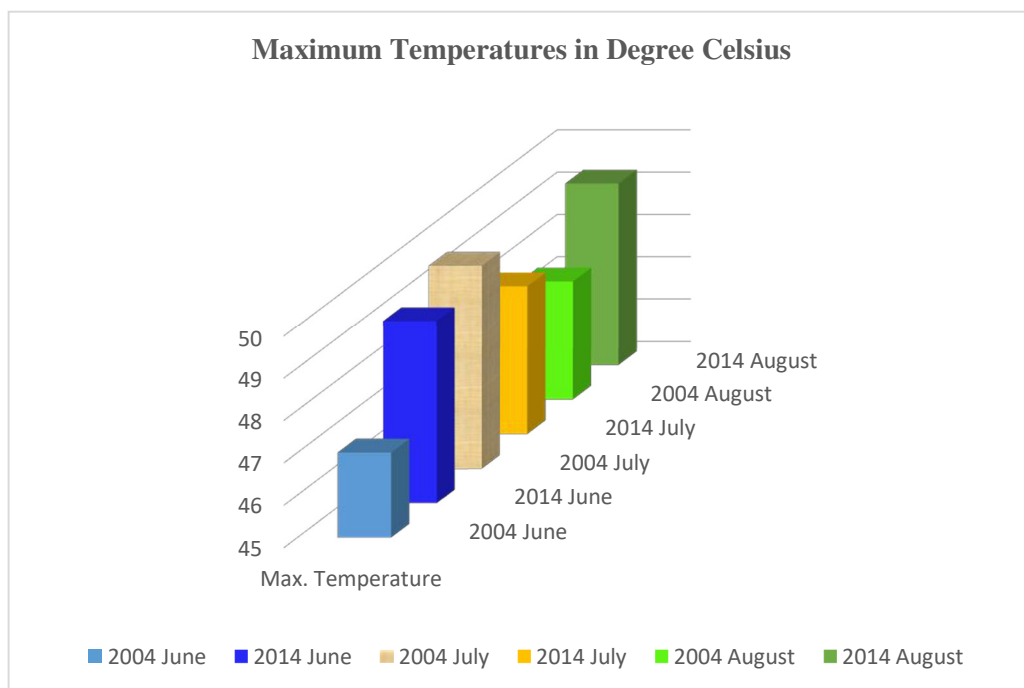


Chart 2. Maximum temperatures during June, July and August, 2004 and 2014

Alahsa station in 2004 and 2014. As mentioned previously the study focuses on the hottest months of the year June, July and August. Chart 2. Below shows the average maximum temperatures measured during June, July and August year 2004 and 2014. The difference in temperature between June 2004 and June 2014 is 2.3°C. While, it is 1.5°C for August. The most astonishing result is that collected for July 2004. It shows the heights temperature recorded. It is even higher than that recorded for July 2014. Which is somehow contradicts the research assumptions that expected increase in temperature in 10 years period.

Nevertheless, it is recognized that this high temperature is accompanied with the heights relative humidity and lowest mean wind speed and velocity during the study period. Therefore, it is excluded. On the other hand, chart 3. below shows the average maximum temperature with respect to average mean wind speed, average wind velocity and population for June 2004 and 2014. The chart confirms that there is an increase of temperature with respect to increase of wind speed, velocity and population.

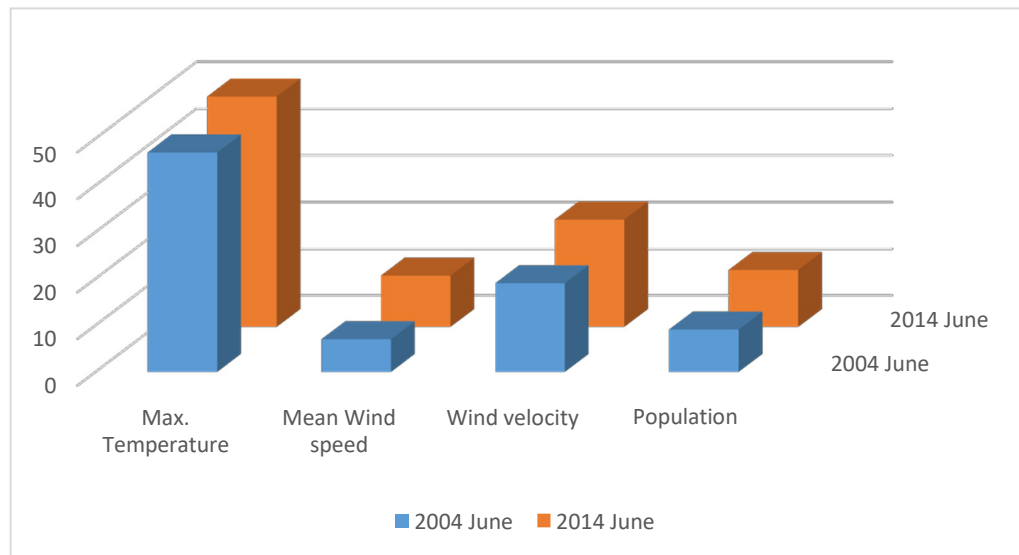


Chart 3. Max. temperature ($^{\circ}\text{C}$), mean wind speed, velocity and population, June 2004 and 2014

CONCLUSION

The results of the study confirms previous studies (Elsayed, I. 2012a &b, Smoyer, K. E. 1997, Valazquez-Lozada, A. 2002) that show that, as the population increases the temperature increases. The study proves that, there is an increase of temperature counted for 2.3°C for one decade period from 2004 to 2014. Moreover, it shows that there is variation in temperature intensity between the two weather stations considered for the research from June to August 2014 counted for 2.0°C difference. The variation in temperature between Alhasah and TAVRC station confirms the availability of UHI within the area under study. Such variation on temperature confirms the need of extensive research to measure the intensity of this UHI, nucleus of UHI and exact number of HUIs available within the Governorate.

The study concludes that, Alahsa Governorate is vulnerable to generate urban heat islands and recommended further studies to locate the nucleus of the UHI. That will contribute much to support decision makers in strategic planning and future development of a governorate that is developing with a high pace and considerable increasing levels of urbanization.

REFERENCES

- Al Zawad, M. F. 2008. *Impact of Climate Change on Evaporation, Surface Runoff and Soil Moisture on a Regional Scale in Saudi Arabia*. M. Sc. Thesis, King Fahd University Of Petroleum and Minerals, Dhahran, Saudi Arabia.
- Alahsa Municipality. 2015. *The Current Conditions of the Present Alahsa: Second Report*. Alahsa Municipality, Eastern Province, Saudi Arabia.
- Elsayed, I. S. 2012a. "A Study on the UHI of the City of Kuala Lumpur, Malaysia." *King Abdul-Aziz University Journal, Sciences of Meteorology Environment and Arid land Agriculture*. 23 (2)

- Elsayed, I. S. 2012b. "Mitigation of the Urban Heat Island of the City of Kuala Lumpur, Malaysia." *Middle-East Journal of Scientific Research, IDOSI Publications*. 11 (11): 1602-1613
- Hafner, J. 1996. *The Development of Urban Heat Islands in the Southeast Region of the United States in the Winter Season (Global Warming)*. Ph. D. Thesis, University of Alabama, Huntsville, AL.
- Ken, D. S., Evans, K., Blane, H., Michele, L., Kallur, S., and James, D. 2015. "Vulnerability to climate change in three hot spots in Africa and Asia: Key issues for policy relevant adaptation and resilience building research." *Springer*.
- Mohamed, F. Atta. 1999. "Climatic Conditions in Alahsa, Saudi Arabia." *Research Consulting Service Center Journal*: 1 (1).
- Mohamed, I. Sharaf. 1996. "Climatic Risk to Agriculture in Oasis of Alahsa." *Journal of Faculty of Arts, Alexandria University, Egypt*.
- Smoyer, K. E. 1997. *Environmental Risk Factors in Heat Wave Mortality in St. Louis*. Ph. D. Thesis, University of Minnesota, Minnesota, MN.
- Streutker, D. R. 2003. *A Study of the Urban Heat Island of Houston, Texas*. Ph. D. Thesis, Rice University, Taxes, TX.
- Valazquez-Lozada, A. 2002. *Urban Heat Island Effect Analysis for San Juan, Puerto Rico*. M. Sc. Thesis, University of Puerto Rico, San Juan.

OPTICAL-ELECTRONIC EQUIPMENTS OF ECOLOGICAL DEDICATION

Ruben Asatryan (National Institute of Metrology, Yerevan, Armenia)

Hamlet Karayan (Yerevan State University, Yerevan, Armenia)

Norayr Khachatryan (National Institute of Metrology, Yerevan, Armenia)

Currently sharply increased interest in environmental issues, which is primarily due to the ever-increasing contamination of the environment. According to the latest data on the study of atmospheric pollution in industrial developed countries, the main sources of pollution are industrial and energy facilities and transport, which accounted for over 80% of the total amount of pollution. The major components of air pollution are gaseous compounds of carbon, nitrogen and sulfur, as well as solid and liquid aerosol formation, which are of particular concern for the normal functioning of humans and other biological objects. Therefore, the creation of optoelectronic devices and systems with the best metrological parameters that enable the operational analysis of basic physical and environmental parameters, and distant monitoring of the atmosphere and air infrared environmental control of vast forest spaces (for detection of fires in the early stages of their development) and pipelines of natural gas is a very important task. The present work is devoted to presenting the results of research and development work on the elaboration and manufacturing of optical-electronic instruments for environmental purposes to explore the basic physical and ecological parameters of the atmosphere, as well as monitoring forest spaces and main gas pipelines.

AN APPROACH FOR ENVIRONMENTAL RISK ASSESSMENT OF ENGINEERED NANOMATERIALS USING ANALYTICAL HIERARCHY PROCESS (AHP) AND FUZZY INFERENCE RULES

Emel Topuz* and C.A.M van Gestel

(VU University Amsterdam, Faculty of Earth and Life Sciences, Amsterdam, The Netherlands)

The usage of Engineered Nanoparticles (ENPs) in consumer products is relatively new and there is a need to conduct environmental risk assessment (ERA) to evaluate their impacts on the environment. However, alternative approaches is required for ERA of ENPs because of the huge gap in data and knowledge compared to conventional pollutants and their unique properties that make it difficult to apply existing approaches. This study aims to propose an ERA approach for ENPs by integrating Analytic Hierarchy Process (AHP) and fuzzy inference model which provide a systematic evaluation of risk factors and reducing uncertainty about the data and information, respectively.

Risk is assumed to be the combination of occurrence likelihood, exposure potential and toxic effects in the environment. A hierarchy was established to evaluate the sub factors of these components. Evaluation was made with fuzzy numbers to reduce uncertainty and incorporate the expert judgements. Overall score of each component was combined with fuzzy inference rules by using expert judgements. Proposed approach reports the risk class and its membership degree such as Minor (0.7). Therefore, results are precise and helpful to determine the risk management strategies. Moreover, priority weights calculated by comparing the risk factors based on their importance for the risk enable user to understand which factor is effective on the risk. Proposed approach was applied for Ag (two nanoparticle with different coating) and TiO₂ nanoparticles for different case studies. Results verified the proposed benefits of the approach.

(Acknowledgement: This study was funded by the Scientific and Technological Research Council of Turkey (TUBITAK) 2211 Grant Program)

**WHAT IS ETHICAL?
AN ANALYSIS OF THE OPPOSING FORCES OF ENVIRONMENTAL SUSTAINABILITY**

Terry L. Polen

(West Virginia Department of Environmental Protection, University of Maryland University College)

ABSTRACT: There is a duality, or triality, between the opposing forces of sustainability; the environmental, economic, and community. By using reinforcing and balancing causal loops we can show that a simple ethical question regarding values of right and wrong regarding the environment is not so simple. This systems thinking analysis will show the ethical, and practical, causes and implications of environmental policy and decision making that surround the current national and international environmental 'climate'. Additionally, an understanding of the drivers both individually and corporately is derived using the Polen Universal Field Management Theorem.

INTRODUCTION

It seems simple enough, what is ethical? Something is ethical or it is not, correct? Well, maybe not. It may be descriptive ethics (thou shalt not cheat on your taxes) or normative ethics (you 'ought' to pay your taxes). Yet life is just not that simple is it? Paying your fair share of taxes is what you are required to do, and what you 'ought' to do, but what is your fair share? Is it really ethical to take all of those deductions knowing that there are starving children in Africa that could be fed by your contribution to the government?

What about the environmental aspects? What 'ought' government to do? What is right? For example, a coal fired electrical utility is critical to the lifestyle that many have and wish to retain. Conversely, what of the pollutants? What about the workers and their livelihood? Will they have another good paying job that they can move into, to or will they be placed out of work and into the public safety net? What of the parks and hospitals? What implication and import will an environmental policy decision really have? Is the greater good, the greater good? Who decides and how do they? These are the seemingly simple, yet oh so deep.

DISCUSSION

To be, or not to be-that is the question: Whether 'tis nobler in the mind to suffer the slings and arrows of outrageous fortune or to take arms against a sea of troubles, and by opposing end them. Shakespeare, Hamlet Act III, Scene I.

This is seemingly the most well-known of all of the Bard's phrases had nothing to do with environmental sustainability. Yet the implication is similar. What is right? What should we do? The ethical conundrum that encompasses most issues is also present in the consideration of environmental sustainability. The commonality of an 'obvious' path is quite uncommon. Environmental, like social and community issues do not lend themselves to simple trite answers:

- Every politician wants 'jobs'
- Every politician wants 'clean air'
- Every politician wants 'strong communities'

But what if these issues are not synergistic? What if these issues actually work against each other? Would the high paying jobs in a commercial sector facility degrade the air? In doing so will that same

manufacturing facility create the tax structure for the park, yet increase the noise and light and pollution around said park?

What was once accepted is now rejected - at least by a segment of the populace. Then what is right? Ethicists and Philosophers and even Engineers have been struggling with this conundrum for millennia.

If we can but understand that there is 'logic' to the other side, then we have already traveled farther down that road than most societies. The implications and interactions of internal and external forces are not, by nature, linear. However, the causes and implications are and can be shown, analyzed, and therefore understood. Consider our own ethics that are described below (Figure 1). Something that is legal and ethical is easy to think of; maybe feeding the homeless. Something that is illegal and unethical is easy to think of; maybe torture. What of something that is legal and not ethical? Some would consider abortion in this bin. What of something that is illegal and ethical? The American Revolution would fill this category for Americans. Not so for the British of the time.

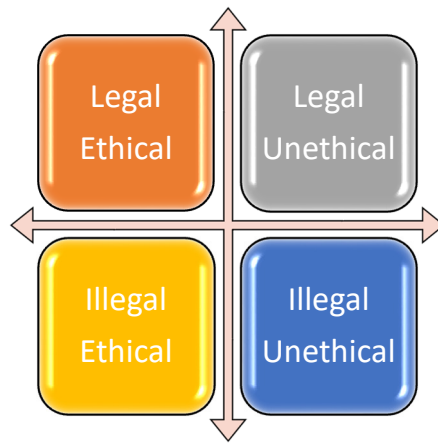


Figure 1. Legal, Illegal, Ethical and Unethical Relations

The common definition of sustainability from United Nations (U.S. EPA, 2011) is that there is a 'sweet spot' in the overlapping priorities of Economic, Environmental, and Societal needs. It is that spot that is the most sustainable and it is this to which we strive. We understand the overshadowing one priority for another can lead to difficulties. Pollution impacts in many places of the world would fit here.

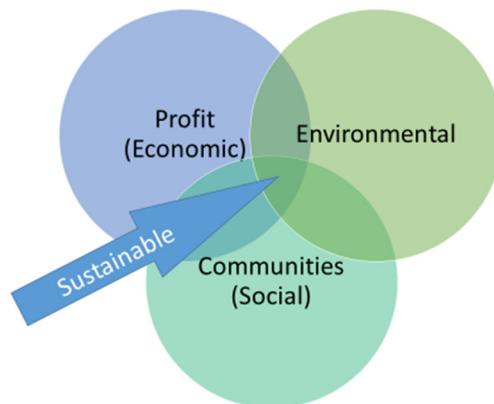


Figure 2. Impact of Economic, Environmental and Social factors on Sustainable Development

A common definition of sustainability speaks of the opposing forces of sustainability i.e. the environmental economic and community issues that interact with each other (Figure 2). However these three forces both support and oppose each other at the same time. If one of them ‘tramples’ over another, difficulties arise, certainly in the societal realm. It is common in the history of the world to see areas where the economic portion has overshadowed that of community and that of society. It is common in the history of the world to see we that are in environmental issues are completely overshadowed by the power of the dollar. In the United Nations interpretation of sustainability, these three opposing forces have the sweet spot, a place within the Venn type diagram whereby all three opposing forces will balance. It is in that space that you will find the greatest sustainability. The above figure shows how this is typically denoted. Yet this mortification of a Venn diagram with its sweet spot can write on his face inaccurate. These opposing forces fight against each other and for area to be sustainable there must be a balance yet that balance is different for each individual as they consider that place. Each culture and subculture will view that ‘sweet spot’ differently. So what is right? What is ethical?

Therefore the second diagram in this analysis shows a further continuation and possibly a more accurate description (Figure 3).

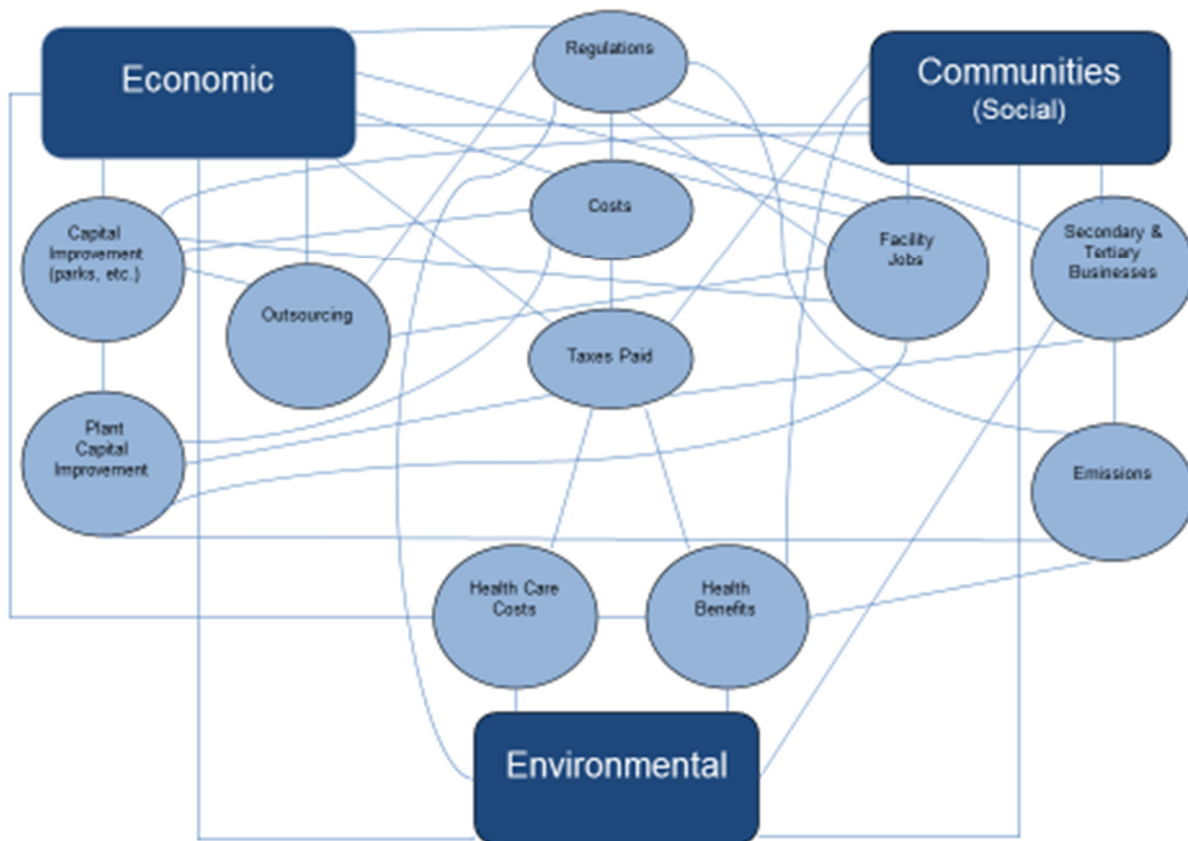


Figure 3. Interactions among Economic, Social and Environmental factors

In previous work (Polen, 2014), it was shown that the model of sustainability is incorrect in that it has many tendrils that pull and push on the environmental, social, and economic spheres. Using the causal loop analysis above, it was shown that there is a strong interrelation of the spheres. Reinforcing loops and balancing loops work like so many carnival attractions. If a new business comes to the community, the tax base will increase which will help build infrastructure (roads, bridges, parks, etc.), but at the same time,

that plant brings increased truck and rail traffic, as well as increased water and air pollution. But that same plant additionally brings needed jobs to the community.

While laborers and construction workers and potential new employees are thrilled, environmentalists worry about the impact on those same individuals and the vegetative and animal species that will be effected by the new facility.

Both sides firmly believe that they are right and well within their rights to encourage, or stop, said facility. They also 'know' that the other side is 'wrong' or even 'nuts'. Their side is only common sense.

- They need jobs.
- They need clean water.
- What good are jobs without clean water?
- What good is water without someone there?
- And the debate roils.

The UN model defines the conjunction of the spheres in some great societal and cultural Venn diagram. Yet, even this view is too simplistic to truly create public policy that is common sense and that is the best for all. Policy makers must understand that yin and yang between the various forces.

While this diagram moves us forward. This too is limited by the two dimensional thinking that has created the problem initially.

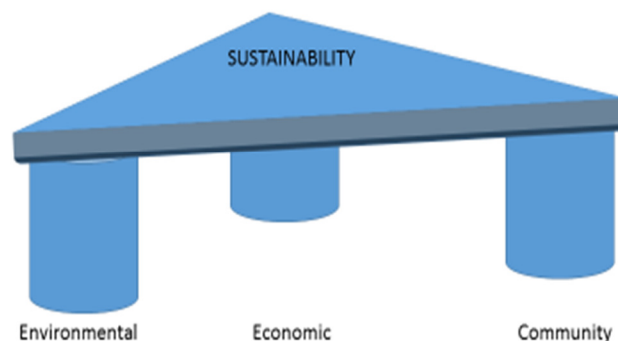


Figure 4. Construction of Solid Sustainability

When we consider 'what is ethical', the triangular table above gives the best representation of the process. Any of the legs of the stool, when limited, can cause the stool itself to be unstable. So a balance of these forces must be maintained to maintain the equilibrium that leads to long term success (Figure 4). Yet this mainlining of equilibrium brings us full circle to the original question of 'is it ethical'?

To whose ethics do we agree? To whose belief structure? Why are you right when I, with a well thought out and passionate argument, wrong?

Ethicist and philosophers from Heraclitus to Socrates to Plato to Aristotle to Bentham to Mill to us posit that we must pursue what is best for the most. Bentham described this as felicitous calculus (Mill, 1863). What makes the most people happy? This is the basis for utilitarianism. The calculation of the best for the most. Consider road construction. While eminent domain is used to remove a few house and homesteads that have been part of that family for generations, additional untold thousands and tens of thousands will be able to use that road for commutes and community. For family, faith, and a better future. The road and the transportation itself will aid in economic development that will create hope and a future for untold multitudes. Yet the road itself destroys wetlands and old growth forests. Protesters stand before bulldozers. What is the balance?

Let us first consider the individual needs and wants of ‘why do they do that’?

The author, in previous works (Polen, 2015) has posited that individuals output or outcomes are derived from the following equation:

$$\begin{aligned} & \textit{Polen's Universal Field Management Theorem (UFMT)} \\ & \textit{Output=Obedience [(Pistos*Agape)+(Leadership*Motivation)]} \\ & \textit{Output=O(PA+LM)} \end{aligned}$$

Where Pistos and Agape are terms from Kione Greek for faith and love respectfully.

In relation to sustainability, this equation can be used to describe not only ‘why do they do that’, but additionally, why they believe that that is ethical.

Let us simplify the sides in the road discussion to environmental groups, economic groups (including businesses, construction workers, and economic developers), and the community (including the public at large and the local politicians).

The environmentalists see a degradation in the air quality and a negative impact to the water and other environmental media. The economic developers see an opportunity for growth to their area. The community sees a resurgence of tax base that will fund parks and hospitals, with a corresponding new need for the tax base, community, and hospitals.

Using the UFMT equation, all sides have a leadership component. Someone has a strong opinion. Someone believes that they are right and the other side is wrong. These groups are well motivated to do the ‘right thing’. The Agape, or love of community (or individual house if the concept is used in that fashion), work, environment, money and etc. along with the faith (Pistos) that what they are doing is not only right, but will do the positive thing is yet another driver.

The individuals involved must be obedient to their cause, or side of the discussion. Obedience is the key to the other terms in the equation. Individuals may well feel strongly, yet never act on those beliefs.

CONCLUSION

Hence the balancing act. It is not a sweet spot that all agree upon. It is a table whose legs must not be unbalanced too far. Otherwise the people and the environment and the society itself will be hurt. So who is right in a contentious situation? Who is wrong? Who is on the side of the greater good? Often lawmakers and policy makers contend that they are completely unbiased, yet their decisions impact without the due course of thought regarding what is really, truly ethical.

The common refrain of it is only ‘common sense’ has become ubiquitous in most political debates, arm chair societal quarterbacks, and new environmental and economic policies. How stridently we attack renewable fuels when we know that coal miners will be on the unemployment lines is a discussion for utilitarians, and should be for policy makers.

REFERENCES

- Gottlieb, A. (2000). *The Dream of Reason*. New York: W. W. Norton & Co.
Mautner, T. (2005). *Dictionary of Philosophy* (2nd ed.). London: Penguin Books.

- Mill, J. S. (1863). *Utilitarianism*. London: Parker, Son, and Bourn.
- Pittenger, D. J. (2002). Deception in Research: Distinctions and Solutions from the Perspective of Utilitarianism. (G. P. Koocher, Ed.) *Ethics and Behavior*, 12(2), 117-142.
- Polen, T. L. (2014). A Systems Thinking Analysis of Environmental and Economic Forces on Sustainable Community Development. *Seventh International Conference on Environmental Science and Technology*. Houston.
- Polen, T. L. (2015). *The Hidden Hand of Management*. Mustang, OK: Tate Publishing and Enterprises.
- Rawls, J. (1955). Two concepts of rules. *The Philosophical Review*, 64, 3-32.
- Russell, B. (1903). *The Principles of Mathematics*. New York: Cambridge University Press.
- Ryckman, T. (n.d.). *Russell's Theory of Descriptions*. Retrieved from Philosophy at Lawrence University: <https://www2.lawrence.edu/fast/ryckmant/Russell's%20Theory%20of%20Descriptions.htm>
- Shakespeare, W. (2005). *William Shakespeare, The Complete Works* (2nd ed.). (S. Wells, & G. Taylor, Eds.) Oxford: Clarendon Press.
- U.S. EPA. (2011). *Sustainability and the U.S. EPA*. Washington, DC: National Academies Press.

**CLIMATE VARIABILITY AND SUSTAINABLE DEVELOPMENT:
THE CASE OF NIGERIA'S NIGER DELTA REGION**

Chika Ogbonna, Eike Albrecht and*René Schönfelder
(Brandenburg University of Technology Cottbus Senftenberg, Germany)
(*University of Lübeck Institute for Software Engineering)

ABSTRACT: Current and future climate associated events endanger sustainable development (SD) in the Nigeria's Niger Delta region. The situation was examined by analyzing a 30-year temperature and rainfall data from 1980 to 2010 obtained from Nigerian Meteorological Agency (NIMET). It was found that temperature trend in different States of the region that made up the study area was increasing while rainfall was variable and declining. Scientific literatures that reveal varying evidence on the effects of climate variability in the region were reviewed and used to complement the results. Nonetheless, the effects of climatic change such as seasonal and erratic flooding, coastal erosion, and variation in temperature and rainfall threaten people's wellbeing and contributed further to environmental degradation. Adaptation measures that need to be addressed to reinforce sustainable development initiatives were suggested. The findings will be useful to decision-makers, non-governmental organizations, relevant institutions, and government agencies in Nigeria.

INTRODUCTION

Climate variability and climate change have become major environmental challenges facing developing countries in the 21st century. The Second National Communication to the UNFCCC (2014) affirms that the Nigeria nation in general faces climate-related impacts such as severe floods, windstorms, heat waves, ocean surges, and a wide range of climate extremes that have negative impact on the country's socio-economic activities. Projections show that a rise of 0.5m in sea level could result in the loss of 35% coastline of the highly-productive delta (INDC 2015). The area faces extensive climate risks ranging from storm surges, increasing risks of flooding, variable but extreme rainfall and heat waves. However, besides seasonal flooding, the 2012 flooding incident in the coastal Niger Delta was devastating in the area. On the other hand, following the global climate temperature trend, observed climate shows that temperature in Nigeria have been increasing in the last five decades and it has become more significant since the 1980s and this is also the case in the Niger Delta (FME 2014). The Fifth Assessment Report of the International Panel on Climate Change (IPCC) concludes that "climate variability and change is a threat to sustainable development" (IPCC 2014a). The concept of sustainable development started in Stockholm, Sweden during the 1972 United Nations Conference on Human Environment. The World Summit on Sustainable Development held in Johannesburg, South Africa from the 2 to the 4 September 2002 reaffirms the commitment to Sustainable development. Sustainable development is a process of development that seeks to achieve, in a balanced manner, the three pillars: social development, economic development and environmental protection. However, the concept of sustainable development was popularized by the Brundtland report published by the World Commission on Environment and Development (WCED) in 1987, also known as "Our Common Future" (UN 2010). The report defined sustainable development as "development which meets the needs of the present without compromising the ability of future generations to meet their own needs" (WCED 1987). While Agenda 21 adopted by more than 178 governments at the 1992 Earth Summit brought a comprehensive plan to table, the 2012 Rio+20 conference asked countries to renew their commitment to sustainable development (IPCC 2014a). The relevance of discussing the potential effects of climate variability and its connection to sustainable development in this paper is due to

the obvious fact that climate change and variability is anticipated to pose major threat to future sustainable development in Nigeria and particularly in the Niger Delta. In essence, such climate impacts make it hard to achieve sustainable development. This study therefore, gives insight into how climate associated events endanger current and future sustainable development and present viable adaptation measures that need to be addressed to reinforce sustainable development initiatives.

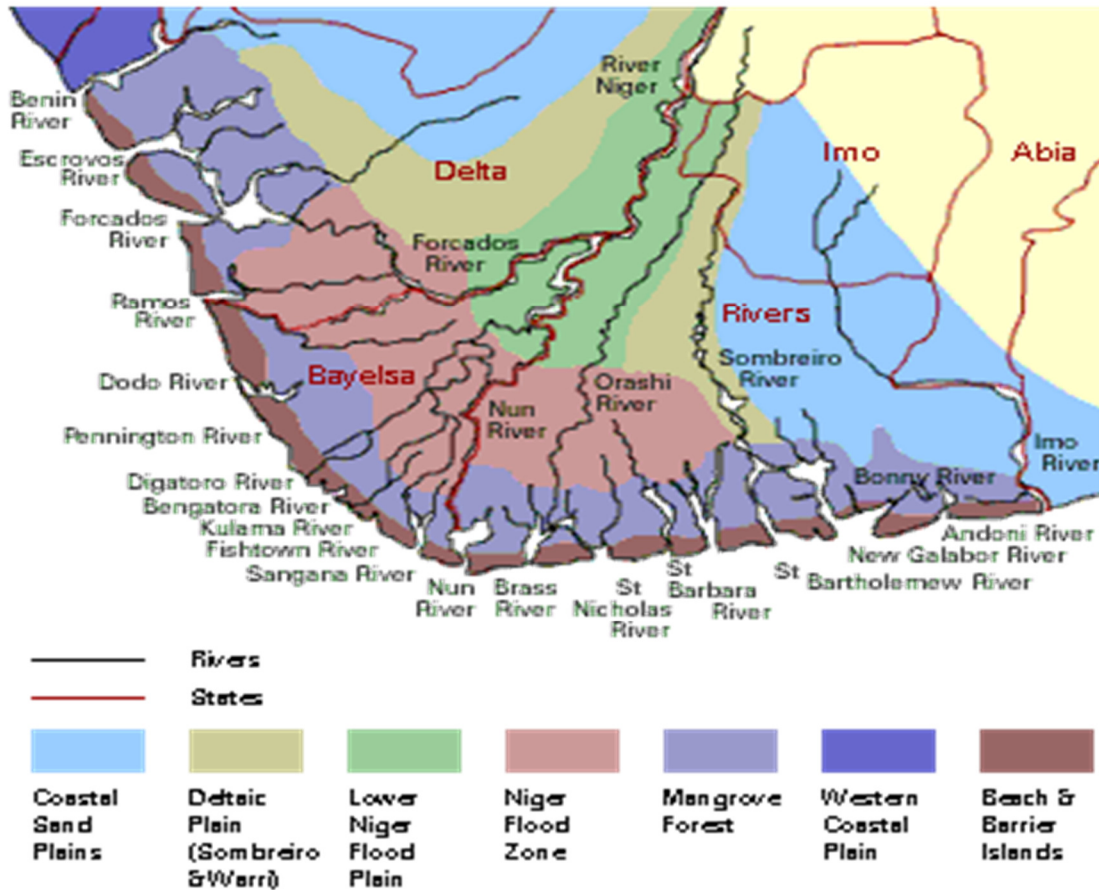


Figure 1. Map of Niger Delta Nigeria (study area) showing, Rivers and Vegetation. Three focal States for this study include Delta, Imo, and Rivers State. Source: UNDP Niger Delta Biodiversity Project.

The Niger Delta region is located on the Atlantic Coast of Southern Nigeria, where the river Niger splits into numerous distributaries (Figure 1). It is one of the largest delta regions in the world and the rich part of Nigeria in terms of natural resources (Ogbonna 2014). For example, it has large oil and gas deposits and biodiversity. The region covers an area of about 70,000 km², starting from a coastal zone of swamps, which extends Northwards towards the rainforest that gradually merges with woodlands and savanna grasslands in central Nigeria (UNEP 2011). The Niger Delta is located on latitudes from 4°25' N to 6°00' N and longitudes from 5° 00' E to 7°5' E.

MATERIALS AND METHODS

The observational data relates to climate variation within a 30-year period ranging from 1980 to 2010. The minimum rainfall data and maximum temperature data used in trend analysis was collected from the Nigerian Meteorological Agency (NIMET), Lagos. The temperature and rainfall data were imported into 'R' statistical software and plotted using ggplot2. The monthly maximum temperature is averaged for an indication of heat waves and the monthly rainfall is added up to get the annual rainfall. These values

were plotted in a line chart and then extended by a linear regression curve showing the trend. The study also relied on the analysis of various secondary materials and literature, relevant journals, government policy papers, research papers, and books that provides evidence of climate impacts and vulnerability in the Niger Delta region.

RESULTS AND DISCUSSION

Trend Analysis of Temperature Data. As can be seen on the result (Figure 2), the average monthly maximum temperature at Warri, Owerri and Port Harcourt showed an increasing trend in temperature patterns. In Warri (Delta State), the lowest temperature of 30.3°C was recorded in 1985 while the highest temperature of 32.3°C was observed in 1994. Results also showed that from 1980 to 2010, the average temperature in Warri, Delta State increased by 0.14°C per decade, whereas the average monthly maximum temperature in Owerri, Imo State over the 30-year period indicated a gradual increase in temperature. The lowest maximum temperature in Owerri was recorded in 1985 at 31.4°C, which rose again rapidly beyond 32°C around 1987, and gradually fluctuated until the highest temperature of 33.10°C was attained by the end of 1998. The linear trend indicates a progressive increase in temperature with time recorded in years. The temperature trend analysis also showed that the average temperature over the years increased by about 0.21°C per decade in Owerri. On the other hand, the monthly maximum temperature at Port Harcourt, Rivers State varied between 1980 and 2010. The lowest temperature recorded within this period was in 1992 with a record of 30.25°C, which rose and fluctuated within 31°C and 31.75°C between 1994 and 2005. After 2005, average temperature increased again and fluctuated until the highest was reached in 2010 at 32.05°C. Overall, temperature did not increase extensively in Port Harcourt in comparison with Owerri and Warri as the trend analysis indicated a slight rise in temperature as the years progressed. Results also show that the monthly maximum temperature in Port Harcourt increased at a rate of 0.042°C per decade.

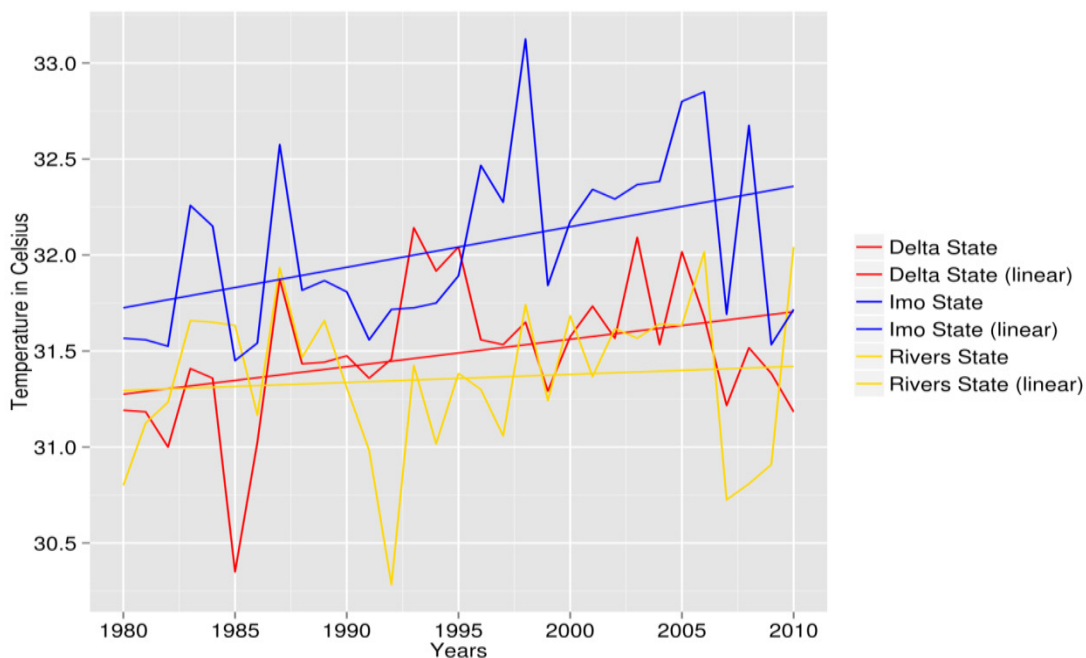


Figure 2: Maximum temperature and yearly average from Owerri (Imo State), Warri (Delta State) and Port Harcourt (Rivers State) synoptic stations respectively.

Trend Analysis of Rainfall Data. The graph (Figure 3) indicates that Delta State experienced a record high of rainfall of about 3400 mm in 1995, whereas a record low of rainfall of about 2,400mm occurred in 1981. Observed rainfall data in Port Harcourt, Rivers State shows a wide variation in rainfall. There was a sharp decline in rainfall pattern recorded in 1982 at 2,200 mm with an all-time record low of 2,000 mm in the years 2000 and 2008, while a peak in rainfall pattern of 2,800 mm was observed in 2007. In Imo State, there was an average rainfall decline to 1,550 mm and 1,650 mm in 1983 and 1998 respectively, a sharp increase to 2,300 mm in 2007 and ultimately, a decline to 2,200 mm in 2010.

The entire results correspond to the existing research on the Niger Delta region (BNRCC 2011; Ike and Ezaziye 2012, Okorie et al. 2012) and with the global predictions of the IPCC 2007 and 2014b. It also strengthens confidence that temperature anomalies in the States follow the same trends of global warming. High values in average monthly maximum temperature clearly depict the intensity of maximum temperature (heat waves) all through the years. The results also corroborated the research conducted by Okorie et al. (2012) in Owerri, Imo State which found that “an increase in surface temperature and torrential rainfall causes flash floods and flood disasters, increasing frequency and intensity of extreme weather events such as thunderstorms and unpredicted rainfall patterns, as well as other climate related disasters.” However, while rainfall data show fluctuating variations, temperature data shows an upward trend. Given the fluctuating rainfall pattern in Figure 3, one may wonder why the flood event in the area is increasing besides other socio-economic factors that may contribute to seasonal flooding. In this vein, the IPCC posits that “if an increase in high-intensity rainfall events is concurrent to the peak of the rainy season, this may result in widespread flooding” (Sylla in IPCC 2015). This is also the case in the coastal Niger Delta communities as information derived from the relevant literature indicates that increase in flood events are recurrent during the peak rainy seasons. The situation is compounded by interactions among multiple environmental stressors.

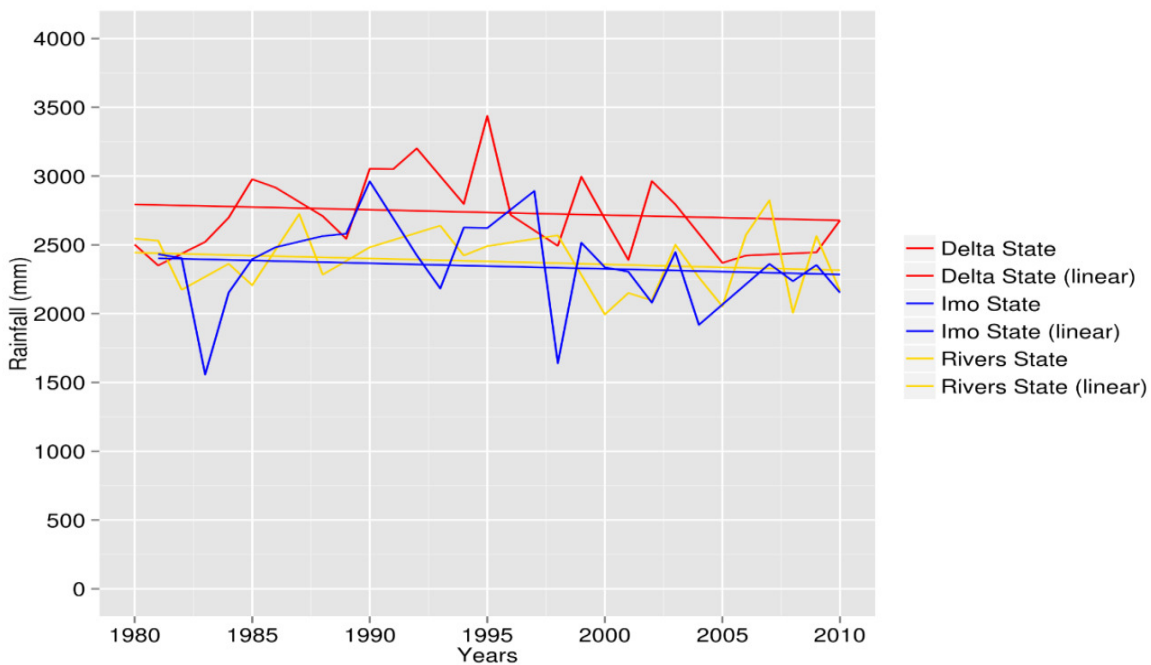


Figure 3. Average annual maximum rainfall for Owerri (Imo State), Port Harcourt (Rivers State) and Warri (Delta State)

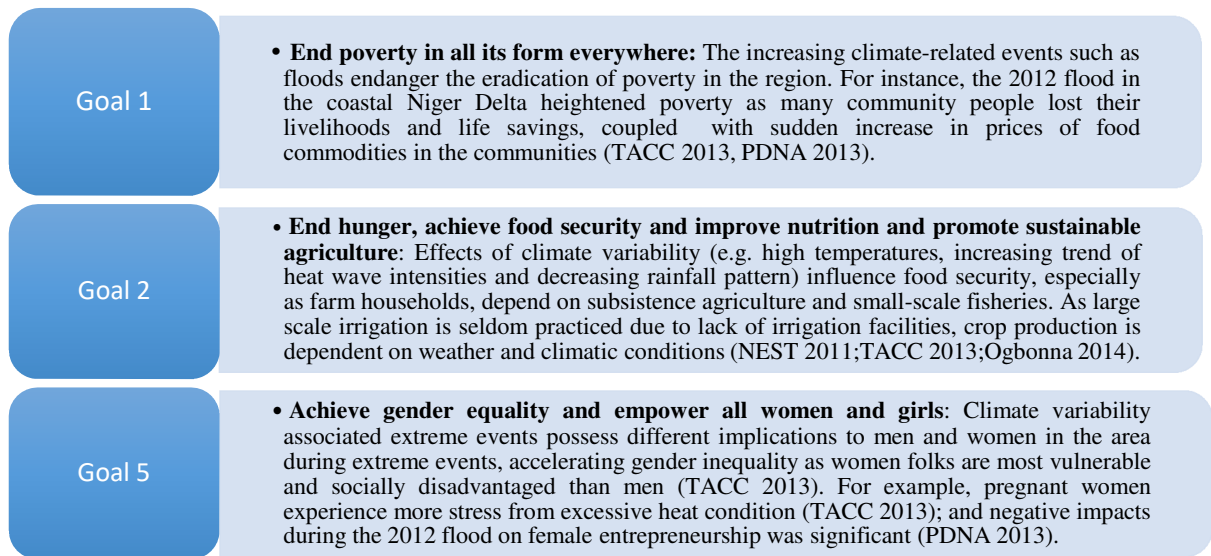


Figure 4. Effects of Climate related events on Sustainable Development
Source: NEST (2011); TACC (2013); PDNA (2013); Ogbonna (2014)

The variability in climate portrayed by both temperature increase and changes in rainfall seasons casts light on how climate variables could affect the human environment and sources of people's livelihoods such as ecosystem services, human health, agricultural activities, and fishing for example. Nonetheless, the study by the United Kingdom Department for International Development (DFID) predicts a rise in temperature of up to 3.2°C by 2050 under a high climate change scenario in every part of Nigeria. It also predicts a significant sea level rise from the 1990 levels to 0.3m by 2020 and 1m by 2050 along the Nigerian coasts (DFID 2009, FME 2014). However, considering the fact that the coastal Niger Delta settlement is a low-lying area, the future predictions of rise in sea levels call for action.

Implications for Sustainable Development. The above analyses show evidence of observed climate variability and its potential risk to people and communities in the area and draw on the Nigeria's Intended National Determined Contribution to the Paris Agreement which states that "climate change poses a significant threat to the achievement of development goals, especially those related to eliminating poverty and hunger and promoting environmental sustainability" (INDC 2015). In other words, achieving sustainable development entails dealing with climate vulnerability (IPCC 2014c). The increasing trend in temperature and irregular yet decreasing trend in rainfall pattern portends extensive negative environmental and socioeconomic implications unless developmental policies consider resilient and robust adaptation actions. For instance, the following three new sustainable development goals are potentially threatened by current and anticipated climate and weather related impacts in the region (Figure 4).

CONCLUSION

Section 20 of the Nigerian 1999 constitution requires that "the state shall protect and improve the environment and safeguard the water, air and land, forest, and wildlife of Nigeria." The United Nations Framework Convention on Climate Change provides the basis to adapt to the impacts of climate change; Nigeria ratified the Convention on the 29 August 1994 (Ogbonna and Albrecht 2015). Article 4.1 of the Convention is crucial for undertaking adaptation and paragraph 1(e) of the Article asked all parties to the Convention to cooperate in preparing for adaptation in the areas of coastal management and agriculture

with particular reference to Africa. Drawing upon the above study analyses, climate variability combined with other environmental stressors exerts potential pressure on current and future sustainable development initiatives in the Niger Delta. Adaptation will enhance social, economic and environmentally sustainable management of the region's natural resources. In this respect adaptation measures that need to be addressed to reinforce sustainable development initiatives include the following but not limited to: provision of accurate weather and climate predictions, though not a panacea to extreme weather events, but will enhance proactive adaptation actions and improve self-protective behaviors; scaling up research that would improve traditional agricultural practices. For example, improved crop species that could be resilient to extreme temperatures and variable rainfall patterns. Such could help avert influences on hunger, food security and poverty. Application of the precautionary principle is imperative to reduce climate risks, protect coastal settlements, infrastructures, and people's livelihoods in the Niger Delta. The provision of appropriate legal and policy frameworks, which will mean bringing together all necessary regulatory tools and environmental instruments that can enhance adaptation implementation, are crucial in this regard.

REFERENCES

- Albrecht, E. and Ogonna, C.U. 2015. Strategic Environmental Assessment as a Tool to Integrate Climate Change Adaptation: A Perspective for Nigeria. In: Leal Filho, W. (ed.), Handbook of Climate Change Adaptation, Springer-Verlag, Berlin Heidelberg, pp. 1239–1260.
- Federal Ministry of Environment (FME). 2010. National Environmental, Economic and Social Development Study (NEEDS) for Climate Change in Nigeria. Federal Ministry of Environment, Abuja, Nigeria. Special Climate Change Unit, pp. 45.
- Federal Ministry of Environment (FME). 2014. Second National Communication on Climate Change. Federal Ministry of Environment of the Federal Republic of Nigeria, Abuja: MEFRN, pp. 132.
- INDC. 2015. Nigeria's Intended Nationally Determined Contribution, available at:<http://www4.unfccc.int/submissions/indc/Submission%20Pages/submissions.aspx>, accessed 05.26.2016.
- IPCC. 2014a. Climate Change 2014. Impacts, Adaptation, and Vulnerability. Cambridge University Press, Cambridge University Press, Cambridge, United Kingdom.
- IPCC. 2014b. Climate Change 2014. Synthesis Report Contribution of Working Groups I, II and III to the Fifth Assessment Report of the Intergovernmental Panel on Climate Change IPCC, Geneva.
- IPCC. 2014c. Climate Change 2014. Mitigation of Climate Change. Contribution of Working Group III to the Fifth Assessment Report of the Intergovernmental Panel on Climate Change. Cambridge University Press, Cambridge, United Kingdom.
- NEST 2011. Reports of Research Projects on Impacts and Adaptation. Building Nigeria's Response to Climate Change. Ibadan, Nigeria: Nigerian Environmental Study/Action Team (NEST), pp. 330.
- Ogonna, C.U. 2014. Adaptation to Climate Change in Developing Countries: A need in the Niger Delta region of Nigeria. In: Albrecht, E. Schmidt, M., Mißler-Behr, M., Spyra, S.P.N. (eds). Implementing Adaptation Strategies by Legal, Economic and Planning Instruments on Climate Change. Springer Berlin Heidelberg, pp. 165–187.
- Okorie F. C, Okeke I., Nnaji A., Chibo, C., and Pat-Mbano, E. 2012. "Evidence of Climate Variability in Imo State of Southern Eastern Nigeria." *Journal of Earth Science Engineering* 2: 544–553.
- Post-Disaster Needs Assessment (PDNA). 2013. Nigeria Post-Disaster Needs Assessment. A Report by the Federal Government of Nigeria, with Technical Support from the European Union, United Nation, World Bank, and other Partners, Nigeria Post-Disaster Need Assessment 2012 floods. Federal Government of Nigeria Abuja, pp. 154.
- Sylla, M.B. 2015. "Regional Climate Change over West Africa: Trends, Shift of Climate Zones and Timing of the Wet Extremes." In: Stocker, T.F., D. Qin, G.-K. Plattner, and M. Tignor (eds.), IPCC. 2015. Workshop Report of the Intergovernmental Panel on Climate Change Workshop on Regional Climate Projections and their Use in Impacts and Risk Analysis Studies, pp. 154–155. IPCC Working Group I Technical Support Unit, University of Bern, Bern, Switzerland.

- Territorial Approach to Climate Change (TACC). 2013. Biophysical and Socio-Economic Assessment of the Nexus of Environmental Degradation and Climate Change, Delta State, Nigeria, pp. 234.
- UNDP Niger Delta Biodiversity Project, available at: http://www.undp.org/content/dam/undp/documents/projects/NGA/Niger%20Delta%20Biodiversity_Prodoc.pdf, accessed 20.05.2016
- United Kingdom Department for International Development (DFID). 2009. Impact of Climate Change on Nigeria's Economy, DFID Abuja, Nigeria.
- United Nations (UN). 2010. Sustainable Development: From Brundtland to Rio 2012. Background Paper Prepared for Consideration by The High Level Panel On Global Sustainability at Its First Meeting, 19 September 2010. International Institute for Sustainable Development (IISD), pp. 26.
- United Nations Environmental Program. 2011. Environmental Assessment of Ogoniland. United Nations Environmental Program, Nairobi, Kenya, pp. 257.
- World Commission on Environment and Development: Our Common Future (WCED). 1987. Report of the World Commission on Environment and Development: Our Common Future, available at <http://www.un-documents.net/our-common-future.pdf>, accessed 05.15. 2016.

**URBAN ENVIRONMENTAL OVERALL PLANNING AND ITS ROLE IN URBAN
SUSTAINABLE DEVELOPMENT IN CHINA**

Luyan Wang, Yang Zhao, Lina Tang, and Jingzhu Zhao
(Institute of Urban Environment, CAS, Xiamen, Fujian Province, 361021, China)

Urbanization is facilitating economic development in China and around the world but is limited by land resources and environmental problems. Unplanned urbanization restricts sustainable development in China. However, the present urban environmental planning only emphasizes the prevention and treatment of the existing civilian and industrial wastes but lacks the efforts in urban environmental overall planning that intends to turnaround environmental degradations from the source. Urban overall planning and land-use overall planning represent technical supports for urban ecological and environmental protection from the angles of spatial pattern and land usage, and make it possible for an environment-development-construction-land integrated planning system of urban sustainable development. The overall planning of urban environment aims at (1) explicit urban resource carrying capacity and environmental capacity, and correctly regulating the rates in urban population growth and economic scale expansion; (2) defining ecological red lines, promoting ecological functions, improving environmental quality, and sustaining resource utilization; (3) comprehensive functional classification of urban environment, realizing classified management and administration of urban environment, and guiding the regulations of industrial distribution and structure; and (4) recognizing major sources of environmental risk, defining red lines of environmental risk, and developing control systems of environmental risk. To ensure the effective role of urban environmental overall planning in urban sustainable development in China, it is essential to clarify legal status of urban environmental overall planning, strengthen the concepts of ecological and environmental spatial management, and attach great importance to the ideas of regional coordination.

**PERFORMANCE ENHANCEMENT OF EVAPORATIVE COOLING TECHNOLOGY IN THE
COMPANY OF LOWER ENVIRONMENTAL IMPACT**

S.P. S. Rajput and Amrat Kumar Dhamneya
(Maulana Azad National Institute of Technology Bhopal, India 462003)

The objective of this paper is to identify the development of different geometry and material of cooling pads used in cooling for performance enhancement of direct evaporative cooling. Nearly everyone discussed that the effectiveness of direct evaporative cooling decreases as temperature increases. Focusing on human thermal comfort at minimum cost, low maintenance, inexpensive, minimum energy consumption and to minimize the emission of greenhouse gases effect, researchers and designers are developing new methods for evaporative cooling technique in place of conventional air-conditioning. India has different weather conditions at different places throughout the year. Central India climate is best favourable for air-conditioning with evaporative cooling. To increase the effectiveness different evaporative cooling method are being used in combined operation with other cooling measures, like indirect/direct evaporative cooling (IDEC) with vapour compression refrigeration system (VCRS), indirect evaporative cooling with desiccant wheel, direct evaporative cooling with desiccant, direct evaporative cooling with ground storage water and direct evaporative cooling with VCRS. In this paper the concluding remark will be on the performance enhancement of direct evaporative cooling technique in favour of cooling effectiveness and better human thermal comfort keeping in mind the minimum consumption of electricity and lower environmental impact. Selection of different evaporative cooling technique for air-conditioning according to the weather conditions will be applied according to appropriate condition. This study will focus on heat exchanger configuration and its material composition, distribution and treatment of water flow, cost-effectiveness and minimum environmental impacts. Emphasis is laid on extracting the heat from atmospheric air by passive technique as well as minimizing the conventional load of air conditioner.

**ADAPTATION STRATEGIES TO MITIGATE CLIMATE CHANGE IMPACTS ON URBAN
STORMWATER.**

Ashantha Goonetilleke (Queensland University of Technology, Brisbane, Queensland, Australia)

An Liu (Shenzhen University, Shenzhen, China)

Erick R. Bandala (Desert Research Institute, Las Vegas, NV, USA)

The water environment is particularly vulnerable to climate change due to the predicted changes to the weather patterns. Studies have shown that even with aggressive mitigation efforts, the impacts of climate change will worsen and, appropriate adaptation efforts are needed. However, attention in relation to climate change impacts on the water environment is primarily focused on water resources with limited attention given to the impacts on stormwater. The need for concern stems from the fact that stormwater runoff exerts a significant influence on freshwater resources. Furthermore, urban stormwater is an important resource for the future as urban areas are facing increasing deficiencies to meet the needs of an ever growing population, which are being further exacerbated by climate change. The predicted climate change impacts will influence the characteristics of the primary stormwater pollutant processes, namely pollutant build-up and pollutant wash-off. Additionally, the changes in rainfall characteristics will result in changes to the stormwater runoff hydrograph. Therefore, understanding the linkages between climate change and stormwater runoff characteristics is important for developing effective adaptation strategies to mitigate the adverse consequences of climate change on the water environment. The paper provides an overview about changes to flow processes and pollutant processes and current knowledge gaps in relation to urban stormwater. Additionally, a broad discussion is provided on the options available for adaptation to cope with climate change impacts on stormwater runoff quality and quantity. It is proposed that adaptation should be viewed as an opportunity to create a sustainable development agenda. Accordingly, two key approaches are proposed to advance the sustainable development agenda: low impact development to underpin urban development; and the identification of water sensitive opportunities in the urban environment based on local needs and imperatives.

ENVIRONMENTAL AND SOCIAL SUSTAINABILITY

Sukhmander Singh

(Santa Clara University, Santa Clara, California 95053, USA)

Sustainable development should include both environmentally and socially sustainable solutions. This is so because environment, society and technology are interlocking parameters. Society's economic system influences the production systems that are appropriate to that society. The production system in turn impacts the ecosystem. It is now well recognized that the production system with an ever increasing per capita consumption can lead to the depletion of resources as well as to the pollution of the ecosystem; and hence the importance of sustainable solutions. Since the production is often motivated by profit- which can be exploited by the rich, even in the use of a sustainable solution, there is a need for a sustainable solution to be both environmentally and socially just. A mode is presented for addressing sustainability in society. It is argued that both environmentally and socially sustainable solutions can be achieved by incorporating locally available renewable or recycling material with the use of local labor. Such an approach would help set up employment base for local people who otherwise may be denied such an opportunity should a large scale system /entrepreneurship is allowed to employ an approach of mass production versus production by masses. In some poor countries where poverty, hunger and poor sanitation exist, environmentally acceptable, economically accessible and socially sustainable solutions must be found to bring about a developed and socially just society. These solutions ought to be simple, inexpensive and environmentally safe. Examples of such solutions are presented in the paper. It is recommended that affordable technologies based on the concept of sustainability be developed to help marginal communities. The paper points out that there's a need for interference between technology and society while developing technology based sustainable solutions.

**ECOTOURISM AND SUSTAINABLE DEVELOPMENT; EVIDENCE FROM LOPE
NATIONAL PARK, GABON**

Cornelius FRIMPONG

(Department of Biological and Environmental Sciences, University of Stirling, Stirling, Stirlingshire,
FK9 4LA, Scotland, UK)

Ecotourism is widely applied to the conservation of tropical forest resources as a means of raising funds for conservation and to support social and economic development of local communities. With these three objectives, ecotourism has been embraced as a sustainable management approach. On this premise, this study has produced a new schematic diagram to guide ecotourism conceptualization. Consequently, using the case of Lope National Park, Gabon, this study engaged a purposive sample of 20 conservation scientists and Park staff (Gabonese and non-Gabonese) to analyse how the three sustainability objectives are achieved and how this is influenced by respondents' nationality. Data analysis and hypotheses testing were conducted through MANOVA, Wilcoxon signed rank test and paired-sample t-test in SPSS Version 21 (IBM). The study found that ecotourism is perceived to fulfil all three objectives of sustainability. However, statistical analysis showed significant difference in the distribution of ecotourism revenue between Gabonese and non-Gabonese [$F(3, 16) = 5.66, p = .008, \text{partial } \eta^2 = .515$]. Follow-up ANOVA conducted revealed that, whereas Gabonese distributed revenue nearly equally across the three pillars, non-Gabonese placed overemphasis on conservation [$F(1, 1.21) = 17.056, p = .001, \text{partial } \eta^2 = .487$]. Consequently, ecotourism management at Lope was found to fall short of meeting international standards. The study concluded with recommendations and a suggestion for further research to broaden this scope by recruiting a larger sample of various stakeholders.

STAKEHOLDER PARTICIPATION IN INTEGRATED WATERSHED MANAGEMENT: MODELS AND PROCESS

*Aysegul Tanik** and Cigdem Kanber
(Istanbul Technical University, ITU, Turkey)

ABSTRACT: Stakeholder participation in sustainable watershed management, the related participation models and process forms the main part of this study. Especially in developing countries, the main concern is to increase public awareness and encourage public representatives to participate in management issues. In that sense, four participation models; Commentary Model, Social Learning Model, Joint Planning Model and Consent/Consensus Model are introduced. Buyukmenderes watershed of Turkey is selected as the pilot watershed. Five main provinces share this watershed making the management a crucial process. Upon investigation, education, socio-economic and development levels are found well above the country's average. The current legal and administrative structure permits the establishment of Watershed Management Committees (WMC); however, the members though limited to 25 exceed 70 in multi-provincial watersheds. A new structure is proposed in this study, namely Watershed Protection Association (WPA) to overcome this participation problem. Training of WMC and WPA members are detailed under the principle of *learning together to manage together*. At the initial phase (2-3 years) of watershed management studies, Social Learning Model is selected for the pilot watershed. After gaining experience on participatory process, Joint Planning Model is recommended. Developing countries may follow a similar pathway to introduce public in watershed studies.

INTRODUCTION

Integrated Watershed Management aims to define the natural resources within its boundaries, and to determine any sectoral conflicts while enabling coordination among any activities and policies related to the current legal and administrative structure with the participation of stakeholders representing the main water-related actors and users in the most compatible manner (Heathcote, 1998; Randhir, 2007; US EPA, 2013a). Practices of different stakeholder participation models heading to increase the well-being of public have so far shown that applicable models may differ among watersheds and that the development level of the watershed is an important concern governing the selection of the appropriate model (US EPA, 2013b; Kanber, 2015). One of the available models may be initially selected and applied for a certain period of time may then be quitted and another model may be preferred. Four of the models are referred in this study. These are; Commentary Model, Social Learning Model, Joint Planning Model and Consent/Consensus Model as shown in Figure 1 (Url-1).

Turkey bearing 25 watersheds is at a stage of preparing the watershed management plans and trying to get acquainted with watershed management principles and policies regarding public participation which is a common case for most of the developing countries. One of the essential strategies to the achievement of the objectives of integrated watershed management relates to the promotion of community participation (ESCAP, 1997; US EPA, 2013c). Public participation is a planned effort to involve citizens in the decision-making process and to present and resolve citizen conflict through mutual two-way communications. Therefore, this research attempts to set a methodology on how public may participate and/or may be represented in watershed management studies. Various participation models will be briefly outlined; suitable ones that seem to best fit the selected watershed of Turkey, namely Buyukmenderes Watershed, will be mentioned. A watershed protection association will be proposed and its structural framework and projected responsibilities will be defined regarding the legal and administrative status of the country.

MATERIALS AND METHODS

Participation Models. Four of the models of public participation are given in Figure 1 and the relationships among these models are schematically shown in Figure 2. All the referred models aim to introduce stakeholders to the participation system. The main concern is to increase public awareness and encourage public representatives to participate in management issues especially in developing countries. In a way, the question is ‘*how can we include different stakeholders in watershed management*’?

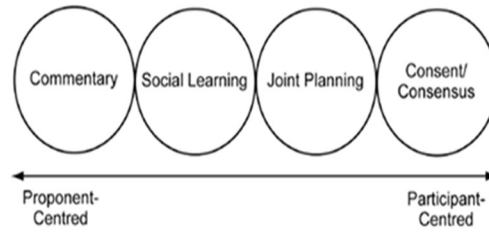


FIGURE 1. Four Models of Public Participation (Url-1)

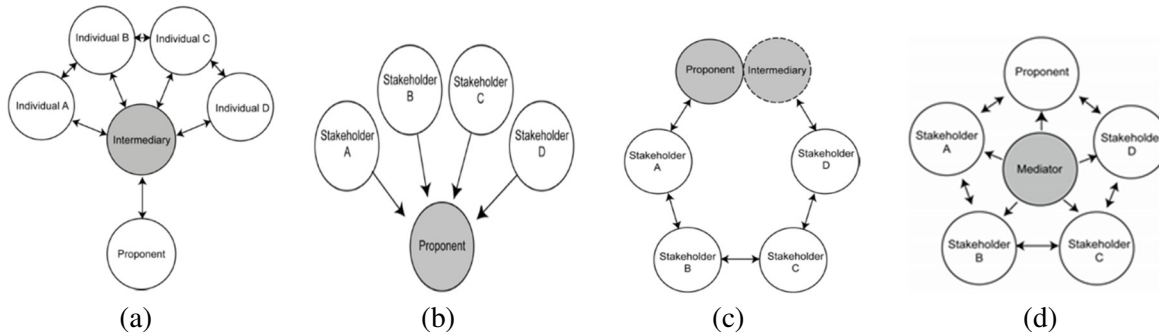


FIGURE 2. Relationship among the participation models; (a) commentary model, (b) social learning, (c) joint planning, (d) consent/consensus (Url-1; Kanber, 2015)

Brief Information on the Watersheds of Turkey. Administratively, the country has 81 provinces with political boundaries that do not match with the hydrological boundaries of 25 watersheds. As might be imagined, the provinces neither bear similar surface areas nor the watersheds. Information defining the watershed characteristics regarding their geographical status, climatic conditions, ecological characteristics as well as the socio-economic welfare may all be gathered on provincial basis. However, the provinces share watersheds but not always fully as seen in Figure 3. Some provinces are shared by more than 2 provinces which make the situation of collecting information quite tiresome. Neighborhood provinces, even though they take place in the same watershed, bear different physical characteristics as well as different financial and social status. Under these circumstances, management becomes more complicated. However, these administrative problems are partly overcome by the publication of two legislations; one is about formation of watershed management committee, duties, working procedures and regulations initially published in 18.06.2013 with no 28681 in the Official Newspaper, and revised in 20.05.2015 with no 29361, and the other is National Watershed Management Strategy (2014-2023) put into force on 04.07.2014 with no 29050.

Physical Structure of Buyukmenderes Watershed. 10 provinces share this coastal watershed located along the Aegean Sea. Aydin Province constituting 27.45% of the basin almost fully lie (95%) within the watershed, and thus acts as the coordinator province. Denizli Province covers 33.65% of Buyukmenderes

Basin and almost 70% of the province is within the basin. These two provinces are followed by Usak, Afyon and Mugla where 67.87%, 23.04% and 19.71% of their respective areas lie within the basin. Apart from these 5 provinces the other 5 have shares less than 5%, thus, they are not considered as important provinces (Figure 4).

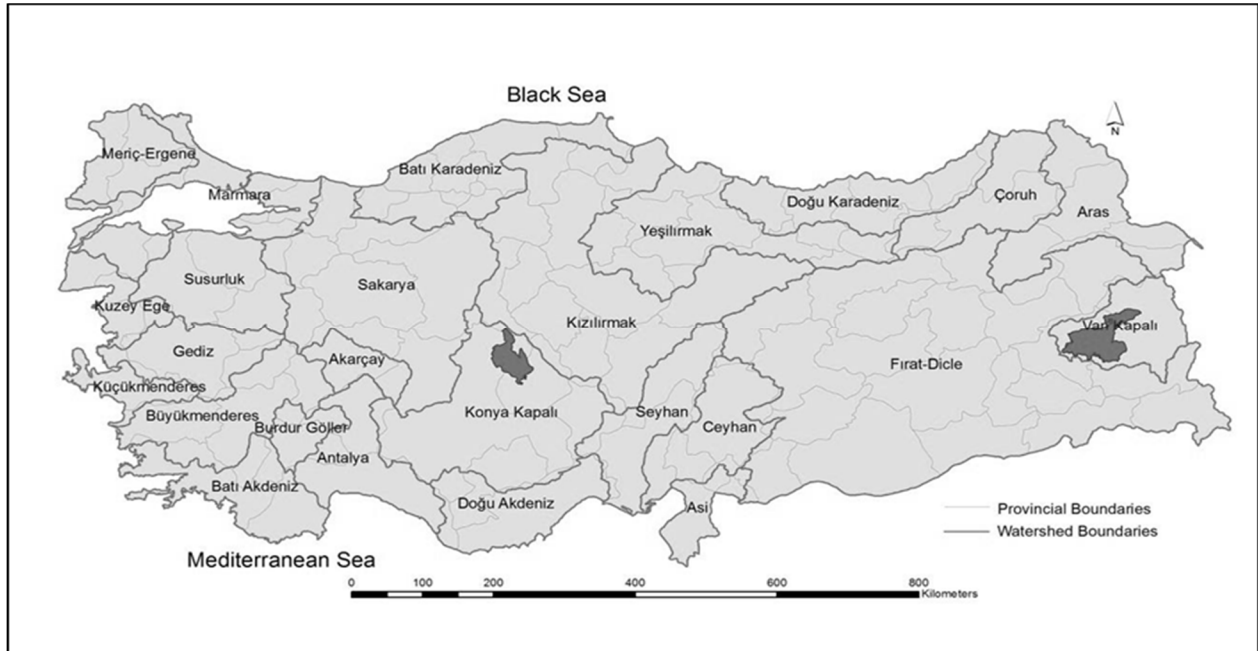


FIGURE 3. Watersheds of Turkey



FIGURE 4. Sharing provinces of Büyükenderes Watershed

Inspecting education level of these 5 major sharing provinces, one can easily observe that the level of education is well above the country's average. In that sense, public awareness and consciousness to environmental and especially to water issues in the basin is quite high in parallel to development level. Similarly, the socio-economic status of the basin is also higher than the other neighborhood coastal basins.

Based on the 2013 values, per capita income level is rated as 'high medium income' according to World Banks criteria in the major provinces of the basin despite some differences in the socio-economical and financial status among the sharing provinces. For example, the coordinator province, Aydin, is ranked as the 3th province of the basin in terms of development level (Gul and Cevik, 2014). However, all the sharing provinces are placed in the first 44 row among the overall number of 81 provinces indicating the above average position of the basin (Kanber, 2015).

Institutional Structure of Buyukmenderes Watershed. According to the current legislation, Watershed Management Committee (WMC) is limited to 25 people including the governor of the coordinator province. However, for this specific basin consisting of 5 major provinces, this number is calculated as 73 (Kanber, 2015). Only the coordinator province authorities are 21 people. Thus, it is for sure that WMC will not be able to fulfil principles like equality, right of representation and transparency. Moreover, convergence of '*public-private sector-people*' cannot be maintained leading to almost no public participation in environmental issues. Therefore, this structure will not be sufficient for involving public to management. A new autonomous system or formation is necessary to work under WMC.

WMC Training and Social Learning Process. Social learning has a basic principle '*learning together to manage together*'. In that sense, a training program for the WMC members at the beginning is proposed. To give training to 73 people is a serious job. Thus, the following questions need to be replied;

- How, when and where these committee members will come together for training?
- Who will give this training?
- What will be the scope and framework of this program?
- Who will cover the expenses of this training program?

It will be quite healthy if this training is given at the early stages of watershed planning process. Thus, the committee members will be furnished with information on the importance of public participation in integrated watershed management studies, and these members on their way back to their sub-basins will communicate with other stakeholders and satisfy the principle of *learning together to manage together*. An establishment of a new structure is also proposed in this study; namely, Watershed Protection Association (WPA), whose structure will be briefly defined in the following part. The training center seems to be better selected by this new association by paying attention to ease of transportation for the committee members. At a start, the place preferred is Regional Directorate of State Water Works in Aydin Province. Probable trainers are recommended to be the team who has already been trained by EU representatives within the context of 'Training the Trainees Project'. The living, accommodation and traveling costs for training the committee members must be covered by the General Directorate of Water Management under the Ministry of Forestry and Water Affairs, and they should be permitted from their work places to attend this training program. Those members who complete this process with success may be awarded by giving certificates of attendance. As such, they will be encouraged to work as volunteers in management studies. Similarly, those who fail must be discarded from the system. The training program may be considered to last 3 days. These programs may be repeated every two years. Certified members and candidate members may lose these lives, may become older, may pose unstable behavior or lose their enthusiasm during the two years' time; thus, repetition of these programs may be a must to gain new trained members.

WMC members may still lead to lack of sufficient public participation and may act as a supreme board at the watershed. Therefore, a new structure is needed to fulfill the participatory management approach.

Formation of Watershed Protection Association (WPA). As defined by the legislation of WMC, the members have to meet monthly. In order to fulfill the requirements of public participation, another association is proposed to be formed under WMC. This formation is named as Watershed Protection Association (WPA) which is actually necessary for a more healthy, fair and consistent public participation.

After the completion of the first run training program to WMC; some of the certified members may take part in the formation of WPA, and WPA members have to be trained by the similar training program. It is then that the successful members of WPA may participate actively in the integrated watershed management efforts and especially in the preparation of watershed management plans, and also in the application of the 'preventive programs' during the application of the management plans. Members of the WPA may consist of public and private sector representatives together with representatives of various other stakeholders like land owners, farmers, fishermen, district or regional representatives, local municipality authorities, various state officers, employers and sectoral representatives, women and youth, public service members, religious officers, universities, colleges, environmental agencies, active NGO's, soil and water protection regional representatives, irrigation associations, national and local media. The association will be a legal personality; therefore, it needs at least a general secretary, office manager and office personnel salaried in its constitution. Furthermore, it will need accounting personnel for arranging the cost of rent and collection of participation shares together with a computer expert, graphic designer and public relations expert (PR). For the field trips and surveys, a vehicle and at least a driver have to be hired. At this point, it is of utmost importance to have sufficient number of representatives of public in WPA. It may be attained through different commissions devoted to training, field applications and PR. Members of these commissions may be represented well by equal distribution of public participation. As such, these commissions will work in close contact with public and feedback gained will increase the consciousness among public towards IWM. Figure 5 shows the schematic diagram of the proposed WPA structure.

RESULTS AND DISCUSSION

High public awareness and participation is expected in this watershed as its development and education levels are comparatively higher than the country's average together with the income rates. In that sense, effective and active participation in IWM attempts will not be surprise and public interest to environmental issues is expected to be high. A similar training program is also suggested to the members of WPA. Successful members of WMC who have passed from this training may train the members of WPA; forming an example of *learning together*.

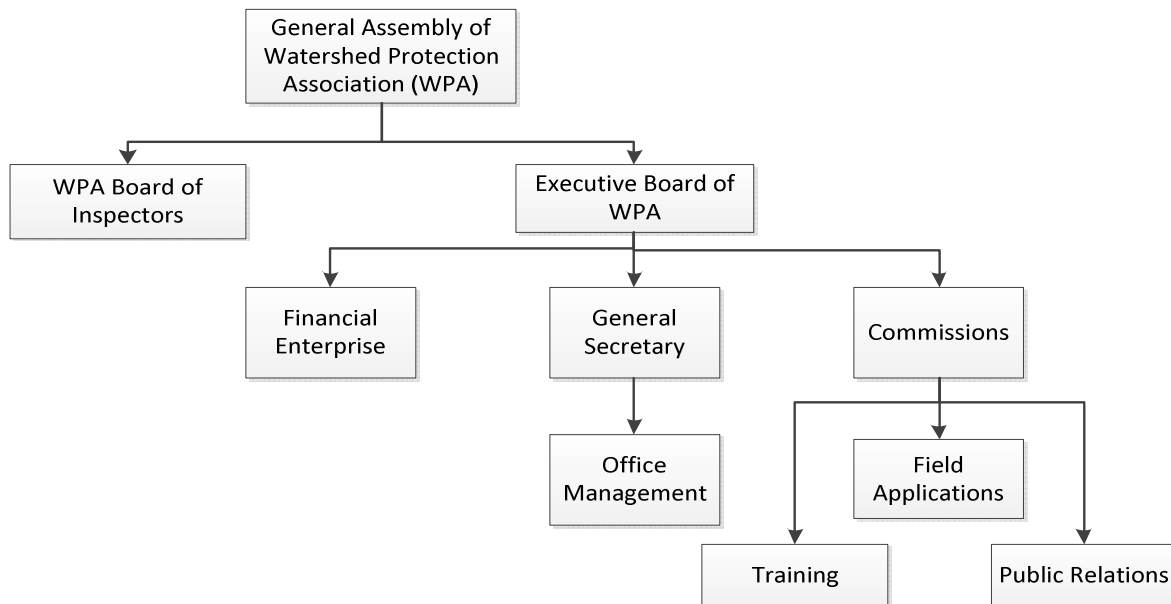


FIGURE 5. Proposed WPA structure

At this stage, one of the referred participation models has to be selected for this purpose. Out of the 4 models referred, it is suggested that Social Learning and Joint Planning Models may best fit to

Buyukmenderes Watershed. In the first 2-3 years of time, Social Learning Model may be practiced; however, after this initial stage as experience will be gained on public participation, Joint Planning Model may be followed considering the high interest of public on IWM.

CONCLUSIONS

Structure of a developing country is always dynamic. Therefore, legal and administrative legislation regarding watershed management tend to change frequently. This study is prepared according to the legislation of April 2015. It is for sure that the legislation of 2013 on the formation of Watershed Management Committee has been an important threshold regarding watershed scale studies. With this legislation for the first time in the country, public participation is encouraged despite many discrepancies. Public awareness and consciousness has still not been widespread, and cooperation and collaboration among various institutions is not at a suitable level. Simply, this study proposes a new structure under the WMC that will communicate more effectively with inhabitants of the watershed. Such an establishment is expected to be successful especially in watersheds where the number of the sharing provinces are high like is the case in this selected watershed.

A fixed participation model is not recommended for all the watersheds of the country as each bears different education, development and socio-economic level. In case of lower education and income levels, proponent-centered commentary model may be preferred. In this model, final decisions are taken by the central authority. The model does not require public participation at the beginning and may be applied by ease.

REFERENCES

- EC-HarmoniCOP. 2005. *Learning Together to Manage Together - Improving Participation in Water Management*, Handbook, EC-funded output of the project Harmonizing Collaborative Planning within the thematic program “Energy, Environment and Sustainable Development” (1998-2002 /Contract No. EVK1-CT-2002-00120).
- Erdogan, R. 2013. “Advances in Landscape Architecture- Chapter 6”, In M. Ozyavuz (Ed.), *Stakeholder Involvement in Sustainable Watershed Management Environmental Sciences*, InTech, DOI: 100.6772/55798. <http://www.intechopen.com/books/advances-in-landscape-architecture/stakeholder-involvement-in-sustainable-watershed-management>
- ESCAP. 1997. *Guidelines and Manual on Land-use Planning and Practices in Watershed Management and Disaster Reduction*, Economic and Social Commission for Asia and the Pacific (ESCAP), United Nations, 133 p.
- Gul, E., and B. Cevik. 2014. *Searching the Development Level of the Turkish Provinces with 2010 and 2012 Data*, Economic Researches Division, February 2014 Report, Turkish IsBank, (in Turkish). http://webcache.googleusercontent.com/search?q=cache:HD4WkK9xrUEJ:https://ekonomi.isbank.com.tr/UserFiles/pdf/ar_03_2012.pdf+&cd=1&hl=tr&ct=clnk&gl=tr
- Heathcote, W. I. 1998. *Integrated Watershed Management Principles and Practice*, Library of Congress Cataloging-in-Publication Data, John Wiley & Sons, Inc., NY, USA.
- Kanber, C. 2015. *Stakeholder Participation in Integrated Watershed Management: Models and Process*, M.S. Thesis, Istanbul Technical University (ITU) Graduate School of Science Engineering and Technology, Istanbul (in Turkish).
- O’Faircheallaigh, C. 2009. “Public Participation and Environmental Impact Assessment: Purposes, Implications, and Lessons for Public Policy Making”, *Environmental Impact Assessment Review*, 30(1):19-27.
- Randhir, T. O. 2007. *Watershed Management Issues and Approaches*, IWA Publishing, UK.
- Url- 1: <http://www.hardystevenson.com/research/articles.php>. Decision making on Controversial Issues of National Scope: Models for Involving the Public.

- US EPA. 2013a. *Getting in Steps: Engaging Stakeholders in Your Watershed*, 2nd Ed. EPA 841-B-11-001, US EPA Office of Water, Nonpoint Source Control Branch (4503T) Washington, DC. <http://cfpub.epa.gov/npstbx/files/stakeholderguide.pdf>
- US EPA. 2013b. *Public Participation Guide*. <http://www2.epa.gov/international-cooperation/public-participation-guide-view-and-print-versions>
- US EPA. 2013c. *A Quick Guide to Developing Watershed Plans to Restore and Protect Our Waters*. http://webcache.googleusercontent.com/search?q=cache:5QYcP7WNE6wJ:water.epa.gov/polwaste/nps/upload/watershed_mgmnt_quick_guide.pdf+&cd=1&hl=tr&ct=clnk&gl=tr
- Webler, T., H. Kastenholz, and O. Renn. 1995. "Public Participation Impact Assessment: A Social Learning Perspective", *Environmental Impact Assessment Review*, 15(5):443-463.

**EFFECTIVENESS OF SOUTH AFRICA'S BIODIVERSITY POLICIES IN PROTECTING THE
INDIGENOUS VEGETATION OF THE SOUTPANSBERG REGION**

Priscilla Ntuchu Kephe

(University of Limpopo, Turfloop, South Africa)

Brilliant M. Petja

(Water Research Commission, Pretoria, South Africa, University of Limpopo, Turfloop, South Africa)

The management of protected areas and biosphere reserves needs to be revised in the light of growing - problems related to the declining biomass and composition of the indigenous vegetation in the Soutpansberg Mountain range. This paper analyses key policies, achievements, gaps and constraints in the implementation of South Africa's key biodiversity policies in the Soutpansberg. Issues examined include threats to vegetation such as habitat transformation (composition and biomass) and changes in the local climate of the area. It was found out that despite remarkable achievements and shifts in conservation paradigms, the development of a widely accepted national policy on biodiversity and an increase in the number of the country's protected areas, Soutpansberg continues to lose plant species and vegetation composition. In order to safeguard what is left of the indigenous vegetation of the Soutpansberg, the protection of plants species and habitats should be prioritise, more especially since the vegetation of the Soutpansberg influences the local climate of the area.

RENEWABLE ENERGY DEVELOPMENT

PHOTO GALVANIC CELL: AN EFFICIENT DEVICE FOR PHOTOCHEMICAL CONVERSION AND STORAGE OF SOLAR ENERGY

Chhagan Lal (Department of Chemistry, Harcourt Butler Technological Institute, Kanpur, India)
E-mail: clal9940@gmail.com

ABSTRACT: Photogalvanic effect was studied in photogalvanic cell containing EDTA as reductant, mixed dyes (combination of two dyes) as photosensitizer i.e. EDTA-NMB-SFO, EDTA-NMB-FG, EDTA-BG-FG, EDTA-BG-CB, EDTA-NMB-CB. The used reductant was Ethylene diamine tetra acetic acid and photosensitizers were new methylene blue (NMB), Safranin-O-(SFO), Fast Green (FG), Brilliant Green (BG), Celestine Blue (CB), in different combinations. The photopotential, photocurrent, conversion efficiency, power of the cell and performance of the photogalvanic cells were determined. The effects of various parameters on the electrical output of the cell were observed and a mechanism has also been proposed for the generation of photocurrent in photogalvanic cells. The photogalvanic cells (system) can be used for 95.0, 90.0, 72.0, 65.0, 45.0 minutes in dark respectively.

Keywords: Photogalvanic cell; Dyes; Fill factor; Conversion Efficiency

INTRODUCTION

Although, the photogalvanic effect was first of all reported by Rideal and Williams (1925) but the iron-thionine system was systematically investigated by Rabinowitch, (1940). Later on, it was investigated by many workers from time to time Fox and Kabir-ud-din (1979), Stevenson and Errelding (1981), Ameta et al (1985). Many workers have used different photosensitizers in different photogalvanic systems and observed a reasonable electrical output as compared to iron-thionine system. Some of the photosensitizers used in solar cells are proflavine (Eisenberg and Silverman, 1961), Tolosafranin (Kaneko and Yamada, 1977), Riboflavin (Murthy et al, 1980), Flavin mononucleotide (Yamase, 1981), Poly(N-acylamido methylthionine (Tamilarasan and Natrajan, 1981), Toluidine blue (Murthy and Reddy, 1983) Brilliant Cresyl blue (Jain et al, 1984) Methylene blue, (Ameta et al, 1989) and Gangotri et al, 1996), Safranin (Gangotri and Regar, 1997) etc. but the use of mixed dyes (Gangotri and Lal, 2005, Yadav and Lal, 2010, Lal and Gangotri 2011, Yadav and Lal, 2013 combinations of two dyes) as photosensitizer and reductant received a little attention. Therefore, present study was undertaken.

In order to increase the electrical output, conversion efficiency and storage capacity of the cells, the different combinations of two dyes (mixed dyes) system have been used in the photogalvanic cells in the present work and the role of mixed dyes has also been investigated.

EXPERIMENTAL

EDTA-disodium salt (MERCK), Sodium hydroxide (Ranbaxy), Methylene blue (NMB), Safranin-O (SFO), Fast green (FG), Brilliant green (BG), Celestine blue (CB), were used in the present work. All the solutions were prepared in the doubly distilled water. A mixture of the solutions of the dyes, reductant, sodium hydroxide was taken in an H-shaped glass cell. A platinum electrode ($1.0 \times 1.0 \text{ cm}^2$) was dipped into one limb of the cell and a saturated calomel electrode (SCE) was kept in the other. The whole system was placed in dark till a stable potential was obtained, then the platinum electrode was exposed to a 200W tungsten lamp (ECE) and the limb containing SCE was kept in dark. A water filter was placed between the exposed limb and the light source to cut off infra-red radiations.

The photochemical bleaching of mixed dyes was studied potentiometrically. The photopotential and photocurrent generated by the system-mixed dyes/ reluctant/ OH/ hv were measured by a digital pHmeter (Model HPG-2001) and a microammeter (Osaw, India) respectively. The (i-v) characteristics of the cells were studied using an external load (Log 470K) in the circuit.

RESULTS AND DISCUSSION

Significant Observations of the Systems. The important observations of different systems are given in Table 1, which are reflecting the overall outcome of the present studies, and justified the significance of these cells from the solar energy conversion and storage point view.

Table 1. Significant Observations of the Systems
 EDTA= $2.2 \times 10^{-3}M$; Temperature = 303K; Light intensity = $10.4mWcm^{-2}$; pH =12.8

Systems→	EDTA-NMB+SFO NMB = 1.08×10^{-5} SFO = 3.6×10^{-5}	EDTA-NMB+FG NMB = 7.2×10^{-5} FG = 4.8×10^{-5}	EDTA-BG+FG BG = 1.32×10^{-5} FG = 2.80×10^{-5}	EDTA-BG+CB BG = 1.24×10^{-5} CB = 4.4×10^{-5}	EDTA-NMB+CB NMB = 8.0×10^{-5} CB = 4.00×10^{-5}
(i) Open Current Voltage Voc (mV)	1235.0	998.0	930.0	894.0	795.0
(ii) Photopotential ΔV (mV)	740.0	738.0	690.0	636.0	580.0
(iii) Potential at Power Point Vpp (mV)	640.0	652.0	580.0	550.0	480.0
(iv) Equilibrium Photocurrent ieq (μA)	108.0	120.0	112.0	93.0	88.0
(v) Maximum Photocurrent Imax(μA)	139.0	142.0	129.0	138.0	101.0
(vi) Current at Power Point ipp (μA)	70.0	90.0	75.0	60.0	65.0
(vii) Short Circuit Current isc (μA)	110.0	120.0	112.0	93.0	88.0
(viii) Rate of Generation (μA)	7.0	5.9	6.1	6.9	8.2
(ix) Power at Power Point (μW)	81.40	88.56	77.28	59.14	51.04
(x) Fill Factor (η)	0.32	0.48	0.41	0.39	0.44
(xi) t _{1/2} (min)	95.0	90.0	72.0	65.0	45.0
(xii) Charge time (min)	112.0	129.0	132.0	117.0	145.0
(xiii) Conversion Efficiency (%)	0.4309	0.5642	0.4182	0.3173	0.3010

Current-Voltage (i-v) Characteristics of the Cell. The short circuit current (i_{sc}) and open circuit voltage (V_{oc}) of the photogalvanic cells were measured with the help of a multimeter (keeping the circuit closed) and with a digital pH meter (keeping the other circuit open), respectively. The current and potential values in between these extreme values were recorded with the help of a carbon pot (log 470K) connected in the

circuit of multimeter, through which an external load was applied .The i-v characteristics of the photogalvanic cells containing mixed dyes – EDTA systems were studied and it was observed that in all the five cases, i-v curves deviated from their expected regular rectangular shape. The power point (a point on the curve where the product of potential and current maximum) in these i-v curves were determined and their fill factor were calculated using the formulae: The i-v characteristics of the photogalvanic cells are given in Table 2.

$$\text{Fill Factor} = \frac{V_{pp} \times I_{pp}}{V_{oc} \times I_{sc}} \quad (1)$$

Where, V_{pp} = Potential at power point; I_{pp} = current at power point; v_{oc} = Open circuit voltage; i_{sc} = Short circuit current

Table 2. i-v Characteristics of the Photogalvanic Cells
 EDTA = $2.2 \times 10^{-3} M$; Light intensity = $10.4 mW/cm^2$; pH = 12.8

EDTA-Dyes Systems	V_{oc} (mV)	I_{sc} (μA)	V_{pp} (mV)	I_{pp} (μA)	η
EDTA-NMB+SFO NMB = 1.08×10^{-5} SFO = 3.6×10^{-5}	1235.0	110.0	640.0	70.0	0.32
EDTA-NMB+FG NMB = 7.2×10^{-5} FG = 4.8×10^{-5}	998.0	120.0	652.0	90.0	0.48
EDTA-BG+FG BG = 1.32×10^{-5} FG = 2.80×10^{-5}	93.0	112.0	580.0	75.0	0.41
EDTA-BG+CB BG = 1.24×10^{-5} CB = 4.4×10^{-5}	894.0	93.0	550.0	60.0	0.39
EDTA-NMB+CB NMB = 8.0×10^{-5} CB = 4.00×10^{-5}	795.0	88.0	480.0	65.0	0.44

On the basis of fill factors calculated, the order of the efficiency of photogalvanic cells in the presence of mixed dyes is: EDTA- NMB + CB >> BG + FG > NMB + SFO > NMB + FG > BG + FG

Conversion Efficiency of the Cells. The conversion efficiency of the all these systems were calculated using the output at power point and the power of incident radiations. The systems at the optimum condition were also exposed to sunlight. The system of optimum conditions was also exposed to sunlight. The conversion efficiency and sunlight conversion data for these photogalvanic cells are reported in Table - 3. The conversion efficiency of these systems were calculated using the formula.

$$\text{Conversion Efficiency (CE)} = \frac{V_{pp} \times I_{pp}}{\text{Light Intensity (mW/cm}^2)} \times 100 \% \quad (2)$$

The observed conversion efficiencies were determined with a tungsten lamp of 200W (as light source), which has a light intensity around 15 times less than direct sunlight. Therefore, the conversion efficiencies have experimentally been observed as 6.46, 8.44, 6.27, 4.75 and 4.50. The observed low conversion

efficiencies in comparison to theoretical conversion efficiency of photogalvanic cells (18%) seems due to the lower stability of dyes, back electron transfer and aggregation of dyes molecules around the electrode, etc.

Table 3. Conversion Efficiency and Sunlight Conversion Data
 EDTA = $2.2 \times 10^{-3} \text{M}$; Light intensity = 10.4mWcm^{-2} ; Temperature = 303K ; pH = 12.8

EDTA-mixed dyes systems	Conversion Efficiency (%)	Sunlight Conversion Data	
		Photopotential (mV)	Photocurrent (μA)
EDTA-NMB+SFO NMB= 1.08×10^{-5} SFO= 3.6×10^{-5}	0.4307	1335.0	130.0
EDTA-NMB+FG NMB= 7.2×10^{-5} FG= 4.8×10^{-5}	0.5632	1360.0	155.0
EDTA-BG+FG BG= 1.32×10^{-5} FG= 2.80×10^{-5}	0.4182	1305.0	110.0
EDTA-BG+CB BG= 1.24×10^{-5} CB= 4.4×10^{-5}	0.3173	1280.0	127.0
EDTA-NMB+CB NMB= 8.0×10^{-5} CB= 4.00×10^{-5}	0.300	1375.0	100.0

Table 4. Performance of the Photogalvanic Cells in Dark
 EDTA = 2.2×10^{-3} ; Light intensity = 10.4mWcm^{-2} ; pH = 12.8

EDTA-mixed dyes systems	Power (μW)	Power at power point (μW)	$T_{1/2}$ (min)
EDTA-NMB+SFO NMB = 1.08×10^{-5} SFO = 3.6×10^{-5}	81.4	44.8	95.0
EDTA-NMB+FG NMB = 7.2×10^{-5} FG = 4.8×10^{-5}	88.5	58.6	90.0
EDTA-BG+FG BG = 1.32×10^{-5} FG = 2.80×10^{-5}	77.2	43.5	72.0
EDTA-BG+CB BG = 1.24×10^{-5} CB = 4.4×10^{-5}	59.1	33.0	65.0
EDTA-NMB+CB NMB = 8.0×10^{-5} CB = 4.00×10^{-5}	51.0	31.2	45.0

Based on all these observations, the fine EDTA-Mixed dyes photogalvanic system are arranged in order of their decreasing efficiencies. EDTA-NMB+FG > EDTA-NMB+SFO > EDTA-BG+FG > EDTA-BG+CB > EDTA-NMB+CB

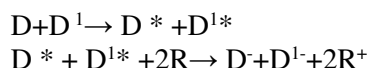
Performance of the Cell. The performance of the photogalvanic cells containing EDTA mixed dyes systems was studied by applying the desired external load to have the potential and current corresponding

to power point, after removing the source of illumination. It was quite interesting to observe that the performance of the cell in dark is affected appreciably in the presence of mixed dyes. The time $t_{1/2}$ was determined after removing the source of power. The time $t_{1/2}$ has been used as the measure of storage capacity of the cells. The performance of cells was studied and comparative results are summarised in the Table 4.

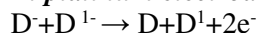
The order of storage capacity or utility of photogalvanic cells in terms of $t_{1/2}$ in the dark was:
EDTA-NMB+SFO>NMB+FG>BG+FG>BG+CB>NMB+CB

Mechanism. On the basis of these observations, a mechanism has also been proposed for the generation of photocurrent in photogalvanic cell as:

Illuminated Chamber:

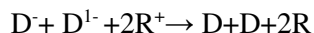
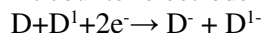


At platinum electrode:



Dark Chamber:

At counter electrode



CONCLUSIONS

According to observed photogalvanic effect in all these five system containing EDTA as reductant and mixed dyes (combination of two dyes molecule) systems, the EDTA-NMB+FG system was most efficient in all the ways and there is still hope to improve the output and storage capacity if it is thoroughly exploited. Through exploration of photogalvanic effect may give a pathway in the field of solar energy conversion and storage and a breakthrough is possible at any movement it is really planned and properly intensified. Workers have developed the photogalvanic cells containing reductant and photosensitizer with reasonable electrical output, but by combining two different photosensitizers the electrical output has increased 1.5-2.0 times as the observations show. More efforts are required to increase conversion efficiency and storage capacity by selecting suitable substances to achieve the desired results for efficient and commercial viability of the photogalvanic cells.

ACKNOWLEDGEMENT

The authors are thankful to the UGC, New Delhi for financial assistance.

REFERENCES

1. Rideal, E.K. and Williams, D.C. 1925. "Photogalvanic effect." *J. Chem. Soc.* 127: 258-269.
2. Rabinowitch, E. 1940. "The Photogalvanic Effect I. The Photochemical Properties of the Thionine-Iron System." *J. Chem. Phys.* 8: 551-59.
3. Rabinowitch, E. 1940. "The Photogalvanic Effect II. The Photogalvanic Properties of the Thionine-Iron System" *J. Chem. Phys.* 18, 560-566.
4. Fox, M.A. and Kabir-ud-din. 1979. "A New Carbonic Photogalvanic Cell." *J. Phys. Chem.* 83: 1800-1801.
5. Stevenson, K.L. and Errelding, W.F.1981. "A Photogalvanic Cell Utilizing the Photodissociation of Iodine in Solution." *Solar Energy.* 27(2): 139-141.

6. Ameta, S.C., Jain P.K., Janu, A.K. and Ameta, R. 1985. "Studies in Photochemical Conservation Of Solar Energy: Use Of Brilliant Cresyl Blue-Mannitol System In Photogalvanic Cell." *Energy J.* 58: 8-12.
7. Eisenberg, M. and Silverman, H.P. 1961. "Photo-electrochemical cells." *Electrochim Acta.* 5(1-2): 1-12.
8. Kaneko, M. and Yamada, A. 1977. "Photopotential and Photocurrent Induced By a Tolusafranin Ethylenediaminetetraacetic Acid System." *J. Phys. Chem.* 81 (12): 1213-1215.
9. Murthy, A.S.N. and Reddy, K.S. 1980. "Photogalvanic Effect in Riboflavin—Ethylenediaminetetraacetic Acid System." *Int. J. Energy Res.*, 4(4): 339-343.
10. Yamase, T. 1981. "Production of Hydrogen by a Photogalvanic Cell with a Flavine Mononucleotide-Edta System." *Photochem. Photobiol.* 34(1): 111-114.
11. Tamilsaram, T. and Natarajan. 1981. "Photovoltaic Conversion by Macromolecular Thionine Films." *Nature*. 292: 224 - 225.
12. Murthy, A.S.N. and Reddy K.S. 1983. "Studies on Photogalvanic Effect in Systems Containing Toluidine Blue." *Solar Energy.* 30(1): 39-43.
13. Jain, P.K. and Ameta, S.C. 1984. "Use of Brilliant Cresyl Blue in Photochemical Conversion Of Solar Energy." *Z. Phys. Chem (Leipzig).* 265(4): 841-2.
14. Ameta, S.C., Chittora, A.K., Gangotri, K.M. and Khamesra, S. 1989. "Use of Azur C-Glucose System In Photogalvanic Cell For Solar-Energy Conversion." *Z. Phys. Chem. (Leipzig).* 270, 607-612.
15. Gangotri, K.M., Regar, O.P., Lal, C., Kalla, P., Genwa, K.R., and Meena, R. 1996. "Use Of Tergitol-7 In Photogalvanic Cell For Solar Energy Conversion And Storage: Toluidine Blue-Glucose System." *Int. J. Energy Res.* 20(7): 581-585.
16. Gangotri, K.M. and Regar, O.P. 1997. "Use of Azine Dye as a Photosensitizer in Solar Cells: Different Reductants-Safranin Systems." *Int. J. Energy Res.* 21(14):1345-1350.
17. Gangotri, K. M. and Lal, C. 2005. "Use of Mixed Dyes in Photogalvanic Cells for Solar Energy Conversion and Storage: EDTA-Methylene Blue and Thionine System." *J. Power and Energy (Part A).* 219: 315-320.
18. Yadav, S. and Lal, C. 2010. "Efficient Solar Energy Conversion and Storage Through Photogalvanic Cell Based on EDTA: Brilliant Green and Fast Green System." *Int. J. of Green Energy*, 8(2): 265-274.
19. Lal, C. and Gangotri, K.M. 2011. "Energy Conversion and Storage Potential of Photogalvanic Cell Based on Mixed Dyes System: Ethylene Diaminetetraacetic Acid-Toluidine Blue-Thionine." *Environmental Progress & Sustainable Energy.* 30(4): 754-761.
20. Yadav, S. and Lal, C. 2013. "Optimization Of Performance Characteristics of A Mixed Dye Based Photogalvanic Cell for Efficient Solar Energy Conversion and Storage." *Energy Conversion and Management.* 66: 271-276.

THE ENVIRONMENTAL BENEFITS OF ACHIEVING HIGH SOLAR PENETRATIONS IN THE UNITED STATES

Ryan Wiser and *Dev Millstein* (Lawrence Berkeley National Laboratory, Berkeley, CA, USA)
Trieu Mai, Jordan Macknick, Alberta Carpenter, Stuart Cohen, Wesley Cole, Bethany Frew, and Garvin Heath (National Renewable Energy Laboratory, Golden, CO, USA)

We assess three key potential environmental benefits of achieving high solar penetrations (14% and 27% of U.S. electricity demand by 2030 and 2050, respectively): greenhouse-gas (GHG) emissions reductions, air-pollution health and environmental impacts, and water-use reductions. To provide context for future scenario analysis, we first assess the recent environmental benefits of the 2014 U.S. solar fleet. In this case, we use the Environmental Protection Agency (EPA)'s Avoided Emissions and geneRation Tool (AVERT) to estimate the characteristics and location of fossil generation sources displaced by year-end 2014 solar capacity. Looking forward, we use a scenario-analysis approach in which the 14%-by-2030 and 27%-by-2050 "SunShot Vision" scenario is compared with a "No New Solar (NNS) baseline" scenario in which no new solar is deployed after 2014. This framework allows us to assess the potential benefits of all incremental solar deployment. We employ the National Renewable Energy Laboratory's Regional Energy Deployment System (ReEDS) electric sector capacity-expansion model to conduct our analysis. For each of the three benefit categories, we take the modeled output from AVERT or ReEDS and then apply additional tools—as necessary—to assess potential benefits in physical and, where feasible, monetary terms. We qualify the study results appropriately, highlighting areas of uncertainty.

Our analysis finds that a future U.S. electricity system in which solar plays a major role would result in enduring environmental benefits globally, nationally and locally, and that the existing fleet of solar power plants is already offering a down-payment towards those benefits. We find that achieving the SunShot Vision scenario from 2015-2050 would reduce 10% of life-cycle GHG emissions from the power sector, reduce premature mortalities from air pollution by 25,000–59,000, and reduce power-sector water withdrawal and consumption by 4% and 9%, respectively.

The total monetary value of the GHG and criteria air pollution benefits of the SunShot Vision scenario exceed \$400 billion in present-value terms under our central estimates, equivalent to roughly 3.5¢/kWh-solar. Focusing on just the existing end-of-2014 fleet of solar power projects, recent annual benefits equal more than \$1.5 billion under our central estimates, equivalent to 4.7¢/kWh-solar. These are central estimates, with a sizable range of uncertainty. GHG reductions are valued based on standard estimates of the global social cost of carbon. U.S. air pollution benefits are valued based on standard estimates of the value of reducing premature mortality and morbidity outcomes. The figures exclude the value of reduced water use—for which monetary quantification was not feasible.

It is important to recognize that the environmental benefits of solar are strongly dependent on not only the amount of solar deployment, but also the location of that deployment—solar that displaces higher-emitting coal generation has substantially larger environmental benefits than solar that displaces lower-emitting gas-fired generation. Although not addressed in this work, decision makers will naturally wish to compare these potential environmental benefits with, among other things, the potential costs and risks introduced by adding solar to the electric system as well as the potential impacts of solar on local ecosystems and communities.

ENERGY CONSUMPTION PATTERN AND GREENHOUSE GASES EMISSION: A CASE STUDY ON POTENTIALITY OF BIOGAS AS A RENEWABLE ENERGY TECHNOLOGY AND ITS ROLE IN REDUCING GREENHOUSE GASES EMISSION

Maheshwor Poudel (Central Department of Environmental Science, Tribhuvan University, KTM, Nepal)
Pabitra Adhikari (College of Applied Sciences-Nepal, Tribhuvan University, Kathmandu, Nepal)
Ramesh Man Singh (Centre for Energy and Environment - Nepal, Kathmandu, Nepal)

ABSTRACT: The study shows the current energy consumption pattern and Green House Gases emission. The study is focused to analyze the status of Biogas as a Renewable Energy Technology (RET) and its role in reducing the consumption of traditional energy resources and GHGs emission. The total energy consumption among the sampled households was found to be 7225.72 GJ per year with 14.06 GJ per capita per year. Fuelwood was found to be the dominant energy resource which comprises 93.73% of the total energy and rest 6.27% of energy was supplied by other sources like electricity, kerosene, solar and LPG. The per capita biomass fuel consumption was 13.18 GJ per year, whereas non-biomass fuel consumption was 0.868 GJ. The per capita Greenhouse Gases (GHGs) emission was found to be of 1209.11 kg CO₂e per year of the study area. The annual GHGs reduction was found 7.62 tCO₂e per biogas plant i.e. GHGs emission of 205.62 tCO₂e per year was reduced from the 27 biogas plants available in the sampled households and the study showed that the possibility of another 57 biogas plants of size 6 m³ which can reduce another 433.20 tCO₂e per year of GHGs emission. The study showed that the use of biogas saved 46.67% of fuelwood and if all the 84 potential biogas plants were constructed from the dung produced annually, the amount of fuelwood saved would be 217.32 tons per year per household. The simple payback period of the biogas plant was found to be 3.06 years excluding the subsidy given by the Government of Nepal. Therefore, the RET used in the study area had either reduced or substituted fuelwood as an energy source. The reduction on GHGs emission by the installation of biogas and high potentiality of biogas on the basis of livestock clearly indicates biogas as a suitable RET in reducing GHGs emission with efficient energy use.

Key words: *Energy Consumption Pattern, Fuelwood, GHGs emission, Biogas, RET*

INTRODUCTION

Energy is an important development indicator, which provides vital inputs for survival and economic development. Human activities particularly the intense use of carbon based energy sources and unsustainable use of biomass resources is increasing greenhouse in the earth's atmosphere resulting global warming in a way that could profoundly affect the global climatic system (Parikh, 2004).

The overall energy consumption of Nepal is largely dominated by the subsistence use of traditional forms of energy such as fuelwood, agricultural residues and animal waste. The intensive use of fossil fuels and unsustainable use of biomass resources from human activities are emitting GHGs which are causing greenhouse effect in the earth's atmosphere resulting global warming process which in turn have resulted the climate change as indicated by various scientific studies (Shakya and Shrestha, 2006). Fuelwood harvesting has been identified as one of the most significant causes of forest decline in rural areas of developing countries (Bhatt and Sachan, 2004). Fuelwood is the biggest energy resources in Nepal providing about 77% of the total energy demand exerting immense pressure on the forest resources (WECS, 2010).

Biogas, solar power, wind power, biobriquettes and micro level hydropower are categorised into renewable energy resources in Nepal. Biogas and biobriquettes are examples of modern interventions,

wherein traditional energy sources undergo transformations into modern types of fuels. In case of Nepal, about 1% of total energy consumption comes from the renewable sources (WECS, 2010). The RETs based on the locally available resources with increased efficiency and environment friendly alternatives seems very feasible for controlling GHGs emission and protecting environment.

The research is focused on determining the amount of energy consumed in terms of firewood and GHGs emission among the biogas user and non user households in the hilly region of Nepal. It will help to calculate the firewood consumption among biogas user and non user households and find out the potentiality of biogas as an alternative source of energy in the study area.

METHODOLOGY

Study Area. The studied site was Sankhupati Chaur VDC of Kavrepalanchok (Figure 1). The area of Sankhupati Chaur VDC is 6.95 km² and is located between the latitude 27°34'24.3"N to 27°57'05" N and longitude 85°33'26.5"E to 84°56'02" E and the elevation of 1523 masl.

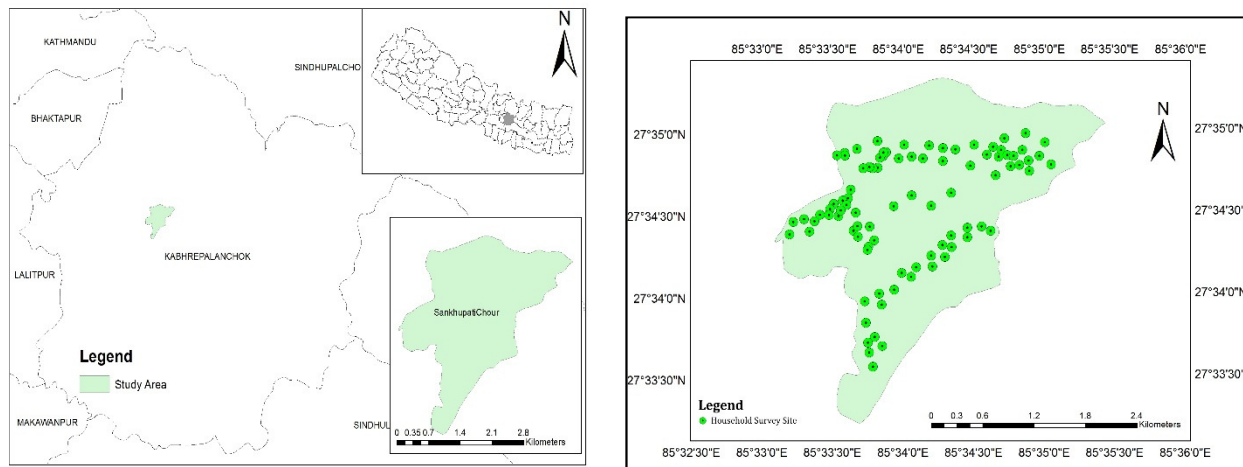


Figure 1. GPS Location of Sampled Household

The VDC is dominated by warm temperate climate with maximum temperature of 32°C and minimum temperature of 0°C. The average annual rainfall is 1200 mm. 41.58% of VDC is covered by forest. The major forest types include *Pinus roxburthii* forest, *Schima castanopsis* forest, *Alnus nepalensis* forest, *Pinus wallichii* forest, *Rhododendron spp.* forest. The species are mainly fodder species like *Dudhilo*, *Uttis*, *Hattipaila*, *Khanayo*, *Mauwa*, *Painyu* and *Bakaino*.

Data Collection. Simple random purposive sampling was used to determine the sample size. Among 722 households of Sankhupati Chaur VDC, 95 households were taken as a sample household (Arkin and Colton, 1963). Out of 95 households, 15 households of marginalized people within the VDC were also selected considering they were not in random selection. It is because marginalized people are using the less efficient technology of energy consumption technology and they have less capacity to adapt with the efficient energy consumption technology.

A semi-structured questionnaire was used for data collection in household survey. Direct observation about the energy consumption practice and its environmental impacts was noted during the field visit. The weight of 1 *bhari* was determined by taking average weight of 10 different *bharis* of fuelwood. Key informants were interviewed with structured checklists in order to verify the gathered relevant information. Focus Group Discussion was also carried out with the local stakeholders to get information about the past and present condition of forest, stoves use, training and awareness campaign on

RETs, their socio-economic status shifting etc. Check list was prepared to include RETs trend, environmental impacts and socioeconomic status.

Data Analysis and Presentation

Estimation of Biogas Potential. The sampled households were asked about the number of cattles owned to determine the daily dung production. Considering the daily dung production of 10 kg per cattle by assuming the animals were partly stall fed and partly grazed (BSP, 2009) and depending on average number of adult and young cattle, the total amount of dung produced in the area was estimated and the gas produced from the dung was calculated considering the gas produced per kg of dung to be 0.032 m³ (Werner et al.1989).

$$\text{Gas produced per kg of dung} = 0.0230 - 0.040 \text{ m}^3$$

(Average value = 0.032 m³)

Calculation of Amount of Dung Required Generating 1m³ of Gas.

$$0.032 \text{ m}^3 \text{ of gas is produced from 1 kg of dung}$$

$$\text{To produce 1 m}^3 \text{ of gas} = 1 / 0.032 \text{ kg of dung is required}$$

$$= 31.25 \sim 31 \text{ kg of dung}$$

Calculation of Amount of Fuelwood Saved. Amount of fuelwood saved was calculated on the basis of energy content on fuelwood as stated by Vaidya and Gautam (2011) which states that 1 ton of dry fuelwood contains 16.75 GJ of energy.

Table 1. Energy Consumption Pattern

Energy Sources	Consumption per day	Consumption per month	Consumption per year	Annual Energy Consumption in GJ	Per Capita Energy Consumption in GJ
Fuelwood	1123.17 kg	33695.20 kg	404.34 ton	6772.86	13.18
Electricity	82 Units	2460 kWh	29.52 MWh	106.27	0.21
Kerosene	1.43 L	42.90 L	0.51 KL	18.49	0.04
LPG	4.70 kg	140.86 kg	1.69 ton	83.22	0.16
Biogas	680.22 MJ	20406.52 MJ	244.88 GJ	244.88	0.48
Total				7225.72	14.06

(Source: Field Data, 2015)

Calculation of Number of Trees Saved and Areas of Forest Protected. The equivalent forest area saved was estimated based on the study of Winrock and Eco Securities (2004) on impact of biogas on forest which states that 1 ha of forest contains 32.81 tons of fuelwood. The estimated number of trees saved through potential biogas plants was based on the estimation of an annual saving of 11.6 trees per biogas plant (Devkota, 2007).

Estimation of GHGs Emission Reduction. 1 kg of fuelwood generates 1.518 kg equivalent of carbon emission (Smith et al., 2000). GHGs emission reduction in terms of carbon dioxide was obtained as follows:

$$\text{GHGs Emission Reduction} = \text{Amount of fuelwood saved} \times \text{GHGs emission per kg of fuelwood.}$$

Calculations and Analytical Process

- Average weight of 1 bhari of fuelwood was determined by weighing randomly 10 bhari of fuelwood and found to be 30.8 kg.
- Annual income saving from reduction in fuelwood was calculated at the local rate of NRs. 140 per bhari.

- Per capita fuelwood consumption = (average fuelwood consumption per family per day X total number of families in the ecosystem) / total number of people in the ecosystem (Maharjan, 2008).
- The estimated number of technically potential biogas plant was based on the daily dung available from cattle as 10 kg dung/cattle (BSP, 2009).
- Emission factor for combustion of fuels were also converted to CO₂e as given by IPCC (1996) and Smith et al. (2000).
- The methane leakage calculation was based on the methane leakage calculated by Devkota (2003).

RESULT AND DISCUSSION

Energy Consumption Pattern. Fuelwood, electricity, kerosene, LPG and biogas were the energy sources used in Sankhupati Chaur VDC. The total annual energy consumption among the sampled household was found to be 7225.72 GJ so that the per capita energy consumption was found to be 14.06 GJ per year (Table 1). The annual per capita energy consumption from the fuelwood was 13.18 GJ, whereas electricity, kerosene, LPG and biogas share 0.21 GJ, 0.04 GJ, 0.16 GJ and 0.48 GJ respectively.

Possibility of Biogas Plant. The study showed that the possibility of total 84 biogas plants among the sampled households. Out of which 27 biogas plants had already been constructed so the study shows that the possibility of another 57 biogas plants of size 6 m³. It was calculated by assuming the total dung produced per animal per day to be 10 kg and the amount of dung required to run one 6 m³ of biogas plant is 31 kg/day (BSP, 2009) (Table 2).

Table 2. Biogas Potentiality

Livestock	No. of Livestock	Total No. of Livestock	Dung produced per animal per day	Total dung produced day	Dung required to run one 6 m ³ plant	Potential of 6 m ³ of biogas plant
Cow / Ox	179	261	10	2610	31	84.19
Buffalo	82					

(Source: Field Data, 2015)

Amount of GHGs Reduction from Biogas Plant. All together 205.62 tCO₂e per year of GHGs emission was reduced from the 27 biogas plants of sampled households of Sankhupati Chaur VDC (Table 3).

Table 3. Amount of GHGs Reduction

Biogas Size (m ³)	Hill (tCO ₂ e/year/plant)	No. of Plants	Total Reduction (tCO ₂ e/year)
4	5.43	4	21.72
6	7.6	18	136.80
8	9.42	5	47.10
Total		27	205.62

(Source: Field Data, 2015)

If all the potential biogas plant of size 6 m³ were constructed from the dung produced annually than the total amount of GHGs reduction will be 638.82 tCO₂e per year.

Estimation of Number of Trees Saved and Areas of Forest Protected. The study showed that the total potentiality of 84 biogas plants was found in Sankhupati Chaur VDC. If all these 84 biogas plant of size 6 m³ were constructed then total number of trees saved will be 974.4 per year. Hence, the forest area protected per household per year will be 0.0789 ha (Table 4).

Table 4. Estimation of Equivalent Area of Forest Protected

Particulars	Comparing Biogas User and Non-Biogas User Households
Annual Fuelwood Saving (tons/year/HH)	2.5872
Equivalent Forest Area Protected (ha/HH/year)	0.0789

(Source: Field Data, 2015)

If all the 84 potential biogas plants were constructed from the dung produced annually, the amount of fuelwood saved would be 217.32 tons per year per household.

Fuelwood Consumption among Biogas User and Non-User Households. The comparison was done between biogas user and non-user households (20 households from each group) which showed that non-biogas user households use 5544 kg of fuelwood annually, whereas biogas users use only 2956.8 kg of fuelwood. Therefore, there was the saving of 2,587.2 kg of fuelwood which is equivalent to NRs. 11,760 per year per household. The study showed that the use of biogas saved 46.67% of fuelwood per year per household (Table 5).

Table 5. Fuelwood Consumption among Biogas User and Non-User Households

Particulars	Biogas User HH	Non-Biogas User HH
Average HH fuelwood consumption per month (kg)	246.4	462
Average HH fuelwood consumption per year (kg)	2956.8	5544
Expenditure in fuelwood per year per household (NRs.)	13,440	25,200
Fuelwood saved per year per household (kg)	2587.2	-
% of fuelwood saved	46.67%	-
Expenses saved per year per household (NRs.)	11,760	-

(Source: Field Data, 2015)

Estimation of GHGs Emission from Energy Sources. The per capita GHGs emission was found to be 1209.11 kg CO_{2e} per year. The study showed that 613791.76 kg CO_{2e} was emitted with the consumption of 404342.40 kg fuelwood annually, whereas 5263.97 kg CO_{2e} was emitted from with 404342.40 kg of LPG. Likewise, consumption of 514.80 L of kerosene per year emits 1278.76 kg CO_{2e}. Similarly, biogas emits 1088.86 kg CO_{2e} from the consumption of 244879.20 MJ of energy. Only 0.53 kg of CO_{2e} emitted with the consumption of 29520 kWh of electricity so electricity is known as a clean form of energy (Table 6).

Economic Analysis. From the field survey it was found that, NRs. 36,000 will cost for the construction of biogas plant of capacity of 6 m³ including all operational cost, maintenance cost and labour cost, excluding the amount of subsidy given by GoN. This shows that the simple payback period in term of fuelwood saved for the construction of 6 m³ biogas plant will be only 3.06 years (Table 7).

Impact of Biogas on Environment and Health. The main cause of pollution in the households is attributed to firewood burning. Apart from this, contamination of faecal waste produces obnoxious smell that is detrimental to human health and environment. Therefore, construction of biogas plant with the connected toilets helps in the better management of animal dung and human waste with better environment.

Table 6. Total CO₂e Emission from Energy Sources

Energy Sources	Annual Energy Consumptions	GHGs	CO ₂ e	Annual GHGs Emission (kg CO ₂ e)
Fuelwood	404342.40 kg	CO ₂	1.406 kg/kg	613791.76
		CH ₄	0.084 kg/kg	
		N ₂ O	0.028 kg/kg	
Electricity	29520 kWh		0.0000179 (ef)	0.53
Kerosene	514.80 L	CO ₂	2.457 kg/L	1278.76
		CH ₄	0.007 kg/L	
		N ₂ O	0.020 kg/L	
LPG	1690.37 kg	CO ₂	3.0689 kg/kg	5263.97
		N ₂ O	0.0452 kg/kg	
Biogas	244879.20 MJ			1088.86
Total				621423.89

(Source: Field Data, 2015)

Table 7. Payback Period of 6 m³ Biogas Plant

Plant Capacity (m ³)	Amount of Fuelwood saved per year per household (kg)	Amount of Expenses saved per year per household (NRs.)	Total cost of the plant excluding subsidy (NRs.)	Pay Back Period in years
6	2587.2	11,760	36,000	3.06

(Source: Field Data, 2015)

Biogas is an alternative form of energy due to easy availability of raw materials and its efficient technology. Therefore, the indoor air pollution can be reduced through biogas stove and reduce the respiratory diseases and eye related problems to those working in the kitchen. On the other hand, there will be conservation of forest resources, wildlife habitat and natural balanced ecosystem.

Besides this, biogas is a clean form of energy, where Nepal is gaining huge amount of revenue from CDM project.

ACKNOWLEDGEMENTS

The authors would like to thank Central Department of Environmental Science for providing the opportunity to carry out this research. The authors are equally thankful to Centre for Energy and Environment Nepal for all the technical support to conduct the research work. The authors are thankful to all the participants of this study for their immense support and providing required information to conduct this research.

REFERENCES

Arkin, H., and Colton, R.R., (1963). *Tables for Statisticians*. New York: Barnes and Noble.

- Aryal, S., (2007). *Adoption of Renewable Energy Technology Towards Sustainable Harvesting of Fuelwood from Community Forest* (Unpublished M.Sc. Thesis). Central Department of Environmental Science, Tribhuvan University, Kathmandu Nepal.
- Bhatta, B.P., and Sachan M.S., (2004). Firewood Consumption along with altitudinal gradient in Mountain Villages of India. *Biomass and Energy*. 27(1):69-75
- BSP, (2009). *Biogas as Renewable Source of Energy in Nepal Theory and Development*. Biogas Support Programme, Lalitpur, Nepal.
- Devkota, G.P. (2007). *Renewable Energy Technology in Nepal*. An Overview and Assessment.
- Devkota, G.P., (2003). *Final Report on Analysis of Biogas Leakages from Household Digesters*. Winrock International, Kathmandu, Nepal
- IPCC, (1996). *Revised Guideline for National Greenhouse Gas Inventory*.
- Maharjan, R., (2008). *Study on Energy Consumption Pattern and its impact on Environment with reference to Okharpauwa VDC, Nuwakot* (Unpublished M.Sc. Thesis), College of Applied Science, Tribhuvan University, Kathmandu, Nepal.
- Parikh, J. (2004). Clean Development Mechanism and Sustainable Development. *Integrated Research and Action for Development*. New Delhi.
- Shakya, S. R., and Shrestha, J. N. (2006). Contribution of renewable energy technology for greenhouse gas emission in Nepal. *Proceeding of first national conference on renewable energy technology for rural development*, 12-14 October, 2006, Kathmandu, Nepal.
- Smith K.R., Uma, R., Kishore, V.V.N., Zhang J., Joshi, V., and Khalil, M.A.K., (2000). Greenhouse Implications of Household Stoves: An Analysis for India. *Annual Reviews Energy Environment* 25, 741-763.
- Vidhya, S., and Gautam, R. M., (2011). *Energy Outlook of Nepal*. Informal Sector Research and Study Centre. First Edition, pp.315.
- Warner, U., Stohr, U., and Hees, N. (1989). *Biogas plants in Animal Husbandary*. GATE/GTZ, GmbH.
- WECS. (2010). *Energy Sector Synopsis Report*. Water and Energy Commission Secretariat, GoN. Kathmandu Nepal.
- Winrock and Eco Securities, (2004). *Nepal Biogas Programme, CDM Baseline Study 2003*.

**CLONING OF GENES ENCODING FOR CELLULOLYTIC ENZYMES FROM
METAGENOME IN GOAT'S RUMEN**

Santosh Thapa, Hui li, Suping Zhou, Sarabjit Bhatti and Roger J. Sauvé

(Department of Agricultural and Environmental Sciences, College of Agriculture, Human and Natural Sciences, Tennessee State University, TN, USA)

The increasing fuel demands has caused in rise in price of crude oil and so the need for alternative source of bioenergy. Among the potential alternative bioenergy resources, cellulosic biomass is considered as a sustainable raw material for biofuel production. The cellulosic bioconversion into fermentable sugar is a complex process and requires the synergistic action of endoglucanases, exoglucanases and β -glucosidases. Those enzymes are hosted in the microbial genomes in the rumen of herbivores. To be able to tap into those resources is expected to have a significant impact on cellulosic biofuel production, but a majority of those microbial species are not accessible using laboratory culture techniques. This study was performed to develop molecular approaches for using these genome resources. Goat rumen fluid was collected immediately after goats were slaughtered. Metagenome DNA was extracted and sequenced using next-generation sequencing. Following assembly and annotation, several gene sequences encoding for cellulases and xylanases were found in the metagenome database. PCR primers were designed to amplify the gene of interests using metagenome DNA as the template. The amplified products were cloned into pET 101 vector. After confirmation of gene sequences, those putative cellulase enzymes were expressed in the BL21 Star (DE3) system. Several genes with high cellulase and hemicellase activities have been isolated on this project. This work has provided the foundation for using these microbial genomic resources in the lignocellulosic bio-ethanol industry. The project was supported by NIFA grant NIFA-2010-02417-223076.

ANAEROBIC AND SUBSEQUENT PHOTOSYNTHETIC PROCESS FOR BIOHYDROGEN AND BIOPLASTIC (PHB) PRODUCTION

Arun. A*, Dinesh. G. H and Satheesh Murugan. R
(Alagappa University, Karaikudi, Tamilnadu, India)

S. Karthik Sundaram
(PSG college of arts and science, Coimabtoe, India)

The faster intake of these non-renewable resources resulted in both, the increase CO₂ concentration in the atmosphere and the rapid depletion of fossil resources. Thus research efforts have been devoted in developing new energy alternatives. Compared with fossil fuels as traditional energy sources, hydrogen (H₂) is a promising candidate as a clean energy carrier in the future because of its high-energy yield (122kJ⁻¹) and producing only water instead of greenhouse gases on burning. Increasing awareness of environmental pollution has generated a resurgence of interest in biological methods for the production of biodegradable polymers.

The present industrial interest of poly-β-hydroxybutyrate (PHB); Hydrogen production via dark fermentation has the greatest potential as a pre-treatment step that can be followed by a suitable secondary process step, such as bioconversion of volatile fatty acids to other products, such as poly hydroxyalkanoates. The present study is carried out for bio hydrogen and PHB production by anaerobic, photo bacterial and their subsequent process using rice straw and husk hydrolysates.

Optimization of substrate (rice straw and husk hydrolysates) (10-100%); pH (5.5-8.0) for anaerobic, photo fermentative and subsequent anaerobic - photo fermentative H₂ and PHB production was carried out using the microbial isolates. In anaerobic condition by *Bacillus subtilis* isolate the maximum volume of cumulative hydrogen production was observed in 70% (14.576 ml) rice husk; 30% (14.576 ml) rice straw hydrolysates at pH 7; while in phototrophic condition the isolate R able to produce maximum volume of cumulative hydrogen production in 70% (76.524 ml) by utilizing rice husk hydrolysate at pH 7. There was 5.25 fold increase in cumulative hydrogen production when comparing anaerobic with photo fermentation. The maximum of PHB (136 mg/l) was produced in 80% of rice husk hydrolysate by under anaerobic fermentation at 80% rice husk hydrolysate at pH 5.5 and the isolate G and R produced 28 mg/l of PHB by utilizing both substrates at various concentrations.

The present work was able to obtain concomitantly the dual benefits of producing bioplastic and alternative energy source such as H₂.

ALGAL OIL PRODUCTION POTENTIAL UNDER DIFFERENT MUNICIPAL WASTEWATER DELIVERY SCENARIOS

Tyler Brown and *Yiwen Chiu*

(California Polytechnic State University, San Luis Obispo, CA, USA)

A lot of research has focused on finding alternative biofuels that are economically and environmentally beneficial to meet the renewable fuel production goals proposed by the Energy Independence and Security Act. Among all the potential biofuel production sources, algae is a prime focus standing apart from other feedstock alternatives resulting from its per-acre production potential. Former studies stated that algae showed promising potential to produce 55 to 341 times more biofuel than other conventional energy feedstock such as corn and soybean. However, algal oil also raises controversial concerns due to negative environmental footprints. One of the significant impacts is the excessive water demand for algae cultivation and refinery maintenance, ranging from 22 to 8357 liters of water per liter of algal oil production. A proposed solution is to introduce municipal wastewater as a nutrient sources for algae cultivation, which can also contribute to the reduction of water demand.

However, a known challenge of using municipal wastewater to aid algal oil production is resulted from the geographically decoupling relation between refinery and wastewater treatment plants. Therefore, to investigate the this concept, we conducted a study aiming to determine the change of algal oil production potential in California under different spatial scenarios varying the distance between refinery sites and existing wastewater plants. We geographically integrated the distribution of suitable land for refinery development with the locations and discharge capacity of existing wastewater plants in California to construct the analytical framework. The results will elaborate upon the feasibility and opportunity of using wastewater to support algal oil production as a water and nutrient source.

**ECONOMICS OF GREEN VERSUS DRY FOREST HARVEST RESIDUE FEEDSTOCK FOR
THE AVIATION FUEL SUPPLY CHAIN**

Rene Zamora-Cristales and *John Sessions*
(Oregon State University, Corvallis, Oregon, USA)

Forest harvest residues are produced as a byproduct of commercial timber harvest and represent a source of readily available material for aviation fuel production. However, these forest harvest residues, when green, contain high moisture content that can increase the costs of processing and transportation and may reduce the yield of potential extractable polysaccharides for biofuel production. Different moisture management strategies can be implemented to reduce the moisture content prior to processing but the most important question is what are the economic and environmental trade-offs between collecting processing and transporting green versus dry residue, moreover what is the opportunity cost of letting the material sit while drying. Our main objective was to estimate the implications in processing, transport and pretreatment of using Douglas-fir green versus dry forest harvest residues. Our analysis was focused on harvest residues ground at the landing and loaded and transported in chip vans. Specifically, we discuss differences in bulk density, bark and needles content, and polysaccharides yield. We processed 150 tons of green and 150 tons of dry forest harvest residues from two similar 45 year-old Douglas-fir stands. Dry residue moisture content when ground was estimated at 15% (wet basis). Green residue was collected immediately after harvest and immediately ground. The green residue had an average moisture content of 60%. Results indicate that the proportion of bark, needles and other substances in green residue is higher than in dry material (14% versus 8%). Chemical analysis from the pretreatment process revealed that polysaccharides content in dry residue are 26% higher than in green residue. Lignin content in dry residue is 17% higher compared to green residue. Implications in processing and transportation economics are discussed.

**CLONING AND CHARACTERIZATION OF GENES ENCODING CELLULOLYTIC ENZYMES
SCREENED FROM GOAT RUMEN METAGENOME**

Santosh Thapa, Hui Li, Sarabjit Bhatti, and Suping Zhou
(Tennessee State University, Nashville, TN, 37209, USA)

One of the major limitations for the efficient bio-conversion of lignocellulosic biomass to bio-fuel is the perverse nature of the plant cell wall, which is composed mostly of cellulose, hemi-cellulose and lignin. Goat rumen harbors an assemblage of microbes hypothesized to evolve a plethora of enzymatic strategies for hydrolyzing cellulose and hemi-cellulose into its constituent sugars for subsequent fermentation to bio-fuels. However, the vast majority of such microbial life remains uncatalogued as they are recalcitrant to in-vitro culture. In this study, we have leveraged a functional metagenomics screen for the identification of cellulolytic enzymes from the bacterial community in the rumen of goat. Metagenome DNA was extracted and sequenced using next-generation sequencing. Following assembly and annotation, 14 gene clones encoding for cellulases, hemicellulases and xylanases have been procured from the metagenome. PCR primers were designed against the assembled gene sequences, and PCR reactions were performed using metagenome DNA as the template. The amplified PCR products were cloned using TA cloning strategy. Gene sequences were confirmed using Sanger sequencing and submitted to NCBI database. The genomic and proteomic analyses of cellulolytic and hemi-cellulolytic bacterial species aim to identify and clone novel hydrolytic enzymes, which can be further sub-cloned and expressed to construct highly active recombinant proteins that render as a potential candidate for various biotechnological applications. The present study shows that a functional metagenomics approach can be an innovative maneuver to isolate previously uncharacterized cellulases from the rumen environment.

PREPARATION AND PROPERTIES OF MA-PA/EG COMPOSITE PHASE CHANGE MATERIAL FOR ENERGY STORAGE

Jianyun Wu¹, Yanping Yuan², Yaguang Yuan²

(1.School of Environmental Science and Municipal Engineering , Lanzhou Jiaotong University , Lanzhou 730070 , China; 2. School of Mechanical Engineering, Southwest Jiaotong University ,Chengdu 611756 , China)

ABSTRACT: Phase change energy storage is an environmental-friendly new technology and the front research direction in energy area, which uses the latent heat that phase change material stored and released can effectively solve the inconsistency between supply and demand of energy in time and space.

This research using the myristic acid(MA) and the palmitic acid(PA) as phase-change material monomers to obtain the MA-PA eutectic mixture, which is based on theoretical calculation and experiment. Besides, using the porous absorbing material, expanded graphite(EG),as primary structure to prepare the MA-PA/EG composite phase-change material(PCM) by porous adsorption method. The performance of phase-change material has been analyzed by the differential scanning calorimetry(DSC), thermal accelerate circulation experiment and heat storing and releasing experiment. The results show that, on the understanding that the best mass ratio of MA-PA eutectic mixture and EG is 15:1, the melting and freezing temperature of the MA-PA/EG composite PCM are 44.42°C and 44.99°C, the latent heat of fusion and solidification are 156.9J/g and 155.3J/g. There is few difference as compared with MA-PA eutectic mixture; after conducting 1000 time's thermal accelerate circulation experiment on the composite PCM, the heat stability and chemical stability of this material is still excellent; the heat storing and releasing rate of composite PCM is improved effectively after adding the EG, also there is no liquid side leakage during the solid-liquid phase-change process. This composite PCM has extensive application in the areas of solar power, energy conservation, air condition and etc.

Key words: composite phase change material; myristic acid- palmitic acid; expanded graphite; porous adsorption method; thermal properties

INTRODUCTION

PCMs absorb and release a great amount of heat in phase change process, its heat storage density is larger than general energy storage material. Additionally, the heat storage and release processes of PCM happen in the same temperature, it also has good thermal stability. Therefore, PCM is appropriate for space heating/cooling applications, for example, it can be used in building envelope, industrial waste heat recovery, solar heat and textile industry, which has a wide application prospects [1-3].

PCMs are divided into organic and inorganic matters, or the combination of them. Among all investigated PCMs, fatty acids are the best, which has many superior properties, including proper melting temperature range, high heat capacity, congruent phase change temperature, little or no supercooling during phase transition, non- corrosive [4]. In addition, mix melting different fatty acids can obtain the eutectic mixture, which decreases the temperature of PCM, and expands the temperature range in its application field [5]. Yuan et al. [4] calculated the temperature and latent heat of phase change of PCMs mix melted with 15 kinds of fatty acids. The temperatures was between 10.2°C and 51.5°C, while the minimum of latent heat is 138.6J/g, and the maximum is 187.5 J/g. Meng et al. [6] obtained the ternary fatty acids/EG composite PCM by canoic acid(CA), lauric acid (LA) and PA, the melting temperature is 16.8°C and the melting enthalpy is 140.5 J/g. Fatty acids PCMs have advantages of inexpensiveness and large latent heat,

but need containers which make extra thermal resistance and leakage[7]. Common methods of encapsulating PCM into containers are sol-gel method, melt infiltration method, porous adsorption method, microcapsule method and polymerization method [8]. Cai et al. [9] used SiO₂ nano-fiber as supporting material to obtain the CA-LA-PA/ SiO₂ nano-fiber composite PCM. Cao et al. [10] used carboxy methyl cellulose-1 as container. Wang et al. [11] chose polymer alloy as matrices. Hadi et al. [12] selected sodium pyruvate and sodium palmitic as supporting materials, and got two kinds of composite PCM. These shape-stabilized materials can effectively prevent the leakage of PCM, furthermore, thermal conductivity increased with the adding of these materials. Zhang et al. [7] selected EG, diatomite and other 7 kinds of high thermal conductivity materials as supporting structures of PCM, the results showed that EG has the most remarkable effect. EG not only enhances the thermal conductivity but also prevents leakage of PCM, therefore, EG has been widely applied.

Two kinds of fatty acids and EG are used to obtain the MA-PA/EG composite PCM, and the mass ratio has been calculated. The properties of PCM has been researched by DSC, the accelerated circulation test of heating and cooling, heat storage and release test and thermal conductivity test.

EXPERIMENTAL

Experiment Materials and Equipment. Experiment materials: Expansible graphite (EG, 80 mesh, expansion ratio:200ml/g, carbon content:99%) was obtained from Jinrilai Electronic Materials Factory, Qingdao, China. Myristic acid (MA, 98% pure), Palmitic acid (PA, AR) were supplied by Aladin Industrial Corporation, Shanghai China.

Experimental equipment: Differential scanning calorimeter (DSC, TA Q20, America), N₂ atmosphere, heating rate 5°C/min, range of temperature:10°C-80°C, the melting temperature and latent heat of PCM in DSC curve are represented by T_m and H_m. The freezing temperature and latent heat are shown as T_f and H_f. Magnetic stirrers with thermostat of heat-collected type (DF-101S) is provided by Yuhua Equipment Limited Liability Company in Gongyi City. KBr tableting, range of tested frequency: 400cm⁻¹-4000cm⁻¹. Metal bath (CHB-T2, BIOER ThermoQ, China). Temperature data logger (Agilent 45980A); Thermostat water bath. Copper-constantan thermocouple (type T). Thermal constant analyzer (Hot Disk 2500-OT) produced by Hot Disk Company in Sweden, the range of thermal conductivity: 0.005-500W/mK, measurement accuracy ≤±3%, type of test probe: Kapton, probe model:5501, radius:6.403mm.

Preparation Process

Preparation of EG. Put a certain amount of EG in to drying oven at 60°C for 16h, then put it in to microwave oven, heat for 30s, which will obtain EG with good adsorption property.

Preparation of Eutectic mixture MA-PA. Put defined amount of MA and PA(68/32 wt%) into beaker, then put the beaker into thermostatic waterbath at 80°C. After the specimen melted, magnetic stir it at the speed of 400r/min for 30min. Make sure that MA and PA are well-mixed. At last, nature cool the mixture, then MA-PA binary eutectic mixture is obtained.

Preparation of MA-PA/EG composite PCM. Put several parts of EG into beakers, each of EG is 0.8g, next add MA-PA with different qualities. Put the beakers in to oven at 70°C for 24h, the mixture should be stirred every 8h to ensure that EG can evenly adsorb MA-PA. After that, cooled down to room temperature, then a series of MA-PA/EG in different ratio is obtained, which named from M1 to M10.

Confirmation of the Ratio of Composite PCM

Confirmation of the theoretical ratio of MA-PA. The phase-transition temperature and quality ratio of MA and PA in MA-PA eutectic mixture can be calculated by Schroder's formula [13]:

$$T_m = \left[\frac{1}{T_i} - \frac{R \ln X_i}{H_i} \right]^{-1} \quad (i=A,B) \quad (1)$$

T_m — the melting point of eutectic system, K;

T_i 、 H_i — the melting point and latent heat of each component, K、 J/g

R — gas constant, 8.315J/(mol•K)

X_i — mole fraction of component i in eutectic system

The latent heat of fusion of MA and PA are 182.6 J/g and 189.6 J/g, and the melting temperatures of MA and PA are 54°C and 62.0°C [5], which is higher than the needed temperature, therefore, the PCM with lower phase-transition temperature is required. In order to obtain the PCM with the proper temperature, the formula (1) is used to calculate the melting temperature of MA-PA, and the mass ratio of MA and PA in eutectic mixture in this situation is 68:32. The melting temperature showed in DSC curves of MA-PA with this mass ratio inosculates theoretical value, which demonstrates that the theoretical ratio is 68:32.

Confirmation of the best ratio of MA-PA/EG. Latent heat of phase change is an important index when PCM used in condense heat recovery system. Under the proper temperature, the larger latent heat, the better heat storage performance will be. Therefore, in MA-PA/EG, the more MA-PA it contains, the larger latent heat of PCM will be. EG serves as supporting material, which has no effect on latent heat of MA-PA, however, the content of EG influences heat-conducting property and side leakage of composite PCM. Therefore, there is a best mass ratio between MA-PA and EG when the content of MA-PA is highest without side leakage. In order to obtain the best composite PCM, MA-PA/EG with EG and MA-PA in different mass ratio (1:11, 1:12, 1:13, 1:14, 1:15, 1:16, 1:17, 1:18, 1:19, 1:20) is prepared, and named them from M1 to M10. Weigh 0.200g MA-PA/EG in different mass ratio on filter paper as fig.1 shows. Put it into oven at 65°C for 90min. The result shows that there are no obvious impressions around M1-M5, which means that there's no MA-PA leaks out under the adsorption of filter paper. While there are impressions around M6-M10, and are growing with the increased content of MA-PA. This is caused by the excessive amount of MA-PA, which is beyond the absorption capacity of EG, therefore, the extra MA-PA leaks out and form the impression. The amount of leaked MA-PA can be reflected by impression. The results show that the best mass ration between MA-PA and EG is 15:1.

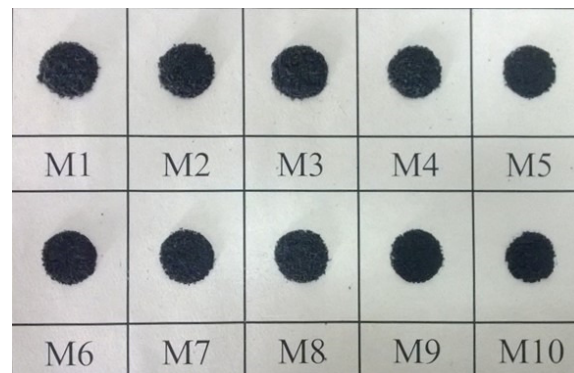


Fig. 1. MA-PA/EG in different mass ratio

RESULTS AND DISCUSSIONS

Phase-transition Temperature and Latent Heat of MA-PA/EG Composite PCM. The phase- transition temperature and latent heat of eutectic mixture MA-PA and MA-PA/EG composite PCM have been tested by DSC. The DSC curves of MA-PA and MA-PA/EG are showed in Fig.2 and Fig.3. The data show in Table.2 and Table.3.

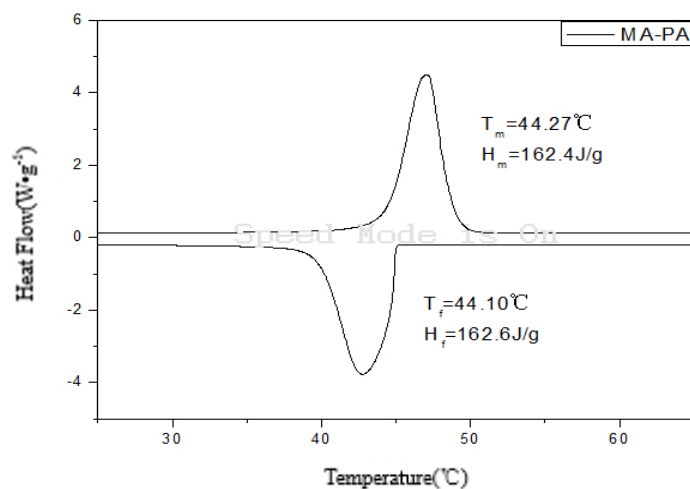


Fig. 2. DSC curves of MA-PA

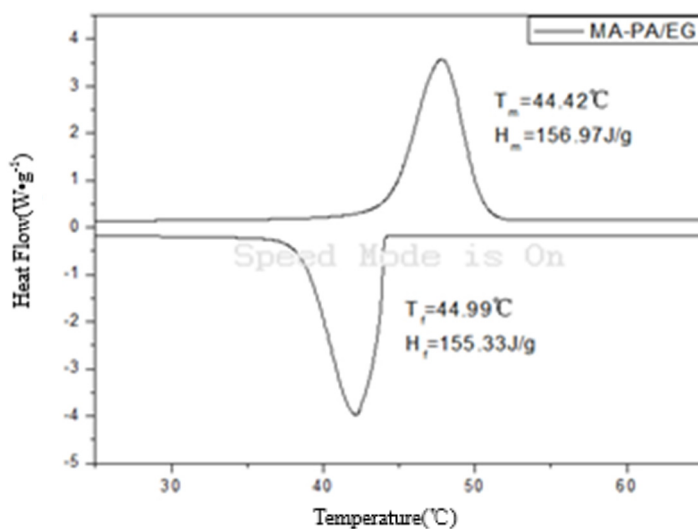


Fig. 3. DSC curves of MA-PA/EG

Table 1. DSC data of MA-PA

Group	Melting temperature °C	Latent heat of fusion J/g	Freezing temperature °C	Latent heat of solidification J/g
1	44.41	159.9	44.00	161.6
2	44.17	163.7	44.20	164.2
3	44.20	163.6	44.11	162.0
Average	44.27	162.4	44.10	162.6

Fig.2 shows that there is only one melting peak of MA-PA on the DSC heating curve, which illustrates that MA and PA are eutectic. Additionally, in the DSC curve of MA-PA/EG, the melting and

freezing temperature are presented as 44.2°C and 44.99°C, the latent heat of fusion and solidification are showed as 156.9J/g and 155.3J/g. Contrasting these thermal properties with MA-PA can find out that the phase-transition temperatures are basically same. Besides, EG has little influence on latent heat of composited PCM, which demonstrates that EG only supports MA-PA but has no effect on the behavior of melting and freezing. The latent heat of phase change is proportional to the content of MA-PA. Since the latent heat and content of MA-PA are known, according to formula 2, the theoretical value of latent heat of composited PCM can be obtained, the results of latent heat of fusion and solidification are 152.25J/g and 152.44J/g. The theoretical value is smaller than the value of actual measurement, which may be caused by experimental error. The results show that, MA-PA/EG composite PCM has a widespread application on solar energy utilization and condense heat recovery.

$$H_{m1} = \eta H_m \quad (2)$$

H_{m1} —the latent heat of MA-PA/EG composited PCM, J/g

H_m —the latent heat of MA-PA, J/g

η —the mass fraction of MA-PA in composited PCM, $\eta = M_m / M_{m1}$ (M_m is the quality of MA-PA, g; M_{m1} is the quality of MA-PA/EG, g.)

Table 2. DSC data of MA-PA/EG

Group	Melting temperature °C	Latent heat of fusion J/g	Freezing temperature °C	Latent heat of solidification J/g
1	44.43	154.2	44.98	151.0
2	44.43	158.2	45.01	157.4
3	44.41	158.5	44.98	157.6
Average	44.42	156.9	44.99	155.3

Heat stability of MA-PA/EG composite PCM. After a long term and multiple times of thermal storage and release process, the composited PCM should still keep a stable thermal property and chemical property, which ensures the long useful life. An experiment of accelerated thermal cycling of MA-PA/EG for 1000 times has been done. The DSC curves of MA-PA/EG after circulation is showed in Fig.4. And the tested melting and freezing temperature of MA-PA/EG after circulation list in Tab. 3, as well as the tested latent heat of fusion and solidification.

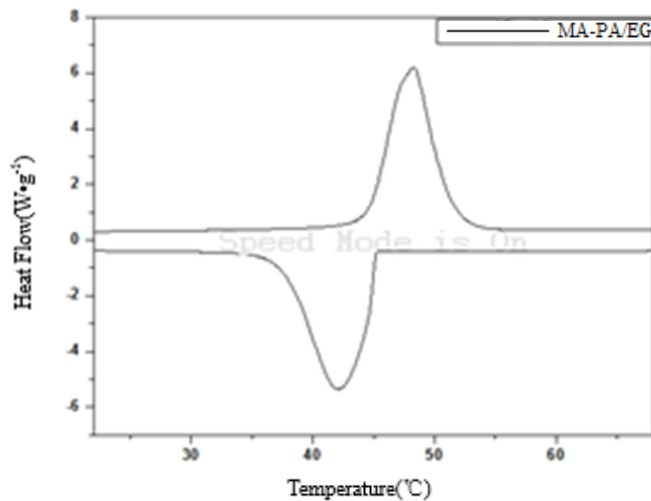


Fig. 4. DSC curves of MA-PA/EG after circulation

The data show that, after 1000 times of circulation, the melting temperature and freezing temperature have changed -0.06°C and 0.32°C , while the latent heat of fusion and solidification have changed -3.25J/g and -3.84J/g . It can be seen that MA-PA/EG composite PCM has a good heat stability.

Table 3. DSC data of MA-PA/EG after 1000 times of circulation

Group	Melting temperature $^{\circ}\text{C}$	Latent heat of fusion J/g	Freezing temperature $^{\circ}\text{C}$	Latent heat of solidification J/g
1	44.43	151.8	45.44	150.82
2	44.29	155.5	45.18	152.1
Average	44.36	153.65	45.31	151.46

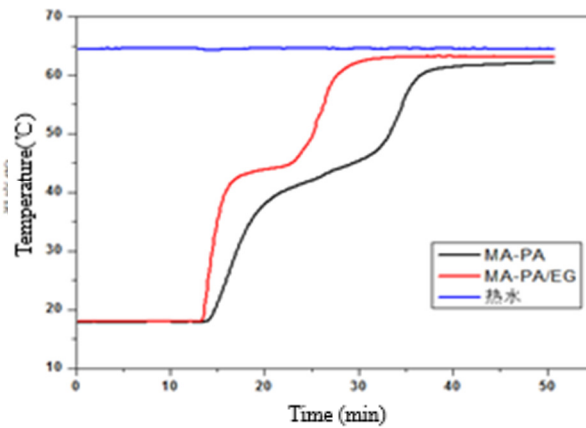


Fig. 5. The melting curves of MA-PA and MA-PA/EG

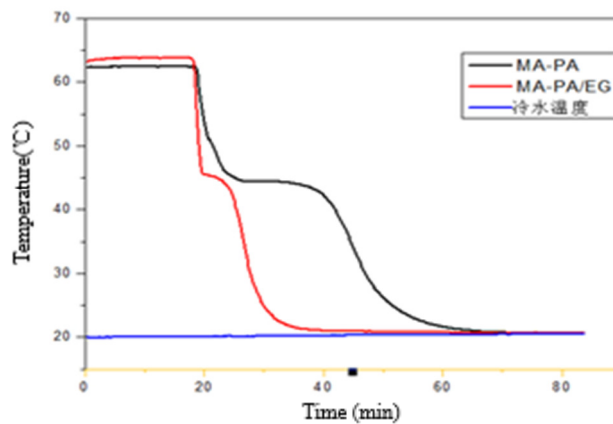


Fig. 6. The freezing curves of MA-PA and MA-PA/EG

Thermal energy stored and discharge performance of MA-PA/EG composite PCM. The speed of thermal energy storage and release of PCM influence its usage. Put the test tubes separately fitted with MA-PA and MA-PA/EG for 45ml into thermostatic waterbath at 65°C . Test the temperatures of MA-PA and

MA-PA/EG by temperature data logger. Record the data every 10s. After about 50min, the temperature of MA-PA and MA-PA/EG achieves a constant. Then put the test tubes separately fitted with MA-PA and MA-PA/EG into thermostatic waterbath at 20°C. Record the data every 10s. After about 70min, the temperature of MA-PA and MA-PA/EG achieves a constant. The data of thermal energy stored and discharge experiment is processed by Origin7.5. The melting and freezing curves of MA-PA and MA-PA/EG are presented in Fig.5 and Fig.6.

Fig. 5 shows that, the temperature of MA-PA/EG increases fast from 20°C to 42°C, the process only takes 3min, while MA-PA spends 9min. In the initial stage, the temperature of MA-PA increased much slower than that of MA-PA/EG. The solid-liquid transition of MA-PA happens when the temperature is between 42°C and 46°C. This process takes about 9min, which is slow. The time increased by 38.9% from MA-PA/EG. With the elevation of temperature, the heating rate of MA-PA is much slower than that of MA-PA/EG when the temperature ranges from 45°C to 65°C. During the whole melting process, MA-PA/EG reaches stability first, which is 10min faster than MA-PA. Similarly, the Fig.6 shows that, the temperature of MA-PA/EG composite PCM reduces quickly when the temperature drop from 63°C to 45°C, which only takes 1.5min, while MA-PA spends about 4.5min. The solid-liquid transition of MA-PA and MA-PA/EG happens when the temperature is between 45°C and 43°C. This process takes MA-PA/EG 5min, while MA-PA 18min. When the temperature ranges from 43°C to 20°C, the freezing rate of MA-PA is much slower than that of MA-PA/EG. During the whole freezing process, MA-PA/EG reaches stability first, which is 30min faster than MA-PA. The results demonstrate that EG serves as primary structure, absorbing MA-PA eutectic mixture into its micro pores, which maintains the energy storage and temperature control properties of PCM, saving much time.

Heat-conducting property of MA-PA/EG composite PCM. Thermal conduction of MA-PA/EG is also an index to evaluate its property. In order to improve it, EG is added into MA-PA. At first, suppress MA-PA and MA-PA/EG into columns (diameter:30mm, quality:9g) by tablet press. Then test the heat-conducting property of MA-PA and MA-PA/EG. The results show as Table 4 and Table 5.

Comparing the heat conductivity coefficients of MA-PA and MA-PA/EG, it is showed that before adding EG, the heat conductivity of MA-PA is 0.3030, after EG added, it rises to 6.462. Obviously, EG enhances the thermal conductivity substantially, which illustrates that adding of EG can effectively improve the heat-conducting property of PCM, it also provides a guarantee of heat storage and stability properties of MA-PA/EG composite PCM.

Table 4. Heat conductivity coefficient of MA-PA

Group	Output power W	Testing time s	Temperature rise K	Characteristic time s	Heat conductivity coefficient
1	0.03	160	0.577	0.622	0.3086
2			0.577	0.638	0.2973
Average					0.3030

Table 4 Heat conductivity coefficient of MA-PA/EG

Group	Output power W	Testing time s	Temperature rise K	Characteristic time s	Heat conductivity coefficient
1	0.5	5	0.674	0.476	6.609
2			0.681	0.479	6.479
3			0.673	0.488	6.298
Average					6.462

CONCLUSION

- (1) The MA-PA eutectic mixture that can be used in air-conditioning condense heat recovery system,

solar energy utilization and phase change wall has been obtained.

(2) The MA-PA/EG composite PCM with the best mass ratio (15:1) has been prepared. Its melting and freezing temperature are 44.42°C and 44.99°C. Its latent heat of fusion and solidification are 156.9J/g and 155.3J/g.

(3) EG has no effects on the phase transition temperature and latent heat, only serves as primary structure.

(4) MA-PA/EG composite PCM has a good thermostability and chemical stability.

(5) Adding of EG holds the temperature control property of PCM, which shorten the phase change time, also enhance the thermal conductivity.

REFERENCES

- [1] Zhang Y P, Hu H P, Kong X D. Phase change energy storage—theory and application[J]. Press of University of Science and Technology of China, Hefei, 1996.
- [2] Li Haijian, Ji Zhijiang, Wang Jing, Xin Zhijun. Research status of phase change composite materials [J]. *Materials Review*,2008,22(Z2): 248-251
- [3] LI Zhisheng, ZHANG Shuting. Research progress and application of phase change materials [J]. *Building Energy Efficiency*,2016,44:57-60
- [4] Yuan Yanping, Zhang Nan, Tao Wenquan, Cao Xiaoling, He Yaling. Fatty acids as phase change materials: a review[J]. *Renewable and Sustainable Energy Reviews*, 2014, 29: 482-498.
- [5] Yuan Yanping, Bai Li, Niu Ben, Theoretic predicton of phase change temperature and latent heat of fatty acids eutectic mixture [J]. *Materials Review*,2010,24(2): 111-113
- [6] Meng Xin, Zhang Huazhi, Zhai Ziming, et al. Preparation, encapsulation and thermal properties of fatty acid /expanded graphite composites as shape-stabilized phase change materials. *Chemical Journal of Chinese Universities*. 2012, 33(03): 526-530
- [7] Zhang Yinping, Ding Jianhong, Wang Xin, et al. Influence of additives on thermal conductivity of shape-stabilized phase change material[J]. *Solar energy materials and solar cells*, 2006, 90(11): 1692-1702.
- [8] Jiang Yunyun, Zhang Yuzhong, Zheng Shuilin. Preparation of composite phase change materials and its application development[J]. *China Non-metallic Minerals Industry*. 2011(3),4-7
- [9] Cai Yibing, Sun Guiyan, Liu Mengmeng, et al. Fabrication and characterization of capric–lauric–palmitic acid/electrospun SiO₂ nanofibers composite as form-stable phase change material for thermal energy storage/retrieval[J]. *Solar Energy*, 2015, 118: 87-95.
- [10] Cao Lei, Tang Yaojie, Fang Guiyin. Preparation and properties of shape-stabilized phase change materials based on fatty acid eutectics and cellulose composites for thermal energy storage[J]. *Energy*, 2015, 80: 98-103.
- [11] Wang Yi, Wang Shaoying, Wang Jianping, Yang Rui. Preparation, stability and mechanical property of shape-stabilized phase change materials[J]. *Energy and Buildings*, 2014, 77: 11-16.
- [12] Fauzi H, Metselaar H S C, Mahlia T M I, et al. Thermal characteristic reliability of fatty acid binary mixtures as phase change materials (PCMs) for thermal energy storage applications[J]. *Applied Thermal Engineering*, 2015, 80: 127-131
- [13] Lv Shilei, Zhu Neng, Feng Guohui. Eutectic mixtures of capric acid applied in building wallboards for heat energy storage [J]. *Energy and Buildings*, 2006,38(6):708-711

ECO-ECONOMICAL NON-CONVENTIONAL METHOD FOR ELECTRICITY GENERATION

Seema Vats

(University of Delhi, New Delhi, INDIA)

Energy is the primary and most universal measure of all kinds of works by human beings and nature. In this world we see the expression of flow of energy in one form or the other. Energy in the form of electricity plays a very important role in our lives. The modern age has, therefore, been truly called the “age of electricity”. So today our whole lifestyle is dependent on electricity but we know that the resources to generate electricity are limited. There is an urgent need to generate electricity through non –conventional methods which are not only non-polluting but also cost effective. Also there is dire need to install multiple non-conventional techniques at one point to extract maximum electrical energy for further use. In the light of above, we have presented the method of clubbing the energy generated from roller as well as from piezoelectric materials at the same installation cost. This will be very cost effective method in a way that it does not require separate arrangement for installing piezoelectric materials. The mechanical energy is being converted into an electrical energy. A wooden prototype model with PZT ceramic for the same has been developed and studied. Also we have tried to explore possibility of generation of electricity by using PVDF films (piezoelectric) as another substitute in combination with roller. The generated electricity can be used at toll gates for charging battery operated vehicles and street lights on highways.

